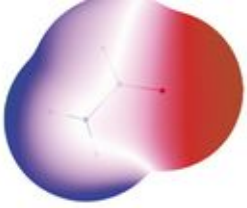

OXFORD

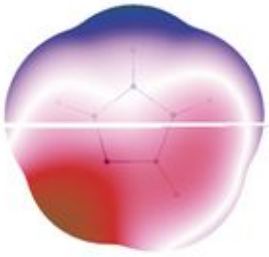

The Theory of Intermolecular Forces

SECOND EDITION

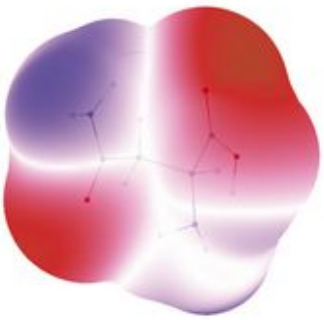

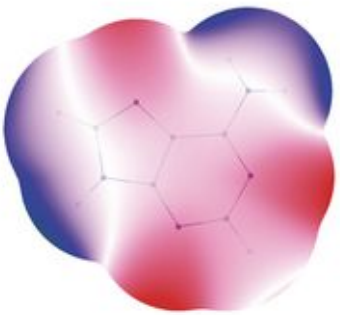

ANTHONY STONE

The Theory of Intermolecular Forces

This page intentionally left blank

The Theory of Intermolecular Forces

Second Edition

Anthony J. Stone
University of Cambridge

OXFORD
UNIVERSITY PRESS

OXFORD
UNIVERSITY PRESS

Great Clarendon Street, Oxford, OX2 6DP,
United Kingdom

Oxford University Press is a department of the University of Oxford.
It furthers the University's objective of excellence in research, scholarship,
and education by publishing worldwide. Oxford is a registered trade mark of
Oxford University Press in the UK and in certain other countries

First Edition published in 1996
Second Edition published in 2013

Impression: 1

British Library Cataloguing in Publication Data
Data available

ISBN 978–0–19–967239–4

Printed and bound by
CPI Group (UK) Ltd, Croydon, CR0 4YY

To Sybil

Preface

The last two decades have seen considerable advances in the understanding of intermolecular forces, in the computational methods used to calculate them, and in the experimental methods used to investigate them. At the time of the first edition, the balance was already shifting from experiment to computation as the prime source of information about intermolecular forces, and this shift has continued. Experiment will continue to have an essential role, but its task now is more to check the validity of calculations and to refine calculated potentials, rather than to provide the principal source of data for them. Density Functional Theory has emerged as a practical tool both for supermolecule calculations, when supplemented by an empirical dispersion term, and as a basis for perturbation theory. It has become possible to calculate interactions between molecules of 20 or 30 atoms to good accuracy, and methods are being developed to describe larger molecules, for example to build proteins from an understanding of their component amino acids. The main changes in this new edition concern these developments. Some issues that were controversial in the 1990s have been resolved and no longer need detailed discussion, and some methods have been superseded and have been mentioned more briefly or omitted.

My own understanding has benefited greatly from several years' enjoyable and fruitful collaboration with Dr Alston Misquitta, and I am glad to be able to acknowledge his considerable contribution. I am indebted both to him and to Professor Sally Price for reading and commenting on drafts of this new edition.

The book is intended to be self-contained as far as the theory of intermolecular forces is concerned. It does assume a sound background in physics, chemistry and mathematics, and in particular in quantum mechanics, but appendices are provided to introduce some of the mathematical techniques. The level of the book is appropriate for graduate students and advanced undergraduates, but it should also be useful for more experienced research workers who require an introduction to the field.

While I have tried to ensure that this edition is free from errors, it is possible that some will have crept through. Any that are found will be reported on my website at http://www-stone.ch.cam.ac.uk/timf.html.

Cambridge A. J. S.
June 2012

Preface to the first edition

There have been many developments in the theory of intermolecular forces over the last twenty years or so that have not so far been collected together in book form. After many years of effort, practical methods have emerged for the accurate calculation of intermolecular interactions by perturbation theory. Increasing computer power is making it possible to pension off the Lennard-Jones potential after 75 years of valuable service and to use more realistic mod-

els; similarly point-charge models are giving way to more sophisticated multipole descriptions. This has come at a time when experimental methods for determining intermolecular potentials are becoming more and more powerful and reliable, and when interest in accurate models of intermolecular interactions is greater than ever before, not least because of the increasing use of computer modelling for simulating systems of biological interest and for designing biologically active molecules for use as drugs and pesticides and the like.

However, these more elaborate descriptions call for corresponding developments in the formalism. The mathematical expressions for interaction energies involving electrostatic multipoles, for instance, are daunting for the beginner, but they can be expressed in a relatively simple form with appropriate mathematical techniques. Forces and torques arising from these interactions can also be manipulated much more easily than is often supposed. I have been interested in these techniques for some time, and I have attempted in this book to set them out in a coherent fashion. The calculation of intermolecular interactions *ab initio* and the construction of accurate potential models are closely related topics that I have described in some detail. The determination of intermolecular potentials from experiment, on the other hand, is not an issue that I have attempted to cover in detail, and I have given only an outline of this aspect of the subject to put the theory in context, together with references to fuller accounts.

It is a pleasure to acknowledge the contributions of my research students and post-doctoral research assistants to the ideas described here, especially those of Sally Price and David Wales, with whom I have had many stimulating discussions and rewarding collaborations in recent years. I thank all my colleagues in the theoretical chemistry group at Cambridge for their support and encouragement; many of them have read parts of the text in draft and made many helpful suggestions. David Buckingham, Nicholas Handy, Ruth Lynden-Bell, David Clary and Roger Amos have all been most agreeable and stimulating people to work with. It is a particular pleasure, as he approaches retirement, to acknowledge the enormous contribution made by David Buckingham to the study of molecular properties and intermolecular forces. I am grateful also to Paul Hoang and Claude Girardet for their hospitality at the Université de Franche Comté in Besançon, where I was Visiting Professor for a time in 1993 and where the first draft of this book was written. I thank Bill Meath for much valuable advice and for permission to reproduce Fig. 8.2. Many others have contributed in various ways; it would be invidious to name a few and impossible to list everyone, but I am grateful to all of them. It goes without saying, but it must be said, that all errors that remain are my responsibility alone.

This book was prepared using LaTeX and BibTeX with the natbib bibliography package, makeindex and hyperref. I am glad to acknowledge the generosity of the TeX community worldwide in making their programs freely available to all.

Cambridge A. J. S.
December 1995

This page intentionally left blank

Contents

1 Introduction 1
- 1.1 The evidence for intermolecular forces 1
- 1.2 Classification of intermolecular forces 4
- 1.3 Potential energy surfaces 6
- 1.4 Coordinate systems 8

2 Molecules in Electric Fields 13
- 2.1 Molecular properties: multipole moments 13
- 2.2 The energy of a molecule in a non-uniform electric field 21
- 2.3 Polarizabilities 24
- 2.4 Hyperpolarizabilities 30
- 2.5 The response to oscillating electric fields 31
- 2.6 Symmetry properties of multipole moments and polarizabilities 34
- 2.7 Change of origin 39

3 Electrostatic Interactions between Molecules 43
- 3.1 The electric field of a molecule 43
- 3.2 Multipole expansion in cartesian form 45
- 3.3 Spherical tensor formulation 47
- 3.4 Examples 52

4 Perturbation Theory of Intermolecular Forces at Long Range 57
- 4.1 Introduction 57
- 4.2 The induction energy 59
- 4.3 The dispersion energy 64

5 Ab Initio Methods 74
- 5.1 Introduction 74
- 5.2 Electron correlation 75
- 5.3 Density functional theory 78
- 5.4 Basis sets 79
- 5.5 Calculation of molecular properties 83
- 5.6 The supermolecule method 87
- 5.7 Density functional theory for interaction energies 92
- 5.8 Semi-empirical methods 95
- 5.9 Potential energy surfaces 95
- 5.10 Energy decomposition analysis 96

6 Perturbation Theory of Intermolecular Forces at Short Range 100
- 6.1 Introduction 100
- 6.2 Symmetric perturbation methods 106

6.3 Symmetry-adapted perturbation theories 110
6.4 The SAPT method 117

7 Distributed Multipole Expansions 122
7.1 Convergence of the multipole expansion 122
7.2 Distributed multipole expansions 123
7.3 Distributed multipole analysis 124
7.4 Other distributed-multipole methods 128
7.5 Simplified distributed multipole descriptions 130
7.6 Examples 131
7.7 Symmetry and distributed multipoles 135
7.8 Point-charge models 136

8 Short-Range Effects 141
8.1 The electrostatic energy at short range: charge penetration 141
8.2 The exchange–repulsion energy 146
8.3 The second-order energy at short range 147
8.4 The hydrogen bond 153
8.5 Halogen bonds 157

9 Distributed Polarizabilities 159
9.1 The Applequist model 161
9.2 Distributed polarizabilities 166
9.3 Computation of distributed polarizabilities 170
9.4 The induction energy in a distributed polarizability description 176
9.5 Distributed dispersion interactions 179

10 Many-body Effects 182
10.1 Non-additivity of the induction energy 182
10.2 Many-body terms in the dispersion energy 187
10.3 Many-body terms in the repulsion energy 190
10.4 Other many-body effects 190
10.5 Intermolecular forces in a medium 191

11 Interactions Involving Excited States 194
11.1 Resonance interactions and excitons 194
11.2 Distributed transition moments 197
11.3 Interactions involving open-shell systems 199

12 Practical Models for Intermolecular Potentials 201
12.1 Potentials for atoms 202
12.2 Model potentials for molecules 209
12.3 Dependence on internal coordinates 219
12.4 A case study: potentials for water 225
12.5 Coarse-grained models 229
12.6 Calculation of energy derivatives 229
12.7 Derivatives with respect to orientation 231

13 Theory and Experiment 240
13.1 Properties of individual molecules 240
13.2 Validation of intermolecular potentials by experimental methods 244
13.3 Simulation methods 247
13.4 Spectroscopic methods 249
13.5 Molecular beam scattering 260
13.6 Measurements on liquids and solids 263

Appendix A Cartesian Tensors 267
A.1 Basic definitions 267

Appendix B Spherical Tensors 271
B.1 Spherical harmonics 271
B.2 Rotations of the coordinate system 273
B.3 Spherical tensors 274
B.4 Coupling of wavefunctions and spherical tensors 275

Appendix C Introduction to Perturbation Theory 277
C.1 Non-degenerate perturbation theory 277
C.2 The resolvent 280
C.3 Degenerate perturbation theory 280
C.4 Time-dependent perturbation theory 281

Appendix D Conversion Factors 283
D.1 Multipole moments 283
D.2 Polarizabilities 284
D.3 Dispersion coefficients 284

Appendix E Cartesian–Spherical Conversion Tables 285

Appendix F Interaction Functions 291

References 298

Author Index 324

Index 331

This page intentionally left blank

1
Introduction

1.1 The evidence for intermolecular forces

The idea that matter is made up of atoms and molecules was known to the Greeks, though the evidence for it did not become persuasive until the eighteenth and nineteenth centuries, when the ideal gas laws, the kinetic theory of gases, Faraday's laws of electrolysis, the stoichiometry of most chemical reactions, and a variety of other indications combined to decide the matter beyond doubt. In the twentieth century, further techniques such as X-ray diffraction and, more recently, high-resolution microscopy, have provided more evidence.

Given the idea that matter consists of molecules, however, the notion that there must be forces between them rests on much simpler evidence. The very existence of condensed phases of matter is conclusive evidence of attractive forces between molecules, for in the absence of attractive forces, the molecules in a glass of water would have no reason to stay confined to the glass. Furthermore, the fact that water has a definite density, and cannot easily be compressed to a smaller volume, shows that at short range the forces between the molecules become repulsive.

It follows that the energy of interaction U between two molecules, as a function of the distance R between them, must take the form shown in Fig. 1.1. That is, it must have an attractive region at long range, where the force $-\partial U/\partial R$ is negative, and a steeply repulsive region at close range to account for the low compressibility of condensed materials. There is a separation R_m where the energy is a minimum, and a closer distance σ where the energy of interaction goes through zero before climbing steeply. These are conventional notations, as is the symbol ϵ for the depth of the attractive well. The precise form of the function $U(R)$ will depend on the particular molecules concerned, but these general features will be almost

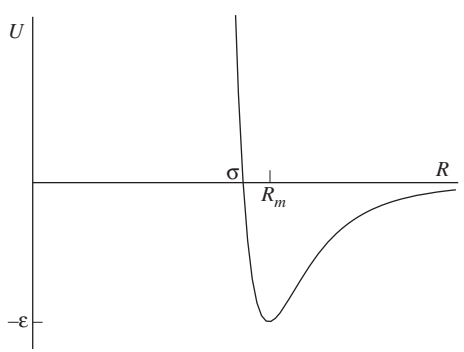

Fig. 1.1 A typical intermolecular potential energy function.

universal. For some pairs of molecules, in some relative orientations, the interaction energy may be repulsive at all distances, but unless the molecules are both ions with the same sign of charge, there will always be orientations where the long-distance interaction is attractive.

Van der Waals was the first to take these ideas into account in describing the departure of real gases from ideality. He suggested that the volume V occupied by a gas included a volume b that was occupied by the incompressible molecules, so that only $V - b$ remained for the free movement of the molecules; and that the attractive forces between the molecules had the effect of reducing the pressure exerted by a gas on its container, by an amount proportional to the square of the density. Thus the 'true' pressure, in the sense of the gas laws, is not the measured pressure P but $P + a/V^2$. The gas law $PV = RT$ then took the form $(P + a/V^2)(V - b) = RT$, where P and V are now the measured pressure and volume rather than the ideal values.

This simple equation gave a remarkably good account of the condensation of gases into liquids, and the values of the constants a and b correspond tolerably well with the properties of molecules as we now understand them. Although this approach has been superseded, the forces of attraction and repulsion between molecules are still often called 'Van der Waals' forces.

1.1.1 Magnitudes

The value of the Van der Waals parameter b has a clear interpretation in terms of molecular size; but more direct methods, such as X-ray crystallography, provide accurate values for the equilibrium separation in the solid. This is not quite the same as R_m, because there are attractive forces between more distant molecules that compress the nearest-neighbour distance slightly. The depth ϵ of the attractive well can be estimated *via* calorimetric data. One simple order-of-magnitude method is based on *Trouton's rule*, an empirical observation which states that the enthalpy of vaporization is approximately related to the boiling point at atmospheric pressure T_b by $\Delta H_\mathrm{vap} \approx 10RT_\mathrm{b}$. Although this is an empirical rule, it can be understood quite easily in a general way: the change in Gibbs free energy $G = H - TS$ between liquid and vapour is zero at the boiling point, so $\Delta H_\mathrm{vap} = T_\mathrm{b}\Delta S_\mathrm{vap}$. We approximate ΔS in terms of the change of volume between liquid and gas, $\Delta S = R\ln(V_g/V_l)$, as if the liquid were just a highly compressed gas. Typically $(V_g/V_l) \approx 10^3$, which gives $\Delta S \approx 7R$; the remaining $3R$ or so can be accounted for by the fact that liquids are more structured than gases, and so have a lower entropy than is assumed in this simple picture.

Now the energy required to separate a condensed liquid into its constituent molecules is approximately ϵ for each pair of molecules that are close together. If each molecule has n neighbours in the liquid, the total energy for N molecules is $\frac{1}{2}Nn\epsilon$ (where the factor of $\frac{1}{2}$ is needed to avoid counting each interaction twice). This is approximately the latent heat of evaporation; we should really correct for the zero-point energy of vibration of the molecules in the liquid, but if we assume that the intermolecular vibrations are classical the energy in these vibrations will be the same as the translational energy in the gas. Thus we find that $\frac{1}{2}N_An\epsilon \approx 10RT_\mathrm{b}$, or $\epsilon/k_B \approx 20T_\mathrm{b}/n$.

Table 1.1 shows the values that result for a few atoms and molecules. The value of the coordination number n has been assumed here to be the same as in the solid; this is probably a slight overestimate in most cases. The results show that the predictions are quite good, and certainly adequate for estimating the order of magnitude of ϵ.

Table 1.1 Pair potential well depths.

	T_b/K	n	$(20T_b/n)$/K	(ϵ_{exp}/k_B)/K
He	4.2	12	7	11
Ar	87	12	145	142
Xe	166	12	277	281
CH_4	111.5	12	186	180–300
H_2O	373.2	4	1866	2400 approx.

We see, then, that the strength of intermolecular interactions between small molecules, as measured by the well depth ϵ, is typically in the region 1–25 kJ mol^{-1} or 100–2000 K. This is considerably weaker than a typical chemical bond, which has a dissociation energy upwards of 200 kJ mol^{-1}, and this is why intermolecular interactions can be broken easily by simple physical means such as moderate heat, while chemical bonds can only be broken by more vigorous procedures.

1.1.2 Pairwise additivity

In this analysis, we have tacitly assumed that the energy of an assembly of molecules, as in a liquid, can be treated as a sum of pairwise interactions; that is, that the total energy W of the assembly can be expressed in the form

$$\begin{aligned} W &= \sum_i W_i + \sum_{i=2}^{N} \sum_{j=1}^{i-1} U_{ij} \\ &= \sum_i W_i + \sum_{i>j} U_{ij} \\ &= \sum_i W_i + \tfrac{1}{2} \sum_j \sum_{i \neq j} U_{ij}, \end{aligned} \tag{1.1.1}$$

where W_i is the energy of isolated molecule i and U_{ij} is the energy of interaction between i and j. We have to be careful to count each pair of molecules only once, not twice, and the sum over pairs can be written in several ways, as shown, the second form being a conventional abbreviation of the first.

This assumption of *pairwise additivity* is only a first approximation. Eqn (1.1.1) is just the leading term in a series which should include three-body terms, four-body terms, and so on:

$$\begin{aligned} U &= W - \sum_i W_i^0 \\ &= \sum_{i>j} U_{ij} + \sum_{i>j>k} U_{ijk} + \sum_{i>j>k>l} U_{ijkl} + \cdots \\ &= W_{2\text{body}} + W_{3\text{body}} + W_{4\text{body}} + \cdots . \end{aligned} \tag{1.1.2}$$

For instance, if there are three molecules A, B and C, the pairwise approximation to the total energy is $U_{AB} + U_{BC} + U_{AC}$, where U_{AB} is evaluated as if molecule C were not present, and so on. However, the presence of molecule C will modify the interaction between the other two

molecules, so there is a three-body correction: $U = U_{AB} + U_{BC} + U_{AC} + U_{ABC}$. When there are four molecules, we have to include a three-body correction for each set of three molecules, and the error that remains is the four-body correction. We hope that the total contribution $W_{3\text{body}}$ of the three-body corrections will be small, and the four-body term smaller still. In most circumstances this is a reasonably good approximation, so most effort is concerned with getting the pair interactions right. However, the many-body terms are not small enough to neglect altogether, and we shall need to consider them later, in Chapter 10. In particular, the three-body terms may be much too large to ignore.

Eqn (1.1.2) ignores a further contribution which may need to be taken into account. Usually the geometry of each interacting molecule is distorted in the environment of its neighbours. The most common example is the hydrogen bond A–H···B, where the AH bond is usually longer in the complex than in the isolated molecule. The distortion away from the equilibrium geometry costs energy, but if the interaction with the neighbour is enhanced the overall energy may be lowered. The difference between the energy of the molecule in its distorted geometry and its energy W_i^0 at equilibrium is called the *deformation energy*. If the molecules are rigid (high vibrational force constants) the cost of even a small distortion outweighs any improvement in binding energy and the deformation energy is negligible. If there are soft vibrational modes, however, the deformation may be significant and the deformation energy may need to be included. This is not easy to do, as the distortion of each molecule depends on all its neighbours, so the deformation energy is a complicated many-body effect, and in practice it is often neglected completely.

1.2 Classification of intermolecular forces

We can identify a number of physical phenomena that are responsible for attraction and repulsion between molecules. Here we give an overview of the main contributions to forces between molecules. All of the important ones arise ultimately from the electrostatic interaction between the particles comprising the two molecules. They can be separated into two main types: 'long-range', where the energy of interaction behaves as some inverse power of R, and 'short-range', where the energy decreases in magnitude exponentially with distance. This apparently arbitrary distinction has a clear foundation in theory, as we shall see.

The long-range effects are of three kinds: *electrostatic*, *induction* and *dispersion*. The electrostatic effects are the simplest to understand in general terms: they arise from the straightforward classical interaction between the static charge distributions of the two molecules. They are strictly pairwise additive and may be either attractive or repulsive. Induction effects arise from the distortion of a particular molecule in the electric field of all its neighbours, and are always attractive. Because the fields of several neighbouring molecules may reinforce each other or cancel out, induction is strongly non-additive. Dispersion is an effect that cannot easily be understood in classical terms, but it arises because the charge distributions of the molecules are constantly fluctuating as the electrons move. The motions of the electrons in the two molecules become correlated, in such a way that lower-energy configurations are favoured and higher-energy ones disfavoured. The average effect is a lowering of the energy, and since the correlation effect becomes stronger as the molecules approach each other, the result is an attraction.

We shall discuss all these effects in much more detail later. For the moment they are summarized in Table 1.2. Two other effects that can arise at long range are included in the

Table 1.2 Contributions to the energy of interaction between molecules.

Contribution	Additive?	Sign	Comment
Long-range ($U \sim R^{-n}$)			
Electrostatic	Yes	±	Strong orientation dependence
Induction	No	−	
Dispersion	approx.	−	Always present
Resonance	No	±	Degenerate states only
Magnetic	Yes	±	Very small
Short-range ($U \sim \mathrm{e}^{-\alpha R}$)			
Exchange-repulsion	approx.	+	Dominates at very short range
Exchange-induction	approx.	−	
Exchange-dispersion	approx.	−	
Charge transfer	No	−	Donor-acceptor interaction

Table: these are resonance and magnetic effects. Resonance interactions occur either when at least one of the molecules is in a degenerate state—usually an excited state—or when the molecules are identical and one is in an excited state. Consequently they do not occur between ordinary closed-shell molecules in their ground states. They will be discussed in Chapter 11. Magnetic interactions involving the electrons can occur only when both molecules have unpaired spins, but in any case are very small. Magnetic interactions involving nuclei can occur whenever there are nuclei with non-zero spin, which is quite common, but the energies are several orders of magnitude smaller still, and are never of any significance in the context of intermolecular forces.

The 'long-range' electrostatic, induction and dispersion contributions are so called because they are the ones that survive at large separations. However, they are still present at short distances, even when the molecules overlap strongly. The electrostatic interaction, for example, being the electrostatic interaction between the unperturbed molecular charge distributions, is well defined at any distance, and remains finite unless nuclei come into contact. However, it is usual to describe all of these contributions as power series in $1/R$, where R is the molecular separation, and such series evidently diverge as $R \to 0$, so they are only valid for sufficiently large R. Even where the series converges, it may still be in error, because the series treats each molecule as if it were concentrated at a point, rather than extended in space. This error is called the 'penetration error'. Furthermore, it is necessary in practice to truncate the series at a finite number of terms, leading to a 'truncation error'.

Further contributions to the energy arise at short range—that is, at distances where the molecular wavefunctions overlap significantly and electron exchange between the molecules becomes possible. The most important is described as exchange-repulsion or just exchange. It can be thought of as comprising two effects: an attractive part, arising because the electrons become free to move over both molecules rather than just one, increasing the uncertainty in their positions and so allowing the momentum and energy to decrease; and a repulsive part, arising because the wavefunction has to adapt to maintain the Pauli antisymmetry requirement that electrons of the same spin may not be in the same place, and this costs energy. The latter dominates, leading to a repulsive effect overall. It is usual to take these effects together. The remaining effects listed in Table 1.2, namely exchange-induction, exchange-dispersion and

charge transfer, also arise when the wavefunctions overlap; the charge-transfer interaction is often viewed as a separate effect but is better thought of as a part of the induction energy. These terms will be discussed in more detail in Chapter 8.

1.3 Potential energy surfaces

Only in the case of atoms is a single distance sufficient to describe the relative geometry. In all other cases further coordinates are required, and instead of contemplating a potential energy curve like Fig. 1.1, we need to think about the 'potential energy surface', which is a function of all the coordinates describing the relative position of the molecules. In the case of two non-linear molecules, there are six of these coordinates (we discuss them below) and the potential energy surface becomes very difficult to visualize. For many purposes, however, we can think in three dimensions: a vertical dimension for the energy, and two horizontal dimensions which are representative of the six or more coordinates that we should really be using. This simplified picture is then like a landscape, with hills and valleys. There are energy minima on the potential energy surface that correspond to depressions in the landscape. In the real landscape such depressions are usually filled with water, to give lakes or tarns; there may be many of them, at different heights. In the quantum-mechanical landscape of the potential-energy surface, there may also be many minima, but there is always one 'global minimum' that is lower than any of the others. (Sometimes there are several global minima of equal energy, related to each other by symmetry.) The rest are 'local minima'; the energy at a local minimum is lower than the energy of any point in its immediate neighbourhood, but if we move further away we can find other points that are lower still.

Just as the depressions in the landscape are filled with water, we might think of the minima in the potential-energy surface as being filled with zero-point energy; and just as lakes may merge into each other, so the zero-point energy may permit molecular systems to move freely between adjacent minima if the barriers between them are not too high. The zero-point energy in molecular complexes is often a substantial fraction of the well depth. In the HF dimer, for example, the well depth ϵ (alternatively described as the dissociation energy from the equilibrium geometry, D_e) is 19.2 kJ mol^{-1} (Peterson and Dunning 1995), while the dissociation energy D_0 from the lowest vibrational level to monomers at their lowest vibrational level is only 1062 cm^{-1} = 12.70 kJ mol^{-1} (Dayton *et al.* 1989). Given enough energy, the molecular system can rearrange, passing from one energy minimum to another via a 'saddle point' or 'transition state' which is the analogue of the mountain pass. The molecular system however can also tunnel between minima, even if the energy of the system is not high enough to overcome the barrier in the classical picture. A well-known example is the ammonia molecule, which can invert via a planar transition structure from one pyramidal minimum to the other. The height of the barrier in this case is 2020 cm^{-1} or about 24 kJ mol^{-1}. If tunnelling is ignored, the lowest-energy stationary states for the inversion vibration have an energy of 886 cm^{-1}, and there are two of them, one confined to each minimum. When tunnelling is taken into account, these two states can mix. If they combine in phase the resulting state has a slightly lower energy; if out of phase, the energy is slightly higher. The difference in energy—the 'tunnelling splitting'—is 0.79 cm^{-1} in this case, and can be measured very accurately by spectroscopic methods. Such tunnelling splittings are a useful source of information about potential energy surfaces.

Along with the minima, then, the barriers constitute the other important features of the surface, corresponding to the mountain passes of the real landscape. To understand the nature

of the potential energy surface, we need to characterize the minima and the transition states. In mathematical terms, these are both 'stationary points', where all the first derivatives of the energy with respect to geometrical coordinates are zero. To distinguish between them, we need to consider the second derivatives. If we describe the energy U in the neighbourhood of a stationary point by a Taylor expansion in the geometrical coordinates q_i, it takes the form

$$U = U(0) + \tfrac{1}{2} \sum_{ij} q_i q_j \left. \frac{\partial^2 U}{\partial q_i \partial q_j} \right|_0 + \cdots ; \tag{1.3.1}$$

the first derivatives are all zero at a stationary point, and we can ignore the higher derivatives if the q_i are small. The matrix of second derivatives is called the 'Hessian'; its components are

$$H_{ij} = \frac{\partial^2 U}{\partial q_i \partial q_j}. \tag{1.3.2}$$

The eigenvalues of the Hessian are all positive at a minimum; in this case the Hessian is said to be 'positive definite'. Whatever direction we walk away from a minimum, we find ourselves going uphill. Such a point is said to have 'Hessian index zero': that is, the Hessian has no negative eigenvalues there. At a saddle point or mountain pass, precisely *one* of the eigenvalues is negative—the Hessian index is 1. If we walk along the eigenvector corresponding to that eigenvalue, in either direction, we find ourselves going downhill, but the other eigenvectors take us uphill. Just as in the real landscape, the saddle points provide the routes from one valley or minimum to another. If two or more of the eigenvalues are negative, there are two orthogonal directions that will take us downhill. In this case (in the real landscape) we are at the top of a hill, and all directions lead downhill; in the many-dimensional system there may be other directions that lead uphill. However, it is never necessary to go over the top of the hill to get to the other side; there is always a lower route round the side of the hill (Murrell and Laidler 1968). If we are interested in characterizing the potential-energy surface, then, the most important stationary points are the minima, with Hessian index 0, and the saddle points, with Hessian index 1. Stationary points with higher values of the Hessian index are much less important.

Often there are several equivalent minima with the same energy, related to each other by the symmetry of the system. In the HF dimer, for example, the equilibrium structure is hydrogen-bonded, with only one of the two H atoms in the hydrogen bond. There are two such structures, one with the H atom of molecule 1 forming the hydrogen bond, the other with the H atom of molecule 2 in that role. For reasons of symmetry they have the same energy; they are distinguishable only if we can label the atoms in some way. The two cases are said to be different 'versions' of the same structure. In the same way there may be several versions of a transition state, related to each other by symmetry (Bone *et al.* 1991).

For large systems, comprising many molecules, the number of stationary points increases exponentially with the size of the system, and detailed characterization of the potential energy surface becomes difficult or impossible. In such cases, a qualitative or statistical description of the nature of the 'energy landscape' is more useful: are the typical barriers high or low compared with the temperature, or with the energy differences between adjacent minima, and what are the consequences for properties such as the rate of rearrangement to the global minimum? Such questions will not be pursued here, but have been addressed in detail by Wales (2004), Wolynes (1997) and others.

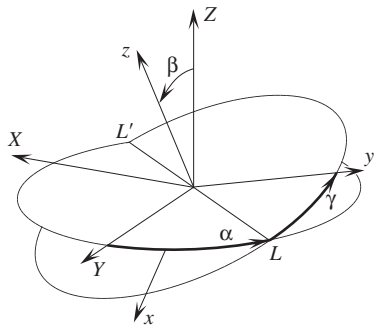

Fig. 1.2 Euler angles α, β and γ defining the orientation of an axis system x, y, z relative to X, Y, Z.

1.4 Coordinate systems

In this book, we shall be particularly concerned with the dependence of intermolecular forces on the orientation of the molecules—indeed, we shall see that the anisotropy of the interaction is a key feature, vital for understanding many aspects of structure and properties—and we shall need to use a variety of coordinate systems to describe the orientations. We summarize the principles here, but the details can be skipped on a first reading.

It is helpful to establish first the idea of 'local' and 'global' coordinate systems, often called 'molecule-fixed' and 'space-fixed' respectively. The 'global' coordinate system is defined by a set of cartesian axes, fixed in space, which we may call X, Y and Z. Their directions may be defined by reference to macroscopic features such as an external electric field, or the directions of the incident and scattered beams in Raman spectroscopy, or the directions of the molecular beam and the laser beam in molecular beam spectroscopy, but often they just provide an abstract frame of reference. Usually it is only the direction of the global axes that matters, and the position of the origin is unimportant.

The 'local' or 'molecule-fixed' axis system is tied to the molecule, and moves with it. Usually the origin is at the centre of mass, but it may be more convenient to put it at one of the nuclei—at the oxygen nucleus in the water molecule, for example. The directions of the coordinate axes are then fixed by reference to atom positions, so in water we might take the z axis along the C_2 symmetry axis, the x axis perpendicular to the plane, and the y axis to form a right-handed orthogonal set. Provided that we treat the molecules as rigid, the definition of local axes is straightforward. Important subtleties arise if we contemplate vibrating molecules, and there are further complications in molecules with large-scale internal motions, such as the torsions around the backbone bonds in a polypeptide. We shall for the most part ignore such issues, but note that the definition of molecule-fixed axes in vibrating molecules is usually achieved by imposing the 'Eckart conditions', which are nearly, but not quite, equivalent to the requirement that the angular momentum of the molecule relative to its local axis system is zero. A detailed discussion can be found in the classic text by Wilson *et al.* (1955, Chapter 11). We return to the question of molecules with large-amplitude internal motions in Chapter 12.

The relationship between global and local axes is described by a rotation and a translation. Starting from a configuration in which the two sets of axes coincide, we first rotate the molecule into the desired orientation, and then translate it to the desired position. The rotation is usually described in terms of Euler angles α, β and γ which are defined as follows.

- Start from an orientation in which the local or molecule-fixed axes x, y and z are parallel to the X, Y and Z axes.
- Rotate through γ about the Z axis (or the z axis—they are parallel initially).
- Rotate through β about the Y axis.
- Rotate through α about the Z axis.

In each case a positive rotation is such as to advance a corkscrew outwards along the specified axis. Fig. 1.2 shows the resulting configuration. The angle between the Z and z axes is β. The other angles, α and γ, can be defined by reference to the *line of nodes*, which is the line of intersection of the XY and xy planes (LL' in Fig. 1.2). α is the angle from the Y axis to the line of nodes, measured corkscrew-wise around the Z axis, while γ is the angle from the line of nodes to the y axis, measured corkscrew-wise around the z axis. If β is zero or π, the xy and XY planes coincide and the line of nodes is undefined, so that α and γ are not individually defined. When $\beta = 0$, their sum, $\alpha+\gamma$, is the angle from the Y axis to the y axis, while if $\beta = \pi$, $\alpha - \gamma$ is the angle from the Y axis to the y axis, measured around the Z axis.

In an alternative definition of the Euler angles, precisely equivalent to the one above, the rotations are taken around the molecule-fixed axes instead. Starting with the axes parallel as before, the rotations are then as follows.

- Rotate through α about the z axis (initially parallel to the Z axis).
- Rotate through β about the y axis (which at this stage is directed along the line of nodes).
- Rotate through γ about the z axis.

Note that the angles are taken in the reverse order in this case. The equivalence of the two definitions can be verified by reference to Fig. 1.2; see Zare (1988, p. 78) for a more formal proof.

Euler angles are not always the most convenient way to describe rotations. One difficulty is that it is not at all straightforward to express the result of two successive Euler-angle rotations as a single Euler-angle rotation. Another is that when $\beta = 0$ or π, the values of α and γ are not unique. This means that a zero rotation can be described with $\beta = 0$ but $\alpha = -\gamma$ non-zero and arbitrary. This makes the Euler-angle description unmanageable in molecular simulations, where each step involves a small rotation, and consequently other descriptions are often used. A simple one is the angle–axis picture: a rotation is described by a unit vector $\mathbf{n} = (n_x, n_y, n_z)$ specifying the axis of rotation and the angle ψ of rotation about that axis. These can be combined into a single vector $\psi\mathbf{n}$. A closely related but more powerful description uses *quaternions*: a rotation through ψ about the axis described by the unit vector $\mathbf{n}$ is specified by the quaternion

$$Q = [\cos \tfrac{1}{2}\psi, n_x \sin \tfrac{1}{2}\psi, n_y \sin \tfrac{1}{2}\psi, n_z \sin \tfrac{1}{2}\psi]. \tag{1.4.1}$$

This appears at first sight to be just a more cumbersome way to express an angle–axis rotation, but it has the great advantage that the result of two or more successive rotations is easily obtained. The product of two successive rotations, $[\beta_0, \beta_1, \beta_2, \beta_3] \equiv [\beta_0, \boldsymbol{\beta}]$ followed by $[\alpha_0, \alpha_1, \alpha_2, \alpha_3] \equiv [\alpha_0, \boldsymbol{\alpha}]$ is the single rotation

$$[\alpha_0, \boldsymbol{\alpha}][\beta_0, \boldsymbol{\beta}] = [\alpha_0\beta_0 - \boldsymbol{\alpha} \cdot \boldsymbol{\beta}, \alpha_0\boldsymbol{\beta} + \boldsymbol{\alpha}\beta_0 + \boldsymbol{\alpha} \times \boldsymbol{\beta}]. \tag{1.4.2}$$

It is also evident from eqn (1.4.1) that the components of a quaternion satisfy $\alpha_0^2 + \alpha_1^2 + \alpha_2^2 + \alpha_3^2 = 1$, so any rotation is represented by a point on the surface of a sphere in four dimensions and the description is well-behaved in the neighbourhood of the identity or zero rotation.

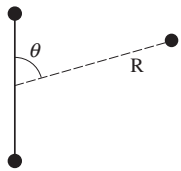

Fig. 1.3 The position of an atom relative to a linear molecule can be described by a distance R and an angle θ.

The relationship between the quaternion $[\alpha_0, \alpha_1, \alpha_2, \alpha_3]$ and the equivalent Euler-angle description (α, β, γ) is

$$\begin{aligned}
\alpha_0 &= \cos\tfrac{1}{2}\beta \cos\tfrac{1}{2}(\gamma + \alpha) \\
\alpha_1 &= \sin\tfrac{1}{2}\beta \sin\tfrac{1}{2}(\gamma - \alpha) \\
\alpha_2 &= \sin\tfrac{1}{2}\beta \cos\tfrac{1}{2}(\gamma - \alpha) \\
\alpha_3 &= \cos\tfrac{1}{2}\beta \sin\tfrac{1}{2}(\gamma + \alpha)
\end{aligned} \tag{1.4.3}$$

Some systems can be described more simply. For linear molecules, we take the local z axis along the molecular axis, and then the configuration is completely described by α and β, and γ is not needed. In this case, the angles α and β are more usually called φ and θ respectively: they are the spherical polar angles that describe the direction of the molecular axis relative to the global frame.

If we are concerned only to describe the interactions of the molecules with each other, rather than with some external field, the 'global' coordinate system may be more conveniently defined by reference to the molecules themselves. Thus for the interaction of an atom with a molecule, we can use a global coordinate system that coincides with the local coordinate system for the molecule, and then use spherical polar coordinates to specify the position of the atom relative to this axis system. If the molecule is linear the energy does not depend on the angle φ, and one distance and one angle suffice to determine the geometry (Fig. 1.3). For an atom interacting with a non-linear molecule we would need φ as well.

In the case of two linear molecules, it is often convenient to use a coordinate system in which one of the molecules is at the origin, and the other is situated on the positive Z axis, at $(0, 0, R)$ (see Fig. 1.4). Here we are defining the global axis system by reference to the positions of the two molecules. The direction of each molecular axis (its local z axis) is then defined by two polar angles, θ and φ. Notice that there is an asymmetry between θ_1 and θ_2: when $\theta_1 = 0$ the z_1 axis points towards molecule 2, but when $\theta_2 = 0$ the z_2 axis points away from molecule 1. This asymmetry in the coordinate system leads to an asymmetry in the formulae for the interaction energy. It is not unduly troublesome, but it means that care must be taken in defining which molecule is which.

A rotation of the entire system about the Z axis leaves the energy unchanged (in the absence of external fields). This has the effect of changing both φ_1 and φ_2 by the same amount, leaving $\varphi_1 - \varphi_2$ unchanged but altering $\varphi_1 + \varphi_2$. It follows that the energy may depend on $\varphi = \varphi_1 - \varphi_2$ but not on $\varphi_1 + \varphi_2$. The relative geometry is described by the four coordinates R, θ_1, θ_2 and $\varphi = \varphi_1 - \varphi_2$.

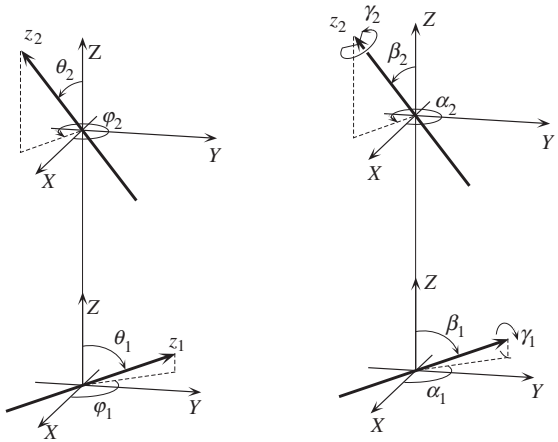

Fig. 1.4 (*Left*) A coordinate system for two linear molecules; (*Right*) A coordinate system for two non-linear molecules.

If either molecule is non-linear, the interaction energy will vary as it is rotated about its molecular axis, and the third Euler angle becomes necessary. Here it is usual to use α, β and γ. If both molecules are non-linear, the description of the geometry requires six angles, but the energy is independent of $\alpha_1 + \alpha_2$. Thus we require the distance R and the five angles $\alpha_1 - \alpha_2$, $\beta_1, \beta_2, \gamma_1$ and γ_2 to describe the configuration.

Sometimes it is more natural to use a genuinely 'global' coordinate system, rather than a coordinate system tied to the molecules under discussion. The vector from molecule 1 to molecule 2 is now defined by three coordinates, R, θ and φ, and the orientation of each molecule is defined as before by three Euler angles. In this case we have nine variables in all, but only six of them are independent, in the absence of external fields, because the energy is unaffected by any rotation of the entire system. Here, however, it is a much more complicated matter to impose this energy invariance. Nevertheless, in spite of its more complicated appearance, such a description is often useful, and the simpler descriptions can be recovered from it by rotating the whole system so that $\theta = \varphi = 0$, i.e., so that the intermolecular vector lies along the global Z axis.

When there are more than two molecules in the system the number of intermolecular degrees of freedom increases further. For a system comprising N molecules, of which L are linear, and A atoms, there are $6(N-1) - L + 3A$ intermolecular degrees of freedom, plus one more if the system as a whole is linear. The simplest description is then to specify the position of each atom and molecule and the orientation of each molecule. This provides $6N - L + 3A$ coordinates, but the energy is unaffected by translation or rotation of the entire system.

1.4.1 Internal coordinates

Intermolecular forces are also affected by the vibrational coordinates of the molecules, which modify the molecular properties on which the intermolecular forces depend. These effects lead to a coupling between intermolecular and intramolecular motions. For the most part we shall not refer explicitly to such effects, since the fundamental theory of the interaction is the

same whatever the molecular geometry may be, and many phenomena are not critically affected by the dependence of the intermolecular forces on the internal coordinates. However, the coupling between internal coordinates and intermolecular coordinates may lead to changes in equilibrium bond lengths and bond angles, and to modification of vibrational frequencies. An example is the well-known vibrational red-shift caused by hydrogen bonding, which cannot be addressed without considering the relationship between the vibrational motion and the intermolecular forces. Even where the internal motions do not affect the phenomena in a fundamental way, however, they will modify them to some degree, so they should be taken into account in principle. Properties on which the intermolecular forces depend, such as multipole moments, should be regarded as functions of the internal coordinates, or at least averaged over the zero-point motion of the molecules. In practice, it is more usual in *ab initio* calculations to evaluate them at the equilibrium geometry of the isolated molecules.

2
Molecules in Electric Fields

2.1 Molecular properties: multipole moments

Of the contributions to the interaction energy listed in Table 1.2, the electrostatic interaction is often the most important, as we shall see in later chapters. However, all of the contributions to the interaction energy between molecules, except for the unimportant magnetic terms, derive ultimately from the Coulombic interactions between their particles. In order to develop the theory of all these effects, we need to be able to describe the way in which the charge is distributed in a molecule. For most purposes, this is done most simply and compactly by specifying its *multipole moments*, and while this description has its limitations it provides an essential part of the language that we use to discuss intermolecular forces.

Multipole moments can be defined in two ways. One uses the mathematical language of cartesian tensors, while the other, the spherical-tensor formulation, is based on the spherical harmonics. The two descriptions are very closely related, and in many applications it is possible to use either. For more advanced work, the spherical-tensor approach is more flexible and powerful, but we begin with the cartesian approach because it is somewhat easier to understand. Later we shall use the spherical-tensor and cartesian tensor definitions more or less interchangeably, using whichever is more convenient.

2.1.1 Cartesian definition

The simplest multipole moment is the total charge: $q = \sum_a e_a$, where e_a is the charge on particle a and the sum is taken over all the electrons and nuclei. If the molecule is placed in an electrostatic potential field $V(\mathbf{r})$, its energy is

$$U_{\text{es}} = \sum_a e_a V(\mathbf{a}),$$

where we are using the vector $\mathbf{a}$ to describe the position of particle a. In a uniform electric field of magnitude F_z in the z direction, the electrostatic potential is $V(\mathbf{r}) = V_0 - zF_z$, and the energy becomes

$$U_{\text{es}} = qV_0 - \sum_a e_a a_z F_z,$$

where V_0 is an arbitrary constant, the electrostatic potential at the origin. In the second term, we are led to introduce the *dipole moment* $\hat{\mu}_z = \sum_a e_a a_z$, and the energy becomes $U_{\text{es}} = -F_z\hat{\mu}_z$. If the electric field also has components F_x and F_y in the x and y directions, the energy becomes

$$U_{\text{es}} = qV_0 - (\hat{\mu}_x F_x + \hat{\mu}_y F_y + \hat{\mu}_z F_z) = qV_0 - \hat{\boldsymbol{\mu}} \cdot \mathbf{F}, \tag{2.1.1}$$

Table 2.1 Examples of dipole moments in atomic units, debye and C m. Positive values correspond to positive charge at the left-hand end of the molecule as written.

	ea_0	D	10^{-30} C m		ea_0	D	10^{-30} C m
HF	0.718	1.826	6.091	H_2O	0.730	1.855	6.188
HCl	0.436	1.109	3.70	H_3N	0.578	1.47	4.90
CO	−0.0431	−0.1096	−0.3656	$(CH_3)_2CO$	1.13	2.88	9.61
OCS	−0.2814	−0.7152	−2.386	C_5H_5N	0.86	2.19	7.31
HCN	1.174	2.984	9.953	CH_3CN	1.539	3.913	13.05

where $\hat{\mu}_x = \sum_a e_a a_x$ and $\hat{\mu}_y = \sum_a e_a a_y$. We can write the three components in one equation using 'tensor notation':

$$\hat{\mu}_\alpha = \sum_a e_a a_\alpha,$$

where α may stand for x, y or z. The caret over the symbol μ is to remind ourselves that this is an operator. If we require the value of the dipole moment in state $|n\rangle$, we construct it by taking the expectation value of this operator:

$$\begin{aligned}\mu_\alpha &= \langle n|\hat{\mu}_\alpha|n\rangle, \\ &= \int \rho_n(\mathbf{r}) r_\alpha \, \mathrm{d}^3\mathbf{r},\end{aligned}$$

where the second form is expressed in terms of the molecular charge density $\rho(\mathbf{r})$, and again α may stand for x, y or z. If we integrate over electronic coordinates only (but include the contribution of the nuclear charge) we get the dipole moment for a fixed nuclear configuration. We have to integrate over nuclear coordinates too (vibrational average) to get a result that corresponds to the value that is measured experimentally. For example, the dipole moment of BH at its equilibrium geometry in the ground state has a magnitude of 0.5511 ea_0, but the vibrationally averaged value is 0.5345 ea_0 (Halkier *et al.* 1999).

Dipole moment values for some small molecules are listed in Table 2.1; for others see McClellan (1963, 1974, 1989) or Gray and Gubbins (1984). The quantity ea_0 is the atomic unit of dipole moment, where e is the elementary charge (the charge on a proton) and a_0 is the Bohr radius. Other common units are the debye, D = 10^{-18} esu, and the SI unit, the coulomb metre; 1 atomic unit = 2.5418 D = 8.478×10^{-30} C m. See Appendix D for other conversion factors. Atomic units are convenient for describing molecular properties, since the numerical values are typically of order unity.

The most accurate experimental technique for the measurement of dipole moments is the Stark effect in microwave spectroscopy. Unfortunately this does not provide the sign of the moment, and although the sign can usually be determined unambiguously on theoretical grounds, this is not always possible. A well-known example is carbon monoxide, for which the very small dipole moment is in the direction $^-CO^+$, contrary to elementary chemical intuition and to *ab initio* calculations at the SCF level, though more accurate calculations allowing for the effects of electron correlation give the correct sign. Experimental determination of the

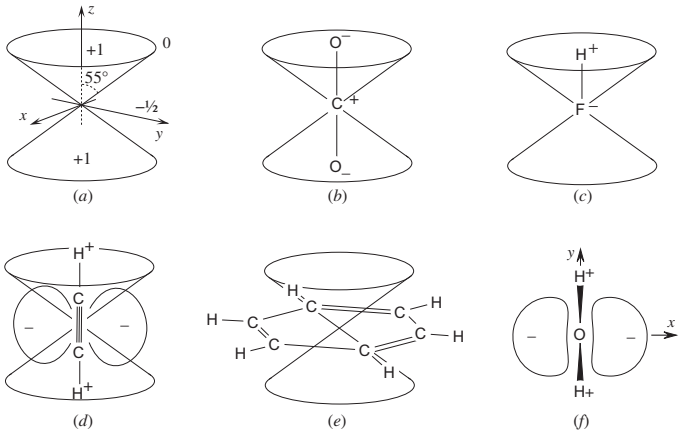

Fig. 2.1 Quadrupole moments. (*a*) the angular part of $\Theta_{zz} = \frac{1}{2}(3\cos^2\theta - 1)$, (*b*) CO_2, (*c*) HF, (*d*) HCCH, (*d*) C_6H_6, (*e*) H_2O.

sign requires a separate experiment; one method involves the determination of the effect of isotopic substitution on the rotational magnetic moment (Townes *et al.* 1955).*

The next of the multipole moments is the *quadrupole moment*, so called because a quadrupolar charge distribution using charges of equal magnitude needs four of them, two positive and two negative.† We define the operator

$$\begin{aligned}\hat{\Theta}_{zz} &= \sum_a e_a(\tfrac{3}{2}a_z^2 - \tfrac{1}{2}a^2),\\ &= \sum_a e_a a^2(\tfrac{3}{2}\cos^2\theta - \tfrac{1}{2}),\end{aligned} \tag{2.1.2}$$

where in the last line the vector **a** has been expressed in spherical polar coordinates. The expectation value of this operator for a particular state has the form

$$\Theta_{zz} = \int \rho(\mathbf{r})r^2(\tfrac{3}{2}\cos^2\theta - \tfrac{1}{2})\ \mathrm{d}^3\mathbf{r}. \tag{2.1.3}$$

The angular factor in parentheses is positive when the angle θ is less than about 54° or more than 126°, and is negative between these values, in the region of the *xy* plane (see Fig. 2.1a). To estimate the quadrupole moment for a particular molecule, we can superimpose the angular

*There is the possibility of confusion about the direction of a dipole moment. As defined here and in virtually all of the recent literature, the direction is from negative to positive charge. However, Debye used a crossed arrow to represent the dipole moment vector, thus: ⟷, the arrow pointing from positive to negative charge, and this convention for the direction of the dipole moment may still occasionally be encountered. It causes much confusion and should be avoided.

†There is some diversity of spelling of 'quadrupole' in the literature. The Latin prefix for four is 'quadri-' (as in quadrilateral, for example) so 'quadripole' would be acceptable. However, 'quadri-' usually becomes 'quadru-' before the letter 'p' (as in 'quadruped') so 'quadrupole' is correct and is the usual spelling. 'Quadrapole' is sometimes seen, but this is definitely incorrect; it is presumably formed by analogy with words like 'quadrangle', but there the 'a' belongs to 'angle' and the prefix has lost its final vowel. 'Octopole' too occurs with alternative spellings. In this case there is no clearcut rule: 'octopole' is more usual, but 'octapole' is also acceptable.

function on the molecular charge distribution and carry out the integration schematically. For CO_2 (Fig. 2.1b) we see that the negatively charged oxygen atoms are in regions where the angular factor is positive, while the positively charged carbon atom occupies the region near the origin (small r) and contributes little to the quadrupole moment. Accordingly we expect a negative quadrupole moment. The experimental value is $-3.3\,ea_0^2$ (Battaglia *et al.* 1981). Once again, we are using atomic units, here ea_0^2. The SI unit is $\mathrm{C\,m^2}$, and the electrostatic unit and debye-ångström are also commonly used. $ea_0^2 = 1.3450 \times 10^{-26}$ esu $= 1.3450\,\mathrm{D\,Å} = 4.487 \times 10^{-40}\,\mathrm{C\,m^2}$. For HF (Fig. 2.1c) the H atom is positively charged, so with the origin at the centre of mass, as shown, we expect a positive quadrupole moment, in agreement with the experimental value of $+1.76\,ea_0^2$. In this case, however, the result depends on the choice of origin; see §2.7 for a detailed discussion.

Other interesting examples are acetylene and benzene. Acetylene (Fig. 2.1d) has a small charge separation between C and H, with the H atoms carrying small positive charges. These charges are in regions where $(3\cos^2\theta - 1)$ is large and positive, and are at relatively large r. There is also a substantial region of negative charge arising from the π-bonding orbitals in the region where $(3\cos^2\theta - 1)$ is negative. Consequently the quadrupole moment is quite large and positive; its value is $5.6\,ea_0^2$—larger than for CO_2. A similar situation arises in benzene (Fig. 2.1e), but here the H atoms are in the xy plane, where $(3\cos^2\theta - 1)$ is negative, and the π electrons are in the region where $(3\cos^2\theta - 1)$ is positive or small in magnitude. In this case, therefore, the quadrupole moment is negative; its value is $-6.7\,ea_0^2$.

The quadrupole moment has other components besides Θ_{zz}, though they are all either zero or related to Θ_{zz} in the molecules discussed so far. They are

$$\begin{aligned}
\Theta_{xx} &= \sum_a e_a(\tfrac{3}{2}a_x^2 - \tfrac{1}{2}a^2),\\
\Theta_{yy} &= \sum_a e_a(\tfrac{3}{2}a_y^2 - \tfrac{1}{2}a^2),\\
\Theta_{xy} &= \sum_a e_a \tfrac{3}{2}a_x a_y,\\
\Theta_{xz} &= \sum_a e_a \tfrac{3}{2}a_x a_z,\\
\Theta_{yz} &= \sum_a e_a \tfrac{3}{2}a_y a_z.
\end{aligned}$$

Notice that $\Theta_{xx} + \Theta_{yy} + \Theta_{zz} = 0$, as a direct consequence of the definition. For linear and axially symmetric molecules, $\Theta_{xy} = \Theta_{xz} = \Theta_{yz} = 0$, while $\Theta_{xx} = \Theta_{yy}$, so that both are equal to $-\frac{1}{2}\Theta_{zz}$. Although there are three non-zero components in this case, namely Θ_{xx}, Θ_{yy} and Θ_{zz}, the value of any one of them determines the others, so there is only one *independent* non-zero component. For molecules with C_{2v} symmetry, like water or pyridine, $\Theta_{xy} = \Theta_{xz} = \Theta_{yz} = 0$ again, but Θ_{xx} and Θ_{yy} may be non-zero and unequal. In such cases it is usual to take the independent non-zero components to be Θ_{zz} and $\Theta_{xx} - \Theta_{yy}$. The consequences of molecular symmetry are discussed in more detail in §2.6.

The water molecule has the charge distribution shown in Fig. 2.1f. The H atoms carry positive charges and are in the yz plane, while the lone pairs are directed in the xz plane and contain substantial amounts of negative charge. These facts fit well with the observed

Table 2.2 Examples of quadrupole moments in atomic units, debye ångström and C m^2. The origin is taken at the centre of mass in each case. For pyridine and H_2O, the z axis is along the C_2 axis and the x axis is perpendicular to the molecular plane.

	ea_0^2		D Å		10^{-40} C m^2	
	Θ_{zz}	$\Theta_{xx}-\Theta_{yy}$	Θ_{zz}	$\Theta_{xx}-\Theta_{yy}$	Θ_{zz}	$\Theta_{xx}-\Theta_{yy}$
CO_2	−3.3	0.0	4.4	0.0	14.8	0.0
HCCH	+5.6	0.0	7.6	0.0	25.1	0.0
C_6H_6	−6.6	0.0	−8.7	0.0	−29.0	0.0
HF	1.75	0.0	2.36	0.0	7.87	0.0
HCl	2.75	0.0	3.7	0.0	12.3	0.0
H_2O	−0.1	−3.8	−0.13	−5.1	−0.4	−17.0
C_5H_5N	−1.9	−9.7	−2.6	−13.0	−8.7	−43.4

quadrupole moments, which are $\Theta_{xx} = -1.86\,ea_0^2$ and $\Theta_{yy} = +1.96\,ea_0^2$. On the other hand, Θ_{zz} is small, with a value of only $-0.10\,ea_0^2$. (These values are origin-dependent; the origin here is taken at the centre of mass.) Note again that $\Theta_{xx}+\Theta_{yy}+\Theta_{zz} = 0$. These values and some others are listed in Table 2.2. Note that measurements of quadrupole moment are not very accurate, and different measurements do not always agree. See Gray and Gubbins (1984, Table D.3) for details and a fuller list.

It is convenient to summarize all these definitions in 'tensor notation':

$$\Theta_{\alpha\beta} = \sum_a e_a(\tfrac{3}{2}a_\alpha a_\beta - \tfrac{1}{2}a^2\delta_{\alpha\beta}). \tag{2.1.4}$$

The subscripts α and β can each be x, y or z. The quantity $\delta_{\alpha\beta}$ is the 'Kronecker delta': $\delta_{\alpha\beta} = 1$ if $\alpha = \beta$ and 0 if $\alpha \neq \beta$. This provides a much more compact way to write down the definitions, and also provides a powerful notation for manipulating them. Appendix A gives a brief summary of tensor notation, which we shall use extensively. The quadrupole moment tensor has nine components, but it is symmetric ($\Theta_{\alpha\beta} = \Theta_{\beta\alpha}$) and together with the 'trace condition' $\Theta_{xx} + \Theta_{yy} + \Theta_{zz} = 0$ this means that there are only five independent non-zero quadrupole components for a molecule with no symmetry.

In the same notation, the octopole moment operator is defined by

$$\hat{\Omega}_{\alpha\beta\gamma} = \sum_a e_a[\tfrac{5}{2}a_\alpha a_\beta a_\gamma - \tfrac{1}{2}a^2(a_\alpha\delta_{\beta\gamma} + a_\beta\delta_{\alpha\gamma} + a_\gamma\delta_{\alpha\beta})], \tag{2.1.5}$$

Here there are 27 components in all, but again they are not all independent: permutation of the subscripts does not change the value, and the definition guarantees that $\hat{\Omega}_{\alpha\beta\beta} = \hat{\Omega}_{\beta\alpha\beta} = \hat{\Omega}_{\beta\beta\alpha} = 0$. (The repeated Greek suffix in each of these expressions implies a summation over that suffix, so that, for example, $\hat{\Omega}_{\alpha\beta\beta} \equiv \sum_\beta \hat{\Omega}_{\alpha\beta\beta}$. This convention was first adopted by Einstein to express the equations of general relativity in a compact form, and is known as the Einstein or repeated-suffix summation convention.) When these relationships are taken into account, we are left with only seven independent components.

As an example, consider methane (Fig. 2.2). The hydrogen atoms carry small net positive charges, while the regions between are negative, so it is not difficult to conclude that Ω_{xyz} is positive when the axes are chosen as shown, with a hydrogen atom in the octant $x > 0$, $y > 0$,

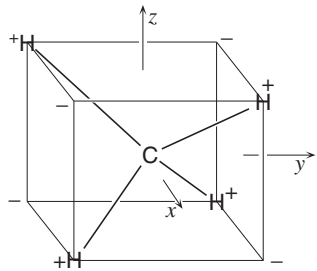

Fig. 2.2 Octopole moment of methane.

$z > 0$. Its value is $+3\,ea_0^3$. (The atomic unit of octopole moment is $ea_0^3 = 0.7118 \times 10^{-34}$ esu = $2.374 \times 10^{-50}\,\mathrm{C\,m^3}$.) The symmetry of the molecule ensures that the remaining components, except for those obtained by permuting the suffixes of Ω_{xyz}, are all zero.

These definitions can be generalized to any rank. The multipole moment operator of rank n has n suffixes, and takes the form

$$\hat{\xi}^{(n)}_{\alpha\beta\ldots\nu} = \frac{(-1)^n}{n!} \sum_a e_a a^{2n+1} \frac{\partial}{\partial a_\nu} \cdots \frac{\partial}{\partial a_\beta} \frac{\partial}{\partial a_\alpha} \left(\frac{1}{a}\right). \tag{2.1.6}$$

It follows at once from this definition that $\hat{\xi}^{(n)}_{\alpha\beta\ldots\nu}$ is symmetric with respect to permutation of its suffixes. Also, because

$$\frac{\partial}{\partial a_\alpha} \frac{\partial}{\partial a_\alpha} \left(\frac{1}{r}\right) = \nabla^2 \frac{1}{r} = 0,$$

it is traceless with respect to any pair of suffixes: $\hat{\xi}^{(n)}_{\alpha\alpha\gamma\ldots\nu} = 0$. We can use these properties to determine the number of independent components. All the components with m x suffixes and $(k - m)$ y suffixes are the same, and can be written as $\xi^{(n)}_{xx\ldots xy\ldots yz\ldots z}$. The value of k (which is the number of x and y suffixes) can range from 0 to n. For each of these values, the number of x suffixes can range from 0 to k, so there are $k + 1$ distinct components for each value of k. The total number of distinct components is therefore $\sum_{k=0}^{n}(k + 1) = \frac{1}{2}(n + 1)(n + 2)$.

This however ignores the trace conditions. Because of the invariance with respect to permutation of suffixes, we can write all the trace conditions in the form

$$\xi^{(n)}_{\alpha\alpha x\ldots xy\ldots yz\ldots z} = 0.$$

By the same argument as before, there are exactly $\frac{1}{2}(n - 1)n$ of these conditions, one for each selection of the $(n - 2)$ x, y and z suffixes. The total number of independent components is therefore reduced from $\frac{1}{2}(n + 1)(n + 2)$ to

$$\tfrac{1}{2}(n + 1)(n + 2) - \tfrac{1}{2}(n - 1)n = 2n + 1.$$

The multipole moment of rank n is sometimes called the '2^n-pole' moment. A dipole requires two charges arranged along a line, and a quadrupole requires four charges arranged in a two-dimensional array. Fig. 2.2 shows that an octopole can be constructed from eight charges, four positive and four negative, arranged in a three-dimensional array. For rank 4 we

would need $2^4 = 16$ charges, arranged in a four-dimensional array, which is not possible in three-dimensional space, but the rank-4 moment is nevertheless called the 2^4-pole or hexadecapole moment.

2.1.2 Spherical tensor definition

It is no accident that the number of independent components of the rank n multipole moment is $2n + 1$, the same as the number of spherical harmonics of that rank. The components of the quadrupole moment are clearly proportional to the spherical harmonics of rank 2 (this is easier to see in the case of Θ_{xx} and Θ_{yy} if we consider $\Theta_{xx} - \Theta_{yy}$ rather than the separate quantities) and the same is true of the higher moments (Tough and Stone 1977). Many advanced applications are easier if the multipole moments are defined at the outset in terms of the spherical harmonics, especially when quadrupoles or moments of higher rank are involved. Unfortunately some of the formulae are more difficult to derive, involving some advanced angular momentum algebra, but they are often much easier to apply than the corresponding cartesian formulae, and it is worth making the effort to master the theory, though perhaps not at a first reading. In the basic treatment, both cartesian and spherical tensor derivations will be given, but later we shall use whichever treatment is most convenient for the purpose. For this reason, it is useful not only to be able to handle both the cartesian and spherical tensor formalisms, but also to be able to switch readily from one to the other. A summary of the basic ideas of the spherical tensor formalism is given in Appendix B, and some familiarity with those ideas is needed in what follows.

We now define the multipole moments in terms of the regular spherical harmonics defined in eqn (B.1.4):

$$\hat{Q}_{lm} = \sum_a e_a R_{lm}(\mathbf{a}) \quad \text{or} \quad Q_{lm} = \int \rho(r) R_{lm}(\mathbf{r})\, \mathrm{d}^3\mathbf{r}. \tag{2.1.7}$$

In practice it is usually more convenient to use the real forms (see eqn (B.1.5)):

$$\hat{Q}_{l\kappa} = \sum_a e_a R_{l\kappa}(\mathbf{a}) \quad \text{or} \quad Q_{l\kappa} = \int \rho(r) R_{l\kappa}(\mathbf{r})\, \mathrm{d}^3\mathbf{r}. \tag{2.1.8}$$

Here and subsequently we use the label κ to denote a member of the series 0, $1c$, $1s$, $2c$, $2s$, ... Where there is a sum over κ in a quantity labelled by $l\kappa$, the sum runs over the values 0, $1c$, $1s$, ..., lc, ls. The relationship between these and the previous, cartesian, definitions is shown in Table E.1.[‡] The inverse relationships can be derived without much difficulty, but it is necessary to use the trace conditions, e.g., $\Theta_{xx} + \Theta_{yy} + \Theta_{zz} = 0$, as well as the relationships in Table E.1. In this way, one finds, for example, that

$$\begin{aligned} \Theta_{xx} &= -\tfrac{1}{2} Q_{20} + \tfrac{1}{2}\sqrt{3} Q_{22c}, \\ \Theta_{yy} &= -\tfrac{1}{2} Q_{20} - \tfrac{1}{2}\sqrt{3} Q_{22c}. \end{aligned} \tag{2.1.9}$$

The octopole and hexadecapole components can be obtained in the same way, and are listed in Table E.2.

[‡]With this definition of the Q_{lm} we have $Q_{l0} = \xi^{(l)}_{zz\ldots z}$ for all l. Some authorities, including the otherwise excellent text by Gray and Gubbins (1984), define the spherical components in terms of the Y_{lm} rather than the C_{lm}. This makes for a much less satisfactory relationship between the cartesian and spherical tensor definitions, and makes the spherical-tensor formalism even more forbidding for most people.

2.1.3 The charge density operator

For some purposes it is convenient to introduce a charge density operator, defined by

$$\hat{\rho}(\mathbf{r}) = \sum_a e_a \delta(\mathbf{a} - \mathbf{r}), \tag{2.1.10}$$

where $\delta(\mathbf{a}-\mathbf{r})$ is the Dirac delta function, which as a function of $\mathbf{r}$ is an infinitely narrow spike of unit volume at $\mathbf{a}$. (Properly, the 'delta function' is not a function at all but a 'distribution'. We should view it as a function of small but finite width, and let the width tend to zero, keeping the volume constant, only after we have integrated over it. See Lighthill (1958) for a full discussion.) The delta function has the important property that for any function $f(\mathbf{r})$, $\int f(\mathbf{r})\delta(\mathbf{r}-\mathbf{a})\,\mathrm{d}^3\mathbf{r} = f(\mathbf{a})$. This happens because $\delta(\mathbf{r}-\mathbf{a})$ is zero except when $\mathbf{r} = \mathbf{a}$, so there is no contribution to the integral unless $\mathbf{r} = \mathbf{a}$, in which case we may as well write $f(\mathbf{r}) = f(\mathbf{a})$. But then the integral reduces to $f(\mathbf{a}) \int \delta(\mathbf{r}-\mathbf{a})\,\mathrm{d}^3\mathbf{r} = f(\mathbf{a})$. Conversely, the delta function may be regarded as a function of $\mathbf{a}$, in which case it is an infinitely narrow spike of unit volume at $\mathbf{r}$, and by the same argument, we may integrate a function of $\mathbf{a}$ to get $\int f(\mathbf{a})\delta(\mathbf{r}-\mathbf{a})\,\mathrm{d}^3\mathbf{a} = f(\mathbf{r})$.

To see that (2.1.10) is indeed the charge density operator, consider the expectation value of the term $\delta(\mathbf{r}_1 - \mathbf{r})$, where $\mathbf{r}$ is some fixed position and $\mathbf{r}_1$ is one of the particle coordinates. This is

$$\begin{aligned}\int \Psi(\mathbf{r}_1, \mathbf{r}_2, \dots)^* \delta(\mathbf{r}_1 - \mathbf{r}) \Psi(\mathbf{r}_1, \mathbf{r}_2, \dots)\,\mathrm{d}^3\mathbf{r}_1\ \mathrm{d}^3\mathbf{r}_2\ \mathrm{d}^3\mathbf{r}_3 \dots \\ = \int \Psi(\mathbf{r}, \mathbf{r}_2, \dots)^* \Psi(\mathbf{r}, \mathbf{r}_2, \dots)\,\mathrm{d}^3\mathbf{r}_2\ \mathrm{d}^3\mathbf{r}_3 \dots\end{aligned} \tag{2.1.11}$$

which is the probability density of particle 1 at $\mathbf{r}$. Multiplying by e_1 gives the contribution of particle 1 to the charge density at $\mathbf{r}$.

In terms of the charge density operator, we may now write the multipole moment operator $\hat{Q}_{l\kappa}$ as

$$\hat{Q}_{l\kappa} = \int \hat{\rho}(\mathbf{r}) R_{l\kappa}(\mathbf{r})\,\mathrm{d}^3\mathbf{r}. \tag{2.1.12}$$

The expectation value of this operator in a state with wavefunction Ψ is then

$$Q_{l\kappa} = \int\int \Psi^* \hat{\rho}(\mathbf{r}) R_{l\kappa}(\mathbf{r}) \Psi\,\mathrm{d}^3\mathbf{r}\,\mathrm{d}\tau = \int\int \Psi^* \sum_a e_a \delta(\mathbf{a} - \mathbf{r}) R_{l\kappa}(\mathbf{r}) \Psi\,\mathrm{d}^3\mathbf{r}\,\mathrm{d}\tau. \tag{2.1.13}$$

Now if we integrate first over $\mathbf{r}$, the delta function replaces $\mathbf{r}$ in each term of the sum by $\mathbf{a}$ to give

$$Q_{l\kappa} = \int \Psi^* \sum_a e_a R_{l\kappa}(\mathbf{a}) \Psi\,\mathrm{d}\tau, \tag{2.1.14}$$

which is the expectation value of the operator $\hat{Q}_{lk}$ as defined in the first of eqns (2.1.8). If on the other hand we integrate first over the particle coordinates $\mathbf{a}$, that integration gives the charge density and we obtain the second of eqns (2.1.8). The charge density operator provides the link between these expressions, and we shall also find it useful later.

2.2 The energy of a molecule in a non-uniform electric field

Consider a molecule in an external potential $V(\mathbf{r})$. Associated with this potential is an electric field $F_\alpha = -\partial V/\partial r_\alpha = -\nabla_\alpha V$. There may be non-zero higher derivatives such as the *field gradient* $F_{\alpha\beta} = -\partial^2 V/\partial r_\alpha \partial r_\beta = -\nabla_\alpha \nabla_\beta V$. We shall use the notation V_α for $\partial V/\partial r_\alpha$, $V_{\alpha\beta}$ for $\partial^2 V/\partial r_\alpha \partial r_\beta$, and so on. We shall work mainly in terms of derivatives of the potential, but the corresponding field or its derivative is obtained merely by changing the sign; that is, $F_\alpha = -V_\alpha$, $F_{\alpha\beta} = -V_{\alpha\beta}$, and so on.

We choose a suitable origin and set of coordinate axes, and expand the potential in a Taylor series:

$$V(\mathbf{r}) = V(0) + r_\alpha V_\alpha(0) + \tfrac{1}{2} r_\alpha r_\beta V_{\alpha\beta}(0) + \frac{1}{3!} r_\alpha r_\beta r_\gamma V_{\alpha\beta\gamma}(0) + \cdots .$$

Once again we are using the Einstein summation convention: a repeated suffix implies summation over the three values x, y and z of that suffix. We note that we should enquire about the convergence of this expansion, but we leave that problem until later. We shall be interested in the energy of our molecule in the presence of this potential. The operator describing this energy is

$$\mathcal{H}' = \sum_a e_a \hat{V}(\mathbf{a}),$$

where the sum is taken over all the nuclei and electrons in the molecule as before; particle a is at position $\mathbf{a}$ and carries charge e_a. Then

$$\mathcal{H}' = V(0) \sum_a e_a + V_\alpha(0) \sum_a e_a a_\alpha + \tfrac{1}{2} V_{\alpha\beta}(0) \sum_a e_a a_\alpha a_\beta + \cdots ,$$

which we write as

$$\mathcal{H}' = \hat{M} V + \hat{M}_\alpha V_\alpha + \tfrac{1}{2} V_{\alpha\beta} \hat{M}_{\alpha\beta} + \cdots , \tag{2.2.1}$$

abbreviating $V_\alpha(0)$ to V_α, etc., and introducing the zeroth moment M, the first moment M_α, the second moment $M_{\alpha\beta}$, and so on. We can immediately identify the zeroth moment $\hat{M} = \sum_a e_a$ with the total charge q, and the first moment $\hat{M}_\alpha = \sum_a e_a a_\alpha$ with the dipole moment $\hat{\mu}_\alpha$.

The second moments are a little more complicated. We are interested only in the energy (2.2.1) of the interaction with the field. We define a new quantity $\hat{M}'_{\alpha\beta} = \hat{M}_{\alpha\beta} - k\delta_{\alpha\beta}$, where k is some constant and $\delta_{\alpha\beta}$ is the Kronecker tensor. Then

$$\begin{aligned} \tfrac{1}{2} V_{\alpha\beta} \hat{M}'_{\alpha\beta} &= \tfrac{1}{2} V_{\alpha\beta} \hat{M}_{\alpha\beta} - \tfrac{1}{2} k \delta_{\alpha\beta} V_{\alpha\beta} \\ &= \tfrac{1}{2} V_{\alpha\beta} \hat{M}_{\alpha\beta} - \tfrac{1}{2} k V_{\alpha\alpha} \\ &= \tfrac{1}{2} V_{\alpha\beta} \hat{M}_{\alpha\beta}, \end{aligned}$$

where the last line follows from Laplace's equation:

$$V_{\alpha\alpha} = \sum_\alpha \frac{\partial^2 V}{\partial a_\alpha^2} = \nabla^2 V = 0.$$

This is true for any value of k. We now choose k so that $\hat{M}'_{\alpha\beta}$ becomes *traceless*: $\hat{M}'_{\alpha\alpha} \equiv \hat{M}'_{xx} + \hat{M}'_{yy} + \hat{M}'_{zz} = 0$. Then $\hat{M}_{\alpha\alpha} - k\delta_{\alpha\alpha} = 0$, or $k = \frac{1}{3}\hat{M}_{\alpha\alpha} = \frac{1}{3}\sum_a e_a a^2$. (Remember that $\delta_{\alpha\alpha} = 3$.) Then we have

$$\hat{M}'_{\alpha\beta} = \sum_a e_a(a_\alpha a_\beta - \tfrac{1}{3}a^2\delta_{\alpha\beta}) = \tfrac{2}{3}\hat{\Theta}_{\alpha\beta}.$$

So by subtracting away the trace of $\hat{M}_{\alpha\beta}$, which does not contribute to the electrostatic energy, we arrive at the quadrupole moment in the form given previously, except for a numerical factor.

The higher moments are manipulated in a similar way. When we modify $\hat{M}_{\alpha\beta\gamma}$ so as to remove the trace terms that do not contribute to the electrostatic energy, we arrive at the octopole moment $\hat{\Omega}_{\alpha\beta\gamma}$ in the form given in eqn (2.1.5), except for the numerical factor $\frac{5}{2}$, while $\hat{M}_{\alpha\beta\gamma\delta}$ leads to the hexadecapole moment $\hat{\Phi}_{\alpha\beta\gamma\delta}$, and so on. The operator describing the interaction becomes

$$\mathcal{H}' = qV + \hat{\mu}_\alpha V_\alpha + \tfrac{1}{3}\hat{\Theta}_{\alpha\beta}V_{\alpha\beta} + \frac{1}{3.5}\hat{\Omega}_{\alpha\beta\gamma}V_{\alpha\beta\gamma} + \frac{1}{3.5.7}\hat{\Phi}_{\alpha\beta\gamma\delta}V_{\alpha\beta\gamma\delta} + \cdots + \frac{1}{(2n-1)!!}\hat{\xi}^{(n)}_{\alpha\beta\ldots\nu}V_{\alpha\beta\ldots\nu} + \cdots, \tag{2.2.2}$$

where $(2n-1)!! \equiv (2n-1)(2n-3)\ldots 5.3.1$ for integer n.

In terms of the spherical-tensor form of the multipole moments, the same expression can be written as

$$\mathcal{H}' = \sum_{lm}(-1)^m\hat{Q}_{l,-m}V_{lm} = \sum_{lm}\hat{Q}^*_{lm}V_{lm} = \sum_{lm}\hat{Q}_{lm}V^*_{lm}, \tag{2.2.3}$$

where $V_{lm} = [(2l-1)!!]^{-1}R_{lm}(\nabla)V\big|_{\mathbf{r}=0}$. By $R_{lm}(\nabla)$ we mean the regular spherical harmonic whose argument is the vector gradient operator ∇, so for example $R_{10}(\nabla) = \nabla_z = \partial/\partial z$. The proof of this result is a little indirect. The general term in eqn (2.2.2) is a scalar (independent of the choice of coordinate axes) and it is the *only* non-zero scalar that can be constructed from the n-th rank tensors $\hat{\xi}^{(n)}_{\alpha\beta\ldots\nu}$ and $V_{\alpha\beta\ldots\nu}$. Similarly, the $l = n$ term in eqn (2.2.3), namely $\sum_{nm}(-1)^m\hat{Q}_{n,-m}V_{nm}$ is a scalar, and is the *only* scalar that can be constructed from the $\hat{Q}_{nm}$ and the V_{nm} (Brink and Satchler 1993, Zare 1988). Since the V_{nm} are linear combinations of the $V_{\alpha\beta\ldots\nu}$, and the $\hat{Q}_{nm}$ are linear combinations of the $\hat{\xi}^{(n)}_{\alpha\beta\ldots\nu}$, these scalars must be the same to within a multiplicative constant. Their identity is confirmed by examining the coefficient of the $\hat{\xi}^{(n)}_{zzz\ldots z}V_{zzz\ldots z}$ term.

A spherical-tensor 'scalar product' of the form $A\cdot B = \sum_m(-1)^m A_{l,-m}B_{lm}$, as in eqn (2.2.3), can be replaced by the scalar product in terms of the real components (see eqn (B.4.3)). That is,

$$\sum_m(-1)^m A_{l,-m}B_{lm} = \sum_\kappa A_{l\kappa}B_{l\kappa}, \tag{2.2.4}$$

so we can write the interaction with the field as

$$\mathcal{H}' = \sum_{l\kappa}\hat{Q}_{l\kappa}V_{l\kappa}. \tag{2.2.5}$$

This is a much more convenient form than (2.2.3) for most purposes.

We can now work out the energy of the molecule using perturbation theory. (See Appendix C for a summary of the principles of perturbation theory.) To first order this is trivial:

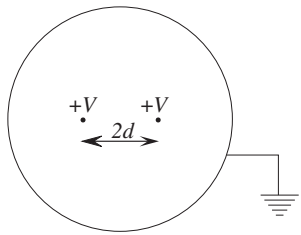

Fig. 2.3 Two-wire cell for quadrupole moment measurements.

we just replace $\mathcal{H}'$ by its expectation value for the state of interest, usually the ground state $|0\rangle$, to obtain

$$\begin{aligned} W' &= \langle 0|\mathcal{H}'|0\rangle \\ &= qV + \mu_\alpha V_\alpha + \frac{1}{3}\Theta_{\alpha\beta}V_{\alpha\beta} + \frac{1}{3.5}\Omega_{\alpha\beta\gamma}V_{\alpha\beta\gamma} + \frac{1}{3.5.7}\Phi_{\alpha\beta\gamma\delta}V_{\alpha\beta\gamma\delta} + \cdots \qquad (2.2.6) \\ &= \sum_{l\kappa} Q_{l\kappa}V_{l\kappa}, \qquad (2.2.7) \end{aligned}$$

where $\mu_\alpha = \langle 0|\hat{\mu}_\alpha|0\rangle$, $\Theta_{\alpha\beta} = \langle 0|\hat{\Theta}_{\alpha\beta}|0\rangle$ and so on. This equation shows that to first order the energy of a dipole depends only on the electric field $F_\alpha = -V_\alpha$, the energy of a quadrupole involves only the field gradient $F_{\alpha\beta} = -V_{\alpha\beta}$, and so on. So the response to a uniform field (as for example in the Stark effect) provides information only about the molecular dipole. To study the molecular quadrupole, we require a potential for which the field is zero but the field gradient is non-zero. Buckingham and his colleagues (Buckingham *et al.* 1983, and references therein) have performed many experiments to determine molecular quadrupole moments and other properties using a cell in which two parallel wires charged to potential V are surrounded by an earthed cylinder (Fig. 2.3). The potential at a distance r from a wire charged to potential V is proportional to $-V \ln r$, so if there are wires at $(x, y) = (\pm d, 0)$, and the enclosing cylinder is far enough away, the potential at a point with coordinates $(x, y) = (\xi d, \eta d)$ close to the origin is

$$\begin{aligned} V_{2\text{wire}} &\propto -V(\ln\sqrt{(d-x)^2+y^2} + \ln\sqrt{(d+x)^2+y^2}) \\ &= -V\ln d - \tfrac{1}{2}V(\ln[1-2\xi+\xi^2+\eta^2] + \ln[1+2\xi+\xi^2+\eta^2] \\ &= -V\ln d - V(\xi^2-\eta^2) + O((\xi^2+\eta^2)^2) \\ &= -V\ln d - V(x^2-y^2)/d^2 + O((x^2+y^2)^2/d^4). \end{aligned}$$

So at the origin, the electric field is zero, but the field gradient has non-zero components $F_{xx} = -F_{yy} \propto 2V/d^2$. In practice, the calculation of the field gradient is more complicated, because the size of the wires and the effect of the earthed cylinder must be taken into account (Buckingham and Disch 1963). This arrangement is used in measurements of the quadrupole moment, discussed further in Chapter 13.

2.3 Polarizabilities

The second-order energy of the ground state is given by the standard Rayleigh–Schrödinger sum over states:

$$\begin{aligned}
W'' &= -\sum_n{}' \frac{\langle 0|\mathcal{H}'|n\rangle\langle n|\mathcal{H}'|0\rangle}{W_n - W_0} \\
&= -\sum_n{}' \frac{\langle 0|\hat{\mu}_\alpha V_\alpha + \tfrac{1}{3}\hat{\Theta}_{\alpha\beta}V_{\alpha\beta} + \cdots |n\rangle\langle n|\hat{\mu}_{\alpha'}V_{\alpha'} + \tfrac{1}{3}\hat{\Theta}_{\alpha'\beta'}V_{\alpha'\beta'} + \cdots |0\rangle}{W_n - W_0} \\
&= -V_\alpha V_{\alpha'} \sum_n{}' \frac{\langle 0|\hat{\mu}_\alpha|n\rangle\langle n|\hat{\mu}_{\alpha'}|0\rangle}{W_n - W_0} \\
&\quad - \frac{1}{3}V_\alpha V_{\alpha'\beta'} \sum_n{}' \frac{\langle 0|\hat{\mu}_\alpha|n\rangle\langle n|\hat{\Theta}_{\alpha'\beta'}|0\rangle}{W_n - W_0} - \frac{1}{3}V_{\alpha\beta}V'_\alpha \sum_n{}' \frac{\langle 0|\hat{\Theta}_{\alpha\beta}|n\rangle\langle n|\hat{\mu}_{\alpha'}|0\rangle}{W_n - W_0} \\
&\quad - \frac{1}{9}V_{\alpha\beta}V_{\alpha'\beta'} \sum_n{}' \frac{\langle 0|\hat{\Theta}_{\alpha\beta}|n\rangle\langle n|\hat{\Theta}_{\alpha'\beta'}|0\rangle}{W_n - W_0} - \cdots .
\end{aligned} \tag{2.3.1}$$

As is customary, the prime on the summation indicates that the state $|0\rangle$ is to be omitted from the sum. Notice that the term qV can be dropped from the perturbation, even if the molecule is charged, because it is a constant and its matrix elements between different eigenstates are zero by orthogonality.

Now we define a set of polarizabilities by

$$W'' = -\tfrac{1}{2}\alpha_{\alpha\beta}V_\alpha V_\beta - \tfrac{1}{3}A_{\alpha,\beta\gamma}V_\alpha V_{\beta\gamma} - \tfrac{1}{6}C_{\alpha\beta,\gamma\delta}V_{\alpha\beta}V_{\gamma\delta} - \cdots ,$$

and by comparing coefficients and relabelling the subscripts we find

$$\alpha_{\alpha\beta} = \sum_n{}' \frac{\langle 0|\hat{\mu}_\alpha|n\rangle\langle n|\hat{\mu}_\beta|0\rangle + \langle 0|\hat{\mu}_\beta|n\rangle\langle n|\hat{\mu}_\alpha|0\rangle}{W_n - W_0}, \tag{2.3.2}$$

$$A_{\alpha,\beta\gamma} = \sum_n{}' \frac{\langle 0|\hat{\mu}_\alpha|n\rangle\langle n|\hat{\Theta}_{\beta\gamma}|0\rangle + \langle 0|\hat{\Theta}_{\beta\gamma}|n\rangle\langle n|\hat{\mu}_\alpha|0\rangle}{W_n - W_0}, \tag{2.3.3}$$

$$C_{\alpha\beta,\gamma\delta} = \frac{1}{3}\sum_n{}' \frac{\langle 0|\hat{\Theta}_{\alpha\beta}|n\rangle\langle n|\hat{\Theta}_{\gamma\delta}|0\rangle + \langle 0|\hat{\Theta}_{\gamma\delta}|n\rangle\langle n|\hat{\Theta}_{\alpha\beta}|0\rangle}{W_n - W_0}. \tag{2.3.4}$$

To understand the significance of these quantities, it is helpful to write down the complete expression for the energy (for a neutral molecule, $q = 0$):

$$\begin{aligned}
W &= W^0 + W' + W'' + \cdots \\
&= W^0 + \mu_\alpha V_\alpha + \tfrac{1}{3}\Theta_{\alpha\beta}V_{\alpha\beta} + \frac{1}{3.5}\Omega_{\alpha\beta\gamma}V_{\alpha\beta\gamma} + \cdots \\
&\quad - \tfrac{1}{2}\alpha_{\alpha\beta}V_\alpha V_\beta - \tfrac{1}{3}A_{\alpha,\beta\gamma}V_\alpha V_{\beta\gamma} - \tfrac{1}{6}C_{\alpha\beta,\gamma\delta}V_{\alpha\beta}V_{\gamma\delta} - \cdots
\end{aligned} \tag{2.3.5}$$

Now

$$\begin{aligned}\frac{\partial W}{\partial V_\xi} &= \mu_\alpha \delta_{\alpha\xi} - \tfrac{1}{2}\alpha_{\alpha\beta}(V_\alpha \delta_{\beta\xi} + V_\beta \delta_{\alpha\xi}) - \tfrac{1}{3}A_{\alpha,\beta\gamma}\delta_{\alpha\xi}V_{\beta\gamma} - \cdots \\ &= \mu_\xi - \alpha_{\xi\beta}V_\beta - \tfrac{1}{3}A_{\xi,\beta\gamma}V_{\beta\gamma} - \cdots \\ &= \mu_\xi + \alpha_{\xi\beta}F_\beta + \tfrac{1}{3}A_{\xi,\beta\gamma}F_{\beta\gamma} + \cdots . \end{aligned} \tag{2.3.6}$$

So $(\partial W/\partial V_\xi)_{V\to 0}$ is the static dipole moment μ_ξ, and indeed this is commonly used as its definition, as well as the basis for some methods of calculating it. $\alpha_{\xi\beta}$ describes the additional dipole induced by an applied electric field F_β, and $A_{\xi,\beta\gamma}$ the dipole induced by an applied field gradient $F_{\beta\gamma}$.

In the same way,

$$3\frac{\partial W}{\partial V_{\xi\eta}} = \Theta_{\xi\eta} + A_{\alpha,\xi\eta}F_\alpha + C_{\alpha\beta,\xi\eta}F_{\alpha\beta} + \cdots , \tag{2.3.7}$$

so that A also describes the quadrupole induced by an electric field, and C describes the quadrupole induced by a field gradient.

In the spherical-tensor treatment, there is a generic polarizability $\alpha_{l\kappa,l'\kappa'}$:

$$\alpha_{l\kappa,l'\kappa'} = \sum_n{}' \frac{\langle 0|\hat{Q}_{l\kappa}|n\rangle\langle n|\hat{Q}_{l'\kappa'}|0\rangle + \langle 0|\hat{Q}_{l'\kappa'}|n\rangle\langle n|\hat{Q}_{l\kappa}|0\rangle}{W_n - W_0}, \tag{2.3.8}$$

and the energy takes the form

$$W = W^0 + \sum_{l\kappa} Q_{l\kappa}V_{l\kappa} - \frac{1}{2}\sum_{l\kappa l'\kappa'} \alpha_{l\kappa,l'\kappa'}V_{l\kappa}V_{l'\kappa'} + \cdots . \tag{2.3.9}$$

The polarizability $\alpha_{l\kappa,l'\kappa'}$ describes the moment $Q_{l\kappa}$ induced by the field $V_{l'\kappa'}$, and also the moment $Q_{l'\kappa'}$ induced by the field $V_{l\kappa}$. To see this, differentiate with respect to $V_{l\kappa}$:

$$\frac{\partial W}{\partial V_{l\kappa}} = Q_{l\kappa} - \sum_{l'\kappa'} \alpha_{l\kappa,l'\kappa'}V_{l'\kappa'} + \cdots . \tag{2.3.10}$$

The components of $\alpha_{1\kappa,1\kappa'}$ correspond precisely with those of the cartesian dipole–dipole polarizability $\alpha_{\alpha\beta}$, with the usual identification $10 \equiv z$, $11c \equiv x$ and $11s \equiv y$. $\alpha_{1\kappa,2\kappa'}$ is the dipole–quadrupole polarizability and corresponds to $A_{\alpha,\beta\gamma}$, and $\alpha_{2\kappa,2\kappa'}$ is the quadrupole–quadrupole polarizability and corresponds to $C_{\alpha\beta,\gamma\delta}$. Notice that one minor advantage of the spherical tensor formalism is that we do not need a new symbol for each rank.

To express the spherical-tensor components of the higher-rank polarizabilities in terms of the cartesian ones, we can start with eqn (2.3.8) and use Table E.1 to replace the spherical-tensor operators by their cartesian equivalents. Finally we refer to eqns (2.3.2)–(2.3.4) to identify the cartesian polarizabilities that result. For example, $\alpha_{20,22c}$ involves the operators $\hat{Q}_{20}$ and $\hat{Q}_{22c}$. In cartesian form,

$$\hat{Q}_{20} = \hat{\Theta}_{zz} \quad \text{and} \quad \hat{Q}_{22c} = \sqrt{\tfrac{1}{3}}(\hat{\Theta}_{xx} - \hat{\Theta}_{yy}).$$

Using eqn (2.3.4) we can then write down immediately that

$$\alpha_{20,22c} = \sqrt{3}(C_{zz,xx} - C_{zz,yy}).$$

Obtaining the cartesian components in terms of the spherical ones is a little more tricky. Where the dipole operators are involved, we can translate directly: $10 \leftrightarrow z$, $11c \leftrightarrow x$ and $11s \leftrightarrow y$. Most of the quadrupole operators similarly translate one to one (see Table E.1) but the tracelessness condition must be invoked to express polarizabilities involving the operators Θ_{xx} and Θ_{yy} in spherical form (see eqn (2.1.9)). In this way we find, for example,

$$\begin{aligned} A_{z,xx} &= -\tfrac{1}{2}\alpha_{10,20} + \tfrac{1}{2}\sqrt{3}\alpha_{10,22c}, \\ A_{z,yy} &= -\tfrac{1}{2}\alpha_{10,20} - \tfrac{1}{2}\sqrt{3}\alpha_{10,22c}. \end{aligned} \tag{2.3.11}$$

A similar procedure can be used to express the cartesian components of the quadrupole–quadrupole polarizability in terms of the spherical ones. Full lists of cartesian components of the dipole–quadrupole and quadrupole–quadrupole polarizabilities are given in Tables E.4 and E.6 respectively.

Readers familiar with spherical tensors may note that it is possible to use the complex components of the multipole moments in the definition of the polarizability. In this case the perturbation takes the form (2.2.3), and the energy to second order is

$$\begin{aligned} W &= W^0 + \sum_{lm}(-1)^m Q_{lm}V_{l,-m} - \frac{1}{2}\sum_{lml'm'}(-1)^{m+m'}\alpha_{lm,l'm'}V_{l,-m}V_{l',-m'} + \cdots \\ &= W^0 + \sum_{lm} Q_{lm}V^*_{l,m} - \frac{1}{2}\sum_{lml'm'}\alpha_{lm,l'm'}V^*_{l,m}V^*_{l',m'} + \cdots, \end{aligned} \tag{2.3.12}$$

with the polarizability given by

$$\alpha_{lm,l'm'} = \sum_n{}' \frac{\langle 0|\hat{Q}_{lm}|n\rangle\langle n|\hat{Q}_{l'm'}|0\rangle + \langle 0|\hat{Q}_{l'm'}|n\rangle\langle n|\hat{Q}_{lm}|0\rangle}{W_n - W_0}. \tag{2.3.13}$$

Note that

$$\frac{\partial W}{\partial V^*_{l,m}} = Q_{lm} - \sum_{l'm'}\alpha_{lm,l'm'}V^*_{l',m'} + \cdots, \tag{2.3.14}$$

so that $\alpha_{lm,l'm'}$ describes the change in moment Q_{lm} induced by the field $V^*_{l',m'} = (-1)^{m'}V_{l',-m'}$, and also (since it is symmetrical in lm and $l'm'$) the moment $Q_{l',m'}$ induced by the field $V^*_{lm} = (-1)^m V_{l,-m}$.

Since $\alpha_{lm,l'm'}$ is defined in terms of the operators Q_{lm} and $Q_{l'm'}$, it transforms under rotations like the product of the spherical harmonics C_{lm} and $C_{l'm'}$. For some purposes it is convenient to recouple the underlying angular momenta represented by the labels $lm, l'm'$. That is, we can construct from the $\alpha_{lm,l'm'}$ a new quantity that transforms according to angular momentum labels kq:

$$\alpha_{ll':kq} = \sum_{mm'}\langle ll'mm'|kq\rangle\alpha_{lm,l'm'}, \tag{2.3.15}$$

where $\langle ll'mm'|kq\rangle$ is a Clebsch–Gordan coefficient. (See §B.4.) This gives, for example, $\alpha_{11:00} = -\sqrt{\tfrac{1}{3}}(\alpha_{xx} + \alpha_{yy} + \alpha_{zz})$ (a scalar, $k = q = 0$) and $\alpha_{11:20} = \sqrt{\tfrac{1}{6}}(2\alpha_{zz} - \alpha_{xx} - \alpha_{yy})$. For linear or axially symmetric molecules these are the only non-zero components (see §2.6.2). The components with $k = 1$ are always zero; for example, $\alpha_{11:10} = \sqrt{\tfrac{1}{2}}i(\alpha_{xy} - \alpha_{yx}) = 0$. It is usual

to use the symbol $\overline{\alpha}$ for the *mean polarizability* $\frac{1}{3}(\alpha_{xx} + \alpha_{yy} + \alpha_{zz})$, so $\alpha_{11:00} = -\sqrt{3}\overline{\alpha}$. We can also define the *anisotropy*, γ or $\Delta\alpha$, by

$$(\Delta\alpha)^2 = \tfrac{3}{2}\sum_q |\alpha_{11:2q}|^2$$
$$= 3(\alpha_{xy}^2 + \alpha_{xz}^2 + \alpha_{yz}^2) + \tfrac{1}{2}[(\alpha_{xx} - \alpha_{yy})^2 + (\alpha_{xx} - \alpha_{zz})^2 + (\alpha_{yy} - \alpha_{zz})^2]. \qquad (2.3.16)$$

$\Delta\alpha$ is invariant with respect to change of axes. Its sign is not defined by eqn (2.3.16), but for linear and axially symmetric molecules, $|\Delta\alpha|$ reduces to $|\alpha_{zz} - \frac{1}{2}(\alpha_{xx} + \alpha_{yy})| = |\alpha_\parallel - \alpha_\perp|$, and it is usual in this case to define $\Delta\alpha$ as $\alpha_\parallel - \alpha_\perp$, retaining the sign.

2.3.1 Units and magnitudes

The atomic unit of dipole–dipole polarizability is obtained from the relationship $\Delta\mu = \alpha F$. Since the atomic units of dipole and electric field are ea_0 and $e/(4\pi\epsilon_0 a_0^2)$, the unit of polarizability is $4\pi\epsilon_0 a_0^3$, i.e., $4\pi\epsilon_0$ times a volume. In the obsolete esu system of units, $4\pi\epsilon_0$ is dimensionless and equal to 1, so the unit of polarizability in this system is just a volume, typically Å^3. Many authors still quote numerical values in such units. In SI, the unit is F m^2, and $4\pi\epsilon_0 a_0^3 = 0.14818\ \text{Å}^3 = 0.16488 \times 10^{-40}\ \text{F m}^2$.

Roughly speaking, the magnitude of the polarizability increases with the molecular volume. However, we can express $\overline{\alpha}$, using eqn (2.3.2), in the form

$$\overline{\alpha} = \frac{2}{3}\sum_n{}' \frac{|\langle 0|\boldsymbol{\mu}|n\rangle|^2}{W_n - W_0},$$

in which the numerator is the intensity of the electric dipole transition between states 0 and n according to Fermi's golden rule, except for a numerical factor. Accordingly the polarizability is larger for molecules that have strong electric dipole transitions to low-lying excited states. Thus the He atom is small and its excited states are high in energy, so its polarizability is very small, at 1.39 a.u. The other inert gas atoms are progressively larger and their excitation energies smaller, so the polarizabilities increase with atomic number, as Table 2.3 shows.

For molecules, the polarizability is related to the freedom of movement of the electrons. In benzene, for example, the electrons can move more freely in the plane of the ring (the xy plane) so α_{xx} and α_{yy} are considerably larger than α_{zz}. Another way to view this is to note that there are low-lying $\pi - \pi^*$ transitions that are polarized in the plane of the ring and contribute to α_{xx} and α_{yy}, while the $\sigma - \pi^*$ and $\pi - \sigma^*$ transitions that are polarized perpendicular to the ring and contribute to α_{zz} lie at higher energy.

The values in Table 2.3 are taken from the useful tabulation of multipole moments and polarizabilities in Gray and Gubbins (1984, Table D.3).

2.3.2 The charge density susceptibility

A useful entity in the theory of molecular polarization and related phenomena is the *charge density susceptibility* $\alpha(\mathbf{r}, \mathbf{r}')$ (Longuet-Higgins 1965, Stone 1985), which can be thought of as the change in charge density at $\mathbf{r}'$ that results from a delta-function change in potential at $\mathbf{r}$. To obtain it, we consider a perturbing potential $V(\mathbf{r}) = V_0\delta(\mathbf{r} - \mathbf{s})$, which is zero everywhere except in an infinitesimal region around $\mathbf{s}$. V_0 is a constant with dimensions of electrostatic

Table 2.3 Examples of polarizabilities in atomic units. For water, the z axis is along the C_2 axis and the y axis is perpendicular to the molecular plane. See Gray and Gubbins (1984) for more details.

	α_{xx}	α_{yy}	α_{zz}	$\overline{\alpha}$	γ
He	1.39	1.39	1.39	1.39	0
Ne	2.67	2.67	2.67	2.67	0
Ar	11.08	11.08	11.08	11.08	0
Kr	16.76	16.76	16.76	16.76	0
Xe	27.2	27.2	27.2	27.2	0
H_2O^a	10.31	9.55	9.91	9.92	0.66
CO_2	28.7	15.2	15.2	19.66	13.5
HCCH	19.1	19.1	32.5	23.55	13.5
C_6H_6	84.2	84.2	46.2	71.5	−38.0

[a] at wavelength $\lambda = 5145$ Å

potential. The perturbation operator is $\int V(\mathbf{r})\hat{\rho}(\mathbf{r})\,\mathrm{d}^3\mathbf{r} = \int V_0\delta(\mathbf{r}-\mathbf{s})\hat{\rho}(\mathbf{r})\,\mathrm{d}^3\mathbf{r} = V_0\hat{\rho}(\mathbf{s})$, where $\hat{\rho}$ is the charge density operator introduced in §2.1.3. Applying Rayleigh–Schrödinger perturbation theory, we find that the first-order change in the wavefunction is

$$|n'\rangle = -{\sum_p}' |p^0\rangle \frac{\langle p^0|V_0\hat{\rho}(\mathbf{s})|n^0\rangle}{W_p^0 - W_n^0} = -{\sum_p}' |p^0\rangle \frac{\langle p^0|V_0\sum_i e_i\delta(\mathbf{r}_i-\mathbf{s})|n^0\rangle}{W_p^0 - W_n^0}. \tag{2.3.17}$$

We may evaluate the change in charge density at $\mathbf{r}'$ for the perturbed wavefunction:

$$\begin{aligned}\Delta\rho(\mathbf{r}') &= \langle n^0 + n' + \cdots | \sum_i e_i\delta(\mathbf{r}_i-\mathbf{r}')|n^0 + n' + \cdots\rangle - \langle n^0|\sum_i e_i\delta(\mathbf{r}_i-\mathbf{r}')|n^0\rangle \\ &= -V_0\frac{\langle n^0|\sum_i e_i\delta(\mathbf{r}_i-\mathbf{r}')|p^0\rangle\langle p^0|\sum_i e_i\delta(\mathbf{r}_i-\mathbf{s})|n^0\rangle + \text{c.c.}}{W_p^0 - W_n^0} + \cdots .\end{aligned} \tag{2.3.18}$$

(where 'c.c.' stands for 'complex conjugate'). We write this as

$$\Delta\rho(\mathbf{r}') = -\int V(\mathbf{r})\alpha(\mathbf{r},\mathbf{r}')\,\mathrm{d}^3\mathbf{r} = -\int V_0\delta(\mathbf{r}-\mathbf{s})\alpha(\mathbf{r},\mathbf{r}')\,\mathrm{d}^3\mathbf{r}, \tag{2.3.19}$$

where

$$\alpha(\mathbf{r},\mathbf{r}') = \frac{\langle n^0|\sum_i e_i\delta(\mathbf{r}_i-\mathbf{r}')|p^0\rangle\langle p^0|\sum_i e_i\delta(\mathbf{r}_i-\mathbf{r})|n^0\rangle + \text{c.c.}}{W_p^0 - W_n^0} \tag{2.3.20}$$

is the *charge density susceptibility*. Note that it is symmetrical between $\mathbf{r}$ and $\mathbf{r}'$.

An important feature of the charge density susceptibility is that it doesn't depend on the multipole approximation. Suppose that a molecule is subjected to a general external perturbing potential $V(\mathbf{r})$. We can view this as $V(\mathbf{r}) = \int V(\mathbf{s})\delta(\mathbf{r}-\mathbf{s})\,\mathrm{d}^3\mathbf{s}$, i.e. as an integral over delta-function potentials, and since the first-order energy is linear in the perturbation we can integrate the response to get

$$\Delta\rho(\mathbf{r}') = -\int V(\mathbf{r})\alpha(\mathbf{r},\mathbf{r}')\,\mathrm{d}^3\mathbf{r}. \tag{2.3.21}$$

The change in energy arises from the interaction between this change in charge density and the perturbing potential, and is

$$\tfrac{1}{2}\int \Delta\rho(\mathbf{r}')V(\mathbf{r}')\,\mathrm{d}^3\mathbf{r}' = -\tfrac{1}{2}\int V(\mathbf{r})\alpha(\mathbf{r},\mathbf{r}')V(\mathbf{r}')\,\mathrm{d}^3\mathbf{r}\,\mathrm{d}^3\mathbf{r}', \tag{2.3.22}$$

where the factor of $\frac{1}{2}$ arises because the distortion in the molecular charge distribution costs energy, which partly cancels the gain in energy of interaction with the external field. This expression is exact, within first-order long-range perturbation theory, and can be evaluated for an arbitrary external potential without recourse to the multipole approximation.

If we do want to use the multipole expansion, however, the charge density susceptibility contains all the information needed to evaluate any of the molecular polarizabilities. The change in charge density induced by a uniform field $\mathbf{E}$, corresponding to an electrostatic potential $-E_\beta r'_\beta$, is $+\int \alpha(\mathbf{r},\mathbf{r}')E_\beta r'_\beta\,\mathrm{d}^3\mathbf{r}'$, and the induced dipole moment is

$$\Delta\mu_\alpha = \int r_\alpha \alpha(\mathbf{r},\mathbf{r}')E_\beta r'_\beta\,\mathrm{d}^3\mathbf{r}\,\mathrm{d}^3\mathbf{r}', \tag{2.3.23}$$

so that the dipole–dipole polarizability is

$$\alpha_{\alpha\beta} = \int r_\alpha \alpha(\mathbf{r},\mathbf{r}')r'_\beta\,\mathrm{d}^3\mathbf{r}\,\mathrm{d}^3\mathbf{r}'. \tag{2.3.24}$$

Substitution of the sum-over-states expression for $\alpha(\mathbf{r},\mathbf{r}')$ now recovers the sum-over-states formula for $\alpha_{\alpha\beta}$, eqn (2.3.2).

For a general external potential, the perturbation operator is $\sum_{l'm'} R_{l'm'}(\mathbf{r}')V^*_{l'm'}$, so that the change in charge density is

$$\Delta\rho(\mathbf{r}) = -\int \alpha(\mathbf{r},\mathbf{r}')\sum_{l'm'} R_{l'm'}(\mathbf{r}')V^*_{l'm'}\,\mathrm{d}^3\mathbf{r}'. \tag{2.3.25}$$

The induced multipole moments are then

$$\begin{aligned}\Delta Q_{lm} &= \int \Delta\rho(\mathbf{r})R_{lm}(\mathbf{r})\,\mathrm{d}^3\mathbf{r} \\ &= -\int R_{lm}(\mathbf{r})\alpha(\mathbf{r},\mathbf{r}')\sum_{l'm'} R_{l'm'}(\mathbf{r}')V^*_{l'm'}\,\mathrm{d}^3\mathbf{r}'\,\mathrm{d}^3\mathbf{r}.\end{aligned} \tag{2.3.26}$$

If we define the polarizability $\alpha_{lm,l'm'}$ by

$$\alpha_{lm,l'm'} = \int R_{lm}(\mathbf{r})\alpha(\mathbf{r},\mathbf{r}')R_{l'm'}(\mathbf{r}')\,\mathrm{d}^3\mathbf{r}'\,\mathrm{d}^3\mathbf{r}, \tag{2.3.27}$$

we recover eqn (2.3.13), and see once again that $\alpha_{lm,l'm'}$ describes the induced moment ΔQ_{lm} resulting from an applied field $V^*_{l'm'}$. In terms of the real spherical-tensor components the equivalent expression is

$$\alpha_{lk,l'\kappa'} = \int R_{lk}(\mathbf{r})\alpha(\mathbf{r},\mathbf{r}')R_{l'\kappa'}(\mathbf{r}')\,\mathrm{d}^3\mathbf{r}'\,\mathrm{d}^3\mathbf{r}. \tag{2.3.28}$$

2.4 Hyperpolarizabilities

The polarizabilities discussed in the previous section describe the linear response of the molecule to external fields: the induced moments are proportional to the strength of the applied field. The atomic unit of electric field, $e/(4\pi\epsilon_0 a_0^2)$, is about $5 \times 10^{11}\,\mathrm{V\,m^{-1}}$. This is very much larger than can be achieved on a macroscopic scale in the laboratory, where the largest static field that can be achieved is in the region of $10^6\,\mathrm{V\,m^{-1}} = 2 \times 10^{-6}$ a.u. However, the most powerful pulsed lasers in current use can produce intensities in the region of $10^{11}\,\mathrm{W\,cm^{-2}}$, corresponding to electric fields of the order of 10^{-3} a.u. (Eberly 1989), while the fields due to other molecules can easily reach magnitudes of 0.1 a.u. In both of these situations it becomes necessary to consider the possibility of non-linear polarizability effects, or hyperpolarizabilities.

If we continue the expansion of the electrostatic energy in powers of the electrostatic field and its derivatives, we obtain (in spherical tensor form)

$$\begin{aligned} W = W^0 &+ \sum_{l\kappa} Q_{l\kappa} V_{l\kappa} - \frac{1}{2} \sum_{l\kappa l'\kappa'} \alpha_{l\kappa,l'\kappa'} V_{l\kappa} V_{l'\kappa'} \\ &+ \frac{1}{3!} \sum_{l\kappa l'\kappa' l''\kappa''} \beta_{l\kappa,l'\kappa',l''\kappa''} V_{l\kappa} V_{l'\kappa'} V_{l''\kappa''} \\ &- \frac{1}{4!} \sum_{l\kappa l'\kappa' l''\kappa'' l'''\kappa'''} \gamma_{l\kappa,l'\kappa',l''\kappa'',l'''\kappa'''} V_{l\kappa} V_{l'\kappa'} V_{l''\kappa''} V_{l'''\kappa'''} + \cdots . \end{aligned} \tag{2.4.1}$$

The quantity β is a (first) *hyperpolarizability*, γ is a second hyperpolarizability, and so on. We can obtain expressions for them from third-order and fourth-order perturbation theory, respectively. For example

$$W''' = \sum_{np}{}' \frac{\langle 0|\mathcal{H}'|n\rangle\langle n|\mathcal{H}'|p\rangle\langle p|\mathcal{H}'|0\rangle}{(W_n - W_0)(W_p - W_0)} - \langle 0|\mathcal{H}'|0\rangle \sum_{n}{}' \frac{\langle 0|\mathcal{H}'|n\rangle\langle n|\mathcal{H}'|0\rangle}{(W_n - W_0)^2},$$

and substituting the expression for $\mathcal{H}'$ in terms of the spherical-tensor moments, eqn (2.2.5), we obtain

$$\begin{aligned} W''' = \sum_{l\kappa l'\kappa' l''\kappa''} V_{l\kappa} V_{l'\kappa'} V_{l''\kappa''} \Bigg\{ &\sum_{np}{}' \frac{\langle 0|\hat{Q}_{l\kappa}|n\rangle\langle n|\hat{Q}_{l'\kappa'}|p\rangle\langle p|\hat{Q}_{l''\kappa''}|0\rangle}{(W_n - W_0)(W_p - W_0)} \\ &- \langle 0|\hat{Q}_{l\kappa}|0\rangle \sum_{n}{}' \frac{\langle 0|\hat{Q}_{l'\kappa'}|n\rangle\langle n|\hat{Q}_{l''\kappa''}|0\rangle}{(W_n - W_0)^2} \Bigg\}. \end{aligned}$$

Hence the first hyperpolarizability is

$$\begin{aligned} \beta_{l\kappa,l'\kappa',l''\kappa''} = 6\mathcal{S} \Bigg\{ &\sum_{np}{}' \frac{\langle 0|\hat{Q}_{l\kappa}|n\rangle\langle n|\hat{Q}_{l'\kappa'}|p\rangle\langle p|\hat{Q}_{l''\kappa''}|0\rangle}{(W_n - W_0)(W_p - W_0)} \\ &- \langle 0|\hat{Q}_{l\kappa}|0\rangle \sum_{n}{}' \frac{\langle 0|\hat{Q}_{l'\kappa'}|n\rangle\langle n|\hat{Q}_{l''\kappa''}|0\rangle}{(W_n - W_0)^2} \Bigg\}. \end{aligned} \tag{2.4.2}$$

Here the initial $\mathcal{S}$ on the right-hand side means 'symmetrize': that is, we average over the 3! permutations of the labels $l\kappa$, $l'\kappa'$ and $l''\kappa''$ in order to obtain an expression that is symmetric

with respect to such permutations. The unsymmetrical part of the expression in braces in (2.4.2) that is removed by this procedure contributes nothing to the energy (2.4.1).

The most important hyperpolarizability is the dipole–dipole–dipole polarizability, where $l = l' = l'' = 1$. In this case the operators are components of the dipole moment, and we can express β in the form

$$\beta_{\alpha\beta\gamma} = 6\mathcal{S}\left\{\sum_{np}{}' \frac{\langle 0|\hat{\mu}_\alpha|n\rangle\langle n|\hat{\mu}_\beta|p\rangle\langle p|\hat{\mu}_\gamma|0\rangle}{(W_n - W_0)(W_p - W_0)} - \langle 0|\hat{\mu}_\alpha|0\rangle \sum_n{}' \frac{\langle 0|\hat{\mu}_\beta|n\rangle\langle n|\hat{\mu}_\gamma|0\rangle}{(W_n - W_0)^2}\right\}. \tag{2.4.3}$$

When these higher polarizabilities are included, the dipole moment takes the form

$$\mu_\alpha = \mu_\alpha^0 + \alpha_{\alpha\beta}F_\beta + \frac{1}{2}\beta_{\alpha\beta\gamma}F_\beta F_\gamma + \frac{1}{3!}\gamma_{\alpha\beta\gamma\delta}F_\beta F_\gamma F_\delta + \cdots$$

(ignoring terms in the derivatives $F_{\beta\gamma}$, etc., of the electric field). So $\beta_{\alpha\beta\gamma}$ and $\gamma_{\alpha\beta\gamma\delta}$ describe the non-linearity in the response to electric fields.

While in principle hyperpolarizabilities can play a part in the interactions between molecules, in practice their contribution is likely to be small. A more serious difficulty is that in all but the simplest cases their inclusion would add very considerably to the complication of evaluating the energy. While there are many studies in the literature of the effect of intermolecular interactions on hyperpolarizability (collision-induced hyperpolarizability), there seem to be none on the effect of hyperpolarizabilities on intermolecular interactions.

2.5 The response to oscillating electric fields

If the applied electric field is not static, but oscillates in time, we have to use time-dependent perturbation theory to determine the response of the molecule. The Hamiltonian $\mathcal{H} = \mathcal{H}^0 + \mathcal{H}'$ consists of a time-independent part $\mathcal{H}^0$ and a time-dependent perturbation $\mathcal{H}' = \hat{V}f(t)$ that is a product of a time-independent operator $\hat{V}$ and a time factor $f(t)$.

According to standard time-dependent perturbation theory (see Appendix C), the wavefunction is written in the form

$$\Psi = \sum_k a_k(t)\Psi_k(t) = \sum_k a_k(t)\psi_k \exp(-\mathrm{i}\omega_k t). \tag{2.5.1}$$

On the assumptions that the perturbation is small and that the system is initially in state $|n\rangle$, the coefficient $a_k(t)$ satisfies the equation

$$\frac{\partial}{\partial t}a_k(t) = -\frac{\mathrm{i}}{\hbar}V_{kn}f(t)\exp(\mathrm{i}\omega_{kn}t), \quad k \neq n, \tag{2.5.2}$$

and integration gives

$$a_k(t) = -\frac{\mathrm{i}}{\hbar}V_{kn}\int_0^t f(\tau)\exp(\mathrm{i}\omega_{kn}\tau)\,\mathrm{d}\tau. \tag{2.5.3}$$

For electric fields at optical frequencies, the wavelength is so long compared with the molecular size that the field gradient and the higher derivatives can be neglected. Also we

suppose that the field is gradually turned on in the distant past, so we take the perturbation to be

$$\mathcal{H}'(t) = 2\hat{V}\exp\epsilon t\cos(\omega t) = \hat{V}(\exp[(\epsilon + \mathrm{i}\omega)t] + \exp[(\epsilon - \mathrm{i}\omega)t]). \tag{2.5.4}$$

Here ϵ is small, and will eventually be allowed to tend to zero, so that we obtain the steady-state response when the oscillating field has been on for a long time.

Now we can integrate (2.5.3) directly to obtain

$$\begin{aligned} a_k(t) &= -\frac{\mathrm{i}}{\hbar}V_{kn}\int_{-\infty}^{t}\Big(\exp[(\epsilon + \mathrm{i}\omega_{kn} + \mathrm{i}\omega)\tau] + \exp[(\epsilon + \mathrm{i}\omega_{kn} - \mathrm{i}\omega)\tau]\Big)\,\mathrm{d}\tau \\ &= -\frac{V_{kn}}{\hbar}\left[\frac{\exp[(\epsilon + \mathrm{i}\omega_{kn} + \mathrm{i}\omega)\tau]}{\omega_{kn} + \omega - \mathrm{i}\epsilon} + \frac{\exp[(\epsilon + \mathrm{i}\omega_{kn} - \mathrm{i}\omega)\tau]}{\omega_{kn} - \omega - \mathrm{i}\epsilon}\right]_{-\infty}^{t} \\ &= -\frac{V_{kn}}{\hbar}\left(\frac{\exp[(\epsilon + \mathrm{i}\omega_{kn} + \mathrm{i}\omega)t]}{\omega_{kn} + \omega - \mathrm{i}\epsilon} + \frac{\exp[(\epsilon + \mathrm{i}\omega_{kn} - \mathrm{i}\omega)t]}{\omega_{kn} - \omega - \mathrm{i}\epsilon}\right) \\ &= -\frac{V_{kn}}{\hbar}\left(\frac{\exp[\mathrm{i}(\omega_{kn} + \omega)t]}{\omega_{kn} + \omega} + \frac{\exp[\mathrm{i}(\omega_{kn} - \omega)t]}{\omega_{kn} - \omega}\right), \end{aligned} \tag{2.5.5}$$

where the last line results from allowing ϵ to tend to zero. We see that the coefficient $\mathbf{a}_k(t)$ remains small at all times provided that V_{kn} is small compared with $\hbar(\omega_{kn} \pm \omega)$.

Now we evaluate the component μ_α of the dipole moment for the molecule in its ground state, in the presence of the perturbation $\mathcal{H}'(t) = 2\hat{V}\cos(\omega t) = -\hat{\mu}_\beta F_\beta\cos(\omega t)$ due to an electromagnetic field polarized in the β direction. To first order, it is

$$\begin{aligned} \mu_\alpha(t) &= \Big\langle \Psi_0 + {\sum_k}' a_k(t)\Psi_k\Big|\hat{\mu}_\alpha\Big|\Psi_0 + {\sum_k}' a_k(t)\Psi_k\Big\rangle \\ &= \langle 0|\hat{\mu}_\alpha|0\rangle + \Big\{{\sum_k}' a_k(t)\langle 0|\hat{\mu}_\alpha|k\rangle\exp(\mathrm{i}\omega_{0k}t) + \text{c.c.}\Big\}. \end{aligned} \tag{2.5.6}$$

(Here 'c.c.' means 'complex conjugate'.) We substitute the expression (2.5.5) for $a_k(t)$, to obtain

$$\begin{aligned} \mu_\alpha(t) &= \langle 0|\hat{\mu}_\alpha|0\rangle + {\sum_k}'\left\{\frac{V_{k0}}{\hbar}\langle 0|\hat{\mu}_\alpha|k\rangle\left(\frac{\exp(\mathrm{i}\omega t)}{\omega_{k0} + \omega} + \frac{\exp(-\mathrm{i}\omega t)}{\omega_{k0} - \omega}\right) + \text{c.c.}\right\} \\ &= \langle 0|\hat{\mu}_\alpha|0\rangle + F_\beta\cos(\omega t){\sum_k}'\frac{\omega_{k0}(\langle 0|\hat{\mu}_\alpha|k\rangle\langle k|\hat{\mu}_\beta|0\rangle + \langle 0|\hat{\mu}_\beta|k\rangle\langle k|\hat{\mu}_\alpha|0\rangle)}{\hbar(\omega_{k0}^2 - \omega^2)} \\ &\quad - \mathrm{i}F_\beta\sin(\omega t){\sum_k}'\frac{\omega(\langle 0|\hat{\mu}_\alpha|k\rangle\langle k|\hat{\mu}_\beta|0\rangle - \langle 0|\hat{\mu}_\beta|k\rangle\langle k|\hat{\mu}_\alpha|0\rangle)}{\hbar(\omega_{k0}^2 - \omega^2)}. \end{aligned} \tag{2.5.7}$$

If the molecule is in a non-degenerate (and therefore real) state, then $\langle 0|\hat{\mu}_\alpha|k\rangle\langle k|\hat{\mu}_\beta|0\rangle$ is real, and the out-of-phase final term in eqn (2.5.7) vanishes. We see that the expectation value of the dipole moment operator is time-dependent:

$$\mu_\alpha(t) = \langle 0|\mu_\alpha|0\rangle + \alpha_{\alpha\beta}(\omega)F_\beta\cos(\omega t),$$

where the polarizability $\alpha_{\alpha\beta}(\omega)$ at frequency ω is

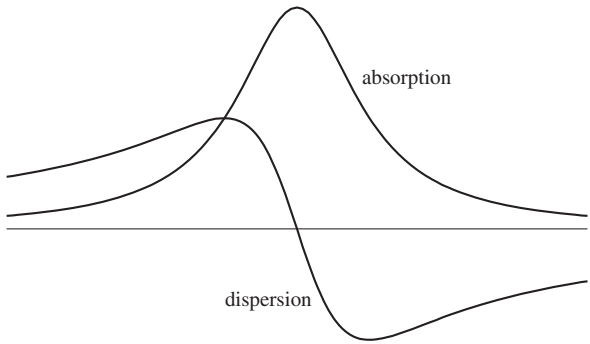

Fig. 2.4 Real and imaginary parts of the polarizability near an absorption frequency.

$$\alpha_{\alpha\beta}(\omega) = \sum_k{}' \frac{\omega_{n0}(\langle 0|\hat{\mu}_\alpha|k\rangle\langle k|\hat{\mu}_\beta|0\rangle + \langle 0|\hat{\mu}_\beta|k\rangle\langle k|\hat{\mu}_\alpha|0\rangle)}{\hbar(\omega_{k0}^2 - \omega^2)}. \tag{2.5.8}$$

Here ω_{k0} is the angular frequency of the transition between state 0 and state k: $\hbar\omega_{n0} = W_k^0 - W_0^0$.

This describes the response of the molecule to the oscillating field, but it leaves out the important effect of *spontaneous emission*. To describe this properly we should use a quantum description of the electromagnetic field. Alternatively, the effect can be included phenomenologically by noting that a system in state k may emit a photon spontaneously and undergo a transition to another state. This is described by adding another term to eqn (2.5.2):

$$\frac{\partial}{\partial t}a_k(t) = -\frac{\mathrm{i}}{\hbar}V_{kn}f(t)\mathrm{e}^{\mathrm{i}\omega_{kn}t} - \tfrac{1}{2}\Gamma_k a_k(t). \tag{2.5.9}$$

Loudon (1973) describes both approaches. In either case, the effect is that the polarizability is slightly modified, and takes the form

$$\alpha_{\alpha\beta}(\omega) = 2\sum_k{}' \frac{\omega_{k0}\langle 0|\hat{\mu}_\alpha|k\rangle\langle k|\hat{\mu}_\beta|0\rangle}{\hbar[\omega_{k0}^2 - (\omega + \frac{1}{2}\mathrm{i}\Gamma_k)^2]}, \tag{2.5.10}$$

where Γ_k is a constant describing the probability of transitions from state k. The singularities in (2.5.8) at the transition frequencies have been removed, because the denominators are now non-zero for all real ω, but they are complex. The frequency dependence $\omega_{k0}/[\omega_{k0}^2 - (\omega + \frac{1}{2}\mathrm{i}\Gamma_k)^2]$ has a real part that goes through zero near ω_{k0} and an imaginary part that peaks near ω_{k0} (see Fig. 2.4). The real part describes anomalous dispersion (variation of refractive index with frequency), and the imaginary part describes absorption. If the matrix elements $\langle 0|\hat{\mu}_\alpha|k\rangle$ are complex, further complications arise (Buckingham 1978), but we do not need to consider them here.

Suppose that in eqn (2.5.8) we set $\omega = \mathrm{i}u$, where u is real. We get

$$\alpha_{\alpha\beta}(\mathrm{i}u) = \sum_k{}' \frac{\omega_{k0}(\langle 0|\hat{\mu}_\alpha|k\rangle\langle k|\hat{\mu}_\beta|0\rangle + \langle 0|\hat{\mu}_\beta|k\rangle\langle k|\hat{\mu}_\alpha|0\rangle)}{\hbar(\omega_{k0}^2 + (u + \frac{1}{2}\Gamma_k)^2)}. \tag{2.5.11}$$

(In practice the Γ_k can be dropped from this expression, since they are small compared with the ω_{k0} and have little effect here, in contrast to eqn (2.5.10).) This is the polarizability at the

imaginary frequency iu. Whether this has a real physical meaning is debatable. If we replace ω by iu in the perturbation operator (2.5.4), the time factor becomes $\cosh(ut)$, so we can think of $\alpha(\mathrm{i}u)$ as the response to an exponentially increasing electric field, but a physical realization of such a situation is hard to envisage. However, as a mathematical entity $\alpha(\mathrm{i}u)$ is well-defined, and moreover it is much better behaved than the polarizability at real frequencies, because the denominators are real, have no zeros, and increase monotonically with u. Consequently $\alpha(\mathrm{i}u)$ decreases monotonically from the static polarizability at $u = 0$ to zero as $u \to \infty$, without any of the near-singularities that afflict $\alpha(\omega)$. We shall see in §4.3.2 that $\alpha(\mathrm{i}u)$ has a useful application in the theory of the dispersion interaction.

A related quantity is the frequency-dependent charge density susceptibility, which describes the response to an oscillating delta-function perturbation. Taking the operator V in the time-dependent perturbation to be the charge-density operator $\hat{\rho}(\mathbf{r}) = \sum_i e_i \delta(\mathbf{r} - \mathbf{r}_i)$, we find that the frequency-dependent charge density susceptibility is

$$\alpha(\mathbf{r}, \mathbf{r}'; \omega) = \sum_k{}' \frac{\omega_{k0}(\langle 0|\hat{\rho}(\mathbf{r})|k\rangle\langle k|\hat{\rho}(\mathbf{r}')|0\rangle + \text{c.c.})}{\hbar(\omega_{k0}^2 - \omega^2)}. \tag{2.5.12}$$

Here too we can replace ω by iu to obtain the charge density susceptibility at imaginary frequency, $\alpha(\mathbf{r}, \mathbf{r}'; \mathrm{i}u)$. Although this notionally describes the response to an exponentially increasing delta-function perturbation, which is physically implausible, it is mathematically well-defined and well-behaved, and also finds application in the theory of dispersion, leading to an expression for the dispersion energy that does not rely on the multipole expansion. When $\omega = 0$ we recover the charge density susceptibility as defined previously in §2.3.2. For clarity it is convenient to refer to that as the *static* charge density susceptibility and to write it as $\alpha(\mathbf{r}, \mathbf{r}'; 0)$.

2.6 Symmetry properties of multipole moments and polarizabilities

If a molecule has any symmetry, some of its multipole moments and polarizabilities will be zero, and we may discover which these are with the help of standard group-theoretical methods. In the following we assume a basic knowledge of such methods, as well as access to point-group character tables in the form given by Tinkham (1964) and many other authors, showing the behaviour under symmetry operations of x, y and z and their products. Accounts of group-theoretical methods may also be found in Hamermesh (1989) or Elliott and Dawber (1979).

If we assume that the molecule is in a non-degenerate state, its charge distribution will be fully symmetric (symmetry species Γ_1 in the molecular point group), so the symmetry species of the multipole moment integral $\langle 0|\hat{Q}_{lk}|0\rangle = \int \rho(\mathbf{r}) R_{lk}(\mathbf{r})\, \mathrm{d}^3 r$ is just the symmetry of the multipole operator itself, and it must vanish unless totally symmetric.

For individual moments it is usually easier to use the cartesian forms. As an example we consider a C_{2v} molecule such as water. The character table is as follows:

C_{2v}	E	C_2^z	σ^{xz}	σ^{yz}			
A_1	1	1	1	1	z		$x^2; y^2; z^2$
A_2	1	1	−1	−1		R_z	xy
B_1	1	−1	1	−1	x	R_y	xz
B_2	1	−1	−1	1	y	R_x	yz

We see that the x, y and z components of the dipole moment transform according to B_1, B_2 and A_1 respectively. Consequently a C_{2v} molecule such as water may have a non-zero μ_z, but μ_x and μ_y must be zero. Similarly the xy, xz and yz components of the quadrupole moment must vanish, since they transform as A_2, B_1 and B_2 respectively, but the xx, yy and zz components may be non-zero. Remember, though, that the xx, yy and zz components are not independent; their sum is zero, so we have only two independent components in this case.

To examine the properties of a whole set of multipole moments of a given rank, we can use the fact that the character of a set of spherical harmonics under rotation through an angle α is independent of the axis of rotation and is given by the formula

$$\chi^{(k)}(\alpha) = \frac{\sin(k + \frac{1}{2})\alpha}{\sin \frac{1}{2}\alpha},$$

where k is the rank of the harmonics. This formula applies to proper rotations; we write an improper rotation as the product of the inversion with a suitable proper rotation, noting that inversion changes the sign of a spherical harmonic if its rank is odd: $\hat{\imath}R_{km} = (-1)^k R_{km}$. In this way we arrive at the following characters for H_2O:

C_{2v}	E	C_2^z	$\sigma^{xz} = \hat{\imath}C_2^y$	$\sigma^{yz} = \hat{\imath}C_2^x$	
Q_{1m}	3	−1	1	1	$A_1 + B_1 + B_2$
Q_{2m}	5	1	1	1	$2A_1 + A_2 + B_1 + B_2$

So we see as before that the dipole moment has one non-zero component and the quadrupole has two.

As another example, we consider a tetrahedral molecule, where the answers are less obvious. The results are

$\mathcal{T}_d$	E	$8C_3$	$3C_2$	$6\sigma_d$	$6S_4 = \hat{\imath}C_4^{-1}$	
A_1	1	1	1	1	1	$x^2 + y^2 + z^2$
A_2	1	1	1	−1	−1	
E	2	−1	2	0	0	$((2z^2 - x^2 - y^2),\ \sqrt{3}(x^2 - y^2))$
T_1	3	0	−1	1	−1	(R_x, R_y, R_z)
T_2	3	0	−1	−1	1	$(x, y, z); (yz, xz, xy)$
Q_{1m}	3	0	−1	1	−1	T_2
Q_{2m}	5	−1	1	1	−1	$E + T_2$
Q_{3m}	7	1	−1	1	1	$A_1 + T_1 + T_2$
Q_{4m}	9	0	1	1	1	$A_1 + E + T_1 + T_2$

So the dipole and quadrupole moments of a tetrahedral molecule like methane are all zero, but there is one non-zero component of the octopole and one of the hexadecapole (rank 4). To find the non-zero components, we use the usual projection formula. It is quite easy to show in this way (using the cartesian form) that the non-zero component of the octopole is $\Omega_{xyz} \propto \Omega_{32s}$. A similar calculation for the hexadecapole gives either $\Phi_{xxxx}+\Phi_{yyyy}+\Phi_{zzzz}$ or $\Phi_{xxyy}+\Phi_{xxzz}+\Phi_{yyzz}$, depending which component one starts from. However this does not mean that there are two *independent* non-zero components; because of the tracelessness property these expressions are equal to within a numerical factor: $\Phi_{xxxx} + \Phi_{yyyy} + \Phi_{zzzz} = -2(\Phi_{xxyy} + \Phi_{xxzz} + \Phi_{yyzz})$. In spherical-tensor form the equivalent expression is $Q_{40} + \sqrt{\frac{5}{14}}(Q_{44} + Q_{4,-4}) = Q_{40} + \sqrt{\frac{5}{7}}Q_{44c}$. In work on tetrahedral molecules it is usual to use the abbreviation Ω for Ω_{xyz} and Φ for Φ_{zzzz}.

General symmetry properties include the results that for all linear molecules $Q_{km} = 0$ unless $m = 0$, and $Q_{k0} = 0$ for odd k when there is a centre of inversion symmetry. If a molecule has axial symmetry of order p, then $Q_{km} = 0$ unless $m = 0 \bmod p$. If in addition there are symmetry planes containing the rotation axis, then only one of Q_{kmc} and Q_{kms} can be non-zero. Which one this is will depend on the choice of axes; if the x axis lies in a symmetry plane it will be Q_{kmc}. If there is a symmetry plane perpendicular to the principal axis, then Q_{kmc} and Q_{kms} both vanish when $k - m$ is odd. The first non-vanishing moment in tetrahedral symmetry is the octopole Ω_{xyz}, as we have seen; in octahedral symmetry it is the hexadecapole $Q_{40} + \sqrt{\frac{5}{7}}Q_{44c}$, and in icosahedral symmetry it is a single combination of the Q_{6m}.

2.6.1 Multipole moments in chiral molecules

In chiral molecules, the multipole moments of the enantiomers are related but not necessarily equal—there may be differences of sign. When dealing with such cases—for example in a racemic crystal—we need to know which multipoles change sign. Suppose we know the multipoles for the R enantiomer, relative to a molecule-fixed set of axes. Recall that we define molecule-fixed axes by some rule such as 'z runs from atom A to B, x runs from A towards C but is orthogonal to z, and y completes a right-handed set'. To get the L enantiomer we reflect in any plane, which with this definition we may take to be the xz plane. If we do this, the x and z axes are unchanged, and as the y axis forms a right-handed set it is unchanged too. In general a particle moves from (x, y, z) to $(x, -y, z)$, and the new charge density ρ^L is related to the old density ρ^R by $\rho^L(x, y, z) = \rho^R(x, -y, z)$.

Now the multipole moments have the form $Q^R_{lk} = \int R_{lk}(x, y, z)\rho^R(x, y, z)\,\mathrm{d}x\,\mathrm{d}y\,\mathrm{d}z$ for the R enantiomer, so for the L enantiomer they are

$$\begin{aligned} Q^L_{lk} = \int R_{lk}(x, y, z)\rho^L(x, y, z)\,\mathrm{d}x\,\mathrm{d}y\,\mathrm{d}z &= \int R_{lk}(x, y, z)\rho^R(x, -y, z)\,\mathrm{d}x\,\mathrm{d}y\,\mathrm{d}z \\ &= \int R_{lk}(x, -y, z)\rho^R(x, y, z)\,\mathrm{d}x\,\mathrm{d}y\,\mathrm{d}z, \end{aligned} \tag{2.6.1}$$

changing the sign of the y dummy integration variable in the last step.

So we see that a multipole moment remains unchanged if $R_{lk}(x, -y, z)$ contains only even powers of y, and changes sign if it contains only odd powers. (All multipole moment operators in real form, i.e. R_{lmc} or R_{lms}, contain either all even powers or all odd powers of y, and likewise for x and z.) This means that Q_{l0} and the Q_{lmc} remain unchanged but the Q_{lms}, i.e. Q_{11s}, Q_{21s}, Q_{22s} etc. change sign.

This applies if we have defined the x and z axes by reference to the molecular structure, leaving y to complete the right-handed set. It is possible to define the y and z axes relative to the molecular structure and reflect in the yz plane. In this case $\rho^L(x,y,z) = \rho^R(-x,y,z)$, and there is a change of sign if the multipole operator contains an odd power of x. This happens for the Q_{lmc} if m is odd and for the Q_{lms} if m is even, so the multipoles that change sign are Q_{11c}, Q_{21c}, Q_{22s}, etc. If the x and y axes are defined relative to the structure and z completes the set, the sign changes if $|l-m|$ is odd, i.e. for Q_{10}, Q_{21s}, Q_{21c}, etc.

It might be supposed that the changes of sign could be avoided by using a left-handed axis system for the left-handed isomer, but this is not an option. The assumption of right-handed axis systems is built into the theory at a very low level, and attempts to use left-handed axes would lead to obscure errors. However, by defining local axes systematically by reference to the molecular structure, we obtain a simple systematic rule for any changes of sign on inversion, and reduce the likelihood of errors.

2.6.2 Symmetry of polarizabilities

The symmetries of the polarizabilities can be determined from those of the multipole moments. The equation defining $\alpha_{l\kappa,l'\kappa'}$ shows that if the set $\{Q_{l\kappa}, \kappa = 0, 1c, 1s, \ldots, ls\}$, for a given l, transforms according to $\Gamma^{(l)}$, then the set $\alpha_{l\kappa,l'\kappa'}$ for given l and l' transforms according to the direct product $\Gamma^{(l)} \otimes \Gamma^{(l')}$. Thus for H_2O, the dipole–quadrupole polarizability transforms as

$$\begin{aligned}\Gamma^{(1)} \otimes \Gamma^{(2)} &= (A_1 + B_1 + B_2) \otimes (2A_1 + A_2 + B_1 + B_2)\\ &= 4A_1 + 3A_2 + 4B_1 + 4B_2,\end{aligned}$$

so that four of the components have A_1 symmetry and can be non-zero.

This is valid when $l \neq l'$. When $l = l'$, the calculation is slightly less straightforward. In this case the polarizability is symmetric with respect to the interchange of κ and κ': $\alpha_{l\kappa,l\kappa'} = \alpha_{l\kappa',l\kappa}$. Thus the antisymmetric combinations $\alpha_{l\kappa,l\kappa'} - \alpha_{l\kappa',l\kappa}$ are all zero, and we have to consider the symmetric combinations $\alpha_{l\kappa,l\kappa'} + \alpha_{l\kappa',l\kappa}$, which transform according to the symmetrized square, $(\Gamma^{(l)} \otimes \Gamma^{(l')})_+$. The standard formula for the character of the symmetrized square is

$$\chi^{(\Gamma\otimes\Gamma)_+}(R) = \tfrac{1}{2}[(\chi^\Gamma(R))^2 + \chi^\Gamma(R^2)].$$

For the dipole–dipole polarizability of water this gives

C_{2v}	E	C_2^z	$\sigma^{xz} = iC_2^y$	$\sigma^{yz} = iC_2^x$	
$\Gamma^{(1)}$	3	−1	1	1	
$(\Gamma^{(1)} \otimes \Gamma^{(1)})_+$	6	2	2	2	$3A_1 + A_2 + B_1 + B_2$

so there are three non-zero components. In the case of methane, the dipole operator transforms according to the T_2 representation, and we find

$\mathcal{T}_d$	E	$8C_3$	$3C_2$	$6\sigma_d$	$6S_4 = \hat{\imath}C_4^{-1}$	
T_2	3	0	−1	1	−1	
$(T_2 \otimes T_2)_+$	6	0	2	2	0	$A_1 + E + T_2$

So the symmetrized square contains the symmetric representation A_1 once, and there is one independent non-zero component of the dipole polarizability.

An alternative approach, which avoids the need for the symmetrized square, is based on the fact that the direct product of two real irreducible representations Γ_1 and Γ_2 contains the symmetric representation exactly once if Γ_1 and Γ_2 are equivalent ($\Gamma_1 \sim \Gamma_2$) and not at all otherwise. Given a set of multipoles Q_i that transform according to Γ_1, and a set Q'_j that transform according to Γ_2, we can construct a set of products $Q_iQ'_j$, and these transform according to $\Gamma_1 \otimes \Gamma_2$. If $\Gamma_1 \sim \Gamma_2$ we can construct just one symmetric combination of these products; and correspondingly there is just one symmetric (and therefore non-zero) combination of the α_{ij}. If Γ_1 and Γ_2 are identical rather than just equivalent, the symmetric combination of the products $Q_iQ'_j$ is $\sum_i Q_iQ'_i$. Taking the dipole–quadrupole polarizability of the water molecule once again, we see that the dipole operator has components of symmetries A_1, B_1 and B_2 ($\hat{\mu}_z$, $\hat{\mu}_x$ and $\hat{\mu}_y$ respectively) while the quadrupole has two components of symmetry A_1 ($\hat{\Theta}_{zz}$ and $\hat{\Theta}_{xx} - \hat{\Theta}_{yy}$) and one each of A_2, B_1 and B_2 ($\hat{\Theta}_{xy}$, $\hat{\Theta}_{xz}$ and $\hat{\Theta}_{yz}$ respectively). Thus we can take A_1 with A_1 to get the symmetric combinations $\hat{\mu}_z\hat{\Theta}_{zz}$ and $\hat{\mu}_z(\hat{\Theta}_{xx} - \hat{\Theta}_{yy})$, or B_1 with B_1 to get $\hat{\mu}_x\hat{\Theta}_{xz}$, or B_2 with B_2 to get $\hat{\mu}_y\hat{\Theta}_{yz}$. Corresponding to each of these symmetric combinations there is a non-zero component of the dipole–quadrupole polarizability, i.e., $A_{z,zz}$, $A_{z,xx} - A_{z,yy}$, $A_{x,xz}$ and $A_{y,yz}$. The same approach for the dipole–dipole case gives the symmetric combinations $\hat{\mu}_z\hat{\mu}_z$, $\hat{\mu}_x\hat{\mu}_x$ and $\hat{\mu}_y\hat{\mu}_y$, corresponding to non-zero polarizabilities α_{zz}, α_{xx} and α_{yy} respectively.

For a higher-symmetry molecule such as methane, there are fewer non-zero components. In this case, the set of $\hat{\mu}_i$ transform as T_2. For the dipole–dipole polarizability, therefore, we can match T_2 with T_2; the set of nine dipole–dipole products $\hat{\mu}_i\hat{\mu}_j$ contains just one symmetric combination, which is $\hat{\mu}_x^2 + \hat{\mu}_y^2 + \hat{\mu}_z^2$. From this we deduce that there is just one non-zero component of the dipole–dipole polarizability, namely $\alpha_{xx} + \alpha_{yy} + \alpha_{zz}$. The fact that $\hat{\mu}_x^2 - \hat{\mu}_y^2$ and $2\hat{\mu}_z^2 - \hat{\mu}_x^2 - \hat{\mu}_y^2$ are not symmetric (they are the components of the E representation that arises from the direct product $T_2 \otimes T_2$) tells us that $\alpha_{xx} - \alpha_{yy} = 0$ and $2\alpha_{zz} - \alpha_{xx} - \alpha_{yy} = 0$, and hence that $\alpha_{xx} = \alpha_{yy} = \alpha_{zz}$.

As a final example of this approach, we note that the quadrupole moment transforms according to $E + T_2$ in tetrahedral symmetry. For the dipole–quadrupole polarizability, we again match T_2 with T_2; the quadrupole components transforming like $\hat{\mu}_x$, $\hat{\mu}_y$ and $\hat{\mu}_z$ are $\hat{\Theta}_{yz}$, $\hat{\Theta}_{xz}$ and $\hat{\Theta}_{xy}$ respectively, and the symmetric combination is $\hat{\mu}_x\hat{\Theta}_{yz} + \hat{\mu}_y\hat{\Theta}_{xz} + \hat{\mu}_z\hat{\Theta}_{xy}$. Consequently the single independent non-zero component of the dipole–quadrupole polarizability is $A_{x,yz} + A_{y,xz} + A_{z,xy}$.

Yet another approach uses the recoupled polarizabilities $\alpha_{ll':kq}$ defined by eqn (2.3.15). They transform under rotations like spherical harmonics of rank k, so we can use the same methods as for the multipole moments. Thus the static dipole polarizability has six components, $\alpha_{11:00}$ and the five $\alpha_{11:2q}$; the components of $\alpha_{11:1q}$ are combinations of the antisymmetric part $\alpha_{\alpha\beta} - \alpha_{\beta\alpha}$ of the polarizability, and are zero. The $k = 0$ component is

$$\alpha_{11:00} = -\sqrt{3}\overline{\alpha} = -\sqrt{\tfrac{1}{3}}(\alpha_{xx} + \alpha_{yy} + \alpha_{zz});$$

it is always symmetric and so is always non-zero. For molecules with axial symmetry, the only other non-zero component is

$$\alpha_{11:20} = \sqrt{\tfrac{1}{6}}(2\alpha_{zz} - \tfrac{1}{2}(\alpha_{xx} + \alpha_{yy})) = \sqrt{\tfrac{2}{3}}\Delta\alpha.$$

It is customary in this case to use the notation $\alpha_\parallel$ for α_{zz} and $\alpha_\perp$ for α_{xx} and α_{yy}, which are equal.

Care must be taken to account correctly for the effects of inversion. For the dipole–quadrupole polarizabilities, for example, the recoupled polarizabilities are $\alpha_{12:kq}$ with $k = 1, 2$ or 3. These behave under rotations like spherical harmonics of rank k, *but they all change sign under inversion, even when* $k = 2$, because the operators $\hat{Q}_{1m}$ in the polarizability expression change sign but the $\hat{Q}_{2m}$ do not. In spherical symmetry, we can classify these polarizability components as P_u, D_u and F_u. It follows that all of them vanish for any centrosymmetric molecule, such as CO_2 or benzene. For a $C_{\infty v}$ molecule, we find by descent in symmetry that P_u reduces to $\Sigma^+ \oplus \Pi$ (one non-zero component), D_u to $\Sigma^- \oplus \Pi \oplus \Delta$ (all zero) and F_u to $\Sigma^+ \oplus \Pi \oplus \Delta \oplus \Phi$ (one non-zero component) so that there are two independent non-zero components in this symmetry.

Where there are only a few non-zero components it is conventional to use a special notation for them (Buckingham 1967). For axially symmetric molecules (linear, or with a unique rotation axis of order 3 or more) we have already met the notations $\alpha_\parallel = \alpha_{zz}$ and $\alpha_\perp = \alpha_{xx} = \alpha_{yy}$ for dipole polarizabilities. In addition, the notation $A_\parallel$ is used for $A_{z,zz}$ and $A_\perp$ for $A_{x,xz} = A_{y,yz}$. Similarly, $\beta_\parallel = \beta_{zzz}$ and $\beta_\perp = \beta_{xxz} = \beta_{yyz}$. In all of these cases, the z direction is parallel to the unique axis. In tetrahedral molecules, where there is only one non-zero dipole–quadrupole polarizability and one non-zero hyperpolarizability, they are usually denoted simply $A = A_{x,yz}$ and $\beta = \beta_{xyz}$ respectively. In the case of the quadrupole–quadrupole polarizability, the symbol C denotes $\frac{1}{5}C_{\alpha\beta,\alpha\beta} = \frac{1}{10}\sum_\kappa \alpha_{2\kappa,2\kappa}$.

2.7 Change of origin

Consider the OH^- ion. It has a negative charge; can we say anything about where the charge resides? It has higher moments too; how do their values depend on our choice of origin? Is there an optimum choice of origin? In many applications it is convenient to take the origin at the centre of mass, but this is not necessarily the optimum choice for describing the electrostatic properties. Indeed, the centre of mass is different for OH^- and OD^-, whereas the charge distribution is the same for both, except for some very small differences due to breakdown of the Born–Oppenheimer approximation.

We take the origin initially at the oxygen nucleus and the z axis from O to H. The total charge $q = -e$. The dipole moment is $\mu_z^O = \langle 0|\sum e_a a_z|0\rangle$ relative to this origin. Now consider a new origin C at $(0, 0, c)$. The dipole moment with respect to this origin is

$$\begin{aligned}\mu_z^C &= \langle 0|\sum_a (a_z - c)|0\rangle \\ &= \mu_z^O - cq. \end{aligned} \tag{2.7.1}$$

So if $q \neq 0$, as in this case, the dipole moment is not invariant under change of origin.

It is possible if $q \neq 0$ to find an origin for which $\mu_z^C = 0$. This happens when $\mu_z^O = cq$ or $c = \mu_z^O/q$. This origin is called the *centre of charge*. If we express the electrostatic potential as a multipole series (as described in Chapter 3), the leading term is the usual point-charge term $q/4\pi\epsilon_0 R$, the next depends on the dipole and is proportional to μ/R^2, the next to Θ/R^3, and so on. Thus the use of the centre of charge as the origin eliminates the dipole contribution and will often be a good choice for an ion. However, it is undefined for a neutral molecule; in this case the dipole moment is independent of origin, as we can see from eqn (2.7.1).

The quadrupole moment too may be affected by change of origin:

$$\begin{aligned}\hat{\Theta}^C_{zz} &= \sum_a e_a\left[\tfrac{3}{2}(a_z - c)^2 - \tfrac{1}{2}(a_x^2 + a_y^2 + (a_z - c)^2)\right] \\ &= \sum_a e_a\left[(\tfrac{3}{2}a_z^2 - \tfrac{1}{2}a^2) - 2a_z c + c^2\right] \\ &= \hat{\Theta}^O_{zz} - 2c\hat{\mu}^O_z + qc^2. \end{aligned} \tag{2.7.2}$$

This is a special case ($c_x = c_y = 0$). A more general expression can be constructed for an arbitrary displacement and for the other components of the quadrupole moment, but the algebra rapidly becomes heavy for higher ranks. This is a case where the spherical-tensor form gives a much more compact expression. There is a standard addition theorem for regular spherical harmonics (Brink and Satchler 1993):

$$\begin{aligned}R_{LM}(\mathbf{a}+\mathbf{b}) = \sum_{l_1 l_2}\sum_{m_1 m_2} \delta_{l_1+l_2,L}(-1)^{L+M}\left[\frac{(2L+1)!}{(2l_1)!(2l_2)!}\right]^{1/2} \\ \times R_{l_1 m_1}(\mathbf{a})R_{l_2 m_2}(\mathbf{b})\begin{pmatrix} l_1 & l_2 & L \\ m_1 & m_2 & -M\end{pmatrix},\end{aligned} \tag{2.7.3}$$

where $\begin{pmatrix} l_1 & l_2 & L \\ m_1 & m_2 & M\end{pmatrix}$ is a Wigner $3j$ coefficient (see Appendix B). When $L = l_1 + l_2$, as here, this $3j$ coefficient can be written in the explicit form

$$\begin{aligned}\begin{pmatrix} l_1 & l_2 & l_1+l_2 \\ m_1 & m_2 & -M\end{pmatrix} = (-1)^{l_1 - l_2 + M}\delta_{m_1+m_2,M}\left[\frac{(2l_1)!(2l_2)!}{(2l_1+2l_2+1)!}\right]^{1/2} \\ \times\left[\binom{l_1+l_2+m_1+m_2}{l_1+m_1}\binom{l_1+l_2-m_1-m_2}{l_1-m_1}\right]^{1/2},\end{aligned} \tag{2.7.4}$$

where $\binom{n}{m}$ is the binomial coefficient $n!/(m!(n-m)!)$, so that we can write

$$R_{lk}(\mathbf{r}-\mathbf{c}) = \sum_{l'=0}^{l}\sum_{k'=-l'}^{l'}\left[\binom{l+k}{l'+k'}\binom{l-k}{l'-k'}\right]^{1/2} R_{l'k'}(\mathbf{r})R_{l-l',k-k'}(-\mathbf{c}). \tag{2.7.5}$$

Using this result we immediately find

$$Q^C_{lk} = \sum_{l'=0}^{l}\sum_{k'=-l'}^{l'}\left[\binom{l+k}{l'+k'}\binom{l-k}{l'-k'}\right]^{1/2} Q^O_{l'k'}R_{l-l',k-k'}(-\mathbf{c}). \tag{2.7.6}$$

From this formula we see that Q_{lk} is invariant under arbitrary changes of origin if and only if $Q_{l'k'} = 0$ for all $l' < l$. For linear molecules, aligned along the z direction, and for the special case $\mathbf{c} = (0, 0, z)$, $k = k' = 0$ and the formula simplifies:

$$Q^C_{l0} = \sum_{l'=0}^{l}(-z)^{l-l'}\binom{l}{l'}Q^O_{l'0} \tag{2.7.7}$$

A similar formula can be derived for change of origin of the real components, using the transformation coefficients $X_{\kappa m}$ (eqn (B.1.7)) to transform to the complex form and back:

$$Q^C_{lk} = \sum_{l'\kappa'} W_{lk,l'\kappa'}(-\mathbf{c}) Q^O_{l'\kappa'}, \tag{2.7.8}$$

where

$$W_{lk,l'\kappa'}(\mathbf{x}) = \sum_{\kappa''} R_{l-l',\kappa''}(\mathbf{x}) \sum_{k=-l}^{l} \sum_{k'=-l'}^{l'} \left[\binom{l+k}{l'+k'} \binom{l-k}{l'-k'} \right]^{1/2} X_{\kappa'',k-k'} X^*_{kk} X_{\kappa' k'}. \tag{2.7.9}$$

This is not quite as complicated as it appears, as there are at most two non-zero terms in each of the sums over k and k'. The coefficients for small values of l are given in Table E.3. General features of these coefficients are that $W_{lk,l'\kappa'}$ is zero if $l' > l$, it is $\delta_{\kappa\kappa'}$ if $l = l'$, and it is $R_{lk}(\mathbf{x})$ if $l'\kappa' = 00$.

Even if a charge distribution can be described exactly in terms of a finite number of multipole moments at one origin, there will be multipole moments of ranks up to infinity if a different origin is chosen. For example, the Na^+ ion has a charge of +1, and all higher moments vanish. If we move the origin from $(0, 0, 0)$ to $(0, 0, c)$ we find, using either the formula for change of origin or (more simply in this case) the original definitions of the multipole moments,

$$\begin{aligned} q^C &= +1, \\ \mu^C_z &= -qc, \\ \Theta^C_{zz} &= +qc^2, \\ \Omega^C_{zzz} &= -qc^3, \end{aligned}$$

and so on. If the new origin is too far from the old one, these multipole moments rapidly become very large. If we wish to calculate the electrostatic potential using multipole moments defined with respect to the new origin, we must include these higher moments. If we were to choose a new origin (such as $(0, 0, c)$ in the example of the Na^+ ion) and calculate the potential of a point charge as if it were at this origin, we would evidently get the wrong answer, even though the magnitude of the charge does not change when we move to this origin. To get the right answer, we have to take account of the higher moments at the new origin too.

This may seem obvious enough in the case of a point charge. It is not always appreciated, however, that the same applies in the case of higher moments such as dipole moments. The energy of a dipole in an electric field $\mathbf{F}$ is $-\boldsymbol{\mu} \cdot \mathbf{F}$; if $\mathbf{F}$ is non-uniform the energy depends on the position ascribed to the dipole moment. If we change the origin, the dipole moment may not change (it will not if the molecule is neutral) but the energy calculated for the new origin will be different. We have to take the higher moments into account if we are to get the same answer in both cases.

Change of origin affects polarizabilities as it does multipole moments. There is one simplification: the matrix elements of the total charge that might occur in the sum over states are all zero, because q is just a constant and the states are orthogonal. This means that the dipole–dipole polarizability is independent of origin, even for ions. However, if we refer the polarizability to a new origin, then the higher-rank polarizabilities will change. We have seen

that the potential due to a charge will be wrong if we calculate it as if it were at a different origin, without taking account of the higher moments that arise at the new origin; it is equally true, though not quite so obvious, that the response to an external field will be calculated incorrectly if we assign the polarizability to a new origin without taking account of the changes to the higher polarizabilities.

The higher polarizabilities are always origin-dependent, because the dipole–dipole polarizability is always non-zero. Consider $A_{z,zz}$ for a linear molecule. It involves the operator $\hat{\Theta}_{zz}$, which is origin-dependent:

$$\hat{\Theta}^C_{zz} = \hat{\Theta}^O_{zz} - 2c\hat{\mu}^O_z.$$

(Again, we are dealing here with the special case of moving the origin from $(0,0,0)$ to $(0,0,c)$.) So

$$\begin{aligned} A^C_{z,zz} &= 2{\sum_n}' \frac{\langle 0|\hat{\mu}^O_z|n\rangle\langle n|\hat{\Theta}^O_{zz} - 2c\hat{\mu}^O_z|0\rangle}{W_n - W_0}, \\ &= A^O_{z,zz} - 2c\alpha_{zz}. \end{aligned}$$

This means that the origin should always be specified when values of $A_{\alpha,\beta\gamma}$ are given. The general formula for change of origin in polarizabilities is obtained by applying (2.7.6) or (2.7.8) to the operators in the formula for the polarizability.

An interesting example of origin dependence and independence arises in the measurement of quadrupole moments of polar molecules, using the method described on p. 23. The experiment leads to a value for the molecular quadrupole moment, but the quadrupole moment of a polar molecule depends on the choice of origin. Somehow the experimental value must be referred to a particular origin, but what is it? Or, to put it another way, the measured quantity (the birefringence induced in the gas by the applied electric field gradient) must depend, not on the quadrupole moment alone, but on some combination of molecular properties that is invariant with respect to change of origin. This problem was investigated by Buckingham and Longuet-Higgins (1968), and in more detail by Lange and Raab (2006), and the conclusion is that the invariant quantity that is being measured is

$$\Theta_{\alpha\beta}\alpha_{\alpha\beta} - \mu_\alpha\Big(A_{\beta,\alpha\beta} + \frac{5c}{\omega}\epsilon_{\alpha\beta\gamma}G'_{\beta,\gamma}\Big) \tag{2.7.10}$$

or, equivalently, that the effective origin to which the measured quadrupole moment is referred is the point where the vector

$$A_{\beta,\alpha\beta} + \frac{5c}{\omega}\epsilon_{\alpha\beta\gamma}G'_{\beta,\gamma} \tag{2.7.11}$$

is zero. Here c is the speed of light, ω the frequency of the light used in the experiment, $\alpha_{\alpha\beta}$ is the dipole–dipole polarizability, $A_{\gamma,\alpha\beta}$ the dipole–quadrupole polarizability, μ_α the dipole moment, and $G'_{\beta,\gamma}$ the tensor describing optical activity.

Gunning and Raab (1997) have shown that origin dependence of the formulae for certain electromagnetic properties can only be achieved if the full second moment $M_{\alpha\beta}$ (eqn (2.2.1)) is used, rather than the traceless quadrupole moment as defined here. However the traceless quadrupole moment is sufficient for all the applications we shall need.

3

Electrostatic Interactions between Molecules

3.1 The electric field of a molecule

Suppose that molecule A is located at position $\mathbf{A}$ in some global coordinate system. The particles of this molecule are at positions $\mathbf{a}$ relative to $\mathbf{A}$, i.e., at positions $\mathbf{A} + \mathbf{a}$. We want to evaluate the potential at a point $\mathbf{B}$ where we shall in due course put another molecule. In terms of the positions and charges of the particles of molecule A, the potential is

$$V^A(\mathbf{B}) = \sum_a \frac{e_a}{4\pi\epsilon_0|\mathbf{B}-\mathbf{A}-\mathbf{a}|} = \sum_a \frac{e_a}{4\pi\epsilon_0|\mathbf{R}-\mathbf{a}|}, \tag{3.1.1}$$

where $\mathbf{R} = \mathbf{B} - \mathbf{A}$. (See Fig. 3.1.) We expand this potential as a Taylor series about $\mathbf{A}$, giving

$$\begin{aligned} V^A(\mathbf{B}) &= \sum_a \frac{e_a}{4\pi\epsilon_0|\mathbf{R}-\mathbf{a}|} \\ &= \sum_a \frac{e_a}{4\pi\epsilon_0}\left\{\frac{1}{R} + a_\alpha\left(\frac{\partial}{\partial a_\alpha}\frac{1}{|\mathbf{R}-\mathbf{a}|}\right)_{\mathbf{a}=0} + \frac{1}{2}a_\alpha a_\beta\left(\frac{\partial^2}{\partial a_\alpha \partial a_\beta}\frac{1}{|\mathbf{R}-\mathbf{a}|}\right)_{\mathbf{a}=0} + \cdots\right\} \\ &= \sum_a \frac{e_a}{4\pi\epsilon_0}\left\{\frac{1}{R} - a_\alpha\left(\frac{\partial}{\partial R_\alpha}\frac{1}{|\mathbf{R}-\mathbf{a}|}\right)_{\mathbf{a}=0} + \frac{1}{2}a_\alpha a_\beta\left(\frac{\partial^2}{\partial R_\alpha \partial R_\beta}\frac{1}{|\mathbf{R}-\mathbf{a}|}\right)_{\mathbf{a}=0} - \cdots\right\} \\ &= \sum_a \frac{e_a}{4\pi\epsilon_0}\left\{\frac{1}{R} - a_\alpha\nabla_\alpha\frac{1}{R} + \frac{1}{2}a_\alpha a_\beta\nabla_\alpha\nabla_\beta\frac{1}{R} - \cdots\right\}. \end{aligned} \tag{3.1.2}$$

As before, we can replace the second moment $M_{\alpha\beta} = \sum_a e_a a_\alpha a_\beta$ by the quadrupole moment $\frac{2}{3}\Theta_{\alpha\beta}$, because $1/R$ satisfies Laplace's equation and there is no contribution to the potential from the trace $M_{\alpha\alpha}$. The higher moments are treated similarly. When we do this, we get

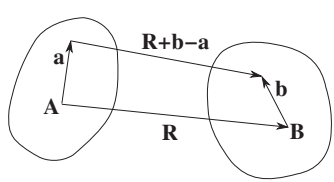

Fig. 3.1 Definition of position vectors in two interacting molecules.

$$V^A(\mathbf{B}) = \frac{1}{4\pi\epsilon_0}\left\{q^A\left(\frac{1}{R}\right) - \hat{\mu}^A_\alpha\nabla_\alpha\left(\frac{1}{R}\right) + \frac{1}{3}\hat{\Theta}^A_{\alpha\beta}\nabla_\alpha\nabla_\beta\left(\frac{1}{R}\right) - \cdots\right\}$$
$$\equiv Tq^A - T_\alpha\hat{\mu}^A_\alpha + \frac{1}{3}T_{\alpha\beta}\hat{\Theta}^A_{\alpha\beta} - \cdots + \frac{(-1)^n}{(2n-1)!!}T^{(n)}_{\alpha\beta\ldots\nu}\hat{\xi}^{A(n)}_{\alpha\beta\ldots\nu} + \cdots, \tag{3.1.3}$$

where

$$4\pi\epsilon_0 T = \frac{1}{R}, \tag{3.1.4}$$

$$4\pi\epsilon_0 T_\alpha = \nabla_\alpha\frac{1}{R} = -\frac{R_\alpha}{R^3}, \tag{3.1.5}$$

$$4\pi\epsilon_0 T_{\alpha\beta} = \nabla_\alpha\nabla_\beta\frac{1}{R} = \frac{3R_\alpha R_\beta - R^2\delta_{\alpha\beta}}{R^5}, \tag{3.1.6}$$

$$4\pi\epsilon_0 T_{\alpha\beta\gamma} = \nabla_\alpha\nabla_\beta\nabla_\gamma\frac{1}{R}$$
$$= -\frac{15R_\alpha R_\beta R_\gamma - 3R^2(R_\alpha\delta_{\beta\gamma} + R_\beta\delta_{\alpha\gamma} + R_\gamma\delta_{\alpha\beta})}{R^7}, \tag{3.1.7}$$

$$4\pi\epsilon_0 T_{\alpha\beta\gamma\delta} = \nabla_\alpha\nabla_\beta\nabla_\gamma\nabla_\delta\frac{1}{R}$$
$$= \frac{1}{R^9}[105R_\alpha R_\beta R_\gamma R_\delta$$
$$- 15R^2(R_\alpha R_\beta\delta_{\gamma\delta} + R_\alpha R_\gamma\delta_{\beta\delta} + R_\alpha R_\delta\delta_{\beta\gamma} + R_\beta R_\gamma\delta_{\alpha\delta} + R_\beta R_\delta\delta_{\alpha\gamma} + R_\gamma R_\delta\delta_{\alpha\beta})$$
$$+ 3R^4(\delta_{\alpha\beta}\delta_{\gamma\delta} + \delta_{\alpha\gamma}\delta_{\beta\delta} + \delta_{\alpha\delta}\delta_{\beta\gamma})] \tag{3.1.8}$$

and in general

$$T^{(n)}_{\alpha\beta\ldots\nu} = \frac{1}{4\pi\epsilon_0}\nabla_\alpha\nabla_\beta\ldots\nabla_\nu\frac{1}{R}. \tag{3.1.9}$$

The superscript (n) specifies the number of subscripts, but is normally omitted when the number is obvious. If we wish to avoid ambiguity when dealing with a system of more than two molecules, we can label the T tensors with the molecular labels: T^{AB}, T^{AB}_α, etc. This tends to make the notation rather cumbersome, however, and we omit the labels in the two-molecule case. Notice though that it is important to establish whether we are dealing with T^{AB} or T^{BA}, i.e., whether $\mathbf{R} = \mathbf{B} - \mathbf{A}$, as above, or $\mathbf{R} = \mathbf{A} - \mathbf{B}$. The definitions above are for the T^{AB}, and show that $T^{BA(n)}_{\alpha\beta\ldots\nu} = (-1)^n T^{AB(n)}_{\alpha\beta\ldots\nu}$.

Returning to eqn (3.1.3), we see that the potential at $\mathbf{R}$ due to a charge q at the origin is $q/4\pi\epsilon_0 R$; the potential at $\mathbf{R}$ due to a dipole $\boldsymbol{\mu}$ at the origin is $-\mu_\alpha T_\alpha = +\mu_\alpha R_\alpha/4\pi\epsilon_0 R^3 = \boldsymbol{\mu}\cdot\mathbf{R}/4\pi\epsilon_0 R^3$, and so on.

Having found the potential as a function of position $\mathbf{R}$, it is now very easy to determine the electric field, the field gradient and the higher derivatives. Thus from the potential qT arising from the charge q, we obtain the electric field at $\mathbf{B}$ due to molecule A as $F^A_\alpha(\mathbf{B}) = -\nabla_\alpha qT = -qT_\alpha$ and the field gradient $F^A_{\alpha\beta}(\mathbf{B}) = -\nabla_\alpha\nabla_\beta qT = -qT_{\alpha\beta}$. For the dipole potential we need to be a little more careful with the suffixes, to avoid clashes; so we write the potential as $-\mu_\gamma T_\gamma$

and then the electric field is $F^A_\alpha(\mathbf{B}) = -\nabla_\alpha(-\mu_\gamma T_\gamma) = +\mu_\gamma T_{\alpha\gamma}$. Similarly the field gradient is $F^A_{\alpha\beta}(\mathbf{B}) = -\nabla_\alpha\nabla_\beta(-\mu_\gamma T_\gamma) = +\mu_\gamma T_{\alpha\beta\gamma}$. In this way we find, for the complete field,

$$\begin{aligned} F^A_\alpha(\mathbf{B}) &= -\nabla_\alpha V^A(\mathbf{B}) \\ &= -T_\alpha q + T_{\alpha\beta}\hat{\mu}_\beta - \frac{1}{3}T_{\alpha\beta\gamma}\hat{\Theta}_{\beta\gamma} + \cdots - \frac{(-1)^n}{(2n-1)!!}T^{(n+1)}_{\alpha\beta\ldots\nu\sigma}\hat{\xi}^{(n)}_{\beta\gamma\ldots\nu\sigma} - \cdots, \end{aligned} \tag{3.1.10}$$

and for the field gradient,

$$\begin{aligned} F^A_{\alpha\beta}(\mathbf{B}) &= -\nabla_\alpha\nabla_\beta V^A(\mathbf{B}) \\ &= -T_{\alpha\beta}q + T_{\alpha\beta\gamma}\hat{\mu}_\gamma - \frac{1}{3}T_{\alpha\beta\gamma\delta}\hat{\Theta}_{\gamma\delta} + \cdots - \frac{(-1)^n}{(2n-1)!!}T^{(n+2)}_{\alpha\beta\ldots\nu\sigma\tau}\hat{\xi}^{(n)}_{\gamma\delta\ldots\nu\sigma\tau} - \cdots. \end{aligned} \tag{3.1.11}$$

This representation is quite compact and economical, but it is rather terse on first acquaintance. We will look at some examples shortly. Notice that T_α describes both the electric field due to a point charge (regarding T_α as a vector function of position) and also the potential due to a point dipole (where we take the scalar product $-\mu_\alpha T_\alpha$ to obtain a scalar function of position, as required for a potential).

Two important general properties of the T tensors with two or more suffixes are: (i) invariance with respect to interchange of suffixes, so that for example $T_{xy} = T_{yx}$; and (ii) tracelessness: $T_{\alpha\alpha\gamma\ldots\nu} = 0$, for any $\gamma\ldots\nu$. These results follow from the fact that the differential operators commute, and from the fact that $\nabla^2(1/R) = 0$ (provided that $R \neq 0$). It follows from these properties that $T^{(n)}_{\alpha\beta\ldots\nu}$, like $\xi^{(n)}_{\alpha\beta\ldots\nu}$, has $2n+1$ components. (See p. 18 for the proof.) It also satisfies Laplace's equation, $\nabla^2 T^{(n)}_{\alpha\beta\ldots\nu} = 0$, and is proportional to R^{-n-1} (because it is obtained by differentiating R^{-1} n times), so its components must be linear combinations of the irregular spherical harmonics of rank n, $I_{nm} = r^{-n-1}C_{nm}$. (See Appendix B.) A detailed discussion of the relationship may be found in Tough and Stone (1977). From this and the orthogonality property of the spherical harmonics a further important property follows: if $T^{(n)}_{\alpha\beta\ldots\nu}$ is averaged over all directions of the intermolecular vector $\mathbf{R}$, the result is zero, except for $n = 0$, i.e., for $T = 1/R$.

3.2 Multipole expansion in cartesian form

We are now in a position to calculate the electrostatic interaction between a pair of molecules in terms of their multipole moments—the multipole expansion. Molecule A has its local origin at position $\mathbf{A}$ in the global coordinate system, and molecule B has its origin at $\mathbf{B}$. We know the potential V^A at $\mathbf{B}$ due to molecule A from eqn (3.1.3), and we can write down the energy of a molecule in a given potential from the results of Chapter 2. Combining these formulae gives the interaction operator:

$$\begin{aligned} \mathcal{H}' &= q^B V^A + \hat{\mu}^B_\alpha V^A_\alpha + \frac{1}{3}\hat{\Theta}^B_{\alpha\beta}V^A_{\alpha\beta} + \cdots \\ &= q^B[Tq^A - T_\alpha\hat{\mu}^A_\alpha + \tfrac{1}{3}T_{\alpha\beta}\hat{\Theta}^A_{\alpha\beta} - \cdots] + \hat{\mu}^B_\alpha[T_\alpha q^A - T_{\alpha\beta}\hat{\mu}^A_\beta + \tfrac{1}{3}T_{\alpha\beta\gamma}\hat{\Theta}^A_{\beta\gamma} - \cdots] \\ &\quad + \tfrac{1}{3}\hat{\Theta}^B_{\alpha\beta}[T_{\alpha\beta}q^A - T_{\alpha\beta\gamma}\hat{\mu}^A_\gamma + \tfrac{1}{3}T_{\alpha\beta\gamma\delta}\hat{\Theta}^A_{\gamma\delta} - \cdots], \\ &= Tq^Aq^B + T_\alpha(q^A\hat{\mu}^B_\alpha - \hat{\mu}^A_\alpha q^B) + T_{\alpha\beta}(\tfrac{1}{3}q^A\hat{\Theta}^B_{\alpha\beta} - \hat{\mu}^A_\alpha\hat{\mu}^B_\beta + \tfrac{1}{3}\hat{\Theta}^A_{\alpha\beta}q^B) + \cdots. \end{aligned} \tag{3.2.1}$$

Notice that some relabelling of subscripts has been necessary to avoid clashes. We are again using $T_{\alpha\beta\ldots}$ rather than $T^{AB}_{\alpha\beta\ldots}$ to avoid overloading the notation. For neutral species, the charges are zero, and the leading term is the dipole–dipole interaction:

$$\begin{aligned}\mathcal{H}' = &-T_{\alpha\beta}\hat{\mu}^A_\alpha\hat{\mu}^B_\beta - \tfrac{1}{3}T_{\alpha\beta\gamma}(\hat{\mu}^A_\alpha\hat{\Theta}^B_{\beta\gamma} - \hat{\Theta}^A_{\alpha\beta}\hat{\mu}^B_\gamma)\\ &- T_{\alpha\beta\gamma\delta}(\tfrac{1}{15}\hat{\mu}^A_\alpha\hat{\Omega}^B_{\beta\gamma\delta} - \tfrac{1}{9}\hat{\Theta}^A_{\alpha\beta}\hat{\Theta}^B_{\gamma\delta} + \tfrac{1}{15}\hat{\Omega}^A_{\alpha\beta\gamma}\hat{\mu}^B_\delta) + \cdots . \end{aligned} \tag{3.2.2}$$

This expression, like the preceding one, is an operator. If we require the electrostatic interaction $U_{\rm es}$ between two molecules in non-degenerate states, then we need the expectation value of this operator, which we obtain by replacing each multipole operator by its expectation value. Thus for two neutral molecules the result is

$$\begin{aligned}U_{\rm es} = &-T_{\alpha\beta}\mu^A_\alpha\mu^B_\beta - \tfrac{1}{3}T_{\alpha\beta\gamma}(\mu^A_\alpha\Theta^B_{\beta\gamma} - \Theta^A_{\alpha\beta}\mu^B_\gamma)\\ &- T_{\alpha\beta\gamma\delta}(\tfrac{1}{15}\mu^A_\alpha\Omega^B_{\beta\gamma\delta} - \tfrac{1}{9}\Theta^A_{\alpha\beta}\Theta^B_{\gamma\delta} + \tfrac{1}{15}\Omega^A_{\alpha\beta\gamma}\mu^B_\delta) + \cdots . \end{aligned} \tag{3.2.3}$$

Eqns (3.2.2) and (3.2.3) have been derived for a pair of molecules, isolated from any others. However, they are based on the Coulomb interactions between nuclear and electronic charges, which are strictly additive, so we can generalize them to an assembly of molecules by summing over the distinct pairs.

Similar expressions have been derived by a number of authors: for example, Hirschfelder *et al.* (1954), Jansen (1957, 1958), Buckingham (1967) and Leavitt (1980).

3.2.1 Explicit formulae

The formulae just derived are general but somewhat opaque, and for practical application we need more transparent forms. We substitute the explicit expression for $T_{\alpha\beta}$, eqn (3.1.9), to obtain the dipole–dipole interaction in the form

$$U_{\mu\mu} = -\mu^A_\alpha\mu^B_\beta\frac{3R_\alpha R_\beta - R^2\delta_{\alpha\beta}}{4\pi\epsilon_0 R^5} \tag{3.2.4}$$

$$= \frac{R^2\boldsymbol{\mu}^A\cdot\boldsymbol{\mu}^B - 3(\boldsymbol{\mu}^A\cdot\mathbf{R})(\boldsymbol{\mu}^B\cdot\mathbf{R})}{4\pi\epsilon_0 R^5}. \tag{3.2.5}$$

It is often convenient to choose coordinates with the z axis along $\mathbf{R}$, with the origin at $\mathbf{A}$. The direction of $\boldsymbol{\mu}^A$ is specified by polar angles θ_A and φ_A and the direction of $\boldsymbol{\mu}^B$ by θ_B and φ_B. (See Fig. 1.4.) Then

$$\begin{aligned}\boldsymbol{\mu}^A\cdot\mathbf{R} &= \mu^A R\cos\theta_A,\\ \boldsymbol{\mu}^B\cdot\mathbf{R} &= \mu^B R\cos\theta_B,\\ \boldsymbol{\mu}^A\cdot\boldsymbol{\mu}^B &= \mu^A\mu^B(\sin\theta_A\cos\varphi_A\sin\theta_B\cos\varphi_A\\ &\qquad + \sin\theta_A\sin\varphi_A\sin\theta_B\sin\varphi_B + \cos\theta_A\cos\theta_B)\\ &= \mu^A\mu^B(\cos\theta_A\cos\theta_B + \sin\theta_A\sin\theta_B\cos(\varphi_B-\varphi_A)),\end{aligned}$$

so that the dipole–dipole interaction becomes

$$U_{\mu\mu} = -\frac{\mu^A\mu^B}{4\pi\epsilon_0 R^3}(2\cos\theta_A\cos\theta_B - \sin\theta_A\sin\theta_B\cos\varphi), \tag{3.2.6}$$

where $\varphi = \varphi_B - \varphi_A$.

Another important interaction is the one between two quadrupolar but non-polar molecules ($\Theta \neq 0$ but $\boldsymbol{\mu} = 0$). A general dipole, like any vector, can be described in terms of a magnitude and two polar angles, but the description of a general quadrupole is rather more complicated and requires five numbers. However, for linear molecules (and symmetric tops) there is only one independent non-zero component. In a coordinate system with the z axis along the molecular axis such a molecule has $\Theta_{zz} = \Theta$ and $\Theta_{xx} = \Theta_{yy} = -\frac{1}{2}\Theta$. In a general coordinate system this can be expressed as

$$\Theta_{\alpha\beta} = \Theta(\tfrac{3}{2}n_\alpha n_\beta - \tfrac{1}{2}\delta_{\alpha\beta}),$$

where $\mathbf{n}$ is a unit vector in the direction of the molecular axis (see Appendix A). So the quadrupole–quadrupole interaction is

$$\begin{aligned} U_{\Theta\Theta} &= \tfrac{1}{9}\Theta^A\Theta^B(\tfrac{3}{2}n^A_\alpha n^A_\beta - \tfrac{1}{2}\delta_{\alpha\beta})T_{\alpha\beta\gamma\delta}(\tfrac{3}{2}n^B_\gamma n^B_\delta - \tfrac{1}{2}\delta_{\gamma\delta}) \\ &= \tfrac{1}{4}\Theta^A\Theta^B n^A_\alpha n^A_\beta T_{\alpha\beta\gamma\delta} n^B_\gamma n^B_\delta, \end{aligned} \tag{3.2.7}$$

where the second form follows from the tracelessness of $T_{\alpha\beta\gamma\delta}$. The evaluation of this expression is straightforward for the case when both molecules lie on the z axis, and gives the result

$$\begin{aligned} U_{\Theta\Theta} = \frac{\Theta^A\Theta^B}{4\pi\epsilon_0 R^5} \cdot \frac{3}{4}[&1 - 5\cos^2\theta_A - 5\cos^2\theta_B - 15\cos^2\theta_A\cos^2\theta_B \\ &+ 2(4\cos\theta_A\cos\theta_B - \sin\theta_A\sin\theta_B\cos\varphi)^2]. \end{aligned} \tag{3.2.8}$$

The interaction between a dipole and a linear quadrupole is calculated in a similar way, and is

$$U_{\mu\Theta} = \frac{\mu^A\Theta^B}{4\pi\epsilon_0 R^4} \cdot \frac{3}{2}[\cos\theta_A(3\cos^2\theta_B - 1) - \sin\theta_A\sin 2\theta_B\cos\varphi]. \tag{3.2.9}$$

Note the R dependence in these formulae. The dipole–dipole interaction is proportional to R^{-3}, the dipole–quadrupole to R^{-4} and the quadrupole–quadrupole to R^{-5}. In general, the interaction between multipoles of ranks l and l' is proportional to $R^{-l-l'-1}$. At large R, therefore, only the lowest-rank non-vanishing moment is important, but the others become increasingly significant as R decreases.

3.3 Spherical tensor formulation

For many purposes, a spherical tensor formulation of the interaction is more convenient. It is best obtained by a somewhat different route. The derivation starts with an expansion of $1/r_{ab}$, just as the cartesian formulation does, but this time we use the expansion in terms of spherical harmonics (the *spherical harmonic addition theorem*), which takes the form

$$\frac{1}{|\mathbf{r}_1 - \mathbf{r}_2|} = \sum_{lm} \frac{r_<^l}{r_>^{l+1}}(-1)^m C_{l,-m}(\theta_1,\varphi_1)C_{lm}(\theta_2,\varphi_2). \tag{3.3.1}$$

In this expression, which is proved in many textbooks of quantum mechanics and mathematical physics (Arfken 1970, Zare 1988), $r_<$ is the smaller and $r_>$ the larger of r_1 and r_2. For our

purposes, we want $1/r_{ab} = 1/|\mathbf{B}+\mathbf{b}-\mathbf{A}-\mathbf{a}|$, and we take $\mathbf{r}_1 = \mathbf{B}-\mathbf{A} = \mathbf{R}$ and $\mathbf{r}_2 = \mathbf{a}-\mathbf{b}$, and assuming that $|\mathbf{a}-\mathbf{b}| < R$ we obtain

$$\frac{1}{|\mathbf{R}+\mathbf{b}-\mathbf{a}|} = \sum_{l=0}^{\infty}\sum_{m=-l}^{l}(-1)^m R_{l,-m}(\mathbf{a}-\mathbf{b})I_{lm}(\mathbf{R}), \tag{3.3.2}$$

where $R_{km}(\mathbf{r})$ and $I_{km}(\mathbf{r})$ are the regular and irregular spherical harmonics. (See Appendix B). We must remember that eqn (3.3.2) is valid only if $|\mathbf{a}-\mathbf{b}| < R$. Now we use the addition theorem already quoted in eqn (2.7.3), and, remembering that $R_{lm}(-\mathbf{r}) = (-1)^l R_{lm}(\mathbf{r})$, we find

$$\begin{aligned}
\mathcal{H}' &= \frac{1}{4\pi\epsilon_0}\sum_{a\in A}\sum_{b\in B}\frac{e_a e_b}{|\mathbf{R}+\mathbf{b}-\mathbf{a}|} \\
&= \frac{1}{4\pi\epsilon_0}\sum_{l_1,l_2}\sum_{m_1 m_2 m}(-1)^{l_1}\left(\frac{(2l_1+2l_2+1)!}{(2l_1)!(2l_2)!}\right)^{1/2} \\
&\qquad \times \sum_{a\in A} e_a R_{l_1 m_1}(\mathbf{a})\sum_{b\in B} e_b R_{l_2 m_2}(\mathbf{b}) I_{l_1+l_2,m}(\mathbf{R})\begin{pmatrix} l_1 & l_2 & l_1+l_2 \\ m_1 & m_2 & m\end{pmatrix} \\
&= \frac{1}{4\pi\epsilon_0}\sum_{l_1,l_2}\sum_{m_1 m_2 m}(-1)^{l_1}\left(\frac{(2l_1+2l_2+1)!}{(2l_1)!(2l_2)!}\right)^{1/2} \\
&\qquad \times \hat{Q}^{A(G)}_{l_1 m_1}\hat{Q}^{B(G)}_{l_2 m_2} I_{l_1+l_2,m}(\mathbf{R})\begin{pmatrix} l_1 & l_2 & l_1+l_2 \\ m_1 & m_2 & m\end{pmatrix},
\end{aligned} \tag{3.3.3}$$

where in the last line we have introduced the multipole moment operators:

$$\hat{Q}^{A(G)}_{lm} = \sum_{a\in A} e_a R_{lm}(\mathbf{a}).$$

Now the expression (3.3.3) is expressed in the global coordinate system, which we have been using throughout; the superscript (G) is to remind us of this fact. As we have seen, however, it is much more convenient to express the interaction in terms of multipole moments defined in the local coordinate system of each molecule. The components in the global system are related to those in the local system by

$$Q^{(L)}_{lk} = \sum_m Q^{(G)}_{lm} D^l_{mk}(\Omega), \tag{3.3.4}$$

where $\Omega = (\alpha,\beta,\gamma)$ is the rotation that takes the global axes to the local axes, and $D^l_{mk}(\Omega)$ is the Wigner rotation matrix element for this rotation. (See eqn (B.2.1)—we take the component $Q^{(L)}_{lk}$ initially in an orientation where the local axes coincide with the global axes, and rotate it and the local axes to the required orientation.) Equivalently, we can write the global components in terms of the local ones:

$$Q^{(G)}_{lm} = \sum_k Q^{(L)}_{lk} D^l_{km}(\Omega^{-1}) = \sum_k Q^{(L)}_{lk}[D^l_{mk}(\Omega)]^*, \tag{3.3.5}$$

where the last step follows because the Wigner matrices are unitary. Making this substitution for the multipole moment operators in global axes that occur in (3.3.3), we get

$$\mathcal{H}' = \frac{1}{4\pi\epsilon_0}\sum_{l_1,l_2}\sum_{k_1k_2}(-1)^{l_1}\left(\frac{(2l_1+2l_2+1)!}{(2l_1)!(2l_2)!}\right)^{1/2}\hat{Q}^{A(L)}_{l_1k_1}\hat{Q}^{B(L)}_{l_2k_2}$$
$$\times\sum_{m_1m_2m}[D^{l_1}_{m_1k_1}(\Omega_1)]^*[D^{l_2}_{m_2k_2}(\Omega_2)]^*I_{l_1+l_2,m}(\mathbf{R})\begin{pmatrix}l_1 & l_2 & l_1+l_2\\ m_1 & m_2 & m\end{pmatrix}. \tag{3.3.6}$$

The multipole moment operators are now referred to local molecular axes (different for the two molecules) and the orientational and distance dependence is all contained in the sum over Wigner functions and irregular spherical harmonics. We define new functions of the orientations by

$$S^{\,k_1k_2}_{l_1\,l_2\,j} = \mathrm{i}^{l_1-l_2-j}\sum_{m_1m_2m}[D^{l_1}_{m_1k_1}(\Omega_1)]^*[D^{l_2}_{m_2k_2}(\Omega_2)]^*C_{jm}(\theta,\varphi)\begin{pmatrix}l_1 & l_2 & j\\ m_1 & m_2 & m\end{pmatrix} \tag{3.3.7}$$

and

$$\overline{S}^{\,k_1k_2}_{l_1\,l_2\,j} = \mathrm{i}^{l_1-l_2-j}\begin{pmatrix}l_1 & l_2 & j\\ 0 & 0 & 0\end{pmatrix}^{-1}$$
$$\times\sum_{m_1m_2m}[D^{l_1}_{m_1k_1}(\Omega_1)]^*[D^{l_2}_{m_2k_2}(\Omega_2)]^*C_{jm}(\theta,\varphi)\begin{pmatrix}l_1 & l_2 & j\\ m_1 & m_2 & m\end{pmatrix}. \tag{3.3.8}$$

Here θ and φ are the polar angles describing the direction of the intermolecular vector $\mathbf{R}$. In terms of the $\overline{S}$ functions, (3.3.6) becomes

$$\mathcal{H}' = \frac{1}{4\pi\epsilon_0}\sum_{l_1l_2}\sum_{k_1k_2}(-1)^{l_1+l_2}\left(\frac{(2l_1+2l_2+1)!}{(2l_1)!(2l_2)!}\right)^{1/2}$$
$$\times\hat{Q}^{A}_{l_1k_1}\hat{Q}^{B}_{l_2k_2}R^{-l_1-l_2-1}\begin{pmatrix}l_1 & l_2 & l_1+l_2\\ 0 & 0 & 0\end{pmatrix}\overline{S}^{\,k_1k_2}_{l_1\,l_2\,l_1+l_2} \tag{3.3.9}$$

(dropping the superscript (L), since we shall be using local axes for the multipoles from now on) and if we insert the explicit formula for the $3j$ symbol (eqn (2.7.4)), this reduces to

$$\mathcal{H}' = \frac{1}{4\pi\epsilon_0}\sum_{l_1,l_2}\sum_{k_1k_2}\begin{pmatrix}l_1+l_2\\ l_1\end{pmatrix}\hat{Q}^{A}_{l_1k_1}\hat{Q}^{B}_{l_2k_2}\overline{S}^{\,k_1k_2}_{l_1\,l_2\,l_1+l_2}R^{-l_1-l_2-1}. \tag{3.3.10}$$

This formulation explicitly separates each term in the interaction into an operator part, involving multipole moment operators in local molecular axes, a factor $\overline{S}^{\,k_1k_2}_{l_1\,l_2\,l_1+l_2}$ that describes the orientation dependence, and a distance dependence $R^{-l_1-l_2-1}$. Notice that the orientational part, eqn (3.3.8), involves a linear combination of products of the Wigner functions and a spherical harmonic, with coefficients that are Wigner $3j$ symbols. This ensures that the result is a scalar, invariant under rotations of the entire system, and takes account of the fact that only five of the eight angular coordinates are independent.

The S and $\overline{S}$ functions differ only by the factor $\begin{pmatrix}l_1 & l_2 & j\\ 0 & 0 & 0\end{pmatrix}^{-1}$ in the latter. This has the effect of normalizing the $\overline{S}$ functions so that $\left|\overline{S}^{\,0\,0}_{l_1\,l_2\,j}\right| = 1$ when both molecules are oriented with their local axes parallel to the global axes and the intermolecular vector is parallel to the

global $+z$ axis. This is a convenient normalization, and leads to a simple numerical coefficient in eqn (3.3.10), but is unusable when $l_1 + l_2 + j$ is odd, since the $3j$ symbol is then zero. Such cases do not arise in the electrostatic interaction, where $j = l_1 + l_2$, but they can occur elsewhere, and in that case it is necessary to use the alternative form, eqn (3.3.7).

Eqn (3.3.10) is a general and powerful formulation, but a little cumbersome for routine use. Also it is at present expressed in terms of the complex components of the multipole moments. Accordingly we first transform to the real components, using eqn (B.1.6):

$$\hat{Q}_{l,k} = \sum_{\kappa} X_{\kappa,k} \hat{Q}_{l,\kappa}, \tag{3.3.11}$$

where the $X_{\kappa,k}$ are defined in eqn (B.1.7). This leads to an expression equivalent to (3.3.10) but in terms of the real components:

$$\mathcal{H}' = \frac{1}{4\pi\epsilon_0} \sum_{l_1,l_2} \sum_{\kappa_1\kappa_2} \binom{l_1 + l_2}{l_1} \hat{Q}^A_{l_1\kappa_1} \hat{Q}^B_{l_2\kappa_2} \overline{S}^{\kappa_1\kappa_2}_{l_1\, l_2\, l_1+l_2} R^{-l_1-l_2-1}, \tag{3.3.12}$$

where

$$\overline{S}^{\kappa_1\kappa_2}_{l_1\, l_2\, j} = \sum_{k_1 k_2} X_{\kappa_1,k_1} X_{\kappa_2,k_2} \overline{S}^{k_1 k_2}_{l_1\, l_2\, j}. \tag{3.3.13}$$

We can now obtain a more compact representation by defining analogues to the T tensors of the cartesian formulation:

$$T_{l_1\kappa_1,l_2\kappa_2} = \frac{1}{4\pi\epsilon_0} \binom{l_1 + l_2}{l_1} \overline{S}^{\kappa_1\kappa_2}_{l_1\, l_2\, l_1+l_2} R^{-l_1-l_2-1}, \tag{3.3.14}$$

and then the interaction is just

$$\mathcal{H}' = \sum_{l_1,l_2} \sum_{\kappa_1\kappa_2} \hat{Q}^A_{l_1\kappa_1} \hat{Q}^B_{l_2\kappa_2} T_{l_1\kappa_1,l_2\kappa_2}. \tag{3.3.15}$$

We can abbreviate this even further by adopting a notation in which the successive multipole components are arranged in a vector, indexed by angular momentum labels 00, 10, 11c, 11s, 20, 21c, 21s, 22c, 22s, 30, ... If we agree always to order the components in this way, we can use a single index, say t or u, to label them, and write the interaction as

$$\mathcal{H}' = \hat{Q}^A_t T^{AB}_{t\,u} \hat{Q}^B_u. \tag{3.3.16}$$

As a final abbreviation we have adopted the repeated-suffix summation convention in this last form. While this may appear excessively terse to the beginner, it is a very compact and convenient form for the manipulation of general formulae. The actual order of the components does not matter as long as it is consistent, so when dealing with only charge and dipole components, for example, it may be convenient to use the labels 0, x, y and z, in that order.

The interaction functions $T^{AB}_{t\,u}$ depend only on the relative positions of the two molecular axis systems, so they can be evaluated once and for all, and tabulated for further use. The functions for $l_1 + l_2 \le 5$, which include all terms in the interaction up to R^{-6}, are tabulated in Appendix F. These formulae were first given by Price *et al.* (1984), in a different form, and by Stone (1991) in the form given here, for $l_1 + l_2 \le 4$. Hättig and Heß (1994) described a much

simpler method for deriving these formulae, and used it to obtain the formulae for $l_1 + l_2 = 5$ and to check the earlier formulae.

One of the important features of these formulae, from the practical point of view, is that they do not involve any trigonometric functions. Although the Wigner functions are usually expressed in terms of sines and cosines, the interaction functions can be expressed entirely in terms of scalar products involving the unit vectors $\mathbf{e}_i^A$ and $\mathbf{e}_j^B$ along the local axes of each molecule, and a unit vector in the direction of $\mathbf{R}$. These vectors are readily available in circumstances such as a molecular dynamics calculation, so the evaluation of the interaction functions is not as time-consuming as might at first appear. Molecular dynamics programs now exist that use distributed multipoles rather than just point charges (Smith *et al.* 2003, Ren and Ponder 2003, Leslie 2008).

A study of the dipole–dipole and quadrupole–quadrupole interactions for linear molecules will perhaps illuminate the difference between this formulation and the cartesian one. The cartesian version of the dipole–dipole interaction is given by eqn (3.2.5), or by (3.2.4), which emphasizes that the expression involves the multipole components μ_α^A and μ_β^B *in the global coordinate system*. In order to evaluate the expression, we need to transform the dipole moments into this coordinate system. The resulting expression involves (in effect) the scalar products $e_z^A \cdot \hat{\mathbf{R}}$, $e_z^B \cdot \hat{\mathbf{R}}$ and $e_z^A \cdot e_z^B$, though we previously used the notation $\mathbf{n}^A$ and $\mathbf{n}^B$ for e_z^A and e_z^B. In the spherical-tensor approach, we use eqn (3.3.15), and the interaction takes the form $\mu_{10}^A \mu_{10}^B T_{10,10}$. The dipole moments are the z components in local axes, while $T_{10,10}$ is obtained from Table F.1. In this case there is little difference between the cartesian and spherical-tensor expressions.

In the case of the cartesian quadrupole–quadrupole interaction the same procedure is required. However, even for Θ_{zz} the transformation to global coordinates is more cumbersome, and the expression involves the interaction tensor $T_{\alpha\beta\gamma\delta}$. In contrast, the spherical tensor expression involves the same scalar products as before:

$$U_{\Theta\Theta} = \frac{\Theta^A \Theta^B}{4\pi\epsilon_0 R^5} \times \frac{3}{4}\big[35(\mathbf{n}^A \cdot \hat{R})^2(\mathbf{n}^B \cdot \hat{R})^2 - 5(\mathbf{n}^A \cdot \hat{R})^2 - 5(\mathbf{n}^B \cdot \hat{R})^2 - 20(\mathbf{n}^A \cdot \hat{R})(\mathbf{n}^B \cdot \hat{R})(\mathbf{n}^A \cdot \mathbf{n}^B) + 2(\mathbf{n}^A \cdot \mathbf{n}^B)^2 + 1\big]. \tag{3.3.17}$$

When both molecules lie on the z axis the scalar products are, as in the dipole–dipole case,

$$\begin{aligned} \mathbf{n}_A \cdot \hat{R} &= \cos\theta_A, \\ \mathbf{n}_B \cdot \hat{R} &= \cos\theta_B, \\ \mathbf{n}_A \cdot \mathbf{n}_B &= \cos\theta_A \cos\theta_B + \sin\theta_A \sin\theta_B \cos(\varphi_B - \varphi_A) \end{aligned}$$

and (3.3.17) is easily evaluated to give (3.2.8).

When electrostatic interactions are to be evaluated by computer, direct use of the formulae in Appendix F is probably not the most efficient procedure. Hättig (1996) has proposed a method that uses recurrence relations to evaluate the higher-rank terms from the lower-rank ones. Furthermore one may transform everything into an axis system in which the formulae simplify. We may, for example, refer everything to a 'site–site' axis system with its z direction running from A to B and with the site x axes parallel to each other. This involves rotating

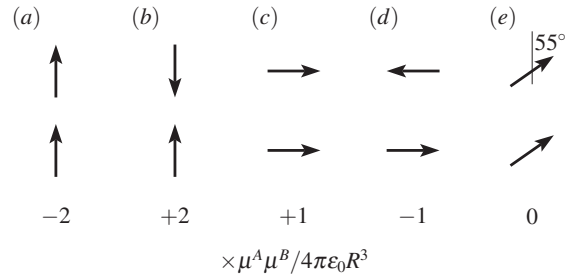

Fig. 3.2 Favourable and unfavourable geometries for dipole–dipole interactions.

the multipoles on each site into the site–site axes, which can be done quite efficiently on the computer. In this axis system, the T functions simplify to

$$4\pi\epsilon_0 T_{l_1\kappa_1,l_2\kappa_2} = (-)^{l_2+k} R^{-l_1-l_2-1} \delta_{\kappa_1\kappa_2} \left[\binom{l_1+l_2}{l_1+k} \binom{l_1+l_2}{l_1-k} \right]^{1/2}, \tag{3.3.18}$$

where $\kappa_1 = \kappa_2 = k = 0$ or $\kappa_1 = \kappa_2 = kc$ or ks. Hättig (1997) has also shown how to use this approach to calculate the forces and torques, and the Hessian, as well as the energy.

3.4 Examples

We noted above that the T tensors are irregular spherical harmonics, and so have the important property that all of them, except T itself, average to zero over all directions of **R**. Thus the angular variation of the electrostatic interaction is much greater than that of other contributions to the interaction energy, such as the dispersion energy, which is always negative. This means that the electrostatic term often has a dominant effect in determining geometry, even when it is not the dominant contribution to the binding energy.

3.4.1 The dipole–dipole interaction

The dipole–dipole interaction has the simple angle-dependence given in eqn (3.2.6). At a given value of R, the most favourable orientation has $\theta_A = \theta_B = 0$. (See Fig. 3.2a.) In this case, the angular factor that multiplies the magnitude $\mu^A\mu^B/4\pi\epsilon_0 R^3$ of the interaction is -2. Conversely the most unfavourable orientation has $\theta_A = \pi$, $\theta_B = 0$ or vice versa, with an angular factor of $+2$ (Fig. 3.2b). If the molecules are linear, however, the orientation with $\theta_A = \theta_B = \pi/2$ and $\varphi = \pi$ may be preferable (Fig. 3.2d); in this case the angular factor is only -1, but it may be possible for the molecules to pack more closely, increasing the R^{-3} factor.

The HCN molecule provides a good illustration of these features. The HCN dimer adopts the linear head-to-tail structure (Fig. 3.2a) with $\theta_A = \theta_B = 0$ (Legon *et al.* 1977), while the crystal structure has chains of HCN molecules arranged head to tail (Dulmage and Lipscomb 1951).

3.4.2 The quadrupole–quadrupole interaction

The quadrupole–quadrupole interaction alone is important in determining the structure of many non-polar molecules, i.e., those with $\mu = 0$. For given R, the energy as a multiple of

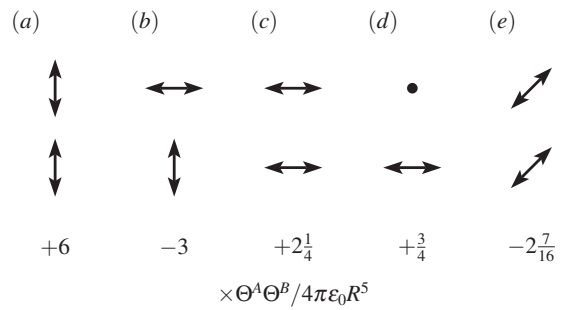

Fig. 3.3 Favourable and unfavourable geometries for quadrupole–quadrupole interactions. The double arrow represents a quadrupole moment Q_{20} with magnitude $\Theta > 0$.

$\Theta^A\Theta^B/4\pi\epsilon_0 R^5$ is largest when $\theta_A = \theta_B = 0$, when the angular factor is +6. (See Fig. 3.3a.) The configurations with $\theta_A = \theta_B = \pi/2$ (Figs 3.3c and 3.3d) are also repulsive, with angular factor +2.25 when $\varphi = 0$ and 0.75 when $\varphi = \pi/2$. There are two common attractive geometries, both planar ($\varphi = 0$): the 'T' structure, with $\theta_A = 0$ and $\theta_B = \pi/2$, or vice versa (Fig. 3.3b); and the 'slipped parallel' structure, with $\theta_A = \theta_B \approx \pi/4$ (Fig. 3.3e). These structures have angular factors of −3 and $-2\frac{7}{16}$ respectively, so they are quite similar in energy. In fact there is a range of attractive geometries with $\theta_B = \pi/2 - \theta_A$, and which of them is preferred in any given case usually depends on the molecular shape. For long narrow molecules, or planar ones, a structure of the slipped parallel type usually gives the smallest intermolecular distance and the lowest energy; for molecules that are more nearly spherical a T structure is usually favoured.

An interesting example is acetylene dimer. *Ab initio* calculations give the total binding energy to be about $400\,\mathrm{cm}^{-1}$(Bone and Handy 1990). In the T structure the separation of the centres of mass is 4.344 Å, and the quadrupole–quadrupole interaction contributes about $-550\,\mathrm{cm}^{-1}$ to the interaction energy, with dispersion, repulsion and higher-rank electrostatic terms making up the difference. In the slipped parallel structure, the centres of mass are slightly closer, at 4.243 Å, which partly offsets the less favourable angular factor. Here the quadrupole–quadrupole term is $-500\,\mathrm{cm}^{-1}$. Consequently the energy difference between the two structures is very small, and there is an interconversion between different T structures via slipped-parallel transition states, the molecules rotating in opposite directions in a geared fashion. (See Fig. 3.4.) The consequences of this isomerization can be seen in the infrared spectrum as a tunnelling splitting (Fraser *et al.* 1988, Ohshima *et al.* 1988), from which the barrier to interconversion is estimated to be only $33\,\mathrm{cm}^{-1}$.

Acetylene trimer is an even more interesting case. Here too the electrostatic interaction dominates the binding, and the equilibrium geometry is a planar C_{3h} structure in which each pair of acetylene molecules is bound in an approximately T-shaped manner, with one H atom of each acetylene directed towards the π orbitals of the next. Here too there are isomerization possibilities, and there is a great variety of rearrangement pathways whose energetics can be well understood in terms of quadrupole–quadrupole interactions (Bone *et al.* 1991).

There are many non-polar linear or planar molecules that show the effects of quadrupole–quadrupole interactions in their crystal structures. Planar aromatic molecules such as benzene, naphthalene and anthracene are examples. Although the molecular packing is important in determining the crystal structure, the influence of quadrupole–quadrupole interactions is often

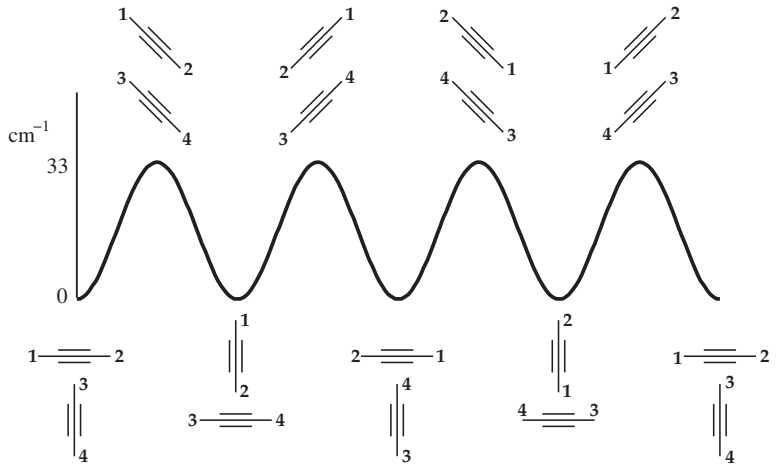

Fig. 3.4 Acetylene dimer: interconversion between different isomers of the T-shaped equilibrium structure via a slipped-parallel structure.

apparent. Structures commonly consist of stacks of tilted parallel molecules, with neighbouring molecules in adjacent stacks often having a T geometry relative to each other.

If the two molecules are different, it is possible for Θ^A and Θ^B to have opposite signs. In the case of dipoles, a change of sign is merely a change of direction, but when Θ^A and Θ^B have opposite signs the preferred geometries are qualitatively different. In this case the preferred geometry for given R is $\theta_A = \theta_B = 0$, with its angular factor of +6 multiplying the negative value of $\Theta^A\Theta^B/4\pi\epsilon_0 R^5$. An example is the complex between benzene ($\Theta = -6.7\, ea_0^2$) and hexafluorobenzene ($\Theta = +7.1\, ea_0^2$). Here the two molecules pack with their planes parallel in a C_{6v} structure (Williams 1993).

For linear molecules, the geometry with $\theta_A = \theta_B = \pi/2$ may be preferred to permit a smaller intermolecular distance. An example of this is the complex between CO_2 and acetylene, which have quadrupole moments of $-3.3\, ea_0^2$ and $5.6\, ea_0^2$ respectively. Here the experimental structure has $\theta_A = \theta_B = \pi/2$, so that the molecules are parallel to each other in a C_{2v} structure, with centre-of-mass separation of 3.29 Å $= 6.22a_0$ (Prichard *et al.* 1988, Muenter 1989, Huang and Miller 1989). In this geometry the quadrupole–quadrupole interaction is $2.25 \times (-3.3 \times 5.6)/6.22^5 = -0.0045$ a.u. $= -980\,\text{cm}^{-1}$. The structure with $\theta_A = \theta_B = 0$—the linear structure—is not observed spectroscopically; *ab initio* calculations (Bone and Handy 1990) predict that it is a local minimum on the potential energy surface, with a centre-of-mass separation of 5.233 Å $= 9.89a_0$. Here the quadrupole–quadrupole energy is much smaller: $(-3.3 \times 5.6 \times 6)/(9.89^5) = -0.0012$ a.u. $= -257\,\text{cm}^{-1}$, the more favourable angular factor being more than outweighed by the increased separation. We should be aware however that such calculations are greatly oversimplified; not only do they ignore other terms in the interaction between the molecules, such as repulsion and dispersion, but even the electrostatic interaction itself is not reliably described by the multipole expansion when the molecules are so close together. We shall return to these matters in later chapters; for the moment we just note that the *ab initio* calculation of Bone and Handy gives binding energies of $568\,\text{cm}^{-1}$ and $358\,\text{cm}^{-1}$ respectively for the C_{2v} and linear structures.

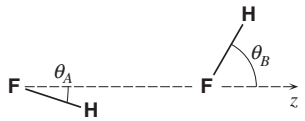

Fig. 3.5 Structure of the HF dimer.

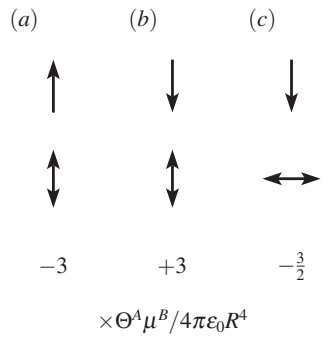

Fig. 3.6 Favourable and unfavourable geometries for dipole–quadrupole interactions.

3.4.3 Competition between electrostatic terms

It might be thought that the HF dimer would be another example where the electrostatic interaction favours a linear structure, because of the dipole–dipole interaction, but the experimental evidence (Dyke *et al.* 1972) leads to a structure (Fig. 3.5) in which the F–H···F hydrogen bond is indeed nearly linear ($\theta_A \approx 0$), but the other hydrogen atom is tilted away from the linear geometry by about 60°. At one time this was adduced as evidence for chemical bonding in the hydrogen bond. However, HF has a significant quadrupole as well as a dipole moment, so we have to consider the effects of dipole–quadrupole and quadrupole–quadrupole interactions as well as dipole–dipole terms. The favourable orientations for dipole–quadrupole interactions are shown in Fig. 3.6. If we postulate a structure in which one of the HF molecules is at the origin and the other on the positive z axis, with $\theta_A = 0$ to give a linear hydrogen bond but with θ_B allowed to be non-zero, it is possible to see from the formulae given above that the linear structure is favoured by the dipole–dipole and quadrupole–dipole ($\Theta^A\mu^B$) terms, but that the dipole–quadrupole ($\mu^A\Theta^B$) and quadrupole–quadrupole terms favour a structure with $\theta_B = \pi/2$.

In fact, there is a competition between these two effects, and the electrostatic energy, for this postulated structure, is minimized at a geometry given by $\cos\theta_B = (2 + 3\lambda)/(9\lambda(1 + 2\lambda))$, where $\lambda = \Theta/\mu R$. For HF, where $\mu = 0.72\, ea_0$, $\Theta = 1.875\, ea_0^2$ and $R = 5.1\, a_0$, this gives $\theta_B = 68°$, in reasonable agreement with the observed value. For HCl, the dipole moment is smaller, $0.433\, ea_0$, the quadrupole moment larger, $2.8\, ea_0^2$, and the separation also somewhat larger at $6.8\, a_0$. In this case the value of θ_B that emerges is also bigger, at 79°. This result too is in agreement with the experimental evidence (Ohashi and Pine 1984). We conclude that there is no need to invoke chemical bonding effects in the description of the hydrogen bond, and that the structure can be understood in a purely classical fashion, provided that the

description of the electrostatics is sufficiently complete and accurate. One of the limitations of conventional treatments is that the multipole expansion in the form that we have used here converges only slowly, or even diverges, for molecules of quite modest size. We return to this theme in Chapter 7.

4

Perturbation Theory of Intermolecular Forces at Long Range

4.1 Introduction

Because intermolecular forces are relatively weak, it is natural to describe them using perturbation theory. If the molecules are far enough apart that the overlap between their wavefunctions can be ignored, the theory becomes relatively simple, so we will study this case first. It was first treated by London (1930*b*, 1937), and has been reformulated by others since then (Margenau 1939, Longuet-Higgins 1956, Buckingham 1967).

The reason for the simplifications has to do with electron exchange. Suppose that we have a wavefunction $\Psi^A(1, 2, \ldots, n_A)$ that describes molecule A (a function of the coordinates of its n_A electrons), and a wavefunction $\Psi^B(1', 2', \ldots, n'_B)$ describing the n_B electrons of molecule B. The primes are used to distinguish the labels of the electrons of molecule B from those of molecule A. By hypothesis, there is a region of space associated with Ψ^A, such that Ψ^A is non-zero only when all its electrons are in this region. Likewise there is another region associated with Ψ^B, and the two regions do not overlap. The wavefunction for the combined system should be written as an antisymmetrized product $\mathcal{A}\Psi^A\Psi^B$. But this antisymmetrized product contains terms like $\Psi^A(1', 2, \ldots, n_A) \times \Psi^B(1, 2', \ldots, n'_B)$, in which electron 1 of molecule A has been exchanged with electron $1'$ of molecule B. The overlap between this and the original product function is

$$\int \Psi^A(1, 2, \ldots, n_A)^* \Psi^B(1', 2', \ldots, n'_B)^* \times \Psi^A(1', 2, \ldots, n_A) \Psi^B(1, 2', \ldots, n'_B)\, \mathrm{d}\tau$$

and when we integrate over the coordinates of electron 1 we get zero, because Ψ^A and Ψ^B are non-zero in different regions of space. So the terms in which the allocation of electrons between the two molecules is different do not mix with each other at all. The effect of this is that calculations may be done without antisymmetrization and the result will be the same.

In practice the overlap is never exactly zero, but the error made by ignoring it decreases exponentially as the distance between the molecules increases. Moreover the error is small enough to neglect at quite modest separations; indeed, if it were not, it would never be possible to discuss the electronic structure of an individual molecule in terms of the behaviour of 'its' electrons. However, it becomes significant when molecules approach each other closely, and we shall have to examine this case later (Chapter 6).

The consequence of all this is that we can identify a set of n_A electrons as belonging to molecule A, and we can define a Hamiltonian $\mathcal{H}^A$ for molecule A in terms of these electrons.

Similarly, the Hamiltonian $\mathcal{H}^B$ for molecule B is defined in terms of its private set of electrons. The unperturbed Hamiltonian for the combined system is then $\mathcal{H}^0 = \mathcal{H}^A + \mathcal{H}^B$, and the perturbation consists of the electrostatic interaction between the particles of molecule A (electrons and nuclei) and those of B:

$$H' = \sum_{a\in A}\sum_{b\in B}\frac{e_a e_b}{4\pi\epsilon_0 r_{ab}}. \tag{4.1.1}$$

Here e_a is the charge on particle a, one of the particles of molecule A, and r_{ab} is the distance between it and particle b in molecule B. This operator can be expressed in several other useful forms. Following Longuet-Higgins (1956) we define a charge density operator $\hat{\rho}^A(\mathbf{r})$ for molecule A:

$$\hat{\rho}^A(\mathbf{r}) = \sum_{a\in A} e_a\delta(\mathbf{r}-\mathbf{a}), \tag{4.1.2}$$

where $\delta(\mathbf{r}-\mathbf{a})$ is the Dirac delta function (§2.1.3), and $\hat{\rho}^B(\mathbf{r})$ similarly. In terms of these operators the perturbation becomes

$$\begin{aligned} H' &= \int \sum_{a\in A}\sum_{b\in B}\frac{e_a\delta(\mathbf{r}-\mathbf{a})e_b\delta(\mathbf{r}'-\mathbf{b})}{4\pi\epsilon_0|\mathbf{r}-\mathbf{r}'|}\ \mathrm{d}^3\mathbf{r}\ \mathrm{d}^3\mathbf{r}' \\ &= \int \frac{\hat{\rho}^A(\mathbf{r})\hat{\rho}^B(\mathbf{r}')}{4\pi\epsilon_0|\mathbf{r}-\mathbf{r}'|}\ \mathrm{d}^3\mathbf{r}\ \mathrm{d}^3\mathbf{r}'. \end{aligned} \tag{4.1.3}$$

Another useful expression results if we notice that the potential at $\mathbf{r}$ due to molecule B is

$$\hat{V}^B(\mathbf{r}) = \int \frac{\hat{\rho}^B(\mathbf{r}')}{4\pi\epsilon_0|\mathbf{r}-\mathbf{r}'|}\ \mathrm{d}^3\mathbf{r}', \tag{4.1.4}$$

so that we can write

$$\mathcal{H}' = \int \hat{V}^B(\mathbf{r})\hat{\rho}^A(\mathbf{r})\ \mathrm{d}^3\mathbf{r}, \tag{4.1.5}$$

or equivalently

$$\mathcal{H}' = \int \hat{V}^A(\mathbf{r}')\hat{\rho}^B(\mathbf{r}')\ \mathrm{d}^3\mathbf{r}'. \tag{4.1.6}$$

(The variable that appears in these integrals is a dummy, so it does not matter whether it is $\mathbf{r}$ or $\mathbf{r}'$; the choice of variable is made simply to retain the connection with the earlier formulae.)

Now the unperturbed states are simple product functions $\Psi^A_m\Psi^B_n$, which we abbreviate to $|mn\rangle$, and they are eigenfunctions of $\mathcal{H}^0$:

$$\begin{aligned} \mathcal{H}^0|mn\rangle &= (\mathcal{H}^A + \mathcal{H}^B)|mn\rangle \\ &= (W^A_m + W^B_n)|mn\rangle \\ &= W^0_{mn}|mn\rangle \end{aligned}$$

For closed-shell molecules, ordinary non-degenerate Rayleigh–Schrödinger perturbation theory gives the energy to second order of the ground state* of the system, labelled by $m = n = 0$:

*In fact this need not be the ground state; it may be a state in which one molecule or both is excited. However, it may not be a degenerate state of the combined system, which excludes all excited states in the case where the two molecules are identical. See the discussion of resonance interactions in Chapter 11.

$$W_{00} = W_{00}^0 + W_{00}' + W_{00}'' + \cdots, \tag{4.1.7}$$

where

$$W_{00}^0 = W_0^A + W_0^B \tag{4.1.8}$$

$$W_{00}' = \langle 00|\mathcal{H}'|00\rangle, \tag{4.1.9}$$

$$W_{00}'' = -\sum_{mn}{}' \frac{\langle 00|\mathcal{H}'|mn\rangle\langle mn|\mathcal{H}'|00\rangle}{W_{mn}^0 - W_{00}^0}. \tag{4.1.10}$$

This is the long-range approximation to the interaction energy, sometimes called in this context the 'polarization approximation' (Hirschfelder 1967). The first-order energy, eqn (4.1.9), is just the expectation value of the electrostatic interaction $\mathcal{H}'$ for the ground state $|00\rangle$, which is the electrostatic interaction that we discussed in Chapter 3. Note, however, that if we write the perturbation in the form (4.1.3) we can express the interaction as

$$W_{00}' = \int \frac{\rho^A(\mathbf{r})\rho^B(\mathbf{r}')}{4\pi\epsilon_0|\mathbf{r} - \mathbf{r}'|}\, \mathrm{d}^3\mathbf{r}\, \mathrm{d}^3\mathbf{r}', \tag{4.1.11}$$

since the integration over the coordinates of the particles in molecule A just replaces the operator $\hat{\rho}^A(\mathbf{r})$ by its expectation value $\rho^A(\mathbf{r})$. This is the exact classical interaction energy of the two molecular charge distributions in a form that does not depend on the multipole expansion.

The second-order energy (4.1.10) describes the induction and dispersion energies. To see this, we first separate it into three parts. Noting that the only term excluded in the sum is the one in which *both* molecules are in the ground state, we consider separately the terms in the sum for which molecule A is excited but B is in its ground state, the terms for which molecule B is excited but A is in its ground state, and the terms where both molecules are excited. This gives

$$W'' = U_{\mathrm{ind}}^A + U_{\mathrm{ind}}^B + U_{\mathrm{disp}},$$

where

$$U_{\mathrm{ind}}^A = -\sum_{m\neq 0} \frac{\langle 00|\mathcal{H}'|m0\rangle\langle m0|\mathcal{H}'|00\rangle}{W_m^A - W_0^A}, \tag{4.1.12}$$

$$U_{\mathrm{ind}}^B = -\sum_{n\neq 0} \frac{\langle 00|\mathcal{H}'|0n\rangle\langle 0n|\mathcal{H}'|00\rangle}{W_n^B - W_0^B}, \tag{4.1.13}$$

$$U_{\mathrm{disp}} = -\sum_{\substack{m\neq 0\\ n\neq 0}} \frac{\langle 00|\mathcal{H}'|mn\rangle\langle mn|\mathcal{H}'|00\rangle}{W_m^A + W_n^B - W_0^A - W_0^B}. \tag{4.1.14}$$

These describe respectively the induction energy of molecule A, the induction energy of molecule B, and the dispersion energy.

4.2 The induction energy

In the long-range theory it is natural to develop the induction energy using the multipole expansion, and this approach is presented first. If the intermolecular distance is too short,

though, the multipole expansion may not converge, even when the molecular wavefunctions do not overlap. One way to deal with this problem is described in §4.2.3; others are discussed in Chapters 7 and 9.

Using the multipole expansion, the operator $\mathcal{H}'$ is given by eqn (3.2.2):

$$\mathcal{H}' = Tq^A q^B + T_\alpha(q^A\hat{\mu}^B_\alpha - \hat{\mu}^A_\alpha q^B) - T_{\alpha\beta}\hat{\mu}^A_\alpha\hat{\mu}^B_\beta + \cdots .$$

(We drop the terms involving the quadrupole for the moment.) Substituting in 4.1.13 gives

$$\begin{aligned} U^B_{\text{ind}} = -\sum_{n\neq 0} &\langle 00|Tq^A q^B + T_\alpha(q^A\hat{\mu}^B_\alpha - \hat{\mu}^A_\alpha q^B) - T_{\alpha\beta}\hat{\mu}^A_\alpha\hat{\mu}^B_\beta + \cdots|0n\rangle \\ &\times \langle 0n|Tq^A q^B + T_{\alpha'}(q^A\hat{\mu}^B_{\alpha'} - \hat{\mu}^A_{\alpha'} q^B) - T_{\alpha'\beta'}\hat{\mu}^A_{\alpha'}\hat{\mu}^B_{\beta'} + \cdots|00\rangle \\ &\times (W^B_n - W^B_0)^{-1}. \end{aligned}$$

Now we can perform the implied integration over the coordinates of molecule A, which just yields the expectation values of the multipole moment operators. We note also that the matrix elements of q^B vanish, because the excited states are orthogonal to the ground state and q^B is just a constant. This gives

$$\begin{aligned} U^B_{\text{ind}} &= -\sum_{n\neq 0} \frac{\langle 0|T_\alpha q^A\hat{\mu}^B_\alpha - T_{\alpha\beta}\mu^A_\alpha\hat{\mu}^B_\beta + \cdots|n\rangle\langle n|T_{\alpha'}q^A\hat{\mu}^B_{\alpha'} - T_{\alpha'\beta'}\mu^A_{\alpha'}\hat{\mu}^B_{\beta'} + \cdots|0\rangle}{W^B_n - W^B_0} \\ &= -(q^A T_\alpha - \mu^A_\beta T_{\alpha\beta} + \cdots)\sum_{n\neq 0}\frac{\langle 0|\hat{\mu}^B_\alpha|n\rangle\langle n|\hat{\mu}^B_{\alpha'}|0\rangle}{W^B_n - W^B_0}(q^A T_{\alpha'} - \mu^A_{\beta'}T_{\alpha'\beta'} + \cdots). \end{aligned} \tag{4.2.1}$$

Now we can recognize here the sum-over-states expression for the polarizability $\alpha_{\alpha\alpha'}$ (see eqn (2.3.2)), so that the induction energy is

$$U^B_{\text{ind}} = -\tfrac{1}{2}(q^A T_\alpha - \mu^A_\beta T_{\alpha\beta} + \cdots)\alpha^B_{\alpha\alpha'}(q^A T_{\alpha'} - \mu^A_{\beta'}T_{\alpha'\beta'} + \cdots). \tag{4.2.2}$$

But the expression $(q^A T_\alpha - \mu^A_\beta T_{\alpha\beta} + \cdots)$ is merely minus the electric field $F^A_\alpha(\mathbf{B})$ at B due to molecule A (eqn (3.1.10)), so the induction energy is $-\frac{1}{2}F^A_\alpha(\mathbf{B})F^A_{\alpha'}(\mathbf{B})\alpha^B_{\alpha\alpha'}$, exactly as we would expect from a straightforward classical treatment of the field. The only part played by the quantum mechanical perturbation theory is to provide the formula for the polarizability.

In this derivation, we ignored all terms in the perturbation except for some of the ones involving the dipole operator for molecule B. It is clear by analogy or by explicit calculation that we shall have other terms in the induction energy, involving the dipole–quadrupole polarizability, the quadrupole–quadrupole polarizability, and so on, so that the induction energy takes the form

$$\begin{aligned} U^B_{\text{ind}} = &-\tfrac{1}{2}F^A_\alpha(\mathbf{B})F^A_{\alpha'}(\mathbf{B})\alpha^B_{\alpha\alpha'} - \tfrac{1}{3}F^A_\alpha(\mathbf{B})F^A_{\alpha'\beta'}(\mathbf{B})A^B_{\alpha,\alpha'\beta'} \\ &- \tfrac{1}{6}F^A_{\alpha\beta}(\mathbf{B})F^A_{\alpha'\beta'}(\mathbf{B})C^B_{\alpha\beta,\alpha'\beta'} - \cdots . \end{aligned} \tag{4.2.3}$$

The simplest case arises when A is a spherical ion, like Na^+. Then the field at B is $-qT_\alpha = qR_\alpha/(4\pi\epsilon_0 R^3)$. For the case where A is at the origin and B at $(0, 0, z)$ the field is $F_z = q/(4\pi\epsilon_0 z^2)$ and the induction energy is $q^2\alpha^B_{zz}/((4\pi\epsilon_0)^2 z^4)$. In this case, therefore, the energy is proportional to R^{-4}. If A is neutral but polar ($\mu \neq 0$), the field is proportional to R^{-3} and the energy to R^{-6}. Notice that the induction energy is always negative.

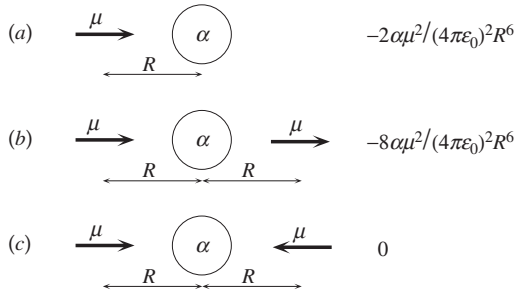

Fig. 4.1 Non-additivity of the induction energy.

4.2.1 Non-additivity of the induction energy

A very important feature of the induction energy emerges when we consider the case of a molecule surrounded by several others. The induction energy still takes the same form, i.e., $-\frac{1}{2}F_\alpha(\mathbf{B})F_{\alpha'}(\mathbf{B})\alpha^B_{\alpha\alpha'}$, but the field is now the total field due to the other molecules. (The simplest way to view this is to regard the rest of the system as comprising 'molecule A'. However, the same result can be obtained by working through the perturbation theory using as perturbation the sum of all intermolecular interactions, and again picking out the terms in which only molecule B is excited.) Now consider the cases illustrated in Fig. 4.1. In Fig. 4.1a we have molecule B in the field of a single polar neighbour, so that $F(\mathbf{B}) = 2\mu/4\pi\epsilon_0R^3$, and the induction energy is $-2\alpha\mu^2/(4\pi\epsilon_0)^2R^6$. In Fig. 4.1b there are two polar neighbours, aligned so that their fields are in the same direction at B. In this case the total field is twice as big as before, $F(\mathbf{B}) = 4\mu/4\pi\epsilon_0R^3$, and the induction energy is $-8\alpha\mu^2/(4\pi\epsilon_0)^2R^6$, four times as big. In Fig. 4.1c there are again two polar neighbours, but aligned this time so that their fields are in opposite directions at B. Now the total field is zero and so is the induction energy.

This simple example illustrates dramatically the severe non-additivity of the induction energy. Both types of situation may occur. For example, the local environment of an ion in an ionic crystal is often centrosymmetric, so that the electric field has to vanish, and in such cases there is no dipole–dipole contribution to the induction energy. In molecular crystals and liquids, the opposite case is common; for example, in the tetrahedral structure found in ice and (approximately) in liquid water, there are two proton donors and two proton acceptors near each molecule, and the fields of these neighbours tend to add rather than cancel. In the case of induction energy, then, the assumption of pairwise additivity fails totally.

If we can simply add together the fields arising from the neighbouring molecules, the calculation of the induction energy would not present any difficulties, even though it is quadratic in the field. Unfortunately this also may fail. The simplest way to see this is to follow the derivation first given by Silberstein (1917) of the polarizability of a pair of neighbouring atoms. Two spherical atoms, with polarizabilities α^A and α^B are placed a distance R apart on the z axis. An external field F in the z direction polarizes both atoms, inducing a dipole moment in both of them. The induced dipole of each atom produces an additional field at the other, and this must be added to the applied field. So the equations for the induced moments are

$$\mu^A = \alpha^A(F + 2\mu^B/(4\pi\epsilon_0 R^3)),$$
$$\mu^B = \alpha^B(F + 2\mu^A/(4\pi\epsilon_0 R^3)).$$

These equations are easily solved to give

$$\mu^A = \alpha^A F \frac{1 + 2\alpha^B/(4\pi\epsilon_0 R^3)}{1 - 4\alpha^A\alpha^B/(4\pi\epsilon_0)^2 R^6}, \quad \mu^B = \alpha^B F \frac{1 + 2\alpha^A/(4\pi\epsilon_0 R^3)}{1 - 4\alpha^A\alpha^B/(4\pi\epsilon_0)^2 R^6}. \tag{4.2.4}$$

So the effective field experienced by each atom is enhanced, and so is the induction energy. This is the case of a uniform external field, but much the same applies when the field is due to other molecules. It follows that we cannot in general expect to be able to add together the fields due to the static moments of the other molecules in order to calculate the induction energy. It may be a reasonable *approximation* to do so, especially if the molecules are not very polar or not very polarizable.

A problem that is apparent from eqn (4.2.4) is that if $R = (4\alpha^A\alpha^B/(4\pi\epsilon_0)^2)^{1/6}$ the denominators vanish, so that the induced moments and the electrostatic energy become infinite. This is known as the *polarization catastrophe*. It is a consequence of ignoring the finite extent of the polarizable charge distribution. Typically, the value of $\alpha/4\pi\epsilon_0$ is comparable to the atomic volume, so the catastrophe arises when the atoms are so close that they overlap. In that case the point-polarizability model fails. One way to avoid this problem will be discussed in §4.2.3, and others in Chapter 8.

In other geometries, the secondary effects of induction can reduce the magnitude of the induction energy. If the external field in the above example is in the x direction rather than the z direction, the equations for the moments become

$$\mu^A = \alpha^A(F - \mu^B/(4\pi\epsilon_0 R^3)),$$
$$\mu^B = \alpha^B(F - \mu^A/(4\pi\epsilon_0 R^3)),$$

and the induced moments are

$$\mu^A = \alpha^A F \frac{1 - \alpha^B/(4\pi\epsilon_0 R^3)}{1 - \alpha^A\alpha^B/(4\pi\epsilon_0)^2 R^6}, \quad \mu^B = \alpha^B F \frac{1 - \alpha^A/(4\pi\epsilon_0 R^3)}{1 - \alpha^A\alpha^B/(4\pi\epsilon_0)^2 R^6}. \tag{4.2.5}$$

However, the electrostatic energy often favours structures in which the induction energy is enhanced rather than reduced, and of course the induction energy itself favours such structures. We return to the question of cooperative induction effects in Chapter 10.

4.2.2 Multipole expansion of the induction energy

A more subtle characteristic of the induction energy emerges when we consider the multipole expansion in more detail. It is enough to consider the simplest case of a hydrogen-like atom A with nuclear charge Z in the field of a proton B. We take $Z > 1$ to avoid resonance effects (see Chapter 11). The perturbation is

$$\mathcal{H}' = \frac{Z}{R} - \frac{1}{|\mathbf{R} - \mathbf{r}|}, \tag{4.2.6}$$

where $\mathbf{R}$ is the position of the proton and $\mathbf{r}$ the position of the electron relative to an origin at the nucleus of atom A. Expressed as a multipole series using eqn (3.3.2), this becomes

$$\mathcal{H}' = \frac{1}{R}\left[Z - \sum_{n=0}^{\infty}\left(\frac{r}{R}\right)^n P_n(\cos\theta)\right], \tag{4.2.7}$$

where r and θ are polar coordinates for the electron in a coordinate system in which the proton is on the z axis.

Dalgarno and Lynn (1957*a*) were able to find an exact expression for the second-order energy of the atom under this perturbation. Their result is

$$W'' = -\sum_{n=1}^{\infty} \frac{(2n+2)!(n+2)}{n(n+1)(ZR)^{(2n+2)}}, \tag{4.2.8}$$

plus some terms that decrease exponentially as R increases; the latter describe the penetration term, which we shall discuss in Chapter 8.

Now we can use the standard ratio test to study the convergence of this series. The ratio of successive terms is $2n(n+3)(2n+3)/[(n+2)(ZR)^2]$, and it becomes infinite as $n \to \infty$, for any value of R. Consequently the multipole series expansion of the induction energy diverges for any R.

This is a very disturbing result. It suggests that in general the multipole expansion of the interaction energy may not converge. However, Ahlrichs (1976), in a more rigorous treatment of earlier work by Brooks (1952), proved that it is always semi-convergent (asymptotically convergent). Specifically, he showed that the interaction energy can be expressed in the form

$$U_{AB}(R) = W_{AB}(R) - W_A - W_B = \sum_{\nu=0}^{N} U_\nu R^{-\nu} + O(R^{-N-1}), \tag{4.2.9}$$

so that the remainder left after truncating the multipole series at any term tends to zero as the intermolecular distance tends to infinity. Ahlrichs also showed that the exchange terms, which arise from overlap of the molecular wavefunctions and which will be discussed in Chapter 8, decrease faster with increasing R than any power of $1/R$. The upshot of all this is that although the multipole expansion cannot be shown to converge at any fixed value of R, and can be shown in some cases to diverge for all R, it gives results that can be made arbitrarily accurate if the intermolecular distance is large enough. In practice, even at distances that are not very large, useful results may be obtained by truncating the multipole series.

4.2.3 Avoiding the multipole expansion

Because of the convergence problems that arise from the use of the multipole expansion, it would be desirable to avoid it. Instead of expressing the interaction with a neighbouring molecule in terms of the multipole expansion, we may write the perturbation in one of the forms (4.1.1–4.1.6). We shall use eqn (4.1.5), which describes the interaction between the charge density of A and an external potential, due to molecule B or in general to the rest of the system. If we are considering the induction energy of A, we sum over states in which A is excited but the rest of the system stays in its ground state, so the operator $\hat{V}^B(\mathbf{r})$ becomes the potential $V(\mathbf{r})$ at some point $\mathbf{r}$ in A due to the rest of the system:

$$\mathcal{H}' = \int V(\mathbf{r})\hat{\rho}^A(\mathbf{r})\ \mathrm{d}^3\mathbf{r}. \tag{4.2.10}$$

When we put this into the perturbation theory, we get

$$U^A_{\rm ind} = -\sum_{m\neq 0}\int V(\mathbf{r})\frac{\langle 0|\hat\rho^A(\mathbf{r})|m\rangle\langle m|\hat\rho^A(\mathbf{r}')|0\rangle}{W^A_m - W^A_0}V(\mathbf{r}')\ \mathrm{d}^3\mathbf{r}\ \mathrm{d}^3\mathbf{r}'$$
$$= \int V(\mathbf{r})\alpha(\mathbf{r},\mathbf{r}';0)V(\mathbf{r}')\,\mathrm{d}^3\mathbf{r}\,\mathrm{d}^3\mathbf{r}'. \qquad (4.2.11)$$

In this way we obtain an expression for the induction energy in terms of the static charge density susceptibility. This expression is quite general, within the long-range approximation. By replacing $V(\mathbf{r})$ and $V(\mathbf{r}')$ by the multipole expansion of the potential due to a neighbouring molecule or set of molecules, we recover the multipole expansion of the induction energy. However, (4.2.11) is more suitable at short distances, where the multipole expansion converges only slowly, if at all. It involves a double integral over position, and is impractical for use in the context of a simulation, where the energy and possibly its derivatives have to be computed at each step, but it can be evaluated quite efficiently to obtain the induction energy of a pair of molecules at particular geometries. We shall explore other solutions to the convergence problem in Chapter 9. We must remember, too, that in the long-range approximation we are ignoring the effects of exchange of electrons between molecules. At short range, these effects become important, and lead to additional terms in the induction energy, which we shall explore in Chapter 8.

4.3 The dispersion energy

4.3.1 Drude model

We turn to the dispersion energy. Because this is a wholly non-classical phenomenon, it may be helpful in understanding it to contemplate a simple model, first introduced by London (1930*a*) (see London (1937) for a version in English). We represent each atom by a Drude model: a one-dimensional harmonic oscillator in which the electron cloud, mass m, is bound to the nucleus by a harmonic potential with force constant k. The Hamiltonian for each atom takes the form $p^2/2m + \frac{1}{2}kx^2$. There is an atomic dipole proportional to the displacement x of the electrons from the nucleus, and for two adjacent atoms the interaction energy of these dipoles is proportional to the product of the dipole moments. Accordingly the Hamiltonian for the complete system takes the form

$$\mathcal{H} = \frac{1}{2m}(p_A^2 + p_B^2) + \frac{1}{2}k(x_A^2 + x_B^2 + 2cx_Ax_B),$$

where c is some coupling constant. This can be separated into two uncoupled oscillators corresponding to the normal modes $x_A \pm x_B$:

$$\mathcal{H} = \frac{1}{4m}(p_A + p_B)^2 + \frac{1}{4}k(1+c)(x_A + x_B)^2$$
$$+ \frac{1}{4m}(p_A - p_B)^2 + \frac{1}{4}k(1-c)(x_A - x_B)^2.$$

The normal mode frequencies are $\omega_\pm = \omega_0\sqrt{1\pm c}$, where $\omega_0 = \sqrt{k/m}$ is the frequency of an isolated oscillator.

Now a classical system would have a minimum energy of zero, whether coupled or not. The quantum system however has zero-point energy, and the energy of the coupled system in its lowest state is

$$\tfrac{1}{2}\hbar(\omega_+ + \omega_-) = \tfrac{1}{2}\hbar\omega_0(\sqrt{1+c} + \sqrt{1-c}) = \tfrac{1}{2}\hbar\omega_0[2 - \tfrac{1}{4}c^2 - \tfrac{5}{64}c^4 - \cdots],$$

so that there is an energy lowering, compared with the zero-point energy $\hbar\omega_0$ of two uncoupled oscillators, of

$$U_{\text{disp}} = -\hbar\omega_0\Big(\frac{1}{8}c^2 + \frac{5}{128}c^4 + \cdots\Big).$$

The interaction between the atoms leads to a correlation between the motion of their electrons, and this manifests itself in a lowering of the energy. Notice that the energy depends on the square of the coupling constant c and is always negative; regardless of the sign of the coupling, the correlation between the motion of the electrons leads to a lowering of the energy. For interacting dipoles, the coupling c is proportional to R^{-3}, so the leading term in the dispersion energy is proportional to R^{-6}.

At very large separations, this picture changes slightly because the speed of light is finite. The correlation between the fluctuations in the two molecules becomes less effective, because the information about a fluctuation in the charge distribution of one molecule can only be transmitted to the other molecule at the speed of light. By the time that the other molecule has responded and the information about its response has reached the first molecule again, the electrons have moved, so that the fluctuations are no longer in phase. Detailed calculation (Casimir and Polder 1948, Craig and Thirumachandran 1984) shows that this 'retardation' effect becomes important when the separation R is large compared with the wavelength λ_0 corresponding to the characteristic absorption frequency of the molecule, and the dispersion energy is then reduced by a factor of the order of λ_0/R and becomes proportional to R^{-7}. However, this only occurs at much larger distances than we are concerned with, since λ_0 is typically several thousand ångström. For a fuller discussion see Israelachvili (1992).

4.3.2 Quantum-mechanical formulation

We return to the perturbation-theory expression, eqn (4.1.14). For simplicity we consider first only the dipole–dipole term in $\mathcal{H}'$:

$$\begin{aligned} U^{(6)}_{\text{disp}} &= -\sum_{m_A\neq 0}\sum_{n_B\neq 0}\frac{\langle 0_A 0_B|\hat{\mu}^A_\alpha T_{\alpha\beta}\hat{\mu}^B_\beta|m_A n_B\rangle\langle m_A n_B|\hat{\mu}^A_\gamma T_{\gamma\delta}\hat{\mu}^B_\delta|0_A 0_B\rangle}{W^A_{m0}+W^B_{n0}} \\ &= -T_{\alpha\beta}T_{\gamma\delta}\sum_{m_A\neq 0}\sum_{n_B\neq 0}\frac{\langle 0_A|\hat{\mu}^A_\alpha|m_A\rangle\langle m_A|\hat{\mu}^A_\gamma|0_A\rangle\langle 0_B|\hat{\mu}^B_\beta|n_B\rangle\langle n_B|\hat{\mu}^B_\delta|0_B\rangle}{W^A_{m0}+W^B_{n0}}, \end{aligned} \tag{4.3.1}$$

where $W^A_{m0} = W^A_m - W^A_0$. This is an inconvenient expression to deal with, because although the matrix elements can be factorized into terms referring to A and terms referring to B, the denominator cannot. There are two commonly used ways to handle it. One was first introduced by London (1930*a*), and uses the *Unsöld* or *average-energy* approximation (Unsöld 1927). Here we first write (4.3.1) as

$$U^{(6)}_{\rm disp} = -T_{\alpha\beta}T_{\gamma\delta}\sum_{m_A\neq 0}\sum_{n_B\neq 0}\frac{W^A_{m0}W^B_{n0}}{W^A_{m0}+W^B_{n0}} \times \frac{\langle 0_A|\hat{\mu}^A_\alpha|m_A\rangle\langle m_A|\hat{\mu}^A_\gamma|0_A\rangle}{W^A_{m0}}\frac{\langle 0_B|\hat{\mu}^B_\beta|n_B\rangle\langle n_B|\hat{\mu}^B_\delta|0_B\rangle}{W^B_{n0}}. \tag{4.3.2}$$

If it were not for the inconvenient factor $W^A_{m0}W^B_{n0}/(W^A_{m0}+W^B_{n0})$, we would be able to factor out the sum-over-states expressions for $\alpha^A_{\alpha\gamma}$ and $\alpha^B_{\beta\delta}$. We therefore approximate this factor using average excitation energies U_A and U_B. Following Buckingham (1967), we use the Unsöld approximation in the form

$$\frac{W^A_{m0}W^B_{n0}}{W^A_{m0}+W^B_{n0}} = \frac{U_AU_B}{(U_A+U_B)}(1+\Delta_{mn}), \tag{4.3.3}$$

where

$$\Delta_{mn} = \frac{1/U_A - 1/W^A_{m0} + 1/U_B - 1/W^B_{n0}}{1/W^A_{m0}+1/W^B_{n0}}. \tag{4.3.4}$$

This is an identity for a particular m and n. If now we can choose U_A and U_B so that Δ_{mn} becomes negligible for all m and n (which requires that all the states $|m_A\rangle$ that make important contributions have excitation energies close to the average energy U_A, and likewise for the $|n_B\rangle$) then eqn (4.3.1) simplifies to

$$U^{(6)}_{\rm disp} \approx -\frac{U_AU_B}{4(U_A+U_B)}T_{\alpha\beta}T_{\gamma\delta}\alpha^A_{\alpha\gamma}\alpha^B_{\beta\delta}. \tag{4.3.5}$$

For atoms, where $\alpha_{\alpha\gamma}$ reduces to $\overline{\alpha}\delta_{\alpha\gamma}$, this becomes

$$\begin{aligned} U^{(6)}_{\rm disp} &\approx -\frac{U_AU_B}{4(U_A+U_B)}\overline{\alpha}^A\overline{\alpha}^BT_{\alpha\beta}T_{\alpha\beta} \\ &= -\frac{3U_AU_B}{2(U_A+U_B)}\frac{\overline{\alpha}^A\overline{\alpha}^B}{(4\pi\epsilon_0)^2R^6}. \end{aligned} \tag{4.3.6}$$

Here we have used the fact that

$$T_{\alpha\beta}T_{\alpha\beta} = \frac{(3R_\alpha R_\beta - R^2\delta_{\alpha\beta})(3R_\alpha R_\beta - R^2\delta_{\alpha\beta})}{(4\pi\epsilon_0)^2R^{10}} = \frac{6}{(4\pi\epsilon_0)^2R^6}. \tag{4.3.7}$$

Eqn (4.3.6) is the London formula for the dispersion energy between two atoms. The same formula can be used for molecules, when it gives the dispersion interaction averaged over relative orientations of the two molecules. It shows that the orientation-averaged dispersion energy takes the form[†] $-C_6R^{-6}$, and that it is larger between more polarizable atoms, but it is evidently not a practical method for determining the dispersion coefficient C_6, since we have no way to determine U_A and U_B. It is usual to put them equal to the ionization energies, but

[†]The sign of the dispersion coefficient C_6 is not a settled convention. Some authors use a convention in which C_6 is positive, in which case a minus sign appears in the expression for the dispersion energy, as here, while others take C_6 to be negative. The definition of C_6 as a positive quantity avoids some irritating semantic difficulties over whether a 'larger' value for a negative quantity is larger in magnitude or less negative, i.e., smaller in magnitude.

this gives no more than a rough approximation to C_6. Alternatively, we can put U_A and U_B equal to the lowest excitation energies of A and B respectively to get an upper bound to the magnitude of the dispersion energy.

A better approach is based on the work of Casimir and Polder (1948), who used quantum electrodynamics to explore the effect of retardation on the dispersion interaction, as mentioned above. Later workers, including Linder (1962), Mavroyannis and Stephen (1962) and McLachlan (1963), showed how to derive a simpler formulation, valid both for $R \ll \lambda_0$ and for $R \gg \lambda_0$, where λ_0 is a characteristic wavelength for the important electronic transitions of the molecules concerned. In the present discussion we are concerned with interactions at relatively short distances, and in this case a simpler approach can be used, still giving an exact formula in the limit $R \ll \lambda_0$. It depends on the following identity, apparently first introduced in this context by McLachlan (1963):

$$\frac{1}{A+B} = \frac{2}{\pi}\int_0^\infty \frac{AB}{(A^2+\nu^2)(B^2+\nu^2)}\,\mathrm{d}\nu. \tag{4.3.8}$$

It is valid for positive A and B, and can be established by a simple contour integration. Applying this formula to the energy denominator in eqn (4.3.1), which we write as $\hbar(\omega_m^A + \omega_n^B)$, we get

$$U_{\mathrm{disp}}^{(6)} = -\frac{2\hbar}{\pi}T_{\alpha\beta}T_{\gamma\delta} \times \int_0^\infty {\sum_m}' \frac{\langle 0_A|\hat{\mu}_\alpha^A|m_A\rangle\langle m_A|\hat{\mu}_\gamma^A|0_A\rangle\omega_m^A}{\hbar((\omega_m^A)^2+\nu^2)} {\sum_n}' \frac{\omega_n^B\langle 0_B|\hat{\mu}_\beta^B|n_B\rangle\langle n_B|\hat{\mu}_\delta^B|0_B\rangle}{\hbar((\omega_n^B)^2+\nu^2)}\,\mathrm{d}\nu. \tag{4.3.9}$$

We can recognize here the polarizabilities of A and B at the imaginary frequency iν (see eqn (2.5.11)), so that the dispersion energy becomes

$$U_{\mathrm{disp}}^{(6)} = -\frac{\hbar}{2\pi}T_{\alpha\beta}T_{\gamma\delta}\int_0^\infty \alpha_{\alpha\gamma}^A(\mathrm{i}\nu)\alpha_{\beta\delta}^B(\mathrm{i}\nu)\,\mathrm{d}\nu, \tag{4.3.10}$$

where $\alpha_{\alpha\gamma}^A(\mathrm{i}\nu)$ and $\alpha_{\beta\delta}^B(\mathrm{i}\nu)$ are polarizability components at imaginary frequency. For spherical atoms, eqn (4.3.10) reduces in the same way as before to give

$$\overline{U}_{\mathrm{disp}}^{(6)} = -\frac{3\hbar}{(4\pi\epsilon_0)^2\pi R^6}\int_0^\infty \overline{\alpha}^A(\mathrm{i}\nu)\overline{\alpha}^B(\mathrm{i}\nu)\,\mathrm{d}\nu. \tag{4.3.11}$$

While the concept of 'polarizability at imaginary frequency' is physically rather bizarre, its mathematical properties are much more civilized than those of the polarizability at real frequencies, as we saw in §2.5: $\alpha_{\alpha\gamma}^A(\mathrm{i}\nu)$ decreases monotonically from the static polarizability when $\nu = 0$, to zero as $\nu \to \infty$. This means that it can be determined quite accurately as a function of frequency, either by *ab initio* computation or from experimental data. In the case of *ab initio* computation, the values of $\alpha_{\alpha\gamma}^A(\mathrm{i}\nu)$ and $\alpha_{\beta\delta}^B(\mathrm{i}\nu)$ are computed at a number of suitable values of ν, and the integral (4.3.10) is evaluated by numerical quadrature. Because the polarizability at imaginary frequency is mathematically well-behaved, the quadrature gives accurate results using a modest number of integration points—typically a dozen or so.

The polarizabilities themselves are unfortunately more difficult to calculate accurately; the calculations require large basis sets in order that the distortion due to the applied field can

be represented accurately. We return to this issue in §5.5. The earliest good calculations of dispersion energies by this method are probably those of Wormer and his colleagues (Rijks and Wormer 1989, Thakkar *et al.* 1992, Wormer and Hettema 1992). More recently, density functional theory has emerged as a surprisingly good source of accurate polarizabilities (Van Caillie and Amos 1998, 2000), though with some limitations—it doesn't handle large conjugated molecules very well, because normal exchange–correlation potentials don't respond appropriately to the external electric field (Champagne *et al.* 1998, van Gisbergen *et al.* 1999).

The important feature of this treatment is that, except for a simple one-dimensional quadrature, the expressions for the dispersion energy coefficients reduce to products of individual-molecule properties. These need only be calculated once, and the resulting dispersion coefficients do not depend on the intermolecular geometry.

Another commonly used formulation of the dispersion interaction is the Slater–Kirkwood formula, which gives the C_6 coefficient for the interaction between atoms A and B as

$$\frac{C_6^{AB}}{E_\mathrm{h} a_0^6} = \frac{3}{2}\frac{\tilde{\alpha}^A \tilde{\alpha}^B}{(\tilde{\alpha}^A/N_A)^{1/2} + (\tilde{\alpha}^B/N_B)^{1/2}}. \tag{4.3.12}$$

Here $\tilde{\alpha} = \alpha/(4\pi\epsilon_0 a_0^3)$, i.e., the numerical value of the polarizability in atomic units, and N_A is an effective number of valence electrons in atom A. E_h is the Hartree energy $e^2/4\pi\epsilon_0 a_0$.

Slater and Kirkwood (1931) obtained this formula by an approximate variational argument, but Mavroyannis and Stephen (1962) showed that it could be obtained from the exact expression (4.3.11) if the polarizability at imaginary frequency is approximated by the simple analytical form

$$\alpha(\mathrm{i}\nu) = \frac{4\pi\epsilon_0 A}{\nu_0^2 + \nu^2}. \tag{4.3.13}$$

For this to work at zero frequency, we need $A/\nu_0^2 = \alpha(0)/4\pi\epsilon_0$, while in the high-imaginary-frequency limit we can use the Thomas–Reiche–Kuhn sum rule (p. 243) to express A as $N^A {E_\mathrm{h}}^2 a_0^3/\hbar^2$, where N_A is now the total number of electrons in atom A. In practice the value of N_A obtained by working back from $\tilde{\alpha}$ and C_6 is usually rather smaller than the number of valence electrons. (Pitzer (1959) reported much higher values, but he was using estimates of the C_6 coefficients that were higher than modern values.) If we compare eqn (4.3.13) with (2.5.11), in fact, we can see that the Slater–Kirkwood formula is equivalent to the assumption that all the important optical transitions occur near frequency ν_0, or in other words that it is just another form of the Unsöld approximation.

If the dispersion coefficient C_6 is known for the $A\cdots A$ and $B\cdots B$ interactions, a value can be estimated for the $A\cdots B$ interaction using various combining rules. The simplest such rule is the geometric mean rule, $C_6^{AB} = [C_6^{AA} C_6^{BB}]^{1/2}$, which can be justified using eqn (4.3.6) if one assumes that $U_A \approx U_B$. If the static polarizabilities are known as well as the homogeneous dispersion coefficients, an alternative approach is to use these values in the Slater–Kirkwood formula to obtain N_A, which is $N_A = (\frac{4}{3} C_6^{AA})^2/(\alpha^A)^3$ if C_6 and α are expressed in atomic units. Then the mixed C_6 coefficient is

$$C_6^{AB} = \frac{2\alpha^A \alpha^B C_6^{AA} C_6^{BB}}{(\alpha^A)^2 C_6^{BB} + (\alpha^B)^2 C_6^{AA}}. \tag{4.3.14}$$

Tang (1969) derived this formula using a variation of Mavroyannis and Stephen's approach.

4.3.3 Non-expanded dispersion energy

As in the case of the induction energy, it is not necessary to use the multipole expansion in deriving the dispersion energy expression. The elementary perturbation is the electrostatic interaction between an element of charge density at $\mathbf{r}_a$ in molecule A and another at $\mathbf{r}_b$ in molecule B:

$$\hat{V} = \frac{\hat{\rho}^A(\mathbf{r}_a)\hat{\rho}^B(\mathbf{r}_b)}{|\mathbf{r}_a - \mathbf{r}_b|}\,\mathrm{d}^3\mathbf{r}_a\,\mathrm{d}^3\mathbf{r}_b. \tag{4.3.15}$$

For the moment, we drop the volume elements, but we shall need to put them back at the end and integrate over the two molecules. The second-order energy, including only the terms in which both molecules are excited, is

$$-\sum_{m_A\neq 0}\sum_{n_B\neq 0}\frac{\langle 0_A 0_B|\hat{\rho}^A(\mathbf{r}_a)\hat{\rho}^B(\mathbf{r}_b)|m_A n_B\rangle\langle m_A n_B|\hat{\rho}^A(\mathbf{r}'_a)\hat{\rho}^B(\mathbf{r}'_b)|0_A 0_B\rangle}{(W^A_{m0}+W^B_{n0})|\mathbf{r}_a-\mathbf{r}_b||\mathbf{r}'_a-\mathbf{r}'_b|}. \tag{4.3.16}$$

On applying eqn (4.3.8) to the energy denominator as before, this becomes

$$\begin{aligned}&-\frac{2\hbar}{\pi}\frac{1}{|\mathbf{r}_a-\mathbf{r}_b||\mathbf{r}'_a-\mathbf{r}'_b|}\\ &\times\int_0^\infty {\sum_m}'\frac{\langle 0_A|\hat{\rho}^A(\mathbf{r}_a)|m_A\rangle\langle m_A|\hat{\rho}^A(\mathbf{r}'_a)|0_A\rangle\omega^A_m}{\hbar((\omega^A_m)^2+v^2)}{\sum_n}'\frac{\omega^B_n\langle 0_B|\hat{\rho}^B(\mathbf{r}_b)|n_B\rangle\langle n_B|\rho^B(\mathbf{r}'_b)|0_B\rangle}{\hbar((\omega^B_n)^2+v^2)}\,\mathrm{d}v.\end{aligned} \tag{4.3.17}$$

We recognize in the two sum-over-states factors the frequency-dependent charge density susceptibilities of A and B (compare eqn (2.5.12)), so that when we integrate over the positions of the interacting charge elements the dispersion energy becomes

$$U_{\mathrm{disp}} = -\frac{\hbar}{2\pi}\iint\frac{\alpha(\mathbf{r}_a,\mathbf{r}'_a;\mathrm{i}v)\alpha(\mathbf{r}_b,\mathbf{r}'_b;\mathrm{i}v)}{|\mathbf{r}_a-\mathbf{r}_b||\mathbf{r}'_a-\mathbf{r}'_b|}\,\mathrm{d}^3\mathbf{r}_a\,\mathrm{d}^3\mathbf{r}'_a\,\mathrm{d}^3\mathbf{r}_b\,\mathrm{d}^3\mathbf{r}'_b\,\mathrm{d}v. \tag{4.3.18}$$

This expression is exact, within the long-range approximation, and can be used to evaluate the dispersion energy between two molecules that are too close together for the multipole expansion to converge. Although it involves a quadruple integration over position, that can be carried out quite efficiently, though not efficiently enough for use on the fly in a simulation.

4.3.4 Spherical tensor formulation

Eqn (4.3.11) gives the orientational average of the R^{-6} term in the dispersion energy, but the method can be used just as easily to obtain the higher-rank terms and to describe the orientation dependence.

If we use the full spherical-tensor form of the interaction Hamiltonian, we obtain, instead of eqn (4.3.1), the expression

$$U_{\mathrm{disp}} = -\sum_{m_A\neq 0}\sum_{n_B\neq 0}\frac{\langle 0_A 0_B|\hat{Q}^A_t T^{AB}_{tu}\hat{Q}^B_u|m_A n_B\rangle\langle m_A n_B|\hat{Q}^A_{t'}T^{AB}_{t'u'}\hat{Q}^B_{u'}|0_A 0_B\rangle}{W^A_{m0}+W^B_{n0}} \tag{4.3.19}$$

(where there is an implied summation over the repeated spherical-tensor suffixes t, t', u and u') and by applying the McLachlan identity (4.3.8) exactly as before, we obtain, instead of (4.3.9),

$$U_{\rm disp} = -\frac{2\hbar}{\pi} T^{AB}_{tu} T^{AB}_{t'u'} \times \\ \times \int_0^\infty {\sum_m}' \frac{\langle 0_A|\hat{Q}^A_t|m_A\rangle\langle m_A|\hat{Q}^A_{t'}|0_A\rangle\omega^A_m}{\hbar((\omega^A_m)^2+v^2)} {\sum_n}' \frac{\omega^B_n\langle 0_B|\hat{Q}^B_u|n_B\rangle\langle n_B|\hat{Q}^B_{u'}|0_B\rangle}{\hbar((\omega^B_n)^2+v^2)}\ {\rm d}v, \tag{4.3.20}$$

and as before we identify components of the polarizability at imaginary frequency to obtain, instead of (4.3.10), the general form

$$U_{\rm disp} = -\frac{\hbar}{2\pi} T^{AB}_{tu} T^{AB}_{t'u'} \int_0^\infty \alpha^A_{tt'}({\rm i}v)\alpha^B_{uu'}({\rm i}v)\ {\rm d}v. \tag{4.3.21}$$

Remember that there is still a sum over t, t', u and u'.

When t, t', u and u' describe dipole components $10 = z$, $11c = x$ or $11s = y$, we have the dipole–dipole contribution to the dispersion energy, almost as before. There is a subtle but important difference: the components $\alpha^A_{tt'}$ and $\alpha^B_{uu'}$ are referred to *molecular* axes, so that the orientation dependence in (4.3.21) is all in the T^{AB}_{tu} and $T^{AB}_{t'u'}$, whereas $\alpha^A_{\alpha\gamma}$ and $\alpha^B_{\beta\delta}$ in eqn (4.3.10) are referred to *global* axes.

If t describes a quadrupole component and the rest are dipole components, then $\alpha^A_{tt'}$ becomes a quadrupole–dipole polarizability. In this case T^{AB}_{tu} is a quadrupole–dipole interaction function, proportional to R^{-4}, while $T^{AB}_{t'u'}$ is a dipole–dipole function as before, proportional to R^{-3}. Accordingly we now have a dispersion term proportional to R^{-7}. There are other R^{-7} terms involving dipole–quadrupole polarizabilities on B. If A and B are atoms or centrosymmetric molecules, these dipole–quadrupole polarizabilities are zero, so there is no R^{-7} term in the dispersion interaction in such cases. Even for non-centrosymmetric molecules, the coefficient C_7 of the R^{-7} term depends on the relative orientation of the molecules, and its average over orientations is zero, if all orientations have equal weight.

The next term, in R^{-8}, involves a quadrupole–quadrupole polarizability on one molecule and a dipole–dipole polarizability on the other, and this is non-zero for atoms as well as molecules. For non-centrosymmetric molecules there can also be an R^{-8} contribution from dipole–quadrupole polarizabilities on both A and B. The R^{-9} term is zero for atoms, like the R^{-7} term, because all the polarizabilities that might contribute to it are zero, so the next term for atoms is the R^{-10} term. Here there are two kinds of contribution, one involving a quadrupole–quadrupole polarizability on both atoms, and the other a dipole–dipole polarizability on one and an octopole–octopole polarizability on the other.

For a general formulation in spherical-tensor form, it is more convenient to use the recoupled polarizabilities, defined in eqn (2.3.15). Also the product of interaction functions $T^{AB}_{tu}T^{AB}_{t'u'}$ contains a product of $\overline{S}$ functions, which can be re-expressed in terms of single S functions and some Wigner $3j$ and $9j$ symbols (Stone 1978*a*). The dispersion energy then takes the form (Williams 2004)

$$U_{\rm disp} = -\sum_{l_A l'_A l_b l'_B} \sum_{L_A L_B J K_A K_B} \overline{C}_n(L_A L_B J; K_A K_B) R^{-n} S^{K_A K_B}_{L_A L_B J}, \tag{4.3.22}$$

where

$$\overline{C}_n(L_AL_BJ;K_AK_B) = \sum_{l_A,l'_A,l_B,l'_B} \mathrm{i}^{L_A-L_B-J}(-1)^{l_A+l'_A}[(2L_A+1)(2L_B+1)]^{1/2}(2J+1)$$
$$\times \begin{pmatrix} l_A+l_B \\ l_A \end{pmatrix}\begin{pmatrix} l'_A+l'_B \\ l'_A \end{pmatrix}\begin{pmatrix} l_A+l_B & l'_A+l'_B & J \\ 0 & 0 & 0 \end{pmatrix}\begin{pmatrix} l_A & l_B & l_A+l_B \\ 0 & 0 & 0 \end{pmatrix}^{-1}\begin{pmatrix} l'_A & l'_B & l'_A+l'_B \\ 0 & 0 & 0 \end{pmatrix}^{-1}$$
$$\times \begin{Bmatrix} l_A & l'_A & L_A \\ l_B & l'_B & L_B \\ l_A+l_B & l'_A+l'_B & J \end{Bmatrix} \frac{\hbar}{2\pi(4\pi\epsilon_0)^2}\int_0^\infty \alpha^A_{L_AK_A(l_Al'_A)}(\mathrm{i}v)\alpha^B_{L_BK_B(l_Bl'_B)}(\mathrm{i}v)\,\mathrm{d}v. \quad (4.3.23)$$

The sum is restricted by the requirement that $l_A + l'_A + l_B + l'_B + 2 = n$, and by the triangle conditions (l_A, l'_A, L_A) and (l_B, l'_B, L_B). The entire coefficient is zero unless the triangle condition (L_A, L_B, J) is satisfied.

The expression (4.3.22) is given in terms of S functions, not the renormalized $\overline{S}$ functions. Recall from eqns (3.3.7) and (3.3.8) that

$$\overline{S}^{k_1k_2}_{l_1\,l_2\,j} = \begin{pmatrix} l_1 & l_2 & j \\ 0 & 0 & 0 \end{pmatrix}^{-1} S^{k_1k_2}_{l_1\,l_2\,j}. \quad (4.3.24)$$

When $l_1 + l_2 + j$ is odd, the $3j$ symbol vanishes and the $\overline{S}^{k_1k_2}_{l_1\,l_2\,j}$ functions cannot be defined. The sum in eqn (4.3.22) does include some terms for which $L_A + L_B + J$ is odd. However, they are often small, and if they can be omitted, we can define

$$C_n(L_AL_BJ;K_AK_B) = \begin{pmatrix} L_A & L_B & J \\ 0 & 0 & 0 \end{pmatrix}\overline{C}_n(L_AL_BJ;K_AK_B), \quad (4.3.25)$$

and write eqn (4.3.22) with C and $\overline{S}$ instead of $\overline{C}$ and S.

For linear molecules and symmetric tops the only non-zero recoupled dipole–dipole polarizabilities are $\alpha_{00(11)}$ and $\alpha_{20(11)}$, and the isotropic and anisotropic dispersion coefficients are

$$C_6 = C_6(000;00) = \frac{3\hbar}{\pi(4\pi\epsilon_0)^2}\int_0^\infty \overline{\alpha}^A(\mathrm{i}v)\overline{\alpha}^B(\mathrm{i}v)\,\mathrm{d}v, \quad (4.3.26)$$
$$\gamma_{202}C_6 = C_6(202;00) = \frac{\hbar}{\pi(4\pi\epsilon_0)^2}\int_0^\infty \Delta\alpha^A(\mathrm{i}v)\overline{\alpha}^B(\mathrm{i}v)\,\mathrm{d}v, \quad (4.3.27)$$
$$\gamma_{022}C_6 = C_6(022;00) = \frac{\hbar}{\pi(4\pi\epsilon_0)^2}\int_0^\infty \overline{\alpha}^A(\mathrm{i}v)\Delta\alpha^B(\mathrm{i}v)\,\mathrm{d}v, \quad (4.3.28)$$
$$\gamma_{220}C_6 = C_6(220;00) = \tfrac{1}{15}\gamma_{22}C_6,$$
$$\gamma_{222}C_6 = C_6(222;00) = \tfrac{2}{21}\gamma_{22}C_6,$$
$$\gamma_{224}C_6 = C_6(224;00) = \tfrac{36}{35}\gamma_{22}C_6,$$

with

$$\gamma_{22}C_6 = \frac{\hbar}{\pi(4\pi\epsilon_0)^2}\int_0^\infty \Delta\alpha^A(\mathrm{i}v)\Delta\alpha^B(\mathrm{i}v)\,\mathrm{d}v. \quad (4.3.29)$$

As usual, $\overline{\alpha} = \frac{1}{3}(\alpha_\parallel + 2\alpha_\perp)$ and $\Delta\alpha = \alpha_\parallel - \alpha_\perp$. The γ notation defined implicitly in eqns (4.3.26–4.3.29) is sometimes used to describe the magnitude of the anisotropy relative to the isotropic term.

The complete R^{-6} dispersion interaction in this case takes the form (Stone and Tough 1984)

$$\begin{aligned} U^6_{\text{disp}} = -\frac{C_6}{R^6}\{1 &+ \gamma_{202}(\tfrac{3}{2}\cos^2\theta_A - \tfrac{1}{2}) + \gamma_{022}(\tfrac{3}{2}\cos^2\theta_B - \tfrac{1}{2}) \\ &+ \gamma_{22}\cdot\tfrac{1}{2}[(2\cos\theta_A\cos\theta_B - \sin\theta_A\sin\theta_B\cos\varphi)^2 \\ &- \cos^2\theta_A - \cos^2\theta_B]\}, \end{aligned} \tag{4.3.30}$$

where the angles θ_A, θ_B and φ are defined as in §3.2.

In fact it is apparent from eqn (4.3.23) that the coefficients of the integrals in the sum are independent of the values of K_A and K_B. In the general case, therefore, the formulae for the C_6 coefficients are very similar to eqn (4.3.29):

$$\begin{aligned} C_6^{AB}(000;00) &= 2W\int_0^\infty \alpha^A_{00(11)}(\mathrm{i}\nu)\alpha^B_{00(11)}(\mathrm{i}\nu)\,\mathrm{d}\nu, \\ C_6^{AB}(022;0K_B) &= -\sqrt{2}W\int_0^\infty \alpha^A_{00(11)}(\mathrm{i}\nu)\alpha^B_{2K_B(11)}(\mathrm{i}\nu)\,\mathrm{d}\nu, \\ C_6^{AB}(220;K_AK_B) &= \frac{1}{5}W\int_0^\infty \alpha^A_{2K_A(11)}(\mathrm{i}\nu)\alpha^B_{2K_B(11)}(\mathrm{i}\nu)\,\mathrm{d}\nu, \\ C_6^{AB}(222;K_AK_B) &= \frac{2}{7}W\int_0^\infty \alpha^A_{2K_A(11)}(\mathrm{i}\nu)\alpha^B_{2K_B(11)}(\mathrm{i}\nu)\,\mathrm{d}\nu, \\ C_6^{AB}(224;K_AK_B) &= \frac{108}{35}W\int_0^\infty \alpha^A_{2K_A(11)}(\mathrm{i}\nu)\alpha^B_{2K_B(11)}(\mathrm{i}\nu)\,\mathrm{d}\nu, \end{aligned} \tag{4.3.31}$$

where $W = \hbar/(2\pi(4\pi\epsilon_0)^2)$.

4.3.5 Numerical values

The numerical value of the dispersion coefficient C_6 increases sharply with molecular size—roughly as the square of the polarizability, as the London formula shows. Some values obtained by Meath and his collaborators using dipole oscillator strength distributions (see Chapter 13) are shown for illustration in Table 4.1. These are in atomic units and are believed to be accurate to about 1%. The atomic unit for the C_6 coefficient is $E_\mathrm{h}a_0^6 = e^2a_0^5/4\pi\epsilon_0$, but a variety of other units is in use, commonly (energy unit) $\times$ Å^6.

The London formula shows that for interactions between unlike molecules, the combining rule $C_6^{AB} \approx (C_6^{AA}C_6^{BB})^{1/2}$ should be quite reliable. For Ar···Xe, for instance, the combining rule gives 135.6 a.u., and for CO···He it gives 10.9 a.u. These numbers are quite close to the accurate values in Table 4.1. Similarly, the combining rule works very well for acetylene and benzene. Where the average excitation energy U is very different for the two molecules, it is likely to be less accurate; thus the combining rule gives $C_6 = 17.26$ a.u. for He···HCCH, whereas the accurate value is 16.50 a.u. In all these cases the Tang formula, eqn (4.3.14), gives rather better values: 134.1 a.u. for Ar···Xe, 10.55 a.u. for CO···He and 16.17 a.u. for He···HCCH, calculated using the static polarizabilities listed by Gray and Gubbins (1984).

The higher dispersion coefficients C_8, C_{10}, etc., may be calculated in much the same way as C_6. If the London approach is used, the result for the isotropically averaged C_8 is

Table 4.1 Some values of dispersion coefficients.

	C_6/ a.u.	C_8/ a.u.	C_{10}/ a.u.
He···He	1.46	13.9	182
Ne···Ne	6.6	57	700
Ar···Ar	64.3	1130	25000
Kr···Kr	133	2500	60000
Xe···Xe	286		
CO···CO	81.4		
SO_2···SO_2	294		
CS_2···CS_2	871		
HCCH···HCCH	204.1		
C_6H_6···C_6H_6	1723		
He···CO	10.7		
Ar···Xe	134.5		
He···HCCH	16.50		
HCCH···C_6H_6	593.0		

$$C_8 = \frac{15U_AU_B(\overline{\alpha}^A\overline{\alpha}_2^B + \overline{\alpha}_2^A\overline{\alpha}^B)}{8(4\pi\epsilon_0)^2(U_A + U_B)},$$

where $\overline{\alpha}_2^A$ and $\overline{\alpha}_2^B$ are the average quadrupole–quadrupole polarizabilities, $\frac{1}{5}\sum_\kappa \alpha_{2\kappa,2\kappa}$. If the same values of U_A and U_B are appropriate here as for C_6, the ratio $C_8/C_6 \approx 5\overline{\alpha}_2/2\overline{\alpha}$. Some numerical values are given in Table 4.1. For Ar, for instance, the ratio $C_8/C_6 = 17.6$, so the C_8/R^8 term becomes equal to C_6/R^6 when $R \approx 4.2\,a_0$. The equilibrium separation R_m for pairs of Ar atoms is $7.1\,a_0$, and at this distance the R^{-8} term is about one third the size of the R^{-6} term, while the R^{-10} term is about a factor of three smaller again. These contributions are by no means insignificant, and have to be included in accurate calculations. However, they are reduced by damping effects, which will be discussed in Chapter 8. If higher values are required, an approximate recursion formula can be used (Tang and Toennies 1978):

$$C_{2n+6} = \left(\frac{C_{2n+4}}{C_{2n+2}}\right)^3 C_{2n}.$$

Thakkar (1988) found that this formula gave values within a few per cent of the accurate values for H atoms.

5
Ab Initio Methods

5.1 Introduction

The term '*ab initio*' is used to describe methods that seek to calculate molecular properties from the beginning, that is, by solving Schrödinger's equation without using any empirical data. Although it is always necessary to make approximations, it may be possible to organize them in such a way that the accuracy of the calculation can be systematically improved, up to the limit allowed by available computing resources.

We shall not attempt to review the principles of *ab initio* methods, but the reader will need to know something of these principles to understand the issues that arise, some of which are quite technical. We give an outline here of the points that affect the calculations of intermolecular forces; for fuller accounts, see for example the books by Szabo and Ostlund (1989), Jensen (1999) and Helgaker *et al.* (2000).

First, we note that the Born–Oppenheimer approximation is used almost universally. That is, the behaviour of the electrons is studied as if the nuclei were clamped in a given geometry. Solving the Schrödinger equation for the electrons then provides the electronic energy for that geometry, together with a wavefunction from which we can calculate properties such as the molecular multipole moments. The energy and the other properties are functions of the nuclear coordinates; in particular, we speak of the 'potential energy surface', which is the electronic energy as a function of nuclear coordinates. This is the potential energy term in the Schrödinger equation describing the nuclear motion. This separation of electronic and nuclear motion is a very good approximation except where there are near-degeneracies or crossings of electronic states.

Secondly, all standard *ab initio* programs ignore relativistic effects of all kinds. The neglect of relativistic effects (principally spin–orbit coupling) is usually a good approximation for calculations on molecules containing only light atoms, especially for closed-shell states. In the cases where it is important, it can be taken into account by perturbation theory.

Ab initio methods are used in the calculation of intermolecular forces in several ways. We have seen that forces at long range depend on molecular properties—multipole moments and polarizabilities—so we need accurate values of these quantities. Alternatively, we might seek the interaction energy as the difference of the energies of the interacting system and the separate molecules, all calculated *ab initio*. This is the so-called 'supermolecule method'. Finally, we can use perturbation theory for systems at distances where the long-range theory becomes invalid because the molecules overlap. In this case, it is no longer possible to write down analytical formulae for the energy, and *ab initio* methods have to be used to evaluate the energy terms. Perturbation methods of this sort are discussed in Chapter 6.

5.2 Electron correlation

The workhorse of *ab initio* calculation is the self-consistent field (SCF) procedure, but this is an independent-electron model—the electrons are treated as if they move in an average field due to the other electrons, and no account is taken of the effect of the electron repulsion in keeping electrons apart. The motion of the electrons is said to be *uncorrelated.* The simplest example of the consequences is the H_2 molecule: in an SCF calculation each electron has probability $\frac{1}{2}$ of being on either atom, so there is a probability $\frac{1}{2} \times \frac{1}{2}$ that they are both on one particular atom. This is true for any internuclear distance, so we are led to conclude that the dissociation products are $H^+\cdots H^-$ and $H^-\cdots H^+$ with probability $\frac{1}{4}$ each, and $H\cdots H$ with probability $\frac{1}{2}$. In the real molecule, the electrons repel each other, so the ionic configurations, in which both electrons are on the same atom, are less probable than this at all distances, and their probability tends to zero as the atoms separate.

Effects such as this are said to be due to *electron correlation.* A satisfactory *ab initio* calculation of intermolecular interactions has to include the effects of electron correlation in one way or another. One of the most important of these is the dispersion interaction, which is wholly a correlation effect, as we saw in §4.3, and is absent from any SCF calculation. The *correlation energy* is defined as the difference between the *Hartree–Fock energy*, i.e. the SCF energy in the limit of an infinite basis set, and the exact energy excluding relativistic effects.

5.2.1 Configuration interaction

The correlation energy can be calculated in many ways, all of them expensive in computer time. This is not the place for a detailed account of all the available methods, but it is necessary to understand the basic principles of some of them. See Helgaker *et al.* (2000) for a very full discussion. The oldest method is 'configuration interaction' (CI), so called because the dominant SCF determinant, or 'root configuration', is allowed to mix with other configurations in which the electrons are assigned to different orbitals. Again, the H_2 molecule provides the simplest example. The SCF wavefunction (ignoring spin) takes the form

$$\begin{aligned}\psi^{\mathrm{SCF}} &= \tfrac{1}{2}[s_A(1) + s_B(1)][s_A(2) + s_B(2)] \\ &= \tfrac{1}{2}[s_A(1)s_A(2) + s_A(1)s_B(2) + s_B(1)s_A(2) + s_B(1)s_B(2)],\end{aligned}$$

in which we see the coefficient $\frac{1}{2}$ for the ionic functions $s_A(1)s_A(2)$ and $s_B(1)s_B(2)$ (probability $(\frac{1}{2})^2 = \frac{1}{4}$). The functions s_A and s_B are atomic orbitals; in an accurate SCF treatment they would not be pure hydrogen $1s$ orbitals but would be modified by bond formation. In the CI method this state is mixed with others, in particular with the configuration σ_u^2 in which both electrons are in the σ_u orbital: $\frac{1}{2}[s_A(1) - s_B(1)][s_A(2) - s_B(2)]$. If we subtract a multiple of this from the original σ_g^2 configuration we get

$$\begin{aligned}\psi^{\mathrm{CI}} &= \sigma_g^2 - \lambda\sigma_u^2 \\ &= \tfrac{1}{2}(1-\lambda)s_A(1)s_A(2) + \tfrac{1}{2}(1+\lambda)s_A(1)s_B(2) \\ &\quad + \tfrac{1}{2}(1+\lambda)s_B(1)s_A(2) + \tfrac{1}{2}(1-\lambda)s_B(1)s_B(2),\end{aligned}$$

so for positive λ the weight of the ionic terms is reduced. λ is a variational parameter which can be chosen to minimize the energy.* Its optimum value depends on the internuclear distance, and at large separations $\lambda \to 1$, so that the ionic terms disappear altogether. This type of correlation, arising from the contamination of the SCF ground state by excited states, is called non-dynamical or long-range correlation. There is also dynamical correlation, which describes the short-range effect of electron repulsion in keeping electrons from approaching each other too closely.

It can be shown that singly excited configurations alone do not introduce any electron correlation, though they can improve the wavefunction in conjunction with more highly excited configurations. Doubly excited configurations are the most important; higher excitations have a significant effect but their inclusion is very expensive. Accordingly the standard method of this type is configuration interaction with single and double excitations, or CISD. Usually the SCF calculation provides a well-defined reference configuration from which the excitations are constructed, but sometimes it is necessary to consider several reference configurations and excited states constructed from them (multireference CI or MRCI), or to treat several configurations on an equal basis in the SCF calculation: a complete active space or CASSCF treatment. See Jensen (1999) or Helgaker *et al.* (2000) for details.

5.2.2 Many-body perturbation theory

CISD is a variational method: the coefficients of the excited configurations are determined variationally, i.e., by minimizing the energy. Many-body perturbation theory (MBPT), in contrast, treats the electron repulsion, or more precisely the difference between the electron repulsion and the average of it that appears in the SCF method, as a perturbation. Methods of this type include Møller–Plesset perturbation theory (MPn for perturbation theory to order n). The zeroth-order Hamiltonian is the Fock operator $\mathcal{F}$, and the perturbation is $\mathcal{H} - \mathcal{F}$. The zeroth-order wavefunction for a closed-shell system is the SCF Slater determinant, and the zeroth-order energy is the sum of the occupied orbital energies. The energy to first order is the expectation value of the full Hamiltonian for the SCF wavefunction, i.e., the SCF energy. Correlation corrections appear at second order and beyond. The MP2 method, for example, gives a correction to the energy that is a sum over all doubly excited configurations:

$$\Delta E_{\mathrm{MP2}} = -\frac{1}{4}\sum_{ijab}\frac{\big((ia|jb) - (ib|ja)\big)^2}{\epsilon_a + \epsilon_b - \epsilon_i - \epsilon_j}, \tag{5.2.1}$$

where the sum runs over occupied spin-orbitals φ_i and φ_j and virtuals φ_a and φ_b. The ϵ_i etc. are the SCF orbital energies, and $(ia|jb)$ is the electron repulsion integral

$$(ia|jb) = \int \varphi_i(\mathbf{r}_1)\varphi_a(\mathbf{r}_1)\frac{1}{r_{12}}\varphi_j(\mathbf{r}_2)\varphi_b(\mathbf{r}_2)\,\mathrm{d}^3\mathbf{r}_1\,\mathrm{d}^3\mathbf{r}_2. \tag{5.2.2}$$

Typically MP2 yields some 80% or so of the correlation energy at near-equilibrium geometries. In the MP3 method the perturbation expansion is taken to third order, in MP4 to fourth

*At first sight it may be difficult to understand how the energy can be lowered by mixing excited states into the wavefunction. There is no difficulty if one understands that the original wavefunction is contaminated by contributions from excited states. The purpose of the CI procedure is to cancel out these contaminating terms.

order, and so on. However, these higher members of the series become rapidly more expensive: the cost of an MP2 calculation scales roughly as the 5th power of the size N of the system (measured as the number of electrons or the number of basis functions), while MP3 scales as N^6 and MP4 as N^7. Moreover the MPn series can be shown to diverge in some cases (Christiansen *et al.* 1996, Olsen *et al.* 1996), so it is unusual nowadays to take the series beyond MP2.

5.2.3 Coupled-cluster theory

The other main class of correlation treatment is the coupled-cluster (CC) scheme (Čižek and Paldus 1980, Bartlett 2010). In the CCSD treatment the correlated wavefunction can be written as $\exp(\hat{T}_1 + \hat{T}_2)\Psi_0$, where Ψ_0 is the SCF wavefunction and $\hat{T}_1$ and $\hat{T}_2$ are operators that transform Ψ_0 into a linear combination of singly excited and doubly excited configurations respectively. The first terms in the expansion of the exponential, $1 + \hat{T}_1 + \hat{T}_2$, give the CISD form of wavefunction, though the coefficients of the terms in the expansion would be different. A commonly used variant incorporates a perturbation-theory estimate of the effect of triple excitations; this is the CCSD(T) method. The effect of triple excitations can be considerable. These again are expensive methods, scaling as N^6 for CCSD and N^7 for CCSD(T), but they are capable of very high accuracy for small systems. The calculations of Patkowski *et al.* (2005) on the potential energy of the argon dimer are almost certainly more accurate than the best experimental data for this very extensively studied system.

5.2.4 Explicitly correlated methods

Unfortunately, while the computation time scales as N^6 or worse, the errors in correlation energy scale as N^{-1} (Helgaker *et al.* 1997), so the improvement in accuracy with increasing basis set size is extremely slow. The reason for this is that conventional basis sets are continuous everywhere, while the true wavefunction has cusps where any electron–electron distance is zero (Kato 1957, Klopper *et al.* 2006):

$$\left\langle \frac{\partial \Psi}{\partial r_{12}} \right\rangle \rightarrow \tfrac{1}{2}\Psi \quad \text{as} \quad r_{12} \rightarrow 0, \tag{5.2.3}$$

where the angle brackets denote spherical averaging around $r_{12} = 0$. To take account of this requirement, the wavefunction needs to vary linearly with r_{ij} near $r_{ij} = 0$. This has been understood since the early days of quantum mechanics—Hylleraas (1929) used a wavefunction of this form to describe the helium atom—but its application to larger molecules was inhibited for a long time by the difficulty of evaluating and handling the three-electron and four-electron integrals that arise. Kutzelnigg (1985) showed how these integrals can be expressed in terms of new two-electron integrals in addition to the electron repulsion integrals of eqn (5.2.2), and following this insight considerable progress has been made in developing 'r_{12} methods' (Klopper *et al.* 2006). At the time of writing it is an active and promising field of research (Neiss and Hättig 2007, Knizia *et al.* 2009, Yang and Hättig 2009, 2010), and it should soon be possible to use this approach routinely to calculate intermolecular interaction energies, but additional classes of difficult integrals are needed for molecular properties.

5.3 Density functional theory

Density functional theory (DFT) has become a very popular method for the calculation of energies and other properties of molecules (Chapter 6 of Jensen 1999, Sholl and Steckel 2009). It is based on a theorem due to Hohenberg and Kohn (1964), which states that a knowledge of the electron density of a system in its ground state is enough to determine the energy: 'the energy is a functional of the density'. An informal understanding of the theorem was provided by Wilson (1968), who remarked that the exact density has cusps only at the positions of the nuclei, and the gradient of the density at the cusp depends on the nuclear charge. Moreover the integral of the density over all space gives the number of electrons. A knowledge of the density therefore allows one to write down the Hamiltonian, from which everything can be determined. This also illustrates that although the theorem is rigorous, it does not in itself provide a practical way to calculate the energy from a given density. If the exact form of the energy functional were known, DFT would be an *ab initio* method, but in practice it is necessary to approximate it, often by fitting to experimental data, and in this form it should properly be regarded as an empirical procedure. An outline of the theory is given here, in order to introduce those aspects that are particularly relevant to the calculation of intermolecular interactions. A much more detailed account is given by Koch and Holthausen (2000).

Formally, the energy of the system is a functional of the density:

$$\begin{aligned} E[\rho] &= V_{ne}[\rho] + T[\rho] + V_{ee}[\rho] \\ &= \int \rho(\mathbf{r}) v(\mathbf{r})\, \mathrm{d}^3\mathbf{r} + T[\rho] + V_{ee}[\rho]. \end{aligned} \tag{5.3.1}$$

(While a *function* is a mapping from a number or set of numbers onto another number, a *functional* is a mapping from a function, in this case the electron density, onto a number. It is usual to use square brackets for the argument of a functional.) In this expression, $T[\rho]$ is the kinetic energy associated with the given electron density, $V_{ee}[\rho]$ is the electron–electron interaction energy and $V_{ne}[\rho]$ is the energy of interaction between the electrons and 'external' fields. V_{ne} normally includes just the interaction between the electrons and the nuclei, but it can include any other fields imposed on the molecule. It is readily expressed in terms of an 'external potential' $v(\mathbf{r})$.

The problem is that the exact forms of the functionals $T[\rho]$ and $V_{ee}[\rho]$ are not known, and at the present time there is no fundamental theory for determining them. The usual route to practical calculations is the method proposed by Kohn and Sham (1965), in which the starting point is a determinantal wavefunction for N *non-interacting* electrons in N orbitals φ_i. For this system the electron density and the kinetic energy are exact:

$$\rho(\mathbf{r}) = \sum_i |\varphi_i(\mathbf{r})|^2, \quad T_s[\rho] = -\tfrac{1}{2} \sum_i \langle \varphi_i | \nabla^2 | \varphi_i \rangle, \tag{5.3.2}$$

while the Coulomb (classical) part $J[\rho]$ of the electron repulsion energy can also be calculated easily. The energy functional now takes the form

$$E[\rho] = V_{ne}[\rho] + T_s[\rho] + J[\rho] + E_{xc}[\rho], \tag{5.3.3}$$

where $E_{xc}[\rho]$ is the *exchange–correlation functional*:

$$E_{xc}[\rho] = T[\rho] - T_s[\rho] + V_{ee}[\rho] - J[\rho]. \tag{5.3.4}$$

The orbitals φ_i satisfy the Kohn–Sham equations:

$$\mathcal{K}\varphi_i = \epsilon_i\varphi_i, \tag{5.3.5}$$

where

$$\mathcal{K} = -\tfrac{1}{2}\nabla^2 + v(\mathbf{r}) + \int \frac{\rho(\mathbf{r}')}{|\mathbf{r} - \mathbf{r}'|}\,\mathrm{d}^3\mathbf{r}' + v_{xc}(\mathbf{r}), \tag{5.3.6}$$

and $v_{xc}(\mathbf{r})$, the exchange–correlation potential, is the functional derivative of $E_{xc}[\rho]$.

The Kohn–Sham equations are very similar to the Hartree–Fock equations, and are solved in a similar way, using an expansion of the orbitals in terms of a suitable basis set. However, the exchange–correlation functional $E_{xc}[\rho]$ and its potential $v_{xc}(\mathbf{r})$ are still unknown. The simplest form uses the local density approximation (LDA), which is based on the theory of the uniform electron gas, and in which the functional depends only on ρ, but this is too inaccurate to be useful for chemistry, and most modern functionals use the 'generalized gradient approximation' (GGA) in which the functional involves $|\nabla\rho|$ as well as ρ. Some functionals, known as 'hybrid functionals' incorporate 'exact exchange', replacing some fraction of the exchange part of $E_{xc}[\rho]$ by the corresponding fraction of the Hartree–Fock expression for the exchange energy, evaluated using the Kohn–Sham orbitals. The best-known and most widely used of these is the B3LYP functional (Becke 1993*a*,*b*, Stephens *et al.* 1994). For the calculation of intermolecular forces by perturbation theory, discussed in Chapter 6, the PBE0 functional (Perdew *et al.* 1996, Adamo and Barone 1999) is favoured at the time of writing.

However, any functional that is to be used in the calculation of intermolecular forces must satisfy a further requirement, in order to achieve an accurate description of the outer regions of molecules, which is essential for the determination of intermolecular forces. It can be shown (Perdew *et al.* 1982, Tozer and Handy 1998*a*) that the exchange–correlation potential should satisfy

$$v_{xc} \sim -\frac{1}{r} + I + \epsilon_{\text{HOMO}} \quad \text{as } r \to \infty, \tag{5.3.7}$$

where I is the ionization potential and ϵ_{HOMO} is the orbital energy of the highest occupied molecular orbital (HOMO). For Hartree–Fock wavefunctions, $\epsilon_{\text{HOMO}} \approx -I$ (this is Koopmans' theorem), but this is not true in Kohn–Sham theory, so v_{xc} should tend to a finite non-zero limit at infinity. Many of the functionals in current use do not satisfy this requirement, but several authors (Tozer and Handy 1998*b*, Casida and Salahub 2000, Allen and Tozer 2000, Gritsenko and Baerends 2004) have described procedures for applying an approximate 'asymptotic correction'. It is the asymptotically corrected version of PBE0, called PBE0-AC, that is recommended for calculation of intermolecular forces (Hesselmann and Jansen 2002*a*).

5.4 Basis sets

In any *ab initio* calculation it is necessary to select a set of basis functions. The choice is a compromise; generally one wishes to use the largest possible basis, but the cost of the calculation increases very sharply with the size of the basis. One reason for this—the main reason,

in the case of self-consistent-field calculations—is the need to calculate the two-electron integrals. These have the form

$$(ij|kl) = \int\int \chi_i(1)^* \chi_j(1) \frac{1}{r_{12}} \chi_k(2)^* \chi_l(2)\ \mathrm{d}\tau_1\ \mathrm{d}\tau_2, \tag{5.4.1}$$

where the χ_i are the basis functions. Typically there are about $\frac{1}{8}N^4$ two-electron integrals for a calculation involving N basis functions, though the number is reduced if symmetry is taken into account, and for a large molecule, many of them may be negligibly small. If conventional methods are used, where the two-electron integrals are stored on disc and read from there as required, there is an absolute upper limit to the size of the calculation, set by the disc space available. 'Direct' methods, in which the integrals are calculated anew every time they are needed, circumvent this limitation, but there is a corresponding increase in the computation time needed. This can be limited to some extent by avoiding the recalculation of integrals whose contribution to the calculation is negligible, and modern direct methods use sophisticated schemes for computing as few integrals as possible. For large molecules, so-called 'order-N' or 'linear-scaling' methods are coming into use. The overlap densities $\chi_i(1)^*\chi_j(1)$ and $\chi_k(2)^*\chi_l(2)$ that appear in eqn (5.4.1) can be represented by multipole expansions if they are far enough apart. In fact a group of overlap densities in the same region of space can be represented by a single multipole expansion. In the 'continuous fast multipole method' of White *et al.* (1994) and a later development by Watson *et al.* (2004), the multipole moments are grouped into boxes, with larger boxes being used at greater distances. In this way the work needed to calculate all the necessary integrals can be carried out in a time that is proportional to N or to $N \log N$. However, the method requires elaborate book-keeping and only becomes faster than more conventional methods for large molecules.

Early calculations used 'Slater-type orbitals' as basis functions. These have the form

$$\chi = R_{lk}(\mathbf{r}) \exp(-\zeta r), \tag{5.4.2}$$

where R_{lk} is a solid harmonic, and the argument $\mathbf{r} \equiv (r, \theta, \varphi)$ is the position of the electron relative to a nucleus. The form of such functions is suggested by the hydrogen-atom wavefunctions; in particular, the s-type functions ($l = 0$) have a cusp at the nucleus. However, they are very awkward to handle computationally, especially in the evaluation of the two-electron integrals (5.4.1), and most modern basis sets use 'contracted gaussian' functions of the form

$$\chi = R_{lk}(\mathbf{r}) \sum_i c_i N_i \exp(-\alpha_i r^2), \tag{5.4.3}$$

where R_{lk} is again the appropriate solid harmonic. The individual $N_i \exp(-\alpha_i r^2)$ (where N_i is a normalizing factor) are called 'primitive gaussian functions' and the c_i are expansion coefficients, usually chosen to optimize the energy of the isolated atom but fixed for the molecule or supermolecule calculation.

Modern *ab initio* programs provide an extensive library of standard basis sets. The minimum quality of basis set that can be contemplated for useful calculations of intermolecular potentials is at about the 6–31G(d,p) level (Hehre *et al.* 1971, Hariharan and Pople 1973, Francl *et al.* 1982). This basis uses a single basis function for the core atomic orbitals, represented by a linear combination of six primitive gaussians. For the valence orbitals, two sets of

basis functions are used, one with three primitives and a more diffuse one consisting of a single primitive. The (d,p) indicates that a set of d functions is added for each heavy (non-hydrogen) atom and a set of p functions for each hydrogen atom. These 'polarization functions' provide for distortion of the atomic orbitals in the molecular environment.

These basis sets use the same primitive exponents α_i for both $2s$ and $2p$ orbitals. The slightly better 'double-zeta plus polarization' or DZP basis sets use different exponents for $2s$ and $2p$, and also use two basis functions for each core orbital. The next step up is the TZ2P basis: 'triple-zeta plus double polarization'. A possible next step beyond this involves introducing higher-rank polarization functions: f functions on heavy atoms (i.e., other than hydrogen) and d functions on hydrogen. Additional diffuse functions are needed for some molecular properties, such as polarizabilities and high-rank multipole moments; they may be specified for the 6–31G family by the notation 6–31G+(d,p) or 6–31G++(d,p).

More elaborate basis sets are needed for accurate calculations, especially if correlation effects are to be included. The most efficient description of correlation effects would involve functions that depend explicitly in the inter-electron distances r_{ij}, but although some calculations have been done using such functions they are not used routinely. Instead, additional gaussian basis functions are added. The spherical harmonic addition theorem, eqn (3.3.1), shows that high-rank spherical harmonics are needed to represent $1/r_{ij}$, and the 'correlation consistent' cc-pVnZ series of basis sets have been devised to meet this need, where n may be D (for double-zeta), T (for triple-zeta) up to 6 (for sextuple-zeta). The error in the correlation energy has been found to be roughly of the order of L^{-3}, where L is the highest angular momentum represented in the basis, and this underlies a common procedure for extrapolating calculations to an estimated 'complete-basis-set' limit (Bak *et al.* 2001). The cc-pVnZ series of basis sets may be augmented by additional diffuse functions to give, for example, the aug-cc-pVTZ basis. A useful catalogue of available basis sets is given in the documentation for the Gaussian series of *ab initio* programs (Frisch *et al.* 2004), and individual basis sets can be obtained from `https://bse.pnl.gov/bse/portal` in the appropriate format for a variety of *ab initio* packages.

In density-functional calculations, on the other hand, these elaborate basis sets are not needed, because the detailed effects of electron repulsion on the wavefunction are washed out of the total electron density. Instead the effects of electron correlation are built into the exchange-correlation functional. Jensen (2001, 2002*a*,*b*, 2003, 2007) has proposed a family of 'polarization-consistent' basis sets suitable for use in DFT calculations. Another possibility is to return to the Slater-type orbital basis, since the integrals cannot in any case be evaluated analytically for the density functionals in common use, and are carried out numerically on a suitable grid (Becke 1988, Murray *et al.* 1993). However, this approach is not possible with the functionals that incorporate exact Hartree–Fock exchange, since in that case the two-electron integrals (5.4.1) are needed.

Since the energy in density functional theory is derived directly from the electron density according to eqn (5.3.3), it is often more efficient to express the density directly in terms of a set of auxiliary basis functions χ_k rather than as a sum over the molecular orbitals:

$$\rho(\mathbf{r}) = \sum_i |\varphi_i(\mathbf{r})|^2 \approx \tilde{\rho}(\mathbf{r}) = \sum_p c_k \chi_k(\mathbf{r}). \tag{5.4.4}$$

The coefficients c_k are chosen by a least-squares procedure, usually by minimizing the integral

$$\Delta = \iint [\tilde{\rho}(\mathbf{r}_1) - \rho(\mathbf{r}_1)] \frac{1}{r_{12}} [\tilde{\rho}(\mathbf{r}_2) - \rho(\mathbf{r}_2)] \, \mathrm{d}^3\mathbf{r}_1 \, \mathrm{d}^3\mathbf{r}_2, \tag{5.4.5}$$

which describes the Coulomb electron-repulsion energy of the difference between the exact and fitted densities (Boys and Shavitt 1959, Dunlap *et al.* 1979, Dunlap 2000). Auxiliary basis sets are available from `https://bse.pnl.gov/bse/portal` for many of the primary basis sets in current use.

A further possibility for the primary basis set, commonly adopted in solid-state calculations, is the use of a plane-wave basis. Here the wavefunction is written as

$$\varphi_i(\mathbf{r}) = N \sum_{\mathbf{g}} c_{\mathbf{g}} \exp(\mathrm{i}\mathbf{g} \cdot \mathbf{r}), \tag{5.4.6}$$

where for calculations in an orthorhombic box with sides L_x, L_y and L_z, the wavevectors $\mathbf{g}$ are

$$\mathbf{g}_{ijk} = \left(\frac{2\pi i}{L_x}, \frac{2\pi j}{L_y}, \frac{2\pi k}{L_z} \right), \tag{5.4.7}$$

for integer i, j and k up to some maximum value. These are unsuitable for calculating intermolecular interactions in the gas phase, as they presuppose that the calculation is carried out under periodic boundary conditions, and the interacting system would need to be contained in a sufficiently large box that interactions with its periodic images could be neglected, which in turn would require an unreasonably large plane-wave basis set. Core electrons, with their strongly peaked wavefunctions, are particularly difficult to describe by plane waves, and it is usual to replace them by pseudopotentials, which attempt to mimic the effect of orbital orthogonality in keeping the valence electrons out of the core region. The use of a mixed gaussian and plane-wave basis may be another way to overcome this problem (VandeVondele *et al.* 2005). On the other hand, the plane wave basis is a natural choice for the study of intermolecular forces in crystals, where the periodicity is present in any case.

In calculations of intermolecular potentials it is necessary to carry out a large number of calculations at different values of the intermolecular coordinates, so it is worth spending some time optimizing the basis for the individual molecules. Other things being equal, the basis that minimizes the energy of the isolated molecule is to be preferred, because this is likely to reduce the effects of basis set superposition error (see §5.6.2). Feller (1992) found that the inclusion of diffuse basis functions was particularly important in this respect. At the same time, it is often necessary to include basis functions that have no effect on the energy of the isolated system, because molecular properties like the polarizability are involved. For example, in complexes of an inert gas atom such as argon with a polar molecule, d and possibly f functions must be included for the argon atom in order that it can respond to the electric field of its partner; otherwise the induction energy will be seriously underestimated.

It is important to ensure that the basis is 'balanced'; that is, that the quality is comparable for all the atoms in the problem, and that the quality of the valence basis and the polarization basis are not too disparate. This is unfortunately an ill-defined criterion. The kind of problem that arises with unbalanced basis sets can be illustrated by the case, already mentioned, of an inert gas atom such as argon interacting with a polar molecule or ion. At the SCF level, the description of the isolated argon atom is unaffected by the addition of d orbitals, because they have the wrong symmetry. However, they are needed in the complex in order to describe the

polarizability of the argon atom and hence the induction energy. The problem with balance arises because if the *d* basis is good but the valence basis not very good, the electron distribution can tip too far into the *d* orbitals under the influence of an electric field, because the electronic energy is artificially high in the poor-quality valence basis. The effect is to exaggerate the polarizability and the induction energy. Evidently a good valence basis with a poor polarization basis leads to an underestimate of the induction energy. Getting the balance right is unfortunately difficult to achieve in a general way, and as with most questions involving basis sets, the choice generally has to be based on experience and intuition. However, it is usually necessary at least to ensure that all atoms are described by basis sets from the same family at the same level of accuracy—for example, all 6–31G(d,p) or all cc-pVTZ.

While one would wish to use the best possible basis set with the highest available level of theory (currently CCSD(T)), the N^7 scaling often makes such calculations impracticable. One solution is to extrapolate from the smaller basis sets to the complete-basis-set limit, as mentioned above; another is to calculate the correlation energy using CCSD(T) with a moderately good basis, and to correct that using the difference between MP2 correlation energies calculated with the moderately good basis and a larger basis (Klopper and Lüthi 1999). Explicitly correlated methods (§5.2.4), which deal with electron correlation much more efficiently, can give good results with small basis sets and show promise for the future.

5.5 Calculation of molecular properties

At long range, intermolecular interactions can be described in terms of properties of the individual molecules, so *ab initio* methods for calculation of properties are an important aspect of the theory of intermolecular forces. First-order properties such as multipole moments can be expressed most simply as expectation values, as for example in eqn (2.1.3). Most *ab initio* programs calculate and print the dipole moment routinely in every calculation, and some calculate the quadrupole moment too. Alternatively, multipole moments can be expressed as energy derivatives. The Hellmann–Feynman theorem (Hellmann 1937, Feynman 1939) states that if the Hamiltonian $\mathcal{H}(\lambda)$ depends on some parameter λ, and $\psi(\lambda)$ is a normalized eigenfunction with eigenvalue $W(\lambda)$, then

$$\begin{aligned}\frac{\partial W}{\partial \lambda} &= \frac{\partial}{\partial \lambda}\langle\psi(\lambda)|\mathcal{H}(\lambda)|\psi(\lambda)\rangle \\ &= \left\langle \frac{\partial\psi}{\partial\lambda}\middle|\mathcal{H}\middle|\psi\right\rangle + \left\langle\psi\middle|\frac{\partial\mathcal{H}}{\partial\lambda}\middle|\psi\right\rangle + \left\langle\psi\middle|\mathcal{H}\middle|\frac{\partial\psi}{\partial\lambda}\right\rangle \\ &= W\frac{\partial}{\partial\lambda}\langle\psi|\psi\rangle + \left\langle\psi\middle|\frac{\partial\mathcal{H}}{\partial\lambda}\middle|\psi\right\rangle \\ &= \left\langle\psi\middle|\frac{\partial\mathcal{H}}{\partial\lambda}\middle|\psi\right\rangle, \end{aligned} \tag{5.5.1}$$

where the last line follows because $\langle\psi|\psi\rangle = 1$ for any λ. It can be shown that the theorem also holds if $\psi(\lambda)$ is a variationally optimized approximate wavefunction, provided that the basis functions do not depend on λ. (See, for example, Jensen (1999), Ch. 10.)

The properties that we are interested in all arise through the effect of perturbations of the form $\lambda\hat{Q}$, where $\hat{Q}$ is some operator such as a dipole or quadrupole moment and λ is a parameter such as the strength of an electric field or field gradient. The derivative of the

energy with respect to the perturbation parameter is then, according to the Hellmann–Feynman theorem,

$$\frac{\partial W}{\partial \lambda} = \left\langle \psi \middle| \frac{\partial \mathcal{H}}{\partial \lambda} \middle| \psi \right\rangle = \langle \psi | \hat{Q} | \psi \rangle, \tag{5.5.2}$$

all in the limit $\lambda \to 0$, and the property can be calculated either as an expectation value or as an energy derivative. For an exact or variationally optimized wavefunction the two results would be the same, but for an MP2 or coupled-cluster wavefunction they can be significantly different.

The usefulness of (5.5.2) appears when we want to calculate a second-order property such as polarizability. From (2.3.5), the polarizability is the second derivative of the energy with respect to electric field:

$$\alpha_{\alpha\beta} = -\frac{\partial^2 W}{\partial E_\alpha \partial E_\beta}\bigg|_{\mathbf{E}=0}. \tag{5.5.3}$$

In general we have a Hamiltonian containing several linear perturbations:

$$\mathcal{H} = \mathcal{H}_0 + \lambda_1 \hat{Q}_1 + \lambda_2 \hat{Q}_2 + \cdots, \tag{5.5.4}$$

and differentiating (5.5.2) again we get

$$\frac{\partial^2 W}{\partial \lambda_1 \partial \lambda_2} = \frac{\partial \langle Q_1 \rangle}{\partial \lambda_2}. \tag{5.5.5}$$

This provides a practical method for determining $\alpha_{\alpha\beta}$. We calculate the wavefunction ψ in the presence of a uniform electric field E_β, and evaluate the expectation value of the dipole moment, $\langle \psi | \hat{\mu}_\alpha | \psi \rangle$. If we repeat this for several values of the field, we can carry out a single numerical differentiation to obtain $\alpha_{\alpha\beta}$, which is numerically much more satisfactory than differentiating the energy twice.

This is the 'finite field' approach to the calculation of properties. Where the required property can be expressed as the derivative of the energy or some other expectation value with respect to an external perturbation, the calculation is carried out for several values of the perturbation and the derivative determined numerically. It is a simple and straightforward method, but needs to be carried out carefully: if the perturbation is too small, the derivative involves a small difference of large numbers, so that precision is lost, while perturbations that are too large introduce non-linear effects.

An alternative approach can also be based on differentiation of (5.5.2), again assuming a Hamiltonian of the form (5.5.4):

$$\begin{aligned} \frac{\partial^2 W}{\partial \lambda_1 \partial \lambda_2} &= \left\langle \frac{\partial \psi}{\partial \lambda_1} \middle| \frac{\partial \mathcal{H}}{\partial \lambda_2} \middle| \psi \right\rangle + \left\langle \psi \middle| \frac{\partial^2 \mathcal{H}}{\partial \lambda_1 \partial \lambda_2} \middle| \psi \right\rangle + \left\langle \psi \middle| \frac{\partial \mathcal{H}}{\partial \lambda_2} \middle| \frac{\partial \psi}{\partial \lambda_1} \right\rangle \\ &= 2 \left\langle \frac{\partial \psi}{\partial \lambda_1} \middle| \frac{\partial \mathcal{H}}{\partial \lambda_2} \middle| \psi \right\rangle, \end{aligned} \tag{5.5.6}$$

if the wavefunctions are real. Now $\partial\psi/\partial\lambda_1$, in the limit $\lambda_1 \to 0$, is the first-order correction to the wavefunction under the perturbation $\hat{Q}_1$, so we could substitute the expression given in eqn (C.1.21), with suitable adjustment of the notation, to arrive at the sum-over-states expression for the second-order property. This is not, however, a good route to accurate numerical

values. Modern methods for calculating wavefunction derivatives, and hence second-order properties, are mainly based on the ideas of 'coupled perturbed Hartree–Fock' or CPHF theory, first set out by Stevens *et al.* (1963) for perturbation by external fields, and later extended by Gerratt and Mills (1968) to deal with changes in nuclear positions. This more elaborate treatment is needed because the perturbation due to an external field or nuclear displacement changes the electronic wavefunction, which in turn affects the electron–electron repulsion energy. Changes in this large term cannot be ignored, and the electronic wavefunction has to be allowed to relax to maintain the self-consistency of the electron repulsion. The technique has been developed greatly since 1968, and an important advance was made by Handy and Schaefer (1984), who showed that the method could be reformulated so that it required the solution of a single set of linear equations, however many perturbations were involved, and that the method could be extended to correlated methods. More details can be found in Jensen (1999, Ch. 10).

Similar methods can be used to calculate response properties via density functional theory calculations (Colwell *et al.* 1993, 1996, Casida 1995). Density functional theory incorporates the effects of electron correlation, and would be exact if only we knew the correct form of the functional, so it can in principle give exact results for molecular properties. As noted in §5.3, the properties that are important for intermolecular forces are sensitive to the outer regions of the molecule, and it is important to use asymptotically corrected functionals. With this proviso, however, perturbation methods based on density functional theory (usually described as 'coupled Kohn–Sham', or CKS, perturbation theory, or as time-dependent density functional theory or TDDFT) are proving to be very successful in the calculation of molecular polarizabilities and dispersion coefficients. For the dispersion coefficients, we need the polarizabilities at imaginary frequency, or equivalently the frequency-dependent charge density susceptibility (FDDS). The detailed derivation of the method is too long to give here; see Casida (1995) or Petersilka *et al.* (1996) or Colwell *et al.* (1996). The FDDS takes the form

$$\alpha(\mathbf{r},\mathbf{r}';\omega) = \sum_{ii'}^{\text{occ}} \sum_{vv'}^{\text{virt}} C_{iv,i'v'}(\omega)\psi_i(\mathbf{r})\psi_v(\mathbf{r})\psi_{i'}(\mathbf{r}')\psi_{v'}(\mathbf{r}'), \tag{5.5.7}$$

where $\psi_i(\mathbf{r})$ and $\psi_{i'}$ are occupied molecular orbitals, ψ_v and $\psi_{v'}$ are virtual orbitals, and the coefficients $C_{iv,i'v'}(\omega)$ are

$$\left[(\mathbf{H}^{(2)}\mathbf{H}^{(1)} - \hbar^2\omega^2\mathbf{I})^{-1}\mathbf{H}^{(2)}\right]_{iv,i'v'}, \tag{5.5.8}$$

where the matrices $\mathbf{H}^{(1)}$ and $\mathbf{H}^{(2)}$, known respectively as the electric and magnetic Hessians, are given by

$$\begin{aligned}\mathbf{H}^{(1)}_{iv,i'v'} &= (e_v - e_i)\delta_{iv,i'v'} + 4(iv|i'v') - \xi[(ii'|vv') + (iv'|i'v)] \\ &\quad + 4\int \varphi_i\varphi_v\varphi_{i'}\varphi_{v'}\frac{\delta(v_{\text{xc}} - \xi v_{\text{x}})}{\delta\rho}\,\mathrm{d}^3\mathbf{r}, \end{aligned} \tag{5.5.9}$$

$$\mathbf{H}^{(2)}_{iv,i'v'} = (e_v - e_i)\delta_{iv,i'v'} + \xi[(ii'|vv') - (iv'|i'v)], \tag{5.5.10}$$

where ξ is the fraction of Hartree–Fock exchange included in the exchange-correlation functional ($\xi = 0$ for a continuum functional), v_{x} is the exchange part of v_{xc}, and $(ij|kl)$ is the two-electron Coulomb integral $\langle\varphi_i(1)\varphi_j(1)\big|(r_{12})^{-1}\big|\varphi_k(2)\varphi_l(2)\rangle$. These formulae apply in the

adiabatic approximation, that is, when $|\hbar\omega|$ is small compared with the energy differences between molecular states. The dispersion coefficient involves an integral, eqn (4.3.21), over imaginary frequency from 0 to ∞, so the adiabatic approximation is not formally valid, but nevertheless the results are very satisfactory. A further and widely used approximation is to replace the correct exchange–correlation potential $v_{\rm xc}$ (i.e., the one used in the calculation of the wavefunction) by the simpler local density approximation (LDA) exchange–correlation potential, with only a small (less than 1%) loss in accuracy (Misquitta *et al.* 2005*b*). These approximations together comprise the ALDA approximation.

The expression for the FDDS given in eqn (5.5.7) involves a quadruple sum over the molecular orbitals. This can be transformed into a quadruple sum over the basis functions by replacing each molecular orbital by its basis set expansion, but it remains cumbersome, especially in the expression (4.3.18) for the dispersion energy. Density-fitting (eqn (5.4.4)) can be used to simplify it. We replace each of the products $\rho_{iv}(\mathbf{r}) = \psi_i(\mathbf{r})\psi_v(\mathbf{r})$ that appears in eqn (5.5.7) by an expansion in terms of an auxiliary basis set $\chi_k(\mathbf{r})$; that is, we approximate $\rho_{iv}(\mathbf{r}) \approx \tilde{\rho}_{iv}(\mathbf{r}) = \sum_k d_k^{(iv)}\chi_k(\mathbf{r})$ and minimize

$$\Delta_{iv} = \iint [\rho_{iv}(\mathbf{r}_1) - \tilde{\rho}_{iv}(\mathbf{r}_1)]\frac{1}{r_{12}}[\rho_{iv}(\mathbf{r}_2) - \tilde{\rho}_{iv}(\mathbf{r}_2)]\,\mathrm{d}^3\mathbf{r}_1\,\mathrm{d}^3\mathbf{r}_2 \tag{5.5.11}$$

by analogy with eqn (5.4.5). This leads to a more compact expression for the FDDS:

$$\alpha(\mathbf{r}, \mathbf{r}'; \omega) = \sum_{kk'} \tilde{C}_{kk'}(\omega)\chi_k(\mathbf{r})\chi_{k'}(\mathbf{r}'), \tag{5.5.12}$$

where the new coefficients $\tilde{C}_{kk'}(\omega)$ are obtained by a straightforward transformation (Misquitta *et al.* 2005*a*).

5.5.1 Basis sets for molecular properties

For calculations of molecular properties other than the energy itself, additional considerations affect the choice of basis set. For the dipole–dipole polarizability, for instance, the sum-over-states expression (2.3.2) shows that matrix elements of the dipole operator between ground and excited states are involved. In the dipole-allowed excited states, p electrons may be excited to d orbitals (as well as $p \to s$ and $s \to p$) so it is essential to include d orbitals in the basis, even if (as in the Ne atom) they are not needed to describe the ground state SCF wavefunction. Werner and Meyer (1976) showed that three sets of d functions are needed to obtain reasonably accurate dipole–dipole polarizabilities for small molecules containing first-row atoms. For quadrupole–quadrupole polarizabilities, $p \to f$ excitations become important, so f functions are required, and so on. This means that high-rank polarizabilities are very difficult to calculate accurately, even for small molecules.

The charge distribution in a molecule is modified by electron correlation. The main effect is to reduce charge separations, so in a distributed-multipole picture (discussed in Chapter 7) the atom and bond charges tend to be smaller. Higher moments are not usually affected so much. Since the electrostatic interaction is often large, the effect of electron correlation on the charge distribution can be important in giving an accurate description of the interaction. The inclusion of electron correlation also affects properties such as polarizabilities, and consequently induction and dispersion energies. That is, although dispersion is itself a correlation

effect, involving the correlated motion of electrons in different molecules, the motion of those electrons can themselves be affected by correlation between electrons in the same molecule. As noted above, the conventional treatment of electron correlation, using methods such as MP2 or CCSD without explicit incorporation of the inter-electron distances r_{ij} into the wavefunction, requires large gaussian basis sets and becomes very expensive. The augmented or doubly augmented correlation-consistent basis sets, aug-cc-pVnZ or daug-cc-pVnZ, are commonly used. This is much less of a problem for density-functional methods, which work with the total electron density, and they can give good results with less elaborate basis sets, though it is still necessary to include enough higher-angular-momentum functions to permit a good description of polarizabilities. For example, the Sadlej basis sets (Sadlej 1988, 1991) give comparable results to aug-cc-pVTZ and are significantly smaller.

5.6 The supermolecule method

There are numerous 'black box' programs available for calculating the energy of a system of electrons and nuclei, either *ab initio*—by solving Schrödinger's equation, making some approximations but using no empirical data—or by semi-empirical methods, in which the calculation is further simplified by additional approximations and the use of some empirical data. In either case there is the possibility of treating a system of two or more interacting molecules as just another assembly of electrons and nuclei—a 'supermolecule'. The interaction energy U_{AB} of a pair of molecules A and B is then just the energy of the supermolecule less the energies of the isolated molecules:

$$U_{AB} = W_{AB} - W_A - W_B. \tag{5.6.1}$$

Nothing apparently could be simpler than to use any of the available programs to calculate W_{AB}, W_A and W_B, and hence to obtain the interaction energy. In fact the approach is a very useful one, but its application is fraught with difficulties, which we shall now discuss.

5.6.1 The variation principle

Ab initio methods are based on the variation principle: the energy of an approximate wavefunction (more precisely, the expectation value of the Hamiltonian, calculated exactly for the approximate wavefunction) cannot be lower than the lowest eigenvalue of the Hamiltonian. This principle holds when the Hamiltonian is the exact Schrödinger Hamiltonian, but also within certain approximations. In particular, it holds within the Born–Oppenheimer approximation. It also holds when the wavefunction is restricted to belonging to a particular class of function; for example within the Hartree–Fock approximation, where the wavefunction is taken to be a single Slater determinant, or perhaps a specific combination of Slater determinants required to ensure that the wavefunction is an eigenfunction of spin. In this case (the self-consistent-field or SCF method) the energy cannot be lower than the energy of the best wavefunction of this type, normally called the Hartree–Fock limit.

The variational principle also holds for certain approximate treatments of electron correlation, in particular for the widely used method of configuration interaction with single and double excitations (CISD), but not for all of them. It does not hold for any semi-empirical method, essentially because the energy calculated by such methods is not the exact expectation value for some Hamiltonian, but only an approximation to the expectation value.

The variational principle is the benchmark that we use to judge the accuracy of most *ab initio* calculations. Although the exact lowest eigenvalue is hardly ever known, we can be confident that a calculation is in some sense better than another if it gives a lower energy. The wavefunction may not be better in all respects—it may for instance give worse results for some molecular properties—but we know that in the limit the energy can only coincide with the true energy if the wavefunction is correct, so that the process of seeking ever lower energies will in principle lead us to the right answer in the end.

In the calculation of interaction energies, however, the variation principle does not provide this kind of assurance. If we do a better calculation using a variational supermolecule method, then W_{AB}, W_A and W_B must improve or at worst remain the same. But we have no way of knowing a priori whether the difference $U_{AB} = W_{AB} - W_A - W_B$ will increase or decrease. Moreover, although W_{AB}, W_A and W_B will all approach their limiting values more closely whenever we improve the wavefunctions, there is no reason why U_{AB} should do the same. In the limit of exact wavefunctions, of course, U_{AB} will be correct, but in a sequence of calculations that approach this limit, U_{AB} need not approach its limit monotonically, but may get worse before it gets better.

This is a general feature of the use of *ab initio* methods to calculate energy differences, and is not confined to intermolecular energy calculations. A well-known example is the ammonia molecule, which has a pyramidal equilibrium geometry but which can invert via a planar configuration some 25 kJ mol^{-1} higher in energy. If a simple basis of atomic s and p functions is used in the calculation, the pyramidal geometry is found to have a lower energy than the planar one. If the sp basis is improved, however, the planar geometry becomes preferred, and remains the preferred geometry even with a complete sp basis (Rauk *et al.* 1970). Only if d functions are added to the N atom basis does the pyramidal geometry become preferred again—essentially because the d functions can all stabilize the pyramidal geometry, but the d_{xz} and d_{yz} functions have the wrong symmetry to affect the energy of the planar geometry.

This example illustrates both that our intuitions may be unreliable, and also that improvements of one sort or another may have very different effects on the energies whose difference we require. Putting the same statement the other way round, we have no reason to expect that the inevitable errors in W_{AB} and $W_A + W_B$ will cancel out. Since the error in a typical *ab initio* calculation is of the order of 1 eV per electron pair, the error in each of W_{AB} and $W_A + W_B$ can easily reach 10 eV or 1000 kJ mol^{-1} (Davidson and Chakravorty 1994). The interaction energy, on the other hand, is typically of the order of 10 kJ mol^{-1}. It is remarkable that the errors cancel as well as they usually do, and the reasons for this are not fully understood, though one reason is that normally only a few electrons on each molecule are involved in the short-range interactions. However there are two well-known ways in which the errors are known not to cancel. These are *basis set superposition error* and lack of *size consistency*.

5.6.2 Basis set superposition error

The principle of basis set superposition error (BSSE) is not difficult to understand. When a calculation is done on an isolated molecule, the energy that can be achieved is limited by the available basis set, which is rarely as good as one would wish and is never complete. If we were to carry out a calculation on molecule A of a complex $A\cdots B$, using the basis functions of both molecules, in the same positions as they would have in the complex, but the electrons and nuclei only of molecule A, we would get an energy that is no higher, and usually lower,

than we would find in a calculation using the basis functions of molecule A alone:

$$W_A(AB) \leq W_A(A).$$

We use the notation $W_A(AB)$ to describe a calculation of the energy W_A of molecule A using the joint (AB) basis, while $W_A(A)$ describes the calculation of the same energy using the A basis alone. When two molecules are brought together and a calculation is carried out on the supermolecule, the basis functions of each molecule become variationally available in this way to improve the description of the other molecule. This is quite separate from any actual physical interaction that may arise; it is an artefact, due to the inadequacy of the original basis sets for the isolated molecules. The result is that the energy of the supermolecule is spuriously low if we calculate it in the obvious way as the difference

$$U^0_{AB} = W_{AB}(AB) - W_A(A) - W_B(B). \tag{5.6.2}$$

A remedy for this defect was proposed by Boys and Bernardi (1970). It is called the 'counterpoise' procedure, and consists simply of using the supermolecule basis (AB) for all the calculations:

$$U^{\mathrm{cp}}_{AB} = W_{AB}(AB) - W_A(AB) - W_B(AB). \tag{5.6.3}$$

The difference between these calculations, $U^{\mathrm{cp}}_{AB} - U^0_{AB} = W_A(A) - W_A(AB) + W_B(B) - W_B(AB)$, is called the 'counterpoise correction' for the basis set superposition error that is present in eqn (5.6.2).

An objection to this procedure has been made on the grounds that in $W_A(AB)$ the basis functions of molecule B are wholly available to molecule A, whereas in the calculation of $W_{AB}(AB)$ they are needed also to describe the wavefunction of molecule B. It is argued that the difference $W_A(A) - W_A(AB)$ is an overestimate of the correction that is needed for molecule A, and that a better formula would be $W_A(A) - W_A(AB')$, where the notation $W_A(AB')$ describes a calculation carried out for molecule A using the basis set of A augmented with only the *virtual* orbitals of B. There has been a great deal of passionate argument over this issue, with both sides claiming that only their method gives the true corrected interaction energy. Probably the most succinct argument in favour of the original Boys–Bernardi scheme is that of Gutowski *et al.* (1987), who remark that in the ideal calculation one would use a *complete* basis for the calculations on AB and on the isolated A and B molecules, and one would not then consider deleting the occupied orbitals of B from the basis for the calculation on A. Van Duijneveldt *et al.* (1994) go further, pointing out that the fact that the electrons of molecule A can use all the orbitals of the basis when A is isolated but are excluded from the occupied orbitals of B in the complex is not an artefact at all but is a true physical effect, leading to phenomena such as Pauli repulsion, as discussed in Chapter 8. On this view, it is manifestly erroneous to exclude the occupied orbitals of B from the calculation of W_A in the dimer basis.

Despite the heat that has been generated by this matter, it is in truth a non-issue. Much of the argument is based on the concept that there is in some sense a 'correct' interaction energy for any given basis. This is a quite meaningless concept for anything but a complete basis; an inadequate basis will give an inadequate result, and no 'correction' can eliminate all its deficiencies. A recent study by Kaczmarek *et al.* (2004, 2006) analyses the sources of error using perturbation theory, and arrives at a similar conclusion.

The only way to get the correct result (at a given level of calculation—SCF, MP2 or whatever it may be) is to use a complete basis, and the only criterion for judging the usefulness

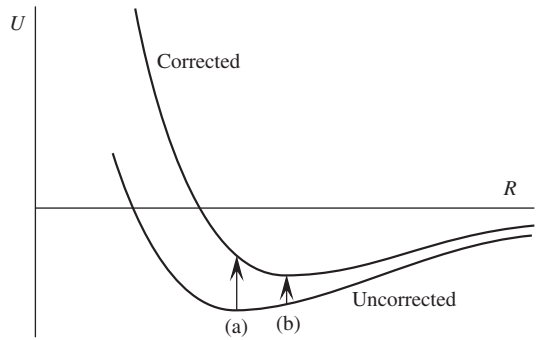

Fig. 5.1 The BSSE correction at the minimum of the uncorrected surface (a) is larger than the correction at the minimum of the corrected surface (b).

of one correction procedure over another is to ask which of them reliably gives results that are closer to the basis set limit. Schwenke and Truhlar (1985) investigated this question, and concluded that neither of the procedures advocated as corrections for BSSE gives results that are consistently closer to the basis set limit than the uncorrected values. They suggest that it is better to use the counterpoise procedure not as a correction device but only as a way of estimating the inadequacy of the basis set. Frisch *et al.* (1986) came to a similar conclusion. The contrary view is held by Szalewicz *et al.* (1988), and by Gutowski *et al.* (1993), who found in a study of He_2 that counterpoise correction according to the original Boys–Bernardi prescription does improve the agreement between the corrected result and the Hartree–Fock limit, while the 'virtuals-only' prescription does not, as expected from van Duijneveldt *et al.*'s argument cited above. More recent work on hydrogen-bonded complexes (Novoa *et al.* 1994) leads to the conclusion that the standard counterpoise procedure gives more consistent results as the basis set is improved than uncorrected SCF or MP2 calculations. However, the corrections are larger for correlated wavefunctions than for SCF at a given level of basis set, and even for the best basis sets they are of the order of 1–3 kJ mol^{-1}.

Most workers currently believe that it is better to correct for BSSE, though few, if any, would see the correction as useful when the basis set is very poor. Indeed, the disagreement on this issue may just be a question of where the line is to be drawn between 'poor' and 'good' basis sets. It is possible to use much better basis sets for He_2 than for the larger systems that Schwenke and Truhlar studied. Probably a reasonable rule of thumb is to apply the counterpoise correction, and to treat the magnitude of the correction as a guide to the reliability of the result, except in cases where the basis set can be improved to the point where the corrected energy varies less with basis than the size of the correction.

One aspect of the BSSE correction process that may have led to the perception that the counterpoise procedure over-corrects is illustrated schematically in Fig. 5.1. The customary procedure is to find the minimum of the uncorrected curve and apply the correction there, as shown schematically by (a) in Fig. 5.1. However, if the error varies with separation, then the minimum of the uncorrected potential curve will occur at a different separation from the minimum of the corrected curve ((b) in Fig. 5.1), and the BSSE correction at the minimum of the uncorrected curve will inevitably be larger than the correction at the minimum of the corrected curve. In some cases the customary procedure can lead to significant errors in the

binding energy and the position of the minimum. Clearly the errors are worst when the BSSE depends strongly on the separation, which seems to happen when the interaction is dominated by dispersion (Eggenberger *et al.* 1991). The correct procedure is evidently to find the minimum of the corrected curve. Simon *et al.* (1996) have described a method for doing this, and find that the relationship between the corrected and uncorrected curves is indeed as shown in Fig. 5.1. Optimization of the geometry using the BSSE-corrected energy can now be carried out, for example using the widely available *ab initio* programs NWChem (Valiev *et al.* 2010) and Turbomole (Ahlrichs *et al.* 2011).

It is unfortunate that so much effort has gone into the subject of BSSE, because it has obscured the fact that there are other errors in a supermolecule calculation that are very imperfectly understood. Indeed, there is very little understanding of what those errors might be. A study by Szalewicz *et al.* (1988) of the binding energy of the water dimer suggested that the uncertainty remaining in the best calculations was at that time of the order of 2.5 kJ mol^{-1}, or 10% of the binding energy in what is a particularly strongly bound complex. With the advent of more powerful computers and better *ab initio* methods, the situation has improved since then, to the point where the uncertainty in the water dimer binding energy is smaller by an order of magnitude (Klopper *et al.* 2000), but our understanding of the remaining errors is still far from complete.

5.6.3 Electron correlation and size consistency

The CISD method is variational, but unfortunately it is not *size consistent*. To explain this technical concept we suppose that we now wish to calculate the energy of a pair of H_2 molecules. At distances where they interact, we use a supermolecule calculation. The reference calculation corresponding to infinite separation involves a counterpoise-corrected calculation for each isolated molecule, using the supermolecule basis in each case. We normally need to do these single-molecule calculations separately, because the supermolecule basis is often the largest basis for which the calculation is feasible, and we cannot do a calculation with a basis that is twice as big. However, we need to be sure that the result we would get by adding the single-molecule energies from the separate calculations is the same as we would get from a supermolecule calculation on the two separated molecules simultaneously. If this is the case, the calculation is said to be size consistent (or *size extensive*).

The H_2 example allows us to see why the CISD method fails this test. For a single molecule, the CISD wavefunction (in the simplified version discussed in §5.2 above) is $\sigma_g^2 - \lambda\sigma_u^2$. If we add the energies for two separate calculations, that is equivalent to using a simple product of a wavefunction like this for molecule A and another for molecule B, i.e., $(\sigma_g^{A\,2} - \lambda\sigma_u^{A\,2})(\sigma_g^{B\,2} - \lambda\sigma_u^{B\,2})$. However, when we multiply this out, we find a term $\lambda^2\sigma_u^{A\,2}\sigma_u^{B\,2}$, in which *four* electrons have been excited out of the ground configuration $\sigma_g^{A\,2}\sigma_g^{B\,2}$ of the two-molecule system. If we were to carry out a CISD calculation on the two-molecule system, however, we would include single and double excitations only, so this configuration would not appear and the answer would be different.

This effect is quite large—much too large to ignore. For a pair of water molecules separated by 5,000 bohr, an SCF calculation using the cc-pVTZ basis gives almost exactly twice the energy calculated for a single molecule using the same basis set. The small difference, of the order of 10^{-10} a.u., can be attributed mainly to rounding errors and incomplete convergence; the physical interaction between the molecules at this distance is dominated by the

dipole–dipole interaction, of order $R^{-3} = 10^{-11}$ a.u. However, the correlation energy calculated by CISD using the cc-pVTZ basis is −0.489 a.u., while the correlation energy calculated for a single molecule by the same method is −0.257 a.u. (The 'correlation energy' is the difference between the energy calculated with correlation effects included, and the energy obtained from the SCF calculation, and is negative.) The difference between the first value and twice the second is 0.025 a.u. = 65 kJ mol^{-1}. That is, if we calculate the interaction energy by the supermolecule method, subtracting twice the energy of a single molecule from the energy of the supermolecule, the result will be in error by an amount of the order of 65 kJ mol^{-1} if we use CISD. Improving the basis doesn't help: with an aug-cc-pVQZ basis the difference is more than 70 kJ mol^{-1}.

It is clear from this example that the calculation of intermolecular interactions must be carried out in a size-consistent way. Fortunately the other main classes of electron correlation method are size consistent. The MP2 energy for an assembly of two or more non-interacting systems is just the sum of the MP2 energies for the individual systems, as required for size consistency. For two widely separated systems the molecular orbitals will be localized on one or other molecule, and the overlap between orbitals on different molecules will all be zero. Consequently a term in the MP2 energy expression (5.2.1) will be zero unless all the orbitals are on the same molecule, in which case it is part of the MP2 energy for that molecule, so the MP2 energy of the widely separated molecules is the sum of MP2 energies for the two individual molecules, as required. The CCSD treatment is size consistent because the product of two CCSD wavefunctions is $\exp(\hat{T}_1^A + \hat{T}_2^A)\Psi_0^A \exp(\hat{T}_1^B + \hat{T}_2^B)\Psi_0^B = \exp(\hat{T}_1^A + \hat{T}_2^A + \hat{T}_1^B + \hat{T}_2^B)\Psi_0^A\Psi_0^B$, which is still of CCSD form.

Neither of these methods is variational; in principle the CCSD wavefunction could be optimized variationally, but that is impractical and a different approach is used. However, size consistency is more important than the variational property; we have seen that a variational calculation of energies provides no particular guarantees as to the quality of energy differences.

5.7 Density functional theory for interaction energies

In view of the simplicity and efficiency of density functional theory, it is natural to use it to calculate intermolecular interaction energies by the supermolecule method. However, numerous early applications found that it failed. Cybulski and Seversen (2003) remarked rather sourly that 'typically, several different functionals are chosen for testing a given problem, and those of them that give results in best agreement with reliable *ab initio* or experimental results are claimed to be satisfactory'. Xantheas (1995) found that the O···O distance in the water dimer varied from 2.6 to 3.3 Å, depending on the functional used, while the binding energy varied from 8.8 to 51.0 kJ mol^{-1}, but he concluded that the B–LYP functional gave results in good agreement with MP2 calculations. Del Bene *et al.* (1995), on the other hand, used DFT to study eight hydrogen-bonded complexes for which experimental data were available, and concluded that 'density functional calculations fail to yield reliable binding energies, intermolecular distances and hydrogen-bonded X–H frequency shifts'. An attempt to apply the method to inert gases was described by Pérez-Jordá and Becke (1995), and the results were very poor. Tsuzuki and Lüthi (2001) showed that DFT gives a very poor account of the relative energies of possible structures of the benzene dimer.

It is now understood that the main reason for such deficiencies is the failure of DFT to describe the dispersion energy, even approximately, for non-overlapping molecules. Cybulski and Seversen (2003) separated the DFT interaction energy of Ar_2 into several components, using several different functionals, and showed that they all decayed with distance in a manner that identified them as overlap effects. Similar results were found for water dimer and the thymine–adenine complex (Cybulski and Seversen 2005). Allen and Tozer (2002) showed that the electron density in each of a pair of interacting helium atoms, calculated using conventional correlated methods, was slightly distorted towards the other, but that no such distortion appeared in the DFT density. It is this slight distortion of the density that leads, through the Hellmann–Feynman principle, to the attractive dispersion force.

The reason for the failure of DFT to reproduce the dispersion energy lies in the nature of the functionals in current use (Strømsheim *et al.* 2011). Functionals based on the generalized gradient approximation are sometimes described as 'non-local', to emphasize the contrast with the local density approximation (LDA), but they are still really local in nature, as they are functionals of the density and its gradient at a single point in space. That is, they take the form

$$E[\rho] = \int K(\rho(\mathbf{r}), \nabla\rho(\mathbf{r}))\, \mathrm{d}^3\mathbf{r}, \tag{5.7.1}$$

where the form of the kernel K of the functional depends on the particular functional that is used. A better term for such functionals is 'semi-local'. The dispersion interaction, however, arises from correlated fluctuations in density at two well-separated points, usually in different molecules, and we can expect that an account of this effect can only be obtained within density functional theory by using a functional that depends on the density at two different points—a genuinely non-local functional. In this case eqn (5.7.1) is replaced by

$$E[\rho] = \iint K(\rho(\mathbf{r}), \nabla\rho(\mathbf{r}), \rho(\mathbf{r}'), \nabla\rho(\mathbf{r}'))\, \mathrm{d}^3\mathbf{r}\, \mathrm{d}^3\mathbf{r}'. \tag{5.7.2}$$

Functionals of this type have been developed by Langreth *et al.* (2009) and more recently by Vydrov and Van Voorhis (2010*a*,*b*). They are not yet in general use but appear to be successful (Hujo and Grimme 2011).

An alternative approach is to return to an old idea: the Hartree–Fock–dispersion (HFD) model, where an *ab initio* SCF calculation is supplemented by an empirical expression for the dispersion (Hepburn *et al.* 1975). This was reasonably successful for inert-gas atoms and non-polar molecules (Meath and Koulis 1991), but because the SCF method lacks intramolecular correlation it gives poor charge distributions and polarizabilities, so the HFD method was not useful for systems involving polar molecules and soon fell out of use.

A DFT+dispersion model should overcome these problems, because DFT can in principle provide exact electron densities, for both isolated molecules and molecules in external fields, so it can yield accurate charge distributions and polarizabilities. Correcting the DFT supermolecule energy for the missing long-range dispersion should therefore give good results. One way to do this is to use Møller–Plesset theory to obtain the dispersion correction. This tends to overestimate it, but an empirical $\Delta C_n R^{-n}$ correction gives good results (Tkatchenko *et al.* 2009).

The more usual procedure has been to use an empirical term for the whole dispersion correction. A difficulty is that the DFT calculation does begin to recover the dispersion contribution in the overlap region, since it is part of the correlation energy, so there is a danger

of double-counting. Claims that such an approach is successful initially met with severe criticism (Cybulski *et al.* 2002), but the method has since been refined considerably (Jurečka *et al.* 2007, Chai and Head-Gordon 2008, Grimme *et al.* 2010, Grimme 2011). In Grimme's DFT-D3 method, the added dispersion term depends only on separation and takes the form

$$E_{\text{disp}}^{\text{DFT-D}} = -\sum_{ab}\sum_{n=6,8,\ldots} s_n \frac{C_n^{ab}}{R_{ab}^n} f_n(R_{ab}). \tag{5.7.3}$$

The sum is taken over all atom pairs, possibly including atom pairs in the same molecule, if there are non-bonded interactions between them. The factor s_n scales the terms for $n > 6$; normally $s_6 = 1$ so that the orientationally averaged dispersion is asymptotically correct. The damping function $f_n(R_{ab})$ has the form

$$f_n(R_{ab}) = \left[1 + 6\left(\frac{R_{ab}}{s_{r,n}R_{ab}^0}\right)^{-\alpha_n}\right]^{-1}, \tag{5.7.4}$$

where R_{ab}^0 is a cutoff radius for atoms types a and b, $\alpha_n = n + 8$, and $s_{r,n}$ scales the cutoff radius for order n. The parameter values depend on the functional. In the DFT-D3 method, the C_6 in the 'dispersion' correction is calculated using time-dependent DFT, and the higher dispersion coefficients by the recursion formula (4.3.5). The interaction energies for the S22 set of small molecular complexes, proposed as a benchmark set by Jurečka *et al.* (2006), differ from good quality *ab initio* calculations with a mean absolute error of about 1 kJ mol^{-1}. The DFT-D method, with a plane-wave basis, has also been successful in the very demanding task of predicting the relative stabilities of different polymorphs of molecular crystals (Neumann and Perrin 2005, Van de Streek *et al.* 2010).

A more fundamental approach to the problem has been proposed by Becke and Johnson (2005, 2006). This uses the idea of the 'exchange hole' or 'Fermi hole'. The Pauli antisymmetry principle implies that two electrons of the same spin may never be in the same place. From the continuity of the electron density we can conclude that if there is an electron (the 'reference electron') at $\mathbf{r}$, the probability of finding another electron of the same spin at a nearby position $\mathbf{r}'$ is reduced relative to the average electron density. This reduction in probability is described by the Fermi hole (Slater 1951):

$$h_{X\sigma}(\mathbf{r},\mathbf{r}') = -\frac{1}{\rho_\sigma(\mathbf{r})}\sum_{ij}\psi_{i\sigma}(\mathbf{r})\psi_{i\sigma}(\mathbf{r})\psi_{j\sigma}(\mathbf{r}')\psi_{j\sigma}(\mathbf{r}'), \tag{5.7.5}$$

where the sum is taken over the occupied orbitals of spin σ. The hole describes a depletion of σ-spin density amounting to exactly one electron around the reference electron, so the electron and its hole have zero total charge. However, the hole is generally not spherical, so the electron with its hole will usually have a dipole moment, easily evaluated by integration over $\mathbf{r}'$. This dipole moment may induce a dipole in another molecule, leading to a dipole–induced-dipole interaction which, integrated over $\mathbf{r}$, comprises the dispersion interaction.

This treatment was admitted to be heuristic and unrigorous. Becke and Johnson (2007) gave a better treatment based on perturbation theory, though it uses the Unsöld approximation and treats the Fermi hole density as a point charge, so is still not rigorous. It has also been criticized on the grounds that the dispersion interaction is usually ascribed to Coulomb

interactions between fluctuating charges in the interacting molecules, rather than to exchange effects. However, Ángyán (2007) has shown that the Coulomb fluctuations are related to the exchange hole, while Hesselmann (2009) showed that a more rigorous approach confirms the validity of the principle, but requires a knowledge of the frequency-dependent density susceptibility, defined in eqn (2.5.12) and used in the exact long-range formulation of the dispersion energy, eqn (4.3.18).

The need to correct for the missing dispersion energy is not the only problem with density functional theory. The difficulty in finding a universal exchange-correlation functional is reflected in the differences between the predictions of the many functionals in the literature. One important deficiency is the description of exchange, which leads the repulsion between electrons to be exaggerated (Cohen *et al.* 2008*a*). This can be corrected to some extent by using a hybrid functional (p. 79), but unfortunately this increases the computational effort considerably (Griffiths *et al.* 2012).

Nevertheless, as our understanding of the strengths and limitations of density functional theory improves, it is becoming clear that it does have a place in the calculation of intermolecular interactions. Its great merit is that it is far more efficient computationally than conventional correlated methods, so it can be applied to much bigger systems. The lack of dispersion energy in standard DFT calculations has been a limitation, but the recent work described above promises to overcome that. Another important approach is provided by recent work, to be discussed in Chapter 6, which has shown that density functional theory provides a basis for efficient and remarkably accurate perturbation-theory methods for intermolecular interactions.

5.8 Semi-empirical methods

Although semi-empirical methods cannot be described as *ab initio*, a brief mention is appropriate here. The most time-consuming step of a true *ab initio* SCF calculation is the computation of the two-electron integrals (eqn (5.4.1)). Semi-empirical methods avoid this computational cost by neglecting most of them and approximating most of the rest. Many of the one-electron integrals are also approximated. The approximations involve empirical parameters which are determined by requiring the calculations to reproduce experimental data, for example on heats of formation of a range of small molecules. The AM1 (Dewar *et al.* 1985) and PM3 (Stewart 1989) methods are two popular examples. As they are calibrated against heats of formation, that is, against enthalpies of reactions involving the making and breaking of large numbers of chemical bonds, they cannot be expected to be reliable for calculating small energy differences such as the binding energies of molecular complexes. However, they are widely used to calculate structures and charge distributions of molecules that are too large for standard *ab initio* methods to be used. They are also sometimes used to obtain a first guess at the structure of a moderately large molecule, to save time in a subsequent geometry optimization using a true *ab initio* method. Semi-empirical methods have reached a high level of sophistication, and are quite reliable provided that they are used for the purposes for which they were designed.

5.9 Potential energy surfaces

Most *ab initio* programs provide facilities for finding the equilibrium geometry of a molecular complex by minimizing the energy with respect to geometrical coordinates. For many purposes, however, this isn't enough; it's often necessary to describe the potential energy surface.

The usual procedure is to calculate the energy at a number of geometries and to fit some sort of analytical function. This is a much more demanding task than finding a single-point energy or an optimized geometry. Up to six coordinates are needed to describe the relative configuration of two rigid molecules, and the set of geometries to be used must be chosen with care to make the best use of the available computing resources. If the molecules are to be treated as non-rigid, so that intramolecular coordinates need to be varied too, the problem becomes much more demanding. For a molecule as simple as water there are three internal vibrational coordinates—two OH distances and the HOH bond angle—so there are 12 coordinates altogether. If five points are chosen in each coordinate there are $5^{12} = 2\frac{1}{2}$ million points, so it is necessary to find a way to cover the space more efficiently. For larger molecules the number of internal coordinates increases rapidly, but it may be possible to treat many of the internal coordinates as fixed.

A possible approach is to calculate an initial PES at a low level of accuracy with a modest number of points, and use that to identify the regions that need to be covered by a more accurate treatment. Alternatively, information from initial calculations can be used to guide the choice of later geometries, for example to exclude high-energy regions of the surface. Collins and his group have developed automated methods of this sort (Jordan *et al.* 1995, Thompson *et al.* 1998).

In their calculations of the PES of water dimer, Huang *et al.* (2006) adopted the following procedure. They started with a choice of 14 O···O distances, concentrated near the known separation at the minimum-energy structure but extending to 100 bohr. At each of these distances, the five angles describing the intermolecular configuration, the four OH distances and the two HOH bond angles were varied, giving up to 2000 points at each distance and 15,000 configurations in all. A further 3000 points were added in regions of low energy (less than 2000 cm^{-1} above the minimum). Finally an analytic functional form was fitted to the energies at these points, and used to carry out a quantum diffusion Monte Carlo calculation of the ground vibrational state. The resulting wavefunction was used to identify regions where more points were needed, and a further 1800 points were added in these regions. In later work (Huang *et al.* 2008), approximately 10,000 more points were added on the basis of further diffusion Monte Carlo calculations.

A further problem with the development of potential energy surfaces is the matter of deformation energy—the correction arising from the distortion of each molecule in the field of its neighbours. As noted in §1.1.2, it can be important in hydrogen-bonded complexes, where the *A*–H bond is longer in an *A*–H···*B* hydrogen bond than in the isolated *A*–H molecule, the cost of stretching the bond being more than compensated by the improvement in binding energy. Taking account of such effects in the construction of potential energy surfaces complicates the calculation very greatly, and they are usually ignored.

5.10 Energy decomposition analysis

One of the limitations of the supermolecule approach is that it provides just a single number, the total interaction energy, at each configuration, in contrast to perturbation methods, which give a number of terms of well-defined physical significance. A number of methods have been proposed for separating the total interaction energy into physically meaningful components.

The first step is to separate out the energy due to geometrical distortion of the monomers. The monomer geometries usually change to some degree on the formation of the complex,

and in a Born–Oppenheimer picture the corresponding energy change, ΔE_{GD}, can be separated from the change in electronic energy. It can be evaluated by optimizing the structure of the complex, allowing the component molecules to distort, and then calculating, for each molecule separately, the electronic energy difference between the equilibrium and distorted configurations:

$$\Delta E_{\mathrm{GD}} = \sum_A (E^A_{\mathrm{dis}} - E^A_{\mathrm{eq}}) \tag{5.10.1}$$

The distorted molecules can now be assembled to form the cluster, and it is the change in electronic energy between the separated and assembled distorted molecules that we seek to break down into components.

Morokuma (1971) proposed a scheme for doing this. The initial scheme involved carrying out the following calculations, after first obtaining the unperturbed wavefunctions Ψ^A_0 and Ψ^B_0 for the two (distorted) molecules. The unperturbed energy for the supersystem is the sum of the energies of the isolated molecules: $E_0 = E^A_0 + E^B_0$.

1. Here the wavefunction is a simple product $\Psi^A_0\Psi^B_0$ of the unperturbed wavefunctions. The expectation value of the energy is $E_1 = E_0 + E_{\mathrm{es}}$; that is, the change in energy yields the electrostatic energy of interaction of the unperturbed charge distributions.
2. Here the wavefunction is still a simple product, antisymmetric only with respect to permutations of electrons within A and B but not with respect to permutations that exchange electrons between the molecules. This is optimized with all integrals deleted that contain overlap between the basis functions of molecule A and those of molecule B. That is, integrals involving products of the form $\chi^A_i(1)\chi^B_j(1)$ are deleted. However, intermolecular Coulomb integrals of the form $\int \chi^A_i(1)\chi^A_j(1)(r_{12})^{-1}\chi^B_k(2)\chi^B_l(2)\,\mathrm{d}\tau_1\,\mathrm{d}\tau_2$ survive, so each molecule's wavefunction distorts under the influence of the other's electrostatic field, but with no mixing of the basis functions of one molecule into the orbitals of the other. The resulting energy contains the induction energy: $E_2 = E_0 + E_{\mathrm{es}} + E_{\mathrm{ind}}$.
3. Here the wavefunction is an antisymmetrized product of the unperturbed wavefunctions: $\Psi_3 = \mathcal{A}\Psi^A_0\Psi^B_0$. As we shall see in Chapter 8, the effect of the antisymmetrization is to introduce the exchange repulsion: $E_3 = E_0 + E_{\mathrm{es}} + E_{\mathrm{er}}$.
4. Finally, the antisymmetrized product is optimized using the full Fock matrix for the supersystem. In the original scheme, the resulting energy was written as $E_4 = E_0 + E_{\mathrm{es}} + E_{\mathrm{ind}} + E_{\mathrm{er}} + E_{\mathrm{ct}}$, so that the remaining part of the interaction energy was ascribed to charge transfer.

This scheme is unsatisfactory, because in step 2 of the calculation, when the wavefunction of each molecule is optimized in the field of the other, the Pauli principle is not satisfied because the wavefunction is not antisymmetrized. The result is an overestimate of the induction energy, which can be quite severe at short range (Gutowski and Piela 1988, Frey and Davidson 1989, Cybulski and Scheiner 1990).

Kitaura and Morokuma (1976, 1981) later suggested a modified approach. They pointed out that parts of the Fock and overlap matrices can be suppressed, at every iteration, and the resulting energy corresponds to the omission of certain terms in the interaction. The Hartree–Fock equations are expressed in the basis of molecular orbitals for the separated molecules, but including all the intermolecular interactions, and can be partitioned according to whether the orbitals belong to molecule A or molecule B, and according to whether they are occupied

$$\mathbf{F} = \begin{array}{c} \\ A_{\text{occ}} \\ A_{\text{virt}} \\ B_{\text{occ}} \\ B_{\text{virt}} \end{array} \begin{array}{c} \begin{array}{cccc} A_{\text{occ}} & A_{\text{virt}} & B_{\text{occ}} & B_{\text{virt}} \end{array} \\ \begin{pmatrix} F_{oo}^{AA} & F_{ov}^{AA} & F_{oo}^{AB} & F_{ov}^{AB} \\ (\text{esx}) & (\text{ind}) & (\text{ex}') & (\text{ct}) \\ F_{vo}^{AA} & F_{vv}^{AA} & F_{vo}^{AB} & F_{vv}^{AB} \\ (\text{ind}) & (\text{esx}) & (\text{ct}) & (\text{ex}') \\ F_{oo}^{BA} & F_{ov}^{BA} & F_{oo}^{BB} & F_{ov}^{BB} \\ (\text{ex}') & (\text{ct}) & (\text{esx}) & (\text{ind}) \\ F_{vo}^{BA} & F_{vv}^{BA} & F_{vo}^{BB} & F_{vv}^{BB} \\ (\text{ct}) & (\text{ex}') & (\text{ind}) & (\text{esx}) \end{pmatrix} \end{array}$$

Fig. 5.2 Partitioning of the Fock matrix for Kitaura–Morokuma energy decomposition.

or virtual. For the Fock matrix the partitioning is shown in Fig. 5.2; the overlap matrix is partitioned in the same way. If now the normal SCF procedure is followed, but with certain terms omitted, we get particular parts of the interaction energy. Specifically:

1. If all the off-diagonal blocks are suppressed, leaving only the 'esx' blocks, the resulting energy contains the electrostatic term plus part of the exchange–repulsion. If in addition we suppress matrix elements that involve products of orbitals on different molecules (i.e., intermolecular exchange integrals), we are left with only the electrostatic term.
2. If the off-diagonal blocks labelled 'ind' are retained, along with the 'esx' blocks, and intermolecular exchange integrals are suppressed, the induction energy is obtained as well as the electrostatic term.
3. If only the 'esx' and 'ex′' blocks are retained, and intermolecular exchange integrals are not suppressed, the exchange energy is obtained.
4. If only the 'esx' and 'ct' blocks are retained, the result contains the charge transfer energy 'ct'.
5. If all the off-diagonal terms are retained, the result is the complete supermolecule energy, which contains all the above effects together with an assortment of cross-terms, which together are denoted by E_{mix}.

It will be apparent that as described, this scheme suffers from the same disadvantage as any other supermolecule calculation: it is affected by basis set superposition error. This manifests itself especially in the charge transfer terms, in which virtual orbitals of one molecule are allowed to mix with occupied orbitals of the other. One cure for this, as in the ordinary supermolecule treatment, is to perform the reference calculations for the isolated molecules in the dimer basis. Such a method was suggested by Sokalski *et al.* (Sokalski *et al.* 1983*a*,*b*, Cammi *et al.* 1985), though Gutowski and Piela (1988) claim that the form of the resulting decomposition is incorrect. The alternative is to use basis sets that are good enough to make BSSE unimportant.

Other problems with this method are that the individual components depend on the choice of basis set, and that the E_{mix} term, which has no clear physical interpretation, may be as large as the other terms (Gutowski and Piela 1988). Nevertheless it has been very widely used.

Bickelhaupt and Baerends (2000) have proposed an energy decomposition scheme for density functional calculations. They separate the interaction energy ΔE into four components:

$$\Delta E = \Delta E_{\text{def}} + \Delta E_{\text{es}} + \Delta E_{\text{Pauli}} + \Delta E_{\text{oi}}. \tag{5.10.2}$$

Here ΔE_{def} is the energy needed to deform the separate molecules from their equilibrium structures into the geometry that they have in the complex; ΔE_{es} is the classical electrostatic interaction between the distorted molecules in the complex; ΔE_{Pauli} is the repulsive interaction between occupied orbitals; and ΔE_{oi} arises from occupied–virtual orbital mixing, and includes induction, charge transfer and dispersion. Cybulski and Seversen (2003) have proposed a similar scheme. The form of the energy expression in DFT makes the decomposition much more straightforward and more detailed than the Morokuma schemes, but its main application has been in highlighting the limitations of DFT in the calculation of intermolecular interactions, as mentioned in §5.7.

Khaliullin *et al.* (2007) have proposed yet another scheme, which has the merit of working with fully antisymmetrized and variationally optimized wavefunctions at each step. They start from a fully antisymmetrized wavefunction that uses the molecular orbitals of the isolated molecules. This gives the electrostatic and exchange-repulsion terms. The induction energy is obtained by carrying out a variational calculation in which the orbitals of each molecule are constrained to be strictly localized on that molecule (no contributions from the atomic orbitals of other molecules) but are not constrained to be orthogonal to the orbitals of other molecules. Finally the charge-transfer energy is obtained from perturbation theory; it can be corrected for BSSE if necessary.

6

Perturbation Theory of Intermolecular Forces at Short Range

6.1 Introduction

The perturbation theory for well-separated molecules described in Chapter 4 (the 'long-range approximation' or 'polarization approximation') is very successful if the molecules are a long distance apart, but at short range it fails completely. Part of the reason for the failure of the theory as usually formulated is that the multipole expansion breaks down, but as we have seen, the multipole expansion is not fundamental to the theory, since it is possible to use a 'non-expanded' treatment. We shall see in Chapter 7 how to overcome the failure of the multipole expansion to converge without resorting to this device.

A more fundamental failure is that the repulsion between molecules that occurs at short range is completely missing from the long-range theory. This failure arises from the fact that if the molecules are close enough for their wavefunctions to overlap, we can no longer ignore exchange, as we did in Chapter 4. To see the effect that this has on the energy, it will suffice initially to study one-electron atoms, and to compare the expectation value of the energy for an antisymmetrized wavefunction with the expectation value for a simple product. We shall see that at long range the result is the same, but at short range new terms appear that can be identified as the repulsion energy.

For two hydrogen atoms in $1s$ states, with parallel spins, the zeroth-order wavefunction in the long-range treatment is $\psi = |a^\alpha(1)b^\alpha(2)\rangle$, a simple product of the normalized $1s$ wavefunction a for atom A and the $1s$ wavefunction b for atom B, both with α spin. In this treatment, electron 1 is associated with atom A and electron 2 with atom B, and exchange is ignored. In the following we drop the spin superscripts, as integration over the spin functions just leads to a factor of +1. We obtain the energy of the system to first order in the usual way, by evaluating $\langle\psi|\mathcal{H}|\psi\rangle/\langle\psi|\psi\rangle$. The Hamiltonian is

$$\begin{aligned}\mathcal{H} &= -\tfrac{1}{2}\nabla_1^2 - \tfrac{1}{2}\nabla_2^2 - \frac{1}{r_{A1}} - \frac{1}{r_{A2}} - \frac{1}{r_{B1}} - \frac{1}{r_{B2}} + \frac{1}{r_{12}} + \frac{1}{r_{AB}} \\ &= \mathcal{H}^A(1) + \mathcal{H}^B(2) - \frac{1}{r_{A2}} - \frac{1}{r_{B1}} + \frac{1}{r_{12}} + \frac{1}{r_{AB}},\end{aligned}$$

so the energy in the long-range approximation is

$$\begin{aligned}
W_{\rm PA} &= \langle\psi|\mathcal{H}|\psi\rangle \\
&= \langle a(1)b(2)\big|\mathcal{H}\big|a(1)b(2)\rangle \\
&= \Big\langle a(1)b(2)\Big|W_a + W_b - \frac{1}{r_{A2}} - \frac{1}{r_{B1}} + \frac{1}{r_{12}} + \frac{1}{r_{AB}}\Big|a(1)b(2)\Big\rangle \\
&= W_a + W_b + U_{\rm es}.
\end{aligned}$$

Here $U_{\rm es}$ is the classical electrostatic interaction energy between the unperturbed charge densities:

$$\begin{aligned}
U_{\rm es} = &-\int \rho^b(2)\frac{1}{r_{A2}}\,\mathrm{d}^3\mathbf{r}_2 - \int \rho^a(1)\frac{1}{r_{B1}}\,\mathrm{d}^3\mathbf{r}_1 \\
&+ \int \rho^a(1)\rho^b(2)\frac{1}{r_{12}}\,\mathrm{d}^3\mathbf{r}_1\,\mathrm{d}^3\mathbf{r}_2 + \frac{1}{r_{AB}},
\end{aligned} \tag{6.1.1}$$

where $\rho^a(1) = |a(1)|^2$ is the electron density for the unperturbed atom A and likewise $\rho^b(1) = |b(1)|^2$.

If the charge densities overlap, however, we should antisymmetrize, so that the wavefunction for the system becomes $\Psi = \big|a(1)b(2) - a(2)b(1)\big\rangle$. This is not normalized; the normalization integral is

$$\int |\Psi|^2\,\mathrm{d}\tau_1\,\mathrm{d}\tau_2 = \langle a(1)b(2) - a(2)b(1)\big|a(1)b(2) - a(2)b(1)\rangle = 2 - 2S^2, \tag{6.1.2}$$

where $S = \langle a(1)\big|b(1)\rangle$. The Hamiltonian is just the same as before, but by reorganizing the terms we can also write it as

$$\mathcal{H} = \mathcal{H}^A(2) + \mathcal{H}^B(1) - \frac{1}{r_{A1}} - \frac{1}{r_{B2}} + \frac{1}{r_{12}} + \frac{1}{r_{AB}},$$

so for the 'symmetric' treatment the energy to first order is

$$\begin{aligned}
W_{\rm S} =& \frac{\langle\Psi|\mathcal{H}|\Psi\rangle}{\langle\Psi|\Psi\rangle} \\
&= \langle a(1)b(2) - a(2)b(1)\big|\mathcal{H}\big|a(1)b(2) - a(2)b(1)\rangle/(2 - 2S^2) \\
&= \langle a(1)b(2)\big|\mathcal{H}\big|a(1)b(2) - a(2)b(1)\rangle/(1 - S^2) \\
&= \frac{1}{1 - S^2}\Big[\Big\langle a(1)b(2)\Big|W_a + W_b - \frac{1}{r_{A2}} - \frac{1}{r_{B1}} + \frac{1}{r_{12}} + \frac{1}{r_{AB}}\Big|a(1)b(2)\Big\rangle \\
&\qquad - \Big\langle a(1)b(2)\Big|W_a + W_b - \frac{1}{r_{A1}} - \frac{1}{r_{B2}} + \frac{1}{r_{12}} + \frac{1}{r_{AB}}\Big|a(2)b(1)\Big\rangle\Big] \\
&= (W_a + W_b) + \frac{1}{1 - S^2}\Big[\Big\langle a(1)b(2)\Big|-\frac{1}{r_{A2}} - \frac{1}{r_{B1}} + \frac{1}{r_{12}} + \frac{1}{r_{AB}}\Big|a(1)b(2)\Big\rangle \\
&\qquad - \Big\langle a(1)b(2)\Big|-\frac{1}{r_{A2}} - \frac{1}{r_{B1}} + \frac{1}{r_{12}} + \frac{1}{r_{AB}}\Big|a(2)b(1)\Big\rangle\Big].
\end{aligned}$$

There has been some juggling of labels here; we can exchange electron labels 1 and 2 provided we do it throughout an integral.

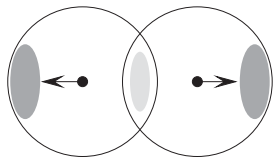

Fig. 6.1 The electron density of a pair of closed-shell atoms is less than the sum of the atomic densities between the nuclei (light shading) and greater in the region remote from the other atom (darker shading).

We can express this result as a sum of the unperturbed energy $W_a + W_b$, the classical electrostatic interaction U_{es} as in the long-range approximation, and some new terms, which are

$$\begin{aligned} U_{\text{er}} &= \frac{S^2}{1-S^2}\Big\langle a(1)b(2)\Big|-\frac{1}{r_{A2}}-\frac{1}{r_{B1}}+\frac{1}{r_{12}}\Big|a(1)b(2)\Big\rangle \\ &\quad -\frac{1}{1-S^2}\Big\langle a(1)b(2)\Big|-\frac{1}{r_{A2}}-\frac{1}{r_{B1}}+\frac{1}{r_{12}}\Big|a(2)b(1)\Big\rangle \\ &= -\frac{S^2}{1-S^2}\Big\{\Big\langle b\Big|\frac{1}{r_A}|b\Big\rangle+\Big\langle a\Big|\frac{1}{r_B}|a\Big\rangle-\Big\langle a(1)b(2)\Big|\frac{1}{r_{12}}\Big|a(1)b(2)\Big\rangle\Big\} \\ &\quad +\frac{1}{(1-S^2)}\Big\{S\Big\langle a\Big|\frac{1}{r_A}+\frac{1}{r_B}\Big|b\Big\rangle-K_{ab}\Big\}. \end{aligned} \tag{6.1.3}$$

$K_{ab} \equiv (ab|ba) \equiv \langle a(1)b(2)|1/r_{12}|a(2)b(1)\rangle$ is the exchange integral between the orbitals a and b, and gives a negative, i.e. attractive, contribution to the energy, while the term $\langle a|1/r_A + 1/r_B|b\rangle$ describes a repulsion arising from the overlap of the electrons from the two molecules. The other terms can be thought of as corrections to the electrostatic energy. The net effect of the whole expression is repulsive, and it is called the *exchange–repulsion* energy. Note that if there is no overlap ($S = 0$) the antisymmetrized wavefunction Ψ gives the same result as the simple product ψ.

It is illuminating to think about these effects in terms of the charge density. For the simple product wavefunction $\big|a(1)b(2)\big\rangle$, the charge density is merely $\rho^a + \rho^b$, the superposition of the unperturbed atomic charge distributions. For the antisymmetrized wavefunction Ψ, however, it is

$$\begin{aligned} \rho(\mathbf{r}) &= \frac{1}{2-2S^2}\int((\delta(\mathbf{r}-\mathbf{r}_1)+\delta(\mathbf{r}-\mathbf{r}_2))\Psi^2\ \mathrm{d}^3\mathbf{r}_1\ \mathrm{d}^3\mathbf{r}_2 \\ &= \frac{1}{1-S^2}((\rho^a(\mathbf{r})+\rho^b(\mathbf{r})-2S\,a(\mathbf{r})b(\mathbf{r})). \end{aligned} \tag{6.1.4}$$

Now on the plane between the atoms and equidistant from them, the two atomic wavefunctions have equal values, and $\rho^a(\mathbf{r}) = \rho^b(\mathbf{r}) = a(\mathbf{r})b(\mathbf{r})$. Consequently the density is $\rho(\mathbf{r}) = 2\rho^a(\mathbf{r})/(1+S)$, which is *less* than the density $\rho^a(\mathbf{r}) + \rho^b(\mathbf{r}) = 2\rho^a(\mathbf{r})$ on the same plane for the simple product wavefunction. At a point on the side of atom A remote from atom B, on the other hand, we have $b(\mathbf{r}) \ll a(\mathbf{r})$ and $\rho^b(\mathbf{r}) \ll \rho^a(\mathbf{r})$, so $\rho(\mathbf{r}) \approx \rho^a(\mathbf{r})/(1-S^2)$, which is *greater* than the density for the product wavefunction.

For the antisymmetrized wavefunction, then, as compared with the product wavefunction, the electron density is decreased between the atoms and increased at the side of each atom

remote from the other. We can now apply the Hellmann–Feynman theorem (eqn 5.5.1), which tells us that the force on a nucleus can be evaluated from the charge distribution as if it were classical, and we see that the change in the charge distribution produces an additional force on each nucleus in the direction away from the other. In other words, the effect of the antisymmetrization is to modify the electron density in such a way as to cause a repulsive force on the nuclei. (See Fig. 6.1.) This is the force corresponding to the exchange–repulsion energy $U_{\rm er}$.

So far we have assumed that the spins associated with orbitals a and b are the same (both α or both β, giving in either case a component of the triplet state $^3\Sigma_u$). If they are different, the overlap integral S becomes zero, and $U_{\rm er}$ vanishes. Thus there is no exchange–repulsion for electrons of opposite spin. In the more usual closed-shell case, therefore, we can regard the repulsion as arising purely between electrons of the same spin, while electrons of opposite spin merely behave like classical charge distributions.

If the spins are different in the hydrogen-atom case, of course, chemical bonding occurs. This arises because there are two states with opposite spin, $|a^\alpha b^\beta\rangle$ and $|a^\beta b^\alpha\rangle$, and they are strongly coupled. The matrix element of the Hamiltonian between them is

$$\begin{aligned}
&\langle a^\alpha b^\beta|\mathcal{H}|a^\beta b^\alpha\rangle \\
&\quad = \tfrac{1}{2}\langle a^\alpha(1)b^\beta(2) - a^\alpha(2)b^\beta(1)\big|\mathcal{H}\big|a^\beta(1)b^\alpha(2) - a^\beta(2)b^\alpha(1)\rangle \\
&\quad = \langle a^\alpha(1)b^\beta(2)\big|\mathcal{H}\big|a^\beta(1)b^\alpha(2) - a^\beta(2)b^\alpha(1)\rangle \\
&\quad = \Big\langle a^\alpha(1)b^\beta(2)\Big|W_a + W_b - \frac{1}{r_{A2}} - \frac{1}{r_{B1}} + \frac{1}{r_{12}} + \frac{1}{r_{ab}}\Big|a^\beta(1)b^\alpha(2)\Big\rangle \\
&\qquad - \Big\langle a^\alpha(1)b^\beta(2)\Big|W_a + W_b - \frac{1}{r_{A1}} - \frac{1}{r_{B2}} + \frac{1}{r_{12}} + \frac{1}{r_{AB}}\Big|a^\beta(2)b^\alpha(1)\Big\rangle \\
&\quad = -S^2(W_a + W_b) - \Big\langle a(1)b(2)\Big|-\frac{1}{r_{A2}} - \frac{1}{r_{B1}} + \frac{1}{r_{12}} + \frac{1}{r_{AB}}\Big|a(2)b(1)\Big\rangle.
\end{aligned}$$

The mixing of these two states produces new states that are the sum and difference: $|a^\alpha b^\beta\rangle \pm |a^\beta b^\alpha\rangle$. The reader may care to verify that one of these is the third component of the $^3\Sigma_u$ state, and has the same energy as the other two components, so it suffers exchange repulsion just as they do, while the other state is substantially lowered in energy and becomes the $^1\Sigma_g$ bonding state of the H_2 molecule.

Thus we see that antisymmetrization introduces new effects that are completely missing when we use a simple product wavefunction. The most important of these for our purposes is that there is a strong repulsion between closed-shell molecules when their wavefunctions overlap significantly. We have to modify the perturbation treatment so as to take this into account correctly.

6.1.1 Short-range perturbation theory

Unfortunately the need for antisymmetrization complicates the theory very considerably. An argument that has often been given is the following. If we assign electrons to individual molecules in order to separate the Hamiltonian into an unperturbed part $\mathcal{H}^0$ and a perturbation $\lambda\mathcal{H}'$ (where $\lambda = 1$ for the perturbed problem), we obtain a zeroth-order Hamiltonian and a perturbation that are not symmetric with respect to permutations P that exchange electrons between the molecules:

$$[P, \mathcal{H}^0] \neq 0, \qquad [P, \lambda\mathcal{H}'] \neq 0, \tag{6.1.5}$$

but the total Hamiltonian is symmetric:

$$[P, \mathcal{H}^0 + \lambda\mathcal{H}'] = 0. \tag{6.1.6}$$

Combining these equations we find

$$[P, \mathcal{H}^0] = -[P, \lambda\mathcal{H}'] \neq 0, \tag{6.1.7}$$

so that we have a non-zero first-order quantity that is equal to a zeroth-order quantity. This appears to contradict the basic assumption that we make when we separate the perturbation equations into their different orders, i.e., that we can collect terms in different powers of the perturbation and equate them separately to zero.

However, Adams (2002*a*) has pointed out that we are contemplating the expansion of the energy and wavefunction as a power series in λ, and that therefore we must treat λ as a variable, not necessarily equal to 1. Indeed, we often think of switching on the perturbation by varying λ from 0 to 1. If λ need not be 1, then eqn (6.1.6) is not true, and the argument fails.

We are still in trouble, though, because the Hamiltonian $\mathcal{H}^0 + \lambda\mathcal{H}'$ is symmetric with respect to all electron permutations only when $\lambda = 1$. For other values of λ we only have symmetry with respect to the intramolecular electron permutations, and it becomes possible for the perturbation theory to lead to unphysical states that do not satisfy the Pauli principle (Claverie 1971).

A closely related problem has to do with the symmetry of the wavefunctions. If the wavefunctions of the two molecules overlap, then, as we have seen, we should antisymmetrize the product functions that we use as zeroth-order wavefunctions, in order to satisfy the Pauli principle. That is,

$$|m_A n_B\rangle = \mathcal{A}|m_A\rangle|n_B\rangle, \tag{6.1.8}$$

where the notation is now to be understood as implying that $|m_A n_B\rangle$ is antisymmetric with respect to all electron permutations, whereas $|m_A\rangle|n_B\rangle$ is antisymmetric with respect only to permutations of the A electrons among themselves and of the B electrons among themselves. But whereas the simple products are orthogonal, even at short range (because $|m_A\rangle$ and $|n_B\rangle$ refer to different electrons) the antisymmetrized products are not. The easiest way to see this is to look at an example. Consider the case of two hydrogen atoms, so that the ground states $|0_A\rangle$ and $|0_B\rangle$ are $1s$ states, and take an excited state $|1_B\rangle$ in which atom B is excited to a $2p$ state. Then

$$\begin{aligned}
\langle 0_A 0_B \big| 0_A 1_B\rangle &= \langle \mathcal{A}s_A(1)s_B(2) \big| \mathcal{A}s_A(1)p_B(2)\rangle \\
&= \tfrac{1}{2}\langle s_A(1)s_B(2) - s_A(2)s_B(1) \big| s_A(1)p_B(2) - s_A(2)p_B(1)\rangle \\
&= \tfrac{1}{2}[\langle s_A(1)\big|s_A(1)\rangle\langle s_B(2)\big|p_B(2)\rangle - \langle s_A(1)\big|p_B(1)\rangle\langle s_B(2)\big|s_A(2)\rangle \\
&\qquad - \langle s_B(1)\big|s_A(1)\rangle\langle s_A(2)\big|p_B(2)\rangle + \langle s_B(1)\big|p_B(1)\rangle\langle s_A(2)\big|s_A(2)\rangle], \\
&= -\langle s_A\big|p_B\rangle\langle s_A\big|s_B\rangle,
\end{aligned} \tag{6.1.9}$$

and this need not be zero.

Now, as we know from elementary quantum mechanics, eigenstates of any hermitian operator with different eigenvalues are orthogonal. If the states $|m_A n_B\rangle$ do not form an orthogonal

set they cannot be eigenstates of any hermitian operator. To put it another way, there can be no hermitian zeroth-order Hamiltonian that has these antisymmetrized products as eigenstates.

This is a serious difficulty. It does not mean that we can no longer use perturbation theory, but it does mean that we cannot use the standard Rayleigh–Schrödinger treatment. In its place we have to put something else, but there is no unique approach, and many different methods have been used. Comparisons between the different methods are difficult, because they use the same terminology for quantities that may be differently defined. For example, all methods yield a quantity that at long range becomes the induction energy. At short range, however, this becomes modified, and the modifications are different in different methods. A short-range term such as the charge-transfer energy may be viewed as a separate effect or included as part of the induction energy. Furthermore, because there is no natural and unambiguous separation into orders of perturbation theory, a term that is second-order in one method may be viewed as including third-order contributions in another.

The view has even been expressed that if Rayleigh–Schrödinger perturbation theory cannot be used then no other approach is valid, because the ideas and nomenclature of this method are so ingrained in the consciousness of the theoretician that other approaches that appear superficially similar but adopt different definitions will be misleading. This can be viewed either as a strictly purist attitude or as a counsel of defeat. It seems more constructive to take the view that intermolecular interactions remain a suitable field for the application of perturbation theory, because the effects are relatively small even in the region of overlap, and to look for some approach that yields satisfactory results, even if the conventional Rayleigh–Schrödinger interpretation of the formulae does not apply. Indeed, one may go further, and take the view that the lack of uniqueness in the theory gives us the flexibility to choose an approach that optimizes the convergence of the perturbation series.

It might be thought possible in principle to carry out ordinary Rayleigh–Schrödinger perturbation theory, starting with the simple unsymmetrized product functions, and using the same functions throughout the calculation, with certain electrons assigned to molecule A and the rest to molecule B. The zeroth-order function for two hydrogen atoms would then be $|a(1)b(2)\rangle$, and the result of the perturbation theory, if it converges, would be close to the antisymmetrized function $\sqrt{1/2}|a(1)b(2) - a(2)b(1)\rangle$. If we use a complete basis on atom A to describe electron 1, we could express $b(1)$ in terms of these basis functions, and conversely $a(2)$ could be expressed in terms of the basis set on atom B. We can see, however, that in practical applications, where the size of the basis set is limited, there would be no possibility of approximating the $a(2)b(1)$ term accurately by this technique. In any case the convergence of such a treatment would be slow, because the difference between the unperturbed function $|a(1)b(2)\rangle$ and the perturbed function $\sqrt{1/2}|a(1)b(2) - a(2)b(1)\rangle$ is not in any sense small. In fact the overlap between them tends to $\sqrt{1/2}$ as the separation increases. In the many-electron case, with n_A electrons on A and n_B on B, there are $(n_A + n_B)!/n_A!n_B!$ ways of assigning the electrons, and the overlap between any particular one of these and the antisymmetrized function, which is a linear combination of all of them, tends to $\sqrt{n_A!n_B!/(n_A + n_B)!}$ at long range, and this becomes smaller and smaller as the number of electrons increases.

Even for the H···H case, Kutzelnigg (1992) showed analytically that the radius of convergence of the Rayleigh–Schrödinger perturbation expansion, viewed as a power series in λ, is only slightly greater than 1—in fact it exceeds 1 by an amount of order e^{-2R}, and so approaches 1 as $R \to \infty$. Cwiok *et al.* (1992) confirmed this result numerically, and found that

to calculate the interaction energy accurately for H···H at 8 bohr, it was necessary to sum the Rayleigh–Schrödinger expansion approximately to infinite order. Clearly this is not possible in practical applications.

However, there is another, more serious, problem with the Rayleigh–Schrödinger expansion, already alluded to above. If we work with wavefunctions that are antisymmetrized with respect to the electrons of A, and with respect to those of B, but we do not impose antisymmetry with respect to exchanges of electrons between A and B, then there are solutions of the Schrödinger equation that do not satisfy the Pauli principle, and that lie lower in energy than all the antisymmetric ones. For the He···H system, for instance, it is possible to write down a wavefunction in which all the electrons, including the one formally assigned to H as well as those assigned to He, occupy the He $1s$ orbital. This Pauli-forbidden, or 'unphysical', state is clearly lower in energy than any correctly antisymmetric physical state. Claverie (1971) was the first to point out this problem; he argued that if the Rayleigh–Schrödinger expansion starting from the lowest-energy unperturbed state converged at all, it would converge to the lowest-energy unphysical state, which he called the 'mathematical ground state', and not to the lowest physical state. Moreover, for any system containing at least one atom with atomic number greater than 2, the physical ground state is buried in a continuum of unphysical states, below which lies an infinite number of discrete unphysical states (Morgan and Simon 1980, Adams 1990).

Consequently it is necessary to find new versions of perturbation theory that overcome these problems. Such methods—methods that deal with intermolecular perturbation theory in the region where exchange cannot be ignored—are generally called 'exchange perturbation theories'. Claverie (1978) gave a very thorough account both of the mathematical issues and of the attempts up to that time to overcome them. A more recent account has been given by Szalewicz *et al.* (2005). The methods so far proposed fall into two main groups. The 'symmetric' methods take as their unperturbed functions the set of antisymmetrized products (6.1.8). These are not orthogonal, as we have seen, and various schemes have been proposed to handle the non-orthogonality. 'Symmetry-adapted perturbation theories', on the other hand, start from the simple product functions $|m_A\rangle|n_B\rangle$, without antisymmetrization, so that in the unperturbed problem each electron is assigned to one or other molecule. These unperturbed functions are orthogonal, but because the perturbed wavefunction must be antisymmetric it is necessary to carry out an antisymmetrization at each order of perturbation theory, or to adopt some other technique to ensure that even if the wavefunction is not antisymmetric the energy is nevertheless correct.

6.2 Symmetric perturbation methods

6.2.1 Expansion in powers of overlap

Since it is to a large degree the non-orthogonality of the antisymmetrized products that causes the difficulties, an approach that has been adopted by some workers is simply to neglect the non-orthogonality at zeroth order. That is, the overlap matrix $\mathbf{S}$ is written in the form $\mathbf{S} = \mathbf{I} + \mathbf{t}$, and the assumption made that the off-diagonal part $\mathbf{t}$ of the overlap matrix is small. (Note that the antisymmetrized product functions require normalization first.) It is then possible to develop a treatment involving expansion in powers of the overlap as well as in powers of the perturbation, and because the unperturbed functions are orthogonal to zeroth order in the overlap, a hermitian unperturbed Hamiltonian can be found. Several methods of this kind have

been proposed (Basilevsky and Berenfeld 1972*a*,*b*, Kvasnicka *et al.* 1974, Stone and Erskine 1980, Mayer and Surjan 1993).

Unfortunately this approach does not give good results. The assumption of small overlap becomes increasingly untenable as the quality of the calculation is improved. Even with basis sets that are far from complete, diffuse basis functions on one molecule may overlap strongly with similar functions on the other, so that the series in powers of overlap converges poorly or not at all (Wilkinson 1965, Gray and Stone 1970).

The methods of this type were for the most part proposed at a time when the capacity of computers was limited, and the problems that arise from the introduction of diffuse basis functions were not apparent. Even without diffuse basis functions, however, the results are not very good. In a calculation using a minimal basis for two H_2 molecules, for example, where the exact result can be calculated analytically, the energy to second order was in error by 50%, even when the intermolecular overlap integrals were only about 0.1 (Hayes and Stone 1984*a*). Since the formulae of perturbation theory become increasingly complicated after second order, any method that is to be useful in practice must give good results at second order.

6.2.2 Orthogonalization of the antisymmetrized-product basis

An alternative way to avoid the difficulties that arise from a non-orthogonal basis might be to construct an orthogonal basis by Schmidt or Löwdin orthogonalization. Unfortunately this suffers from similar difficulties. It is easier to think about it in terms of molecular orbitals rather than many-electron states. We have a set of orbitals ψ_k^A for molecule A, orthogonal among themselves, and a similar set $\psi_{k'}^B$ for molecule B, also orthogonal among themselves but not to the ψ_k^A. In each case there is a set of occupied orbitals and a set of vacant (virtual) orbitals. In order to make $\psi_{k'}^B$ orthogonal to the ψ_k^A it is necessary to add a little of each ψ_k^A to it. In a Schmidt treatment, we might have

$$\tilde{\psi}_{k'}^B = \psi_{k'}^B - \sum_k \psi_k^A \langle \psi_k^A | \psi_{k'}^B \rangle.$$

Inevitably, there is a contamination of the orbitals of B by those of A. This particular formulation is unsymmetrical between A and B, so it is not a satisfactory method. We might seek to improve it by a procedure such as the following. Take a Slater determinant describing the SCF ground state of the unperturbed $A + B$ system. First orthogonalize the occupied orbitals of A with those of B, using a symmetrical method such as Löwdin orthogonalization (Löwdin 1950). This ensures that the SCF description of the ground state is unchanged, because it merely mixes the columns of the Slater determinant. Then Schmidt orthogonalize the virtual orbitals of A and B to all the occupied orbitals. This will modify the virtual orbitals but leave the occupied orbitals unchanged. Finally, orthogonalize the virtual orbitals of A symmetrically with those of B. This procedure achieves orthogonality of the orbitals, and hence of the states constructed from them, while changing the low-lying states as little as possible, and the ground state not at all. Reed *et al.* (1986) described a variant of this procedure suitable for correlated wavefunctions, in which the natural orbitals for the unperturbed molecules were used as a starting point, and their procedure preserved the form of the orbitals with occupation numbers near 2 as far as possible consistent with achieving orthogonality. Nevertheless all such schemes show the same feature: there is inevitably a contamination of the orbitals

of each molecule by those of the other. This means that it becomes difficult to regard molecular states constructed from these orbitals as unperturbed states in any natural sense, and this makes the physical interpretation of numerical results difficult and very misleading. In particular, it seems to lead to much larger estimates of the charge transfer energy than other methods (Reed *et al.* 1986, 1988, King and Weinhold 1995).

6.2.3 Biorthogonal functions

An alternative approach has been proposed by Surjan *et al.* (1985), following earlier work by Gouyet (1973). Denoting a member $|m_A n_B\rangle = \mathcal{A}|m_A\rangle|n_B\rangle$ of the set of antisymmetrized products by $|I\rangle$, we can construct the overlap matrix, with elements $S_{IJ} = \langle I|J\rangle$. We define a new 'biorthogonal' set of functions $|\bar{I}\rangle = \sum_J |J\rangle(S^{-1})_{JI}$. By construction these satisfy $\langle\bar{K}|I\rangle = \delta_{KI}$, as can easily be verified. We now define an operator $\mathcal{H}^0 = \sum_J |J\rangle W_J^0\langle\bar{J}|$. Its eigenvectors are the $|I\rangle$: $\mathcal{H}^0|I\rangle = W_I^0|I\rangle$. $\mathcal{H}^0$ is not hermitian, but the *matrix* $\mathbf{H}$ with elements $H_{JI} = \langle\bar{J}|\mathcal{H}^0|I\rangle$ is not only hermitian but diagonal. (If this appears to be contradictory, note that the matrix elements are constructed with the biorthogonal functions $\langle\bar{J}|$ on the left and the original functions $|I\rangle$ on the right. If $\mathcal{H}^0$ were hermitian, we would have $\langle\bar{J}|\mathcal{H}^0|I\rangle^* = \langle I|\mathcal{H}^0|\bar{J}\rangle$, but the elements of $\mathbf{H}$ satisfy $\langle\bar{J}|\mathcal{H}^0|I\rangle^* = \langle\bar{I}|\mathcal{H}^0|J\rangle$.)

It is now possible to work through the standard Rayleigh–Schrödinger perturbation theory formalism, using the $|I\rangle$ as ket vectors in every matrix element and the $\langle\bar{I}|$ as bra vectors, to obtain expressions for the perturbed energy (Surjan *et al.* 1985). The method was applied to a number of examples (Kochanski and Gouyet 1975*a*,*b*, Surjan and Poirier 1986), and gave good results in some cases, but not in all. It was thought at one time that the poor results were a consequence of the biorthogonal formalism, since the overlap matrix S may become singular or ill-conditioned when the basis set becomes large, but Surjan and Mayer (1991) later argued that they arose not from overlap problems but from an incorrect formulation of the perturbation operator. Nevertheless the energy expressions involve matrix elements in which the $\langle\bar{I}|$ appear on the left, and the problems of contamination of the orbitals of each molecule by those of the other are just as severe as they are in procedures that involve orthogonalization.

6.2.4 Non-orthogonal perturbation theory

The use of orthogonal expansion functions is a convenience in carrying out calculations, and is a natural consequence of conventional Rayleigh–Schrödinger perturbation theory, where the functions used as a basis for expanding the first-order wavefunction are eigenfunctions of the zeroth-order Hamiltonian. However, it is not necessary to use an orthogonal expansion set, and at the cost of somewhat greater complexity in the calculations a non-orthogonal set can be used. It is also possible to formulate the problem in such a way that no separation into zeroth-order Hamiltonian and perturbation is necessary. In the case of intermolecular interactions, the natural basis is the set of antisymmetrized product functions. Taking the pragmatic view that we can only ever handle a finite number of them in numerical calculations, we regard them as a basis for a matrix treatment of the problem. That is, we seek to solve the matrix equation

$$(\mathbf{H} - W\mathbf{S})\mathbf{c} = 0, \tag{6.2.1}$$

where $\mathbf{H}$ is the matrix of the Hamiltonian between the unperturbed functions, $\mathbf{S}$ is the overlap matrix, W the perturbed energy, and $\mathbf{c}$ the vector of coefficients. This is then solved perturbatively by splitting $\mathbf{H}$ into a zeroth-order part $\mathbf{H}^0$ and a perturbation $\mathbf{H}'$. It is possible to choose

both $\mathbf{H}^0$ and $\mathbf{H}'$ to be hermitian, but the $|m_A n_B\rangle$ cannot all be eigenfunctions of $\mathbf{H}^0$ for the reasons already discussed. If $\mathbf{H}^0$ is chosen to comprise the diagonal part of $\mathbf{H}$, the following expression emerges for the perturbed energy of the system (Hayes and Stone 1984*a*):

$$W = H_{00} - \sum_k{}' \frac{(H_{0k} - H_{00}S_{0k})(H_{k0} - H_{00}S_{k0})}{H_{kk} - H_{00}} + \cdots, \tag{6.2.2}$$

where the label k denotes one of the antisymmetrized products $|m_A n_B\rangle$ and 0 denotes $0_A 0_B\rangle$. The choice of $\mathbf{H}^0$ as the diagonal part of $\mathbf{H}$ is not the only possibility. Any diagonal matrix can be used, and if $\mathbf{H}^0$ has diagonal elements E_k the energy to second order has the same form, i.e.,

$$W = H_{00} - \sum_k{}' \frac{(H_{0k} - E_0 S_{0k})(H_{k0} - E_0 S_{k0})}{E_k - E_0} + \cdots. \tag{6.2.3}$$

Higher-order terms will be different, and evidently the convergence of the perturbation series may be improved or (more likely) degraded by such a change.

If SCF wavefunctions, i.e., single Slater determinants in the closed-shell case, are used as the single-molecule basis, the antisymmetrized product functions are simply Slater determinants constructed from the molecular orbitals of the two molecules. In this case a choice for the E_k which does not appear to affect the convergence adversely is the Møller–Plesset formula: $E_k = \sum_i n_{ik}\epsilon_i$, with n_{ik} the occupation number of orbital i in determinant k, and ϵ_i the orbital energy. The formulae needed for manipulating these determinantal functions in the context of perturbation theory have been worked out (Hayes and Stone 1984*b*), and a perturbation theory using these formulae has been developed (Hayes and Stone 1984*a*) and implemented to second order. Subsequently, Magnasco and Figari (1986) described a similar method, also to second order, and also showed how to generalize the manipulation of the determinantal functions (Figari and Magnasco 1985), so that the perturbation theory could in principle be extended to higher order. The method is quite successful, and behaves well at short distances, but the use of SCF zeroth-order wavefunctions means that intramolecular correlation effects are ignored, and for accurate work this is a serious deficiency.

6.2.5 Expansion in orders of exchange

A further approximation which has often been used is based on the premise that if exchange is negligible at long range its effects will be small at shorter range. The long-range approximation is equivalent to replacing the antisymmetrized wavefunction $|m_A n_B\rangle = \mathcal{A}|m_A\rangle|n_B\rangle$ by $|m_A\rangle|n_B\rangle$. The antisymmetrizer $\mathcal{A}$ can be written in the form

$$\mathcal{A} = N(1 - P^{(1)} + P^{(2)} - \cdots), \tag{6.2.4}$$

where $P^{(1)}$ describes permutations that exchange one of the electrons of A with one of the electrons of B, $P^{(2)}$ describes permutations that exchange two electrons from A with two electrons from B, and so on. N is a normalizing factor to ensure that $\mathcal{A}^2 = \mathcal{A}$. The overlap between a product function $|m_A\rangle|n_B\rangle$ and the function obtained from it by exchanging one of the electrons of A with one of the electrons of B is of order S^2, where S represents the magnitude of overlap integrals between orbitals on A and orbitals on B. S^2 decreases exponentially with distance, roughly like $\mathrm{e}^{-\alpha R}$, where R is the distance between atoms on the two molecules and α is typically in the range 1.5–2.5 bohr^{-1}. The overlap between $|m_A\rangle|n_B\rangle$ and a function obtained from

it by two electron exchanges is of order S^4, so if S^2 is small, the contributions of these double exchanges may be negligible. The contributions of triple exchanges will be even smaller, and so on. Consequently the approximation is made that only single exchanges need be considered. This single-exchange approximation becomes necessary when correlated zeroth-order wavefunctions are used, because the formulae become intractable when exchanges of more than one pair of electrons are included, but it is not needed for SCF zeroth-order wavefunctions, where the standard procedures for handling Slater determinants can be used, modified to cope with the non-orthogonality of the orbitals. An obvious limitation of the approximation is that when the molecules are very close, S is no longer small, and the neglect of terms of order S^4 may no longer be justifiable. Korona *et al.* (1997) found that for He_2 at the equilibrium separation of 5.6 bohr the errors were only about 10^{-3} K for the exchange–repulsion and exchange–induction terms, and 5×10^{-3} K for the exchange–dispersion, compared with a total interaction energy of about −11 K. The errors were larger at shorter distances, but still small compared with the total energy. Schäffer and Jansen (2012) have described a method for calculating the full exchange energy without expanding in orders of exchange, and found that the errors were still small for Ne_2 but rather larger for water dimer, where it is about 0.2 kJ mol^{-1} at the minimum and 3.8 kJ mol^{-1} where the total energy goes through zero. The exchange–repulsion energy in the latter case is about 100 kJ mol^{-1}, so the error in the single-exchange approximation is still relatively small.

6.3 Symmetry-adapted perturbation theories

The difficulties that appear in formulating the symmetric perturbation theories arise from the fact that there can be no hermitian zeroth-order Hamiltonian which has the antisymmetrized products as eigenfunctions, because of their non-orthogonality. Symmetry-adapted perturbation theories avoid these difficulties by taking as their expansion functions the simple products $|m_A\rangle|n_B\rangle$, without antisymmetrization. These are eigenfunctions of a well-defined zeroth-order Hamiltonian in which some of the electrons are assigned to molecule A and the rest to molecule B. However, because the true wavefunction for the system must be antisymmetric, it is necessary to work with the antisymmetrized functions $|m_An_B\rangle = \mathcal{A}|m_A\rangle|n_B\rangle$ alongside the unsymmetrized ones. The first theory of this sort was given by Eisenschitz and London (1930) in the early days of quantum mechanics. Van der Avoird (1967*a*,*b*) gave a version of this treatment in more modern notation. Although very elegant, it suffers from a lack of rigour, and Van der Avoird (1967*c*) also gave a more rigorous treatment. To second order, the results are the same: in a notation using ψ_k to denote a member of the set of unperturbed simple product functions $|m_A\rangle|n_B\rangle$, with ψ_0 for the unperturbed ground-state function $|0_A\rangle|0_B\rangle$, the first-order energy is

$$W' = \frac{\langle\mathcal{A}\psi_0|\mathcal{A}\mathcal{H}'\psi_0\rangle}{\langle\mathcal{A}\psi_0|\mathcal{A}\psi_0\rangle}, \tag{6.3.1}$$

and the second-order energy is

$$W'' = \frac{1}{\langle\mathcal{A}\psi_0|\mathcal{A}\psi_0\rangle}\sum_k{}' \frac{\langle\mathcal{A}(\mathcal{H}'-W')\psi_0|\mathcal{A}\psi_k\rangle\langle\mathcal{A}\psi_k|\mathcal{A}(\mathcal{H}'-W')\psi_0\rangle}{W_0^0-W_k^0}. \tag{6.3.2}$$

It is instructive to compare these formulae with those of the symmetric non-orthogonal treatment, eqn (6.2.2). At first sight they look different, but in fact they are the same. From (6.3.1) the energy to first order is

$$W^0 + W' = \frac{\langle \mathcal{A}\psi_0 | \mathcal{A}(W^0 + \mathcal{H}')\psi_0 \rangle}{\langle \mathcal{A}\psi_0 | \mathcal{A}\psi_0 \rangle} = \frac{\langle \mathcal{A}\psi_0 | \mathcal{A}\mathcal{H}\psi_0 \rangle}{\langle \mathcal{A}\psi_0 | \mathcal{A}\psi_0 \rangle}, \tag{6.3.3}$$

and this is the same as H_{00} if ψ_0 is normalized and antisymmetric, as it is in the symmetric non-orthogonal treatment. In the second-order energy, eqn (6.3.2), note that $(\mathcal{H}^0 - W_0^0)\psi_0 = 0$, so we can replace $(\mathcal{H}' - W')\psi_0$ by $(\mathcal{H}^0 + \mathcal{H}' - W_0^0 - W')\psi_0 = (\mathcal{H} - H_{00})\psi_0$ to give the second-order term of (6.2.2).

6.3.1 Iterative symmetry-forcing procedures

There is a family of related perturbation methods of the symmetry-adapted type. One method of deriving them is to seek a primitive function ψ which is not symmetric, but from which the true perturbed wavefunction Ψ may be derived by antisymmetrization: $\Psi = \mathcal{A}\psi$. The primitive function ψ is not uniquely defined, and by imposing different conditions on it one obtains different perturbation expansions (Amos 1970). These include the Van der Avoird version of the Eisenschitz–London theory mentioned above, and the equivalent treatment due to Hirschfelder (1967) (these methods being usually referred to together as EL–HAV), the HS method of Hirschfelder and Silbey (1966), and the MS–MA method, derived independently by Murrell and Shaw (1967) and Musher and Amos (1967), their two methods being later shown to be equivalent (Johnson and Epstein 1968). The convergence of these methods was compared for a simple model problem by Epstein and Johnson (1968); a discouraging result of this comparison was that the radius of convergence of the power series in the perturbation parameter λ was in many cases much smaller than the value of 1 needed to describe the perturbed problem. Jeziorski *et al.* (1978) also compared the convergence, using the more realistic example of H_2^+, and showed that the MS–MA method diverges.

Jeziorski and Kołos (1977) proposed a different approach to the derivation of these perturbation methods. We start with the unperturbed Hamiltonian $\mathcal{H}^0 = \mathcal{H}^A + \mathcal{H}^B$, with some electrons assigned to molecule A and the rest to molecule B. Assume that we have a set of zeroth-order eigenfunctions ψ_k and eigenvalues W_k:

$$\mathcal{H}^0\psi_k = W_k\psi_k, \tag{6.3.4}$$

where as before ψ_k is an unsymmetrized product of unperturbed functions for the two isolated molecules. Now define the 'reduced resolvent' R_0 (see Appendix C), which acts like the inverse of the operator $\mathcal{H}^0 - W_0$ for functions orthogonal to ψ_0 but gives zero when operating on ψ_0:

$$R_0\psi_k = \begin{cases} (W_k - W_0)^{-1}\psi_k, & k \neq 0, \\ 0, & k = 0. \end{cases} \tag{6.3.5}$$

In operator notation, this can be expressed in the form

$$\begin{aligned} R_0(\mathcal{H}^0 - W_0) &= 1 - P_0, \\ R_0P_0 &= 0, \end{aligned} \tag{6.3.6}$$

where $P_0 = |\psi_0\rangle\langle\psi_0|$. In terms of the complete set of eigenvalues and eigenvectors of $\mathcal{H}^0$, R_0 may be expressed in the form

$$R_0 = \sum_{k\neq 0} |\psi_k\rangle (W_k - W_0)^{-1} \langle \psi_k|. \tag{6.3.7}$$

Now we look for a solution Ψ to the perturbed problem:

$$\mathcal{H}\Psi = W\Psi, \tag{6.3.8}$$

subject to the usual intermediate normalization condition $\langle \psi_0|\Psi\rangle = 1$. Writing $W = W_0 + \Delta W$ and $\mathcal{H} = \mathcal{H}^0 + \mathcal{H}'$, we have

$$(\mathcal{H}^0 + \mathcal{H}' - W_0 - \Delta W)\Psi = 0, \tag{6.3.9}$$

and when we operate on this equation with R_0 and use (6.3.6) we get

$$(1 - P_0 + R_0(\mathcal{H}' - \Delta W))\Psi = 0, \tag{6.3.10}$$

or

$$\Psi = \psi_0 + R_0(\Delta W - \mathcal{H}')\Psi. \tag{6.3.11}$$

Also from (6.3.9) we see that

$$\Delta W = \langle \psi_0|\mathcal{H}'|\Psi\rangle. \tag{6.3.12}$$

Now we may attempt to solve these equations iteratively, through the scheme

$$\Delta W_n = \langle \psi_0|\mathcal{H}'|\Psi_{n-1}\rangle, \tag{6.3.13}$$

$$\Psi_n = \psi_0 + R_0(\Delta W_n - \mathcal{H}')\Psi_{n-1}. \tag{6.3.14}$$

This scheme may or may not converge; whether it does or not will depend on the function that we use to start the iterations. If we choose $\Psi_0 = \psi_0$, the first iterations yield

$$\begin{aligned}
\Delta W_1 &= \langle \psi_0|\mathcal{H}'|\psi_0\rangle, \\
\Psi_1 &= \psi_0 + R_0(\Delta W_1 - \mathcal{H}')\psi_0, \\
&= \psi_0 + {\sum_k}' \psi_k \frac{\langle \psi_k|\mathcal{H}'|\psi_0\rangle}{W_0 - W_k}, \\
\Delta W_2 &= \langle \psi_0|\mathcal{H}'|\psi_0\rangle + \langle \psi_0|\mathcal{H}' R_0 \mathcal{H}'|\psi_0\rangle \\
&= \langle \psi_0|\mathcal{H}'|\psi_0\rangle + {\sum_k}' \frac{\langle \psi_0|\mathcal{H}'|\psi_k\rangle\langle \psi_k|\mathcal{H}'|\psi_0\rangle}{W_0 - W_k},
\end{aligned}$$

which are the standard results of Rayleigh–Schrödinger perturbation theory. Clearly this initial choice is a bad one, because Ψ is antisymmetric and is very different from ψ_0, which is not. We have already seen that Rayleigh–Schrödinger perturbation theory converges badly for just this reason. If we start instead from the antisymmetrized function $\mathcal{A}\psi_0$ we should do better. Because of the normalization condition we have to set $\Psi_0 = \langle \psi_0|\mathcal{A}\psi_0\rangle^{-1}\mathcal{A}\psi_0$. Jeziorski and Kołos (1977) showed that this generates the MS–MA perturbation scheme.

Even if we start from an antisymmetric Ψ_0, eqn (6.3.14) does not maintain the antisymmetry, so Ψ_n is not in general antisymmetric for finite n, and indeed it need not be antisymmetric in the limit $n \to \infty$, even if the process converges. This does not matter so long as the energy

expression is right, but it seems intuitively that it would be more satisfactory if the antisymmetry could be maintained. Jeziorski and Kołos (1977) proposed to improve the convergence by forcing the correct symmetry on Ψ_{n-1} before using it in the calculation of ΔW_n or Ψ_n or both. The iteration scheme becomes

$$\Delta W_n = \langle \psi_0 | \mathcal{H}' | \mathcal{G}\Psi_{n-1} \rangle, \tag{6.3.15}$$

$$\Psi_n = \psi_0 + R_0(\Delta W_n - \mathcal{H}')\mathcal{F}\Psi_{n-1}, \tag{6.3.16}$$

where $\mathcal{F}$ and $\mathcal{G}$ are the symmetry-forcing operators. They must satisfy $\mathcal{G}\Psi = \mathcal{F}\Psi = \Psi$, but otherwise they are arbitrary. In practice the available choices are, for $\mathcal{F}$, either 1 or $\mathcal{A}$; and for $\mathcal{G}$, either 1 or a modified antisymmetrizer defined by $\mathcal{G}\chi = \langle \psi_0 | \mathcal{A}\chi \rangle^{-1} \mathcal{A}\chi$, this form being needed in order to preserve the intermediate normalization of the antisymmetrized function. A wide variety of perturbation schemes, including the MS–MA, HS and EL–HAV schemes, can be generated using suitable choices for the symmetry-forcing (which does not have to be the same at every iteration) and for the starting function. In a subsequent paper, Jeziorski *et al.* (1978) found that the choice $\mathcal{G} = 1$, $\mathcal{F} = \mathcal{A}$, $\Psi_0 = \langle \psi_0 | \mathcal{A}\psi_0 \rangle^{-1} \mathcal{A}\psi_0$, suggested by Jeziorski and Kołos (1977) and called the JK scheme, was the most satisfactory for strong interactions, while a scheme in which the symmetry is forced only in the evaluation of the energy is most successful at longer range where the interaction is weaker. This scheme, called the symmetrized Rayleigh–Schrödinger (SRS) scheme, takes the form

$$\Delta W_n = \langle \psi_0 | \mathcal{H}' | \mathcal{G}\Psi_{n-1} \rangle, \tag{6.3.17}$$

$$\Psi_n = \psi_0 + R_0(\langle \psi_0 | \mathcal{H}' | \Psi_{n-1} \rangle - \mathcal{H}')\Psi_{n-1}, \tag{6.3.18}$$

with $\Psi_0 = \psi_0$ and $\mathcal{G}$ defined by $\mathcal{G}\chi = \langle \psi_0 | \mathcal{A}\chi \rangle^{-1} \mathcal{A}\chi$, as above. In diagram form the procedure is then

$$\begin{array}{ccccc} \Psi_0 & \longrightarrow & \mathcal{G}\Psi_0 & \longrightarrow & E_1 \\ \big\downarrow \text{RS} & & & & \\ \Psi_1 & \longrightarrow & \mathcal{G}\Psi_1 & \longrightarrow & E_2 \\ \big\downarrow \text{RS} & & & & \\ \vdots & & & & \end{array}$$

The corrections to the wavefunction have the same form as in the ordinary Rayleigh–Schrödinger scheme, and it is only in the formula for the energy that the antisymmetrizer appears. This method has been used successfully for $(H_2O)_2$ and $(HF)_2$ (Rybak *et al.* 1991) and Ar···H_2 (Williams *et al.* 1993), but its success is not yet fully understood (Adams 1994). One may obtain a power series expansion of the interaction energy by replacing $\mathcal{H}'$ in any of these schemes by $\lambda\mathcal{H}'$ and picking out powers of λ from the resulting expressions. If this is done for the SRS scheme, the resulting power series for the ground state of H_2 has a radius of convergence of 1.0000000031 at the Van der Waals minimum (Cwiok *et al.* 1992), and so converges extremely slowly for $\lambda = 1$. Moreover the radius of convergence can be shown to be less than 1 if either of the monomers has more than two electrons (Kutzelnigg 1980), so the series diverges for $\lambda = 1$. Nevertheless Patkowski *et al.* (2001*b*) showed that the SRS series gives good results at low order for Li···H, and excellent results if summed using the standard

procedure for asymptotically convergent series. It provides the basis for the very successful SAPT and SAPT-DFT methods, described in §6.4 below. The same approach can be used with the HS scheme, which also diverges in this case, but the results are no better and the method is much more complicated.

6.3.2 Regularized symmetry-forcing methods

The importance of the symmetry-forcing approach lies in the fact that it is possible to develop a satisfactory perturbative treatment of intermolecular forces by means of an iterative scheme rather than a conventional power series expansion. In this way, the difficulties that arise from the ambiguities in the definition of perturbation order can be circumvented, and the arbitrariness that remains in the formulation of the iterative scheme is seen to be not a fundamental problem but merely a flexibility that can be exploited to achieve the most effective convergence of the process.

Nevertheless, a fundamental difficulty remains with all of these methods, namely that the physical ground state of the system lies in a continuum of unphysical (non-antisymmetric) states. Two problems ensue. First, the symmetry-forcing procedures do not usually force the antisymmetry completely. The symmetry-forced energy, as for example in eqn (6.3.17), involves the matrix element of the perturbation between ψ_0 and an antisymmetrized Ψ_{n-1}. The antisymmetrization involves exchange of electrons between the interacting molecules, and in typical cases leads to a very large number of terms. It is not usually practicable to calculate all of them, and in practice it is usual to use the single-exchange approximation, that is to take only the leading term (no exchanges) and the single-exchange term, which in magnitude is of the order of the square of the overlap S between wavefunctions on the two molecules. Omission of the remaining terms means that the result may still be contaminated by unphysical effects. In practice, however, it seems that it does not lead to significant errors.

The problem caused by failure to antisymmetrize completely lies in the fact that the electrons of either molecule are subject to a perturbation that includes the nuclear attraction to the nuclei of the other molecule. Thus, in the case of Li···H, it is possible to construct an unphysical wavefunction in which the H electron occupies the Li 1s orbital, along with the two Li 1s electrons, while the third Li electron occupies the H 1s orbital. This state clearly has a much lower energy than any state in which the H electron stays on the H atom. There are infinitely many other unphysical states in which an electron is excited, and above those there is a continuum of states in which the Li atom is ionized. The true physical ground state is embedded in this continuum. If no symmetry is imposed, the unsymmetrized perturbed state will include contributions from neighbouring unphysical states which have to be projected out. If the projection is incomplete, because of the use of the single-exchange approximation to the antisymmetrizer, the resulting energy will be incorrect.

A cure for this problem was proposed by Patkowski *et al.* (2001*a*, 2004) and Adams (2002*b*). The idea is to weaken the attraction between the electrons of each molecule and the nuclei of the other, by subtracting a short-ranged attractive term, so that all the unphysical states are moved up in energy, above the lowest physical states. Then any mixing of the unphysical states with the physical ones will be small, and deficiencies in the antisymmetrization will not be important. The resulting Hamiltonian is not symmetric with respect to electron permutations, since the attraction between the A nuclei and the B electrons is different in form from the attraction between the A nuclei and the A electrons. However, the true Hamiltonian

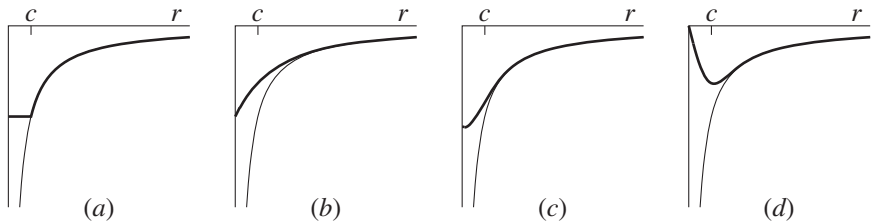

Fig. 6.2 Regularized Coulomb potentials. (*a*) eqn (6.3.19), (*b*) $r^{-1}[1 - \exp(-r/c)]$, (*c*) $r^{-1}\,\mathrm{erf}(r/c)$, (*d*) $r^{-1}[1 - \exp(-(r/c)^2)]$.

can be used to evaluate the energy of the antisymmetrized wavefunction, and since that is no longer contaminated significantly by unphysical states, the results should be much more satisfactory.

The form of the short-ranged term appears not to be critical, except that it must decay rapidly to zero so that it has no effect at large separations, ensuring that the energy is asymptotically correct as $R \to \infty$. Patkowski *et al.* (2001*a*) used a form equivalent to replacing r^{-1} by $r^{-1}[1 - \exp(-(r/c)^2)]$, while Adams (2002*b*) replaced r^{-1} by

$$\begin{cases} 1/c, & r \le c, \\ 1/r, & r > c. \end{cases} \tag{6.3.19}$$

Adams also tried $r^{-1}[1 - \exp(-r/c)]$ and Patkowski *et al.* (2001*a*) tried $r^{-1}\,\mathrm{erf}(r/c)$. These 'regularized Coulomb' functions are shown in Fig. 6.2. The results were almost independent of the function chosen. The rather strange choice of $r^{-1}[1 - \exp(-(r/c)^2)]$ has the advantage that the resulting integrals are similar to ones that already occur in *ab initio* programs, but this is also the case for $r^{-1}\,\mathrm{erf}(r/c)$.

6.3.3 The treatment of electron correlation

It must be said that the flexibility of symmetry-forcing procedures is to a large degree academic, since practical calculations on systems of any size cannot be carried out beyond second order, and even then considerable practical difficulties remain. The most important of these is that the iterative scheme is formulated in terms of the reduced resolvent R_0, which is defined in terms of a sum over states, and these states are products of the exact eigenstates of the isolated molecules, which we do not know.

Accordingly it is necessary, if we are to make any progress, to start from a simplified treatment of the isolated molecules. A natural choice is the self-consistent-field approximation, in which the effects of electron correlation are ignored (see Chapter 5). It is a practicable treatment for molecules of significant size, and although it too is not exactly soluble, it is possible to get quite close to the exact solution (the 'Hartree–Fock limit') using modern basis sets. Electron correlation is then treated as a perturbation. This leads to the particular version of symmetry-adapted perturbation theory known as SAPT, which will be discussed in §6.4.

The rapid developments in density-functional theory have offered an alternative approach. Here the electron correlation is incorporated into the Kohn–Sham operator $\mathcal{K}$ (eqn (5.3.6)), and it is possible to write down the equations of a symmetry-adapted perturbation theory,

using Kohn–Sham orbitals and energies rather than Hartree–Fock ones. This approach, known variously as DFT-SAPT, SAPT(DFT) or SAPT-DFT, is discussed in §6.4.1.

6.3.4 The treatment of induction

One of the reasons for the slow convergence of the perturbation theory of intermolecular interactions is the behaviour of the induction energy. We have seen (§4.2.2) that the long-range perturbation expansion of the induction energy is only asymptotically convergent. A classical approach, to be discussed in detail in §9.4, and illustrated in Fig. 9.3, helps to clarify the problem. Each molecule is polarized by the electrostatic field of its neighbours, and the corresponding energy is the second-order induction energy of long-range perturbation theory. However, the polarization modifies the multipole moments of each molecule, and the induced moments further polarize neighbouring molecules, leading to a third-order energy term in perturbation theory. The process continues through higher-order contributions. Unfortunately the third-order and higher terms are often too large to ignore; in the water dimer, for example, they contribute some 2.5 kJ mol^{-1} to the total energy.

The δ^{HF} correction. One way to deal with this problem is to use the Hartree–Fock energy of the system, which contains all induction effects, though without correlation corrections. The 'δ^{HF} correction' is defined (Jeziorska *et al.* 1987, Moszynski *et al.* 1996) as

$$\delta^{\mathrm{HF}} = E^{\mathrm{HF}} - E^{\mathrm{HF}}_{\mathrm{es}} - E^{\mathrm{HF}}_{\mathrm{er}} - E^{\mathrm{HF}}_{\mathrm{indcx}}. \tag{6.3.20}$$

The idea is that everything in the Hartree–Fock interaction energy, except for the first-order electrostatic and exchange–repulsion terms, involves the response of the charge distribution of each molecule to the electric field of its neighbours, i.e. the induction energy. Perturbation theory gives a good estimate of the second-order induction energy, if we calculate it using coupled perturbation theory and include the exchange corrections, so we can subtract that off too, i.e. the term $U^{\mathrm{HF}}_{\mathrm{indcx}}$, to leave an estimate of the higher-order terms in the induction energy. In practice this method does appear to provide a reasonably accurate estimate of these higher-order terms (Misquitta and Stone 2008), except for very weakly bound clusters, but unfortunately it may be impracticable even for a dimer, as it requires a supermolecule SCF calculation of the dimer and each molecule in the dimer basis, to avoid BSSE, as well as the SAPT calculation. It is even more impracticable for larger clusters, where induction effects often dominate the many-body contributions to the interaction energy.

The classical polarizable model. If we have a good description of the molecular polarizabilities, we can use the classical multipole expansion for the induction energy, as set out in §4.2, or better a version using local atomic polarizabilities which will be developed in Chapter 9. The leading term in this expansion corresponds to the second-order energy in perturbation theory, and the remaining terms provide an estimate of the higher-order terms in the perturbation-theory description. An advantage of this approach is that it involves only single-molecule properties, which are relatively easy to calculate and can include correlation effects. However, it is a long-range approximation, and needs to be corrected for overlap and exchange effects at short range. This is usually done by applying a damping function, but it is not clear what the form of the damping function should be for induction. The classical form also assumes linear response of each molecule to external fields (that is, it neglects hyperpolarizabilities). The

damped classical expansion seems to underestimate the higher-order terms in dimers quite severely, possibly because of deficiencies in the damping function, but it gives a good account of many-body effects in clusters of polar molecules, such as small water clusters. We return to this in Chapter 10.

The ZI method. Adams (2002*b*) has proposed another approach to the problem of induction. For a dimer, this method starts by calculating a wavefunction for each molecule using a modified Hamiltonian that includes the electrostatic field of the partner molecule, regularized as described above (§6.3.2) so as to avoid unphysical effects arising from the singularities at the nuclei of the partner. The resulting energies and wavefunctions include the main effects of induction. These wavefunctions are then used as the starting point for the SAPT calculation. The method has some attractive features, and appears to work well in some small test cases, but its application to polyatomic molecules and especially to clusters would be very difficult.

6.3.5 Summary

Following a long period of neglect by all but a few research groups, the perturbation approach to the calculation of intermolecular forces at short range was revived in the 1980s and has proved successful and practicable. The symmetric method of Hayes and Stone (1984*a*) has been applied to systems as large as the benzene-tetracyanoethylene complex, and while it does not handle correlation corrections (except for the dispersion energy itself) it provides an efficient route to the uncorrelated terms. The lack of correlation corrections and the uncoupled treatment of the second-order terms are serious deficiencies, but it is still useful for some applications (Fischer *et al.* 2008). Symmetry-forcing methods have become the preferred approach, in particular the symmetry-adapted perturbation theory (SAPT) of Jeziorski, Szalewicz and their collaborators, and the density functional variants of Misquitta *et al.* and Hesselmann and Jansen. We examine these in more detail in the next section.

6.4 The SAPT method

SAPT stands for 'symmetry-adapted perturbation theory', but the term is used for a particular symmetry-adapted perturbation theory in which the starting point is the self-consistent-field approximation, and electron correlation effects, as well as the intermolecular interaction, are incorporated by perturbation theory. Szalewicz (2012) gives a detailed account. The procedure is to separate the complete Hamiltonian in the following way:

$$\mathcal{H} = \mathcal{F}^A + \mathcal{F}^B + \zeta^A\mathcal{G}^A + \zeta^B\mathcal{G}^B + \lambda\mathcal{H}', \tag{6.4.1}$$

where $\mathcal{F}^A$ and $\mathcal{F}^B$ are the Fock operators for the isolated molecules A and B, respectively, $\mathcal{G}^A = \mathcal{H}^A - \mathcal{F}^A$ describes the effects of electron correlation in molecule A and similarly $\mathcal{G}^B = \mathcal{H}^B - \mathcal{F}^B$, and $\mathcal{H}'$ is the intermolecular interaction, as before. It is now necessary to carry out a triple perturbation expansion, the coefficients ζ_A, ζ_B and λ being used to identify orders of perturbation. The theory becomes extremely complicated, and has been described in detail by Jeziorski *et al.* (1993, 1994). It yields an expansion of the interaction energy in powers of the parameters λ, ζ_1 and ζ_2 appearing in eqn (6.4.1), and the interaction terms can be classified accordingly. Jeziorski *et al.* use a notation in which $E^{(ijk)}$ is the term of order i in the interaction, j in the intramolecular correlation for A, and k in the intramolecular correlation for B. A subscript 'exch' denotes the exchange correction, while the subscript 'resp' indicates

Table 6.1 Summary of perturbation terms in symmetry-adapted perturbation theory.

Symbol	Name	Physical interpretation
$E^{(10)}_{\text{elst}}$	Electrostatic energy	Electrostatic energy of interaction, calculated classically from the unperturbed Hartree–Fock charge distributions.
$E^{(12)}_{\text{elst,resp}} + E^{(13)}_{\text{elst,resp}}$	Electrostatic energy: correlation corrections	Correction to the electrostatic energy arising from second-order and third-order intramolecular correlation corrections to the charge distributions.
$E^{(10)}_{\text{exch}}$	Exchange repulsion	'Closed-shell repulsion': the modification to the first-order energy of the Hartree–Fock monomers arising from exchange of electrons between them.
$\epsilon^{(1)}_{\text{exch}}(\text{CCSD})$	Exchange repulsion: correlation corrections	Contribution to the closed-shell repulsion arising from CCSD corrections to the monomer wavefunctions.
$E^{(20)}_{\text{ind,resp}}$	Induction energy	Energy arising from the distortion of each molecule in the field due to the unperturbed Hartree–Fock charge distribution of the other.
$E^{(20)}_{\text{exch-ind,resp}}$	Exchange induction	Modification to the induction energy when exchange effects are taken into account.
$E^{(22)}_{\text{ind}} + E^{(22)}_{\text{exch-ind}}$	Induction energy: correlation corrections	Correlation corrections to induction and exchange–induction.
$E^{(20)}_{\text{disp}}$	Dispersion energy	Energy arising from the correlated fluctuations of the Hartree–Fock electron distributions of each molecule.
$E^{(20)}_{\text{exch-disp}}$	Exchange dispersion	Modification to the dispersion energy when exchange effects are taken into account.
$E^{(21)}_{\text{disp}} + E^{(22)}_{\text{disp}}$	Dispersion energy: correlation corrections	Correction to the dispersion energy arising from intramolecular correlation.

that coupled perturbation theory is used. They also use a notation with only two superscripts, where $E^{(il)}$ is the sum of the terms $E^{(ijk)}$ with $j + k = l$, so that l describes the total order of intramolecular correlation. A summary of the terms that are normally included is given in Table 6.1.

One of the advantages of using perturbation theory in this way is that it is only necessary to carry out the correlation corrections to the order that is appropriate for each term sepa-

rately. The electrostatic interaction is very sensitive to correlation effects, and Jeziorski *et al.* recommend using correlation corrections up to $j + k = 3$ or 4. The induction energy, on the other hand, is often a small term, and if that is so the correlation corrections may be negligible. Dispersion is dominated by the Hartree–Fock term*, but correlation corrections up to $j + k = 2$ may be significant, and the exchange–dispersion is a small but not negligible repulsive contribution. The exchange–induction term, on the other hand, is often large and positive, cancelling out most of the $E^{(20)}_{\mathrm{ind,resp}}$ term. It seems likely that this is a symptom of the contamination of the perturbed state by non-physical contributions, discussed in §6.3.2, but this has not been explored in any detail. Recall that $E^{(20)}_{\mathrm{exch\text{-}ind,resp}}$ is obtained using the single-exchange approximation, so the non-physical contributions may not be completely projected away. In practice the induction energy term $E^{(20)}_{\mathrm{ind,resp}}$ is often modelled by a multipole expansion, while the exchange term is ignored. This is more successful than might be expected, because the penetration error in $E^{(20)}_{\mathrm{ind,resp}}$ and the truncation error in its multipole approximation seem to largely cancel the neglect of the exchange term.

The exchange–repulsion is also affected by correlation. Calculations on small systems such as Ar···H_2 (Williams *et al.* 1993) showed that the correlation correction up to $j + k = 2$ is about 10–15% of the uncorrelated exchange–repulsion, and is usually positive, i.e., it increases the repulsion. However, the percentage change in U_{er} is not the same at all distances, and is unlikely to be the same for all systems. Indeed, Moszynski *et al.* (1995*b*) found that for HCCH···He, it was necessary to include correlation terms up to $j + k = 4$ to achieve satisfactory convergence, and although the correlation correction is repulsive in the linear geometries, where it increases the repulsion energy by about 20%, it is attractive for the T geometry, where the He atom interacts with the π bond. Here the correction decreases the repulsion by about 10%.

6.4.1 The SAPT-DFT method

The triple perturbation theory used in the SAPT method, together with the coupled-cluster treatment of electron correlation, makes for a very complicated treatment that is difficult to implement on the computer and very demanding in computational resources. Density functional theory offers an attractive alternative, since correlation effects are included from the outset, and there is only a single perturbation, the intermolecular interaction. Consequently the triple perturbation theory of SAPT is not required, and the theory is very much simpler. A perturbation method based on this approach was first proposed by Williams and Chabalowski (2001), but was not very successful. It was soon realized that it is necessary to use an asymptotically corrected functional—otherwise the electron density is too diffuse and this leads to errors in both the first-order terms. In addition, the second-order terms were calculated using uncoupled perturbation theory and were also poor.

The method was soon improved by Hesselmann and Jansen (2002*a*, 2002*b*, 2003) and Misquitta *et al.* (2002, 2003, 2005), independently. Their methods, called respectively DFT-SAPT and SAPT(DFT), are essentially identical, and use the asymptotically corrected PBE0-AC functional, with coupled Kohn–Sham perturbation theory for the second-order terms. To avoid apparently favouring one over the other, the acronym SAPT-DFT will be used here to

*It is difficult to find a satisfactory terminology here. Dispersion is a correlation effect, so it seems contradictory to speak of a 'Hartree–Fock' dispersion term. What we mean by this expression is the contribution to the dispersion energy that is obtained using the long-range approximation with Hartree–Fock unperturbed wavefunctions.

Table 6.2 Summary of perturbation terms in SAPT-DFT.

Symbol	Name	Physical interpretation
$E^{(1)}_{\text{elst}}$	Electrostatic energy	Electrostatic energy of interaction, calculated classically from the unperturbed Kohn–Sham charge distributions.
$E^{(1)}_{\text{exch}}$	Exchange repulsion	'Closed-shell repulsion': the modification to the first-order energy of the Kohn–Sham monomers arising from exchange of electrons between them.
$E^{(2)}_{\text{ind,resp}}$	Induction energy	Energy arising from the distortion of each molecule in the field due to the unperturbed Kohn–Sham charge distribution of the other.
$E^{(2)}_{\text{exch-ind,resp}}$	Exchange induction	Modification to the induction energy when exchange effects are taken into account.
$E^{(2)}_{\text{disp,resp}}$	Dispersion energy	Energy arising from the correlated fluctuations of the Kohn–Sham electron distributions of each molecule.
$E^{(2)}_{\text{exch-disp}}$	Exchange dispersion	Modification to the dispersion energy when exchange effects are taken into account.
δ^{HF}	Induction correction	Estimate of higher-order terms in the induction energy (see §6.3.4).

refer to both. A summary of the terms that arise is in Table 6.2. The second-order induction and dispersion energies are calculated from the frequency-dependent density susceptibility (eqn (2.5.12)), but this approach does not take account of exchange effects, which have to be estimated using the single-exchange approximation.

The Kohn–Sham formulation of density functional theory would lead to the exact electron density if we knew the exact functional, so we can expect that practical functionals will give a good description of the density and hence of the electrostatic interaction. It is not obvious that the rest of the first-order term, the exchange–repulsion, should be given correctly, since it depends on the two-electron density matrix, not just on the density, and the Kohn–Sham density matrix derives from the Kohn–Sham independent-electron ansatz (see §5.3) and is not the same as the true two-electron density matrix. However, the exchange–repulsion is known to be closely related to the overlap of electron densities (see §12.2.2), so we expect a good description of this term too. In practice it turns out that it is important to use an asymptotically corrected functional, because the exchange–repulsion is sensitive to the outer regions of the electron density (Misquitta and Szalewicz 2002).

One might expect that the second-order perturbation terms, induction and dispersion and their exchange counterparts, would not be as well described, because the perturbation-theory expressions involve the molecular orbitals, and the Kohn–Sham orbitals are not the same as

the Hartree–Fock orbitals. However, it turns out that the results are very good, giving interaction energies in excellent agreement with CCSD(T) (Tekin and Jansen 2007), provided that coupled perturbation theory is used to derive the static and imaginary-frequency density susceptibilities (see §5.5). Indeed, the performance of these DFT-based methods seems to be better than that of the more conventional SAPT using triple perturbation theory. The reason for this may be that density-functional theory treats correlation effects exactly, in principle, while conventional correlation methods provide an incomplete treatment.

6.4.2 Basis sets for SAPT and SAPT-DFT

For accurate calculations of interaction energies, good quality basis sets are needed. The interaction energies depend strongly on the outer regions of the wavefunction, and basis sets of augmented triple-zeta quality are needed for a good description.

The simplest form of basis set to use in a calculation of intermolecular interactions is a 'monomer' or 'monomer-centred' (MC) basis, in which each molecule is described by the same basis set that would be used for the isolated molecule. The excited states that are mixed with the ground state by the perturbation are then constructed from each molecule's own virtual orbitals, so this limits the excited states that can be included. In particular, it excludes excited states corresponding to transfer of an electron from one molecule to the other (charge-transfer states), which can make a significant contribution to the interaction. Excitations from occupied orbitals of A to virtual orbitals of B cannot be allowed, however, because they are the source of basis set superposition error (BSSE). The solution is to use a basis set for A that includes basis functions on B (ghost orbitals), and vice versa. This is the 'dimer' or 'dimer-centred' (DC) basis.

In addition, it is found that the dispersion energy is obtained more accurately if further basis functions are provided in the region between the molecules (so-called 'mid-bond' functions). A small set of s and p functions at a single site is sufficient, but can make a significant difference, sometimes accounting for as much as 20% of the dispersion energy.

6.4.3 Three-body corrections

All of the perturbation theory methods discussed so far have been confined to the calculation of pair interactions. The assumption of pair additivity is an approximation, however, and many-body corrections are often important, as we shall see in Chapter 10. Calculation of these corrections by perturbation theory is difficult and time-consuming, but some progress has been made. The general symmetry-adapted perturbation theory of three-body interactions has been set out by Moszynski *et al.* (1995*a*) and applied to the Ar_2–HF system (Moszynski *et al.* 1998). Podeszwa and Szalewicz (2007) have adapted SAPT to calculate the first-order three-body corrections, with second-order (dispersion and induction) terms calculated by coupled Kohn–Sham perturbation theory, as in SAPT-DFT. The method has been applied to benzene trimer (but only in a configuration with threefold symmetry) and to endohedral complexes of one or two H_2 molecules enclosed in C_{60} or C_{70} (Korona *et al.* 2009).

7
Distributed Multipole Expansions

7.1 Convergence of the multipole expansion

The multipole expansion of the electrostatic interaction is based on a power series expansion of $1/(\mathbf{B}+\mathbf{b}-\mathbf{A}-\mathbf{a}) = 1/(\mathbf{R}+\mathbf{b}-\mathbf{a})$, initially in powers of $|\mathbf{b}-\mathbf{a}|/R$ (eqn (3.3.2)). If this is to converge absolutely, at a particular R, it must converge for arbitrary orientations of both molecules. This means that the series must converge for the worst-case orientation of **a** and **b**, i.e., for the largest value of $|\mathbf{b}-\mathbf{a}|$, which is $a+b$. Since the angular factors multiplying $|\mathbf{b}-\mathbf{a}|^k$ and R^{-k-1} are Racah spherical harmonics, with maximum magnitude 1, the series will converge absolutely if $a+b<R$ and will diverge if $a+b>R$ (Amos and Crispin 1976*a*).

For classical assemblies of point charges, this result can easily be expressed in pictorial form. We construct a sphere with its centre at **A**, just large enough to enclose all the charges belonging to A, and a similar sphere for B. Then we enquire whether the spheres intersect for a given R. If they do, it is possible to find particles a and b, on the surface of each sphere, such that $a+b>R$, and the multipole expansion will diverge. (See Fig. 7.1.) If we increase R so that the spheres no longer intersect, then $a+b<R$ for all pairs of particles, and the series will converge.

For those readers accustomed to the concept of radius of convergence as it applies to a series in powers of a complex variable, it is worth emphasizing that we are dealing here with a series in powers of $1/R$. For this reason, the small-R region, where the spheres overlap, is where the series *diverges*, and we shall use the term 'divergence sphere' to emphasize this fact. In contrast to the case of a circle of convergence in the theory of complex variables, which one wishes to be as large as possible, we require the spheres of divergence to be as *small* as possible for optimum convergence.

For atoms and molecules the implication at first sight is that the multipole series must always diverge, because the charge distribution of any molecule extends formally to infinity,

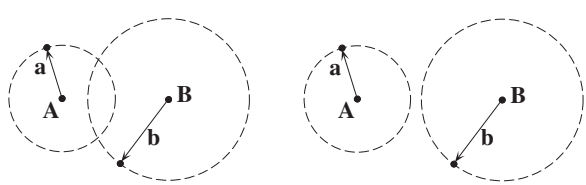

Fig. 7.1 Convergence of the multipole series for the interaction of two charges displaced by **a** and **b** from the respective local origins **A** and **B**. We construct spheres with centres at **A** and **B** that are just large enough to enclose the two charges. The series diverges if the spheres intersect (*left*), and converges if they do not (*right*).

even though it dies away exponentially with distance. Consider, however, the interaction between two Li^+ ions. Both particles have charge +1, but they are spherical (^1S) atoms, and all their higher multipole moments vanish. Consequently the multipole expansion comprises the single term $q^A q^B/R$ and converges trivially. We have to remember that if the ions are close enough for their charge distributions to interpenetrate significantly, this expression for the electrostatic interaction is in fact incorrect, but that is a separate issue which we shall discuss in Chapter 8. The 'penetration error' in the multipole expansion decreases exponentially as the distance between the ions increases.

The electronic wavefunction can be represented by an expansion in terms of gaussian functions of the form $R_{lm}(\mathbf{r}-\mathbf{p})\exp(-\alpha|\mathbf{r}-\mathbf{p}|^2)$, centred at one or more arbitrary points $\mathbf{p}$, usually at the nuclei. When the wavefunction takes this form, it can be shown that the divergence sphere for a molecule is the sphere enclosing just the *nuclei* (Stone and Alderton 1985, Vigné-Maeder and Claverie 1988), a much less demanding condition. The proof of this important result will be given at the end of §7.3 (p. 126).

Nevertheless convergence problems remain. It is still possible to find cases where the multipole series will certainly diverge. For example, the radius of a sphere enclosing all the nuclei of benzene has a radius of about 2.4 Å. For hexafluorobenzene the radius needs to be about 2.8 Å. The multipole expansion of the electrostatic interaction between benzene and hexafluorobenzene will therefore converge only if their centres are more than 5.2 Å apart. In the $C_6H_6\cdots C_6F_6$ complex, however, the molecular planes are about 3.5 Å apart. This means that the multipole expansion cannot be used to describe the interaction.

Even when the divergence spheres do not overlap, the multipole expansion will converge slowly if they are not widely separated, so we have a problem even for molecules smaller than benzene.

7.2 Distributed multipole expansions

The solution to this problem is to use, not a molecular or single-site multipole expansion in which we describe the entire molecular charge distribution by an expansion about a single point, but a *distributed multipole expansion*, in which the molecule is divided into regions, each described by its own multipole moments. A region will usually be an atom or a small group of atoms like a methyl group. Sometimes, for accurate work, it is helpful to have separate regions associated with the bonds. Each region has its own origin, usually at the nucleus for an atomic region. We use the term 'site' for the origin of a region.

The interaction between two molecules A and B then takes the form

$$\mathcal{H}' = \sum_{a\in A}\sum_{b\in B}[T^{ab}\hat{q}^a\hat{q}^b + T^{ab}_\alpha(\hat{q}^a\hat{\mu}^b_\alpha - \hat{\mu}^a_\alpha\hat{q}^b) + T^{ab}_{\alpha\beta}(\tfrac{1}{3}\hat{q}^a\hat{\Theta}^b_{\alpha\beta} - \hat{\mu}^a_\alpha\hat{\mu}^b_\beta + \tfrac{1}{3}\hat{\Theta}^a_{\alpha\beta}\hat{q}^b) + \cdots] \tag{7.2.1}$$

(compare eqn (3.2.1)). The sum runs over the sites a of molecule A and the sites b of molecule B, and $\hat{q}^a$, $\hat{\mu}^a_\alpha$, etc., are the operators for the charge, dipole moment, etc., of region a.

There are several ways to obtain this kind of expansion.

7.2.1 Empirical models

At sufficiently long range, the central multipole expansion is valid, and in this case the distributed multipole description and the central multipole description must agree. If we use

eqn (2.7.6) to change the origin of all the distributed moments to the molecular centre, the resulting multipoles must be the central moments. This provides a constraint on the distributed moments that may be used to help determine their values.

The difficulty with this approach is that the information contained in the central moments is not usually sufficient to determine the distributed moments, or to discriminate between alternative models. Consider, for example, the quadrupole moment of the N_2 molecule, which has a value of -1.09 ± 0.05 a.u. (Buckingham *et al.* 1983, Huot and Bose 1991). We may contemplate a number of distributed-multipole models that reproduce this value. A point-charge model, with a charge of q at the N nuclei and a balancing charge of $-2q$ at the centre of the bond, has a quadrupole moment of $2q(\frac{1}{2}l)^2$, where l is the bond-length, so we require $q = -0.51\,e$. (The bond length is $2.0674\,a_0$.) Alternatively, we might assign a point dipole of magnitude μ to each N atom. In this case, eqn (2.7.2) shows that the quadrupole moment is $2 \times 2\mu(\frac{1}{2}l)$ (if the positive direction of the dipole moment is outwards) so we need $\mu = -0.26\,ea_0$. A third possibility is to assign a point quadrupole Θ to each atom, in which case the total quadrupole is just 2Θ, so we need $\Theta = -0.55\,ea_0^2$.

How can we tell which, if any, of these is right? Occam's razor might favour the simplest model, the point-charge picture, were it not for the fact that everything we know about chemical bonding contradicts a model in which a charge of +1 is assigned to the centre of a triple bond. Most chemists have a less well developed intuition about atomic dipole and quadrupole moments, so it is less easy to assess the merits of the other two models. One possibility is to examine the hexadecapole moment. It is not very well determined experimentally; a value of -10.4 ± 1 a.u. has been deduced from collision-induced infrared spectra of gaseous N_2 (Poll and Hunt 1981), but this is a rather indirect method and depends on an assumed intermolecular potential for N_2. *Ab initio* calculation yields a value of -6.75 a.u. (Amos 1985, Maroulis 2003). The charge, dipole and quadrupole models give central hexadecapole moments of -1.2, -2.4 and -7.2 respectively. This provides some support for the quadrupole model, but is far from conclusive. In fact we shall see that all of these models are wrong. The experimental data are just not complete enough to distinguish between these or the many other models that we might contemplate. This is by no means an unusual case; it is usually possible to measure only the first one or two non-zero moments, and usually only the first with any accuracy.

7.3 Distributed multipole analysis

We therefore need to make some use of computational results. One possibility would be to fit a model to computed central moments, and some workers have done this, but a much better approach is to compute the distributed moments directly. The method of *distributed multipole analysis* (Stone 1981, Stone and Alderton 1985) will be described here, but similar procedures have been used by Rein (1973), Sokalski and Poirier (1983) and Vigné-Maeder and Claverie (1988). An alternative procedure based on the use of localized molecular orbitals has been proposed by Amos and Crispin (1976*b*).

It is customary nowadays to express computed wavefunctions in terms of gaussian functions of the form $\chi = R_{lm}(\mathbf{r} - \mathbf{a})\exp[-\zeta(\mathbf{r} - \mathbf{a})^2]$, centred at one or more arbitrary points $\mathbf{a}$, usually at the nuclei, though additional functions are sometimes used, for example at the centres of bonds. Then a one-electron wavefunction such as a molecular orbital takes the form

$$\psi(\mathbf{r}) = \sum_s c_s \chi_s(\mathbf{r} - \mathbf{a}_s). \tag{7.3.1}$$

The charge density then takes the form of a sum of products, with coefficients which are elements of the density matrix P_{st}:

$$\rho(\mathbf{r}) = \sum_{st} P_{st}\chi_s(\mathbf{r}-\mathbf{p}_s)\chi_t(\mathbf{r}-\mathbf{p}_t). \tag{7.3.2}$$

This form for the charge density does not depend on any particular assumptions about the form of the electronic wavefunction; for example it may include electron correlation.

We need to examine the form of a typical product of basis functions, say

$$\chi_a\chi_b = R_{lm}(\mathbf{r}-\mathbf{a})\exp[-\alpha(\mathbf{r}-\mathbf{a})^2] \times R_{l'm'}(\mathbf{r}-\mathbf{b})\exp[-\beta(\mathbf{r}-\mathbf{b})^2].$$

The product of two spherical gaussian functions $\exp[-\alpha(\mathbf{r}-\mathbf{a})^2] \times \exp[-\beta(\mathbf{r}-\mathbf{b})^2]$ can be written as a single gaussian centred at a point on the line from **a** to **b**:

$$\begin{aligned}&\exp[-\alpha(\mathbf{r}-\mathbf{a})^2]\exp[-\beta(\mathbf{r}-\mathbf{b})^2]\\ &\qquad = \exp\Big[-\frac{\alpha\beta}{\alpha+\beta}(\mathbf{a}-\mathbf{b})^2\Big]\exp[-(\alpha+\beta)(\mathbf{r}-\mathbf{p})^2],\end{aligned} \tag{7.3.3}$$

where **p** is the point $(\alpha\mathbf{a}+\beta\mathbf{b})/(\alpha+\beta)$. This formula was first derived by Boys (1950), and used by him as the basis for the practical application of gaussian wavefunctions in *ab initio* calculations. The basis function χ_a also contains regular spherical harmonics $R_{lm}(\mathbf{r}-\mathbf{a})$. These can be moved to **p** using eqn (2.7.5):

$$R_{lm}(\mathbf{r}-\mathbf{a}) = \sum_{k=0}^{l}\sum_{q=-k}^{k}\left[\binom{l+m}{k+q}\binom{l-m}{k-q}\right]^{\frac{1}{2}} R_{kq}(\mathbf{r}-\mathbf{p})R_{l-k,m-q}(\mathbf{p}-\mathbf{a}),$$

giving a linear combination of regular spherical harmonics of ranks up to l. We do the same with the $R_{l'm'}(\mathbf{r}-\mathbf{b})$ in χ_b, to give a linear combination of spherical harmonics of ranks up to l'. The product of two spherical harmonics of ranks k and k' is a linear combination of spherical harmonics of ranks from $|k-k'|$ to $k+k'$ (Clebsch–Gordan series; see Appendix B). When we multiply all of these expressions together, we obtain a rather complicated linear combination of terms of the form $R_{kq}(\mathbf{r}-\mathbf{p})\exp[-\zeta(\mathbf{r}-\mathbf{p})^2]$, involving spherical harmonics R_{kq} of ranks from 0 to $l+l'$.

Now the term $R_{kq}(\mathbf{r}-\mathbf{p})\exp[-\zeta(\mathbf{r}-\mathbf{p})^2]$ in the charge distribution has multipole moments, evaluated with origin at **p**, that are all zero except for Q_{kq}, because of the orthogonality of the spherical harmonics. Accordingly the product distribution $\chi_a\chi_b$ of basis functions of angular momentum l and l' has multipole moments, with respect to an origin at **p**, of ranks from 0 to $l+l'$ only. Thus an exact multipole representation of the charge distribution consists of a set of multipoles like this for each product of primitive gaussians appearing in the expansion of the charge density.

This may seem extremely complicated at first sight. Fortunately there are two features which make the practical application of this result very much simpler than might be expected. The first of these is that for most molecules of interest, the angular momentum of the basis functions is quite small. The valence orbitals of small molecules are constructed principally from s and p orbitals, and although d, f and higher angular momentum functions may be needed to describe polarization effects, their contributions are relatively small. We see that the

overlap of two s functions ($l = l' = 0$) leads only to a point charge at the overlap centre **p**; the overlap of an s function with a p function generates a charge and a dipole; and the overlap of two p functions generates charge, dipole and quadrupole. For a qualitative understanding of distributed multipoles, nothing further is needed, though the moments that arise from the polarization functions have to be included in accurate calculations.

The second simplifying feature is that in the numerical computation of the distributed multipole moments it is not necessary to carry out the algebraic manipulations explicitly. If we know that the multipole moments relative to **p** are limited in rank to $l + l'$, we can evaluate all of them by standard techniques, using Gauss–Hermite quadrature. Standard theory shows that $(l + l' + 1)$-point Gauss–Hermite quadrature gives exact results for all the moments that arise.

However, one complication remains: the formula for the position of the overlap centre **p** shows that it depends on the exponents α and β of the two gaussian functions, and will in general be different for every pair of gaussians. We deal with this problem by choosing a small number of *sites* at suitable positions in the molecule, and using eqn (2.7.6) to move the moments at the overlap centre to one or other of the chosen sites. The way in which this is done—the allocation algorithm—varies between different implementations of the theory.

Before exploring allocation algorithms, we note that the point $\mathbf{p} = (\alpha\mathbf{a} + \beta\mathbf{b})/(\alpha + \beta)$ lies on the line between **a** and **b**. If we use atom-centred gaussian basis functions, as is usual, we see that all the multipoles in the exact multipole representation lie on lines joining the nuclei. Accordingly, they all lie within any sphere that encloses the nuclei. The convergence sphere for a single-site multipole description of an assembly of point multipoles has its centre at the single site, and a radius just large enough to enclose all the multipoles. The required sphere therefore just encloses all the nuclei, as previously stated. The observant reader will notice that this begs the question of whether the atom-centred gaussian expansion of the wavefunction is itself convergent. We do not attempt to answer this question, but merely observe that in practice the expansion appears to converge quite quickly.

7.3.1 Allocation algorithms for distributed multipole analysis

The importance of a correct choice of allocation algorithm arises from the fact that, as explained in §2.7, there is a penalty for shifting the origin for multipole moments too far. If a moment Q_{km} at one origin is described by a multipole expansion about a new origin at a distance s from the old one, the new expansion contains moments of all ranks $l \geq k$, multiplied by a numerical factor proportional to s^{l-k}, so the higher moments rapidly become unacceptably large if s is too big.

To quantify this effect, we can define a divergence sphere for each site in a distributed multipole expansion, just as we did previously for the complete molecule. The sphere is centred at the site origin, and has to be just large enough to enclose all the multipoles that are to be transferred there.

Several allocation algorithms have been proposed. The *Mulliken* algorithm, which is used in the cumulative atomic multipole moment (CAMM) method (Sokalski and Poirier 1983), is a generalization of the method used to calculate Mulliken populations (Mulliken charges), and involves allocating half of the multipoles to each of the sites **a** and **b** from which the basis functions came. The *nearest-site* algorithm involves transferring all of the multipoles to the nearest site, which may be **a** or **b** or some other site entirely. The Mulliken algorithm has

the merit of simplicity, but there is nothing else to be said in its favour. Its disadvantage is that it may involve relatively large movements of the multipoles, especially if the two sites concerned are fairly far apart. If one of the basis function exponents α and β is much larger than the other, the overlap centre **p** will be very close to either **a** or **b**, and it is much more satisfactory in this case to move all the multipoles to the nearest site rather than half of them to the other. In terms of divergence spheres, we can easily see that the divergence sphere of each site for the Mulliken algorithm will reach nearly to the most distant atom with which there is a significant degree of basis-function overlap. Since modern high-quality basis sets include a number of very diffuse functions on each atom, the divergence spheres are typically quite large. Even for a small molecule such as N_2, the divergence spheres for each site have a radius equal to the bond length when sites are placed at each atom. This may be compared with the central multipole expansion, where the divergence sphere has only to enclose the two nuclei and has a radius equal to half the bond length. We have to conclude that the Mulliken algorithm can actually be worse than the central-multipole description, and this is confirmed by detailed calculation (Stone and Alderton 1985).

For the nearest-site algorithm, on the other hand, each divergence sphere extends just halfway to the nearest other site. If for N_2 we take two sites, one at each nucleus, the divergence spheres have radius equal to half the bond length. In this case the distributed-multipole treatment is no better in terms of convergence than the single-site multipole expansion. However, we can do much better if we add a further site at the centre of the bond. Now the divergence spheres have a radius of only one quarter of the bond length, and the convergence is very much better (Stone and Alderton 1985).

One minor problem with the nearest-site algorithm arises in the case where $\alpha = \beta$, which is common in symmetrical molecules. In this case sites **a** and **b** are equidistant from the overlap centre, and to preserve the symmetry it is necessary to divide the multipoles equally between the two sites, but this causes no practical difficulty, and in particular has an insignificant effect on the radius of the divergence spheres.

A more serious problem is that the values for the distributed multipoles are very sensitive to the choice of basis set. This happens because a change of basis set involves changes in the exponents of the basis functions (α and β in eqn (7.3.3)), so the overlap centres **p** are different for different basis sets. The allocation of a particular set of overlap multipoles to one site or another depends on whether the corresponding **p** falls to one side or the other of the dividing surface between the sites, so small changes in the positions of the overlap centres can have dramatic effects on the multipole moments. In one sense this is not a serious problem, because the convergence properties of the nearest-site algorithm ensure that the distributed multipoles always give the optimum description of the electrostatic interactions, and sets of distributed multipoles that look very different may in fact yield similar interaction energies. It is however a practical inconvenience in two ways. First, it makes it much more difficult to compare distributed multipoles from different basis sets and to assess whether improvements in the basis are making a significant difference; and secondly, the effect of truncating the description, for example by discarding all moments above quadrupole, may be different for different basis sets. Indeed, the errors may be greater for better basis sets containing functions with high angular momentum, because these make larger contributions to the higher moments.

A hybrid approach overcomes these problems by using grid-based quadrature for the diffuse basis functions (Stone 2005). The quadrature procedure is essentially the same as

that used in DFT calculations: a grid of points is constructed around each atom, each point weighted according to a suitable algorithm. Each point is then further weighted by reference to the distances from it to every atom (Murray *et al.* 1993, Becke 1988). In a normal DFT quadrature this is done in such a way that there is a sharp cutoff between the regions of space assigned to each atom, but for the calculation of distributed multipoles it is better to use a softer cutoff, so that the atom regions interpenetrate and are more nearly spherical. This approach is less satisfactory for sharply peaked basis functions, so the original nearest-site algorithm is used for those. The resulting hybrid algorithm is much less sensitive to the choice of basis set, and the site charges and higher moments are more likely to be in line with chemical intuition, but unfortunately the grid-based quadrature is much more time-consuming than Gauss–Hermite quadrature, and the convergence of the multipole series is not as good. For the purposes of calculating intermolecular interactions, the original nearest-site algorithm remains the preferred choice.

Wheatley has suggested another allocation algorithm that appears to overcome the problems of basis set dependence to some extent (Wheatley 1993*b*), but it only applies to linear molecules. According to this prescription, the maximum rank of multipole that is to be retained, $l_{\max}$, is chosen in advance. The z axis of coordinates is chosen to lie along the molecular axis, so that only the Q_{lm} with $m = 0$ are non-zero (see §2.6); we abbreviate Q_{l0} by Q_l. Then an overlap multipole Q_l at position $z = p$ is represented by moments at each of the n sites, with the moment $Q_{l'}^{\text{new}}(a)$ for the site at a being given by

$$Q_{l'}^{\text{new}}(a) = \frac{(l_{\max}-l)!}{(l_{\max}-l')!}\frac{(l_{\max}+n-l'-1)!}{(l_{\max}+n-l-1)!}\binom{l'}{l}(p-a)^{l'-l}Q_l\frac{\Pi_{a'\neq a}(p-a')}{\Pi_{a'\neq a}(a-a')}. \tag{7.3.4}$$

This applies for $l \le l' \le l_{\max}$. In addition, there are correction terms that account for overlap multipoles of ranks from $l_{\max}+1$ to $l_{\max}+n-1$ by modifying the site multipoles with rank $l_{\max}$.

This procedure has not been used extensively, but early results (Wheatley 1993*b*) suggested that the sensitivity to basis set is greatly reduced, and the accuracy of the multipole description is enhanced.

7.4 Other distributed-multipole methods

An alternative approach to the calculation of distributed multipoles uses a procedure due to Hirshfeld (1977) which he called 'stockholder partitioning'. The idea is to partition the molecular electron density between its atoms in proportion to the densities of the isolated atoms. He constructed a weighting function for each atom a in the molecule in the form

$$w_a(\mathbf{r}) = \rho_a^0(\mathbf{r})/\rho_{\text{pro}}(\mathbf{r}), \tag{7.4.1}$$

where $\rho_a^0(\mathbf{r})$ is the spherically averaged electron density of the free atom a and $\rho_{\text{pro}}(\mathbf{r})$ is the *promolecule density* $\sum_a \rho_a^0(\mathbf{r})$, with the sum taken over all atoms in the molecule. Then the electron density $\rho_a(\mathbf{r})$ to be assigned to atom a in the actual molecule, with electron density $\rho(\mathbf{r})$, is

$$\rho_a(\mathbf{r}) = w_a(\mathbf{r})\rho(\mathbf{r}), \tag{7.4.2}$$

and the multipole moments to be assigned to atom a can be evaluated by integration over this density in the usual way.

While this is an attractive idea, its original form has been criticized. The atom charges that are obtained in this way are smaller than those obtained by other methods, and this has been viewed as a deficiency, as indeed it is if a model based only on charges is required. Inclusion of the higher moments, as originally envisaged by Hirshfeld, would give a better model. A more serious criticism is that the expression of the promolecule in terms of isolated atoms is somewhat arbitrary, depending on the electron configuration chosen for the atom. In LiF, for example, the charges obtained when the promolecule is constructed from neutral Li and F (namely ±0.57) are very different from those obtained when it is constructed from Li^+ and F^- (±0.98).

Bultinck *et al.* (2007) proposed an iterative modification of the method which gives improved charges, though higher atomic moments were not considered. Their method still requires the calculation of isolated atom densities, however, and Lillestolen and Wheatley (2008, 2009) described a procedure that obtains the promolecule atom densities iteratively, starting from an arbitrary set of weight functions and converging to a unique solution. At each iteration new atom densities are calculated using the current set of weight functions in eqn (7.4.2), and the spherical averages of the new atom densities are used in eqn (7.4.1) to derive new weight functions. Lillestolen and Wheatley showed that this procedure is guaranteed to converge. The resulting localized atomic densities can be used to obtain atomic charges and higher moments.

For completeness, we mention two other methods for calculating distributed multipoles, though they are less suitable for application to intermolecular forces because they have poor convergence properties. One is to associate a region of physical space with each site using Voronoi polyhedra. The Voronoi polyhedron of a given site is the region of space that is closer to that site than to any other. Then distributed multipoles can be defined for each site:

$$Q_{lm}^a = \int_{V_a} R_{lm}(\mathbf{r} - \mathbf{a})\rho(\mathbf{r})\ \mathrm{d}^3\mathbf{r}. \tag{7.4.3}$$

Here a labels the site, with its centre at $\mathbf{a}$, and V_a denotes the volume enclosed by the Voronoi polyhedron. Guerra *et al.* (2004) described such a method, but they were only concerned with atom charges. The trouble with this approach is that although it seems logical to divide space up in this way, it does not lead to an efficient (that is, rapidly convergent) multipole description. For N_2, for example, with a site at each N nucleus, the dividing surface between the two regions is the plane through the centre of the molecule perpendicular to the axis. The nitrogen molecule as a whole is not far from spherical, but the two halves obtained by this bisection are very non-spherical, and their multipole moments increase rapidly with increasing rank (Stone and Alderton 1985). Even the central-multipole model provides a very much better description. The hybrid method described above uses a similar partitioning, but with a softer transition between one atom and the next, and this gives better results.

Another approach which suffers from similar problems is Bader's 'atoms in molecules' (AIM) treatment. In this method, the dividing surface between two atoms is the 'zero-flux' surface, which is determined directly from the charge density (Bader 1990, Popelier 2000). As a method for analysing molecular charge densities it has many attractive features. However, it leads to atomic regions or 'basins' that are highly non-spherical, and although the multipole moments for these atomic regions can be evaluated (Cooper and Stutchbury 1985) (at considerable computational expense, though there are ingenious techniques for improving the efficiency of the calculation) they suffer from the same disadvantages as those for the polyhedral dissection. In the case of N_2, in fact, the dividing surface is the same in both methods,

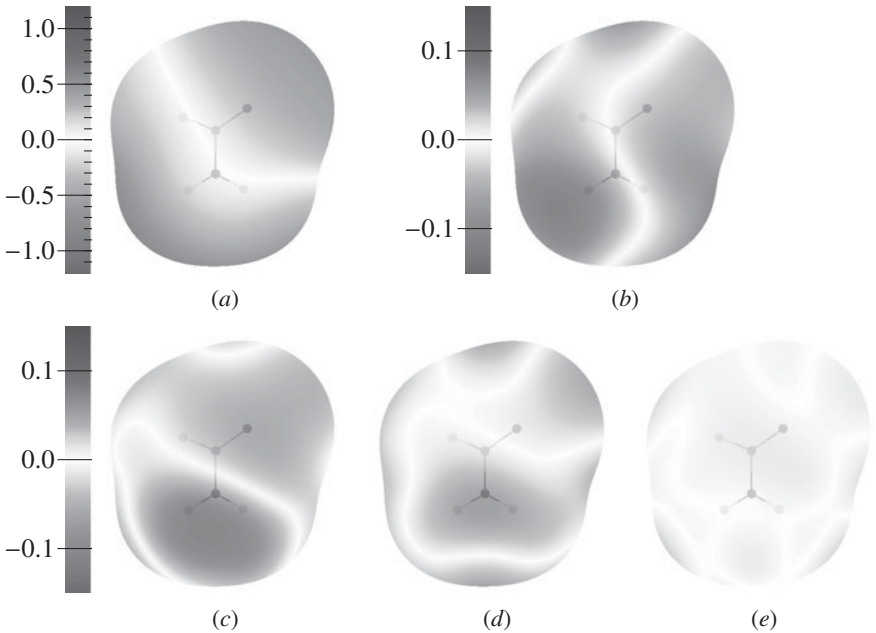

Fig. 7.2 Distributed-multipole models for formamide, $HCONH_2$. The maps show the electrostatic potential on the vdW×1.8 surface. The O atom is at the top right of each picture and the NH_2 group at the bottom. The scales are in volts, numerically equal to the energy in eV of a unit charge. (*a*) shows the total electrostatic potential using a rank-4 DMA. The other pictures show the difference between this and various simpler models: (*b*) CHELPG potential-derived charges, (*c*) Mulfit charges, (*d*) Mulfit charges and dipoles, (*e*) Mulfit charges, dipoles and quadrupoles on heavy atoms, charges and dipoles on H atoms. (See also Plate 1.)

for symmetry reasons. A further limitation is that by definition the AIM method deals with atomic sites only, though Joubert and Popelier (2002) have shown that the convergence can be improved by shifting a fraction of the moments to off-atom sites, while in condensed phases the electron distribution of any particular molecule is enclosed by surrounding molecules, so the atom basins no longer extend to infinity and convergence is better.

7.5 Simplified distributed multipole descriptions

Distributed multipole analysis readily provides a description that includes site multipoles up to hexadecapole or even higher. This description is often too elaborate, either because of the computation time needed to evaluate the interactions involving the higher moments, or because the distributed-moment description is needed in an application where these interactions have not been included. In particular, many applications are designed for use with point-charge models and cannot handle higher moments at all. Methods for constructing point-charge models are discussed in §7.8, but here we consider the general issue of constructing a low-rank distributed-multipole model from a high-rank one.

One possibility is simply to truncate the distributed-multipole description at the required rank. This is generally unsatisfactory, since it suppresses all the effects of the higher moments. A better strategy is to approximate the effects of the higher moments by modifying the lower moments. For example, a dipole on one site may be represented approximately by charges on other sites, and these charges may be added to the ones already present. Repeating the procedure for other sites gives a charge-only model that incorporates the effects of the site dipoles, albeit approximately. Similarly, site quadrupoles can be represented approximately by charges, or charges and dipoles, at other sites.

This approach is used in the Mulfit program of Ferenczy *et al.* (1991, 1997). A distributed multipole model using multipoles up to hexadecapole or higher can be approximated using multipoles of lower rank. Different ranks can be used for different atoms; for instance, hydrogen atoms may be limited to charges only, but other atoms allowed to carry dipoles and quadrupoles as well.

Examples of this procedure are shown for formamide in Fig. 7.2. The surface is the vdW×1.8 surface of the heavy atoms: that is, the union of spheres drawn around the heavy atoms at 1.8 times the Van der Waals radius, with the junctions between the spheres smoothed over. (The smoothing is done as follows. A sphere at radius R_a around atom a comprises points that satisfy $r_a = R_a$, where r_a is the distance from nucleus a, or equivalently $\exp[-\xi(r_a - R_a)] = 1$ for any ξ. We define the surface for the molecule by $\sum_a \exp[-\xi(r_a - R_a)] = 1$. The effect is as if an elastic membrane were stretched over the atomic spheres, with the tightness of the membrane defined by ξ. In this case $\xi = 2\,\text{bohr}^{-1}$.) The potential-fitted charges (CHELPG, see §7.8, p. 138) yield a potential that is in error near the NH_2 hydrogen atoms by about 0.15V, corresponding to an energy for a unit charge of $0.15e$V or about $15\,\text{kJ mol}^{-1}$. The Mulfit charges reduce the error significantly, and adding dipoles and quadrupoles reduces it further. Whether the gain in accuracy justifies the additional complication of the more elaborate potential would depend on the application.

7.6 Examples

We return to the N_2 molecule. The distributed multipoles, obtained using three sites, with the hybrid allocation algorithm, are shown in Table 7.1. The sites are the two N atoms, at $z = \pm 1.0337 a_0$ in the local coordinate system, and the centre of the bond. The values were calculated using the cc-pVQZ basis set. The left-hand column of numbers shows the central moments, while the next three columns show the distributed multipole analysis. The final column in each row shows the contribution of the moments in that row to the overall molecular quadrupole moment. The different levels of calculation give somewhat different results, but the general features are clear. Evidently none of the simple models discussed earlier (§7.2.1) comes anywhere near being an accurate description. The atomic charges are positive, in agreement with chemical expectations, not negative, as would be required by the three-charge model. The dipole moments on the atoms are nearly four times as big as would be required for the simple model involving dipoles only. The value of around 0.95 a.u. is quite large in chemical terms—it is about 2.4 D, a value significantly larger than the molecular dipole moment of HF. These dipoles have their positive ends directed towards the centre of the molecule and the negative ends outwards, so they can be regarded as describing the σ lone pair orbitals on each N atom. Finally, the atomic and bond quadrupoles are positive, as expected for the relatively diffuse π orbitals, but they have the opposite sign to the over-

Table 7.1 Distributed multipoles for N_2. cc-pVQZ basis. The last column shows the contributions to the overall molecular quadrupole from the distributed charges, dipoles and quadrupoles.

	Total moments	Distributed multipole analysis			ΔQ_2
Site:	centre	N	centre	N	
Position/bohr:	0.0	−1.0337	0.0	1.0337	
SCF:					
Q_0	—	0.439	−0.878	0.439	0.938
Q_1	—	0.927	—	−0.927	−3.833
Q_2	−0.983	0.808	0.296	0.808	1.912
MP2:					
Q_0	—	0.427	−0.854	0.427	0.913
Q_1	—	0.955	—	−0.955	−3.949
Q_2	−1.251	0.752	0.281	0.752	1.785
CCSD:					
Q_0	—	0.430	−0.860	0.430	0.919
Q_1	—	0.943	—	−0.943	−3.899
Q_2	−1.163	0.766	0.285	0.766	1.817
B3LYP:					
Q_0	—	0.427	−0.854	0.427	0.913
Q_1	—	0.947	—	−0.947	−3.916
Q_2	−1.170	0.775	0.283	0.775	1.833
Experimental (Buckingham *et al.* 1968):					
Q_2	−1.09 ± 0.07				

all molecular quadrupole moment. Notice that the atomic and bond quadrupole moments are somewhat larger for the SCF wavefunction than for the correlated ones; the wavefunction contracts slightly when correlation is included, because the effects of electron repulsion are reduced. It is evident that the overall quadrupole moment arises from a balance between these three contributions, and that each of them is readily understandable in simple physical terms.

The CO molecule provides an interesting comparison. If the numbers in Table 7.2 are compared with those in Table 7.1, a broadly similar pattern can be seen. However, the negative charge in the bond is balanced by a positive charge that is mostly on the C atom, in agreement with electronegativity considerations. This effect alone would give a fairly large dipole with the wrong sign, though significantly smaller when MP2 corrections are included, in line with the general observation that SCF calculations tend to exaggerate charge separations. However, there is an atomic dipole on each atom (with negative end directed outwards, as in N_2), and the dipole on the C atom is considerably larger than the one on oxygen. The net dipole moment for the whole molecule is much smaller as a result, and in the case of the MP2 calculation has the correct sign. However, MP2 is apt to over-correct for the excessive charge separation, so the dipole moment is now too large. The coupled cluster and density functional calculations give a very similar charge distribution to the MP2, but now the dipole moment is in good agreement with the experimental value.

Table 7.2 Distributed multipoles for CO. cc-pVQZ basis.

	Total moments	Distributed multipole analysis		
Site:	c. of m.	C	centre	O
Position/bohr:	0.0	−1.218	−0.152	0.914
SCF:				
Q_0	—	0.637	−0.851	0.214
Q_1	−0.104	1.169	−0.032	−0.791
Q_2	−1.532	0.225	0.281	1.143
MP2:				
Q_0	—	0.529	−0.834	0.305
Q_1	+0.111	1.162	−0.029	−0.784
Q_2	−1.500	0.411	0.276	1.048
CCSD:				
Q_0	—	0.563	−0.839	0.275
Q_1	+0.026	1.149	−0.030	−0.787
Q_2	−1.467	0.366	0.277	1.072
B3LYP:				
Q_0	—	0.556	−0.832	0.276
Q_1	+0.036	1.159	−0.030	−0.796
Q_2	−1.515	0.377	0.274	1.068
Experiment (Meerts *et al.* 1977):				
Q_1	+0.043			
Q_2	−1.4			

The quadrupole moments are much less affected by electron correlation. The main feature to notice is that in comparison with N_2, the quadrupole moment on O is greatly increased and the quadrupole on C is reduced. These features are a consequence of the concentration of the π electrons on the O atom, for electronegativity reasons, and are associated with the strong π-acceptor properties of the C atom in carbon monoxide.

Here again we see that the pattern of distributed moments is readily understandable in simple physical terms. We also see that the small dipole moment does not signify a breakdown of simple electronegativity ideas, as is sometimes suggested, but that it is the consequence of competing effects, easily understood if we allow for the effects of atomic electronic distortions.

Another example is the HF molecule. Distributed multipoles up to rank 12 for a three-site model, using nearest-site allocation, are shown in Table 7.3, together with the total moments. This table illustrates very clearly the superior convergence properties of the distributed-multipole treatment when the nearest-site algorithm is used. The magnitude of the central moments, referred to the centre of mass, increases steadily with increasing rank. In fact the ratio between successive moments is close to 1.6, which is the distance from the centre of mass to the most distant atom, i.e., the hydrogen. The odd moments, Q_7 and above, not shown in the Table, follow the same pattern. For the three-site distributed model, on the other hand,

Table 7.3 Distributed multipoles for HF (atomic units). B3LYP, cc-pVQZ basis. Odd moments of rank 7 and above are not shown. The experimental dipole moment is 0.7093 a.u. (Ogilvie 1988).

	Total moments	Distributed multipole analysis		
Site:	c. of m.	F	centre	H
Position:	0.0	−0.087	0.779	1.645
Q_0	—	**−0.016**	**−0.572**	**0.588**
Q_1	0.715	**0.265**	**−0.112**	0.038
Q_2	1.628	**0.430**	0.041	0.003
Q_3	2.404	−0.015	−0.028	−0.014
Q_4	4.65	−0.0006	0.017	0.018
Q_5	8.10	−0.0013	−0.009	−0.016
Q_6	13.90	−0.0004	0.0052	0.012
Q_8	39.97	0.0000	0.0016	0.0048
Q_{10}	114.73	0.0000	0.0005	0.0017
Q_{12}	332.50	0.0000	0.0001	0.0005

the moments decrease steadily with increasing rank, and the higher moments are quite negligible. Indeed, a description of the charge distribution in HF that is quite accurate as well as physically understandable is obtained from just the moments shown in bold in Table 7.3. These include a substantial positive charge on the H atom, balanced by a negative charge in the bond and a much smaller negative charge on F. These charges correspond well with conventional ideas of electronegativity and chemical bonding. Then there is a significant positive dipole moment on the F atom, which is associated with the σ lone pair, and a small negative dipole in the bond, describing the asymmetry of the charge distribution there. Finally there is a quadrupole moment on the F atom, which is associated with the π electrons.

For larger molecules, we can improve considerably on the central-multipole model without going to the extent of putting sites at the centre of every bond or even at every atom. For benzene, for example, a six-site model with a site at each carbon atom is very satisfactory. In this case the divergence spheres extend to the nearest H atom, and so have a radius of about 1 Å, instead of the 2.4 Å for the central model. This is small enough to ensure convergence of the distributed multipole expansion at accessible distances. In this model, each site has a quadrupole moment representing the anisotropy arising from the p-π electrons. In conjunction with a suitable repulsion model, again using six sites, this gave good results in Monte Carlo simulations of the orthorhombic and the high-pressure monoclinic phases of crystalline benzene, and of the liquid (Yashonath *et al.* 1988).

An even simpler six-site model, again in conjunction with a suitable repulsion and dispersion model, was able to account for the very diverse crystal structures of benzene and the azabenzenes (Price and Stone 1983, 1984). Here the electrostatic properties can be described very satisfactorily by a model in which there is a movement of 0.23 electrons along every CN bond, so that the C atoms become positively charged and the N atoms negatively charged. No higher multipoles are needed, except in benzene, which has no charge flow of this type, and where a quadrupole moment $Q_{20} = -0.8376\, ea_0^2$ was assigned to each C atom.

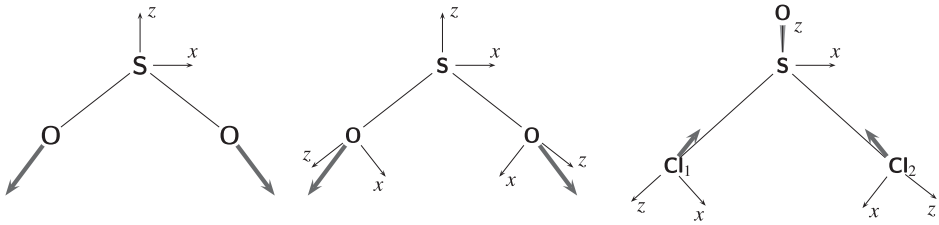

Fig. 7.3 (a) Molecule-fixed axes for SO_2, (b) site-fixed axes for SO_2, and (c) site-fixed axes for $SOCl_2$. Atomic dipole moments are shown schematically, for the O atoms only in SO_2 and for the Cl atoms only in $SOCl_2$.

7.7 Symmetry and distributed multipoles

The symmetry properties of multipole moments were discussed in §2.6. Some additional issues arise with distributed multipoles: the symmetry of a particular site (the 'site symmetry') may be lower than the overall molecular symmetry, and different sites may be related by symmetry. Careful choice of local axes can take advantage of any local symmetry, and simplify the relationships between sites.

For example, the SO_2 molecule in its equilibrium geometry has C_{2v} symmetry, and while a multipole site at the S atom has the full C_{2v} symmetry, the O atom sites have only C_s symmetry. Suppose that we choose molecular axes with z along the C_2 axis and x in the molecular plane (Fig. 7.3), and describe all the site multipoles in terms of these axes. The local C_{2v} symmetry at the S site implies that the components μ_x and μ_y of the S atom dipole must be zero. The symmetry at the O sites, however, is lower—only the σ_{xz} reflection plane—and this C_s symmetry implies only that μ_y must be zero for the O atoms.

However, the C_{2v} symmetry of the molecule means that the multipole moments of the two O atoms are related. In molecular axes (Fig. 7.3a) μ_z is the same for both O atoms, while μ_x has the same magnitude but opposite sign. Such sign differences are inconvenient, especially for higher moments, and a potential source of error. If we use symmetry-related local axes for each site (as for example in Fig. 7.3b), the magnitude and sign of both x and z components are the same for both O atoms.

Unfortunately it is not always possible to choose local axes so that signs are the same for all symmetry-related atoms. Consider the case of thionyl chloride, $SOCl_2$ (Fig. 7.3c). It is pyramidal—the O atom is above the SCl_2 plane in the Figure. We can define local axes for the Cl atoms as shown. In these axes μ_x and μ_z are the same for the two Cl atoms, but consider the μ_y components. They have the same magnitude, and both are directed up out of the SCl_2 plane, but in local axes μ_y is positive for Cl_1 and negative for Cl_2, because the local y axes point in opposite directions.

This behaviour is similar to that of enantiomers of chiral molecules, discussed in §2.6.1, and occurs when the only symmetry operation relating two sites is a reflection or other improper operation. As in the case of chiral molecules, defining the local axes differently doesn't help; the result is just that different multipole components change sign. The issue doesn't arise in the case of SO_2, because the higher symmetry requires μ_y to be zero for the O atoms in the local axes of Fig. 7.3b.

7.8 Point-charge models

Although distributed multipole analysis describes the charge distribution very accurately, it has the disadvantage—a serious one in the view of some workers—of using dipoles, quadrupoles and so forth as an essential feature of the description. The disadvantage here is that the interactions involving these moments are anisotropic. This means that not only does the energy depend on orientation, but as a result there are torques on the atoms. In an energy optimization or dynamical simulation it then becomes necessary to keep track of the orientation as well as the position of each atom. It will be argued in Chapter 12 that this level of complication is inevitable if we are to attempt accurate descriptions of molecules, and further that there are advantages to offset the complications—in particular, the possibility of using fewer sites.

Nevertheless, the scientific community has generally preferred to use point-charge models, avoiding the use of higher moments. We examine here some of the ways of obtaining such models. Storer *et al.* (1995) proposed to classify the methods as follows:

I Methods that extract the charges directly from experiment;
II Methods that extract them from a wavefunction by analysing the wavefunction itself;
III Methods that extract them from a quantum-mechanical calculation by analysing properties predicted from the wavefunction.

Few methods of type I exist. One is the use of X-ray diffraction data, which in principle yields directly a three-dimensional map of the charge density which can be integrated to provide atom charges. In practice the route from the measured diffraction intensities to the charge density involves a number of assumptions and approximations which reduce the reliability of the results (Spackman 1992).

Another is the atomic polar tensor (APT) approach. If each atom k can be treated as carrying a fixed point charge q_k and no dipole, the overall dipole moment is

$$\mu_\alpha = \sum_k q_k r_{k\alpha}, \tag{7.8.1}$$

where $\mathbf{r}_k$ is the position of atom k. We can immediately see that

$$\frac{\partial \mu_\alpha}{\partial r_{k\beta}} = q_k \delta_{\alpha\beta}, \tag{7.8.2}$$

and the derivative of the dipole moment with respect to a normal coordinate Q is

$$\frac{\partial \mu_\alpha}{\partial Q} = \sum_{k\beta} \frac{\partial \mu_\alpha}{\partial r_{k\beta}} \frac{\partial r_{k\beta}}{\partial Q} = \sum_{k\beta} q_k \frac{\partial r_{k\beta}}{\partial Q}. \tag{7.8.3}$$

The infrared intensity is proportional to the square of the dipole derivative, so a knowledge of the infrared intensities and the normal modes is sufficient to determine the q_k (Gussoni *et al.* 1986).

The difficulty with this idea goes back to its initial assumption, eqn (7.8.1). The dipole moment is more accurately represented as

$$\mu_\alpha = \sum_k (q_k r_{k\alpha} + \mu_{k\alpha}), \tag{7.8.4}$$

where $\boldsymbol{\mu}_k$ is the atomic dipole moment of atom k, and its derivative is not eqn (7.8.2) but

$$\frac{\partial \mu_\alpha}{\partial r_{k\beta}} = q_k \delta_{\alpha\beta} + \sum_{k'} \left(r_{k'\alpha} \frac{\partial q_{k'}}{\partial r_{k\beta}} + \frac{\partial \mu_{k'\alpha}}{\partial r_{k\beta}} \right), \tag{7.8.5}$$

because both the charge q_k and the dipole μ_k vary with geometry. These additional terms cannot usually be neglected. If, for example, we take the simple case of the HF molecule, a Kohn–Sham calculation of the dipole moment using the cc-pVQZ basis set with the B3LYP functional gives a dipole moment of $0.715\, ea_0$ at the equilibrium bond length of 0.9171 Å = $1.733a_0$. The dipole derivative with respect to the F–H bond length is $0.317e$, and this is therefore the charge to be assigned to the H atom in the APT scheme. This leads to a dipole moment of $0.317e \times 1.733a_0 = 0.55\, ea_0$, 23% too low. A distributed multipole analysis shows that the discrepancy is mainly accounted for by the dipole moment on the F atom: its variation with bond length contributes substantially, and negatively, to the dipole derivative.

A further issue with eqn (7.8.2) is that there are three derivatives $\partial\mu_\alpha/\partial r_{k\beta}$ with $\alpha = \beta$, and they need not be equal to each other. Consequently q_k is not well defined by this equation. However, Dinur and Hagler (1989) have pointed out that in *planar* molecules the derivatives of the atom charges with respect to displacement normal to the plane are zero by symmetry. That is, if the molecule lies in the xy plane, $\partial q_{k'}/\partial z_k = 0$. They further imposed the arbitrary condition that $\sum_k \boldsymbol{\mu}_k = 0$, so that the last term of eqn (7.8.5) vanishes. Then eqn (7.8.5) reduces to $q_k = \partial\mu_z/\partial z_k$. Dinur and Hagler viewed this as a *definition* of the atomic charge. They were able to relate the atomic dipole moments to derivatives of the molecular quadrupole in a similar fashion, obtaining a model comprising atomic charges and dipoles that by construction reproduces the molecular dipole and quadrupole moments exactly. This however takes the method beyond type I to type III, since it requires *ab initio* information.

Cioslowski (1989*a*,*b*) has proposed a generalized atomic polar tensor scheme (GAPT), according to which the atomic charge is defined in terms of the trace of the tensor $\partial\mu_\alpha/\partial r_{k\beta}$. However, this gives

$$\frac{1}{3}\frac{\partial}{\partial r_{k\alpha}}\mu_\alpha = q_k + \frac{1}{3}\sum_{k'}\left(r_{k'\alpha}\frac{\partial q_{k'}}{\partial r_{k\alpha}} + \frac{1}{3}\frac{\partial \mu_{k'\alpha}}{\partial r_{k\alpha}} \right). \tag{7.8.6}$$

Even if we impose the Dinur–Hagler condition, $\sum_k \boldsymbol{\mu}_k = 0$, we see that there are additional terms that vanish only if the charges are independent of geometry. This is clearly unphysical in the limit of dissociation, and implausible even near equilibrium, and the charges obtained this way are unrealistic (Solheim *et al.* 2004).

For our purposes the criterion against which any point-charge model is to be judged is its adequacy for describing intermolecular interactions. The Dinur–Hagler approach has the merit in this respect of reproducing the molecular dipole moment exactly, so it is guaranteed to get the dipole–dipole interaction correct. At short range, however, this is not enough.

In fact it will be clear from the previous discussion on N_2 that point-charge models may need to be quite elaborate to describe small molecules accurately. Atomic sites are not enough. The simplest point-charge model that reproduces the quadrupole moment of N_2 not only fails to reproduce the hexadecapole but is wholly unacceptable physically, because it assigns a positive charge to the bond. The APT approach also fails, since it assigns zero charges to the atoms, and if atomic dipoles are added the quadrupole is reproduced but again not the hexadecapole. The simplest adequate point-charge description of N_2 is a five-charge model

due to Murthy *et al.* (1983). This uses charges of q and q' at $\pm z$ and $\pm z'$ respectively, with a balancing charge of $-2(q + q')$ at the centre. The four parameters—two charges and two positions—were chosen to reproduce the lowest four calculated central multipole moments. This model is successful in accounting for the lattice vibrations in the solid.

For larger molecules, especially biological molecules such as proteins and nucleic acids, point-charge models have been used for a long time with reasonable success, and there are several commercially available programs that use them. However, the quality of model varies greatly (Roterman *et al.* 1989*a*,*b*), and it is worth examining the criteria for a reliable model.

If we start notionally from the viewpoint of a distributed-multipole model with sites on all the atoms, the simplest route to a point-charge model is to throw away the higher moments. It is not difficult to see that this will not work. Such a truncation of the multipole series will be satisfactory only if the discarded moments are small, but the distributed-multipole picture includes atomic dipole moments, describing lone-pair electrons and other atomic distortions, and atomic quadrupole moments, arising usually from π electrons. The construction of the valence orbitals from *s* and *p* atomic orbitals guarantees that such atomic dipoles and quadrupoles will arise except in very symmetrical environments. They will be particularly important in the polar groups that are common in proteins, nucleic acids and other biological systems.

Historically, one of the popular sources of point-charge models has been the Mulliken population analysis provided by virtually all semi-empirical and *ab initio* wavefunction programs. This provides a count of the number of electrons formally assigned to each atom, and can be used, following Mulliken's original suggestion, to provide some information about the nature of the bonding. In distributed-multipole terms, the Mulliken charges are just the charges that arise when the Mulliken allocation algorithm is used for the calculation of distributed multipoles, this algorithm being in fact a generalization of Mulliken population analysis. We have already seen that this algorithm provides a poorly convergent description, so it is a particularly bad approximation to throw away the dipoles and higher moments in this case. It should be noted that Mulliken suggested his method of population analysis for a quite different purpose, and would probably have deplored the use of Mulliken charges in point charge models.

However, the use of only the charges from any distributed-multipole model will be subject to errors, if to a lesser degree, because the dipoles and quadrupoles (though not usually the higher moments) are intrinsic to the description. The examples discussed above of CO (Table 7.2) and HF (Table 7.3) illustrate this very clearly. The MP2 DMA charges for CO give a molecular dipole moment of −0.24 a.u., compared with the overall MP2 dipole moment of +0.11 a.u.; while the charges alone for HF give a dipole moment of 0.52 a.u. compared with the overall dipole moment of 0.72 a.u. The error in the case of CO is 0.35 a.u., or 0.9 D, even though this is not a particularly polar molecule.

It is therefore necessary, if a point-charge model is to be used, to modify the charges so as to take into account as far as possible the effects of these omitted moments. One way to do this is to fit atomic charges so as to reproduce the molecular electrostatic potential. This approach was introduced by Momany (1978) and refined by Cox and Williams (1981), Singh and Kollman (1984) and Breneman and Wiberg (1990). It is now widely used under the name CHELPG (for CHarges from ELectrostatic Potentials using a Grid based method). The potential is obtained directly from an *ab initio* molecular charge density, using eqn (4.1.4), evaluated on a grid of points surrounding the molecule, and a least-squares fitting procedure is used to obtain a set of atom charges which reproduce the potential at the grid points as closely

as possible. The charges are constrained so that the total charge on the molecule is correct, and sometimes so that the molecular dipole moment is also reproduced. It is important to choose the grid points so that they lie outside the molecular charge distribution, otherwise the potential contains penetration effects (see Chapter 8) which cannot be represented by any multipolar description. Usually the points are chosen so that they are all at least 1 Å outside the Van der Waals surface of the molecule. Unfortunately the higher moments—octopoles, hexadecapoles, and so on—make only a small contribution to the potential at such distances, and their effects on the potential at short range may be poorly reproduced by the point charges. Furthermore, Francl *et al.* (1996) showed that the CHELPG procedure is ill-conditioned, so that the charges are not well-determined, though they also showed how to use singular value decomposition to improve the condition number of the problem.

Another method, the Mulfit procedure, already discussed in §7.5, uses an accurate distributed multipole analysis as the source of the potential to be fitted. This has two advantages: the potential obtained this way is completely free from penetration effects, and the generation of the potential from the DMA is much faster than from the charge density. In fact, it is possible to use an analytical procedure which bypasses the intermediate step of generating the potential, but only by treating the multipole potential of each atom individually, and the fit to the total potential seems to be less accurate if this procedure is adopted (Chipot *et al.* 1994).

All of these methods suffer from the disadvantage that atomic dipoles and quadrupoles have to be represented by point charges, some of which are necessarily on other atoms. This leads to inaccuracies in the potential close to polar and quadrupolar atoms, which often occur in just the regions where an accurate description is needed, for example near the active sites of enzymes. Wiberg and Rablen (1993) investigated a number of schemes for assigning atom charges, and concluded that 'the charge distribution in a molecule is much too anisotropic to be successfully modelled by *any* single set of atom-centred charges unless only long-distance interactions are of interest. Otherwise it is necessary to include at least atomic dipole terms, and possibly higher terms as well.'

One way to overcome this problem within the framework of a point-charge model is to introduce additional sites near such atoms (Williams 1993), but this increases the number of sites to be handled, and the choice of additional sites is often somewhat arbitrary. Alemán *et al.* (1994) added charges in lone-pair and bond positions. The charges are then fitted to the electrostatic potential in the usual way. They found that the r.m.s. error in the point-charge potential can be reduced by a factor of five or so, but there does not seem to be any systematic procedure for choosing the positions of the additional charges.

A more elaborate form of point-charge model, derived from cumulative atomic multipole moments (CAMM) has been used by Sokalski and Sawaryn (1992) who use an array of point charges near the nucleus of each atom. By choosing appropriate values for the charges, it is possible to reproduce the atomic charge, dipole and quadrupole. If the point charges are too far from the nucleus, spurious higher moments are introduced, while if they are too close, the charges have to become very large, and numerical problems can arise in calculating the interactions, which become small differences of very large quantities. Displacements of 0.25 a.u., as used by Sokalski and Sawaryn, are probably a reasonable compromise, but the charges can be as large as 200 a.u. However, the main disadvantage of the method is that because there are nine sites for each atom, the number of site–site interactions is increased by a factor of 81 over a simple point-charge model. Distributed-multipole descriptions are computationally

much more efficient than this. A further inefficiency is that for linear molecules, where three charges on the axis suffice to describe the only non-zero moments Q_{00}, Q_{10} and Q_{20}, the method assigns off-axis charges, so increasing the number of charges unnecessarily and also destroying the cylindrical symmetry.

Nevertheless models using off-atom charges can be useful. In aromatic systems, each C atom carries a quadrupole moment of about $-1.1\, ea_0^2$. This cannot usually be represented satisfactorily by point charges on neighbouring atoms, because there are no atoms above and below the plane. Hunter and Sanders (1990) represented it by negative charges above and below the aromatic plane and a positive charge at the C atom. This simple picture provides a very effective treatment of π–π interactions in aromatic systems (Hunter 1994); it has been used for example to account for the geometry of interactions between phenylalanine residues in proteins, where the pattern of observed orientations of pairs of neighbouring phenyl rings matches almost exactly the pattern of electrostatically attractive orientations (Hunter *et al.* 1991), and for the way in which the structure of DNA depends on the base-pair sequence (Hunter 1993).

8
Short-Range Effects

The interaction energy terms between molecules at long range can be expressed straightforwardly and accurately at long range in terms of power series in $1/R$, and this description is relatively easy to understand and to manipulate. At short range, however, the description is complicated by the effects of overlap and exchange, as we have seen. We explore some of these complications here.

In spite of the plethora of perturbation treatments, the first-order energy is essentially the same in all methods: it is the difference between the expectation value of the full Hamiltonian $\mathcal{H}$ for the antisymmetrized product function $|0_A 0_B\rangle$ and the zeroth-order energy. The latter is unambiguously $W_A^0 + W_B^0$ without any need to specify a zeroth-order Hamiltonian. We have seen that there are two contributions to the first-order energy: the electrostatic energy and the exchange–repulsion energy.

8.1 The electrostatic energy at short range: charge penetration

The electrostatic energy can be described at any distance by the expression 4.1.3; it is defined in terms of the unperturbed charge densities of the two molecules. At long range, the multipole expansion provides a satisfactory alternative, but often fails to converge at shorter distances. The distributed multipole expansion can always be constructed so as to converge at all configurations of interest, but when the molecular charge distributions overlap, the converged result is in error by an amount called the *penetration energy*. Consider as an illustration the interaction between a proton and a hydrogen-like atom of nuclear charge Z. The wavefunction of the latter is $\sqrt{Z^3/\pi}\exp(-Zr)$, so that the electron charge density is $-e(Z^3/\pi)\exp(-2Zr)$. The potential at the proton due to this electron density is the solution of Poisson's equation:

$$\nabla^2 V = -\frac{\rho}{\epsilon_0} = 4Z^3 \exp(-2Zr), \tag{8.1.1}$$

since $4\pi\epsilon_0 = 1$ in atomic units. Since the charge density is spherically symmetric, the potential is also spherically symmetric, so this equation becomes

$$\frac{1}{r^2}\frac{\partial}{\partial r} r^2 \frac{\partial V}{\partial r} = 4Z^3 \exp(-2Zr),$$

which can be solved by standard methods to give

$$V(r) = -\frac{1}{r} + \exp(-2Zr)\Big(Z + \frac{1}{r}\Big). \tag{8.1.2}$$

Note that this does not include the potential Z/r due to the nucleus. We see that there are two terms. One is proportional to $-1/r$ and is the multipole expansion of the potential due to the

spherical electron cloud. We note that this is trivially convergent at all non-zero values of r. The other term contains a factor $\exp(-2Zr)$ and describes the correction to the potential at short distances that arises from the finite extent of the charge distribution. This is the penetration correction. Note that when $r \to 0$ the potential remains finite, as it should; there is no singularity in the electron charge distribution, and therefore no singularity in the potential. In the general case, the complete penetration correction cancels out all the r^{-n} singularities that arise from the multipole expansion of the potential due to the electrons, leaving only the Z/r terms from the nuclei.

Note also that the term in $\exp(-2Zr)$ does not contribute to the multipole expansion. Viewed as a function of $z = 1/r$, $\exp(-2Zr) = \exp(-2Z/z)$ has an essential singularity at $z = 0$: it tends to zero as $z \to 0$ from positive values, but to infinity as $z \to 0$ from negative real values, so it has no Taylor expansion in powers of z.

At moderate distances the penetration term is approximately proportional to $\exp(-2Zr)$, i.e., to the charge density. It is a positive correction to the potential, so it yields a negative correction to the interaction energy in the usual case where the electron distribution of one molecule penetrates into another. If we may assume that the penetration correction to the potential of molecule A, ΔV^A_{pen}, is proportional to the charge density ρ^A in the general case, then the correction to the energy is

$$\Delta U_{\text{pen}} \approx \int \Delta V^A_{\text{pen}}(\mathbf{r})\rho^B(\mathbf{r})\ \mathrm{d}^3\mathbf{r} \propto \int \rho^A(\mathbf{r})\rho^B(\mathbf{r})\ \mathrm{d}^3\mathbf{r}.$$

Note that the 'constant' of proportionality includes the nuclear charge Z, so this is unlikely to be very accurate as a general formula. Nevertheless it provides some guidance to the behaviour of the effect, and moreover suggests that the penetration correction can be modelled for practical purposes as part of the repulsion energy, which has a similar behaviour, as we shall see.

It is possible to write eqn (8.1.2) in the form

$$\begin{aligned} V(r) &= -\frac{1}{r}[1 - \exp(-2Zr)(1 + rZ)] \\ &= -\frac{1}{r} f_1(2Zr), \end{aligned} \tag{8.1.3}$$

in which the quantity in square brackets is treated as a *damping function* $f_1(2Zr)$ that is 1 at long range and tends to zero at short range in such a way as to suppress the singularity in the multipole term. The dispersion and induction terms, where similar effects arise (see §8.3.1) have been treated this way for many years, but the treatment of electrostatic penetration by means of damping functions has been explored only recently. A way to approach this possibility is through the concept of Gaussian multipoles.

8.1.1 Gaussian multipoles

A gaussian multipole is a charge density that is obtained as a derivative of an ordinary spherical gaussian charge distribution (Wheatley 1993*a*):

$$G^{\zeta}_{abc}(\mathbf{r} - \mathbf{r}_P) = \left(\frac{\zeta}{\pi}\right)^{3/2} \frac{(-1)^{a+b+c}}{(a+b+c)!} \frac{\partial^a}{\partial x^a} \frac{\partial^b}{\partial y^b} \frac{\partial^c}{\partial z^c} \exp[-\zeta(\mathbf{r} - \mathbf{r}_P)^2]. \tag{8.1.4}$$

The multipole expansion of this charge density about $\mathbf{r}_P$ contains only terms of rank $n = a + b + c$. In particular, the gaussian multipole $G^{\zeta}_{00n}(\mathbf{r} - \mathbf{r}_P)$ produces the same multipolar potential as a spherical tensor multipole Q_{n0} of magnitude 1 sited at $\mathbf{r}_P$.

A gaussian multipole can be viewed as a component of a cartesian tensor of rank n:

$$G^{\zeta}_{i_1 i_2 \ldots i_n} = \left(\frac{\zeta}{\pi}\right)^{3/2} \frac{(-1)^n}{n!} \nabla_{i_1} \nabla_{i_2} \ldots \nabla_{i_n} \exp[-\zeta(\mathbf{r} - \mathbf{r}_P)^2]. \tag{8.1.5}$$

This tensor is symmetric in all its indices, since the ∇ operators commute. Its components can be re-expressed in spherical tensor form, as products of a radial function with a regular spherical harmonic. For example (taking $\mathbf{r}_P = 0$),

$$G^{\zeta}_{00} = G^{\zeta} = \left(\frac{\zeta}{\pi}\right)^{\frac{3}{2}} \mathrm{e}^{-\zeta r^2} R_{00}(\mathbf{r}), \tag{8.1.6}$$

$$G^{\zeta}_{10} = G^{\zeta}_{z} = \left(\frac{\zeta}{\pi}\right)^{\frac{3}{2}} 2\zeta \mathrm{e}^{-\zeta r^2} R_{10}(\mathbf{r}). \tag{8.1.7}$$

These correspond to unit charge and unit μ_z respectively; that is, the multipole expansion of G^{ζ}_{00} contains the single term $Q_{00} = 1$, while the multipole expansion of G^{ζ}_{10} contains the single term $Q_{10} = 1$. In the limit $\zeta \to \infty$, these become point charge and point dipole respectively, but for finite ζ their interactions involve penetration terms as well as multipole terms.

For higher rank, additional non-multipolar components occur. A symmetric second-rank tensor has both rank 2 and rank 0 components. We can define

$$G^{\zeta}_{20} = \tfrac{1}{3}(2G^{\zeta}_{zz} - G^{\zeta}_{xx} - G^{\zeta}_{yy}) = \frac{4\zeta^2}{3}\left(\frac{\zeta}{\pi}\right)^{\frac{3}{2}} \mathrm{e}^{-\zeta r^2} R_{20}(\mathbf{r}), \tag{8.1.8}$$

$$G^{\zeta}_{(2)00} \equiv G^{\zeta}_{\alpha\alpha} = \left(\frac{\zeta}{\pi}\right)^{\frac{3}{2}} (2\zeta^2 r^2 - 3\zeta) \mathrm{e}^{-\zeta r^2}. \tag{8.1.9}$$

It is easy to verify by direct integration, using eqn (2.1.7), that G^{ζ}_{20} has a multipole moment $Q_{20} = 1$. $G^{\zeta}_{(2)00}$ is spherically symmetrical, so all its multipole moments vanish except for its charge Q_{00}; but integration shows that the charge too is zero, so $G^{\zeta}_{(2)00}$ does not contribute to the multipole expansion of rank 2 gaussian multipoles. However, it does contribute to the penetration part of the interaction.

Similarly, for rank 3 we have

$$G^{\zeta}_{30} = \tfrac{1}{5}(5G^{\zeta}_{zzz} - 3G^{\zeta}_{\alpha\alpha z}) = \frac{8}{15}\left(\frac{\zeta}{\pi}\right)^{\frac{3}{2}} \zeta^3 \mathrm{e}^{-\zeta r^2} R_{30}(\mathbf{r}), \tag{8.1.10}$$

$$G^{\zeta}_{(3)10} = G^{\zeta}_{\alpha\alpha z} = \frac{1}{3}\left(\frac{\zeta}{\pi}\right)^{\frac{3}{2}} (4\zeta^3 r^2 - 10\zeta^2) \mathrm{e}^{-\zeta r^2} R_{10}(\mathbf{r}), \tag{8.1.11}$$

$$\tag{8.1.12}$$

and for rank 4:

$$G^{\zeta}_{40} = \tfrac{1}{35}(8G^{\zeta}_{zzzz} - 24G_{xxzz} - 24G_{yyzz} + 3G_{xxxx} + 3G_{yyyy} + 6G_{xxyy})$$
$$= \frac{16}{105}\left(\frac{\zeta}{\pi}\right)^{\frac{3}{2}} \zeta^4 \mathrm{e}^{-\zeta r^2} R_{40}(\mathbf{r}), \tag{8.1.13}$$

$$G^{\zeta}_{(4)20} = 2G^{\zeta}_{zz\alpha\alpha} - G^{\zeta}_{xx\alpha\alpha} - G^{\zeta}_{yy\alpha\alpha} = \left(\frac{\zeta}{\pi}\right)^{\frac{3}{2}} \zeta^3(2\zeta r^2 - 7)\mathrm{e}^{-\zeta r^2} R_{20}(\mathbf{r}), \tag{8.1.14}$$

$$G^{\zeta}_{(4)00} = G^{\zeta}_{\alpha\alpha\beta\beta} = \left(\frac{\zeta}{\pi}\right)^{\frac{3}{2}} \zeta^2(4\zeta^2 r^4 - 20\zeta r^2 + 15)\mathrm{e}^{-\zeta r^2}. \tag{8.1.15}$$

G^{ζ}_{30} has multipole moment $Q_{30} = 1$, but $G^{\zeta}_{(3)10}$, although having dipolar angular behaviour, has zero dipole moment and does not contribute to the multipolar potential. Similarly, G^{ζ}_{40} has multipole moment $Q_{40} = 1$, but $G^{\zeta}_{(4)20}$ and $G^{\zeta}_{(4)00}$ have zero multipole moments. Again, these non-multipolar terms do contribute to the penetration term.

It is usual in modern density functional programs to represent the electron density using a basis set of gaussian functions, since the energy is a functional of the density and it is more efficient to represent the density in this way than in terms of the wavefunction. Consequently basis sets have been developed specifically for density fitting, and the density-fitted form can be used directly in the calculation of the electrostatic interaction. The charge density can then be represented, not by point charges, dipoles and so forth, but by a superposition of gaussian multipoles, since they are essentially the same as the gaussian basis functions used in *ab initio* calculations (eqn (5.4.3)). However, the electrostatic interaction between gaussian multipoles differs in several ways from the point-multipole expressions developed in §3.3 (Stone 2011). The first difference is that the point-multipole expression in (3.3.10) or (3.3.12) or (3.3.14) for the interaction between multipoles of ranks l_1 and l_2 is multiplied by a damping function $g_{l_1+l_2}(R/\lambda)$, where $\lambda = (\zeta_1^{-1} + \zeta_2^{-1})^{1/2}$ and ζ_1 and ζ_2 are the exponents of the two gaussian multipoles. The quantity λ can be thought of as a penetration length, characterizing the distance below which penetration effects become significant. The damping function $g_n(z)$ is related to the error function $\mathrm{erf}(z)$, in the following way. The error function can be represented by a power series (Abramowitz and Stegun 1965):

$$\mathrm{erf}(z) = \frac{2}{\sqrt{\pi}}\mathrm{e}^{-z^2} \sum_{k=0}^{\infty} \frac{2^k}{(2k+1)!!} z^{2k+1}, \tag{8.1.16}$$

which converges for all z, and the damping function $g_n(z)$ is this series with the first n terms deleted.

The second difference from the normal point-multipole expression is that there are additional terms involving the functions $\overline{S}^{\kappa_1\kappa_2}_{l_1\,l_2\,j}$ with $j = l_1 + l_2 - 2, l_1 + l_2 - 4, \ldots, 1$ or 0. These terms also involve a linear combination of some of the first few terms of the series expansion (8.1.16), so they decay to zero exponentially as the argument $z = R/\lambda$ increases.

It may seem surprising that the damping functions depend only on the separation R and not on orientation. In fact this must be so, as the energy is described as an expansion in terms of the $\overline{S}$ functions, which constitute a complete set in orientational space. The coefficient of each $\overline{S}$ function must be a function only of R, and the damping can only modify the R^{-n} behaviour that is seen at long range. There are new orientation-dependent penetration effects, but they are described by the new terms with $j \neq l_1 + l_2$.

The third difference is that the expansion of the density in terms of gaussian orbitals uses several primitive gaussian functions for each orbital, and therefore gaussian multipoles with several different values of ζ. The interaction described by a single point-multipole interaction at long range will therefore become a sum of terms involving several different values of ζ_1 and ζ_2 and hence of λ. It is possible to combine the terms into an expression involving a single damping function, but the damping can no longer be described by a simple analytic function. Moreover charge-multipole interactions involve differences between the electron–electron and electron–nucleus interactions, since $\zeta = \infty$ for the point-charge nucleus, so that the penetration length λ is smaller for the electron–nucleus terms.

In practice it seems to be possible to simplify the approach considerably. Elking *et al.* (2010) have found that fitting the density to the molecular electrostatic potential gives a good description of the penetration energy with relatively few gaussian basis functions, compared with the usual procedure of minimizing the error in the electron-electron repulsion (eqn (5.4.5)). Another approach is to use a relatively crude description of the density, possibly even using only *s*-type gaussians, which is used only to calculate the penetration-energy correction (Cisneros *et al.* 2007).

8.1.2 Other treatments of charge penetration

Freitag *et al.* (2000) proposed damping functions for the electrostatic interaction, obtained by fitting a one-parameter empirical damping function to the electrostatic potential around each isolated molecule. They used separate damping functions for the electron–nucleus and electron–electron interaction terms, and found that a fair description of the penetration effect (errors less than about 4 kJ mol^{-1}) was obtained with charge–charge damping only. Piquemal *et al.* (2003) used similar damping functions to refine the electrostatic energy term in their SIBFA scheme, and Piquemal *et al.* (2006) used an expansion of the charge density in terms of spherical gaussian functions to describe the exchange–repulsion and induction energy as well as the electrostatic energy. Slipchenko and Gordon (2006) used a penetration correction based on eqn (8.1.2) in their effective fragment potentials. Spackman (2006) found that good estimates of the penetration energy can be obtained from the Coulombic interactions between promolecule electron densities (see §7.4).

Charge penetration effects only arise between atoms whose electron densities overlap, so it is possible to use the distributed-multipole model for most atom pairs, using more elaborate treatments for nearby atoms only. Volkov *et al.* (2004, 2006) described such a method, using exact evaluation of the electrostatic interaction between atoms closer than 4 Å, or rather between transferable model representations of the atoms. They note that the penetration correction is particularly large for hydrogen bonds. The method is more time-consuming than the use of damping functions, but much faster than the calculation of the full electrostatic interaction between *ab initio* wavefunctions. Rob *et al.* (2007) described a similar method, but used exact evaluation of the interaction between the nearby atoms. Accounting for the separation between the regions of density to be treated by exact and multipole methods needs careful consideration, and Rob *et al.* found that they needed to use augmented basis sets for the atoms in the exact region but non-augmented sets sufficed for the rest.

8.2 The exchange–repulsion energy

The main part of the first-order energy is normally described as 'exchange–repulsion', and is a combination of two effects, as we saw in eqn (6.1.3). The 'exchange' energy is a consequence of the fact that the electron motions are free to extend over both molecules, and is an attractive term, while the 'repulsion' arises when the electrons attempt to occupy the same region of space, and are forced to redistribute because the Pauli principle forbids electrons of the same spin to be in the same place. The exchange–repulsion is termed 'exchange' by some authors.

For single-determinant (SCF) wavefunctions, we can write the exchange–repulsion energy in the form (Hayes and Stone 1984*a*)

$$U_{\rm er} = U_{\rm exch} + U_{\rm rep}, \tag{8.2.1}$$

where

$$U_{\rm exch} = -\tfrac{1}{2}\sum_{k\in A}\sum_{l\in B}(kl|lk), \tag{8.2.2}$$

$$U_{\rm rep} = \sum_{kl}\langle k|h_A + h_B - \tfrac{1}{2}\nabla^2|l\rangle(T_{kl} - \delta_{kl}) + \tfrac{1}{2}\sum_{klmn}(kl|mn)[T_{kl}T_{mn} - \delta_{kl}\delta_{mn} - T_{kn}T_{ml} + \delta_{kn}\delta_{ml}]. \tag{8.2.3}$$

Here h_A is the electron–nuclear attraction for molecule A, $(kl|mn)$ is a two-electron integral $\int k(1)l(1)r_{12}^{-1}m(2)n(2)\,{\rm d}\tau_1\,{\rm d}\tau_2$, and T is the inverse of the overlap matrix between the occupied spin-orbitals of the system. The sums are taken over the occupied spin-orbitals. Notice that T_{kl} is zero if orbitals k and l have different spin. In the interaction of two hydrogen atoms that we discussed in §6.1, exchange–repulsion arises only if the two electrons have the same spin. If they have opposite spins, chemical bonding could occur. In an interaction between two closed-shell molecules, this is not a possibility, and in this case there is an exchange repulsion between pairs of electrons of the same spin, while pairs of electrons of opposite spin merely interact like classical charge densities.

Fig. 8.1 shows the exchange–repulsion on a semi-logarithmic plot for a number of simple examples, calculated using SAPT-DFT with the aug-cc-pVQZ or aug-cc-pVTZ basis and the PBE0 functional with asymptotic correction. R is the distance between the adjacent heavy (non-hydrogen) atoms. For water dimer, the geometry is based on the equilibrium geometry, with the O···O distance varied. The other geometries are linear, except for the Cl_2 dimer geometry shown. From these we can draw some important conclusions. First, the variation of $\log U_{\rm er}$ with distance is close to linear. Secondly, the slope of the line is very nearly the same for the cases shown, though the intercept of the line with any given energy value depends on the system and on its orientation. These observations suggest that the exchange–repulsion can be quite accurately represented by a function of the form

$$U_{\rm er} = K\exp[-\alpha(R-\rho)], \tag{8.2.4}$$

where K is an arbitrary fixed constant. α describes the slope of the logarithmic plot, and is about 2 bohr^{-1}, varying between 1.75 and 2.1 for the examples shown. When $R = \rho$ the repulsion energy has the fixed value K. In fact ρ provides a description of the size and shape of the

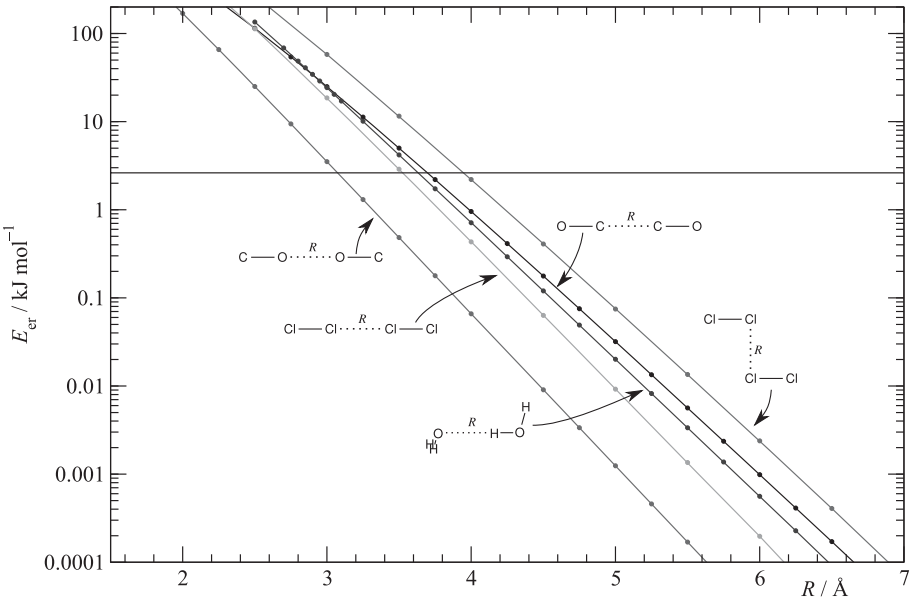

Fig. 8.1 The dependence of the exchange–repulsion energy U_{er} on separation for several pairs of small molecules. Calculated using SAPT-DFT with an aug-cc-pVQZ basis for CO and H_2O, aug-cc-pVTZ for Cl_2. (See also Plate 3.)

molecules concerned. The horizontal line at an energy of 1 millihartree (about 2.626 kJ mol^{-1} or 316 K) intersects the plots at a separation corresponding roughly to a Van der Waals diameter. It is notable that the effective diameter of a chlorine atom in Cl_2 is significantly greater perpendicular to the bond than parallel to it.

In fact an important feature of the exchange–repulsion is that it is not adequately described in terms of spherical atoms. Moreover, since the factor α in eqn (8.2.4) is around 2 bohr^{-1}, the exchange–repulsion varies by a factor of e over a distance of about 0.5 bohr, and since exchange–repulsion energies of 30 kJ mol^{-1} are common near equilibrium, a difference in atomic radius of even 0.1 bohr can make a difference of around 5 kJ mol^{-1} to the energy.

8.3 The second-order energy at short range

The detailed predictions of the theory at second order depend on the form of perturbation theory that is used, but there are common features that are generally agreed to be physically valid. We recall that at long range there are two contributions to the second-order energy, namely the induction energy and the dispersion energy, and that these are normally expanded as power series in $1/R$. The features that we have discussed for the first-order energy also arise here, but in a form that is very much less amenable to calculation.

These features are penetration, exchange and poor convergence. In the case of the electrostatic interaction, it is quite easy to show that there is a region where the multipole expansion converges (see Chapter 7), though convergence may be slow at short range, and that there is an error in the multipole expansion, even when it does converge—this is the penetration effect.

In the case of the induction energy, it can be shown, both in general (Brooks 1952, Ahlrichs 1976) and by example (Dalgarno and Lynn 1957*a*, Kreek and Meath 1969) that the R^{-n} expansion of the induction energy never converges, as we saw in Chapter 4. It is asymptotically convergent, which means that the terms in the series decrease to a minimum magnitude and then increase again, and in series of this type it is often the case that a good estimate can be obtained by truncating the series at its smallest term, the truncation error being of the order of the first neglected term.

This feature means that the convergence characteristics of the multipole expansion of the induction energy are much less well defined than they are for the electrostatic interaction, and the same is true for the dispersion energy.

The second-order energy at short range is given by eqn (6.3.2). We can rewrite this in the following form, using the fact that the antisymmetrizer $\mathcal{A}$ satisfies $\mathcal{A}^2 = \mathcal{A}$:

$$W'' = \frac{1}{\langle\psi_0|\mathcal{A}\psi_0\rangle}\sum_k{}' \frac{|\langle\psi_k|\mathcal{A}(\mathcal{H}' - W')\psi_0\rangle|^2}{W_0^0 - W_k^0}. \tag{8.3.1}$$

If we ignore the effect of all the permutations in $\mathcal{A}$ except the identity, we recover the formula of the long-range approximation. If this is evaluated without using the multipole expansion, we obtain non-expanded expressions for the induction and dispersion energy in the long-range approximation. (Remember that the induction energy and the dispersion energy are separated according to the nature of the excited state ψ_k in the sum over states: if ψ_k describes a state in which A alone is excited, it contributes to the induction energy of A, and so on.) The difference between each of these expressions and the corresponding multipole approximation is a penetration term, analogous to the penetration term in the electrostatic energy.

When we take the electron exchanges into account, the normalization integral $\langle\psi_0|\mathcal{A}\psi_0\rangle$ and the matrix elements in the sum over states change. If the overlap between the molecules is small, the changes will be of order S^2, where S is a measure of the overlap of molecular orbitals of A with those of B. The difference between the induction energy when exchange is taken into account, and the induction energy calculated using the (non-expanded) long-range approximation, is the 'exchange–induction' energy. Similarly, there is an 'exchange–dispersion' energy. These terms are normally calculated using the single-exchange approximation, since the effects of multiple exchanges are of order S^4 and are both small and very difficult to calculate.

8.3.1 Damping functions

The short-range perturbation theories discussed in Chapter 6 do not make use of the multipole expansion, so the terms listed in Tables 6.1 and 6.2 are in 'non-expanded' form. Consequently they remain finite as the molecular separation tends to zero; they are components of the electronic energy of the whole system, which remains finite for any nuclear configuration. (The only singularities in the total energy are terms like $Z_aZ_be^2/4\pi\epsilon_0R$, arising from electrostatic repulsion between the nuclei.) However, if we use the long-range theory and the multipole expansion, the dispersion energy appears as a power series in $1/R$, with leading term $-C_6R^{-6}$. At short distances this cannot be correct. The proper behaviour can be achieved by expressing the dispersion energy in the form (for atoms)

$$U_{\text{disp}} = -f_6(R)\frac{C_6}{R^6} - f_8(R)\frac{C_8}{R^8} - f_{10}(R)\frac{C_{10}}{R^{10}} - \cdots, \tag{8.3.2}$$

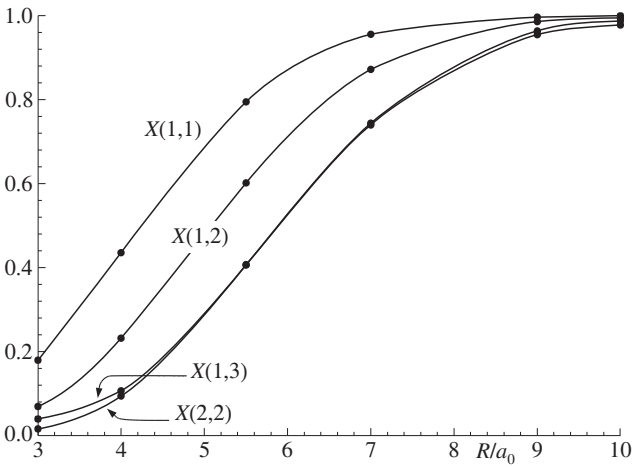

Fig. 8.2 Dispersion damping functions for Ar···Ar. $X(1,1)$: dipole–dipole, $X(1,2)$: dipole–quadrupole, $X(2,2)$: quadrupole–quadrupole and $X(1,3)$: dipole–octopole.

where $f_6(R)$, $f_8(R)$, etc., are 'damping functions' that tend to 1 as $R \to \infty$, and to zero as $R \to 0$. Each damping function $f_n(R)$ must suppress the corresponding R^{-n} singularity, so it must tend to zero like R^n as $R \to 0$. For non-centrosymmetric molecules there will be similar terms in odd powers of $1/R$.

Knowles and Meath (1986*a*,*b*, 1987) carried out *ab initio* calculations of the dispersion interaction $U^0_{\rm disp}$ between atoms and small molecules, and determined the form of the damping functions. Fig. 8.2 shows the results for Ar···Ar. The notation $X(1,2)$ indicates that the damping function shown is for the dispersion term involving the dipole–dipole polarizability (rank 1) on one atom and the quadrupole–quadrupole polarizability (rank 2) on the other. These curves all have a broadly similar shape, but the effect of the higher-rank damping functions extends to greater distances. For molecules, the dispersion energy is orientation dependent, and the orientation dependence can be described by an expansion in S functions. As for the penetration energy, the damping function for a particular S-function term must be a function only of R, but we can expect additional terms involving different S functions combined with exponentially decaying functions of R.

The induction energy behaves similarly; for ions the leading term in the multipole expansion behaves like R^{-4}, while for neutral polar molecules it is proportional to R^{-6}. Again, satisfactory behaviour can in principle be achieved by multiplying each term in the multipole expansion by a damping function that suppresses the singularity.

The damped dispersion energy calculated by Knowles and Meath is a representation of the dispersion energy in the long-range theory, without including any exchange effects, and without allowing for electron correlation in the separated molecules. In the multipole-expanded treatment, electron correlation just modifies the polarizabilities at imaginary frequency that appear in the Casimir–Polder formulae for the dispersion coefficients, eqns (4.3.26–4.3.29). Consequently, the form of eqn (8.3.2) should be equally valid for the correlation-corrected dispersion energy, but both the damping functions and the dispersion coefficients will be different in the correlated case. Exchange effects do not arise at long range, because they decay

exponentially with increasing separation, so they do not affect the dispersion coefficients, but it may be possible to include their effects in the damping factors.

8.3.2 Charge transfer and basis set superposition error

Perturbation theories of intermolecular interactions commonly identify a further contribution to the interaction energy. This is the charge transfer term. It is the source of a good deal of error and confusion, and it may be as well to make it plain at the outset that first, it is not a new term but is part of the short-range induction energy; and second, as commonly formulated it is a serious source of basis set superposition error.

The charge-transfer phenomenon was first identified by Mulliken (1952) in the electronic spectra of molecular complexes. A 'charge-transfer complex' comprises an electron acceptor A with a high electron affinity A_A and an electron donor D with a low ionization potential I_D. The ionic system $A^-\cdots D^+$ then has an energy $I_D - A_A$ at infinite separation that is not much higher than the energy of the neutral system $A\cdots D$, and at finite separations its energy is lowered by the electrostatic interaction, which is $-e^2/4\pi\epsilon_0 R$ plus higher-rank terms. When the molecules are close enough for their wavefunctions to overlap, these states can mix, so that the ground state becomes $|AD\rangle + \epsilon|A^-D^+\rangle$, in an obvious notation, and the excited state becomes approximately $|A^-D^+\rangle - \epsilon|AD\rangle$. (We are not concerned here with cases such as NaCl, where the ionic state becomes the ground state at short distances.)

There is an allowed electronic transition between these two states. Its intensity is proportional to the square of the matrix element of the dipole operator, which is

$$\mu_{\rm ct} = (\langle AD| + \epsilon\langle A^-D^+|)\hat{\mu}(|A^-D^+\rangle - \epsilon|AD\rangle). \tag{8.3.3}$$

The dominant term in this expression is $\epsilon\langle A^-D^+|\hat{\mu}|A^-D^+\rangle$, i.e., ϵ times the dipole moment of the ionic state, which is approximately eR if the molecules are separated by R. If the mixing coefficient ϵ becomes significant, therefore, there is an intense electronic transition between the ground state $|AD\rangle$ of the complex and the ionic state $|A^-D^+\rangle$. A very characteristic feature of a charge-transfer transition is that it does not correspond to any electronic transition in either isolated molecule, because it involves the state $|A^-D^+\rangle$, which is unique to the complex.

This simple idea of Mulliken's was very successful in explaining the phenomenon of charge-transfer spectra, and many examples are known. For instance, tetracyanoquinodimethane (TCNQ) and anthracene are both colourless, but when mixed they yield an intensely coloured deep green complex. Unfortunately Mulliken also noted that if the neutral and charge transfer states become mixed, then there must be a stabilization associated with this mixing, and it was assumed that it was this stabilization that was responsible for binding the complex together. At the time, it was not possible to carry out reliable calculations to confirm this assumption. Dewar and Thompson (1966) warned against it, pointing out that it was not consistent with observations of binding energies and charge-transfer transition frequencies, and that the electrostatic interaction would be big enough in many of these systems to provide strong bonding.

Nevertheless, the concept of 'charge-transfer stabilization' has entered the collective consciousness of the chemical community and has become firmly established. This view was reinforced by a paper describing Compton scattering from ice (Isaacs *et al.* 1999). (Compton scattering is inelastic X-ray scattering, and provides a direct experimental probe of the

electron momentum distribution.) The experimental results were interpreted as showing evidence of covalency in the hydrogen bond in ice. Unfortunately the interpretation was faulty, and was comprehensively refuted by Ghanty *et al.* (2000). The essence of the argument in favour of covalency was that a density-functional calculation of the wavefunction for a 12-molecule supercell successfully reproduced the observed anisotropy of the Compton profile, while a sum of the contributions of the 12 molecules, treated individually, was in poor agreement with the data. To treat the molecules individually, however, is a fundamental error, and Ghanty *et al.* showed that merely antisymmetrizing the product of single-molecule wavefunctions, as required by the Pauli principle, led to excellent agreement with experiment, very little different from a full quantum mechanical calculation. Moreover, detailed analysis of the full wavefunction showed that although there were features that could be described as covalent, they corresponded to *repulsion*, that is to the Pauli exclusion effect discussed in §6.1, and that there was no evidence of an attractive feature that could be described as a charge-transfer stabilization. Regrettably, the refutation did not receive as much publicity as the original claim, and some textbooks still assert the covalent nature of the hydrogen bond.

Now that it has become possible to carry out accurate calculations of the terms in the interaction energy, it can be shown that the charge-transfer component of the binding energy is usually small compared with other contributions (Stone 1993, Stone and Misquitta 2009), and this is in line with experimental results (Cozzi *et al.* 1993).

However, it is crucial in carrying out these calculations to be aware of the way in which the charge-transfer energy appears in the calculations. We have seen that the induction energy arises from states in which one of the molecules, say D, is excited. It is also possible to identify states in which one of the electrons of D becomes excited into an orbital that is localized not on D but on the electron acceptor A, and if the molecules are close enough together, such states will contribute to the interaction. It has been supposed that the sum of contributions of this sort may then be identified as the charge-transfer energy.

There are serious errors in this view. First of all, observe that the effect on the wavefunction of mixing in such excited states is to mix virtual orbitals of A into the occupied orbitals of D. This is precisely the process of using the basis functions of A to improve the description of D that leads to basis set superposition error. Accordingly, the charge-transfer energy will be heavily contaminated with BSSE unless steps are taken to compensate for it or to prevent it occurring. Secondly, notice that as we improve the basis for D, it will eventually become possible to describe any orbital of A in terms of basis functions on D, so that the charge-transfer state, with an electron from D occupying an orbital of A, can be described entirely in terms of the D basis set. Consequently, the genuine charge-transfer effect, as distinct from the BSSE component, will eventually be described as part of the induction energy when the basis set is good enough.

In practice, any basis set chosen for the purpose of describing D is unlikely to be good enough to describe orbitals for A at all adequately. If however we use the dimer basis to determine the unperturbed wavefunctions for both A and D, in the style of Boys and Bernardi (1970), we provide enough flexibility in the basis set of D to describe the charge-transfer states and the charge-transfer energy with good accuracy. At the same time, we ensure that no purely variational improvement can occur as a side-effect of the perturbation calculation, so that BSSE is absent. But the charge-transfer states will then formally be excited states of D, and their contributions to the interaction will appear as part of the induction energy.

The $D \rightarrow A$ charge-transfer term may then be defined as the difference between the induction energy of D calculated using the dimer basis on D, and the same quantity calculated with the monomer basis. This gives the $D \rightarrow A$ charge transfer energy. There will usually be an $A \rightarrow D$ charge-transfer energy too, even though A is nominally the electron acceptor and D the donor. It is possible to separate out the 'charge-transfer' terms from the total induction energy in this way (Stone 1993, Stone and Misquitta 2009). The separation is basis-set dependent, but the charge-transfer component turns out to be not very sensitive to basis set. The remaining part of the induction energy is more sensitive to basis, since it describes the distortion of the wavefunction in the electric field of the other molecule, and requires high-rank polarization functions if it is to be described accurately, but the charge-transfer energy describes the occupation of a low-lying valence orbital on the other molecule, and a reasonably good account of that can be given without polarization functions.

In SAPT-DFT, the 'induction energy' is taken to be the result of the long-range or polarization approximation, and the exchange-induction is treated separately, normally using the single-exchange approximation. In the Hayes–Stone treatment, on the other hand, the wavefunctions are fully antisymmetrized from the outset, so the induction energy includes all exchange effects.

Now, both the charge-transfer term, and the exchange-induction term in SAPT-DFT, depend on overlap between the wavefunctions of the two molecules, and the magnitude of the overlap decays exponentially with increasing separation. Consequently both the charge-transfer energy and the exchange-induction energy are expected to decay exponentially with separation, and indeed they do. A decaying exponential $\exp(-aR)$ cannot be expressed as a power series in $1/R$, as noted in §8.1, since it has an essential singularity when $1/R$ is zero. Consequently it is convenient to separate the complete induction expression, evaluated in the dimer basis, into three terms:

(i) The long-range or polarization term evaluated in the monomer basis. This depends only on monomer properties, and it can be represented by a power series in $1/R$ involving monomer polarizabilities and multipole moments.

(ii) The charge-transfer term, defined as the difference between the long-range term evaluated first in the dimer basis and then in the monomer basis.

(iii) The exchange induction term, evaluated in the dimer basis.

When numerical values are calculated, it turns out that the exchange-induction term, which is positive, approximately cancels the charge-transfer term, so that the sum of the two is only of the order of 1 kJ mol^{-1}or so at equilibrium separations (Stone and Misquitta 2009). For the water dimer at its equilibrium geometry, for instance, the charge-transfer term, calculated as above using an augmented cc-pVQZ basis set, is -5.9 kJ mol^{-1}, while the exchange-induction energy is $+7.8$ kJ mol^{-1}.

An alternative approach to the calculation of charge-transfer energies has been given by Khaliullin *et al.* (2007). It is a form of energy decomposition analysis, using localized molecular orbitals and formulated to avoid BSSE. When Hartree–Fock calculations are used, the charge-transfer energy of the water dimer at its equilibrium geometry is found to be about -3.5 kJ mol^{-1}. Density-functional calculations give estimates two or three times as big, but this is attributed to the tendency of density functionals to underestimate the separation between the highest occupied and lowest unoccupied molecular orbitals (the 'HOMO–LUMO gap').

An implication of all this is that the importance attached to 'frontier-orbital' effects in organic reactions is probably misplaced. In this approach, due to Klopman and Hudson (1967), Klopman (1968), Salem (1968) and Fukui and Fujimoto (1968), the energy change in the early stages of an organic reaction is expressed as a sum of three parts: the electrostatic interaction, the exchange–repulsion, and a second-order term which is wholly charge-transfer. The charge-transfer term is commonly approximated by the term with the lowest energy denominator, describing the transfer of an electron from the highest occupied molecular orbital, or 'HOMO', of the electron donor (or nucleophile) to the lowest unoccupied molecular orbital, or 'LUMO', of the electron acceptor (electrophile). The HOMO and LUMO are the 'frontier orbitals'. This idea has been a valuable unifying concept in understanding a wide range of organic reactions (Fleming 1976, 2009), but numerical calculations of the frontier-orbital component of the interaction energy, which is part of the charge-transfer term, show it to be small (Stone 1993, Craig and Stone 1994). At present, it is not clear why frontier-orbital theory is so successful. In one particularly important case where the theory is commonly used, namely in justifying the Woodward–Hoffmann rules for electrocyclic reactions (Woodward and Hoffmann 1970), there are many quite different explanations that do not invoke frontier-orbital ideas (Stone 1978*b*), but no alternative has been found for predicting stereoselectivity and regioselectivity effects.

8.4 The hydrogen bond

One of the important unifying concepts in physical chemistry is the hydrogen bond (Pimentel and McClellan 1960, Buckingham *et al.* 2008). It has been recognized for many years that there is a significant attraction between a hydrogen atom attached to an electronegative atom, such as oxygen or a halogen, and another electronegative atom. There has been some controversy over the years about what constitutes a hydrogen bond. IUPAC has recently defined it rather broadly as 'an attractive interaction between a hydrogen atom from a molecule or a molecular fragment X–H in which X is more electronegative than H, and an atom or a group of atoms in the same or a different molecule, in which there is evidence of bond formation' (Arunan *et al.* 2011). This deliberately includes extremes such as FHF^-, with a binding energy relative to $F^- + HF$ of 167 $kJ\,mol^{-1}$, and Ne···HF, with a binding energy of less than 1 $kJ\,mol^{-1}$, but most hydrogen bonds have energies in the range 10–25 $kJ\,mol^{-1}$.

An early treatment of the hydrogen bond due to Pauling (1928) viewed it as electrostatic in nature, assigning point charges to the atoms involved. By and large, this remains the general view, though an oversimplified electrostatic model fails in many cases, and this has led some to the conclusion that some form of 'incipient chemical bonding' is involved. The HF dimer, for instance, is incorrectly predicted to be linear if the electrostatic interaction is described simply in terms of point dipoles on each molecule (see the discussion in §3.4.3) or point charges on each atom. Legon and Millen (1982) gave a rule for determining hydrogen bonded structures, based on their observations using microwave spectroscopy:

> The gas-phase geometry of B···HX can be obtained ... as follows:
> (i) The axis of the HX molecule coincides with the supposed axis of a non-bonding pair as conventionally envisaged,
> or, if B has no non-bonding pairs but has π-bonding pairs,
> (ii) the axis of the HX molecule intersects the internuclear axis of the atoms forming the π bond and is perpendicular to the [nodal] plane ... of the π orbital.

However, the Legon–Millen rule, and the general observation that oversimplified electrostatic models do not predict hydrogen-bonded structures correctly, can be interpreted in two ways. One possibility is that charge transfer occurs, electron density moving from the proton acceptor to the proton. For this to be effective, it is clearly favourable for the proton to approach a region of high electron density in the proton acceptor, in accordance with the Legon–Millen rule. The other possibility is to acknowledge that a crude electrostatic description is inadequate, and seek to improve it. We saw in §3.4.3 that inclusion of the HF quadrupole moment leads to a structure of HF dimer in agreement with experiment. More generally, we can see that a structure in which the proton approaches a region of high electron density in the proton acceptor is sure to have a very favourable electrostatic interaction, without any need to postulate charge transfer.

We saw in §8.3.2 that the charge-transfer energy is not a well-defined quantity, and is merely a basis-dependent part of the induction energy. Nevertheless, we saw that we can contemplate, and calculate in a reasonably well-defined way, a distinction between polarization effects in which electrons are perturbed while remaining on the same molecule (classical induction) and effects involving the transfer of electrons from one molecule to the other (charge transfer).

All of these effects—charge transfer, induction and electrostatics—evidently have a part to play in forming the hydrogen bond, as does the dispersion energy. Their relative importance can be estimated by exploring a model in which only one of them is included.

8.4.1 The Buckingham–Fowler model

Buckingham and Fowler (1983) formulated a simple but very successful model for predicting the structures of small molecular complexes. This model has two elements:

- An accurate description of the electrostatic interaction, using a distributed multipole expansion as described in §7.2 above;
- A crude description of the repulsion, consisting of a hard-sphere repulsion for each heavy (non-hydrogen) atom, with standard Van der Waals radii as listed by Pauling (1960) or Bondi (1964).

The hydrogen atom forming the hydrogen bond is not assigned a radius; it is contained within the Van der Waals sphere of the heavy atom to which it is attached.

Optimization of the energy of a complex then gives predictions of the structure. The model evidently has no predictive power as far as interatomic separations are concerned, but it can predict the orientational aspects of the geometry, and does so with very good accuracy. Errors in angles are typically of the order of a few degrees—typically within experimental error, since these complexes are usually rather floppy and the equilibrium geometry may be different from the average geometry determined by the experiment.

Many successful predictions were made by Buckingham and Fowler (1985), and the method has been used to study many complexes involving polar molecules, not just hydrogen-bonded ones. The model is also the basis for the prediction of the azabenzene crystal structures cited on p. 134, and has been used to predict the equilibrium structures of complexes involving aromatic molecules (Price and Stone 1987).

The success of the model emphasizes the importance of the electrostatic interaction in determining structures. The repulsion and the other components of the interaction, neglected in

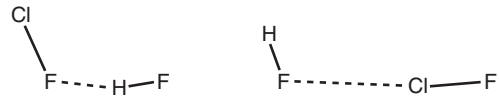

Fig. 8.3 Possible structures for HF/ClF: (left) the hydrogen-bonded structure ClF···HF, and (right) the 'anti-hydrogen-bonded' structure HF···ClF.

this model though implicit in the values used for the hard-sphere radii, are much less sensitive to orientation. One example of the failure of the model does however show that in some cases the other components can be decisive in selecting the best structure. The example is the complex formed between HF and ClF, for which two structures can be considered. One is the hydrogen-bonded structure ClF···HF, and the other is an 'anti-hydrogen-bonded' structure HF···ClF (Fig. 8.3). The model predicts that both of these structures are minima on the potential energy surface, with electrostatic energies of $-13.5\,\mathrm{kJ\,mol^{-1}}$ and $-7.5\,\mathrm{kJ\,mol^{-1}}$ respectively. However, the observed structure (Novick *et al.* 1976) is the 'anti-hydrogen-bonded' one.

The reason for this incorrect prediction has to do with the atomic separations. The sum of Van der Waals radii for F and Cl is 3.15 Å, but the observed separation in HF···ClF is only 2.76 Å. We shall see in Chapter 12 that the standard Van der Waals radius for chlorine is too large for end-on approach, as in HF···ClF, where the heavy atoms are approximately collinear. At the shorter F···Cl distance the electrostatic interaction is stronger, and the HF···ClF structure is favoured. However, the total energy includes repulsion, induction and dispersion, and also charge-transfer energy if that is viewed separately from the rest of the induction energy. The energy difference between the two structures is small—a few $\mathrm{kJ\,mol^{-1}}$ according to *ab initio* calculations—though decisive at the low temperatures of the molecular beam experiment.

We should therefore be cautious in using the predictions of the Buckingham–Fowler model when there are two or more possible structures. Usually one of them will be the correct one, but the relative energies may be incorrect as in the HF/ClF case.

8.4.2 Other contributions to the energy of the hydrogen bond

The success of the Buckingham–Fowler model, in which the charge-transfer, induction and dispersion effects are omitted, suggests that they are less important in determining structure. However, all three effects are expected to act in concert, favouring similar structures, so it could be argued that charge transfer alone, or induction alone, might be equally successful. Because of the difficulty of calculating these terms reliably this conjecture has not been tested extensively. Against it there is the argument that the electrostatic interaction is much more strongly orientation-dependent, being attractive in some geometries and repulsive in others, while the charge-transfer, induction and dispersion terms are always attractive, less sensitive to geometry and therefore less likely to be structure-determining. Calculations on the water dimer using SAPT-DFT show that the charge-transfer term is in fact quite sensitive to geometry, but is much smaller in magnitude than the electrostatic term. At the equilibrium structure the contributions to the interaction energy, in $\mathrm{kJ\,mol^{-1}}$, are as follows (aug-cc-pVQZ basis). The terms are as listed in Table 6.2, except that the charge-transfer term has been separated from the total induction by the procedure described in §8.3.2:

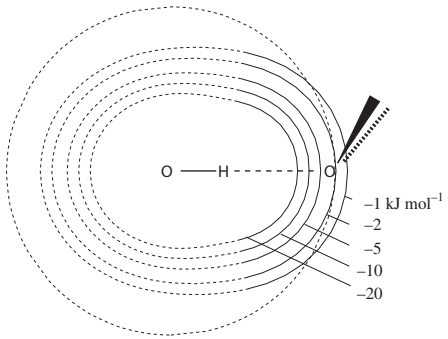

Fig. 8.4 Contours of the charge-transfer energy for the hydrogen bond in the water dimer.

Electrostatic	−33.4
Exchange–repulsion	31.5
Dispersion	−12.2
Induction	−8.0
Charge transfer	−5.9
Exchange–dispersion	2.3
Exchange–induction	7.8
δ_{HF} correction	−3.4
Total	−21.5

The form of the charge-transfer term is quite interesting (Millot and Stone 1992, Stone 1993). It can be fitted accurately to an attractive term that is exponential in form:

$$U_{\mathrm{ct}} = \sum_{\mathrm{H-bonds}} -K \exp[-\alpha(R_{\mathrm{OH}} - \rho(\Omega)],$$

where K is a constant and ρ is a distance that depends on the relative orientation of the molecules. (See Chapter 12 for a fuller discussion of this type of model, which is also used to describe repulsion.) The contours of this function are shown in Fig. 8.4 as a function of the position of the acceptor oxygen, the orientation of the acceptor molecule being relatively unimportant. It is apparent that in the region of the hydrogen-bonded geometry the contours are nearly spherical and centred on the H atom. (The dashed parts of the contours lie within the repulsive region, where few calculations were done, and are less well determined.) In conjunction with the repulsion, for which the contours are also approximately spherical but centred on the oxygen (as shown by the dashed circle at the O···O Van der Waals distance) this acts to favour a linear hydrogen bond. It is apparent from the table above, however, that this is a relatively minor effect.

The importance or otherwise of charge transfer, or incipient chemical bonding, in hydrogen bonding has long been a controversial issue. Reed *et al.* (1988) claimed that charge transfer dominates the hydrogen-bonding energy, but as we saw in §6.2.2, this is probably an artefact of their method. More recently, as noted in §8.3.2, Isaacs *et al.* (1999) interpreted measurements of Compton scattering in ice as 'direct evidence for the substantial covalent nature of the hydrogen bond', but their interpretation was refuted by Ghanty *et al.* (2000). The

evidence strongly supports the view that the electrostatic term is the major attractive contribution to hydrogen bonding in most cases, and the dominant factor determining structures of hydrogen bonded complexes, but that induction, charge transfer and dispersion all contribute to the bonding. The very broad IUPAC definition clearly encompasses exceptions to this rule, specifically Ne···HF, where the binding is due to dispersion and induction, and FHF^-, where it is covalent.

The induction energy is a relatively minor contribution to the hydrogen bond energy in the dimer, but its importance increases in larger clusters of hydrogen-bonded molecules and in condensed phases. The induction energy is strongly non-additive, and it acts cooperatively in hydrogen-bonded networks of molecules. Its contribution must certainly be taken into account in such systems. Indeed it accounts almost entirely for the three-body correction to the energy in such systems. This is discussed more fully in Chapter 10.

The full model of the hydrogen bond, including all the effects listed above, can account qualitatively and often quantitatively for the characteristic properties that are observed experimentally. For a hydrogen bond X–H···Y these include: (i) a lengthening of the X–H bond, (ii) a very large red-shift of the X–H infrared absorption accompanied by (iii) substantial broadening in the case of liquids and (iv) an increase in intensity by an order of magnitude. The other main effect is (v) deshielding of the proton NMR resonance. The lengthening of the bond can be attributed to electrostatic attraction between the proton and the negatively charged Y atom, together with electrostatic and exchange repulsion between the X and Y atoms. Because of the anharmonicity of the X–H bond, this stretching also has the effect of reducing the force constant, thus causing a red shift of the vibration frequency (Buckingham 1960). It is likely that charge transfer effects contribute by weakening the bond. The broadening also is attributed to anharmonicity (Sandorfy 1976), together with the disorder that occurs in the liquid. The deshielding of the proton NMR resonance can also be understood in fairly simple terms (Pople *et al.* 1959): the electric field at the proton due to the neighbouring Y atom causes the bond to stretch, as we have seen, and this inhibits the diamagnetic circulation of the electrons around the proton, especially in a magnetic field perpendicular to the bond. Since it is the diamagnetic current that is responsible for the shielding, this effect reduces it.

The large change in intensity of the X–H infrared absorption is a more subtle phenomenon (McDowell *et al.* 1992). When the X–H bond stretches in the course of vibration, the dipole moment of the X–H bond changes. This is the effect that is responsible for the normal intensity, which is proportional to the square of the dipole derivative. However, in the complex there is also an induced dipole moment in the proton acceptor Y, and this depends strongly on the position of the proton. Thus the dipole derivative for the whole complex with respect to the X–H bond length is greatly enhanced, and the intensity is increased. McDowell *et al.* found that a calculation of the intensity enhancement for HF dimer using distributed multipoles and polarizabilities gave excellent agreement with an SCF supermolecule calculation.

8.5 Halogen bonds

The structure of HF···ClF (Fig. 8.3) is now viewed as an example of *halogen bonding* (Legon 2010), recognized in recent years as a widespread phenomenon with close analogies to hydrogen bonding. It involves a molecule XY, in which X is a halogen atom and Y is either another X atom or a more electronegative atom or group of atoms. The intermolecular bond B···XY is formed with another electronegative atom B and is close to linear, with a geometry similar

to the hydrogen-bonded analogue $B\cdots HY$. As in the case of the hydrogen bond, the geometry can be attributed largely to electrostatic effects, comprising in part repulsion between the electronegative atoms B and Y, but also a strongly directional interaction between the B atom and the dipole and quadrupole moments of X, which both favour linearity. Another factor that favours linearity is that bonded halogen atoms, except fluorine, are markedly non-spherical, having a smaller effective radius in the direction away from the bond than in the perpendicular direction. This allows a closer approach in the axial direction, and consequently larger magnitudes for the other interaction terms.

The energy terms for HF···ClF, calculated using SAPT-DFT with the Sadlej basis, are, in $kJ\,mol^{-1}$,

Electrostatic	−17.3
Exchange–repulsion	21.3
Dispersion	−10.0
Induction	−4.4
Charge transfer	−8.9
Exchange–dispersion	1.3
Exchange–induction	10.3
δ_{HF} correction	−2.6
Total	−10.3

The charge-transfer term has been separated from the total induction energy by the procedure described in §8.3.2. There is a substantial charge-transfer component, though it is cancelled out by the exchange-induction, and dispersion also makes an important contribution.

9
Distributed Polarizabilities

Polarizabilities, like multipole moments, are commonly ascribed to the molecule as a whole, but they describe movements of charge density within the molecule, and are often associated with particular regions. The polarizabilities describe changes in the charge distribution arising from external fields, and a single-centre multipole description of these changes is subject to the same convergence problems as the ordinary multipole expansion. A distributed treatment can be expected to give better results here too.

A further consideration is that we are often concerned with the response of the molecular charge distribution to external fields from other molecules. Such fields are usually very non-uniform, so that the strength of the field varies considerably from one part of the molecule to another. We can allow for this by using higher-rank polarizabilities to describe the response to the field gradient and the higher derivatives of the field, but the Taylor series describing the variation of the field across the molecule converges poorly or not at all when the molecule is large—the sphere of convergence extends to the nearest multipole source of the field, which may be closer to the origin than the most distant part of the molecule. Here too a distributed treatment automatically takes account of variations in the strength of the field, since we use the value of the field at each site rather than the value at some arbitrary origin, and the sphere of convergence around each site only has to extend far enough to enclose the region belonging to the site.

It has been known for many years that molecular polarizabilities are additive, in the sense that the mean polarizability of a molecule can be expressed as a sum of contributions from its individual atoms or functional groups. Table 9.1, for instance, shows that the mean polarizabilities of the alkanes increase steadily with the length of the chain. The values were obtained from a study of dipole oscillator strength distributions (Thomas and Meath 1977, Jhanwar *et al.* 1981) (see §13.1.2); similar results have been obtained for polarizabilities derived from depolarization ratios in rotational Raman spectroscopy (Haverkort *et al.* 1983). Clearly there is a sense in which we can assign a polarizability of 12 a.u. to the CH_2 unit. This can be viewed either as a sum of atomic contributions, from a carbon and two hydrogens (atomic polarizabilities), or as a sum of contributions from two C–H bonds and one C–C bond

Table 9.1 Mean polarizabilities for the normal alkanes, C_nH_n (Thomas and Meath 1977, Jhanwar *et al.* 1981).

Chain length, n	1	2	3	4	5	6	7	8
$\overline{\alpha}$/a.u.	17.27	29.61	42.09	54.07	66.07	78.04	90.02	102.00
Difference		12.34	12.48	11.98	12.00	11.97	11.98	11.98

(bond polarizabilities). Using polarizabilities for a large number of molecules it is possible to assign atom and bond polarizabilities for a wide range of atoms and bonds. In doing this, one naturally distinguishes between different kinds of atom or bond involving the same element. For instance, the bond polarizabilities for C–C, C=C and C≡C bonds will clearly be different. Le Fèvre (1965) was probably the most thorough compiler of such data, and in addition to determining mean polarizabilities he also obtained polarizability anisotropies. More recently Miller (1990) has produced an extensive tabulation of molecular polarizabilities and expressed them in terms of bond polarizabilities.

While this work clearly established that it is possible to attach a meaning to atom or bond polarizabilities, it is necessary to understand that it does not, except in a very limited way, meet our present needs. Let us suppose for the moment that we can apply an electric field to just one of the atoms in a molecule. Such a field would polarize the atom in question, distorting its charge distribution; it would induce a dipole moment, but also higher moments. These induced moments are the sources of further fields, which extend over the whole molecule and cause the charge distributions of the other atoms to distort also. These in turn cause further distortions. So the end result is that the multipole moments on all the atoms in the molecule are affected by a field applied to just one atom, though naturally the effects are smaller for atoms some distance away.

It is not physically possible to apply a field to a single atom of a molecule, but in the linear-response approximation the response to a field that extends over the whole molecule is the sum of the responses to the fields at individual atoms. Le Fèvre's data refer to the total molecular dipole induced by a *uniform* field—either a static field or the field of a light wave at an optical frequency, which is essentially uniform on the molecular scale. The contribution to the overall induced molecular dipole from the field at a particular CH_2 group will be a sum of the induced dipoles at that CH_2 group and its neighbouring atoms. If the environment of each CH_2 group is the same, the response will be the same. This is why each additional CH_2 group adds a constant amount to the overall polarizability. It does not mean that each responds as if it were an isolated entity.

As soon as we deal with non-uniform fields that vary significantly from one part of a molecule to another, the simple additive picture breaks down. It is no longer possible to speak of 'the' electric field at the molecule, because it is different for different parts of the molecule. It becomes necessary to divide the molecule into regions, and to determine the response of each region and its neighbours to its own local field.

The induction energy, $-\frac{1}{2}\alpha_{\alpha\beta}F_\alpha F_\beta$, can be written as $-\frac{1}{2}\Delta\mu_\alpha F_\alpha$. In a uniform external field, F_α is constant, so the position of the induced dipole is immaterial. If F_α varies with position, however, the magnitude of the induction energy depends on the position of the induced dipole. Thus we cannot suppose that the induced dipoles of a CH_2 group and its neighbours can be treated as if they were all at the CH_2 group; we must take account of their positions explicitly.

A final difference between a single-site treatment of polarizability and a distributed treatment is that if we divide a molecule into regions, we have to contemplate the possibility that electronic charge may flow from one region to another under the influence of an external field. That is, we have changes in charge arising in response to differences in electrostatic potential. Such 'charge-flow' polarizabilities are not provided for in most distributed-polarizability treatments, but they can be incorporated quite naturally and consistently, as we shall see later, in §9.2.

9.1 The Applequist model

Silberstein (1917) was the first to address the description of molecular polarizabilities in terms of atomic polarizabilities, as we saw in §4.2, and Applequist *et al.* (1972) generalized his approach. In their treatment, each atom in a molecule is assigned a polarizability $\alpha^a_{\alpha\beta}$. (They used isotropic atom polarizabilities, but the general case is no more difficult to derive; see Birge (1980).) In an external field, each atom becomes polarized, and develops an induced dipole moment $\Delta\mu^a_\alpha$, in addition to any static dipole that may exist in the absence of a field. These induced dipoles are caused not only by the external field but by the fields arising from induced dipoles on the other atoms. The field at a due to the induced dipole on b is $T^{ab}_{\alpha\beta}\Delta\mu^b_\beta$, and the total field at atom a is the sum of the external field F^a_α and the fields due to the other atoms, so that the induced moment on atom a is

$$\Delta\mu^a_\gamma = \alpha^a_{\gamma\alpha}\Big(F^a_\alpha + \sum_{b\neq a} T^{ab}_{\alpha\beta}\Delta\mu^b_\beta\Big). \tag{9.1.1}$$

Note that the external field need not have the same value at each atom. We see that the equation for each induced moment depends on the induced moments at all the other atoms. We rewrite this set of coupled equations in the form

$$(\alpha^a)^{-1}_{\alpha\beta}\Delta\mu^a_\beta - \sum_{b\neq a} T^{ab}_{\alpha\beta}\Delta\mu^b_\beta = F^a_\alpha, \tag{9.1.2}$$

or

$$\sum_{b\beta} B^{ab}_{\alpha\beta}\Delta\mu^b_\beta = F^a_\alpha, \tag{9.1.3}$$

where the elements of the matrix B are

$$B^{ab}_{\alpha\beta} = \begin{cases} (\alpha^a)^{-1}{}_{\alpha\beta} & \text{if } a = b, \\ -T^{ab}_{\alpha\beta} & \text{if } a \neq b. \end{cases} \tag{9.1.4}$$

B here is a $3N \times 3N$ matrix if there are N atoms in the molecule.* Its rows are labelled by a and α and its columns by b and β. The solution of (9.1.3) is just

$$\Delta\mu^a_\alpha = \sum_{b\beta} (B^{-1})^{ab}_{\alpha\beta} F^b_\beta, \tag{9.1.5}$$

or

$$\Delta\mu^a_\alpha = \sum_{b\beta} A^{ab}_{\alpha\beta} F^b_\beta, \tag{9.1.6}$$

where the matrix $\mathbf{A} = \mathbf{B}^{-1}$ is a generalized polarizability matrix, sometimes called the *relay matrix*. The total induced moment is

$$\Delta\mu^{\text{tot}}_\alpha = \sum_a \Delta\mu^a_\alpha = \sum_{ab\beta} A^{ab}_{\alpha\beta} F^b_\beta, \tag{9.1.7}$$

*I have interchanged the notation used by Applequist for the matrices **A** and **B** since it seems more satisfactory to use **A** for the generalized polarizability rather than for its inverse.

and in a *uniform* external field, with $F^b_\beta = F_\beta$, the same for every atom, the polarizability for the whole molecule is

$$\alpha^{\rm tot}_{\alpha\beta} = \sum_{ab} A^{ab}_{\alpha\beta}. \tag{9.1.8}$$

Notice that **B** depends only on the atomic polarizabilities and on their arrangement in space, as described by the interaction tensors, and not on the external field. Consequently it can be evaluated once and for all for a given molecule. As an example, let us consider a diatomic molecule with bond length R. Taking the molecular axis to be the z axis, labelling the atoms as a and b, and abbreviating $1/4\pi\epsilon_0 R^3$ as p, we find without difficulty that **B** is the matrix

$$\begin{array}{c} \\ a\ x \\ \quad y \\ \quad z \\ b\ x \\ \quad y \\ \quad z \end{array}
\begin{array}{c}
\begin{array}{cccccc} a & & & b & & \\ x & y & z & x & y & z \end{array} \\
\begin{pmatrix}
(\alpha^a_\perp)^{-1} & 0 & 0 & p & 0 & 0 \\
0 & (\alpha^a_\perp)^{-1} & 0 & 0 & p & 0 \\
0 & 0 & (\alpha^a_\parallel)^{-1} & 0 & 0 & -2p \\
p & 0 & 0 & (\alpha^b_\perp)^{-1} & 0 & 0 \\
0 & p & 0 & 0 & (\alpha^b_\perp)^{-1} & 0 \\
0 & 0 & -2p & 0 & 0 & (\alpha^b_\parallel)^{-1}
\end{pmatrix}
\end{array} \tag{9.1.9}$$

Inversion of this matrix is straightforward (it consists of three interlaced 2×2 matrices) and the result is the matrix **A**:

$$\begin{pmatrix}
\dfrac{\alpha^a_\perp}{1-X} & 0 & 0 & -\dfrac{p\alpha^a_\perp\alpha^b_\perp}{1-X} & 0 & 0 \\
0 & \dfrac{\alpha^a_\perp}{1-X} & 0 & 0 & -\dfrac{p\alpha^a_\perp\alpha^b_\perp}{1-X} & 0 \\
0 & 0 & \dfrac{\alpha^a_\parallel}{1-4Z} & 0 & 0 & \dfrac{2p\alpha^a_\parallel\alpha^b_\parallel}{1-4Z} \\
-\dfrac{p\alpha^a_\perp\alpha^b_\perp}{1-X} & 0 & 0 & \dfrac{\alpha^b_\perp}{1-X} & 0 & 0 \\
0 & -\dfrac{p\alpha^a_\perp\alpha^b_\perp}{1-X} & 0 & 0 & \dfrac{\alpha^b_\perp}{1-X} & 0 \\
0 & 0 & \dfrac{2p\alpha^a_\parallel\alpha^b_\parallel}{1-4Z} & 0 & 0 & \dfrac{\alpha^b_\parallel}{1-4Z}
\end{pmatrix} \tag{9.1.10}$$

where

$$X = p^2\alpha^a_\perp\alpha^b_\perp, \quad Z = p^2\alpha^a_\parallel\alpha^b_\parallel. \tag{9.1.11}$$

We can now see that the response to a uniform field in the z direction is

$$\Delta\mu_z = \Delta\mu^1_z + \Delta\mu^2_z = \frac{\alpha^a_\parallel + \alpha^b_\parallel + 4p\alpha^a_\parallel\alpha^b_\parallel}{1-4Z}F_z, \tag{9.1.12}$$

while a uniform field in the x direction gives

$$\Delta\mu_x = \Delta\mu^1_x + \Delta\mu^2_x = \frac{\alpha^a_\perp + \alpha^b_\perp - 2p\alpha^a_\perp\alpha^b_\perp}{1-X}F_x. \tag{9.1.13}$$

These results may be compared with (4.2.4) and (4.2.5). The molecular polarizabilities are

$$\alpha_{\parallel}^{\mathrm{mol}} = \frac{\alpha_{\parallel}^{a} + \alpha_{\parallel}^{b} + 4p\alpha_{\parallel}^{a}\alpha_{\parallel}^{b}}{1 - 4p^{2}\alpha_{\parallel}^{a}\alpha_{\parallel}^{b}},$$
$$\alpha_{\perp}^{\mathrm{mol}} = \frac{\alpha_{\perp}^{a} + \alpha_{\perp}^{b} - 2p\alpha_{\perp}^{a}\alpha_{\perp}^{b}}{1 - p^{2}\alpha_{\perp}^{a}\alpha_{\perp}^{b}}.$$

This procedure gives expressions for the parallel and perpendicular polarizabilities of the diatomic in terms of the values $\alpha_{\parallel}$ and $\alpha_{\perp}$ for the individual atoms. Given the experimental polarizabilities for the molecule, we can work back to the atom polarizabilities. For a heteronuclear diatomic, the two components of the molecular polarizability would not provide enough information to characterize an $\alpha_{\parallel}$ and $\alpha_{\perp}$ for each atom, but from experimental data for many molecules, together with assumptions about transferability of the atom polarizabilities, it is possible to assign polarizabilities for a variety of atoms. Alternatively, the number of parameters to be found can be reduced by assuming that the atom polarizabilities are isotropic, as Applequist *et al.* (1972) originally did.

This treatment can very easily be extended to handle higher-rank fields and polarizabilities. Applequist (1983, 1985) did this in cartesian notation, which necessitates an elaborate scheme to cope with the redundancies resulting from the symmetry of the higher moments with respect to permutation of subscripts, and the tracelessness property. The spherical-tensor approach gives a much more compact and straightforward treatment. All we have to do is to replace $\Delta\mu_{\alpha}^{a}$ by the general induced moment ΔQ_{t}^{a}, where t as usual runs over the sequence 00, 10, 11c, 11s, etc., of multipole suffixes, and the field F_{α}^{a} by $-V_{t}^{a}$. The interaction tensor $T_{\alpha\beta}^{ab}$ becomes T_{tu}^{ab}, and we get

$$\Delta Q_{t'}^{a} = -\alpha_{t't}^{a}\Big(V_{t}^{a} - \sum_{b\neq a} T_{tu}^{ab}\Delta Q_{u}^{b}\Big), \tag{9.1.14}$$

(with an implied summation over the repeated suffixes t and u) or

$$(\alpha^{a})^{-1}{}_{tu}\Delta Q_{u}^{a} - \sum_{b\neq a} T_{tu}^{ab}\Delta Q_{u}^{b} = -V_{t}^{a}. \tag{9.1.15}$$

As before, we define a matrix $\mathbf{B}$ by

$$B_{tu}^{ab} = \begin{cases} (\alpha^{a})^{-1}{}_{tu} & \text{if } a = b, \\ -T_{tu}^{ab} & \text{if } a \neq b, \end{cases} \tag{9.1.16}$$

and the generalized polarizability matrix $\mathbf{A}$ is the inverse of this.

This then provides a reasonably simple and straightforward formalism for treating a molecule as an assembly of polarizable atoms. In the case where the atoms are far removed from each other (an assembly of isolated atoms rather than a molecule) the value of $p = 1/4\pi\epsilon_{0}R^{3}$ in eqn (9.1.9) becomes zero, and $A_{\alpha\beta}^{ab}$ (eqn (9.1.10)) becomes a diagonal matrix, with diagonal elements $(\alpha_{\perp}^{a}, \alpha_{\perp}^{a}, \alpha_{\parallel}^{a}, \alpha_{\perp}^{b}, \alpha_{\perp}^{b}, \alpha_{\parallel}^{b})$. The overall polarizability is then just the sum of the polarizabilities of the individual atoms. When the atoms approach, the overall polarizability is modified, and when they become very close, the elements of the $\mathbf{A}$ matrix diverge. The explicit expression (9.1.10) shows that this happens, so that $\mathbf{A}$ becomes undefined, if $4p^{2}\alpha_{\parallel}^{a}\alpha_{\parallel}^{b}$

or $p^2\alpha_\perp^a\alpha_\perp^b$ becomes equal to 1; that is, if $R^6 = 4\alpha_\parallel^a\alpha_\parallel^b/(4\pi\epsilon_0)^2$ or $R^6 = \alpha_\perp^a\alpha_\perp^b/(4\pi\epsilon_0)^2$. Since $\alpha/4\pi\epsilon_0$ for an atom is typically comparable with the atomic volume, and bond lengths are rather smaller than Van der Waals radii, this can very easily happen. Furthermore, if R^6 is less than either of these critical values, the matrix **B** ceases to be positive definite (that is, one or more of its eigenvalues becomes negative) and the matrix **A** is then also not positive definite. Thole (1981) pointed out that this situation is unphysical.

As with most cases of this sort, the mathematical singularity reflects a failure in the physical model. In this case the problem is that when atoms are close together it is no longer valid to use a multipole expansion to describe the interaction between them. In the terminology used at the beginning of Chapter 7, the convergence spheres overlap.

9.1.1 Thole damping

Two methods have been used to overcome this difficulty. One is an empirical fix; the other involves a more fundamental review of the theory, and is discussed in the next section. The empirical approach, due to Thole (1981), recognizes that the interaction between the charge distributions of two atoms remains finite as they approach, except for the nucleus–nucleus terms which are not involved in electronic induction effects, and incorporates a damping term to suppress the singularity in the multipole–multipole interaction. Thole obtained the damped interaction by replacing the point-charge potential $1/(4\pi\epsilon_0 R)$ in the usual definition of $T_{\alpha\beta}$ (eqn (3.1.6)) by the potential V_{Thole} arising from a smeared-out spherical charge distribution ρ_{Thole} having unit total charge, and treated as a universal function of the dimensionless quantity $u = R/S_{ab}$, where $S_{ab} = (\alpha_a\alpha_b/(4\pi\epsilon_0)^2)^{1/6}$ for atoms a and b with mean polarizabilities α_a and α_b. This leads to a damped interaction of the form

$$\tilde{T}_{\alpha\beta}^{ab} = \frac{f_e R^2\delta_{\alpha\beta} - 3f_t R_\alpha R_\beta}{4\pi\epsilon_0 R^5} \tag{9.1.17}$$

where f_e and f_t are the damping coefficients. The simplest form of charge density suggested by Thole varies linearly from a finite value at the origin to zero at $u = \lambda$:

$$\rho = \begin{cases} 3(\lambda - u)/\pi\lambda^4, & u < \lambda, \\ 0, & u \geq \lambda. \end{cases} \tag{9.1.18}$$

The parameter λ controls the damping strength. Then eqn (9.1.18) leads to the undamped form ($f_e = f_t = 1$) when $R > \lambda S_{ab}$, and the damped form when $R < \lambda S_{ab}$, with damping coefficients

$$f_e = 4\nu^3 - 3\nu^4, \quad f_t = \nu^4, \tag{9.1.19}$$

where $\nu = R_{ab}/\lambda S_{ab}$. Thole fitted λ and the atomic polarizabilities to experimental data, and found that 1.662 was a suitable value for λ.

An alternative form also proposed by Thole starts from the density $\rho = a^3\exp(-aR)/8\pi$, and leads to

$$f_e = P(3,\nu), \quad f_t = P(4,\nu), \tag{9.1.20}$$

where $P(n,x)$ is the incomplete gamma function of order n:

$$P(n,x) = 1 - \exp(-x)\sum_{k=0}^{n-1}\frac{x^k}{k!}. \tag{9.1.21}$$

Table 9.2 Applequist polarizabilities for CO.

α_{tu}^{ab}		b	C	O	α_{tu}^{ab}		b	C	O
		u	z	z			u	x	x
a	t				a	t			
C	z		8.64	6.00	C	x		4.78	−1.44
O	z		6.00	6.08	O	x		−1.44	3.37

Table 9.3 Damped Applequist polarizabilities for CO.

α_{tu}^{ab}		b	C	O	α_{tu}^{ab}		b	C	O
		u	z	z			u	x	x
a	t				a	t			
C	z		9.48	0.09	C	x		11.78	−4.07
O	z		0.09	5.82	O	x		−4.07	7.23

Yet another possible form is $\rho = (3a/4\pi)\exp(-au^3)$, which leads to

$$f_e = 1 - \exp(-\lambda u^3), \quad f_t = 1 - (1 + \lambda u^3)\exp(-\lambda u^3). \tag{9.1.22}$$

Thole's method can be applied to interactions involving higher multipoles, simply by replacing $1/R$ by V_{Thole} in the definitions of $T_{\alpha\beta\gamma}$, $T_{\alpha\beta\gamma\delta}$, etc.

Other versions of the method use Thole damping but suppress the dipole–dipole coupling completely for pairs of atoms separated by only one or two bonds.

The only change required to the theory with any of these damped interaction tensors is now to replace the interaction tensor $T_{\alpha\beta}^{ab}$ in the matrix $\mathbf{B}$ by the damped tensor $\tilde{T}_{\alpha\beta}^{ab}$. It is possible, using this approach, to assign isotropic atomic polarizabilities that lead to molecular polarizabilities in quite good agreement with *ab initio* or experimental values (Voisin and Cartier 1993, Wang *et al.* 2011). It cannot be assumed, however, that a good description of the molecular polarizability (the *molecular* dipole response to a *uniform* external field) guarantees a good description of the local response to a non-uniform external field.

As an example of the Applequist dipole–induced-dipole scheme and the damped version of it, some results for CO are given in Tables 9.2 and 9.3. The left-hand table of each pair gives longitudinal polarizabilities, and the right-hand table gives transverse ones. The local z axis is along the internuclear axis from C to O. Table 9.2 gives the results for the original Applequist model, based on isotropic atomic polarizabilities of 4.16 a.u. for C and 2.93 a.u. for O. Notice that the dipole–induced-dipole formalism leads to a value of 6.00 a.u. for $\alpha_{z\,z}^{\mathrm{CO}}$, describing the dipole induced on O by a field at C or vice versa, that is almost as large as the value of 8.64 a.u. for $\alpha_{z\,z}^{\mathrm{CC}}$, which describes the dipole induced at C by a field at C. $\alpha_{z\,z}^{\mathrm{CO}}$ has the same sign as $\alpha_{z\,z}^{\mathrm{CC}}$, because in the dipole–induced-dipole picture an electric field in the z direction at the C atom induces a dipole moment in the same direction, and the field from that induced dipole at O is also in the same direction. Similarly, $\alpha_{x\,x}^{\mathrm{CO}} = -1.44$ a.u. is quite comparable in magnitude with $\alpha_{x\,x}^{\mathrm{CC}} = 4.78$ a.u., but is negative, because, with a transverse applied field at C, the field at O due to the induced dipole on C is in the opposite direction to the applied field.

The overall polarizabilities for the molecule according to this model are $\alpha_{\parallel} = \sum_{ab}\alpha_{z\,z}^{ab} = 26.7$ a.u. and $\alpha_{\perp} = \sum_{ab}\alpha_{x\,x}^{ab} = 5.3$ a.u. These should be compared with the experimental values,

which are $\alpha_\parallel = 15.75$ a.u. and $\alpha_\perp = 12.16$ a.u. at an optical frequency of 15,800 cm^{-1} (Bridge and Buckingham 1966). Characteristically the Applequist model exaggerates the anisotropy in the molecular polarizability, even though it starts from isotropic atomic polarizabilities.

Thole's damped dipole–induced-dipole model performs much better (Table 9.3). Here isotropic atomic polarizabilities of 9.48 a.u. for C and 5.82 a.u. for O lead to the values shown, giving $\alpha_\parallel = 15.5$ a.u., $\alpha_\perp = 10.86$ a.u. for the molecule, in quite good agreement with the experimental values. The value of α_{zz}^{CO} in this scheme is a good deal smaller, but the transverse polarizabilities are much larger in magnitude, and the values are not justified by the accurate treatment that we shall now explore.

9.2 Distributed polarizabilities

The Applequist approach, either in its original form or with Thole damping, treats the atoms of a molecule as distinct isolated entities, interacting only through multipole interactions. In reality, they are much more intimately connected, and a multipole description of their interactions is inadequate. In particular, it is possible for electrons to move from one atom to another in response to the external field. A more complete treatment can be derived using perturbation theory (Stone 1985), or in terms of the charge density susceptibility, §2.3.2. We use the latter approach here. In the following account we consider the static charge density susceptibility $\alpha(\mathbf{r}, \mathbf{r}'; 0)$, written as $\alpha(\mathbf{r}, \mathbf{r}')$ for brevity, but all of the methods described can be applied to the density susceptibility at imaginary frequency, $\alpha(\mathbf{r}, \mathbf{r}'; \mathrm{i}\omega)$.

Recall that the charge density susceptibility $\alpha(\mathbf{r}, \mathbf{r}')$ describes the change in charge density at $\mathbf{r}'$ resulting from a change in electrostatic potential at $\mathbf{r}$, or vice versa. We obtain a molecular polarizability from it by integrating over the molecule. The induced moment is the integral of the appropriate spherical harmonic over the induced change in charge density:

$$\Delta Q_t = \int R_t(\mathbf{r}') \Delta\rho(\mathbf{r}') \, \mathrm{d}^3\mathbf{r}, \tag{9.2.1}$$

and the induced change in charge density is the integral of the charge density susceptibility times the external potential:

$$\Delta\rho(\mathbf{r}') = -\int \alpha(\mathbf{r}', \mathbf{r}) V(\mathbf{r}) \, \mathrm{d}^3\mathbf{r}. \tag{9.2.2}$$

Expanding the external potential in a multipole series $\sum_u V_u R_u(\mathbf{r})$ allows us to pick out the ΔQ_t response to the particular component V_u, i.e. the polarizability α_{tu}:

$$\alpha_{tu} = \int R_t(\mathbf{r}') \alpha(\mathbf{r}', \mathbf{r}) R_u(\mathbf{r}) \, \mathrm{d}^3\mathbf{r} \, \mathrm{d}^3\mathbf{r}'. \tag{9.2.3}$$

For a distributed treatment, we divide the molecule into regions, in some manner to be discussed below, and use a multipole expansion of the potential in each region with respect to its own local origin. That is, we can write

$$V(\mathbf{r}) = \sum_t R_t(\mathbf{r} - \mathbf{a}) V_t^a, \tag{9.2.4}$$

where R_t is the operator for moment t of region a, and V_t^a is the t derivative of the potential at the origin of region a (i.e., at site a). If the regions are small enough, this description will

converge rapidly within each region, even if it would not converge for the molecule as a whole. Then the perturbing potential can be expressed as

$$V(\mathbf{r}) = \sum_a w^a(\mathbf{r}-\mathbf{a}) \sum_t R_t(\mathbf{r}-\mathbf{a}) V_t^a, \tag{9.2.5}$$

where w^a is a weight function that is 1 within region a and zero outside it. We do not need to have a sharp cutoff between regions as long as the sum of the weight functions is 1 everywhere.

The change in charge density at $\mathbf{r}'$ is now

$$\Delta\rho(\mathbf{r}') = -\int \alpha(\mathbf{r}', \mathbf{r}) \sum_a w^a(\mathbf{r}-\mathbf{a}) \sum_t R_t(\mathbf{r}-\mathbf{a}) V_t^b \, \mathrm{d}^3\mathbf{r}. \tag{9.2.6}$$

This charge density response can also be separated into regions, as for a distributed multipole analysis. The change in multipole t' of region a' involves integration over the region in the usual way:

$$\begin{aligned} \Delta Q_{t'}^{a'} &= \int w^{a'}(\mathbf{r}-\mathbf{a}') R_{t'}(\mathbf{r}'-\mathbf{a}') \Delta\rho(\mathbf{r}') \, \mathrm{d}^3\mathbf{r}' \\ &= -\int\int w^{a'}(\mathbf{r}-\mathbf{a}') R_{t'}(\mathbf{r}'-\mathbf{a}') \alpha(\mathbf{r}', \mathbf{r}) \sum_a w^a(\mathbf{r}-\mathbf{a}) \sum_t R_t(\mathbf{r}-\mathbf{a}) V_t^a \, \mathrm{d}^3\mathbf{r} \, \mathrm{d}^3\mathbf{r}', \end{aligned} \tag{9.2.7}$$

where the same weight functions are used to define the regions in order to preserve the symmetry between perturbation and response that we expect to see in formulae for polarizabilities. Separating the integral over r into the contributions from the regions, we get

$$\Delta Q_{t'}^{a'} = -\sum_{at} \alpha_{t't}^{a'a} V_t^a, \tag{9.2.8}$$

where $\alpha_{t't}^{a'a}$ is a distributed polarizability:

$$\alpha_{t't}^{a'a} = \int\int w^{a'}(\mathbf{r}-\mathbf{a}') R_{t'}(\mathbf{r}'-\mathbf{a}') \alpha(\mathbf{r}', \mathbf{r}) w^a(\mathbf{r}-\mathbf{a}) R_t(\mathbf{r}-\mathbf{a}) \, \mathrm{d}^3\mathbf{r} \, \mathrm{d}^3\mathbf{r}'. \tag{9.2.9}$$

We see that $\alpha_{t't}^{a'a}$ describes the response of the multipole component $Q_{t'}^{a'}$ at site a' to the component V_t^a of the external field at site a. In this formulation the interactions between the different regions of the molecule are treated exactly, and we use the multipole approximation only to describe the interaction between each region of the molecule and the external field, where it is very accurate. Notice that the distributed polarizabilities are symmetric, in the sense that $\alpha_{t't}^{a'a} = \alpha_{tt'}^{aa'}$.

One important difference between distributed polarizabilities and conventional molecular polarizabilities is that the change in total charge of any given region in response to the external perturbation need not be zero, unlike the total charge of the molecule. Consequently there are polarizabilities describing changes in atom charges induced by the external field, for example by the potential difference between atoms. We use the term 'charge-flow polarizabilities' to emphasize that these new polarizabilities describe the movement of charge between atoms in

Table 9.4 Distributed polarizabilities for CO. Calculated by the method of §9.3, using PBE0 with asymptotic correction, d-aug-cc-pVTZ basis.

α^{ab}_{tu}		b	C	C	O	O
		u	0	z	0	z
a	t					
C	0		0.006	0.022	−0.006	−0.018
C	z		0.022	5.575	−0.022	2.747
O	0		−0.006	−0.022	0.006	0.018
O	z		−0.018	2.747	0.018	3.883

α^{ab}_{tu}		b	C	O
		u	x	x
a	t			
C	x		4.504	1.666
O	x		1.666	3.778

response to the field. The total charge on the molecule must be conserved, and this implies that

$$\sum_b \alpha^{ab}_{t0} = 0 \quad \text{for all } a, t. \tag{9.2.10}$$

Here and in the following discussion we use subscript 0 rather than 00 to denote the charge components. Because of the symmetry of the distributed polarizabilities with respect to exchange of at with $a't'$, this equation also describes the requirement that the charge density is unaffected by a uniform change in electrostatic potential across the molecule.

Let us compare distributed polarizabilities for CO, given in Table 9.4, with the Applequist results in Tables 9.2 and 9.3. The distributed polarizabilities were calculated using the method to be described in §9.3.1, and are very different from either of the Applequist models. Notice first that the transverse polarizability $\alpha^{\mathrm{CO}}_{x\,x}$ is *positive*. This emphasizes the limitations of the dipole–induced-dipole model, which even if damped is certain to give a negative value here; in that model, as we have seen, the secondary field at O arising from the dipole induced at C by a transverse applied field must be in the opposite direction to the applied field. In reality, the behaviour of the electron distribution cannot be described by such an oversimplified model when the atoms are so close together. The distributed polarizability method treats the response of the electrons properly, without using the multipole approximation.

The longitudinal polarizabilities are more complicated, because of the charge-flow polarizabilities. It is helpful in understanding the terms in the table to calculate the response of the molecule to a uniform electric field F in the z direction. The electrostatic potential is $-F(z - z_0)$, for some arbitrary z_0. The change in charge at b due to the potential at a is $\Delta Q^b_0 = +F(z_a - z_0)\alpha^{ab}_{00}$, and the change in dipole moment due to all the charges induced by the potential at a is $\sum_b z_b F(z_a - z_0)\alpha^{ab}_{00}$. The total change in dipole, due to the potential at all sites, is

$$\Delta\mu_z = \sum_{ab} z_b F(z_a - z_0)\alpha^{ab}_{00} = F\sum_{ab} z_a\alpha^{ab}_{00}z_b - Fz_0\sum_b z_b\sum_a \alpha^{ab}_{00}. \tag{9.2.11}$$

The last term vanishes by charge conservation (eqn (9.2.10)), so the charge-flows contribute $\sum_{ab} z_a\alpha^{ab}_{00}z_b$ to the overall molecular polarizability.

The potential at a also contributes directly to the change in dipole at b through the charge-dipole polarizability α^{ab}_{0z}: this contribution is $\Delta Q^b_z = +(z_a - z_0)F\alpha^{ab}_{0z}$, and the total contribution to the molecular polarizability is $\sum_{ab} z_a\alpha^{ab}_{0z}$, the term in z_0 once again vanishing.

There is a further change in charge at b due to the field at a. It is $\Delta Q_0^b = F\alpha_{z0}^{ab}$. In a similar way this leads to a contribution $\sum_{ab} \alpha_{z0}^{ab} z_b$ to the polarizability. Finally the field at a induces a dipole $F\alpha_{zz}^{ab}$ at b, with a total contribution to the polarizability of $\sum_{ab} \alpha_{zz}^{ab}$.

The total molecular polarizability α_{zz} is then

$$\alpha_{zz} = \sum_{ab} (z_a \alpha_{00}^{ab} z_b + z_a \alpha_{0z}^{ab} + \alpha_{z0}^{ab} z_b + \alpha_{zz}^{ab}). \tag{9.2.12}$$

For CO, we can take the C atom at $z_C = 0$ and the O atom at $z_O = d = 2.132$ bohr, to obtain

$$\begin{aligned} \alpha_{zz} &= d^2 \alpha_{00}^{OO} + d(\alpha_{0z}^{OC} + \alpha_{0z}^{OO}) + \alpha_{zz}^{CC} + \alpha_{zz}^{CO} + \alpha_{zz}^{OC} + \alpha_{zz}^{OO} \\ &= 0.006d^2 + d(-0.022 + 0.018) + (5.575 + 2 \times 2.747 + 3.883) \\ &= 14.97. \end{aligned} \tag{9.2.13}$$

This is identically equal to the value that is obtained from a conventional coupled Kohn–Sham calculation with the same functional and basis. There are several reasons, besides computational limitations, for the difference of about 5% between this and the experimental value of 15.75 a.u. (Bogaard *et al.* 1978): this value is for the equilibrium bond length rather than a vibrational average, and the experimental value was obtained at optical frequency (see §13.1.2).

For the transverse polarizability, we can take $x_C = x_O = 0$, so $d = 0$ and the total polarizability is just

$$\alpha_{xx} = \alpha_{xx}^{CC} + \alpha_{xx}^{CO} + \alpha_{xx}^{OC} + \alpha_{xx}^{OO} = 4.504 + 1.666 + 1.666 + 3.778 = 11.614, \tag{9.2.14}$$

which may be compared with the experimental value of 12.15 a.u.

In the general case, the total molecular polarizability is

$$\alpha_{\alpha\beta} = \sum_{ab} (r_\alpha^a r_\beta^b \alpha_{00}^{ab} + r_\alpha^a \alpha_{0\beta}^{ab} + r_\beta^b \alpha_{\alpha 0}^{ab} + \alpha_{\alpha\beta}^{ab}), \tag{9.2.15}$$

where $\mathbf{r}^a$ is the position of site a.

This detailed description of the response of the charge distribution to an applied field may seem unnecessarily elaborate, and it is certainly overkill if we only require the dipole response to a uniform field. However, fields around molecules are far from uniform, and even for such a small molecule the more detailed description does make a difference. The induced dipole moments in complexes of HCl with CO (Altman *et al.* 1983*a*) and N_2 (Altman *et al.* 1983*b*) could not be understood using a conventional treatment of the polarizability (Altman *et al.* 1982). These complexes are linear: ClH···CO and ClH···NN. The electric field of the HCl decreases sharply with distance, so the response to a polarizability sited at the C atom of CO is much larger than to the same polarizability sited at the O atom, say, or at the centre of mass. The fact that the polarizability is formally independent of origin does not relieve us of the need to choose the origin carefully. In the case of CO, we can see that the C atom, with a longitudinal polarizability of 5.6 a.u., is 40% more polarizable than the O atom; and if we want to calculate the response accurately we have to assign the polarizability to the correct origin. The situation is analogous to a change of origin for a point charge (§2.7): we can use

the 'wrong' origin only at the expense of including higher-rank terms which could be omitted if a better origin were chosen.

The induced dipole moments of ClH···CO and ClH···N_2 are obtained in good agreement with experiment when the distributed polarizabilities are used (Buckingham *et al.* 1986); it turns out that the dipole moment induced in the HCl by the other molecule makes a significant contribution, larger in the case of CO. Good results have been obtained for the induced moments of a number of other complexes, including some complexes involving BF_3 and the HF complexes H_2CO···HF and NNO···HF (Fowler and Stone 1987), and several acetylene complexes (Le Sueur *et al.* 1991). In the case of the NNO···HF complex, it was possible to determine the sign of the small dipole moment of nitrous oxide, then unknown, and since confirmed experimentally (Jalink *et al.* 1987).

The distributed polarizability picture, then, gives more insight into the response of the charge distribution to an external field than can be obtained from an overall molecular polarizability, and it does so without invoking the multipole approximation to describe the interactions between regions of the molecule.

9.3 Computation of distributed polarizabilities

Eqn (9.2.9) provides an expression for the distributed polarizabilities in terms of the charge density susceptibility, which can be calculated readily using coupled Hartree–Fock theory (Stevens *et al.* 1963, Gerratt and Mills 1968) or, more accurately, by coupled Kohn–Sham perturbation theory. We do however need to explore the nature of the weight functions w^a that define the regions, or equivalently the effective multipole operators $w^a R_t(\mathbf{r} - \mathbf{a})$ for each region.

As in the case of distributed multipoles, the definition of the distributed multipole moment operators is not unique; it is only necessary to ensure that they yield the correct matrix elements for the molecular multipole moments. The criteria for the definition are that first, the distributed polarizabilities should have good convergence properties; secondly, they should be insensitive to the choice of basis set; and thirdly, the computation should be reasonably tractable.

A natural procedure is to take the weight functions w^a to define regions of physical space. For linear molecules, this is easy if the atom boundaries are taken to be planes perpendicular to the molecular axis; the necessary integrals, for gaussian basis functions, are incomplete gamma functions, and are easily evaluated. The same technique can be used for molecules like formaldehyde, if a two-site model is sufficient; in this case, sites are taken at the C and O nuclei, and the regions are separated by a plane perpendicular to the CO bond. Other non-linear molecules where the sites lie on a straight line can be treated the same way. The case where the sites do not lie on a straight line is more difficult to handle. Le Sueur and Stone (1993) described a method in which the contributions from Gauss–Hermite integration points are partitioned between the regions of the molecule. Ángyán *et al.* (1994) used Bader partitioning (Bader 1990), which is less sensitive to changes in basis set, but the integration over the atomic basins is time-consuming and the numerical precision is only of the order of 0.001 a.u. Although both of these schemes provide only an approximate partitioning between the regions, they are exact in the sense that the overall molecular polarizabilities can be correctly recovered from the distributed polarizabilities.

9.3.1 Distributed polarizabilities by density-fitting methods

A rather different approach avoids the difficulties of these real-space partitioning methods. We start from the frequency-dependent density susceptibility, calculated by coupled Kohn–Sham perturbation theory, and use a modification of the density-fitting procedure set out in eqns (5.4.4) and (5.4.5). The FDDS is expanded in terms of the density-fitting basis as in eqn (5.5.12), but we change the notation to emphasize that each of the expansion functions is associated with a particular atom:

$$\alpha(\mathbf{r},\mathbf{r}';\omega) = \sum_{ab}\sum_{k\in a}\sum_{k'\in b}\tilde{C}_{kk'}(\omega)\chi_k(\mathbf{r}-\mathbf{a})\chi_{k'}(\mathbf{r}'-\mathbf{b}), \tag{9.3.1}$$

and then a distributed form is obtained by restricting the summations to include only basis functions on particular atoms:

$$\alpha^{ab}(\mathbf{r},\mathbf{r}';\omega) = \sum_{k\in a}\sum_{k'\in b}\tilde{C}_{kk'}(\omega)\chi_k(\mathbf{r}-\mathbf{a})\chi_{k'}(\mathbf{r}'-\mathbf{b}). \tag{9.3.2}$$

Distributed polarizabilities can now be obtained by a simple integration involving the appropriate spherical harmonics:

$$\alpha^{ab}_{tu}(\omega) = \sum_{k\in a}\sum_{k'\in b}\tilde{C}_{kk'}(\omega)\int R_t(\mathbf{r}-\mathbf{a})\chi_k(\mathbf{r}-\mathbf{a})\,\mathrm{d}^3\mathbf{r}\int R_u(\mathbf{r}-\mathbf{a})\chi_{k'}(\mathbf{r}'-\mathbf{b})\,\mathrm{d}^3\mathbf{r}'. \tag{9.3.3}$$

In effect, we interpret the weight function w_a as 1 when multiplying an auxiliary basis function centred on atom a and zero otherwise. That is, the integral over region a includes only the functions centred on atom a.

In its simplest form, this approach is not very successful: the resulting distributed polarizabilities are physically implausible, with unreasonably large charge-flow polarizabilities, counterbalanced by large dipole polarizabilities. The reason for this seems to be that the large basis sets needed for accurate polarizabilities are 'almost over-complete': some basis functions on a particular atom, especially the diffuse ones, can be expressed quite accurately in terms of the basis functions on other atoms. It is then possible to change the wavefunction coefficients significantly without changing the wavefunction itself very much, and if such a change occurs in response to an applied field, it will appear that a substantial movement of charge between atoms has occurred. This problem is similar to the difficulty in distributed multipole analysis with large basis sets, but exacerbated by the sensitivity of the wavefunction coefficients to the applied field.

However, a modification of the density-fitting procedure leads to much more sensible results. Instead of minimizing the quantity Δ_{iv}, as in eqn (5.5.11), we minimize

$$\Xi_{iv} = \Delta_{iv} - \eta\sum_{a,b\neq a}E^{ab}_{iv} + \lambda\left(\int\tilde{\rho}_{iv}(\mathbf{r})\,\mathrm{d}^3\mathbf{r}\right)^2. \tag{9.3.4}$$

The transition density $\rho_{iv} = \psi_i(\mathbf{r})\psi_v(\mathbf{r})$ satisfies $\int\rho_{iv}(\mathbf{r})\,\mathrm{d}^3\mathbf{r} = 0$, because the orbitals $\psi_i(\mathbf{r})$ and $\psi_v(\mathbf{r})$ are orthogonal to each other, but the density-fitted approximation $\tilde{\rho}_{iv}$ obtained from eqn (5.5.11) may not. The last term in eqn (9.3.4) imposes this condition. Properly, λ is a

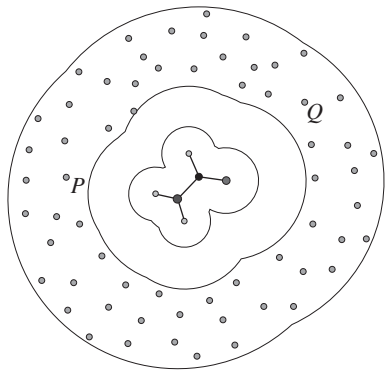

Fig. 9.1 An array of points around the formamide molecule. (Schematic; the array extends in three dimensions around the molecule.)

Lagrange multiplier, but in practice it is sufficient to treat the term as a penalty function, using a value of λ large enough to enforce the orthogonality constraint to sufficient accuracy.

The quantity E_{iv}^{ab} in the middle term in eqn (9.3.4) is defined by

$$E_{iv}^{ab} = \iint \frac{\tilde{\rho}_{iv}^{a}(\mathbf{r}_1)\tilde{\rho}_{iv}^{b}(\mathbf{r}_2)}{r_{12}} \, \mathrm{d}^3\mathbf{r}_1 \, \mathrm{d}^3\mathbf{r}_2. \tag{9.3.5}$$

The inclusion of this middle term is difficult to justify, but it does have the effect of favouring a more localized description. Suitable values for the parameters η and λ are found empirically to be about 0.0005 and 1000.0, respectively.

9.3.2 Fitting distributed polarizability models to induction responses

It is also possible to determine distributed polarizabilities by fitting them to computed polarization responses. Celebi *et al.* (2000) calculated the induction energy of a point charge at each of an array of positions around a molecule, and fitted a local polarizability model to the results. The fitting procedure is numerically ill-conditioned, however, and a better approach is to calculate the response (change in electrostatic potential) arising at each position in the array from a point charge at each position (Williams and Stone 2003).

The electric field from a unit point charge at some point P near the molecule (Fig. 9.1) induces a change in the molecular charge density:

$$\Delta\rho(\mathbf{r}') = \int \frac{1}{|\mathbf{r}_P - \mathbf{r}|} \alpha(\mathbf{r}, \mathbf{r}') \, \mathrm{d}^3\mathbf{r}, \tag{9.3.6}$$

and this change in charge density results in a change in electrostatic potential at another point Q:

$$\Delta V(\mathbf{r}_Q) = \int \Delta\rho(\mathbf{r}') \frac{1}{|\mathbf{r}' - \mathbf{r}_Q|} \, \mathrm{d}^3\mathbf{r}'. \tag{9.3.7}$$

We can denote this response at Q to a charge at P by α_{PQ}:

$$\alpha_{PQ} = \int \frac{1}{|\mathbf{r}_P - \mathbf{r}|} \alpha(\mathbf{r}, \mathbf{r}') \frac{1}{|\mathbf{r}' - \mathbf{r}_Q|} \, \mathrm{d}^3\mathbf{r} \, \mathrm{d}^3\mathbf{r}'. \tag{9.3.8}$$

If $\alpha(\mathbf{r}, \mathbf{r}')$ is expressed in density-fitted form (eqn (9.3.1)), α_{PQ} becomes

$$\alpha_{PQ} = \sum_{kk'} \tilde{C}_{kk'} J_{Pk} J_{Qk'}, \tag{9.3.9}$$

where

$$J_{Pk} = \int \frac{1}{|\mathbf{r} - \mathbf{r}_P|} \chi_k(\mathbf{r}) \, \mathrm{d}^3\mathbf{r}. \tag{9.3.10}$$

α_{PQ} is clearly symmetric with respect to interchange of P and Q.

Now we can seek to describe these responses by some polarizability model comprising distributed multipoles $\tilde{\alpha}^{aa'}_{tt'}$. For such a model, the response is

$$\tilde{\alpha}_{PQ} = \sum_{aa'tt'} T^{Pa}_{0\,t} \tilde{\alpha}^{aa'}_{tt'} T^{a'Q}_{t'\,0}. \tag{9.3.11}$$

We can now determine the $\tilde{\alpha}^{aa'}_{tt'}$ by a least-squares fitting procedure (Williams and Stone 2004), minimizing the quantity

$$S = \sum_{P>Q} (\tilde{\alpha}_{PQ} - \alpha_{PQ})^2 \tag{9.3.12}$$

with respect to the $\tilde{\alpha}^{aa'}_{tt'}$. This approach has the advantage that the fitted model can be as simple or as elaborate as the circumstances require, and the fitting procedure provides a direct measure of the accuracy of any particular model. In particular, it is possible to use it to obtain localized polarizability models, which we now consider.

9.3.3 Localized polarizabilities

We have seen that the polarization of one atom of a molecule by a local field will inevitably produce secondary fields at the other atoms that will polarize them too. However, we have also seen that the secondary polarizations are small—much smaller than the simple Applequist dipole–induced-dipole picture would suggest. If we describe these secondary polarizations by multipole expansions about the primary atom, representing a secondary induced dipole by dipole, quadrupole, etc. components on the original atom according to eqn (2.7.6) or (2.7.8), we can obtain a 'local polarizability' description in which all the secondary effects have been transformed away. The method first proposed for carrying out this procedure (Le Sueur and Stone 1994) described a non-local distributed polarizability α^{ab}_{tu} by polarizabilities $\alpha^{aa}_{t't''}$ and $\alpha^{bb}_{u'u''}$, i.e. only on the atoms a and b. Some work on the alkanes and alkenes led to the following conclusions (Stone *et al.* 1996, Williams and Stone 2004):

1. The transformation procedure is in principle exact; that is, the overall molecular polarizabilities are left unchanged.
2. The resulting description has less satisfactory convergence properties, making it more important to include higher-rank polarizabilities for accurate work.
3. Care must be taken with the charge-flow polarizabilities to ensure that the sum rules for charge conservation are preserved.
4. Care must also be taken to ensure that the polarizabilities remain symmetric, in the sense that $\alpha^{ab}_{tu} = \alpha^{ba}_{ut}$.

5. Pure charge-flow polarizabilities (i.e., the α^{ab}_{00}, describing the charge-flows induced by potential differences) are quite large, even for atoms some distance apart, and the resulting localized description is rather poor.

Lillestolen and Wheatley (2007) proposed a method in which α^{ab}_{tu} is represented by local polarizabilities on all atoms, in principle, rather than just on a and b. For example, a charge-flow polarizability between atoms at the ends of an alkene chain would be represented by dipole–dipole and higher polarizabilities on all atoms along the chain. This approach has not been extensively tested on large molecules, but it appears to provide a more satisfactory description. In any case, the charge-flow polarizabilities obtained from the density-fitting approach described in §9.3.1 are smaller and so less troublesome than those given by the earlier methods.

In an alternative procedure due to Garmer and Stevens (1989), the SCF molecular orbitals are transformed to localized orbitals using the Boys (1960) procedure, and a local dipole polarizability is assigned to each occupied orbital. Each orbital carries a charge of $-2e$, and the centroid of charge is taken as the local origin, so that the unperturbed dipole moment is zero. A uniform electric field applied to the molecule modifies the localized orbital, which acquires a dipole moment with respect to the fixed local origin. The change in dipole $\Delta\mu_\alpha$ in response to a field F_β defines a local polarizability through $\Delta\mu_\alpha = \alpha_{\alpha\beta}F_\beta$. This approach defines the local-molecular-orbital (LMO) polarizability as a local response to a uniform field applied to the whole molecule, so it is unsymmetrical, and in general $\alpha_{\alpha\beta} \neq \alpha_{\beta\alpha}$ when $\alpha \neq \beta$. Since the polarizabilities were obtained from finite-field perturbed Hartree–Fock calculations they do not include correlation effects, but the same approach could be adopted using localized Kohn–Sham orbitals.

Local distributed polarizabilities have many attractions. They eliminate the need to take account of secondary polarizations, since they are fully described within the local polarizabilities for each site, and they provide a model that is much simpler to handle than the full distributed-polarizability picture, and require far fewer parameters to characterize the system.

9.3.4 A hybrid approach

Neither of the methods described in §9.3.1 and §9.3.2 is entirely satisfactory on its own. It is usual to use the FDDS in density-fitted form, but that is not exact, and there is a further loss of accuracy if local polarizabilities are required. It is also not very flexible: it normally provides non-local polarizabilities on every specified site up to rank 3 or 4, but if a simpler model is needed it is necessary to carry out further manipulations, for example by dropping the higher polarizabilities.

The fitting procedure has the great advantage that the polarizability model can be as elaborate or as simple as required, and in the case of simple models it can give a better result than just dropping the high-rank terms, since in the fitting procedure the low-rank terms can incorporate some of the higher-rank effects. However, it does have a major disadvantage: it is not sensitive to the polarizabilities of 'buried' atoms, for which all the J_{Pk} (eqn (9.3.10)) are small. The consequence of this is that such polarizabilities are not reliably determined, and may even be unphysical (not positive definite) so that it is possible to envisage an external field that would lead to a positive induction energy. In such cases the external field that would be required to do this is extremely unrealistic, and the induction energies that would be ob-

Table 9.5 Local polarizabilities for CO. Calculated by the method of §9.3.4, using PBE0 with asymptotic correction, d-aug-cc-pVTZ basis.

α_{tu}^{ab}		b	C	O
		u	z	z
a	t			
C	z		8.12	0.00
O	z		0.00	6.82

α_{tu}^{ab}		b	C	O
		u	x	x
a	t			
C	x		6.23	0.00
O	x		0.00	5.38

tained for realistic fields are not only physical but accurate, but nevertheless this is not very satisfactory.

The solution to this problem is to use a combination of the two methods (Misquitta and Stone 2008, Misquitta *et al.* 2008*a*). The density-fitted polarizabilities are not very inaccurate, so we can use them as 'anchors' for the fitting procedure, applying penalty functions that prevent the fitted values from straying far from the anchor values. Instead of (9.3.12) we now minimize

$$S = \sum_{P>Q} (\tilde{\alpha}_{PQ} - \alpha_{PQ})^2 + \sum_{pp'} (\tilde{\alpha}_p - \tilde{\alpha}_p^0) g_{pp'} (\tilde{\alpha}_{p'} - \tilde{\alpha}_{p'}^0), \tag{9.3.13}$$

where the $\tilde{\alpha}_p$ are the parameters $\tilde{\alpha}_{tt'}^{aa'}$ that appear in the polarizability model and the $\tilde{\alpha}_p^0$ are the corresponding anchor values. The $g_{pp'}$ are the elements of a positive definite weight matrix, usually diagonal. Quite mild constraints are sufficient to keep the polarizabilities from taking on unphysical values, while the fit to the responses is almost as good as before. The recommended procedure is therefore to start with the density-fitting procedure, carry out the localization, and finally to refine the localized model by a constrained fit to polarization responses, using the values from the localization stage as anchor values. This procedure has been implemented in the computer package CamCASP (Misquitta and Stone 2012).

The polarizabilities for CO using this approach are shown in Table 9.5, and may be compared with the values in Tables 9.2, 9.3 and 9.4. The secondary intramolecular polarizations are taken fully into account in these values, so the molecular polarizabilities are now $\alpha_{\parallel} = 8.12 + 6.82 = 14.94$ and $\alpha_{\perp} = 6.23 + 5.38 = 11.61$.

9.3.5 Examples

These methods can be illustrated by examining the induction energy of a molecule in the presence of a point charge. As a reference we take the induction energy as calculated by coupled Kohn–Sham perturbation theory. Although this is not exact, it is an appropriate reference, since the various distributed polarizability models all seek to reproduce the Kohn–Sham polarizability. We construct a surface around the molecule at twice the Van der Waals radius from the nearest atom, smoothed where Van der Waals spheres intersect (Misquitta and Stone 2008), and evaluate the induction energy arising from a point charge of magnitude $0.4e$ at points on this surface. The value of $0.4e$ is at the high end of atom charges that might typically be found on neighbouring molecules. For the N-methyl propanamide molecule, the resulting induction energy is mapped in Fig. 9.2a. The remaining maps in Fig. 9.2 show the differences between the induction energies for various models and the reference. The lower scale applies to all of these.

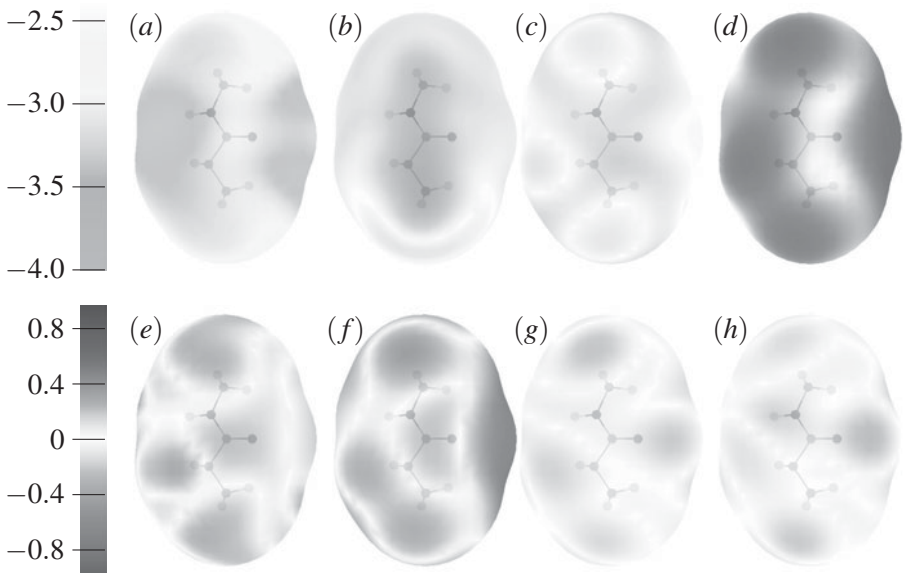

Fig. 9.2 (*a*) (upper scale): Induction energy of N-methyl propanamide in the presence of a point charge $0.4e$ on the vdW×2 surface, computed using Kohn–Sham perturbation theory. (*b*)–(*h*) (lower scale): Differences between induction energies for various distributed polarizability models and the reference induction energy shown at (*a*). (*b*) non-local rank 3, (*c*) non-local rank 2, (*d*) non-local rank 1, (*e*) local rank 2, (*f*) local rank 1, (*g*) refined local rank 1, (*h*) refined constrained local rank 1. Scales are in kJ mol^{-1}. (See also Plate 2.)

We see that the non-local model to rank 2 gives a good account of the induction energy, but the rank 3 model is slightly worse and the rank 1 model underestimates the magnitude of the induction energy quite badly. After localization, the rank 2 model is not as good, but the rank 1 model is, surprisingly, rather better than the rank 1 non-local model. The refined local rank 1 model is good, with a maximum error of about 0.3 kJ mol^{-1}, but it has a couple of negative polarizabilities. The refined model with constraints performs equally well, and has no unphysical polarizabilities. This example and others (Misquitta *et al.* 2008*a*) show that the local atomic dipole–dipole polarizabilities give a good account of the polarization of a molecule by its neighbours, but it is easy to include higher-rank polarizabilities in the model if required.

9.4 The induction energy in a distributed polarizability description

First, we develop the classical electrostatic energy of an assembly of polarizable molecules. In this we follow to some extent the treatment of Barker (1953) and Böttcher *et al.* (1972), who discuss an assembly of polarizable dipoles, but do not treat higher-rank moments and polarizabilities.

In an external field, the perturbation experienced by molecule A takes the form

$$\sum_{a\in A}\sum_{t}\hat{Q}_t^a V_t^a, \tag{9.4.1}$$

where $\hat{Q}_t^a$ is the operator for multipole moment t of region a of the molecule, and the V_t^a are the potential V_{00}^a and its derivatives, evaluated at the origin of region a. The electrostatic interaction between molecule A and its neighbours B takes the following form (see eqn (3.3.15)), which gives the corresponding operator):

$$\mathcal{H}' = \sum_{B \neq A} Q_t^a T_{tu}^{ab} Q_u^b. \tag{9.4.2}$$

We are using a repeated-index summation convention for the multipole suffixes t, u etc., and for the site indices a, b etc., but sums over the molecules themselves will be indicated explicitly. We see by comparing eqn (9.4.2) with eqn (9.4.1) that the V_t^a are given in this case by

$$V_t^a = \sum_{B \neq A} T_{tu}^{ab} Q_u^b. \tag{9.4.3}$$

When polarization is taken into account the moments of each molecule change under the influence of the electrostatic field due to its environment. Let us consider first the case where only molecule A is polarizable. In the field described by the V_t^a the moment Q_t^a changes by ΔQ_t^a. Now the value of ΔQ_t^a is determined by a competition between two effects. There is a positive energy required to distort the molecule's charge distribution from its equilibrium form in zero field, and this is counteracted by a lowering of the energy of interaction with the field. The latter becomes

$$E_f = (Q_t^a + \Delta Q_t^a) V_t^a, \tag{9.4.4}$$

while the internal energy of the molecule must depend bilinearly (in lowest order) on the ΔQ:

$$\Delta E_A = \tfrac{1}{2} \Delta Q_t^a \zeta_{tt'}^{aa'} \Delta Q_{t'}^{a'}. \tag{9.4.5}$$

(If there was a linear term it would be possible to lower the internal energy in zero field by choosing a non-zero ΔQ, but the ΔQ are defined to be zero in zero field.) Accordingly the total energy of molecule and field is minimized when

$$\partial(E_A + E_f)/\partial(\Delta Q_t^a) = 0,$$

i.e. when

$$\zeta_{tt'}^{aa'} \Delta Q_{t'}^{a'} + V_t^a = 0,$$

or equivalently when

$$\Delta Q_t^a = -\alpha_{tt'}^{aa'} V_{t'}^{a'}, \tag{9.4.6}$$

where α, the polarizability matrix, is the inverse of ζ. The polarizability $\alpha_{tt'}^{aa'}$ describes the change in moment t of region a that results from the t'th derivative of the potential at site a', as we saw in §9.2.

In terms of α the internal energy of the molecule is

$$\Delta E_A = \tfrac{1}{2} \alpha_{tt'}^{aa'} V_t^a V_{t'}^{a'}, \tag{9.4.7}$$

while the change in the energy of interaction between the molecule and the field as a result of polarization is (from eqns (9.4.4) and (9.4.6))

$$\Delta E_f = -\alpha^{aa'}_{tt'} V^a_t V^{a'}_{t'}. \tag{9.4.8}$$

The generalization to the case when all molecules are polarizable is not quite obvious. The electrostatic energy in the field takes the form

$$E_f = \sum_{A>B} (Q^a_t + \Delta Q^a_t) T^{ab}_{tu} (Q^b_u + \Delta Q^b_u), \tag{9.4.9}$$

while the internal energy of the molecules is

$$E_m = \tfrac{1}{2} \sum_A \Delta Q^a_t \zeta^{aa'}_{tt'} \Delta Q^{a'}_{t'}. \tag{9.4.10}$$

The ΔQ are found as before by minimizing the total energy to give

$$\frac{\partial (E_f + E_m)}{\partial (\Delta Q^a_t)} = \sum_{B \neq A} T^{ab}_{tu} (Q^b_u + \Delta Q^b_u) + \zeta^{aa'}_{tt'} \Delta Q^{a'}_{t'} = 0 \tag{9.4.11}$$

or

$$\Delta Q^a_t = -\sum_{B \neq A} \alpha^{aa'}_{tt'} T^{a'b}_{t'u} (Q^b_u + \Delta Q^b_u). \tag{9.4.12}$$

This is just the same as eqn (9.4.6) except that the fields V^a_t are given not by eqn (9.4.3) but by

$$V^a_t = \sum_{B \neq A} T^{a'b}_{t'u} (Q^b_u + \Delta Q^b_u). \tag{9.4.13}$$

That is, the fields depend on the polarized moments of the other molecules, and a solution of the problem requires the solution of the coupled equations (9.4.12), as we saw in §9.1. In practical applications, it is usual to solve them iteratively, since a self-consistent solution is usually reached after only half a dozen iterations or so.

Now the energy of the system is

$$E_m + E_f = -\tfrac{1}{2} \sum_A \Delta Q^a_t \sum_{B \neq A} T^{ab}_{tu} (Q^b_u + \Delta Q^b_u) + \tfrac{1}{2} \sum_A \sum_{B \neq A} (Q^a_t + \Delta Q^a_t) T^{ab}_{tu} (Q^b_u + \Delta Q^b_u), \tag{9.4.14}$$

where eqn (9.4.11) has been used to eliminate ζ from eqn (9.4.10). This includes the electrostatic energy of the unpolarized system, which is

$$E_{\text{es}} = \tfrac{1}{2} \sum_A \sum_{B \neq A} Q^a_t T^{ab}_{tu} Q^b_u,$$

so the induction energy is

$$\begin{aligned} E_{\text{ind}} &= \tfrac{1}{2} \sum_A \sum_{B \neq A} \{2 \Delta Q^a_t T^{ab}_{tu} Q^b_u + \Delta Q^a_t T^{ab}_{tu} \Delta Q^b_u - \Delta Q^a_t T^{ab}_{tu} (Q^b_u + \Delta Q^b_u)\} \\ &= \tfrac{1}{2} \sum_A \sum_{B \neq A} \Delta Q^a_t T^{ab}_{tu} Q^b_u. \end{aligned} \tag{9.4.15}$$

This separates conveniently into a sum of induction energies, one for each molecule:

$$E^A_{\text{ind}} = \tfrac{1}{2} \sum_{B \neq A} \Delta Q^a_t T^{ab}_{tu} Q^b_u. \tag{9.4.16}$$

This is only a formal separation, since the induction energy is not additive in the ordinary sense; remember that the induced moments that appear in this expression depend on the total

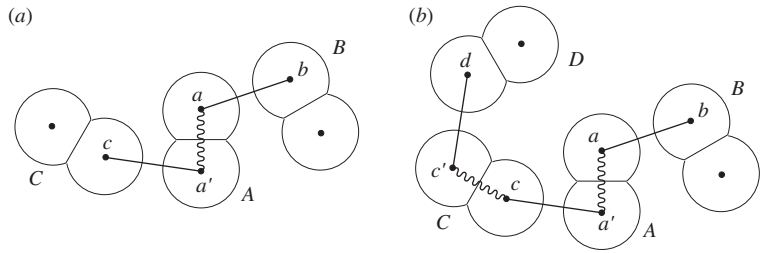

Fig. 9.3 (*a*) A first-order term in the induction energy of molecule *A*, involving the static moments of two other molecules, *B* and *C*. (*b*) A second-order term, in which molecule *A* is perturbed by the moment induced in *C* by the static moment of molecule *D*.

field due to the neighbouring molecules. Nevertheless it is a convenient form for computation, if the induced moments have been found by an iterative solution of eqn (9.4.12). Notice that eqn (9.4.16) involves the *unpolarized* moments on the other molecules.

An alternative approach uses eqn (9.4.12) to develop an expansion of eqn (9.4.16) in powers of the polarizability analogous to the expansion given by Barker (1953) for the dipole-polarizability case:

$$\begin{aligned} E^A_{\text{ind}} &= \tfrac{1}{2}\sum_{B\neq A} \Delta Q^a_t T^{ab}_{tu} Q^b_u \\ &= -\tfrac{1}{2}\sum_{B\neq A}\sum_{C\neq A} (Q^c_v + \Delta Q^c_v) T^{ca'}_{vt'} \alpha^{a'a}_{t't} T^{ab}_{tu} Q^b_u \\ &= -\tfrac{1}{2}\sum_{B\neq A}\sum_{C\neq A} Q^c_v T^{ca'}_{vt'} \alpha^{a'a}_{t't} T^{ab}_{tu} Q^b_u \\ &\quad + \tfrac{1}{2}\sum_{B\neq A}\sum_{C\neq A}\sum_{D\neq C} (Q^d_w + \Delta Q^d_w) T^{dc}_{wv'} \alpha^{c'c}_{v'v} T^{ca'}_{vt'} \alpha^{a'a}_{t't} T^{ab}_{tu} Q^b_u. \end{aligned} \tag{9.4.17}$$

This procedure can evidently be continued to arbitrary order in the polarizabilities to give a generalization of Barker's expression. The first term in eqn (9.4.17) involves only the static multipole moments and provides a 'first-order' approximation to the induction energy, while the subsequent terms allow for the induced moments. Fig. 9.3 shows this schematically: Fig. 9.3a represents one of the contributions $Q^c_v T^{ca'}_{vt'} \alpha^{a'a}_{t't} T^{ab}_{tu} Q^b_u$ to the leading term of eqn (9.4.17), in which multipoles on sites *b* and *c* interact with the polarizabilities $\alpha^{a'a}_{t't}$, while Fig. 9.3b describes a higher-order term $Q^d_w T^{dc'}_{wv'} \alpha^{c'c}_{v'v} T^{ca'}_{vt'} \alpha^{a'a}_{t't} T^{ab}_{tu} Q^b_u$ in which the moment at site *c* is modified by the field from Q^d_w on site *d*.

9.5 Distributed dispersion interactions

It is natural to look for a distributed description of the dispersion energy along the lines of the distributed treatment of polarizabilities. In fact we can write it down at once: taking the distributed-multipole form of the electrostatic interaction from eqn (7.2.1), we can follow the working of eqns (4.3.19)–(4.3.21) to obtain (Stone and Tong 1989)

$$U_{\text{disp}} = -\frac{\hbar}{2\pi} \sum_{a,a' \in A} \sum_{b,b' \in B} T_{tu}^{ab} T_{t'u'}^{a'b'} \int_0^\infty \alpha_{tt'}^{aa'}(\mathrm{i}v) \alpha_{uu'}^{bb'}(\mathrm{i}v)\, \mathrm{d}v \tag{9.5.1}$$

(with an implicit summation over the repeated suffixes t, t', u and u'). This is exact, subject as usual to convergence of the distributed multipole expansions, but unfortunately it is very cumbersome in practice, because it involves a quadruple sum over the sites. Nevertheless it is instructive to study its behaviour. Because it is expressed in terms of distributed polarizabilities, there are charge-flow terms, and if $t = t' = u = u' = 00$, the interaction functions T_{tu}^{ab} and $T_{t'u'}^{a'b'}$ become $1/4\pi\epsilon_0 R_{ab}$ and $1/4\pi\epsilon_0 R_{a'b'}$ respectively, so we have terms in the dispersion energy that behave like R^{-2} (McWeeny 1984, Stone and Tong 1989). There are also mixed charge-flow and dipole polarizability terms in R^{-3}, R^{-4} and R^{-5}. It is not difficult to show that because of the charge-conservation sum rules for the charge-flow polarizabilities, these terms cancel in the long-range limit, and if they are expanded in Taylor series about the molecular origins, the R^{-n} terms with $n < 6$ all cancel, so that the leading term is in $(R_{AB})^{-6}$, in agreement with the conventional treatment. Nevertheless the description is unsatisfactory, not only because of the large number of terms but also because a description involving many nearly cancelling terms is numerically troublesome.

These unfamiliar features can be transformed away by localizing the polarizabilities that occur in (9.5.1), using the methods described above, which apply to the imaginary-frequency polarizabilities in exactly the same way as to the static ones. This leads to a site–site form of the dispersion interaction:

$$U_{\text{disp}} = \sum_{a \in A} \sum_{b \in B} U_{\text{disp}}^{ab}, \tag{9.5.2}$$

where

$$\begin{aligned} U_{\text{disp}}^{ab} &= -\frac{\hbar}{2\pi} \sum_{tt'uu'} T_{tu}^{ab} T_{t'u'}^{ab} \int_0^\infty \alpha_{tt'}^{aa}(\mathrm{i}v) \alpha_{uu'}^{bb}(\mathrm{i}v)\, \mathrm{d}v \\ &= -\frac{C_6^{ab}(\Omega^{ab})}{R_{ab}^6} - \frac{C_7^{ab}(\Omega^{ab})}{R_{ab}^7} - \frac{C_8^{ab}(\Omega^{ab})}{R_{ab}^8} - \cdots, \end{aligned} \tag{9.5.3}$$

and so provides a justification for the widely assumed site–site model for the dispersion interaction (see Chapter 12).

As implied by the notation, the dispersion coefficients occurring in (9.5.3) are anisotropic in general (Stone and Tong 1989, Misquitta and Stone 2008). It is more convenient for practical calculations to express the orientational behaviour in terms of S functions, as in eqn (4.3.22), with dispersion coefficients expressed by eqn (4.3.23) (Williams 2004).

The derivation leading to eqn (9.5.3) is based on some approximations, in particular that the localized polarizability model is valid. In cases where substantial charge-flow can occur over long distances, there must be doubts about this. Indeed it can be shown clearly that there are cases where the model fails. For infinitely long parallel molecules, treated as continuous distributions of material with R^{-6} interactions between infinitesimal elements, it is not difficult to show that the dispersion energy per unit length is proportional to R^{-5}, but there is evidence that the dispersion energy per unit length for conducting and semiconducting wires is in fact proportional to R^{-2} (Dobson 2007). The same behaviour is observed for long conjugated molecules at distances that are comparable with their length or less, though in this case

R^{-6} behaviour is recovered at greater distances (Misquitta *et al.* 2010). From the above discussion we can expect that the anomalous behaviour arises from a failure of the charge-flow terms to cancel.

The question then arises of whether the atom–atom dispersion model is always valid for interactions between normal molecules, or at least whether any errors in it are likely to be important. The anomalies are generally associated with small band gaps (small HOMO–LUMO separations) (Misquitta *et al.* 2010), so we can be reasonably confident that saturated molecules, or ones containing small conjugated groups, such as proteins, will not pose any problems, but it is advisable to be wary of the atom–atom dispersion model for large conjugated molecules with small band gaps, such as organic conductors.

10
Many-body Effects

In Chapter 1 we assumed that the interaction energy of an assembly of molecules can be written in the form of a series starting with pairwise interaction terms and continuing with three-body terms, four-body terms and so on:

$$\begin{aligned} U &= W - \sum_i W_i \\ &= \sum_{i>j} U_{ij} + \sum_{i>j>k} U_{ijk} + \sum_{i>j>k>l} U_{ijkl} + \cdots \\ &= W_{2\text{body}} + W_{3\text{body}} + W_{4\text{body}} + \cdots . \end{aligned}$$

We have assumed further that this series converges rapidly, so that the pairwise interactions dominate and the many-body corrections are relatively small. In many cases this is true, but we have already seen in §4.2.1 that the induction energy is inherently non-additive, and in §9.4 we developed an expansion of the induction energy in which many-body contributions appear even in the leading term. In this chapter we study first a case where the non-additive effects of the induction energy dominate, and then go on to examine other non-additive effects.

10.1 Non-additivity of the induction energy

How far do we need to take this many-body expansion to account adequately for the effects of induction? To get a qualitative answer, consider the induction energy of molecule A:

$$U^A_{\text{ind}} = -\tfrac{1}{2}\alpha^A \mathbf{F}(\mathbf{A})^2 - \cdots , \tag{10.1.1}$$

where $\mathbf{F}(\mathbf{A})$ is the total electric field at molecule A. This is made up of contributions from all the neighbouring molecules, so that

$$\begin{aligned} \mathbf{F}(\mathbf{A})^2 &= \left(\mathbf{F}^B(\mathbf{A}) + \mathbf{F}^C(\mathbf{A}) + \cdots\right)^2 \\ &= \mathbf{F}^B(\mathbf{A})^2 + \mathbf{F}^C(\mathbf{A})^2 + \cdots + 2\mathbf{F}^B(\mathbf{A}) \cdot \mathbf{F}^C(\mathbf{A}) + \cdots , \end{aligned} \tag{10.1.2}$$

where $\mathbf{F}^X(\mathbf{A})$ is the field at $\mathbf{A}$ due to molecule X. So the induction energy of A includes terms like $-\alpha^A \mathbf{F}^B(\mathbf{A}) \cdot \mathbf{F}^C(\mathbf{A})$. These are three-body terms and can be large and of either sign.

Now $\mathbf{F}^B(\mathbf{A})$ arises from the charge distribution of B, which is itself modified by the fields of other molecules, as illustrated schematically in Fig. 9.3. However, these modifications, which lead to four-body, five-body and higher-order terms, are smaller than the main three-body term, which can lead to a doubling or cancellation of the sum of pair interaction terms. It follows that although we cannot neglect the three-body induction terms, it may be a good

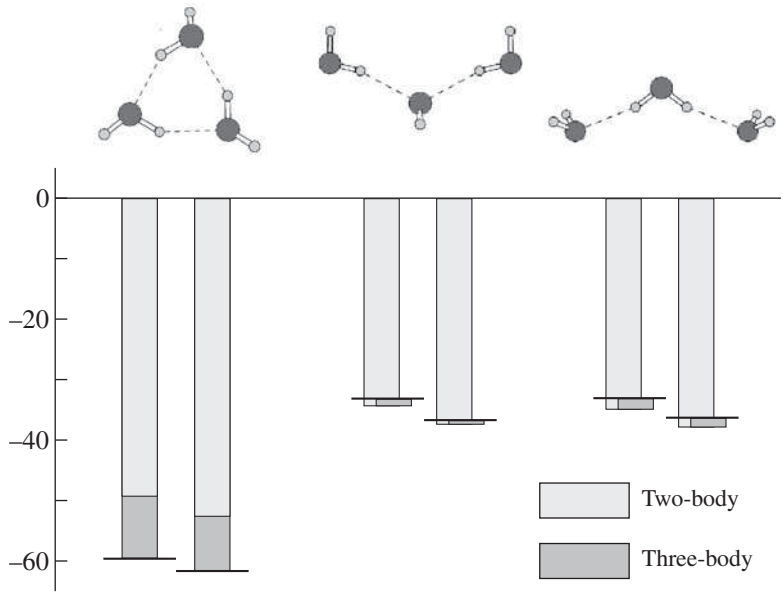

Fig. 10.1 Two-body and three-body energies (in kJ mol^{-1}) for water trimer in three geometries. The extended horizontal line shows the total binding energy. The left-hand bar of each pair shows the energies from SCF+MP2 *ab initio* calculations with an aug-cc-pVDZ basis set; the right-hand one shows the energies obtained from the ASP-W4 water potential in the *ab initio* geometries. (See also Plate 4.)

Table 10.1 Many-body contributions, in kJ mol^{-1}, to the total interaction energy for the ring, prism and cage isomers of water hexamer, calculated using the ASP-W4 potential model (Millot *et al.* 1998).

	Total	2-body	3-body	4-body	5-body	6-body
ring	−180.7	−137.7	−35.7	−6.30	−0.914	−0.090
prism	−196.9	−163.6	−30.4	−3.11	0.251	0.009
cage	−191.8	−160.3	−29.3	−2.27	0.120	−0.015
book	−188.3	−150.6	−33.1	−4.35	−0.196	−0.027

approximation to neglect the higher-order terms in the many-body expansion of the induction energy.

This is illustrated for small water clusters in Figs 10.1 and 10.2 (Hodges *et al.* 1997). In these Figures, the left-hand bars of each pair show the sum of the pair interactions, the three-body correction and (in Fig. 10.2) the four-body correction, calculated by *ab initio* SCF theory with MP2 corrections. The right-hand bars of each pair show the corresponding quantities calculated using the ASP-W4 model for the water dimer (Millot *et al.* 1998), in which the only many-body term is the induction energy. Note that the three-body correction is positive, reducing the binding energy, for many of the examples shown.

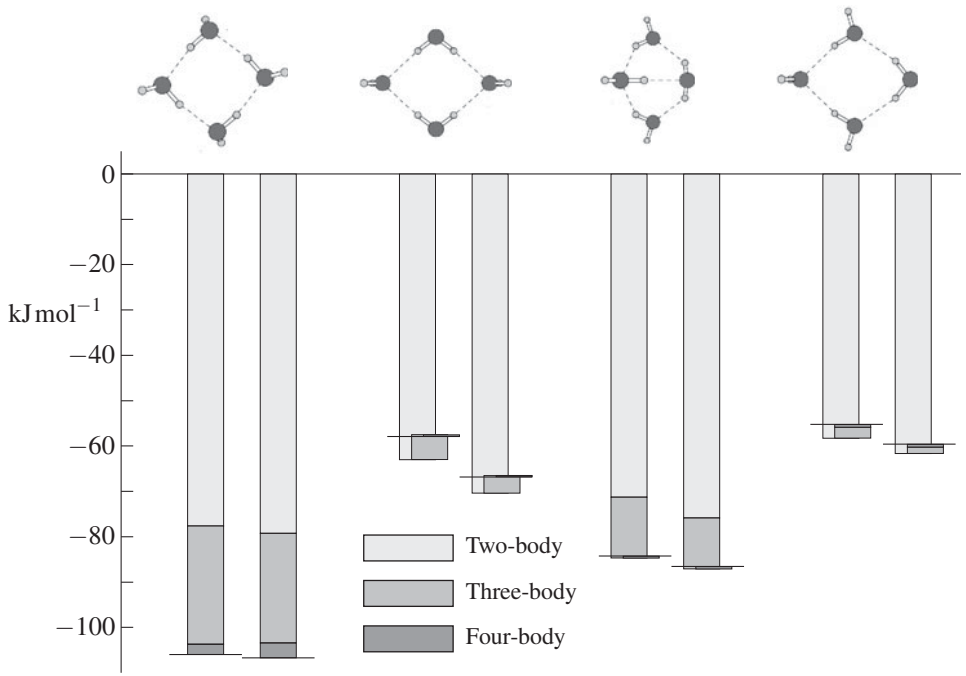

Fig. 10.2 Two-body, three-body and four-body energies (in kJ mol^{-1}) for water tetramer in four geometries. The extended horizontal line shows the total binding energy. The left-hand bar of each pair shows the energies from SCF+MP2 *ab initio* calculations with an aug-cc-pVDZ basis set; the right-hand one shows the energies obtained from the ASP-W4 water potential in the *ab initio* geometries. (See also Plate 5.)

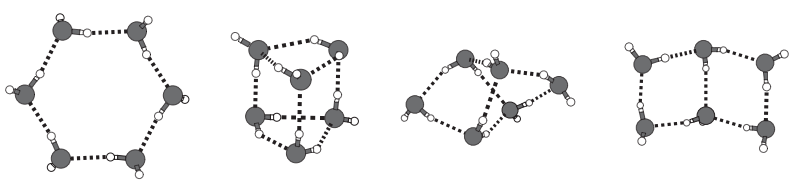

Fig. 10.3 Some low-energy structures of the water hexamer. From left: ring, prism, cage and book. (See also Plate 6).

These results show, first, that almost all of the three-body correction and probably also the four-body correction are accounted for by the induction energy; and secondly that the four-body terms are in most cases very much smaller than the three-body terms. The exception to the latter result is the left-hand structure for the tetramer, where the hydrogen bonds act co-operatively to enhance the induction energy. The same cooperative effect stabilizes the cyclic ring structure in the pentamer and hexamer, but in the hexamer other more compact structures are more stable than the ring, the additional hydrogen bonds making a larger two-body

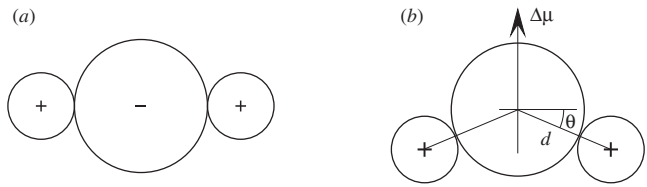

Fig. 10.4 Symmetrical and unsymmetrical arrangements of ions in a lattice.

contribution that outweighs the smaller three-body contribution. (See Table 10.1.) The lowest-energy structures are the 'prism', 'cage' and 'book' structures, with the cyclic 'ring' structure lying somewhat higher (Fig. 10.3). There are several variants of each of these, with different hydrogen-bonding patterns. Temelso *et al.* (2011) carried out CCSD(T) calculations on examples of each, extrapolated to complete basis sets, and found that the cage, prism and book had energies within 0.2 kJ mol^{-1} of each other after correction for zero-point energy, while the ring was about 1.6 kJ mol^{-1}higher. Experimental work using chirped microwave pulse Fourier transform rotational spectrometry (§13.4, p. 251) has confirmed the cage as the lowest-energy structure, but found that the prism and book structures are only slightly higher in energy.

One of the most striking examples of the non-additivity of the induction energy occurs in work by Wilson and Madden (1994) on the halides (except the fluorides) of the alkaline earths, such as $MgCl_2$. These comprise small and quite highly charged cations and relatively large and polarizable anions. Simple chemical intuition leads us to expect these compounds to be purely ionic, and conventional radius-ratio considerations predict the fluorite (CaF_2) structure for radius ratios between 1 and 1.37, the rutile (TiO_2) structure between 1.37 and 2.44, and a four-coordinated structure for larger values. While these predictions are correct for the smaller radius ratios, the structures at higher ratios are chain or layer structures in which the cations are symmetrically coordinated but the environment of the anions is very unsymmetrical.

This phenomenon has been attributed to the onset of 'covalent' bonding or to 'charge transfer'; Wells (1975) attributes it to the large polarizability of the anions, though without an explanation of how this leads to the observed structure. In fact the fundamental mechanism is very simple. Consider an anion X with polarizability α, placed symmetrically between two cations M (Fig. 10.4a). We ignore the polarizability of the cations, which is much smaller than that of the anions. (The polarizability of Cl^- in NaCl, for instance, is about 20 a.u., while the polarizability of the Na^+ ion is about 1 a.u. (Fowler and Madden 1984), and that of Mg^{2+} is about 0.5 a.u. (Fowler and Madden 1985).) In this configuration the induction energy is zero because the total electric field at the anion is zero. Now consider a distorted configuration (Fig. 10.4b) in which the X–M–X bond angle changes from π to $\pi - 2\theta$. The electric field at the anion is now $2(q/4\pi\epsilon_0 d^2)\sin\theta$, where q is the charge on each cation. The induction energy is

$$U_{\text{ind}} = -\tfrac{1}{2}\alpha F^2 = -\alpha\frac{2q^2}{(4\pi\epsilon_0)^2 d^4}\sin^2\theta,$$

while the electrostatic repulsion between the cations is

$$E_{\text{es}} = \frac{q^2}{4\pi\epsilon_0.2d\cos\theta}.$$

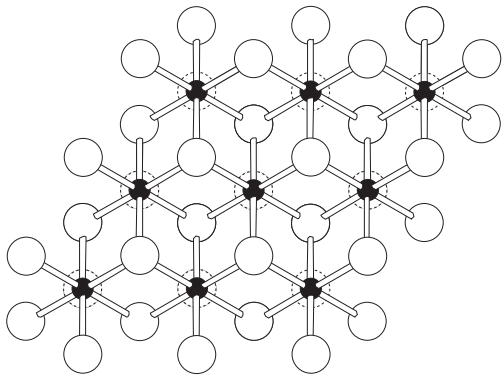

Fig. 10.5 Crystal structure of $CdCl_2$ and $MgCl_2$. One layer of the crystal is shown, comprising a plane of anions (nearest, open circles), a plane of cations (filled circles) and another plane of anions. The nearest plane of anions in the layer below is indicated by dashed open circles.

(We need not consider the attraction between the anion and cations, which does not depend on θ.) The total energy is stationary with respect to variations of θ when

$$-\alpha \frac{2q^2}{(4\pi\epsilon_0)^2 d^4}.2\sin\theta\cos\theta + \frac{q^2}{4\pi\epsilon_0.2d}\frac{\sin\theta}{\cos^2\theta} = 0,$$

i.e., when $\sin\theta = 0$ or $\cos^3\theta = 4\pi\epsilon_0 d^3/8\alpha$. If there are n cations arranged in a regular polygon, each M–X bond making an angle θ with the plane of the cations, the second solution becomes

$$\cos^3\theta = 4\pi\epsilon_0 d^3/(2n^2\alpha\sin(\pi/n)). \tag{10.1.3}$$

In the $MgCl_2$ crystal, each Cl^- ion has three Mg^{2+} ions coordinated to it, with Mg–Cl–Mg angles close to 90°. (See Fig. 10.5.) This corresponds to $\theta \approx 35°$. The Cl^- ion in a crystal has a polarizability of about 20 a.u. (Fowler and Madden 1984), so a minimum other than $\theta = 0$ is possible with three cations if $d^3 < 300$ approximately, or $d < 6.7$ bohr. The Mg−Cl distance in $MgCl_2$ is about 2.52 Å = 4.76 bohr, and the minimum in the energy occurs for $\theta = 45°$. Consequently we can very easily attribute the unexpected structures of the alkaline-earth halides to the effects of induction, and in particular to its non-additivity. We can see from eqn (10.1.3) that the effect increases as the cation becomes smaller (reducing d) and as the anion polarizability increases. This is precisely in accordance with the observed trends.

Notice that the charge on the cation drops out of this calculation, which may therefore seem to suggest that salts involving singly charged cations are as likely to exhibit distorted structures as those involving more highly charged cations. In fact that is not the case, and the reason for this has to do with the other remarkable and apparently highly unfavourable feature of these structures. The $CdCl_2$ structure, for instance, which is also that of $MgCl_2$, can be derived from the NaCl structure by deleting alternate (111) planes of cations (Wells 1975), so it contains adjacent layers of anions, which might be expected to repel each other very strongly. However, this repulsion is greatly reduced by polarization effects. There is a substantial dipole induced in each anion by the electric field of the three cations coordinated to it:

$$\Delta\mu = 3\alpha(q/4\pi\epsilon_0 d^2)\sin\theta.$$

If $\alpha = 20$ a.u., $d = 4.76$ bohr and $\theta \approx 35°$, the magnitude of the induced dipole is about 3 a.u. or 7.5 D. The interaction between anions in two adjacent layers includes a repulsive charge–charge term $+1/4\pi\epsilon_0 R$, an attractive dipole–charge term $-2\Delta\mu\cos\theta'/4\pi\epsilon_0 R^2$, and a repulsive dipole–dipole term $+(\Delta\mu)^2(3\cos^2\theta' - 1)/4\pi\epsilon_0 R^3$, where θ' is the angle between the anion–anion vector and the normal to the anion sheets. In the $MgCl_2$ structure, the anions form a cubic close-packed lattice, so an anion in one sheet fits into a hole between three adjacent anions in the adjacent sheet, the four ions forming a nearly regular tetrahedron (see Fig. 10.5). In this geometry, $\sin\theta' = \sqrt{1/3}$, while R is 6.7 bohr, so the values of these three terms are $1/R = 0.15$, $-6\sqrt{2/3}/R^2 = -0.12$ and $9/R^3 = 0.03$. This is a grossly oversimplified calculation, but it shows how the attraction between the induced dipoles in one layer and the charges in the next compensate to a large degree for the repulsion between the ion charges, while the repulsion between the induced dipoles is relatively small because of the $3\cos^2\theta' - 1$ factor. Notice that the magnitude of the induced dipole is proportional to the cation charge, so that the compensating effect is stronger for structures containing highly charged cations.

This simplified approach does no more than suggest the way in which polarization effects can stabilize the layer structure. It is necessary to perform a sum over all the ions in the lattice to arrive at a quantitatively useful result, and the induced moments on the anions need to be determined by solving eqn (9.4.12). A better calculation also needs to take into account the damping of the induction interaction at short range, which reduces the effects just discussed, and the effect of dispersion, especially the dispersion interaction between anions in adjacent layers, which contributes greatly to the stability of the structure. Wilson and Madden (1994) discuss the contribution of these effects in detail, and describe calculations in which they are taken into account and which lead to very satisfactory predictions of the observed structures. Nevertheless the fundamental feature is the effect of induction non-additivity in stabilizing what seem at first sight to be very improbable structures.

10.2 Many-body terms in the dispersion energy

In interactions between neutral spherical atoms, induction cannot contribute, and the main non-additive effects are many-body repulsion and dispersion terms (Elrod and Saykally 1994). If the long-range perturbation theory is continued to third order, in a system with three or more atoms or molecules, terms arise of the form

$$\sum_{m\neq 0}\sum_{n\neq 0}\sum_{p\neq 0}\frac{\langle 000|\mathcal{H}'_{AB}|mn0\rangle\langle mn0|\mathcal{H}'_{BC}|m0p\rangle\langle m0p|\mathcal{H}'_{CA}|000\rangle}{(\Delta W_m^A + \Delta W_n^B)(\Delta W_m^A + \Delta W_p^C)},$$

where for example $\mathcal{H}'_{AB}$ is the interaction Hamiltonian between A and B. The states $|mnp\rangle$ are simple products of single-molecule states with molecule A in state m, B in state n, and C in state p. (We are using the long-range theory, so no antisymmetrization is needed, though this may not be a very good approximation at the distances where these terms are important.) Notice that molecule A is different from the others in this expression, since it is excited in both intermediate states; there are other terms in which this is true of B or C. If all terms of this sort are collected together, and the perturbation is truncated at the dipole–dipole term, the result

is the Axilrod–Teller–Muto triple-dipole dispersion interaction, first given independently by Axilrod and Teller (1943) and by Muto (1943):

$$U_{3\mu} = C_9 \frac{(1 + 3\cos\widehat{A}\cos\widehat{B}\cos\widehat{C})}{R_{AB}^3 R_{BC}^3 R_{AC}^3}, \tag{10.2.1}$$

where R_{AB}, etc., are the lengths of the sides and $\widehat{A}$, $\widehat{B}$ and $\widehat{C}$ are the angles of the triangle formed by the three atoms or molecules. (In the case of a molecule, the reference point forming the vertex of the triangle is the origin that has been chosen for the molecule.) The coefficient C_9 can be expressed using an average-energy formula of London type:

$$C_9 = 3\overline{U}\alpha^A\alpha^B\alpha^C, \tag{10.2.2}$$

where

$$\overline{U} = \frac{U_A U_B U_C (U_A + U_B + U_C)}{(U_A + U_B)(U_B + U_C)(U_A + U_C)}, \tag{10.2.3}$$

or in terms of an integration over imaginary frequencies:

$$C_9 = \frac{3\hbar}{\pi} \int_0^\infty \alpha^A(\mathrm{i}u)\alpha^B(\mathrm{i}u)\alpha^C(\mathrm{i}u)\ \mathrm{d}u. \tag{10.2.4}$$

The latter form can be used to evaluate triple-dipole coefficients from dipole oscillator strength distributions (see §13.1.2, p. 243), and Kumar and Meath (1984, 1985) have tabulated values for interactions involving a number of atoms and small molecules. One advantage of this approach is that it is just as easy to evaluate the coefficients for the mixed interactions, involving two or three different molecules, as for the unmixed ones. The C_9 coefficient can also be estimated from the C_6 coefficient and the polarizability (Tang 1969), using the same approach that provides a combining rule for the C_6 coefficient:

$$C_9^{ABC} \approx \frac{2S^A S^B S^C (S^A + S^B + S^C)}{(S^A + S^B)(S^B + S^C)(S^C + S^A)}, \tag{10.2.5}$$

where

$$S^A = C_6^{AA}\alpha^B(0)\alpha^C(0)/\alpha^A(0),$$

and similarly for S^B and S^C.

The principal feature that distinguishes the triple-dipole dispersion from the ordinary two-molecule dispersion terms is that it has a geometrical factor whose sign depends on the configuration of the three molecules. Also, as (10.2.2) and (10.2.4) show, C_9 is positive, whereas the ordinary dispersion interaction is negative. For three atoms in contact, forming an equilateral triangle, the geometrical factor is $(11/8)R^{-9}$, so the triple-dipole dispersion energy is repulsive in a close-packed solid, where such configurations dominate. The angular factor is negative, though much smaller, for isosceles triangles where one of the angles is 120°, which also occur in the close-packed solid, but then the distance between two of the atoms is significantly greater; while for three atoms in a line with separations of R the geometrical factor is $-\frac{1}{4}R^{-9}$. Configurations where there is only one atom–atom contact, or none, make a much smaller contribution, because of the R^{-3} factors. The upshot is that the triple-dipole dispersion makes

a repulsive contribution to the total energy of the solid. In the case of argon, its contribution is estimated to be about 7% of the total binding energy.

In liquid water or ice, on the other hand, the constraints arising from hydrogen bonding ensure that one of the angles in a triangle of nearest neighbours is close to the tetrahedral angle. This is close to the angle (117°) where the angular factor changes sign, and the geometrical factor is smaller by a factor of 20 in the case when one of the angles is tetrahedral than it is for an equilateral triangle. Accordingly, the triple-dipole term is likely to be negligible in water and ice. Goldman and Saykally (2004) have pointed out, however, that it has quite significant effects on the structures of small water clusters. This is partly because the energy differences between alternative structures are quite small, and also because in these small clusters the geometries of neighbouring sets of three water molecules can be distorted away from the tetrahedral geometry found in ice, so that some of the individual triple-dipole contributions may be larger in magnitude. If the triple-dipole dispersion is treated using eqn (10.2.1) with the C_9 coefficient derived from the water DOSD by Margoliash *et al.* (1978), the energies for the low-lying structures of the water hexamer are, in $\mathrm{kJ\,mol^{-1}}$,

ring	prism	cage	book
0.04	1.62	1.45	0.67

Note the very small value for the ring structure, where the angles in the ring are all 120°.

The expressions (10.2.2) and (10.2.4) involve average polarizabilities. If the polarizabilities are anisotropic, (10.2.1) becomes (Stogryn 1971),

$$U_{3\mu} = -\frac{\hbar}{\pi} T^{AB}_{\beta\gamma} T^{BC}_{\delta\epsilon} T^{CA}_{\varphi\alpha} \int_0^\infty \alpha^A_{\alpha\beta}(\mathrm{i}u)\alpha^B_{\gamma\delta}(\mathrm{i}u)\alpha^C_{\epsilon\varphi}(\mathrm{i}u)\ \mathrm{d}u. \tag{10.2.6}$$

An expression for the three-body dispersion in terms of frequency-dependent density susceptibilities avoids the multipole expansion:

$$U^{(3)}_{\mathrm{disp}} = -\frac{\hbar}{\pi} \int_0^\infty \frac{\alpha^A(\mathbf{r}_1, \mathbf{r}'_1, \mathrm{i}u)\alpha^B(\mathbf{r}_2, \mathbf{r}'_2, \mathrm{i}u)\alpha^C(\mathbf{r}_3, \mathbf{r}'_3, \mathrm{i}u)}{|r'_1 - r_2||r'_2 - r_3||r'_3 - r_1|}\ \mathrm{d}u, \tag{10.2.7}$$

and this provides the basis for *ab initio* calculation of three-body dispersion energies, though a full treatment needs to include exchange terms (Podeszwa and Szalewicz 2007).

The Axilrod–Teller–Muto triple-dipole dispersion is only the leading term in a multipole expansion of the non-additive third-order energy:

$$U^{\text{long-range}}_{\text{three-body}} = U_{111} + U_{112} + (U_{122} + U_{113}) + (U_{222} + U_{123} + U_{114}) + \cdots, \tag{10.2.8}$$

where subscripts 1, 2, 3,... refer to dipole, quadrupole, octopole, etc. The distance dependence of U_{jkl} is $R^{-(2j+2l+2k+3)}$, so the higher terms are only significant at short range, and they are strongly anisotropic (Bell 1970, Doran and Zucker 1971), but for small clusters of inert-gas atoms they contribute around 20% of the triple-dipole term (Etters and Danilowicz 1979). There is also a fourth-order dispersion term involving the three dipole–dipole interactions between three atoms; this is attractive, and for inert gases, especially Ar and Kr, it largely cancels the higher-rank third-order terms.

Four-body and higher many-body terms are expected to be less important because the N-body dipole–dipole interaction contains a factor of R^{-3N}, and no more than four atoms can be

in mutual contact. Kim *et al.* (2006) have explored dispersion interactions between clusters, using a Drude dipole–dipole dispersion model with a full summation over the many-body terms, and found that for some geometries the three-body term was cancelled by the higher many-body terms, while in others the contribution of the three-body and higher terms was about the same as the two-body term.

10.3 Many-body terms in the repulsion energy

We have seen how the overlap of the wavefunctions of adjacent molecules, and the consequent antisymmetrization and renormalization, leads to a repulsion between the molecules. If three molecules overlap in this way, the renormalization is different in form, and the energy of the three interacting molecules is not just the sum of the three two-body interactions. We have

$$W_{ABC} = W_A + W_B + W_C + U_{AB} + U_{BC} + U_{AC} + U_{ABC}, \tag{10.3.1}$$

where U_{ABC} is a three-body correction. Wells and Wilson (1986) estimated the magnitude of this correction by *ab initio* calculation, and concluded that for three neon atoms in an equilateral triangle it is negative, i.e., attractive, but smaller in magnitude for the crystal as a whole than the repulsive contribution of the triple-dipole dispersion term. Chałasiński *et al.* (1997) analysed the three-body exchange–repulsion energy by expansion in orders of exchange (see §6.2.5), and found that for inert gas atoms in an equilateral triangle, the three-body term is positive in the single-exchange approximation, but the triple-exchange term is negative and dominates, so that the total three-body correction is negative. For Ne_3 the correction was −534 microhartree at an Ne···Ne separation of 4 bohr, but only −0.5 microhartree at 6 bohr. (The Ne···Ne separation in the crystal is 5.96 bohr.) In the linear configuration, on the other hand, the triple-exchange term and the total three-body correction are positive.

For four atoms in contact, there is a further four-body correction, which is repulsive and somewhat smaller in magnitude than the three-body term (Wells and Wilson 1989*a*). The total four-body contribution is estimated to amount to 40% of the three-body contribution for the He crystal (Wells and Wilson 1989*b*). The many-body corrections are largest for those configurations where the atoms are all in contact. For four Ne atoms in a tetrahedral geometry with an Ne···Ne distance of 4 bohr, the four-body correction is 129 microhartree, and it decreases to less than 2 microhartree at a distance of 5 bohr (Wells and Wilson 1989*a*). Since it is not possible to arrange more than four atoms so that each is in contact with all the others, it is reasonable to hope that the many-body expansion of the repulsion energy converges. However, there appears to have been no investigation of the rate of convergence after the four-body term. There has been some dispute over the relative importance of the exchange–repulsion and dispersion three-body terms (Meath and Aziz 1984, Barker 1986, Meath and Koulis 1991). Hinde (2008) found that they cancelled approximately in solid *para*-hydrogen.

10.4 Other many-body effects

Potential-energy surfaces for small Van der Waals clusters can be obtained very accurately by fitting them to infrared spectra (see Chapter 13). Such work has demonstrated the existence of other many-body effects, small but not negligible. The spectrum of the $HCl\cdots Ar_2$ complex cannot be fitted satisfactorily by a potential model unless a term is included that describes the generation of an overlap quadrupole moment when the two Ar atoms are close together. This

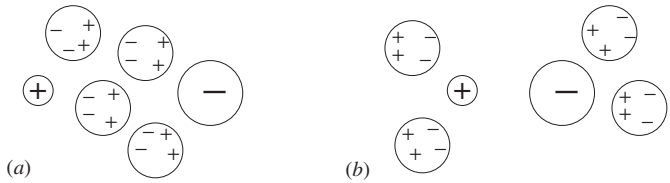

Fig. 10.6 The effect of a polarizable solvent on electrostatic interactions.

is readily understood in terms of the qualitative description of repulsion given in Chapter 8: at short range there is a redistribution of the electron charge away from the region between the argon atoms towards the ends of the Ar_2 unit. This corresponds to a negative quadrupole moment, and contributes repulsively to the energy of the otherwise favourable structure in which the H atom of the HCl points between the two Ar atoms (Cooper and Hutson 1993, Ernesti and Hutson 1994). While this was evidently an important effect, Chałasiński and Szczęśniak (2000) found that a detailed calculation of the three-body terms was needed to give the full picture. The general symmetry-adapted perturbation theory of three-body interactions (§6.4.3) includes mixed induction–dispersion terms as well as third-order induction and dispersion, and at short range there are mixed exchange terms too.

10.5 Intermolecular forces in a medium

One important instance of many-body effects is the modification of intermolecular forces between molecules in a solvent. These modifications occur in various ways.

In the first place, the presence of a polarizable solvent changes the interactions between solute molecules. If two solute molecules carry opposite charges, for example, and there is a polarizable solvent molecule between them, its polarization has the effect of increasing the attraction between the solute ions (Fig. 10.6a). Solvent molecules in other positions, on the other hand, can cause the attraction to decrease (Fig. 10.6b). If the solvent can be treated as if it were a continuous medium, these effects can be described by assigning a dielectric constant ϵ to the medium, but in many cases the distance scale is too small for this to be a reasonable approximation. Indeed, a detailed study has revealed that a pair of ions with the same sign in a polarizable solvent experience an attraction, on average, due to the polarization of the solvent, while ions of opposite sign experience a repulsion (Jarque and Buckingham 1989, 1992). If the solvent polarizability is large enough, the effect can overcome the Coulomb interaction at intermediate distances.

The reorientation of solvent molecules in the field of the solute also has substantial effects on their interactions. Ions in a polar solvent are normally surrounded by a shell of solvent molecules (Fig. 10.7) and these become in effect part of the solute, so that the interaction is not between bare ions or molecules but between 'dressed' ones. The coordination shell is not rigid but constantly in motion, so that the dressed ion involves a statistical average over the positions and orientations of the solvent molecules.

In fact the interaction between molecules in solution is not properly an energy (enthalpy) but a free energy, called the *potential of mean force*:

$$G(\mathbf{R}, T) = H(\mathbf{R}, T) - TS(\mathbf{R}, T). \tag{10.5.1}$$

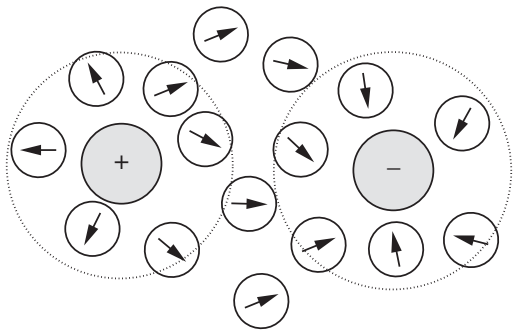

Fig. 10.7 Ions in a polar solvent.

Both the enthalpy term H and the entropy S involve a statistical average over the solvent, and so depend on the temperature, and the entropy as well as the energy depends on the positions of the solute molecules, specified by the coordinates $\mathbf{R}$.

10.5.1 The hydrophobic effect

An important example of the way in which entropy affects solutions is the *hydrophobic effect* (Ben-Naim 1980, Chandler 2005). This is seen in the tendency for oil and water to segregate, for amphiphilic molecules (such as detergents, with a water-attracting end and a water-repelling end) to form micelles, and for protein molecules to fold in water in such a way that the hydrophobic residues go to the centre while the hydrophilic residues end up on the surface.

The change in free energy on solvation is $\Delta G = \Delta H - T\Delta S$. The enthalpy change arises from intermolecular interactions of all kinds, the pV term in the enthalpy being usually unimportant. However, a small volume V_s of solute can dissolve in a large volume V of solvent, even if the enthalpy change is unfavourable, because there is a large increase in the entropy of the solute, of the order of $R\ln(V/V_s)$ per mole (where R is the molar gas constant), as its available volume increases. Hydrophobic effects may reduce the change in entropy and so reduce the solubility. They may also modify the enthalpy and entropy of the solvent. According to Chandler (2005), water molecules can still form a hydrogen-bond network around a small solute molecule, but it is constrained by the presence of the solute, so the solvent entropy is reduced while the enthalpy is unaffected. This effect is roughly proportional to the volume of the solute. Water near a hydrophobic surface, however, behaves much like water at the liquid–vapour interface, with loss of hydrogen bonding and a consequent increase in enthalpy, proportional to the surface area of the interface. The crossover between these effects occurs at a length scale of around 1 nm.

One example on the smallest scale is seen in mixtures of methanol and water. They mix freely at any volume ratio, but the entropy of solution is less than it would be if the water and methanol molecules were randomly distributed. Dixit *et al.* (2002) studied a concentrated solution of methanol in water by both neutron diffraction and molecular simulation, and found that the hydrogen-bonding structure is much the same as in liquid water, but that the oxygen atoms, whether of the water or the methanol, tend to form chains and clusters separately from the carbon atoms of the methyl groups, so that there is incomplete mixing at the molecular level and a reduced entropy of mixing.

Examples of the loss of hydrogen-bonding structure near a large hydrophobic solute were found by Du *et al.* (1994), who studied the interfaces between water and several hydrophobic materials using sum-frequency generation spectroscopy, and found that they were characterized by a large number of dangling hydroxyl groups—approximately one for every four water molecules. Thus the insertion of a large hydrophobic molecule into water requires energy to break or distort hydrogen bonds between water molecules. Also, recent work by Rezus and Bakker (2007) shows that the water molecules near to methyl groups in hydrophobic solute molecules display much slower reorientational dynamics than those in the bulk, so that they are effectively immobilized and have a lower entropy. This is thought to happen because it is more difficult for a fifth water molecule to approach and disrupt the tetrahedral coordination. The picture is reminiscent of the 'iceberg model' proposed by Frank and Evans (1945) to account for the hydrophobic effect, but the water molecules around hydrophobic groups are ice-like only in lack of mobility, not in structure.

As a consequence, there is a tendency towards 'dewetting' or 'drying' around a hydrophobic solute molecule; that is, the solvent molecules tend to move away from the surface of the solute, forming an interface that is similar to the liquid–vapour interface of water. As two separated solute molecules approach, the drying zones around them overlap. The area of the interface between solute and solvent consequently decreases, so that the enthalpy effect associated with disruption of hydrogen bonding and the entropic effect arising from lack of mobility of the hydrogen bonded network both favour solute aggregation. In addition, there is a 'depletion' force: the overlap of regions from which the solvent molecules are excluded increases the volume that is accessible to the solvent, so that the solvent entropy increases and further favours aggregation. Overall, the creation of an interface between a hydrophobic solute and water requires a free energy per unit area comparable with the liquid–vapour surface energy of water, though it is somewhat lower because of the attraction energy, mainly dispersion, between the water and solute molecules (Huang and Chandler 2002). The reduction in the surface energy that results from aggregation has to be set against the reduction in free energy, via the entropy term, that would result from dispersing the solute throughout the solvent. In the case of hydrocarbons in water, the balance favours aggregation. In the case of detergents, micelle formation avoids completely the creation of an interface between the hydrophobic parts of the molecules and the water, and the same applies when a protein folds so that the hydrophobic side-chains are embedded within the protein, leaving the hydrophilic side-chains at the surface. In the presence of a hydrophobic surface, however, the unfolded protein may be stabilized to some extent by aggregation of its hydrophobic residues with the surface (Patel *et al.* 2011).

11
Interactions Involving Excited States

11.1 Resonance interactions and excitons

When one of a pair of identical molecules is in an excited state, a new type of interaction becomes possible. Since either molecule can be excited, with the other in the ground state, there are two states involved, and they can mix under the influence of the intermolecular perturbation, one combination being stabilized and the other raised in energy. This effect operates at long range; there is no need for the molecular wavefunctions to overlap.

If the two states are $|1^A0^B\rangle$ (molecule A excited) and $|0^A1^B\rangle$ (molecule B excited), we can write down secular equations for a mixed state $c_A|1^A0^B\rangle + c_B|0^A1^B\rangle$:

$$\begin{aligned}(H_{AA} - W)c_A + H_{AB}c_B &= 0,\\ H_{BA}c_A + (H_{BB} - W)c_B &= 0,\end{aligned} \tag{11.1.1}$$

where

$$\begin{aligned}H_{AA} &= \langle 1^A0^B|\mathcal{H}|1^A0^B\rangle = W_1^A + W_0^B,\\ H_{BB} &= \langle 0^A1^B|\mathcal{H}|0^A1^B\rangle = W_0^A + W_1^B,\\ H_{AB} &= \langle 1^A0^B|\mathcal{H}|0^A1^B\rangle.\end{aligned} \tag{11.1.2}$$

Here $\mathcal{H} = H^0 + \mathcal{H}' = \mathcal{H}^A + \mathcal{H}^B + \mathcal{H}'$, and we have ignored the perturbation $\mathcal{H}'$ in the diagonal matrix elements. The zeroth-order Hamiltonian does not contribute to the off-diagonal matrix element H_{AB}, because, for example, $\langle 1^A0^B|\mathcal{H}^A|0^A1^B\rangle = W_0^A\langle 1^A|0^B\rangle\langle 0^B|1^B\rangle = 0$. Using just the dipole–dipole term in the perturbation (see eqn (3.2.2)), we have

$$\begin{aligned}H_{AB} &= -\langle 1^A0^B|T_{\alpha\beta}\hat{\mu}_\alpha^A\hat{\mu}_\beta^B|0^A1^B\rangle\\ &= -\langle 1^A|\hat{\mu}_\alpha^A|0^A\rangle T_{\alpha\beta}\langle 0^B|\hat{\mu}_\beta^B|1^B\rangle\\ &= -(\mu_\alpha^A)_{01}T_{\alpha\beta}(\mu_\beta^B)_{01},\end{aligned} \tag{11.1.3}$$

where $(\mu_\alpha^A)_{01}$ is the transition dipole between states 0 and 1.

If the molecules are identical, $W_1^A + W_0^B = W_0^A + W_1^B$ and we can drop the superscripts. Solving the secular equations, we find that the states and their energies are

$$\sqrt{\tfrac{1}{2}}\Big(|1^A0^B\rangle \pm |0^A1^B\rangle\Big), \qquad W = W_0 + W_1 \mp (\mu_\alpha^A)_{01}T_{\alpha\beta}(\mu_\beta^B)_{01}. \tag{11.1.4}$$

We conclude that even if the molecules are non-polar, so that there is no dipole–dipole interaction between them when both are in their ground states, there can be an interaction of

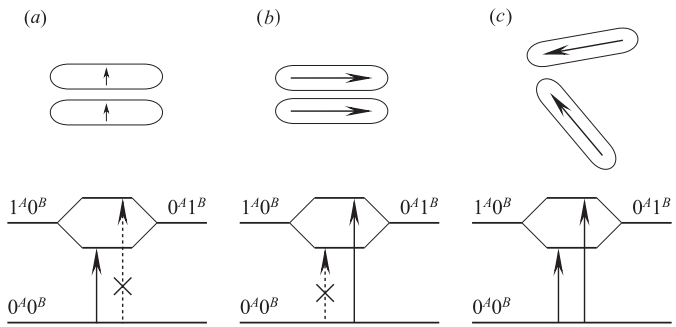

Fig. 11.1 Energy levels and allowed transitions resulting from the resonance interaction between a pair of molecules.

dipole–dipole form when one molecule is in an excited state, provided that there is an allowed electric dipole transition to that state. The splitting of the excited states that occurs is called an *exciton* splitting. It is proportional to $T_{\alpha\beta}$ and hence to R^{-3}, so it tends to attract the molecules to each other if the system is in the lower of the two excited states. Notice again that this is a long-range type of interaction—there is no need for the molecules to overlap. However, the molecules need to be identical; if they are not, then the energies $W_1^A + W_0^B$ and $W_0^A + W_1^B$ of the two excited states will usually be very different, and the energy change due to the interaction will be much smaller.

Consider, for example, a dipole-allowed $\sigma - \pi^*$ transition in an aromatic molecule. The transition dipole is perpendicular to the plane of the molecule, so there is an attractive interaction if the planes of the molecules are parallel (Fig. 11.1a). In this case the transition moment to the lower state is

$$\left\langle 0^A0^B\middle|\mu^A + \mu^B\middle|\sqrt{\tfrac{1}{2}}(1^A0^B + 0^A1^B)\right\rangle = \sqrt{\tfrac{1}{2}}((\mu^A)_{01} + (\mu^B)_{01}) = \sqrt{2}\mu_{01}, \tag{11.1.5}$$

and the intensity of this transition is twice as great as for a single molecule. For the upper state, on the other hand, the wavefunction is $\left|\sqrt{\tfrac{1}{2}}(1^A0^B - 0^A1^B)\right\rangle$, so the transition moments cancel out and the transition is forbidden.

Low-lying excited states of aromatic molecules are more commonly due to $\pi - \pi^*$ transitions, and then the transition moment lies in the plane of the molecule (Fig. 11.1b). There is still an attractive interaction, in spite of the repulsive geometry of the transition dipoles, but now it is the state $\left|\sqrt{\tfrac{1}{2}}(1^A0^B - 0^A1^B)\right\rangle$ that has the lower energy. However, the transition to this state is still forbidden, and the upper state now takes all the intensity.

In fact the sign of the transition dipole is arbitrary, because it depends on the arbitrary phase assigned to the ground and excited-state wavefunctions. Consequently the geometrical features of such interactions are somewhat different from those for static moments. There are just two possibilities for the signs, since changing both of them has no effect. In example (a) above, we can have *either* transition dipoles parallel, giving the attractive lower state, *or* antiparallel, giving the repulsive upper state. In (b), transition dipoles parallel gives the repulsive upper state, while the antiparallel arrangement gives the attractive lower state. In both cases it is the state with parallel transition dipoles that has all the intensity.

Of course other orientations are possible in which the dipoles are neither parallel nor antiparallel, but related in some other way (Fig. 11.1c). In this case there will again be an attractive state and a repulsive one, but usually both will have non-zero intensity.

11.1.1 Excitons

The resonance interaction is often important in excited states of molecular crystals. Here matters become a little more complicated, because all the molecules in the crystal are involved. Davydov's classic book (1962) gives a detailed account. If there is just one molecule per unit cell, then we can label them by the cell coordinate $\mathbf{t}$ which gives the position of the cell relative to some arbitrary origin. If the state with the molecule in cell $\mathbf{t}$ excited is denoted $|1,\mathbf{t}\rangle$, then the excited states of the crystal are the Bloch functions

$$|1,\mathbf{k}\rangle = N^{-\frac{1}{2}} \sum_{\mathbf{t}} |1,\mathbf{t}\rangle \exp(\mathrm{i}\mathbf{k}\cdot\mathbf{t}), \tag{11.1.6}$$

where $\mathbf{k}$ is the wavevector of the state and N is the number of unit cells in the crystal.* Now an optical spectrum uses light whose wavelength is long compared with the size of the unit cell—typically 100–1000 times as long—so the oscillating electric field is uniform over a macroscopic region of crystal. In this case the only Bloch function for which the intensity is non-zero is the state with $\mathbf{k} = 0$, because the $\exp(\mathrm{i}\mathbf{k}\cdot\mathbf{t})$ factors otherwise cause the transition dipole to cancel out. However, the $\mathbf{k} = 0$ transition acquires all the intensity of the transitions for the N molecules, just as in the two-molecule case already considered. The spectrum therefore contains a single line for the transition in question, as for an isolated molecule.

When there are two molecules in the unit cell, we are still concerned only with $\mathbf{k} = 0$ states, but now there are two of them:

$$\begin{aligned} |1^A0^B\rangle &= N^{-1/2} \sum_{\mathbf{t}} |1^A0^B,\mathbf{t}\rangle, \\ |0^A1^B\rangle &= N^{-1/2} \sum_{\mathbf{t}} |0^A1^B,\mathbf{t}\rangle. \end{aligned} \tag{11.1.7}$$

We have dropped the $\mathbf{k}$ label, but we should remember that we are dealing with states with $\mathbf{k} = 0$. The ket $|1^A0^B,\mathbf{t}\rangle$ denotes the state in which molecule A in cell $\mathbf{t}$ is excited and all others are in the ground state; similarly $|0^A1^B,\mathbf{t}\rangle$ has just molecule B in cell $\mathbf{t}$ excited.

Now, as before, there is an interaction between these two states, and only these, because states with different $\mathbf{k}$ cannot mix. The matrix element is

$$\begin{aligned} \langle 1^A0^B|\mathcal{H}'|0^A1^B\rangle &= N^{-1} \sum_{\mathbf{tt}'} \langle 1^A0^B,\mathbf{t}|\mathcal{H}'|0^A1^B,\mathbf{t}'\rangle \\ &= \sum_{\mathbf{t}} \langle 1^A0^B,\mathbf{t}|\mathcal{H}'|0^A1^B,0\rangle. \end{aligned}$$

We have replaced the sum over $\mathbf{t}'$ by a factor N, since the translational symmetry of the crystal ensures that all values of $\mathbf{t}'$ give the same result. The matrix elements in the remaining sum

*Some knowledge of the elementary theory of solids is being assumed here. If it is unfamiliar, this discussion may be skipped, or a suitable introduction may be found in, e.g., Kittel (1987).

are dipole–dipole interactions between transition dipoles, as before. In each of these, one of the transition dipoles is that of molecule B in cell 0, while the other is that of molecule A in the same cell or one of the neighbouring ones. Because of the R^{-3} factor in the dipole–dipole interaction, only the nearest neighbours contribute significantly. Note that all these A transition moments are parallel because $\mathbf{k} = 0$; there is no arbitrariness about their relative phases, though as before the relative phase of the A and B transition moments is arbitrary. The number of neighbouring A molecules that contribute significantly to the matrix element will depend on the details of the crystal structure, but because the two $\mathbf{k} = 0$ states are initially degenerate, the resonance interaction causes them to mix, just as for two isolated molecules; and the intensity may all attach to the lower state, or all to the upper state, or be divided between them, again just as for two isolated molecules. The delocalized excitation represented by eqns (11.1.7) is called an *exciton*, and the splitting between the states is an *exciton splitting*.

11.1.2 Excimers

One of the most interesting consequences of the resonance interaction is the formation of dimers in which one of the molecules is excited. Because of the resonance interaction such an excited dimer, or *excimer*, may be much more firmly bound than when both molecules are in their ground state. Indeed the ground-state molecules may not form a stable complex at all. Excimers were first observed by Forster and Kasper (1955) in solutions of pyrene in benzene. Here the fluorescence spectrum at low concentration (2×10^{-4} M) shows the emission from the isolated molecule, with peaks at 3725 Å, 3840 Å and 3920 Å. As the concentration is increased, a broader emission band appears at about 4780 Å; this is due to emission from the red-shifted state of the excimer. At a concentration of 2×10^{-2} M the monomer fluorescence virtually disappears, leaving only the excimer fluorescence.

However, the most important application is in the excimer laser (Milonni and Eberly 1988). In the xenon excimer laser, for example, some of the atoms in xenon gas at high pressure are excited by a pulsed electron beam, and combine with ground-state atoms to form $Xe\cdots Xe^*$ excimers. They are quite strongly bound, and persist in the gas for some time. When a radiative transition to the ground state occurs, the repulsive form of the ground-state potential curve ensures that the dimer immediately falls apart. (See Fig. 11.2.) This means that a population inversion can easily be maintained, and laser action can occur; also, because there are no well-defined vibration–rotation states on the repulsive potential-energy surface, the radiation is broad-band and can be tuned.

11.2 Distributed transition moments

In deriving the expression for the matrix elements between the exciton states, we used the multipole expansion of the interaction and truncated it at the dipole–dipole term. We have seen enough to suggest that such a treatment may be invalid when the molecules are as close together as they are in an excimer or a crystal. It is likely that the multipole expansion will fail to converge, especially when large molecules are involved.

An example is the 'special pair' that forms a component of chlorophyll and related molecules. This essentially comprises two bacteriochlorophyll units, each of which has a conjugated system of the form shown in Fig. 11.3 (M = Mg). The precise geometry varies, as indeed does the detailed molecular structure, but usually the two units are stacked one above the other with

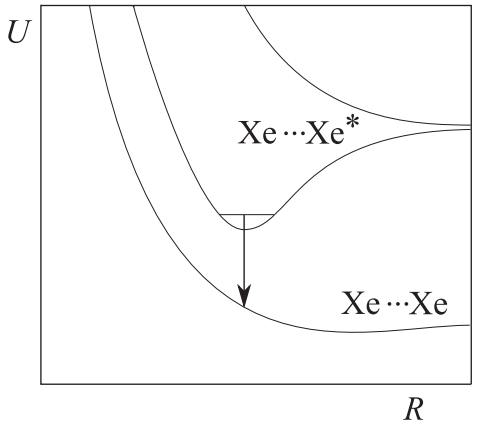

Fig. 11.2 Potential curves for Xe···Xe and Xe···Xe* (schematic).

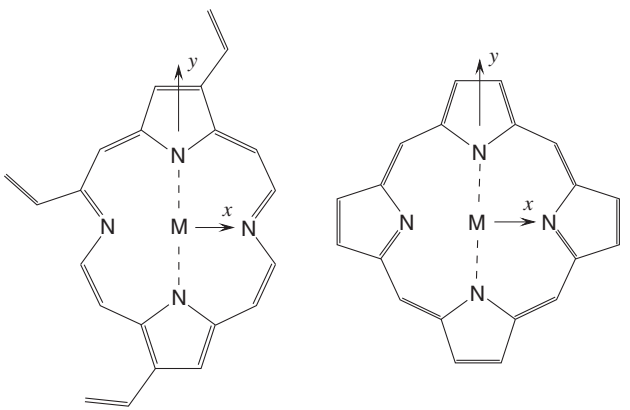

Fig. 11.3 Structure of bacteriochlorophyll (left) and porphin (right).

their planes approximately parallel and approximately 3.5 Å apart, and they are offset by about 7 Å in the *y* direction (see Fig. 11.3), so that the centre of one molecule is approximately above a pyrrole ring of the other (Warshel and Parson 1987). The bacteriochlorophyll molecule is some 12 Å across, compared with the separation between centres of about 8 Å, so this is a case where the multipole expansion cannot be expected to converge and the dipole–dipole model of the resonance interaction will give poor results.

A similar situation arises in some model compounds designed to mimic the special pair (Leighton *et al.* 1988). They comprise two porphin units (Fig. 11.3, either with M = Zn or with M = −H···H−, i.e., the free base) joined by flexible linking side-chains. In these compounds the porphin units are parallel, and offset in the *y* direction relative to each other by a distance of the order of 3.5 Å. (This is an example of a structure that is successfully predicted as a consequence of the electrostatic interaction, provided that a distributed-multipole model is used (Hunter 1994).) A more rigid structure can be made using the bifunctional ligand $N(CH_2CH_2)_3N$, which binds to the two Zn atoms. In this way the two porphin units are held

parallel to each other, with the two Zn atoms directly over each other (Hunter *et al.* 1989) and 7 Å apart. There is a $\pi - \pi^*$ transition, the Soret band, at 415 nm in the isolated porphin molecule; in the complex it is blue-shifted to 409 nm. As the transition dipole lies in the plane of the molecule, we have case (*b*) of Fig. 11.1, and the red-shifted band is forbidden. In this case the porphin planes are 7 Å apart, but this is still small compared with the molecular size, so again we cannot use the dipole–dipole model. Instead we can use a distributed multipole model, as follows.

The transition of interest is a $\pi \leftrightarrow \pi^*$ transition. We can write the two orbitals as

$$\psi_0 = \sum c_i^0 \varphi_i, \qquad \psi_1 = \sum c_i^1 \varphi_i, \tag{11.2.1}$$

where the φ_i are p_π orbitals on the atoms of the conjugated system, and the c_i^k are molecular orbital coefficients. We need the matrix element

$$\langle \psi_1^A \psi_0^B | \mathcal{H}' | \psi_0^A \psi_1^B \rangle = \langle \psi_1^A \psi_0^B | \sum_{a\in A} \sum_{b\in B} (T^{ab} \hat{q}^a \hat{q}^b - T_\alpha^{ab} (\hat{q}^a \hat{\mu}_\alpha^b - \hat{\mu}_\alpha^a \hat{q}^b) - \cdots | \psi_0^A \psi_1^B \rangle. \tag{11.2.2}$$

Here we are using a distributed-multipole expression for the interaction operator. The summation runs, as usual, over the sites a of molecule A and the sites b of molecule B. In view of the form of the wavefunction it is natural to choose these sites to be at the atoms involved in the π system. Then the matrix element of one of the distributed charge operators is

$$\langle \psi_1^A | \hat{q}^a | \psi_0^A \rangle = \sum_{ii'} \langle c_i^1 \varphi_i | \hat{q}^a | c_{i'}^0 \varphi_{i'} \rangle = -c_a^1 c_a^0, \tag{11.2.3}$$

because only the atomic orbital on atom a contributes to the matrix element of $\hat{q}^a$ (if we ignore overlap) and it is normalized to 1. The minus sign takes account of the negative charge on the electron. Similarly,

$$\langle \psi_1^A | \hat{\mu}_\alpha^a | \psi_0^A \rangle = \sum_{ii'} \langle c_i^1 \varphi_i | \hat{\mu}_\alpha^a | c_{i'}^0 \varphi_{i'} \rangle = 0, \tag{11.2.4}$$

since the π-orbital distribution has zero dipole moment relative to an origin at the nucleus. There would be a non-zero quadrupole term but we neglect it. Thus (11.2.2) becomes

$$\langle \psi_1^A \psi_0^B | \mathcal{H}' | \psi_0^A \psi_1^B \rangle = \sum_{a\in A} \sum_{b\in B} c_a^1 c_a^0 c_b^1 c_b^0 / 4\pi\epsilon_0 R_{ab}. \tag{11.2.5}$$

If we know the geometry of the complex and the wavefunctions, this is easily evaluated. For most purposes a Hückel or Pariser–Parr–Pople treatment of the π orbitals is adequate, but the method is readily extended to more accurate wavefunctions.

In the case of the rigid porphin dimer complex, the point-dipole treatment, using the observed intensity to determine the magnitude of the transition dipole, predicts an exciton shift of −19 nm for the Soret band, whereas the distributed-monopole treatment, again scaled according to the observed intensity, predicts a shift of −6 nm, in exact agreement with experiment.

11.3 Interactions involving open-shell systems

Many molecules occurring in gas-phase reactions have unpaired electrons. They are said to be in *open-shell* states, as compared with most molecules, in which each orbital contains a

pair of electrons, one with α and one with β spin, giving a *closed-shell* configuration with total spin zero—a singlet state. The most common open-shell molecule is O_2, which has two antibonding π orbitals each containing one electron, giving total spin $S = 1$, a triplet state with term symbol $^3\Sigma_g^-$. The spins on a pair of neighbouring molecules couple to give overall spin of 0, 1 or 2, and for each of these there is a potential energy surface that depends on the relative positions and orientations of the molecules. In the case of $S = 1$ or 2 there is a small splitting of the potential energy surface due to spin-orbit coupling. The interaction between O_2 molecules was first explored by van Hemert *et al.* (1983) and Wormer and van der Avoird (1984), who showed that the Heisenberg Hamiltonian $\mathcal{H} = -2J_{AB}S_A \cdot S_B$ gave a good qualitative account of the interaction, where J_{AB} depends on the relative configuration. No new terms arise, apart from the small spin-orbit couplings: the interaction is described by the normal first-order exchange term, though the calculation is more complicated than usual. Accurate calculations are relatively straightforward for the quintet state, $S = 2$, because it is well described by a single configuration, and Bartolomei *et al.* (2008) found that the most satisfactory treatment was to use CCSD(T) to calculate the quintet potential energy surface, and to calculate the singlet–quintet and triplet–quintet differences separately.

The $O_2 \cdots O_2$ system is unusual in having four open-shell electrons. A more common case comprises a molecule with a single unpaired electron interacting with a closed-shell molecule. Zuchowski *et al.* (2008) have shown that SAPT-DFT can be used in such cases, and also where both fragments have one unpaired spin and the complex has $S = 1$. The principles of SAPT-DFT are the same as in the closed-shell case, but the computer programs have to be modified to handle the open-shell case.

Where there is orbital degeneracy as well as spin degeneracy in one of the components of the complex, the degeneracy is lifted by the interaction. Wormer *et al.* (2005) studied the complex between HCl and OH ($^2\Pi$), and found that the interaction could be well described by a multipole expansion. However, in addition to the ordinary multipole moments, there are matrix elements of the multipole moment operators between the states of the OH radical with orbital angular momentum $\Lambda = 1$ and $\Lambda = -1$, leading to splittings between the two potential energy surfaces.

12
Practical Models for Intermolecular Potentials

The computation of the interaction energy *ab initio* is very time-consuming, whether it is done by perturbation theory or the supermolecule method, and it is impractical in many applications. In molecular dynamics, for instance, it is necessary to calculate the forces and torques on all the molecules in an assembly of several hundred or more, in order to obtain the equations of motion, and this has to be repeated for each step in the simulation, which typically requires millions of steps. For this sort of problem, we usually need to use much simpler models of the interaction. For the most basic properties of condensed phases, it is sufficient to use extremely simple models—for example, the hard-sphere model provided much useful information about the behaviour of inert-gas liquids—but if we want more detailed information, we have to use better models.

Potential models are of two kinds. One kind is a simplification of the *ab initio* approach; the potential is still computed from first principles, but approximations are made in order to make the calculation more tractable. In a sense all *ab initio* calculations fall into this category, since it is virtually never possible to perform the calculation exactly; but one can distinguish between true *ab initio* calculations, where it is possible to identify a path towards better and eventually arbitrarily accurate calculations, and a model in which an approximation is imposed that offers no hope of improvement but is merely a more or less accurate prescription. One such model is the 'exchange-Coulomb' or XC model (discussed in more detail below) which makes use of the empirical observation that for inert gas atoms the repulsion (exchange) energy E_X is closely related to the electrostatic penetration (Coulomb) energy E_C: $E_X = -\gamma(1 + aR)E_C$, where a and γ are empirical constants. This relationship is quite successful in many cases, but no-one supposes that it is exact, or that it could be developed towards a relationship that would reliably yield exact values of E_X while avoiding computational effort. Its usefulness lies in the fact that E_X, which is time-consuming to calculate, can be determined reasonably accurately in terms of E_C, which can be calculated much more easily.

The other kind of model is more empirical: a suitable function, of a relatively simple form, is proposed to describe the interaction, and the parameters in the model are fitted to experimental data or to accurate calculations. In practice, a combined approach is often used. The HFD or Hartree–Fock–dispersion model, for example, uses an approximate *ab initio* treatment, namely an SCF supermolecule calculation, and corrects for the worst deficiency of such a calculation—the fact that it includes no correlation and therefore no dispersion—by adding an empirical dispersion term. This again is quite successful in some cases, but it is intrinsically limited in accuracy, however good the SCF calculation and the dispersion model may be, because its success depends crucially on the assumption, not always valid, that other correlation

effects may be neglected. The modern and much more successful variant of this method is the DFT-D method described in §5.7, where a dispersion term is added to density-functional-theory energies. This procedure includes correlation effects, but the 'dispersion' term is used to correct for other deficiencies of the functional as well as the lack of dispersion, so its form and parametrization is different for different functionals. The latest version is very accurate, but although it is much cheaper in computational resources than the best *ab initio* methods it is still expensive.

Empirical models can be further subdivided. Some seek to describe a particular system, and are intended for use in calculations on that system alone. Such models can be as complicated as is necessary to describe the potential, subject to constraints imposed by the computation in which they are to be used. Indeed those constraints may determine the form of the potential; for example, calculations of the scattering of an atom with a diatomic are most easily carried out if the potential is a spherical-harmonic expansion:

$$U(R,\theta) = \sum_{k=0}^{n} V_k(R) P_k(\cos\theta)$$

and this is then a natural way to express the potential, though it does not provide any separation into contributions such as dispersion and repulsion.

Other kinds of model are intended for use with a whole set of systems, with their parameters very often determined from properties of a subset. In particular one often wishes to determine potentials for mixed ($A\cdots B$) interactions from properties of pure substances only, which in principle lead only to information about interactions between like molecules. Models of this kind need to be simpler in form, and are more usefully composed of identifiable terms such as dispersion, repulsion and so on. The reason for this is that the derivation of potentials for mixed systems is often based on 'combining rules', and these are more successful if they can be closely based on fundamental theory. We have seen, for instance, that the geometric-mean combining rule for C_6 dispersion coefficients is derived directly from the London formula for the dispersion energy. The determination of accurate dispersion coefficients for mixed systems via dipole oscillator strength distributions (DOSDs) for the individual molecules, described in §13.1.2, can be thought of as a rather refined combination rule, though it differs from most combining rules in being exact in principle. Neither approach is useful if a potential model is used in which the dispersion energy is not clearly distinguishable from the rest of the model.

In the following sections we explore models in more detail, first for atoms and then for molecules.

12.1 Potentials for atoms

12.1.1 Hard-sphere atoms

In this approach, each atom is treated as an impenetrable hard sphere, so that the potential is infinite if atoms overlap, and zero otherwise. The radius of the sphere is usually a standard Van der Waals radius, taken from Pauling (1960), Bondi (1964) or Mantina *et al.* (2009). This is a very simple treatment of the repulsion, but it is sufficient, as remarked above, to account for some of the properties of inert gas fluids, such as some of their transport properties. When applied to molecules, it is enough to account for the structures of a wide range of Van der Waals complexes when combined with an accurate electrostatic description, as we saw in

§8.4.1 (Buckingham and Fowler 1983, 1985). Of course it has no predictive value whatever in terms of intermolecular separations, and it is successful in structural predictions for these complexes only because the structure is usually much more sensitive to the angular behaviour of the electrostatic interaction than to the precise interatomic separations. As a part of such models the hard-sphere repulsion still has a limited but useful contribution to make; it has the merit that it requires only one parameter, the atomic radius, that is readily and directly determinable from crystal-structure data. It has the obvious limitation that atoms in molecules are neither hard nor spheres.

12.1.2 Lennard-Jones potentials

The Lennard-Jones potential, first proposed in 1906 by Mie and adopted by Lennard-Jones in the early 1920s, has a repulsive term A/R^n and an attractive term $-B/R^m$, with $n > m$. Following London's work on dispersion forces it became usual to set $m = 6$, and although several values of n have been used, the most common choice is $n = 12$, which is computationally convenient and reasonably successful. The Lennard-Jones potential then takes the form

$$U_{\mathrm{LJ}} = 4\epsilon\Big(\frac{\sigma^{12}}{R^{12}} - \frac{\sigma^6}{R^6}\Big) = \epsilon\Big(\frac{R_m^{12}}{R^{12}} - \frac{2R_m^6}{R^6}\Big), \tag{12.1.1}$$

where ϵ is the depth of the well and R_m the position of the minimum. $\sigma = 2^{-1/6}R_m$ is the position where the repulsive branch crosses zero.

This potential has been remarkably successful, as is shown by its continued widespread use 90 years after Lennard-Jones first introduced it. The attractive term has a sound theoretical justification as the leading term in the R^{-1} expansion of the dispersion energy, though the value of $C_6 = 4\epsilon\sigma^6$ that is obtained by fitting ϵ and σ (or R_m) to experimental data is much too large, typically by a factor of about 2, compared with direct experimental or theoretical determination. This is in part because the Lennard-Jones potential contains no R^{-8} or R^{-10} terms, so the R^{-6} term has to be larger to compensate. The repulsive term, on the other hand, has no theoretical justification at all, beyond its steeply repulsive form.

When the atoms are different, it is common to use 'combining rules' to estimate the parameters, often using a geometric mean for ϵ (the 'Berthelot' rule) and an arithmetic mean for σ (the 'Lorentz' rule):

$$\epsilon_{ab} \approx (\epsilon_{aa}\epsilon_{bb})^{1/2}, \qquad \sigma_{ab} \approx \tfrac{1}{2}(\sigma_{aa} + \sigma_{bb}). \tag{12.1.2}$$

The theoretical basis for these rules is very flimsy. The Berthelot rule is known to overestimate the well depth. More elaborate rules have been proposed (see Maitland *et al.* (1981) for a discussion) but still with rather dubious justification. The main reason for the continued use of these combining rules is that experimental data sufficiently good to validate or falsify them are very difficult to obtain, and meanwhile some way of estimating the parameters in mixed systems is required.

We have seen that a geometric-mean combining rule for C_6 should be successful, so an alternative possibility would be to apply a geometric-mean combining rule to the R^{-6} coefficient, i.e. to $4\epsilon\sigma^6$, even though this is not a true C_6 but contains various other effects as well. Waldman and Hagler (1993) have shown that such a combining rule is successful for the inert gases, but only if it is used in conjunction with an arithmetic-mean combining rule for σ^6 rather than for σ itself.

12.1.3 Born–Mayer potential

Not long after the introduction of the Lennard-Jones potential, Born and Mayer (1932) suggested that the repulsion between atoms would have a roughly exponential dependence on distance, because of its relationship to the overlap between the wavefunctions:

$$U_{\mathrm{BM}} = A\mathrm{e}^{-BR}. \tag{12.1.3}$$

If this is combined with the London formula for the dispersion, we get the exp-6 potential:

$$U_{\mathrm{exp6}} = A\mathrm{e}^{-BR} - C/R^6. \tag{12.1.4}$$

A variant proposed by Buckingham and Corner (1947) has an R^{-8} dispersion term as well.

The exp-6 and Buckingham–Corner potentials have a deficiency which makes them unsuitable for some calculations: although the exponential term rises steeply as R decreases, it remains finite at $R = 0$, so the dispersion term dominates at very small R, and the potential reaches a maximum and then tends to $-\infty$ as $R \to 0$. This can be overcome by damping the dispersion term (see below) at the cost of complicating the form of the function. However, the main disincentive to its widespread use in the days of mechanical hand-operated calculating machines, and even with early computers, was the computational inconvenience of the exponential. For this reason the Lennard-Jones potential won an early popularity which it has still not lost in spite of its obvious deficiencies.

12.1.4 Accurate potentials for atoms

A great variety of empirical potential functions have been proposed, especially for the inert gases. Many of these have no particular basis in theory, but use mathematical devices such as spline functions to reproduce the experimental data as accurately as possible.

For the inert gases, especially argon, the experimental data are sufficiently diverse and reliable to characterize the potentials quite well. There is a wide range of potentials fitted to such data, such as the Barker–Fisher–Watts potential for argon (Barker *et al.* 1971):

$$U(R) = \exp[\alpha(1-\bar{R})]\sum_{k=0}^{5} A_k(\bar{R}-1)^k - \sum_{n=6,8,10} C_n/(\delta + \bar{R}^n), \tag{12.1.5}$$

where $\bar{R} = R/R_m$, R_m being the separation at the minimum, and δ is a small non-physical parameter introduced to suppress the spurious singularity that would otherwise arise at $R = 0$. A detailed account of such potentials has been given by Maitland *et al.* (1981), and since our interest is primarily in molecular potentials we shall not review them fully here. However, there are some general issues that are relevant to molecules as well as atoms.

Eqn (12.1.5) shares with many atom–atom potential models a separation of the interaction into a term of the form $\exp(-\alpha R)$ that can be loosely identified with the repulsion, and a series in inverse powers of R that describes the dispersion. The theory gives good grounds for separating the potential in this way. However, there is no clean separation between the terms when they are derived from experimental data—the distinction between repulsion and dispersion is a theoretical one, and they are not separately observable—and any deficiencies in one tend to be taken up by the other. Notice that the 'dispersion' part of eqn (12.1.5) is undamped (the parameter δ is too small to provide any real damping) so although the potential

must include dispersion damping in order to agree satisfactorily with the experimental data, it must here be contained in the 'repulsion' term. Whether or not this is viewed as a satisfactory way to treat the Ar···Ar interaction, it does not provide a useful starting point for constructing potentials for other systems. Other potentials that have been proposed for Ar···Ar are even less useful in this respect. A more robust strategy in the long term is to use functional forms for the terms in the potential that are as closely based on theory as practical constraints will allow.

12.1.5 Dispersion

We have seen that the dispersion term in a model potential must include a damping function to suppress the singularity as $R \to 0$. One function that has been proposed for this purpose is part of the Hartree–Fock–dispersion (HFD) model, proposed originally by Hepburn *et al.* (1975) and modified slightly by Ahlrichs *et al.* (1977). Here the interaction between two atoms is described by two terms: a Hartree–Fock part, obtained from a supermolecule SCF calculation, and a dispersion part, represented by a term of the form $-F(R)(C_6/R^6 + C_8/R^8 + C^{10}/R^{10})$. The damping function $F(R)$ is

$$F(R) = \begin{cases} \exp[-(1.28(R_m/R) - 1)^2], & R < 1.28R_m, \\ 1, & R > 1.28R_m. \end{cases} \tag{12.1.6}$$

This function was obtained by fitting to the dispersion interaction in the $b\ ^3\Sigma_u^+$ state of H_2, that is, to the dispersion interaction between two H atoms with parallel spins, which can be calculated accurately (Kołos and Wolniewicz 1974). (In the rest of this section we refer to this for brevity as the H···H interaction.) While it fits the calculated points quite well, its behaviour at $R = 0$ is unsatisfactory (it is non-analytic) and, more seriously, the same function is used for all the dispersion terms. The calculations of Kreek and Meath (1969) had already shown that different damping functions are needed for each term in the R^{-n} expansion.

A later version of the HFD model (Douketis *et al.* 1982) corrected this deficiency, writing the dispersion energy in the form

$$U_{\text{disp}} = -\sum_{n=6,8,10} F_n(R)\frac{C_n}{R^n}, \tag{12.1.7}$$

with

$$F_n(R) = g(\rho R) f_n(\rho R), \tag{12.1.8}$$

where f_n is supposed to be a universal damping function correcting for charge-overlap effects (penetration) in the R^{-n} term, g is a universal function correcting for exchange effects in all the dispersion terms, and ρ is a distance scaling factor. These functions, like the earlier one, were found by an empirical fit to the damping functions calculated by Kreek and Meath (1969) for the H···H dispersion interaction, where $\rho = 1$ by definition, and are

$$g(R) = 1 - R^{1.68}\exp(-0.78R),$$
$$f_n(R) = [1 - \exp(-2.1R/n - 0.109R^2/n^{1/2})]^n.$$

Table 12.1 Coefficients for Koide–Meath–Allnatt damping functions, with C_n coefficients for H···H.

n	a_n/a_0^{-1}	$10b_n/a_0^{-2}$	$10^3 d_n/a_0^{-3}$	C_n/ a.u.	$\lim_{R\to 0} f_n C_n R^{-n}$
6	0.3648	0.3360	1.651	6.499	0.0153
8	0.3073	0.2469	1.227	124.399	0.0099
10	0.2514	0.2379	0.5664	3285.8	0.0033
12	0.2197	0.4168	0.4168	121486.0	0.0015

Another form of damping function was proposed by Koide *et al.* (1981), who recalculated the accurate damping functions for the H···H dispersion interaction and fitted them to the form

$$f_n^0(R) = [1 - \exp(-a_n R - b_n R^2 - d_n R^3)]^n. \tag{12.1.9}$$

The coefficients in these functions, for $n \leq 12$, are listed in Table 12.1; the paper gives coefficients for n up to 20.

However, the most widely used damping functions by far are those proposed by Tang and Toennies (1984) and shown in Fig. 12.1. The C_n/R^n term was replaced as usual by $f_n(R)C_n/R^n$, and f_n was required to tend to 1 for large R and to zero as $R \to 0$. Tang and Toennies further assumed that $f_n(R) - 1$ has the form of a polynomial multiplied by a decaying exponential (an assumption based on the form of the exchange correction to the dispersion for the H···H system) and were led to the conclusion that $f_n(R)$ is an incomplete gamma function of order $n + 1$:

$$f_n(R) = P(n + 1, bR) = 1 - \exp(-bR) \sum_{k=0}^{n} \frac{(bR)^k}{k!}. \tag{12.1.10}$$

Here b is a distance scaling factor, usually taken to be the same as the parameter B in the Born–Mayer repulsion, on the grounds that both the repulsion and the dispersion damping are consequences of wavefunction overlap. Although f_n behaves like R^{n+1} at small R, so that it has the effect of suppressing the dispersion entirely at $R = 0$ rather than making it tend to the

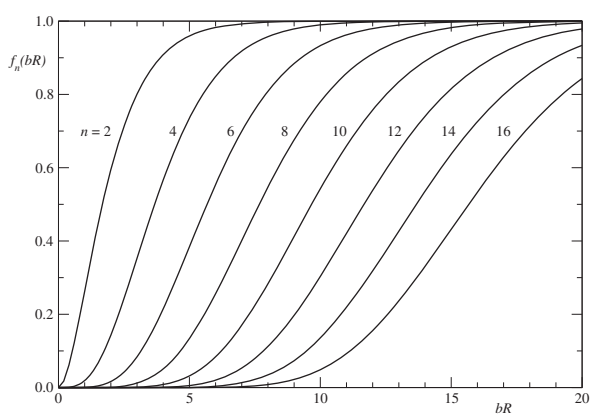

Fig. 12.1 Tang–Toennies damping functions $f_n(bR)$ for $n = 2, 4, \ldots, 16$.

appropriate part of the united-atom correlation energy, this is a trivial flaw by comparison with errors in other potential terms at very small R. The Tang–Toennies functions have the merit of using no adjustable parameters, if the parameter b is taken from the repulsion term, and only one if it is fitted to the data.

These damping functions, being all derived from the H···H potential, are all rather similar. It was assumed from the outset that they are 'universal' damping functions and can be transferred to other systems simply by scaling the distance. Douketis *et al.* (1982) acknowledged that this assumption is 'difficult, and perhaps impossible, to justify rigorously'. They remark that the accuracy of the Law of Corresponding States makes the assumption seem plausible, and indeed the reduced potential curves $U(R)/U(R_m)$ *vs.* R/R_m for the H···H interaction and the most reliable inert-gas potentials (Aziz 1984) are very similar. The damping functions also have a very similar R dependence to the *ab initio* damping functions determined by Knowles and Meath (1986*a*,*b*, 1987) from the ratio of the non-expanded dispersion terms to the C_n/R^n formula. The Tang–Toennies damping functions shown in Fig. 12.1 may be compared with the Knowles–Meath *ab initio* damping functions for Ar···Ar, shown in Fig. 8.2. Wheatley and Meath (1993*a*) also found that damping functions for other systems can be obtained by scaling the H···H functions of Koide *et al.* (1981):

$$f_n^{\mathrm{AB}}(R) = f_n^{\mathrm{HH}}(S^{AB}R),$$

where S^{AB} is a suitable scaling factor for the $A\cdots B$ interaction. The *ab initio* calculations use time-dependent coupled Hartree–Fock (TDCHF) perturbation theory in the polarization approximation, so they include penetration (charge-overlap) effects but not exchange. The original H···H calculations, on the other hand, are essentially exact within the non-relativistic Born–Oppenheimer model.

The various HFD-type models that have been proposed for inert-gas atoms all represent the interaction as the sum of a repulsive part and an attractive (dispersion) part, but they differ in the description of the repulsive part of the potential, so that the attractive part necessarily differs also. For example, the factor $g(\rho R)$ that appears in eqn (12.1.8) describes exchange-correlation effects, but these may in other models be regarded as part of the repulsive term. Such differences between the models have been discussed in detail by Meath and Koulis (1991), who remark that it is consequently inappropriate to use a damping function designed for one model in a different context.

12.1.6 Repulsion

The near linearity of the semi-log plots of Fig. 8.1 shows that the simple exponential (Born–Mayer) form provides a remarkably accurate description of the repulsion at moderate energies. The HFD model in its simplest form uses a Born–Mayer repulsion fitted to the SCF energy, together with a damped dispersion term of the form discussed in the previous section. A variant uses the form $A\exp[-\alpha R-\beta R^2]$ to describe the repulsion; the parameter β is quite small. See, for example, Dham *et al.* (1989).

The exchange-Coulomb (XC) repulsion model for inert-gas dimers is based on the idea that the repulsion (exchange) energy and the electrostatic (Coulomb) energy are closely related in such systems (Ng *et al.* 1979, Meath and Koulis 1991). The long-range electrostatic energy (the multipole expansion) is zero in such cases, and the first-order electrostatic energy E_C arises purely from penetration (see §8.1). The XC model uses the semi-empirical relationship

$$E_X = -\gamma(1 + aR)E_C, \tag{12.1.11}$$

where a and γ are parameters. The Coulomb energy is evaluated as an integral over the charge densities: $E_C = \int \rho^A(\mathbf{r}_1) r_{12}^{-1} \rho^B(\mathbf{r}_2)\ \mathrm{d}r_1\ \mathrm{d}r_2$, using accurate *ab initio* (SCF) charge densities for the atoms, and fitted to a function of the form

$$E_C = -\exp[a_0 R + a_1 + a_2 R^{-1} + a_3 R^{-2}]. \tag{12.1.12}$$

This then gives a quite elaborate expression for the repulsion energy, which is quite satisfactory for the case to which it is fitted, and which describes the short-range, high-energy part of the potential curve where the simple Born–Mayer form is inadequate (Dham *et al.* 1989). It can be extended to other systems quite easily, because it starts from the monomer charge density, which is relatively easy to calculate accurately, and the calculation of the Coulomb integral is not very time-consuming.

A further model of this type is the Tang–Toennies one, which is simpler in form, using a plain Born–Mayer repulsion together with a damped dispersion with damping functions that are incomplete gamma functions, as described above:

$$U_{\mathrm{TT}} = A \exp(-bR) - \sum_{k=3}^{K} f_{2k}(bR) C_{2k} / R^{2k}. \tag{12.1.13}$$

As originally formulated, the repulsion term was fitted to SCF *ab initio* data, but if A and b are determined by fitting to the accurate potentials available for systems such as Ar_2, somewhat larger values of A are found, though the values of b do not change much. This is consistent with the observation from *ab initio* perturbation theory that the inclusion of correlation effects increases the magnitude of the repulsion by a ratio that is more or less independent of distance.

12.1.7 Induction

For neutral atoms, induction plays a very minor role. It is zero in the long-range approximation, because no atom provides an electric field to polarize any other. When the atoms overlap, there are penetration and exchange induction contributions, but these can be absorbed into the exchange–repulsion model. However, atomic ions have large electric fields, and in ionic fluids it is essential to take account of induction.

Just as point-charge models have long been used to give a simple description of the charge distribution, simplified models of polarization have also been used. Probably the simplest of such treatments is the 'shell model' of Dick and Overhauser (1958) and Cochran (1959). In this approach, widely used to describe ions in solids, the valence electrons are viewed as a charged massless spherical shell (equivalent for the purposes of electrostatic interactions to a point charge at the centre of the shell) and the core of the atom or ion is treated as another point charge. The two charges, the shell and the core, are taken to be attached to each other by a harmonic 'spring'. In a uniform electric field, the negatively charged shell moves in one direction and the positively charged core in the other, producing a dipole whose magnitude depends on the strength of the spring. It is a simple matter to choose the spring constant so as to reproduce the dipole polarizability of the ion. The mass of the ion is attributed to the positive core, and the shell carries the repulsive interactions.

This model has been extensively used for modelling ionic solids, where it is reasonably successful. For example, the SYMLAT program (Leslie 1983) uses an ionic model that includes the shell–model description of polarization. Freyriafava *et al.* (1993) found that it agreed well with Hartree–Fock calculations on defects in MgO. The shell model accounts only for dipole polarization, and the Hartree–Fock calculations also showed evidence of quadrupolar polarization and spherical 'breathing' distortions of the oxide anions, but their effects appeared to be unimportant in this case. Whether this was fortuitous or not could not be determined.

The shell model has not been found useful in calculations on molecules, and where induction is too important to ignore it is usual to include the dipole–dipole polarizability explicitly. In this case it is necessary to solve eqn (9.4.12) iteratively, which is time-consuming. A rather different approach was used by Sprik and Klein (1988) in a polarizable model of water. The polarizability was represented using a tetrahedral array of four sites, with the centre of the tetrahedron on the bisector of the HOH angle, 0.6 Å from the O atom. Two of the sites were in the plane of the molecule, displaced in the general direction of the H atoms, and the other two were out of plane, displaced in the 'lone-pair' directions. In this case, the magnitude of the charges, rather than their positions, change in response to an electric field, so this is a distributed-polarizability model, limited to charge flows. The merit of this formulation is that it is easy to describe the induction by adding a suitable term to the Lagrangian for the system, which in turn makes it easy to write down the classical equations of motion of a system containing a number of such water molecules. Wilson and Madden (1994) used a similar approach in their work on the alkaline-earth halides (§10.1). By treating the charges as extended gaussian charge distributions rather than point charges, Sprik and Klein also introduced damping into the model.

12.2 Model potentials for molecules

As in the treatment of purely electrostatic interactions, it is possible to view each molecule as a unit, with a single interaction centre, or to regard the interactions as distributed over the molecule. For brevity we call the former treatment a 'molecule–molecule' description, and the latter an 'atom–atom' or 'site–site' treatment. We may expect that, as for electrostatic interactions, a molecule–molecule description will suffice for small molecules but will become unsatisfactory for larger ones.

A natural way to obtain a molecule–molecule description is to allow the parameters in a potential for atoms to become functions of the relative molecular orientation. For instance, an extension of the hard-sphere model to molecules was proposed by Kihara (1978), who treated a molecule as a convex hard solid—an ellipsoid, spherocylinder, disc or other shape. He was able to gain a useful understanding of the packing of molecules in crystals using mechanical models of this kind, but the approach has not been much used in calculations because it is difficult to manipulate mathematically.

Corner (1948) seems to have been the first to suggest using a variant of the Lennard-Jones potential in which the well depth ϵ and the range parameter σ or R_m are allowed to vary with orientation. In the gaussian overlap model (GOM) of Berne and Pechukas (1972), the form of the angle-dependence of ϵ and R_m is taken from the expression for the overlap integral of two ellipsoidal gaussian charge distributions. This model has been widely used to explore the generic properties of liquid crystals, where the molecules can be approximated as ellipsoids,

but its only merit for real molecules is its mathematical convenience. Pack (1978) explored potentials for Ar···CO_2 in which $\epsilon = \epsilon_0(1 + aP_2(\cos\theta))$ and $R_m = R_0(1 + bP_2(\cos\theta))$, where P_2 is a Legendre polynomial and θ is the angle between the C···Ar direction and the OCO axis (see Fig. 1.3), and he was able to understand some of the features of Ar···CO_2 scattering using these potentials. A similar approach has been used to describe the interaction between inert gases and SF_6 (Pack *et al.* 1982, 1984).

The Lennard-Jones potential is not a very good model for atoms, so this is not a very promising strategy for molecules if accurate potentials are needed. The exp-6 model should be better. Moreover, molecules differ from atoms in having non-zero multipole moments, so it becomes necessary to include electrostatic interactions; and even if one of the components is an inert gas, there will be an induction energy term, which may be important if the other component is strongly polar. This line of argument leads to the type of model that has been used extensively, for example by Hutson (1989*a*, 1989*b*), to describe the potentials for complexes between hydrogen halides and inert gases. These potentials take the form

$$U(R,\theta) = A(\theta)\exp[-\beta(\theta)R] + U_{\rm ind} + \sum_{n=6,7,8} f_n(R)C_n(\theta)/R^n, \tag{12.2.1}$$

where the induction energy expression is the ordinary multipole expansion up to terms in R^{-7}. Such potentials have been very successful in accounting for the spectra of small Van der Waals complexes, where the molecules are nearly spherical. We shall return to this theme in Chapter 13.

12.2.1 Atom–atom potentials: repulsion and dispersion

For all but the smallest molecules, repulsion and dispersion are usually treated in atom–atom form. A Lennard-Jones atom–atom potential, for example, would take the form

$$U_{\rm LJ} = \sum_{a\in A}\sum_{b\in B} 4\epsilon_{ab}\left(\frac{\sigma_{ab}^{12}}{R_{ab}^{12}} - \frac{\sigma_{ab}^{6}}{R_{ab}^{6}}\right), \tag{12.2.2}$$

where the sum is over the atoms of each molecule, and ϵ_{ab} and σ_{ab} are suitable parameters for atoms of types a and b. Similarly, an exp-6 atom–atom potential takes the form

$$\begin{aligned} U_{\exp 6} &= \sum_{a\in A}\sum_{b\in B} A^{ab}\exp(-B^{ab}R_{ab}) - \frac{C_6^{ab}}{R_{ab}^6} \\ &= \sum_{a\in A}\sum_{b\in B} K\exp(-\alpha^{ab}(R_{ab}-\rho^{ab})) - \frac{C_6^{ab}}{R_{ab}^6}. \end{aligned} \tag{12.2.3}$$

The Born–Mayer parameters A^{ab} and B^{ab} describing the repulsive part of the exp-6 site–site interaction must not be confused with the labels A and B that we have been using throughout to label molecules. The alternative formulation shown in eqn (12.2.3) uses $\alpha^{ab} = B^{ab}$ and $\rho^{ab} = \ln(A^{ab}/K)/\alpha^{ab}$. Here K is not a parameter but a convenient energy unit, usually 10^{-3} hartree. This corresponds to a temperature of about 316 K, so is a suitable unit for potentials that are to be used to describe interactions occurring at ambient temperatures. ρ^{ab} is then the distance at which the repulsion energy of atoms a and b has a value equal to the constant K, which gives it a direct physical interpretation.

Table 12.2 Atom types for the Williams W99 force field.

H(1)	hydrogen in C–H group
H(2)	hydrogen in alcoholic group
H(3)	hydrogen in carboxyl group
H(4)	hydrogen in N–H group
C(4)	carbon bonded to four other atoms
C(3)	carbon bonded to three other atoms
C(2)	carbon bonded to two other atoms
N(1)	nitrogen with triple bond
N(2)	nitrogen with no bonded hydrogen (except triple bond)
N(3)	nitrogen with one bonded hydrogen
N(4)	nitrogen with two or more bonded hydrogens
O(1)	oxygen bonded to one other atom
O(2)	oxygen bonded to two other atoms

Table 12.3 Exp-6 parameters for the W99 force field (eqn (12.2.3) with $K = 10^{-3}$ hartree).

Atom type	C_6 a.u.	α a_0^{-1}	ρ a_0
H(1)	4.83	1.88	4.503
H(2)	0.00	1.88	2.614
H(3)	0.00	1.88	2.010
H(4)	0.00	1.88	3.012
C(4)	16.97	1.91	5.681
C(3)	29.52	1.91	6.059
C(2)	24.89	1.91	5.553
N(1)	24.41	1.84	5.707
N(2)	24.25	1.84	5.740
N(3)	41.22	1.84	6.082
N(4)	97.65	1.84	6.488
O(2)	22.30	2.10	5.533
O(1)	21.87	2.10	5.453

Williams (1965, 1967) derived atom–atom Born–Mayer parameters for H···H, C···H and C···C interactions from data on crystalline hydrocarbons, and a set covering a wider range of atom types was provided by Mirsky (1978). These have been superseded by a later set compiled by Williams (1999, 2001), known as the W99 force field, and intended to be used in conjunction with a point-charge description of the electrostatic interactions. Williams identified several different atom types for each element, as set out in Table 12.2. The parameter values are listed in Table 12.3. Parameters for mixed interactions are to be obtained using combining rules: the geometric mean for C_6, the arithmetic mean for B (α) and the geometric mean for A, equivalent to the arithmetic mean for $\alpha\rho$.

An alternative set has been assembled by Filippini and Gavezzotti (1993). This is intended for use in predicting crystal structures, but is designed for use on its own, i.e., without any electrostatic terms in the potential, and is inappropriate for use when the electrostatic effects are included explicitly. The same is true of the exp-6 potentials proposed to describe hydrogen bonding (Gavezzotti and Filippini 1994).

Such models treat the atoms as spherical, and there is now extensive evidence that the isotropic-atom approximation is inadequate in some cases, and can give qualitatively incorrect results. Probably the most direct evidence is the paper by Nyburg and Faerman (1985), which was based on distances of closest approach between atoms in a very large number of crystal structures. These showed, for instance, that iodine atoms in molecules containing C–I bonds were about 0.7 Å closer in the crystal if they were in end-on contact (C–I···I–C) than if they approached side-on. More evidence comes from the crystal structure of Cl_2. Many attempts to account for this structure using simple potentials with spherical atoms failed, predicting a cubic *Pa*3 structure instead of the observed *Cmca* structure, and the only simple model to account satisfactorily for the observed structure is one in which the Cl atoms are assumed to be slightly non-spherical, being some 5% larger in the direction perpendicular to the Cl–Cl bond than parallel to it (Price and Stone 1982). This model was also very successful in accounting for the properties of liquid Cl_2, and a similar model gave a good account of liquid and solid Br_2 and I_2 (Rodger *et al.* 1988*a*,*b*).

The anisotropy of the repulsion can be determined by *ab initio* calculation, using one of the perturbation methods described in Chapter 6, and fitted to a suitable analytic function for use in other applications. One possibility is to make the parameters of the Born–Mayer potential depend on orientation:

$$U(R,\Omega) = A(\Omega)\exp(-B(\Omega)R). \tag{12.2.4}$$

(Here and subsequently we use Ω to stand for the relative orientation of the molecules, however we choose to describe it. See the discussion of coordinate systems in §1.4.) Consider the behaviour of B. It appears to describe the range of the potential, but if we evaluate the radial force we find that $-\partial U/\partial R = BA\exp(-BR) = BU$. Thus for a particular value of the repulsion energy U, the repulsive force is proportional to B, which therefore describes the steepness or hardness of the potential. This means that the molecular shape has to be described by $A(\Omega)$. The usual way to do this would be to expand $A(\Omega)$ in terms of spherical harmonic functions of the angular coordinates, but this leads to a very slowly convergent series, because the repulsion energy varies very sharply as a function of orientation and is not at all well described by a few terms of a spherical harmonic series.

These considerations led to the suggestion (Stone 1979, Price and Stone 1980) that the repulsive potential should take the form

$$\begin{aligned} U_{\rm rep}^{AB} &= \sum_{a\in A}\sum_{b\in B} U_{\rm rep}^{ab} \\ &= K\sum_{a\in A}\sum_{b\in B}\exp[-\alpha^{ab}(\Omega_{ab})(R_{ab}-\rho^{ab}(\Omega_{ab}))]. \end{aligned} \tag{12.2.5}$$

Here α^{ab} is the hardness parameter for the interaction between atoms a and b, and ρ^{ab} describes the shape. As before, K is not a parameter but a convenient energy unit, usually 10^{-3} hartree. Since $U_{ab} = K$ when $R_{ab} = \rho^{ab}(\Omega_{ab})$, the parameter ρ^{ab} describes the shape of the contour on which the repulsion energy between atoms a and b has a value equal to this energy unit.

The variation of atomic radius and hardness with orientation is quite small, even though it can be very significant in determining structures, and spherical-harmonic expansions of α and ρ can be expected to converge very quickly. The appropriate expansion functions are again the $\overline{S}$ functions:

$$\rho^{ab}(\Omega) = \sum_{l_a l_b j k_a k_b} \rho^{k_a k_b}_{l_a l_b j} \overline{S}^{k_a k_b}_{l_a l_b j},$$
$$\alpha^{ab}(\Omega) = \sum_{l_a l_b j k_a k_b} \alpha^{k_a k_b}_{l_a l_b j} \overline{S}^{k_a k_b}_{l_a l_b j}. \tag{12.2.6}$$

Often α^{ab} can be taken to be constant, so that all the anisotropy is contained in ρ^{ab}.

The $\overline{S}$ functions that can appear in this expression are restricted by the symmetry of the system, and the expansion converges rapidly, so that only a few terms are normally needed (Price and Stone 1982, Rodger *et al.* 1988*a*,*b*, Wheatley and Price 1990*b*, Day and Price 2003). However, the index j is not restricted to the value $l_a + l_b$, as it is for electrostatic interactions. One of the largest sets of $\rho^{k_a k_b}_{l_a l_b j}$ parameters has been fitted to the water dimer potential of Millot and Stone (1992). In that work a satisfactory fit was obtained using only $\overline{S}^{k0}_{l0l}$ or $\overline{S}^{0k}_{0ll}$ functions up to $l = 4$. Such functions have a particularly simple form. Consider $\overline{S}^{k0}_{l0l}$, and adopt a coordinate system that coincides with the local axes for site a. Then $\Omega_a = (0, 0, 0)$, so

$$\begin{aligned}
\overline{S}^{k0}_{l0l} &= \sum_{m_a m} \left[\begin{pmatrix} l & 0 & l \\ m_a & 0 & m \end{pmatrix} \Big/ \begin{pmatrix} l & 0 & l \\ 0 & 0 & 0 \end{pmatrix} \right] [D^{l_a}_{m_a k_a}(0,0,0)]^* [D^0_{00}(\Omega_2)]^* C_{lm}(\theta,\varphi) \\
&= \sum_{m_a m} (-1)^m \delta_{m_a,-m} \delta_{m_a,k_a} C_{jm}(\theta,\varphi) \\
&= (-1)^k C_{l,-k}(\theta,\varphi) \\
&= C_{l,k}(\theta,\varphi)^*.
\end{aligned} \tag{12.2.7}$$

If we express this in terms of the real components, using eqn (3.3.13), we find that

$$\overline{S}^{\kappa 0}_{l0l} = C_{l,\kappa}(\theta_a, \varphi_a),$$

where we have labelled the arguments of the spherical harmonic to emphasize that they are the polar coordinates describing the direction of the site–site vector in the local axis system of site a. In the same way,

$$\overline{S}^{0\kappa}_{0ll} = C_{l,\kappa}(\theta_b, \varphi_b),$$

where θ_b and φ_b here describe the direction of the vector to site a from site b in the local coordinate system of site b.

If ρ can be expressed purely in terms of these functions, then, it takes the form

$$\rho^{ab}(\Omega) = \rho^{ab}_{00} + \sum_{l>0} \sum_{\kappa} \rho^a_{l\kappa} C_{l,\kappa}(\theta_a, \varphi_a) + \sum_{l>0} \sum_{\kappa} \rho^b_{l\kappa} C_{l,\kappa}(\theta_b, \varphi_b),$$

and it is natural to express this as

$$\rho^{ab}(\Omega) = \rho^a(\theta_a, \varphi_a) + \rho^b(\theta_b, \varphi_b), \tag{12.2.8}$$

where

$$\rho^a = \sum_{l\kappa} \rho^a_{l\kappa} C_{l,\kappa}(\theta_a, \varphi_a),$$
$$\rho^b = \sum_{l\kappa} \rho^b_{l\kappa} C_{l,\kappa}(\theta_b, \varphi_b),$$

and $\rho^{ab}_{00} = \rho^a_{00} + \rho^b_{00}$. That is, there is a function ρ for each atom (or site) that describes its radius as a function of direction, and the parameter $\rho(\Omega)$ that appears in eqn (12.2.5) is then the sum of the radii of each site in the direction of the other. This is a very simple and physically appealing description, and offers obvious possibilities for transferable potentials, but it is important to remember that it is based on the approximation that only the $\overline{S}^{k0}_{l0l}$ or $\overline{S}^{0k}_{0ll}$ functions are needed in the expansion of $\rho(\Omega)$.

12.2.2 Approximate methods for determining repulsive potentials

One of the disadvantages of the anisotropic atom–atom model is that the parameters describing the orientation dependence of α and ρ have to be determined, usually by fitting to *ab initio* or experimental data. *Ab initio* calculations become expensive for large molecules at a reasonable level of accuracy, and have to be repeated at many different relative orientations to give an adequate coverage of the six-dimensional coordinate space. Methods that require less computational effort can therefore be very useful, even if less accurate. Three such methods are the exchange-Coulomb (XC) model, the test particle method and the density overlap model. The XC model has been discussed above, in the context of atoms. When it is applied to molecules, it is important to appreciate that the 'Coulomb' term is the electrostatic penetration energy, which depends on the overlap of the wavefunctions, and does not include the long-range part of the electrostatic energy, described by the multipole expansion. In fact, the only applications of the XC model to molecules (Wheatley and Meath 1993*b*) deal with cases where one component is an inert gas atom, so that the multipolar contribution to the electrostatic energy is zero. Even here, however, it is necessary to remove from the electrostatic interaction the repulsion between the nuclei, which becomes singular as their separation tends to zero. The uncorrected relationship (12.1.11) must break down in this limit because the exchange energy remains finite even when two nuclei are superimposed.

The test particle model is based on the assumption that in the exponential expression (12.2.5) for the repulsive potential, the effective diameter ρ can be expressed to a good approximation in the additive form (12.2.8), that is, $\rho^{ab} = \rho^a(\theta_a, \varphi_a) + \rho^b(\theta_b, \varphi_b)$. Since ρ^a describes the shape of atom a, it is natural to hope that it is a transferable quantity. If so, we can determine ρ^p for a spherical probe or test particle p, such as the He atom, by studying the $p\cdots p$ interaction, which depends only on the distance between the atoms. If the additive model is valid, then $\rho^{pp} = 2\rho^p$. Then an investigation of the $a\cdots p$ interaction provides $\rho^{ap} = \rho^a(\theta_a, \varphi_a) + \rho^p$, and hence $\rho^a(\theta_a, \varphi_a)$. This is much more efficient computationally than exploring the $a\cdots b$ interaction directly: in the general case that would require calculations over a six-dimensional space (one distance and five angles) whereas the probe calculation requires only three variables (a distance and two angles).

If this procedure is to work, we need to use a similar combining rule for the hardness parameter α. There are several possibilities, but the choice is not very critical because values of α fall in quite a narrow range—typically from 1.8 to 2.3 bohr^{-1}. Böhm and Ahlrichs

Table 12.4 Repulsion parameters $\eta = 1/\alpha$ and ρ for He, N_2, Cl_2, acetylene and H_2S. Values in atomic units (bohr).

Molecule:	He	N_2	Cl_2	HCCH	H_2S
Site:	He	N	Cl	C	S
η_{00}	0.21086	0.2433	0.2711	0.2748	0.3309
ρ_{00}	2.0817	2.955	3.427	3.415	3.998
ρ_{10}		−0.075	0.102	0.098	0.389
ρ_{20}		0.107	−0.227	0.185	−0.003
ρ_{22c}					0.012
ρ_{30}			−0.106	0.270	−0.184
ρ_{32c}					−0.469

(1982), using a nitrogen atom in its average-of-terms state as the probe, and Stone and Tong (1994), using a helium atom, found that the so-called 'energy-dependent hard-core model' was slightly more successful than other possibilities. This model is a simplification of the 'atomic distortion model' developed by Sikora (1970), in which the atoms are treated as classical deformable solids, and it leads to additivity for $\eta = 1/\alpha$: $\eta^{ab} = \eta^a + \eta^b$.

The choice of test particle is rather limited. Inert-gas atoms are obvious possibilities, together with other spherical atoms such as the N atom used by Böhm and Ahlrichs (1982), which is a spherical average of the terms arising from the ground $(2s)^2(2p)^3$ configuration. The merit of the He atom is that at the SCF level it has only one occupied molecular orbital, and since the repulsion is a first-order perturbation term, the virtual orbitals are irrelevant. Consequently the $1s$ orbital can be thoroughly optimized and the calculation carried out with a contracted basis comprising just this one basis function, greatly reducing the number of two-electron integrals needed in the calculation.

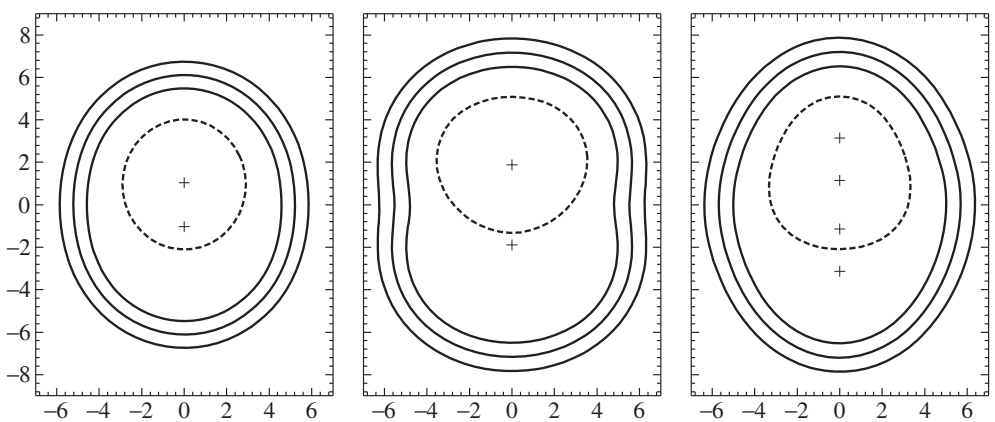

Fig. 12.2 Atom shapes. The continuous lines are contours of the $M\cdots$He repulsion energy for (left to right) $M = N_2$, Cl_2 and HCCH. The dashed lines show the site shape functions ρ^a for N, Cl and CH respectively. The scale is in bohr.

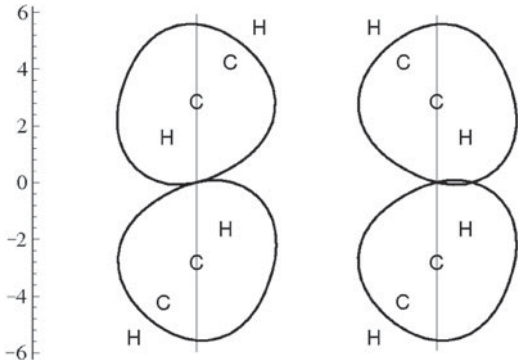

Fig. 12.3 When the site functions ρ^a and ρ^b are anisotropic, as illustrated here for the CH unit in acetylene, the point of contact may not be along the line from site to site, and a correction is needed to the formula $\rho^{ab} = \rho^a + \rho^b$. The scale is in bohr.

Calculations for N_2, Cl_2, acetylene and H_2S give the repulsion parameters shown in Table 12.4 (Stone and Tong 1994). For N_2, the repulsion energies derived from these agree very well with direct calculations of the dimer repulsion energy at mildly repulsive geometries (up to about $20\,\mathrm{kJ\,mol^{-1}}$), with an r.m.s. error in the energy of about $0.1\,\mathrm{kJ\,mol^{-1}}$. For the other molecules the agreement is not so good. The r.m.s. error in the distance at which the model matches the dimer calculation at a given orientation leads to similar conclusions: this error is about 0.02 bohr for N_2, but several times larger for the other molecules.

The reasons for this are interesting, as they highlight a fundamental limitation of the simple additive model, eqn (12.2.8). On this model, the parameters in Table 12.4 can be regarded as describing the shape of each site. Fig. 12.2 shows these shapes, as well as the contours of the repulsion between each molecule and a helium atom. We see that the N atom is nearly spherical according to this picture, but the Cl atom is distinctly non-spherical and the CH group in acetylene even more so. Now, if we allow two acetylene molecules to approach in a tilted geometry, the parameter ρ in the additive model depends only on the effective radius of each site in the direction of the other, and is the same for the orientation in Fig. 12.3a ($\varphi = 0°$) as for that in Fig. 12.3b ($\varphi = 180°$). The Figure shows that this is not correct; there should be a difference of about 0.2 bohr.

We have to conclude that although eqn (12.2.8) is a useful approximation, it will be inadequate in some cases. The problem can be avoided in the acetylene case by using separate sites for C and H, but it is unavoidable in the case of Cl and other halogen atoms.

In the density overlap model, some guidance on the form of the anisotropy in the repulsive potential is gained by a rather empirical route. It has been observed that the repulsion between pairs of inert-gas atoms is closely related to the overlap S_ρ between their charge densities. (Notice that this is a different quantity from the usual overlap between wavefunctions.)

$$U_{\mathrm{er}} \approx kS_\rho^\gamma, \qquad S_\rho = \int \rho^A(\mathbf{r})\rho^B(\mathbf{r})\,\mathrm{d}^3\mathbf{r}. \tag{12.2.9}$$

The value of γ was empirically found to be close to 1; it is typically between 0.96 and 0.99 (Kita *et al.* 1976, Kim *et al.* 1981). Wheatley and Price (1990*a*) found that this was true for

small molecules too. There are grounds for believing that for DFT densities calculated with asymptotic correction the exponent γ should be exactly 1 (Misquitta and Stone 2012). The charge density of each molecule can be expressed as a sum of densities for the atoms of the molecule:

$$\rho^A(\mathbf{r}) = \sum_{a\in A} \rho^a(\mathbf{r}), \tag{12.2.10}$$

and if $\gamma = 1$ the repulsion energy can be expressed as a sum of atom–atom terms. In the case of molecules the atom densities are anisotropic. Wheatley and Price were able to express the density overlap between two molecules as a sum of site–site terms, in the form

$$S_\rho = \sum_{a\in A}\sum_{b\in B} \exp(-\alpha^{ab} R_{ab}) \sum_{l_a l_b j} C_{l_a l_b j} \overline{S}_{l_a l_b j}, \tag{12.2.11}$$

where the $\overline{S}$ functions describe the orientation dependence in the usual way. The coefficients $C_{l_a l_b j}$ are treated as constant, though in fact they vary slightly with separation.

This method gives results comparable in accuracy with the test-particle model for N_2, and is much better for Cl_2, where the test-particle model is relatively unsuccessful. Indeed, the density overlap method gives better results for Cl_2 than a potential of the form of eqn (12.2.5) with the same number of parameters fitted directly to the calculated repulsion energies.

With continuing improvements in computing performance, it is becoming practicable to calculate repulsive potentials using *ab initio* calculations on pairs of interacting molecules of significant size—each containing up to 20 or so heavy (non-hydrogen) atoms. One approach is to separate the electron density of each molecule into atomic contributions, using stockholder density partitioning (§7.4), and use the density overlap model to obtain an atom–atom repulsion model for each pair of atoms. The resulting atom–atom repulsion model for the pair of molecules can then be refined, if necessary, by fitting to SAPT-DFT calculations of the molecule–molecule repulsion energy. It is not usually possible to fit all the parameters of the atom–atom model directly to the molecule–molecule repulsion, as there are too many of them and they are strongly correlated, so the fitting procedure often leads to unphysical solutions. Consequently some sort of limited or constrained optimization must be used for this final step.

12.2.3 Dispersion

It is usual to express the dispersion interaction for molecules in atom–atom form:

$$U_{\text{disp}} = -\sum_{a\in A}\sum_{b\in B}\left\{ f_6(R_{ab})\frac{C_6^{ab}}{R_{ab}^6} + f_8(R_{ab})\frac{C_8^{ab}}{R_{ab}^8} + f_{10}(R_{ab})\frac{C_{10}^{ab}}{R_{ab}^{10}} + \cdots \right\}. \tag{12.2.12}$$

The $f_n(R_{ab})$ are damping functions (see §12.1.5). In principle, there will be C_7 and C_9 terms for atoms whose local symmetry is not centrosymmetric, but their coefficients are smaller than those for the even terms and they are often omitted. Indeed it is usual to include only the C_6 term.

The use of a damped dispersion formula removes the negative singularity of the exp-6 potential (though a spurious minimum may remain at short distances), and makes it possible to use potentials of this type in any application, and in particular for interactions between molecules as well as atoms. It is evident, however, that for molecules the potential must depend on orientation as well as on distance; that is, it must be anisotropic. The anisotropy of the

dispersion was discussed in §4.3, and is satisfactorily understood at long range, but the form of the damping in the anisotropic case is not well understood. As in the case of the electrostatic interaction, the S-function expansion comprises, by definition, S-functions each multiplied by some function of R, so the damping function for each S-function term must be a function only of R, though it may be a different function for each S-function term. There may also be additional S-function terms that only appear at short range.

12.2.4 Induction

Induction is often ignored altogether in simple treatments, partly because it usually makes a relatively small contribution to the energy, and partly because its non-additive characteristics make it awkward to handle. Even in strongly polar systems like water, where the effects of induction are significant, it is common to omit any explicit treatment of induction and instead to use an electrostatic model with an enhanced dipole moment to describe its effects in an average way. The dipole moment of water in such cases may be increased from the isolated-molecule value of 1.8 D to 2.3 D or more.

The induction energy is awkward to describe accurately, as its calculation involves either a matrix inversion or an iterative treatment, as explained in §9.4, in both cases involving all the molecules in the system, and either method increases the computation time considerably. For many years it has been common to neglect it altogether, and if it is small this can be an acceptable approximation, but it is increasingly becoming clear that it can have significant effects. An easily understood example is the case of crystal structure prediction for hydrogen-bond-forming crystals. Here there may be candidate crystal structures in which the hydrogen bonds are intramolecular, and others where they are intermolecular. In the former case the effects of induction in the hydrogen bonding are taken into account in evaluating the energy of the isolated molecule. If in the latter case the effects of induction in the intermolecular hydrogen bonds are neglected, the calculated lattice energy is too high, so structures with intramolecular hydrogen bonding are spuriously favoured (Welch *et al.* 2008). In the study of biological systems such as proteins, too, there is an increasing recognition that induction needs to be taken into account.

Methods for doing this are broadly of two types. One is the damped Applequist method, in which polarizabilities are assigned to individual sites, usually atoms but sometimes at the centroids of localized molecular orbitals, and interactions between them are described by dipole–dipole coupling, usually with Thole damping (§9.1.1). The other is to use distributed polarizabilities, where the intramolecular coupling effects are treated exactly and only the intermolecular coupling needs to be handled explicitly, though damping is usually needed here too.

12.2.5 *Ab-initio*-derived potentials

Several schemes have been proposed for assembling the various components of the intermolecular interaction into a model potential. They involve analytic representations of the separate contributions to the full interaction energy, with parameters evaluated *ab initio* or fitted to *ab initio* data. The energy is typically expressed as

$$E = E_{\mathrm{es}} + E_{\mathrm{ind}} + E_{\mathrm{er}} + E_{\mathrm{disp}} + E_{\mathrm{ct}} + E_{\mathrm{pen}}, \tag{12.2.13}$$

where the terms are the familiar electrostatic, induction, exchange–repulsion, dispersion, charge-transfer and penetration contributions discussed in Chapter 6. The methods differ in the formulation of the individual terms and whether they appear at all. The penetration and exchange–repulsion terms are often modelled together.

Probably the oldest scheme of this type is SIBFA (sum of interactions between fragments calculated ab-initio), first described by Gresh *et al.* (1984), but it has evolved over the years since then. In the current version (Piquemal *et al.* 2007) the electrostatic term is described by damped interactions between distributed multipoles up to quadrupole at atom and bond-centre sites. The repulsion and penetration terms are represented separately by bond–bond, bond–lone-pair and lone-pair–lone-pair orbital overlap contributions (Gresh 1995). Induction is described using local-molecular-orbital (LMO) polarizabilities (see §9.3.3).

In the effective fragment potential (EFP) method Gordon *et al.* (2012), the model potential takes a similar form. The fragments may be single molecules, or parts of molecules. The electrostatic term is described by a distributed multipole analysis of each fragment, and the induction term using LMO polarizabilities. The dispersion term is of site–site form, $-\sum C_6^{ab} R_{ab}^{-6}$, with estimated R^{-8} terms. The dispersion coefficients are evaluated from LMO polarizabilities at imaginary frequency. The exchange–repulsion term is obtained from an expansion involving intermolecular orbital overlap integrals (Jensen and Gordon 1996). Variants of this approach include the fragment molecular orbital (FMO) method of Kitaura *et al.* (1999), and the effective fragment molecular orbital (EFMO) of Steinmann *et al.* (2010).

Collins and his group have described a systematic procedure for separating a large molecule into functional groups such as amide or carboxyl by breaking the molecule at single bonds and attaching hydrogen atoms at the breaks (Addicoat and Collins 2009). The properties of each fragment (distributed multipoles, polarizabilities, etc.) can then be evaluated. The effects of the fragmentation can be estimated by comparing the properties of fragments HG_1H and HG_2H with those of the recombined fragment HG_1G_2H. In practice a more elaborate hierarchical fragmentation scheme is used. In this way the interaction of a large molecule with its neighbours can be described in terms of the properties of the small fragments. The through-space interactions between different fragments of the same molecule can also be evaluated, as in eqn (12.2.13). The method has given good results for the isomerization energies of a range of large organic molecules.

The CamCASP program package of Misquitta and Stone (2012) uses the methods described in §9.3 to compute both static and imaginary-frequency distributed polarizabilities and hence distributed dispersion coefficients. The exchange–repulsion is obtained from the density overlap model, eqn (12.2.9), using local atomic densities, fitted to the exponential repulsion form of eqn (12.2.5), and refined by reference to exchange–repulsion energies derived using SAPT-DFT. Distributed multipoles were calculated using the GDMA program (Stone 2005). This scheme was used to predict the crystal structure of 1,3-dichloro-2-bromo-5-fluorobenzene successfully in the 2007 blind test (Misquitta *et al.* 2008*b*). The SIMPER method of Wheatley *et al.* (2004, 2007) uses a combination of calculations on the separate molecules and the supermolecule, and an extrapolation scheme to improve the accuracy.

12.3 Dependence on internal coordinates

All of the models discussed so far have been of 'rigid-body' type: that is, the molecules have been treated as rigid bodies with no internal degrees of freedom. Even the fragmentation pro-

cedure of Addicoat and Collins (2009), described in the previous section, uses rigid geometries for the fragments, though they may be combined in different ways to construct several isomers, or in different conformations of a particular isomer. For many purposes, the rigid-body picture is adequate; the frequencies associated with internal vibrational motions are often very different from those of the intermolecular degrees of freedom, so that the two kinds of motion are coupled only weakly. In other cases, however, the interaction of intramolecular and intermolecular motions may be significant, and for some properties, such as the red-shift of the OH vibrational frequency caused by hydrogen bonding, the explicit treatment of the vibrational motion is essential. For large flexible molecules, such as polypeptides, the energy of even an isolated molecule includes interactions of an 'intermolecular' type between parts of the molecule that may be separated by many chemical bonds but are close to each other in space, so the description of the intramolecular potential energy surface has to include these terms as well as the conventional bond stretching, bending and twisting forces. Conversely, the interaction of flexible molecules with each other is often facilitated by distortions of their structures, which may for example allow a substrate molecule to squeeze into the active site of an enzyme.

12.3.1 Molecular mechanics

The simplest way to describe these effects is to suppose that the internal vibrations of the molecules are the same as in the isolated molecule, and to assume that the intermolecular interaction can be described by an atom–atom model whose parameters do not depend on internal coordinates. In this picture, the internal motion of the molecules affects the intermolecular interactions only because it modifies the positions of the atoms.

There has been a great deal of interest over the last thirty or so years in the study of biological molecules by computer simulation. Such molecules are generally large and flexible, so it is essential to take the internal coordinates of the molecule into account. The method used is usually described as 'molecular mechanics': a function is chosen to describe the energy of the system, and then the coordinates may be varied to find an energy minimum, or the classical equations of motion of the system may be solved to explore the dynamics of the molecular motion. For biological systems it is usually necessary to include water in the simulation, either explicitly or by treating the system as embedded in a dielectric continuum (the polarizable continuum model). Often only a small region of the molecules is of interest—for example, the active site of an enzyme—and this region may be treated quantum mechanically, while molecular mechanics is used to treat the surrounding parts of the molecule and the solvent. In this way the influence of the surroundings on the active site is taken into account, without the need to apply the quantum mechanical treatment to the whole system (Acevedo and Jorgensen 2009). The method is generally known as QM/MM. In an extension of this idea known as ONIOM, there may be several layers. For example the region of interest may be described by an accurate *ab initio* method, its immediate surroundings by a simpler *ab initio* method, and the more remote regions by molecular mechanics (Svensson *et al.* 1996). The details of such methods would take us beyond the field of intermolecular forces, and here we only summarize the nature of the force fields (energy functions) used in molecular mechanics.

The energy of the system is described by a function such as

$$U = \sum_{\text{bonds}} k_r(r - r_0)^2 + \sum_{\text{angles}} k_\theta(\theta - \theta_0)^2 + \sum_{\text{torsions}} \tfrac{1}{2}V_n(1 + \cos(n\varphi - \gamma))$$

$$+ \sum_{i<j}^{\text{non-bond}} \left(\frac{A_{ij}}{R_{ij}^{12}} - \frac{B_{ij}}{R_{ij}^{6}} + \frac{q_i q_j}{\epsilon R_{ij}} \right). \tag{12.3.1}$$

This is the form of the classical AMBER force field. The first version (Weiner *et al.* 1984) was a united-atom description, in which the hydrogen atoms were not described explicitly but were incorporated into the neighbouring heavy atom. In the subsequent 'all-atom' version (Weiner *et al.* 1986), the hydrogen atoms were included explicitly, and further developments followed (Case *et al.* 2005). The first three terms in eqn (12.3.1) describe the energies of intramolecular bond stretches, angle bends and dihedral torsions respectively, while the remaining terms describe the through-space interactions. There is a Lennard-Jones repulsion–dispersion term, which is applied to pairs of atoms in the same molecule as well as to intermolecular interactions. However, it is usual to omit intramolecular interactions between atoms that are separated by three or fewer bonds, since such interactions are included in the earlier terms.

The electrostatic interaction is described by atom–atom point-charge terms only, the charges usually being obtained by fitting to the molecular electrostatic potential (see §7.8). Some early versions included an additional interaction between the H atom of a hydrogen bond and the proton acceptor atom, to provide additional flexibility and accuracy in the description of hydrogen bonds, but it was dropped from later versions.

This is evidently quite an elaborate potential. Although each of the terms is simple in form, and indeed has serious inadequacies, very many parameters are needed to describe all the interactions that may occur. In the Lennard-Jones term, for example, parameters A_{ij} and B_{ij} must be provided for each pair of atom types. This may not seem too serious a problem until one realizes that the general AMBER force field (Wang *et al.* 2004), a general-purpose version with 'a limited number of atom types', provides for eight types of nitrogen atom and six types of hydrogen. Although some parameters are shared between different types, the number of parameters that is needed to characterize the force field is still very large. Moreover it has been found necessary to construct different parameter sets for different types of system, and even for a particular type of system, such as nucleic acids, several parameter sets are available (Cheatham and Young 2000).

The AMBER family of force fields is only one of many in the literature. Ponder and Case (2003) have given a detailed review. The earliest still in use is probably the MM*n* series: MM1 (Allinger 1976), developed by Allinger's group at the University of Georgia, later superseded by MM2 (Allinger 1977), MM3 (Allinger *et al.* 1989, Lii and Allinger 1991) and MM4 (Nevins *et al.* 1996). The last of these versions used 15 different types of term, including coupling terms between different vibrational modes, and has since been extended further. Other force fields include CHARMM (Brooks *et al.* 1983) from Karplus's group at Harvard, ECEPP (Némethy *et al.* 1983, Sippl *et al.* 1984, Arnautova *et al.* 2006) from Scheraga's group at Cornell, GROMOS from Groningen (Hermans *et al.* 1984) and OPLS (Jorgensen and Tirado-Rives 1988). They are all broadly similar, but differ in various ways. For example, the earliest version of ECEPP used fixed bond lengths and bond angles, though this constraint was removed in some later versions. The MM*n* force fields use an exp-6 formulation of the repulsion–dispersion term, but the rest all use Lennard-Jones, though the parameters differ between models. The latest version of GROMOS aims to evaluate the Gibbs free energy rather than the energy. The parameters for the interactions between unlike atoms are

usually obtained from combining rules; some models use the Lorentz–Berthelot combining rules (see §12.1.2), while OPLS (for example) uses the geometric-mean combining rule for the dispersion coefficient B and the repulsion coefficient A of eqn (12.3.1), and ECEPP uses the Slater–Kirkwood combining rule (eqn (4.3.12)) for the dispersion coefficients. The more important of the unlike-atom parameters in all force fields are directly fitted, and not obtained from combining rules.

The description of the internal degrees of freedom also varies. The MM4 force field uses anharmonic stretch and bend potentials, including terms up to quartic, and also includes quite a number of cross terms between bend and stretch, between bends involving different bond angles involving the same atom, and between bends and torsions. The other force fields include only the harmonic (quadratic) terms, with no cross terms between different coordinates. This is an example of how differences in formulation of the force fields arise from differences in objectives; an objective of MM4 was to obtain reliable vibration frequencies, so a good description of the vibrational potential was essential. Many of the other force fields were devised for accurate prediction of folded protein structures, for which reliable non-bonded interactions are more important.

The treatment of the electrostatic term differs in the value used for the dielectric constant ϵ. In some work it is taken to be equal to the distance R_{ij} in ångström. This has no valid theoretical justification, but has been claimed to take some account of the effect of the aqueous solvent. A more significant reason for its inclusion at the time when the early force fields were introduced was that the electrostatic interaction then became proportional to R_{ij}^{-2}, so that the energy expression included only even powers of R_{ij} and it was not necessary to evaluate any square roots. Nowadays this is no longer a problem. It is now generally agreed that the solvent molecules should if possible be included explicitly in the simulation, and then the dielectric constant should be set equal to 1, or perhaps to a slightly higher value to take account of polarization effects; for example MM3 uses $\epsilon = 1.5$ for gas-phase simulations.

Another difference concerns the description of hydrogen bonds: some models include explicit hydrogen-bond terms, while others have no special hydrogen-bond functions and rely on the electrostatic terms to recover the special features of the hydrogen bond. Sometimes the charge and repulsion centres for the H atoms are placed part of the way along the bond rather than at the position of the proton. The force fields also differed originally in the model used to describe explicitly included water molecules: CHARMM used ST2, GROMOS SPC and OPLS TIP4P. (See §12.4 below.)

Note that the same name is often used for the force field itself—the energy function—and for the computer program used to evaluate and optimize the energy. Thus AMBER can mean either the family of force fields or the computer program. The AMBER force fields can be used in many other programs, and the AMBER program can handle other force fields. The development of the programs has proceeded alongside the development of the force fields, with much attention given to the fast and accurate evaluation of the energies and forces. For example, particle-mesh-Ewald (PME) summation is now widely used to evaluate long-range electrostatic interactions both more accurately and more efficiently (Darden *et al.* 1999). The capabilities of the programs have also broadened, so that, for example, explicit water molecules can be described by any of a range of simple models. All the force fields have been extensively refined and validated over the years, and force fields intended for specialized applications—proteins, or nucleic acids, or carbohydrates—have evolved.

The variations in detail between the force fields make it impossible to compare their parameter values directly, since the parameters are all interdependent, and also make it difficult to compare their reliability. Roterman *et al.* (1989*a*,*b*) compared the CHARMM, AMBER and ECEPP force fields, and concluded that their predictions were significantly different. The review by Ponder and Case (2003) describes other differences. Lindorff-Larsen *et al.* (2012) compared the predictions of several force fields with a variety of experimental data, and concluded that there had been an improvement over the past decade. Nevertheless, comparisons of force fields continue to appear in the literature (e.g. Pu *et al.* 2011, Garrido *et al.* 2011), often emphasizing the need to use the 'right' force field for the problem or recommending adjustment of parameters to achieve the 'right' result. It has been found, for example, that some protein force fields favour α-helix secondary structure over β-sheet, while others do the opposite (Best *et al.* 2008). An empirical parameter adjustment using data for the helix-coil equilibrium has been found to reduce this bias. However, other shortcomings remain, particularly with respect to reproducing thermodynamic quantities (Best and Hummer 2009). Sherrill *et al.* (2009) compared CHARMM, AMBER, MM3 and OPLS with high-quality *ab initio* calculations and found that none of the empirical force fields reproduced the *ab initio* results consistently. Piana *et al.* (2011) found that while the rate of folding of some proteins and the structure of their native states were in good agreement with experiments, the folding mechanism and the properties of the unfolded state depended substantially on the choice of force field. As Stouch (2012) has forcefully pointed out, applications such as drug design and crystal structure prediction deal with energy differences of $1\,\mathrm{kJ\,mol^{-1}}$ or so, and the errors in current force fields are at least comparable with this and probably significantly larger.

12.3.2 Polarizable force fields

The main approximations that are applied in most of the widely used force fields are the use of isotropic Lennard-Jones terms for repulsion and dispersion, the use of point charge models for electrostatics, and the treatment of induction in a mean-field manner, by modification of the electrostatic parameters, or by the use of a dielectric constant in the electrostatic interactions. Such approximations were necessary when computer simulation stretched the capabilities of even the most powerful computers, and are still needed for the largest systems, but advances in computer power have made it possible to move beyond these approximations. Methods for incorporating polarizability effects into force fields have been discussed by Söderhjelm and Ryde (2009). The AMBER ff02 force field provides for polarization by assigning dipole polarizabilities to each atom. Another example is AMOEBA, developed first for water (Ren and Ponder 2003) and then more generally (Ponder *et al.* 2010), which describes electrostatics using atomic dipoles and quadrupoles as well as point charges. Polarization is described using the Applequist model with dipole–dipole polarizabilities and the version of Thole damping functions given in eqn (9.1.22). In this approach, implemented in the TINKER program (Ponder 2009), the atomic multipole moments (obtained using distributed multipole analysis) have to be modified so that the consistent polarization of the multipoles by the intramolecular fields recovers the DMA values (Ren and Ponder 2002). The evaluation of the induction energy from such force fields can be carried out by the iterative solution of the induction equations, as described in §9.4, or by using a Drude model, comprising a fictitious particle carrying mass and charge and attached to the polarizable site by a spring. The fictitious particles are included in the Lagrangian equations of motion for the system, along with the real particles.

12.3.3 Conformational dependence of potential parameters

One of the limitations of all these models for large flexible molecules is that they cannot easily describe the way in which the charge distribution of the molecule depends on the molecular structure. Consider a molecule such as acrolein, $H_2C{=}CH{-}CH{=}O$. We can describe its charge distribution in terms of distributed multipoles, using a local coordinate system for each atom—for instance, the local axis system for the O atom might have the z axis perpendicular to the plane of the C–C=O unit, the y axis from C to O along the C=O bond, and the x axis forming a right-handed set. If the molecule is twisted around the central bond, the oxygen multipoles are approximately unchanged in this local coordinate system, but this is not a very good approximation, because the change in the central bond (especially the loss of conjugation as it is twisted out of plane) causes a redistribution of the electron density. Consequently the multipole moments of the O atom depend on the torsion angle around the central bond. The same is true for the other atoms, particularly the C atoms at each end of the bond being twisted. Koch *et al.* (1995) found that the electrostatic potential on a grid of points 1.4 Å from the Van der Waals surface, calculated at one value of the torsion angle using multipole moments obtained at another, is in error by as much as 0.1 V (r.m.s.) (10 kJ mol^{-1} for a charge of 1e). If the multipole moments, as functions of the torsional angle, are fitted to Fourier series truncated at the $\cos 3\theta$ term, the r.m.s. error is reduced to less than 0.01 V.

If the charge distribution is represented using point charges, the dependence on torsion angle has to include not only the intrinsic change in the charge distribution arising from the change in bonding, but the effects of moving the atoms relative to one another, since the dipoles and higher moments on each atom have to be represented in terms of point charges on other atoms. The use of charges for one conformation in calculating the potential for a different conformation leads to large errors, as one would expect. Reynolds *et al.* (1992*a*) found that by averaging the charges over conformations, weighting each conformation by its Boltzmann factor, an improved point-charge description could be obtained. Nevertheless, the errors are still large, and calculations of the difference between the free energy of hydration for ethanol and propanol showed very large variations in the calculated value depending on the choice of point-charge model (Reynolds *et al.* 1992*b*). In fact these variations dominated all other sources of error.

A description of the charge distribution in terms of low-rank multipoles rather than just charges is likely to be less sensitive to geometry than a description using only charges, while it may be possible to describe much of the variation in charge distribution with geometry by the polarization of atoms by neighbouring polar groups. This is the approach used in the AMOEBA force field, but it is still under development, and it is too early to say whether it is the answer. Söderhjelm *et al.* (2011) found that the local polarizabilities themselves vary by about 0.5 a.u. on average as the conformation is varied, while the uncertainty in assigning transferable atomic polarizabilities would be as much as 2.75 a.u., leading to errors of the order of 36 kJ mol^{-1} in relative conformational energies if such fixed values are used. Jankowski (2004) described the potential energy at a given position in intermolecular coordinate space as a Taylor expansion in intramolecular coordinates around the molecular equilibrium geometries. The method proved accurate, but was only applied to very small systems. Le and Bettens (2011) described a more general method in which the distributed multipoles were obtained by Shepard interpolation following Thompson *et al.* (1998): the multipoles are calculated at a number of geometries (data points), and the multipoles at some other geometry are expressed

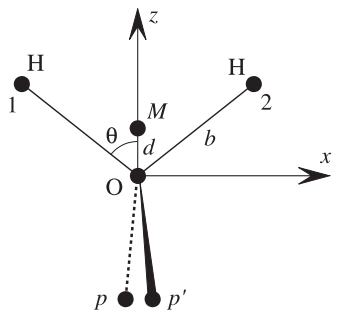

Fig. 12.4 Interaction sites for water models.

as a weighted sum of Taylor expansions about the data points. Applied to glycine and alanine, the method predicted r.m.s. errors in the potential on the solvent-accessible surface as small as 2×10^{-5} a.u., or 5×10^{-4} V, using multipoles up to rank 5, but 0.64×10^{-3} a.u., or 20 mV, for multipoles only up to quadrupole. A similar procedure has been used to tabulate and interpolate information acquired during crystal structure optimization for use in optimizing related structures (Kazantsev *et al.* 2011*a*, Braun *et al.* 2011), and this approach has been successfully used in a blind structure prediction for a very flexible model pharmaceutical (Kazantsev *et al.* 2011*b*).

12.4 A case study: potentials for water

Because of its obvious importance, the intermolecular potential for water has been an objective for theoreticians for many years (Finney 2001). The anomalous properties of water also make it the most difficult small molecule to describe well. Guillot (2002) listed about 50 proposed potentials from 1933 to 2001, and more have been added since then. The reason for this large number is not just the need for better potentials, but also the need to describe water in a number of different roles. Reproducing the spectroscopic properties of the water dimer and small water clusters to cm^{-1} accuracy calls for a very detailed and inevitably complicated description—more so for the small clusters than for the dimer, because many-body terms have then to be included. For a description of water in its condensed phases, compromises have to be made, because time-consuming molecular dynamics or Monte Carlo methods are needed, so the potentials become simpler in form and less accurate. On the other hand, the properties to be calculated do not require such high accuracy. Frequently the focus of interest is not on the water but on a solute, and then the water model can be simpler still, unless the interactions between the solute and the water are important. Sometimes it is enough for the water model to provide a dielectric environment for the system of interest, for example where that involves the interaction between the active site of an enzyme and a ligand, but even here there are several methods for describing the interaction of the system with the dielectric continuum (Strodel and Wales 2008).

The first attempt at a water model was made by Bernal and Fowler (1933), who used three point charges, two at the H nuclei (points 1 and 2 in Fig. 12.4) and one on the symmetry axis (point M) together with an oxygen–oxygen Lennard-Jones term. Rowlinson (1949) used a Stockmayer potential—that is, a Lennard-Jones interaction with an embedded dipole—and in

a later version (1951) he added a quadrupole. However, the Bernal–Fowler type of model has been generally preferred, with variations in the position and magnitude of the charges and the parameters of the Lennard-Jones term. They include the ST2 potential (Stillinger and Rahman 1974), which has four charges in a tetrahedral array (two of them at the positions p and p' in Fig. 12.4, corresponding notionally to the lone pairs), the family of potentials known as TIPS2, TIP3P, TIP4P (Jorgensen *et al.* 1983) and TIP5P (Mahoney and Jorgensen 2000) and the simple point charge (SPC) model (Berendsen *et al.* 1981). Most of these potentials have been used in molecular dynamics and Monte Carlo calculations (see Chapter 13) on liquid water, ice and hydrated proteins, with reasonable success. Such potentials cannot be expected to perform well in a variety of applications. They are very simple in form, and do not reproduce the true potential at all accurately, so agreement with experiment depends on a cancellation of errors. In particular, they do not describe the polarization of the water molecule, which can contribute substantially to the interaction energy, and is strongly non-additive, as we saw in Chapter 10. Such non-additive effects are only incorporated in an averaged way; thus, for example, all of these models except Rowlinson's assign a dipole moment to the water molecule that is substantially higher than the gas-phase value of 1.85 debye—typically 20–30% higher, sometimes more. It follows that they should not be used in circumstances for which they were not designed, and having been designed for liquid water they cannot be expected to give good results for other systems, such as an isolated pair of water molecules. Indeed, Berweger *et al.* (1995) found that even for liquid water, the optimum parameters in the SPC model depend quite strongly on the temperature and pressure. No doubt this is true of other models of this type also. Since the applications are frequently of a biological nature, the potentials are usually parameterized for ambient temperature (around 300K) and atmospheric pressure.

An alternative to this purely empirical approach is to use *ab initio* calculations to obtain a potential energy surface, which is then fitted with a suitable analytic function. One of the best-known potentials of this type is due to Matsuoka *et al.* (1976). Their potential, commonly known as the MCY potential, is more realistic in some respects, having an exponential repulsion term between every pair of atoms, but the electrostatic interaction is still represented by three point charges. It also has attractive exponential terms between the hydrogen and oxygen atoms, which were introduced to describe electron correlation effects. Although it was derived from calculations on the water dimer, it gives very poor results for the virial coefficient of water vapour (Reimers *et al.* 1982), which is a purely pair-potential property (see §13.2.1). We have to conclude that either the *ab initio* calculations were not good enough or the analytic function used to represent the results was not sufficiently flexible.

In fact we know that the intermolecular electron correlation leads to the dispersion interaction, so an attractive exponential representation for it is inappropriate. Reimers *et al.* (1982) attempted to improve matters by replacing the attractive exponential terms by the damped R^{-6}, R^{-8} and R^{-10} dispersion terms of the HFD model, but the calculated second virial coefficient was still very poor. Reimers *et al.* attributed this to the errors in fitting the analytic function to the *ab initio* data, rather than to errors in the calculation itself, but the calculations were not corrected for BSSE so there must be errors from this source. Matsuoka *et al.* estimated the BSSE to be about 0.8 kJ mol^{-1} at SCF level, and assumed that the correlation contribution would be about the same, as had been found for a smaller basis set. In fact it is now known that the correlation contribution to BSSE does not decrease as rapidly as the SCF contribution when the basis is improved.

Another potential of this type is the RWK2 model of Reimers *et al.* (1982). This too described the electrostatics by using three point charges, chosen to reproduce the monomer dipole and quadrupole moments, but it included the accurate dispersion term from the HFD model, exponential repulsions for O···O and H···H interactions, and Morse terms for O···H interactions. This model was intended to give a good account of water in all three phases, but the authors were only able to claim 'reasonable accuracy'.

12.4.1 Polarizable models

A serious limitation of all these potentials is that they have no explicit description of induction, usually treating its effects in an average way by using an enhanced dipole moment. A number of authors have sought to rectify this omission. An early attempt was the polarizable electropole (PE) model of Barnes *et al.* (1979), which has an isotropic dipole–dipole polarizability, a Lennard-Jones term and point dipole and quadrupole, all at the same site. The use of an isotropic polarizability is quite a good approximation for water, for which the experimental polarizability components are (in a.u.) $\alpha_{xx} = 10.31$, $\alpha_{yy} = 9.55$ and $\alpha_{zz} = 9.91$. The PE model gave a better account of the second virial coefficient of steam and of the structure of liquid water than other models in use at the time, and Barnes *et al.* showed that the indirect effects of the induction term on the long-range interaction between pairs of molecules were considerable, and that the mean dipole of each water molecule was about 2.5 debye, even higher than the enhanced value used in most unpolarizable models. Another model of this type is the POL3 model of Caldwell and Kollman (1995), based on the SPC model but with reduced point charges and isotropic atomic polarizabilities.

Sprik and Klein (1988, 1991) modelled the induction by distributed charge-flow polarizabilities, as described in §12.1.7, the other features of their potential being similar to the TIP4P potential, except that the charges were chosen to reproduce the true molecular dipole moment rather than the enhanced value that is needed when the induction is not included explicitly.

With the emergence of more accurate *ab initio* methods, it has become possible to build model potentials based on *ab initio* calculations (Szalewicz *et al.* 2009). Burnham and Xantheas (2002*a*) used accurate supermolecule calculations on the water dimer at relatively few dimer geometries to parametrize a model potential. Their model includes polarization explicitly. This first version was not particularly successful, but a later parametrization (Burnham and Xantheas 2002*b*,*c*) was able to give a good account of the dimer potential energy surface, the second virial coefficient, and properties of small water clusters as well as liquid water and ice.

For some years, the most elaborate analytical potentials proposed for water evolved from that of Millot and Stone (1992). They made no attempt to simplify the potential so that it could be used in conventional molecular dynamics calculations, but sought to describe the interaction as accurately as possible. Their potential used distributed multipoles to describe the charge distribution (up to quadrupole on oxygen, charges only on hydrogen) and central polarizabilities up to quadrupole–quadrupole. (Distributed polarizabilities offer no advantage for this near-spherical molecule.) The dispersion interaction was described using the anisotropic dispersion coefficients C_6 to C_{10} calculated by Rijks and Wormer (1989), though the smaller coefficients were neglected. Repulsion was described by anisotropic atom–atom exponential terms, fitted to the repulsion–penetration energy calculated using the *ab initio* intermolecular perturbation theory (IMPT) described in §6.2.4. This anisotropic site potential (ASP) model

gave a good account of the equilibrium geometry and of the tunnelling splittings and second virial coefficient in the water dimer. Improved ASP-W2 and ASP-W4 potentials (Millot *et al.* 1998) included a charge transfer term, which has an attractive exponential form (see Fig. 8.4), and used corrected dispersion coefficients (Rijks and Wormer 1990). Goldman *et al.* (2002, 2005) refined the earlier ASP potential using spectroscopic data on vibration-rotation-tunnelling (VRT) energy levels for the water dimer. They were able to carry out Monte Carlo simulations of liquid water with this VRT(ASP-W)III potential, obtaining good agreement with some experimental liquid properties, as well as reproducing the VRT spectra of the dimer and small clusters.

Mas *et al.* (2000) used a wholly non-empirical method. They calculated interaction energies using SAPT at 2510 dimer geometries and fitted them to a relatively simple (SAPT-5s) analytic function. This gave good results for dimer properties such as the virial coefficient and the dimer VRT spectrum, but it has no explicit polarization term. A later model (Bukowski *et al.* 2008*a*,*b*) included an isotropic dipole–dipole polarizability, and was fitted to energies calculated at the same 2510 grid points using CCSD(T), extrapolated to the complete basis set limit. This potential gave results for the VRT spectra that were slightly better than those from the VRT(ASP-W)III potential, although not fitted to the VRT data, and also gave better results for liquid properties. An important conclusion from this work was that practically all of the many-body effects could be accounted for by induction, though there were small contributions from three-body exchange–repulsion. Three-body dispersion was not included. A further improvement in the fit was obtained by using additional interaction sites, giving eight symmetry-unique sites including the O and H nuclei—25 sites in all—and using B-splines to describe the site–site pair interaction terms (Cencek *et al.* 2008). This CC-pol-8s potential gave very good agreement with the VRT spectrum, but at the cost of a potential function that is less closely related to the underlying theory.

A different approach was used by Huang *et al.* (2005, 2006, 2008) to obtain a potential that describes molecular vibration and dissociation as well as the intermolecular interaction. They used a potential of the form

$$V = p(\mathbf{x}) + \sum_{i<j} q_{ij}(\mathbf{x}) \exp(-r_{ij})/r_{ij}, \tag{12.4.1}$$

where r_{ij} is the distance between nuclei i and j, $\mathbf{x}$ is the set of 'Morse variables' $x_{ij} = \exp(-r_{ij}/a)$, and p and q_{ij} are polynomials, of degree 7 and 4 respectively, in the x_{ij}. The parameter a was taken to be 3. The function V was constructed to be invariant with respect to nuclear permutations, so for example the q_{HH} functions were the same for all HH pairs, whether in the same molecule or in different ones. The parameters in V were fitted to more than 30,000 energies calculated using CCSD(T) with an aug-cc-pVTZ basis. The resulting potential was used to calculate intermolecular vibration-rotation-tunnelling energy levels, and gave excellent agreement with experiment, but Leforestier *et al.* (2009) found that the intramolecular vibrational frequencies were less well reproduced. A later version was modified to give better agreement with vibrational spectrum of the monomer, and the long-range potential and dissociation energy D_e for the dimer (Shank *et al.* 2009), and in a further development three-body terms were added (Wang *et al.* 2009). The dimer potential leads to dissociation energies $D_e = 20.8\,\mathrm{kJ\,mol^{-1}}$ and $D_0 = 1103\,\mathrm{cm^{-1}} = 13.2\,\mathrm{kJ\,mol^{-1}}$ (see §13.4.5, p.259) which compares very well with the experimental value of $D_0 = 1105 \pm 10\,\mathrm{cm^{-1}}$ (Rocher-Casterline

et al. 2011) (see §13.4, p. 250). The best estimate of D_e is close to 21.1 kJ mol^{-1} (Klopper *et al.* 2000, Burnham and Xantheas 2002*a*), giving a zero-point energy of 7.9 kJ mol^{-1}.

The various analytic water potentials are commonly used in classical calculations of properties. In simulations, for example, the equations of motion of the water molecules are solved as though they were classical particles. Since they are in fact quantum particles this is not correct, and Kuharsky and Rossky (1985) used Feynman path-integral techniques to estimate the quantum corrections. They found that the quantum liquid was less structured than the classical one, and that at ambient temperature the difference between the quantum and classical radial distribution functions was the same as the change induced by an increase in temperature of 50°. The second virial coefficient (§13.2.1) is another property where quantum corrections are important, especially at low temperatures.

12.5 Coarse-grained models

The models described in the previous sections are mostly atomistic: they describe the atoms and the interactions between them individually. For very large systems such as viruses, the number of atoms makes such a treatment impractical, and an alternative is to use a 'coarse-grained' model, in which a group of atoms is described by a single interaction centre or 'bead'. A protein, for example, might be modelled using a single bead for each residue. The interaction between beads attempts to summarize the interactions involving all the atoms comprising each bead, and because it is averaged over the motions of those atoms it is properly viewed as a potential of mean force (see §10.5), i.e., a free energy, and so is temperature-dependent. Lu and Voth (2011) have shown that it is possible to use the temperature dependence to separate the enthalpy and entropy components of the coarse-grained potential.

For more details of coarse-graining methods, see, for example, Hills *et al.* (2010), or the journal special issue *PCCP* 2009 or the Faraday discussion *Faraday* 2010.

12.6 Calculation of energy derivatives

If we wish to optimize the structure of a system, we need to evaluate not only the energy but its derivatives. For molecular dynamics calculations, in which the evolution of the system is explored by solving the classical equations of motion, the first derivatives of the energy—forces and torques—suffice. The same is true if we seek a local minimum in the energy. If we want to find saddle points on the potential energy surface, as is the case when isomerization pathways are of interest, the most effective procedure for finding them is the eigenvector-following technique of Cerjan and Miller (1981) (see also Wales (1991)). In its original form this requires second derivatives (the Hessian matrix), but in a later modified version it is only necessary to evaluate the search direction, i.e., the eigenvector corresponding to the lowest Hessian eigenvalue, and this can be done numerically (Munro and Wales 1999). However, second derivatives are needed to calculate harmonic frequencies at local minima and transition rates between minima.

When the potential is described by one of the more accurate models discussed above, in which dipoles and higher moments appear, and the repulsion and dispersion may also be orientation dependent, we require derivatives of the orientation-dependent terms. The perceived difficulty of evaluating these derivatives has been one of the reasons for the continued use of potentials that depend only on the distance between sites, but they are neither as difficult

nor as time-consuming to evaluate as is often supposed. Programs that use anisotropic site–site potentials in molecular dynamics calculations include DL_MULTI (Leslie 2008) and TINKER (Ponder 2009).

12.6.1 Derivatives of the electrostatic energy

The first derivatives of the energy comprise the forces on each molecule, which are (minus) the derivatives of the energy with respect to translations of the molecular centre of mass, and the torques, which are (minus) the derivatives with respect to rotations about axes through the centre of mass. For a pair-additive energy the forces are also pair-additive, so we consider a pair of molecules A and B, with centres of mass at $\mathbf{A}$ and $\mathbf{B}$, and we consider the interaction between the multipole moments on site a, at position $\mathbf{A} + \mathbf{a}$, and site b, at position $\mathbf{B} + \mathbf{b}$. As the molecule rotates, the local position vectors $\mathbf{a}$ and $\mathbf{b}$ rotate with it, and we have to take this into account as well as the rotation of the multipoles on each site.

The electrostatic interaction U^{ab} between sites a and b is:

$$U^{ab} = \sum_{tu} Q_t^a Q_u^b T_{tu}^{ab},$$

where Q_t^a and Q_u^b are multipole moments on sites a and b, referred to the local coordinate system for each site, so their values are independent of orientation.

The function T_{tu}^{ab} depends on the relative orientations of the site axis systems and the intersite vector $\mathbf{R}$. More specifically, as we saw in §3.3 (eqn (3.3.14)) it can be expressed in terms of the distance R between the sites and an $\overline{S}$ function, which in turn depends on the direction cosines

$$\begin{array}{cccc} \mathbf{x}^a \cdot \mathbf{x}^b, & \mathbf{x}^a \cdot \mathbf{y}^b, & \mathbf{x}^a \cdot \mathbf{z}^b, & \mathbf{x}^a \cdot \hat{\mathbf{R}}, \\ \mathbf{y}^a \cdot \mathbf{x}^b, & \mathbf{y}^a \cdot \mathbf{y}^b, & \mathbf{y}^a \cdot \mathbf{z}^b, & \mathbf{y}^a \cdot \hat{\mathbf{R}}, \\ \mathbf{z}^a \cdot \mathbf{x}^b, & \mathbf{z}^a \cdot \mathbf{y}^b, & \mathbf{z}^a \cdot \mathbf{z}^b, & \mathbf{z}^a \cdot \hat{\mathbf{R}}, \\ -\hat{\mathbf{R}} \cdot \mathbf{x}^b, & -\hat{\mathbf{R}} \cdot \mathbf{y}^b, & -\hat{\mathbf{R}} \cdot \mathbf{z}^b, & \end{array}$$

where $\hat{\mathbf{R}}$ is the unit vector in the direction of the intersite vector $\mathbf{R} = \mathbf{B} + \mathbf{b} - \mathbf{A} - \mathbf{a}$, , while $\mathbf{x}^a$, $\mathbf{y}^a$ and $\mathbf{z}^a$ are the unit vectors of the local axis system of site a and $\mathbf{x}^b$, $\mathbf{y}^b$ and $\mathbf{z}^b$ those of site b. The minus sign appears in the last three direction cosines to make the S-function formulae symmetrical—in effect we use the vector from a to b with the local axes on a, but the vector from b to a with the local axes on b. Following Willock *et al.* (1993, 1995), we regard these scalar products and the distance R as a set of intermediate variables $\mathbf{q} = \{q_i,\ i = 1, \ldots, 16\}$. The expression for T_{tu}^{ab} in terms of these quantities is not unique, because there are some relationships between them, such as $[\mathbf{x}^a \cdot \hat{\mathbf{R}}]^2 + [\mathbf{y}^a \cdot \hat{\mathbf{R}}]^2 + [\mathbf{z}^a \cdot \hat{\mathbf{R}}]^2 = 1$, but this is not a problem for the differentiation procedure.

To differentiate an interaction term, we use the chain rule. If C_K is one of the rigid-body coordinates, we have

$$\frac{\partial}{\partial C_K} T_{tu}^{ab} = \sum_i \frac{\partial q_i}{\partial C_K} \frac{\partial}{\partial q_i} T_{tu}^{ab}. \tag{12.6.1}$$

Now the form of T_{tu}^{ab} is a polynomial in the direction cosines q_i multiplied by an inverse power of R (see Appendix F), so its derivatives are very easy to evaluate. Formulae for the T functions and their derivatives in terms of the q_i can be determined with the help of an algebra program such as Mathematica or Maple (Hättig and Heß 1994), or for computational

purposes recursion formulae can be used (Hättig 1996). The derivatives of the q_i with respect to the molecular positions and orientations are more complicated, but formulae for them only have to be calculated once.

The variables q_i depend on the rigid-body translational and rotational coordinates of each molecule. This set of $6N$ external coordinates for the N molecules are the independent variables with respect to which we require derivatives of the total energy. It is convenient to introduce the alternative notation $\{A_X, A_Y, A_Z\}$ for the coordinates of the centre of mass of molecule A in the global axis system. It is also convenient to define an orthogonal matrix $\mathbf{W}_a$ which describes the orientation of the local axes of site a relative to the global axes. Its columns are the unit vectors $\mathbf{x}_a$, $\mathbf{y}_a$ and $\mathbf{z}_a$ defining the local axes of site a in global coordinates.

12.6.2 Derivatives with respect to position

In this notation, the derivatives with respect to the position of A are easily obtained:

$$\begin{aligned}
&\frac{\partial}{\partial A_\alpha} R^2 = \frac{\partial}{\partial A_\alpha} |\mathbf{B} + \mathbf{b} - \mathbf{A} - \mathbf{a}|^2 = -2(B_\alpha + b_\alpha - A_\alpha - a_\alpha) = -2R_\alpha, \\
&\frac{\partial R}{\partial A_\alpha} = \tfrac{1}{2}(R^2)^{-1/2} \frac{\partial R^2}{\partial A_\alpha} = -\frac{R_\alpha}{R}, \qquad (12.6.2) \\
&\frac{\partial}{\partial A_\alpha} R_\beta W^s_{\beta\gamma} = -W^s_{\alpha\gamma}, \quad s = a \text{ or } b, \\
&\frac{\partial}{\partial A_\alpha} \hat{R}_\beta W^s_{\beta\gamma} = \frac{\partial}{\partial A_\alpha}\left(\frac{R_\beta}{R} W^s_{\beta\gamma}\right) = -\frac{1}{R} W^s_{\alpha\gamma} + \frac{R_\alpha R_\beta}{R^3} W^s_{\beta\gamma}, \quad s = a \text{ or } b, \\
&\frac{\partial}{\partial A_\alpha} (\mathbf{W}^a)^{-1} \mathbf{W}^b = 0. \qquad (12.6.3)
\end{aligned}$$

Similar formulae apply for the derivatives with respect to the position of B, but there are some sign changes:

$$\begin{aligned}
&\frac{\partial R}{\partial B_\alpha} = +\frac{R_\alpha}{R}, \\
&\frac{\partial}{\partial B_\alpha} \hat{R}_\beta W^s_{\beta\gamma} = +\frac{1}{R} W^s_{\alpha\gamma} - \frac{R_\alpha R_\beta}{R^3} W^s_{\beta\gamma}, \quad s = a \text{ or } b.
\end{aligned}$$

The K component of the force on molecule A arising from its interaction with molecule B is then

$$\begin{aligned}
F^A_K &= -\frac{\partial}{\partial A_K} U^{AB} \\
&= -\sum_{ab} Q^a_i Q^b_u \frac{\partial}{\partial A_K} T^{ab}_{tu} \\
&= -\sum_{ab} Q^a_i Q^b_u \sum_i \frac{\partial q_i}{\partial A_K} \frac{\partial}{\partial q_i} T^{ab}_{tu}. \qquad (12.6.4)
\end{aligned}$$

12.7 Derivatives with respect to orientation

The orientation of a molecule can be described in a number of ways, as explained in §1.4; for example by angle-axis coordinates or quaternions. We denote by $\mathbf{M}^A$ the rotation matrix

describing the orientation of A. That is, $\mathbf{M}^A$ is the rotation that takes molecule A to its current orientation from a reference orientation with its molecular axes parallel to the global axes. For the moment we assume that $\mathbf{M}^A$ is expressed in terms of some set of orientation coordinates p_k^A, and that we can evaluate the derivatives

$$\mathbf{M}_k^A = \frac{\partial M^A}{\partial p_k} \text{ and } \mathbf{M}_{jk}^A = \frac{\partial}{\partial p_j^A}\frac{\partial}{\partial p_k^A} M^A. \tag{12.7.1}$$

Note that $\mathbf{M}_{jk}^A$ may be different from $\mathbf{M}_{kj}^A$, since differentiations with respect to different rotation axes do not commute.

It is convenient to write $\mathbf{a} = \mathbf{M}^A(\mathbf{M}^A)^{-1}\mathbf{a} \equiv \mathbf{M}^A\tilde{\mathbf{a}}$, so that $\tilde{\mathbf{a}}$ is the position of site a in molecular axes relative to the molecular origin $\mathbf{A}$, and is constant. Similarly we can write $\mathbf{b} = \mathbf{M}^B(\mathbf{M}^B)^{-1}\mathbf{b} \equiv \mathbf{M}^B\tilde{\mathbf{b}}$.

We also write $\mathbf{W}_a = \mathbf{M}^A\widetilde{\mathbf{W}}^a$, where $\widetilde{\mathbf{W}}^a = (\mathbf{M}^A)^{-1}\mathbf{W}_a$ is the orientation of the local axes for site a relative to the molecular axes, and is unchanged by rotations of the molecule. Similarly $\mathbf{W}_b$ describes the orientation of the local axes of site b relative to the global axes, and $\widetilde{\mathbf{W}}^b = (\mathbf{M}^B)^{-1}\mathbf{W}_b$ is a constant matrix describing the orientation of site b relative to the molecular axes of B.

Then the intersite distance R can be written as

$$R^2 = \mathbf{R}\cdot\mathbf{R} = |\mathbf{B}+\mathbf{b}-\mathbf{A}-\mathbf{a}|^2 = |\mathbf{B}+\mathbf{b}-\mathbf{A}|^2 - 2(\mathbf{B}+\mathbf{b}-\mathbf{A})\cdot\mathbf{a} + \mathbf{a}\cdot\mathbf{a}. \tag{12.7.2}$$

The first and last terms on the r.h.s. are constant with respect to rotations of A, as is the factor $\mathbf{B}+\mathbf{b}-\mathbf{A}$ in the middle term, while $\mathbf{a} = M^A\tilde{\mathbf{a}}$ and $\tilde{\mathbf{a}}$ is also constant. Consequently

$$\frac{\partial}{\partial p_k^A}(R^2) = -2\frac{\partial}{\partial p_k^A}(\mathbf{B}+\mathbf{b}-\mathbf{A})\cdot\mathbf{a} = -2(\mathbf{B}+\mathbf{b}-\mathbf{A})\cdot(\mathbf{M}_k^A\tilde{\mathbf{a}}), \tag{12.7.3}$$

and

$$\frac{\partial R}{\partial p_k^A} = \tfrac{1}{2}(R^2)^{-1/2}(R^2)_k = -\frac{1}{R}(\mathbf{B}+\mathbf{b}-\mathbf{A})\cdot(\mathbf{M}_k^A\tilde{\mathbf{a}}), \tag{12.7.4}$$

or in suffix notation,

$$\frac{\partial R}{\partial p_k^A} = -\frac{1}{R}(\mathbf{B}+\mathbf{b}-\mathbf{A})_\alpha(\mathbf{M}_k^A)_{\alpha\beta}\tilde{a}_\beta. \tag{12.7.5}$$

Next we need derivatives of the set of direction cosines $\hat{\mathbf{R}}\cdot\mathbf{W}_a$ between the intersite unit vector $\hat{\mathbf{R}}$ and the local axes $\mathbf{W}_a$ for site a. Using suffix notation, and working initially with the vector $\mathbf{R}$ rather than the unit vector $\hat{\mathbf{R}}$, we have

$$\begin{aligned} R_\alpha\mathbf{W}_{\alpha\beta}^a &= (B_\alpha + b_\alpha - A_\alpha - a_\alpha)\mathbf{M}_{\alpha\gamma}^A\widetilde{\mathbf{W}}_{\gamma\beta}^a \\ &= (B_\alpha + b_\alpha - A_\alpha)\mathbf{M}_{\alpha\gamma}^A\widetilde{\mathbf{W}}_{\gamma\beta}^a - \mathbf{M}_{\alpha\delta}^A\tilde{a}_\delta\mathbf{M}_{\alpha\gamma}^A\widetilde{\mathbf{W}}_{\gamma\beta}^a. \end{aligned} \tag{12.7.6}$$

In the last term, $(\mathbf{M}^A)_{\alpha\delta}(\mathbf{M}^A)_{\alpha\gamma} = \delta_{\delta\gamma}$, so this term becomes $\tilde{a}_\gamma\widetilde{\mathbf{W}}_{\gamma\beta}^a$ and is independent of the molecular orientation. Consequently

$$\frac{\partial}{\partial p_k^A}(R_\alpha\mathbf{W}_{\alpha\beta}^a) = (B_\alpha + b_\alpha - A_\alpha)(\mathbf{M}_k^A)_{\alpha\gamma}\widetilde{\mathbf{W}}_{\gamma\beta}^a. \tag{12.7.7}$$

The derivative of the scalar product $\mathbf{R}\cdot\mathbf{w}_b$ is different. Here we have

$$\begin{aligned}-R_\alpha \mathbf{W}^b_{\alpha\beta} &= -(B_\alpha + b_\alpha - A_\alpha - \mathbf{M}^A_{\alpha\gamma}\tilde{a}_\gamma)\mathbf{W}^b_{\alpha\beta}\\ &= -(B_\alpha + b_\alpha - A_\alpha)\mathbf{W}^b_{\alpha\beta} + \mathbf{M}^A_{\alpha\gamma}\tilde{a}_\gamma \mathbf{W}^b_{\alpha\beta}.\end{aligned} \tag{12.7.8}$$

This time the first term is constant with respect to rotation of A and the second term provides the derivative:

$$-\frac{\partial}{\partial p^A_k}(R_\alpha \mathbf{W}^b_{\alpha\beta}) = +(\mathbf{M}^A_k)_{\alpha\gamma}\tilde{a}_\gamma \mathbf{W}^b_{\alpha\beta}. \tag{12.7.9}$$

Similarly, for the derivatives with respect to rotation of B, we have

$$\begin{aligned}\frac{\partial}{\partial p^B_k}(R_\alpha \mathbf{W}^a_{\alpha\beta}) &= \frac{\partial}{\partial p^B_k}((B_\alpha + M^B_{\alpha\gamma}\tilde{b}_\gamma - A_\alpha - a_\alpha)\mathbf{W}^a_{\alpha\beta})\\ &= (M^B_k)_{\alpha\gamma}\tilde{b}_\gamma \mathbf{W}^a_{\alpha\beta},\end{aligned} \tag{12.7.10}$$

and

$$\begin{aligned}\frac{\partial}{\partial p^B_k}(-R_\alpha \mathbf{W}^b_{\alpha\beta}) &= -\frac{\partial}{\partial p^B_k}((B_\alpha - A_\alpha - a_\alpha)M^B_{\alpha\gamma}\widetilde{\mathbf{W}}^b_{\gamma\beta} + b_\alpha \mathbf{W}^b_{\alpha\beta})\\ &= -(B_\alpha - A_\alpha - a_\alpha)(M^B_k)_{\alpha\gamma}\widetilde{\mathbf{W}}^b_{\gamma\beta}.\end{aligned} \tag{12.7.11}$$

Eqns (12.7.7)–(12.7.11) provide derivatives of the scalar products $R_\alpha \mathbf{W}^a_{\alpha\beta}$ and $-R_\alpha \mathbf{W}^b_{\alpha\beta}$, but we need the scalar products with the unit vector $\hat{\mathbf{R}}$. For example,

$$\begin{aligned}\frac{\partial}{\partial p^A_k}(\hat{R}_\alpha \mathbf{W}^a_{\alpha\beta}) &= \frac{\partial}{\partial p^A_k}\left(\frac{1}{R}R_\alpha \mathbf{W}^a_{\alpha\beta}\right)\\ &= \frac{1}{R}\frac{\partial}{\partial p^A_k}(R_\alpha \mathbf{W}^a_{\alpha\beta}) - \frac{R_\alpha}{R^2}\mathbf{W}^a_{\alpha\beta}\frac{\partial R}{\partial p^A_k}.\end{aligned} \tag{12.7.12}$$

The derivative in the first term is given by eqn (12.7.7), and the derivative in the second term by eqn (12.7.5). Similarly, for the derivative with respect to rotation of B:

$$\frac{\partial}{\partial p^B_k}(\hat{R}_\alpha \mathbf{W}^a_{\alpha\beta}) = \frac{1}{R}(M^B_k)_{\alpha\gamma}\tilde{b}_\gamma \mathbf{W}^a_{\alpha\beta} - \frac{R_\alpha}{R^2}\mathbf{W}^a_{\alpha\beta}\frac{\partial R}{\partial p^B_k}. \tag{12.7.13}$$

Finally we need the derivatives of the direction cosines between the local axes of site a and those of site b. Again writing the local axis matrix for site a as $\mathbf{W}^a = \mathbf{M}^A\widetilde{\mathbf{W}}^a$, these direction cosines are the elements of the matrix

$$(\mathbf{W}^a)^T\mathbf{W}^b = (\mathbf{M}^A\widetilde{\mathbf{W}}^a)^T\mathbf{M}^B\widetilde{\mathbf{W}}^b, \tag{12.7.14}$$

where T denotes transpose, and the derivatives with respect to rotations of A are then just

$$\frac{\partial}{\partial p^A_k}(\mathbf{W}^a)^T\mathbf{W}^b = (\mathbf{M}^A_k\widetilde{\mathbf{W}}^a)^T\mathbf{M}^B\widetilde{\mathbf{W}}^b. \tag{12.7.15}$$

12.7.1 Angle-axis coordinates

We now need the derivatives $\mathbf{M}_k$ of the rotation matrices with respect to the orientation coordinates. We give here the case of angle-axis coordinates, following Chakrabarti and Wales (2009). Rotations are described by a vector $\mathbf{p}$, whose direction is the axis of rotation and whose magnitude is the rotation angle ψ (in radians). We define $\mathbf{n} = \mathbf{p}/\psi$, the unit vector in the direction of the rotation axis. Associated with the vector $\mathbf{n}$ is the matrix

$$\mathbf{N} = \begin{pmatrix} 0 & -n_3 & n_2 \\ n_3 & 0 & -n_1 \\ -n_2 & n_1 & 0 \end{pmatrix}, \tag{12.7.16}$$

so that $N_{ij} = -\epsilon_{ijk} n_k$. The rotation matrix corresponding to the rotation $\mathbf{p}$ is

$$\mathbf{M} = \mathbf{I} + \mathbf{N}^2(1 - \cos\psi) + \mathbf{N}\sin\psi, \tag{12.7.17}$$

where $\mathbf{I}$ is the identity matrix (Altmann 1986, p. 75).

Now $\psi = \sqrt{p_1^2 + p_2^2 + p_3^2}$, so $\partial\psi/\partial p_k = p_k/\psi = n_k$, and the derivative of the rotation matrix $\mathbf{M}$ with respect to the component p_k of $\mathbf{p}$ is

$$\mathbf{M}_k = \mathbf{N}^2 n_k \sin\psi + (\mathbf{N}_k\mathbf{N} + \mathbf{N}\mathbf{N}_k)(1 - \cos\psi) + \mathbf{N} n_k \cos\psi + \mathbf{N}_k \sin\psi, \tag{12.7.18}$$

where $\mathbf{N}_k$ is the derivative of $\mathbf{N}$ with respect to p_k:

$$\mathbf{N}_k = \frac{\partial}{\partial p_k}\mathbf{N} = \frac{\partial}{\partial p_k}\frac{1}{\psi}\begin{pmatrix} 0 & -p_3 & p_2 \\ p_3 & 0 & -p_1 \\ -p_2 & p_1 & 0 \end{pmatrix} = -\frac{n_k}{\psi}\mathbf{N} + \frac{1}{\psi}\begin{pmatrix} 0 & -\delta_{3k} & \delta_{2k} \\ \delta_{3k} & 0 & -\delta_{1k} \\ -\delta_{2k} & \delta_{1k} & 0 \end{pmatrix}. \tag{12.7.19}$$

When the rotation angle ψ is zero, $\mathbf{n}$ and the matrix $\mathbf{N}$ become undefined, but for small ψ,

$$\mathbf{M} = \mathbf{I} + \psi\mathbf{N} + \tfrac{1}{2}\psi^2\mathbf{N}^2 + O(\psi^3), \tag{12.7.20}$$

so the limit of $\mathbf{M}_k$ as $\psi \to 0$ is well defined:

$$\lim_{\psi\to 0}\mathbf{M}_k = \begin{pmatrix} 0 & -\delta_{3k} & \delta_{2k} \\ \delta_{3k} & 0 & -\delta_{1k} \\ -\delta_{2k} & \delta_{1k} & 0 \end{pmatrix}. \tag{12.7.21}$$

12.7.2 Torques

The torque on molecule A arising from its interaction with B is a vector with components $(-\partial U_{AB}/\partial\xi_X^A, -\partial U_{AB}/\partial\xi_Y^A, -\partial U_{AB}/\partial\xi_Z^A)$, where ξ_X^A etc. are rotations of A about axes through its centre parallel to the global coordinate directions $\mathbf{e}_X$ etc. To obtain the derivatives of the direction cosines, we use the operator

$$\frac{\partial}{\partial\xi_K} = \lim_{\xi\to 0}\frac{(\mathbf{M}(\xi\mathbf{e}_K) - \mathbf{I})}{\xi} = \begin{pmatrix} 0 & -\delta_{3K} & \delta_{2K} \\ \delta_{3K} & 0 & -\delta_{1K} \\ -\delta_{2K} & \delta_{1K} & 0 \end{pmatrix}. \tag{12.7.22}$$

Then from the first term on the r.h.s. of eqn (12.7.7) we get, for example,

Table 12.5 First derivatives of R and the scalar products $\mathbf{w}^a \cdot \mathbf{R}$, $\mathbf{w}^b \cdot \mathbf{R}$ and $\mathbf{w}^a \cdot \mathbf{w}^b$ (where $\mathbf{w}^a$ is $\mathbf{x}^a$, $\mathbf{y}^a$ or $\mathbf{z}^a$, and $\mathbf{w}^b$ similarly) with respect to the twelve external coordinates (translation and rotation) necessary to describe a pair of rigid interacting molecules. The differential operators are given in the left column and their arguments in the top row.

	R	$\mathbf{w}^a \cdot \mathbf{R}$	$\mathbf{w}^b \cdot \mathbf{R}$	$\mathbf{w}^a \cdot \mathbf{w}^b$
$\partial/\partial A_K$	$-\hat{R}_K$	$-w_K^a$	$-w_K^b$	0
$\partial/\partial\xi_K^A$	$(\hat{\mathbf{R}} \times \mathbf{a})_K$	$-[(\mathbf{R}+\mathbf{a}) \times \mathbf{w}^a]_K$	$(\mathbf{w}^b \times \mathbf{a})_K$	$(\mathbf{w}^a \times \mathbf{w}^b)_K$
$\partial/\partial B_K$	$\hat{R}_K$	w_K^a	w_K^b	0
$\partial/\partial\xi_K^B$	$-(\hat{\mathbf{R}} \times \mathbf{b})_K$	$-(\mathbf{w}^a \times \mathbf{b})_K$	$-[(\mathbf{R}-\mathbf{b}) \times \mathbf{w}^b]_K$	$-(\mathbf{w}^a \times \mathbf{w}^b)_K$

$$\frac{\partial}{\partial\xi_Z^A}(\mathbf{B}+\mathbf{b}-\mathbf{A}) \cdot \mathbf{x}^a = (\mathbf{B}+\mathbf{b}-\mathbf{A}) \cdot \begin{pmatrix} 0 & -1 & 0 \\ 1 & 0 & 0 \\ 0 & 0 & 0 \end{pmatrix} \mathbf{x}^a = -((\mathbf{B}+\mathbf{b}-\mathbf{A}) \times \mathbf{x}^a))_Z. \tag{12.7.23}$$

This approach, or the original method of Popelier and Stone (1994), leads to the derivatives of the q_i given in Table 12.5. Here $\mathbf{w}_a$ stands for $\mathbf{x}^a$, $\mathbf{y}^a$ or $\mathbf{z}^a$. Now the K component of the torque on A arising from the electrostatic interaction between sites a and b is

$$\begin{aligned} G_K^A &= -\frac{\partial}{\partial\xi_K^A} U^{AB} \\ &= -\sum_{ab} Q_t^a Q_u^b \frac{\partial}{\partial\xi_K^A} T_{tu}^{ab} \\ &= -\sum_{ab} Q_t^a Q_u^b \frac{\partial q_i}{\partial\xi_K^A} \frac{\partial}{\partial q_i} T_{tu}^{ab}. \end{aligned} \tag{12.7.24}$$

12.7.3 Second derivatives

We can compute all the second derivatives in a similar manner by consecutive applications of the chain rule. To evaluate the Hessian matrix element H_{KL}, that is, the second derivative of the energy U with respect to two external coordinates C_K and C_L, which may refer to the same molecule or to different ones, we have

$$\begin{aligned} \frac{\partial^2 U}{\partial C_K \partial C_L} &= \frac{\partial}{\partial C_K} \sum_j \frac{\partial U}{\partial q_j} \frac{\partial q_j}{\partial C_L} \\ &= \sum_i \sum_j \frac{\partial^2 U}{\partial q_i \partial q_j} \frac{\partial q_i}{\partial C_K} \frac{\partial q_j}{\partial C_L} + \sum_j \frac{\partial U}{\partial q_j} \frac{\partial^2 q_j}{\partial C_K \partial C_L}. \end{aligned} \tag{12.7.25}$$

Each term here is a product of a factor that is specific to the nature of the interaction and a factor that depends only on the geometry. The former set includes $\partial U/\partial q_i$, which is a first derivative and has already been calculated, and $\partial^2 U/\partial q_i \partial q_j$. The latter comprises the derivatives $\partial q_i/\partial C_K$, which have already been evaluated in the course of finding the forces and torques, and the $\partial^2 q_j/\partial C_K \partial C_L$, which like the first derivatives can be calculated analytically

once and for all. For angle-axis coordinates this requires the matrix $\mathbf{M}_{jk}$ obtained from a further differentiation of eqn (12.7.18):

$$\begin{aligned}\mathbf{M}_{jk} = {} & \mathbf{N}^2 n_{jk} \sin\psi + \mathbf{N}^2 n_j n_k \cos\psi + ((\mathbf{N}_j\mathbf{N} + \mathbf{N}\mathbf{N}_j)n_k + (\mathbf{N}_k\mathbf{N} + \mathbf{N}\mathbf{N}_k)n_j)\sin\psi \\ & + (\mathbf{N}_{jk}\mathbf{N} + \mathbf{N}_j\mathbf{N}_k + \mathbf{N}_k\mathbf{N}_j + \mathbf{N}\mathbf{N}_{jk})(1 - \cos\psi) + (\mathbf{N}_j n_k + \mathbf{N}_k n_j)\cos\psi \\ & - \mathbf{N} n_j n_k \sin\psi + \mathbf{N} n_{jk} \cos\psi + \mathbf{N}_{jk} \sin\psi, \end{aligned} \tag{12.7.26}$$

where

$$N_{jk} = \frac{\partial}{\partial p_j}\mathbf{N}_k = \left(\frac{2n_j n_k}{\psi^2} - \frac{n_{jk}}{\psi}\right) - \frac{n_j + n_k}{\psi^2}\begin{pmatrix} 0 & -\delta_{3k} & \delta_{2k} \\ \delta_{3k} & 0 & -\delta_{1k} \\ -\delta_{2k} & \delta_{1k} & 0 \end{pmatrix}, \tag{12.7.27}$$

and

$$n_{jk} = \frac{\partial}{\partial p_j} n_k = \frac{\partial}{\partial p_j}\frac{p_k}{\psi} = \frac{\delta_{jk} - n_j n_k}{\psi}. \tag{12.7.28}$$

Expressions for the second derivatives with respect to rotations about the global axis directions are given in Table 12.6. Note that these derivatives are not in general symmetric. As an example we see from Table 12.6 that $\partial^2(\mathbf{w}^b \cdot \mathbf{R})/\partial\xi_K^A\partial\xi_L^A = a_L w_K^b + \delta_{KL}(\mathbf{w}^b \cdot \mathbf{a})$, while $\partial^2(\mathbf{w}^b \cdot \mathbf{R})/\partial\xi_L^A\partial\xi_K^A = a_K w_L^b + \delta_{KL}(\mathbf{w}^b \cdot \mathbf{a})$. These expressions are clearly not the same unless $K = L$. In fact, all the rotation–rotation derivatives in Table 12.6 exhibit this asymmetry. This result, at first unexpected, is easily understood in terms of the infinitesimal rotation operators (angular momentum operators) $J_K = -\mathrm{i}\partial/\partial\xi_K$. These satisfy the familiar commutation relation $[J_K, J_L] = \mathrm{i}\epsilon_{KLM}J_M$. It follows that, for example,

$$\left(\frac{\partial}{\partial\xi_X}\frac{\partial}{\partial\xi_Y} - \frac{\partial}{\partial\xi_Y}\frac{\partial}{\partial\xi_X}\right)U = -\frac{\partial}{\partial\xi_Z}U = \tau_Z. \tag{12.7.29}$$

When the system is at a stationary point the rotation–rotation asymmetry disappears because the torques vanish. At such a point the diagonalized Hessian yields real eigenvalues and orthogonal eigenvectors, in line with the physics of normal modes. Elsewhere the Hessian is not symmetric, but optimization methods like the Cerjan–Miller method (Cerjan and Miller 1981) can still function if a symmetrized Hessian is used. This asymmetry in the rotation–rotation block has been previously observed in the context of isotropic electrostatic and Lennard-Jones potentials (Wales 1991).

12.7.4 Repulsion and dispersion

As we saw in §12.2.1 (eqn (12.2.5)), the repulsive potential between two molecules A and B is represented to good accuracy by the empirical expression

$$U_{\mathrm{rep}}^{AB} = K\sum_{a\in A}\sum_{b\in B}\exp[-\alpha^{ab}(\Omega^{ab})(R_{ab} - \rho^{ab}(\Omega^{ab}))]. \tag{12.7.30}$$

Here R_{ab} is the intersite distance, Ω^{ab} represents the set of orientational coordinates describing the relative orientation of the two sites a and b, $\alpha^{ab}(\Omega^{ab})$ describes the hardness of the repulsion as a function of orientation, and $\rho^{ab}(\Omega^{ab})$ is a sum of the effective radii of the sites. They are conveniently expanded in the set of $\overline{S}$ functions (see eqn (12.2.6)), which are polynomials in the direction cosines q_i. The derivatives of α^{ab} and ρ^{ab} are therefore easily determined

Table 12.6 Second derivatives of $\mathbf{R}\cdot\mathbf{R}$ and the scalar products $\mathbf{w}^a\cdot\mathbf{R}$, $\mathbf{w}^b\cdot\mathbf{R}$ and $\mathbf{w}^a\cdot\mathbf{w}^b$ (where $\mathbf{w}^a$ is $\mathbf{x}^a$, $\mathbf{y}^a$ or $\mathbf{z}^a$, and $\mathbf{w}^b$ similarly) with respect to the twelve external coordinates (translation and rotation) necessary to describe a pair of rigid interacting molecules. The summation convention is used here.

C \ C'	A_L	ξ^A_L	B_L	ξ^B_L
$\partial^2(\mathbf{R}\cdot\mathbf{R})/\partial C\partial C'$				
A_K	$2\delta_{KL}$	$2\epsilon_{KLJ}a_J$	$-2\delta_{KL}$	$-2\epsilon_{KLJ}b_J$
ξ^A_K	$-2\epsilon_{KLJ}a_J$	$-2(R_K+a_K)a_L$ $+2\delta_{KL}(\mathbf{R}+\mathbf{a})\cdot\mathbf{a}$	$2\epsilon_{KLJ}a_J$	$2a_Lb_K-2\delta_{KL}(\mathbf{a}\cdot\mathbf{b})$
B_K	$-2\delta_{KL}$	$-2\epsilon_{KLJ}a_J$	$2\delta_{KL}$	$2\epsilon_{KLJ}b_J$
ξ^B_K	$2\epsilon_{KLJ}b_J$	$2a_Kb_L-2\delta_{KL}(\mathbf{a}\cdot\mathbf{b})$	$-2\epsilon_{KLJ}b_J$	$2(R_K-b_K)b_L$ $-2\delta_{KL}(\mathbf{R}-\mathbf{b})\cdot\mathbf{b}$
$\partial^2(\mathbf{w}^a\cdot\mathbf{R})/\partial C\partial C'$				
A_K	0	$-\epsilon_{KLJ}w^a_J$	0	0
ξ^A_K	$\epsilon_{KLJ}w^a_J$	$(R_K+a_K)w^a_L$ $-\delta_{KL}(\mathbf{R}+\mathbf{a})\cdot\mathbf{w}^a$	$-\epsilon_{KLJ}w^a_J$	$-b_Kw^a_L+\delta_{KL}(\mathbf{w}_a\cdot\mathbf{b})$
B_K	0	$\epsilon_{KLJ}w^a_J$	0	0
ξ^B_K	0	$-b_Lw^a_K+\delta_{KL}(\mathbf{w}_a\cdot\mathbf{b})$	0	$b_Lw^a_K-\delta_{KL}(\mathbf{w}_a\cdot\mathbf{b})$
$\partial^2(\mathbf{w}^b\cdot\mathbf{R})/\partial C\partial C'$				
A_K	0	0	0	$-\epsilon_{KLJ}w^b_J$
ξ^A_K	0	$-a_Lw^b_K+\delta_{KL}(\mathbf{w}_b\cdot\mathbf{a})$	0	$a_Lw^b_K-\delta_{KL}(\mathbf{w}_b\cdot\mathbf{a})$
B_K	0	0	0	$\epsilon_{KLJ}w^b_J$
ξ^B_K	$\epsilon_{KLJ}w^b_J$	$a_Kw^b_L-\delta_{KL}(\mathbf{w}_b\cdot\mathbf{a})$	$-\epsilon_{KLJ}w^b_J$	$(R_K-b_K)w^b_L$ $-\delta_{KL}(\mathbf{R}-\mathbf{b})\cdot\mathbf{w}^b$
$\partial^2(\mathbf{w}^a\cdot\mathbf{w}_b)/\partial C\partial C'$				
A_K	0	0	0	0
ξ^A_K	0	$w^a_Lw^b_K-\delta_{KL}(\mathbf{w}^a\cdot\mathbf{w}^b)$	0	$-w^a_Lw^b_K+\delta_{KL}(\mathbf{w}^a\cdot\mathbf{w}^b)$
B_K	0	0	0	0
ξ^B_K	0	$-w^a_Kw^b_L+\delta_{KL}(\mathbf{w}^a\cdot\mathbf{w}^b)$	0	$w^a_Kw^b_L-\delta_{KL}(\mathbf{w}^a\cdot\mathbf{w}^b)$

by the methods already described, and the derivatives of the repulsive potential then require merely another application of the chain rule.

The atom–atom dispersion can be handled in the same way. The dispersion takes the form

$$U^{AB}_{\mathrm{disp}}=\sum_{a\in A}\sum_{b\in B}\left(f_6(R)\frac{C^{ab}_6(\Omega^{ab})}{R^6_{ab}}+f_7(R)\frac{C^{ab}_7(\Omega^{ab})}{R^7_{ab}}+\cdots\right),$$

where the $f_n(R)$ are damping functions (see §12.1.5), and the dispersion coefficients C_n can be expanded in terms of $\overline{S}$ functions. Differentiation of the dispersion coefficients follows the same procedure as for α^{ab} and ρ^{ab}, while the damping functions depend only on R.

12.7.5 Induction

Finally, we consider the induction energy, which is a more awkward term to handle. The calculation is based on eqn (9.4.16), which we write in the form

$$E^A_{\rm ind} = \tfrac{1}{2}\Delta Q^a_t V^a_t, \tag{12.7.31}$$

where the induced moments are given by eqn (9.4.12),

$$\Delta Q^a_t = -\sum_{B\neq A} \alpha^{aa'}_{tt'} T^{a'b}_{t'u}(Q^b_u + \Delta Q^b_u), \tag{12.7.32}$$

and V^a_t is the total field at site a due to the unpolarized moments of all the other molecules,

$$V^a_t = \sum_{B\neq A} T^{ab}_{tu} Q^b_u. \tag{12.7.33}$$

As usual, repeated suffixes imply summation. Calculation of the induction energy and its derivatives is then a two-stage process. The fields V^a_t at each site in each molecule, and their derivatives, are evaluated in the same loop over site pairs as the electrostatic terms, since they involve the same interaction functions T^{ab}_{tu}. The induced moments and their derivatives can also be evaluated in this loop, since (12.7.32) is also a sum over site pairs involving the same interaction functions. The polarizabilities $\alpha^{aa'}_{tt'}$, like the unpolarized multipole moments, are expressed in the local coordinate system for each site and are constant. The fields and induced moments are then combined at the end of the calculation to give the induction energy according to (12.7.31), and its derivatives are easily obtained by applying the formulae for differentiation of a product.

The difficulty in this procedure arises from the coupled form of (12.7.32). Each induced moment depends on the induced moments in all the other molecules, and its derivatives depend on the derivatives of the other moments. Several options are available. One is to use a first-order treatment, in which the induced moments on the r.h.s. of (12.7.32) are simply neglected. This is a good approximation when the molecules are not very polarizable or the electrostatic fields are relatively small. In this case the calculation is straightforward. The second option is to solve (12.7.32) iteratively. This is more time-consuming, though the process often converges in half a dozen or so iterations. For geometry optimizations, the convergence can be improved by using the induced moments from the previous step of the optimization, and their derivatives, in the r.h.s. of (12.7.32) and its derivatives. Indeed it is possible to do this without iterating at each step. In this case, the induced moments and their derivatives are slightly in error at each step, but as the optimization procedure approaches convergence the induced moments also converge to the correct final values. This means that the iterated version of eqn (12.7.32) can be used in a geometry optimization with virtually no additional effort. Unfortunately this method is not suitable for a molecular dynamics calculation, because it does not conserve the energy of the system, so it is necessary either to use the first-order approximation throughout, or to iterate the moments to convergence at every step. A third option, for a molecular cluster or a crystal, would be to solve (12.7.32) in the manner of the Applequist treatment (§9.1), which requires a matrix inversion but might be simpler and more efficient than the iterative procedure. Rewriting (12.7.32) gives

$$\left[(\alpha^{-1})^{ab}_{tu}\delta_{ab} + T^{ab}_{tu}(1-\delta_{ab})\right]\Delta Q^b_u = T^{ab}_{tu}(1-\delta_{ab})Q^b_u. \tag{12.7.34}$$

Here a and b are any two sites in the system, on the same or different molecules. For a distributed multipole treatment, α would be the complete polarizability matrix for a particular molecule, and δ_{ab} would be 1 if sites a and b were on the same molecule, zero otherwise. For an Applequist model, α would be the site polarizability and δ_{ab} would be 1 if $a = b$ and zero otherwise, as usual. For the derivatives, writing the matrix in square brackets in (12.7.34) as M, we have

$$M\frac{\partial \Delta Q^b_u}{\partial C} + \frac{\partial M}{\partial C}\Delta Q^b_u = \frac{\partial}{\partial C}\left(T^{ab}_{tu}(1-\delta_{ab})Q^b_u\right). \tag{12.7.35}$$

All the derivatives in this equation are already available at this point.

13
Theory and Experiment

For the most part, this account has concentrated on methods of calculating intermolecular interactions, either analytically or from *ab initio* computations. However, the purpose of such calculations is to make it possible to predict the behaviour of molecules, in small aggregates or in the bulk, and in principle a knowledge of intermolecular potentials should allow us to predict the outcome of any experiment on molecules that does not involve actual chemical reaction. Comparison of theory with experiment in cases where the result is known allows us to validate the theory and, in some cases, to calibrate unknown parameters. At one time, accurate information about intermolecular interactions depended entirely on experimental data, but only a few small systems can be treated reliably in this way, and intermolecular potential energy surfaces are no longer constructed directly from experimental data. Rather the starting point is *ab initio* calculation, and experimental data are used to provide a check on the calculations, to refine parameters in model potential energy surfaces fitted to the *ab initio* results, and to expose limitations in the potentials and the methods used to calculate observable quantities. In this chapter we survey the experimental techniques that are useful in the study of intermolecular potentials. The focus is not on the experimental techniques themselves, but rather on the theoretical methods that can be used to relate the observable quantities to the intermolecular potential energy surfaces. The increasing precision of experimental methods has set new challenges for theory, as summarized for example by Chałasiński and Szczęśniak (2000). This is not intended to be a detailed account; a fuller treatment may be found, for example, in Gray and Gubbins (1984) and Gray *et al.* (2011).

13.1 Properties of individual molecules

Although experimental data on intermolecular interactions are difficult to use in the construction of intermolecular potentials, an important source of data for intermolecular forces lies in the properties of isolated molecules. We have seen that at long range, the interactions between molecules can be described entirely in terms of such properties, so that methods of measuring them are of great importance.

13.1.1 Multipole moments

Dipole moments are usually obtained from measurements of the dielectric constant or from the Stark effect in rotational spectroscopy, where the absorption lines are split by the application of a static electric field, though McClellan (1963, 1974, 1989) lists a large number of other techniques in his tabulations of dipole moments. Many of these measurements give only the magnitude of the dipole moment, not its direction; in the case of the Stark effect, the experiment gives the magnitude, but not the sign, of the components of the dipole moment

along the inertial axes. Often *ab initio* calculation, or even chemical intuition based on electronegativity arguments, is accurate enough to give the sign reliably. One way to determine the sign independently uses the effect of isotopic substitution on the rotational magnetic moment (Townes *et al.* 1955), though this has rather large errors and in the case of ClF gave the wrong sign (Ewing *et al.* 1972, McGurk *et al.* 1973, Janda *et al.* 1976). (Jalink *et al.* 1987) used another method to determine the sign of the dipole moment of nitrous oxide, N_2O. They used an electric field to align the molecules in a molecular beam, or rather to focus only the molecules with a particular alignment, and observed the rate of reaction with barium atoms in a crossed beam. The rate increases when the N_2O molecules are aligned with the O atom leading, and it is possible to deduce the sign of the dipole moment from the direction of the field needed to cause an increase. It is also possible to deduce the sign from measurement of the dipole moment of a Van der Waals complex with another polar molecule if the structure of the complex and the sign of the dipole moment of the other molecule are known (Janda *et al.* 1976, Fowler and Stone 1987). A more direct approach is to use X-ray diffraction data for crystals, from which the electron density map can be determined. This gives the sign and magnitude of all the components. Spackman (1992) gave an account of the capabilities and limitations of this method. Since the electron distributions of the molecules overlap, it is necessary to partition the electron density obtained from X-ray diffraction between the molecules, and the moments assigned to the molecules are very dependent on how this is done. Partitioning based either on Bader's theory of atoms in molecules (Bader 1990) or Hirshfeld analysis (Spackman and Jayatilaka 2009) can be used. The electron density in the crystal is polarized by the fields of the neighbouring molecules, so that the dipole moments obtained in this way differ from those of the free molecules, sometimes substantially (Spackman *et al.* 2007).

The same technique can be used to determine quadrupole moments, and values have been reported for a number of molecules (Spackman 1992). Schnieders *et al.* (2009) have gone further, using a version of the AMOEBA polarizable electrostatic model in which the point multipoles are replaced by Gaussian multipoles (§8.1.1) and polarization by neighbouring molecules in the crystal is taken into account. Then the Fourier transform of the resulting charge density can be compared directly with the X-ray structure factors and the multipole description refined accordingly.

More accurate values of quadrupole moments are obtained from measurements of the induced birefringence (Buckingham 1967), that is, of the anisotropy in the refractive index induced by a non-uniform external electric field. In the non-uniform field of a two-wire cell (see Fig. 2.3), quadrupolar molecules in a gas become partially aligned. A molecule such as CO_2, for example, positioned midway between positively charged wires, will tend to lie with its molecular axis in the plane of the wires and perpendicular to them. Since its polarizability along the molecular axis ($\alpha_\parallel$) is greater than the component perpendicular to it ($\alpha_\perp$), the refractive index of the gas for light polarized in the plane of the wires will be slightly different from the refractive index perpendicular to the plane. The effect of this birefringence on a laser beam parallel to the wires can be measured; it is proportional to the quadrupole moment and to the polarizability anisotropy $\alpha_\parallel - \alpha_\perp$, so if the anisotropy is known, the quadrupole moment can be measured. For the field produced by a two-wire source, $F_{zz} = 0$ and $F_{xx} = -F_{yy}$, and the birefringence is

$$n_x - n_y = \frac{4\pi F_{xx}}{15}\Big(B_{\alpha\beta,\alpha\beta} + \frac{1}{kT}\alpha_{\alpha\beta}\Theta_{\alpha\beta}\Big). \tag{13.1.1}$$

The quantity $B_{\alpha\beta,\gamma\delta}$ in the temperature-independent term is the dipole–dipole–quadrupole hyperpolarizability. The temperature-dependent term involves a contraction of the quadrupole moment with the polarizability. Because the quadrupole moment is traceless, only the anisotropy of the polarizability enters this expression; for linear molecules $\alpha_{\alpha\beta}\Theta_{\alpha\beta} = (\alpha_\parallel - \alpha_\perp)\Theta_{zz}$. If $\alpha_\parallel - \alpha_\perp$is known, this technique provides both the magnitude and the sign of Θ_{zz}. Further details of the experimental technique and the underlying theory are given by Buckingham and Disch (1963). The use of the method to determine quadrupole moments of polar molecules raises the question of origin of coordinates; see the discussion on p. 42.

Methods for determining higher moments are indirect and not very accurate. One of the more reliable methods involves the study of the collision-induced infrared spectrum of the gas. In gaseous methane, for example, there is no allowed pure rotational spectrum for the isolated molecule, or for the gas at very low pressure, but at higher pressures there is an infrared spectrum whose intensity is proportional to the square of the density. This arises from interactions between pairs of molecules, each inducing fluctuating dipole moments in the other (Birnbaum and Cohen 1975, Joslin *et al.* 1985). The magnitude of the induced moments depends mainly on the molecular octopole and hexadecapole, in this case, so measurements of the intensity lead to values for these moments. They can be distinguished because the octopole moment is associated with rotational transitions with $\Delta J = 0, \pm1, \pm2$ and ±3, while the hexadecapole also leads to $\Delta J = \pm4$. The transitions are not resolvable because there are also translational contributions to the spectrum which broaden the lines, but from the frequency dependence of the spectrum the octopole and hexadecapole can be determined separately. However, the induced moments also depend on the polarizability and on the intermolecular potential—the latter because the magnitude of the induced moment is affected by the distance to which the molecules can approach. In fact Birnbaum and Cohen (1975) point out that the quantities determined from the spectrum are Ω^2/σ^7 and Φ^2/σ^9, where σ is the size parameter in the Lennard-Jones potential that they used, and Ω and Φ are the octopole and hexadecapole moments, Ω_{xyz} and Φ_{zzzz}. (Recall (§2.6) that there is only one independent non-vanishing component of each for a tetrahedral molecule.)

13.1.2 Polarizabilities

The dipole–dipole polarizability α can be measured by a variety of methods. The mean polarizability $\overline{\alpha}$ at frequency ω is related to the refractive index n at the same frequency by the Lorentz–Lorenz equation:

$$\frac{n^2-1}{n^2+2} = \frac{\rho\overline{\alpha}}{3\epsilon_0}, \tag{13.1.2}$$

where ρ is the number density. For a gas at low pressure, where $n \approx 1$, this becomes

$$n - 1 = \frac{\rho\overline{\alpha}}{2\epsilon_0}. \tag{13.1.3}$$

The polarizability $\overline{\alpha}(\omega)$ for the frequency at which the refractive index is measured will normally be different from the static electronic polarizability, though not very different if there are no low-lying absorption bands. Measurements of the dielectric constant also yield values of the polarizability, but these include a contribution from the movement of the nuclei under the influence of the electric field (the vibrational or 'atomic' polarizability) and this contribution can be quite large for molecules with low-frequency vibrations. Some typical values, taken

Table 13.1 Values of the mean polarizability (a.u.) at zero frequency and at a frequency ω of 15,800 cm^{-1}.

Molecule	$\alpha(0)$	$\alpha(\omega)$
CH_4	2.593	2.607
CF_4	3.84	2.85
C_6H_6	10.6	10.39
SF_6	6.56	4.50

from the book by Gray and Gubbins (1984) (a useful source of numerical values of multipole moments and polarizabilities) are given in Table 13.1.

Experimental data on electric-dipole absorption spectra can be used to obtain accurate values of mean polarizabilities. The average polarizability at frequency ω is, from eqn (2.5.8),

$$\overline{\alpha}(\omega) = \frac{1}{3}\alpha_{\alpha\alpha}(\omega) = \frac{2}{3}{\sum_n}' \frac{\omega_n \left|\langle 0|\hat{\boldsymbol{\mu}}|n\rangle\right|^2}{\hbar(\omega_n^2 - \omega^2)}, \tag{13.1.4}$$

and the numerator $\left|\langle 0|\hat{\boldsymbol{\mu}}|n\rangle\right|^2$ of each term is related to the intensity of the corresponding electric dipole transition. It is customary to define a dimensionless number called the *oscillator strength* of a transition by

$$f_n = \frac{2}{3}\frac{\hbar\omega_n}{E_\mathrm{h}}\frac{\left|\langle 0|\hat{\boldsymbol{\mu}}|n\rangle\right|^2}{e^2 a_0^2}. \tag{13.1.5}$$

Here E_h is the Hartree energy $e^2/4\pi\epsilon_0 a_0$. From a knowledge of the dipole oscillator strengths at all frequencies (the 'dipole oscillator strength distribution' (DOSD)), a number of properties can be determined. Other sources of information about oscillator strengths include molar refractivities and inelastic scattering cross sections of charged particles (Meath *et al.* 1981, Kumar and Thakkar 2010). It is useful to define a set of oscillator strength sums by

$$S_k = \sum_n f_n \left(\frac{\hbar\omega_n}{E_\mathrm{h}}\right)^k. \tag{13.1.6}$$

The Thomas–Reiche–Kuhn sum rule states that S_0 is equal to the number of electrons in the system, and this can be used as an additional constraint on the data, while comparison of eqns (13.1.4) and (13.1.5) shows that $S_{-2} = \overline{\alpha}(0)/4\pi\epsilon_0 a_0^3$, numerically equal to the mean static polarizability in atomic units.

The polarizability as a function of real frequency has singularities at every absorption frequency, according to eqn (13.1.4), and although the singularities are moved off the real axis when the finite lifetime of the excited states is taken into account (see eqn (2.5.10)), the polarizability is still strongly frequency-dependent near absorption frequencies. However, these singularities are all near the real axis, and the polarizability as a function of imaginary frequency is very well-behaved, as we saw in §4.3.2. Consequently it can be accurately represented in terms of oscillator strengths and transition frequencies, and is much less sensitive to errors in these quantities than the polarizability at real frequencies. In fact, it is possible

to represent the polarizability at imaginary frequency to good accuracy in terms of 'pseudo dipole oscillator strength distributions':

$$\overline{\alpha}(iv) = 4\pi\epsilon_0 a_0^3 \frac{{E_\mathrm{h}}^2}{\hbar^2} \sum_{k=1}^{N} \frac{\tilde{f}_k}{\tilde{\omega}_k^2 + v^2}, \tag{13.1.7}$$

where the parameters $\tilde{f}_k$ and $\tilde{\omega}_k$ are chosen to fit the experimental DOSD. Usually a good fit can be found with quite a small number of parameters; $N = 10$ is typical (Kumar and Meath 1992).

The importance of this approach to the determination of polarizabilities at imaginary frequency is that it provides a route to accurate values of isotropic C_6 dispersion coefficients, via eqn (4.3.11). Moreover it is just as easily applied to interactions between unlike molecules; most experimental methods for determining interactions between unlike systems are difficult and inaccurate. The method can also be used to calculate C_9 triple-dipole dispersion coefficients, using eqn (10.2.4). The method was first used by Dalgarno and Lynn (1957*b*), and applied to the inert gases, to some spherical ions, and to a number of small molecules to obtain values of the C_6 dispersion coefficients, both for like and unlike pairs (Dalgarno 1967). Meath and his collaborators (Jhanwar and Meath 1982, Kumar and Meath 1992, Kumar and Thakkar 2010) have used the method extensively to determine dipole oscillator strength distributions for a number of atoms and small molecules, and have given values of polarizabilities, C_6 dispersion coefficients and C_9 triple-dipole dispersion coefficients.

It is possible to obtain the anisotropic terms in the same way if the polarization associated with each oscillator strength can be determined. For a linear molecule, separate oscillator-strength distributions are needed for transitions polarized parallel and perpendicular to the molecular axis. Meath and Kumar (1990) determined these distributions for N_2 and H_2, and derived anisotropic C_6 coefficients for interactions involving these molecules and the inert gases. CO, O_2 and NO have been treated similarly (Kumar and Meath 1994, Kumar *et al.* 1996, Bundgen *et al.* 1997).

13.2 Validation of intermolecular potentials by experimental methods

The determination of the intermolecular potential, as distinct from the constants that enter the long-range part of the potential, is a much more difficult matter. The experiments are all to a greater or lesser degree indirect; that is, they do not measure the potential itself, but some property that in turn depends on the potential. This dependence invariably involves some sort of configurational average, so that it is very difficult to work back from the measurement to the potential. Instead it is usual to assume some more or less plausible functional form for the potential, and to adjust the parameters in that by reference to the experimental data. If this is to be successful, the functional form that is chosen must be a realistic one, but it cannot contain too many adjustable parameters if numerical instabilities are to be avoided. The traditional source of data for this type of approach consists of measurements on the physical properties of gases, but in recent years spectroscopy of small molecular clusters has proved very fruitful, especially for the region near the minimum of the potential surface, while simulation of fluids by molecular dynamics or Monte Carlo techniques has become very widely used.

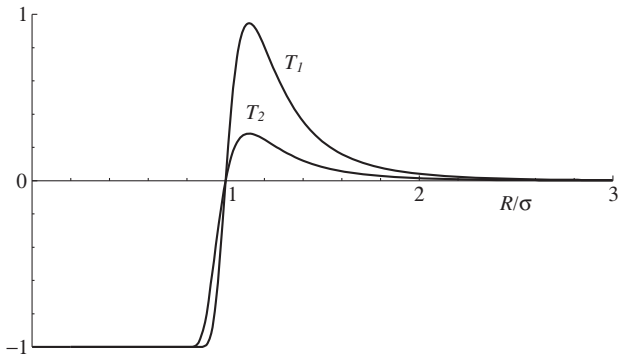

Fig. 13.1 The Mayer f-function for a Lennard-Jones potential at temperatures $T_1 = 1.5\epsilon/k$ and $T_2 = 4\epsilon/k$, as a function of $R^* = R/\sigma$.

13.2.1 The virial coefficient

One of the classical sources of data about intermolecular potentials is the second (pressure) virial coefficient. The quantity PV/RT is 1 for an ideal gas and for real gases at the limit of zero density, but at finite densities it deviates from this value, and we can describe this by an expansion in powers of the density, or inverse powers of the molar volume V. The coefficients in this expansion depend on the temperature:

$$\frac{PV}{RT} = 1 + \frac{B(T)}{V} + \frac{C(T)}{V^2} + \cdots . \tag{13.2.1}$$

$B(T)$ is the second virial coefficient, and an expression for it can be obtained from statistical mechanics (McQuarrie 1976). It depends rigorously on the pair potential only, even if many-body terms occur in the total energy. For atoms:

$$B(T) = -2\pi N_A \int_0^\infty [\exp(-U(R)/kT) - 1]R^2 \, \mathrm{d}R. \tag{13.2.2}$$

The quantity in square brackets here is the *Mayer f-function*, $f(R)$. Its radial dependence is illustrated for a Lennard-Jones potential in Fig. 13.1 for two temperatures, $kT = 1.5\epsilon$ and $kT = 4\epsilon$. At all temperatures, $f(R) = -1$ when $R = 0$, passes through zero when $R = \sigma$ to a maximum at $R = R_m$ and then decays to zero. The virial coefficient is an integral of this over all space, i.e., over all positions of a second atom. It is negative at low temperature, where the positive tail of $f(R)$ dominates, and positive at high temperatures, where the small-R region wins. The temperature T_B at which the virial coefficient is zero is called the Boyle temperature.

For atoms, the virial coefficient, as a function of temperature, is an integral transform of the Mayer function, and it is possible in principle to invert this transform to recover the Mayer function, and hence the potential, from measurements of the virial coefficient over a range of temperatures. More detailed investigation has revealed (Keller and Zumino 1959, Frisch and Helfand 1960) that inversion of the virial coefficient yields only the width of the well as a function of depth, though the region where the potential is positive can be determined uniquely. In practice $B(T)$ cannot be measured accurately enough or over a wide enough temperature range. Moreover the formula is a classical one which requires correction for quantum

effects. Maitland *et al.* (1981) give a detailed discussion. For molecules, the virial coefficient is again an integral of the Mayer function over all positions of the second molecule, but now it takes six coordinates (a distance and five angles) to describe the position of the second molecule relative to the first, if both are non-linear. Consequently the virial coefficient is a six-dimensional integral, and there is no hope of inverting virial coefficient data to obtain the potential. Moreover the experimental measurement of the virial coefficient is difficult, being subject to systematic errors that are hard to avoid, and in the compilation of virial coefficient data for water by Harvey and Lemmon (2004) values calculated from an accurate *ab initio* potential are considered more reliable than the limited high-temperature experimental data. The comparison of values of the mixed water–nitrogen second virial coefficient calculated by Wheatley and Lillestolen (2009) with the very scattered experimental values suggests that here too the calculations are more reliable than the experiments.

Nevertheless, virial coefficient data provide an important test of a potential. The virial coefficient depends rigorously on the pair potential only, and contains no contributions from three-body corrections. These appear in the third virial coefficient C, which involves a similar integration over all configurations of three molecules, while the four-body terms first appear in the fourth virial coefficient, and so on. Accurate measurement of C is even more difficult than B, and because the pair-potential terms appear in the expression for C as well as the three-body terms, it has not so far proved possible to extract useful three-body data from this source.

13.2.2 Transport coefficients

The viscosity, thermal conductivity and diffusion coefficient of a gas at low pressure also depend only on the pair potential, but like the second virial coefficient they can usually be used only to gauge the validity of a given potential and not to determine it in the absence of other information. They involve a more complicated sequence of integrations than the virial coefficient. For example, the thermal conductivity λ of a monatomic gas may be expressed in the form

$$\lambda = \frac{75}{64}\left(\frac{k_B^3 T\pi}{m}\right)^{1/2}\left(\overline{\Omega}^{(2,2)}(T)\right)^{-1} f_\lambda, \tag{13.2.3}$$

where m is the molecular mass, $\overline{\Omega}^{(2,2)}(T)$ is a 'collision integral' and f_λ is a correction factor that normally differs from unity by only 1 or 2 per cent. The collision integrals are defined by

$$\overline{\Omega}^{(2,2)}(T) = \frac{1}{6(k_B T)^4}\int_0^\infty Q^{(2)}(E)\mathrm{e}^{-E/k_B T}E^3\ \mathrm{d}E, \tag{13.2.4}$$

where E is the relative kinetic energy of a collision between two atoms and $Q^{(2)}(E)$ is the 'transport cross-section', given by

$$Q^{(2)}(E) = 3\pi\int_0^\infty (1-\cos^2\chi)b\ \mathrm{d}b. \tag{13.2.5}$$

Here χ is the classical deflection angle for a collision with energy E and impact parameter b (see §13.5):

$$\chi(E,b) = \pi - 2b\int_{R_0}^\infty \frac{dR}{R^2\sqrt{1-b^2/R^2-U(R)/E}}, \tag{13.2.6}$$

where $U(R)$ is the interatomic potential and R_0 is the distance of closest approach in the collision.

The viscosity can be expressed in terms of the same collision integrals:

$$\eta = \frac{5}{16}\left(m\pi k_B T\right)^{1/2}\left(\overline{\Omega}^{(2,2)}(T)\right)^{-1} f_\eta, \tag{13.2.7}$$

where f_η, like f_λ, is a correction factor close to unity. The self-diffusion coefficient D can be expressed in a similar way but involves a different collision integral. For full details the reader is referred to Hirschfelder *et al.* (1954) or Maitland *et al.* (1981).

In spite of the complexity of this formulation, it is possible to use it in reverse to determine the potential for monoatomic gases from viscosity or thermal conductivity data. The procedure is iterative, but converges rapidly if the first guess at the potential function has the correct well depth (Maitland *et al.* 1981).

Methods of this sort have been important in the past in determining accurate potentials for inert gases, where the potential depends on one coordinate only, but they are much less useful for studying interactions between molecules. The difficulty in applying them to molecules is two-fold: the calculation of the physical property from the potential is very much more difficult, because of the orientation dependence of the interaction potential, and there is the complication of inelastic collisions, where energy is transferred to or from the rotational and vibrational degrees of freedom of the molecules. In any case the experimental data do not provide enough information to characterize the many-dimensional potential surface. The usual practice nowadays is to carry out molecular dynamics calculations (see §13.3) with a trial potential, and to use the transport coefficients and other properties derived from the simulation to assess the quality of the potential.

13.3 Simulation methods

Some properties of liquids as well as gases can be calculated by the methods of analytical statistical mechanics (McQuarrie 1976), but generally it is necessary to assume that the interaction potential depends only on the separation. It is now usual to calculate such properties by computer simulation methods, in which a collection of molecules in an imaginary box is allowed to interact under the influence of a potential. A random configuration of the molecules is chosen initially, and then either a sequence of new configurations is generated randomly (Monte Carlo method) or the classical equations of motion of the system are integrated numerically (molecular dynamics method). The only limitation on the potential is that it must be possible to compute the energy of an arbitrary configuration of the molecules, and also, for molecular dynamics, the forces and torques on the molecules. In either case the system is initially allowed to reach equilibrium, after which a sequence of configurations is collected and the appropriate averages calculated. A detailed account of simulation methods is beyond the scope of this book, but the book by Allen and Tildesley (1987) provides an excellent introduction to the field.

It is usual to apply periodic boundary conditions, in which the imaginary box of molecules is replicated infinitely many times in all directions, so that the box can be considered as being immersed in an infinite medium. The calculation is still only carried out with the original finite box, but molecules leaving at one side are replaced by their images at the opposite side, and molecules near a side of the box interact with images of molecules at the opposite side,

so there are no surface effects. There may however be artefacts arising from the periodicity of the arrangement. A recent development is the construction of a computer, called Anton, using hardware specifically designed to carry out molecular mechanics simulations at very high speed (Shaw *et al.* 2008), but the speed is obtained at the cost of limiting the potential model to the specific form of eqn (12.3.1).

In the Monte Carlo treatment, it is usual to use the Metropolis method of sampling. Here a new configuration is obtained randomly, usually by changing some of the coordinates by small amounts, and its energy is computed. If the new energy is lower than the previous energy the new configuration is retained, while if it is higher by an amount ΔE it is retained with probability $\exp(-\Delta E/kT)$ and otherwise rejected. A retained configuration becomes the reference for the next trial. It can be shown that this procedure leads to a Boltzmann distribution for temperature T if continued for long enough. The retained configurations are used as the basis for the averaging.

One useful property of a fluid is the radial distribution function, which for atom types a and b is evaluated as the ratio of the probability $g_{ab}(r)$ of finding a b atom in an element of volume dV at a distance r from an a atom, to the mean probability of finding a b atom in an element dV anywhere in the system. Then $g_{ab}(r)$ for a fluid is zero for short distances, and typically has a peak at a distance corresponding to the first shell of b neighbours around a atoms, followed by a few lower peaks corresponding to further shells, before reaching a limit of 1 at larger r. The area under the first peak is the number of b atoms in the first shell, i.e. the coordination number. The shape of the radial distribution function is quite sensitive to details of the interaction potential, so it is often used as a guide to the validity of the potential. Unfortunately agreement between the calculated and experimental $g(r)$ does not guarantee that the potential is correct, while any discrepancies are not readily translated into improvements in the potential. For example, the first peak in the radial distribution function for the Cl atoms in liquid Cl_2 is asymmetric, with a shoulder to larger r that could not be explained in terms of any simple potential. Agreement with experiment was only obtained with a potential that took account of the non-spherical shape of the Cl atoms (Rodger *et al.* 1987).

Transport coefficients can be obtained from time correlation functions, which can be calculated using molecular dynamics. The time correlation function $C_{PQ}(t)$ for properties P and Q is $\langle P(0)Q(t)\rangle / \sqrt{\langle P(0)^2\rangle\langle Q(0)^2\rangle}$, where the angle brackets denote ensemble averages. If P and Q are the same, $C_{PP}(t)$ is called an autocorrelation function, and its time integral from 0 to ∞ is the correlation time for property P. The diffusion coefficient D is related to the correlation time for the velocity:

$$D = \frac{1}{3}\int_0^\infty \langle \mathbf{v}_i(0)\cdot\mathbf{v}_i(t)\rangle \,\mathrm{d}t, \tag{13.3.1}$$

where $\mathbf{v}_i$ is the velocity of molecule i. In practice this would be averaged over the molecules in the system. The viscosity can be obtained in a similar way from the time correlation functions of the pressure tensor (Allen and Tildesley 1987). This approach is conceptually much simpler than the analytical methods described in the previous section, but there are statistical uncertainties in quantities calculated by simulation that need to be estimated carefully.

A widely used simulation method is the Car–Parrinello molecular dynamics technique (Car and Parrinello 1985), in which the motion of the nuclei is handled classically, but the energy and forces at each configuration of the system are found by solving the electronic problem 'on the fly' using density functional theory. It was initially used for systems in which the

electronic structure is sensitive to the nuclear geometry—generally ones with loosely bound valence electrons—but it is now used for a wide range of applications, in particular for cases involving closed-shell molecules where the interaction is conventionally regarded as intermolecular or Van der Waals in nature rather than chemical reaction. Marx and Hutter (2009) have given a good account of the method, with emphasis on the CPMD computer program, which uses a plane-wave basis set for the valence electrons and pseudopotentials to account for the core electrons. At present such methods suffer from the usual problem with DFT, namely the failure to describe the dispersion energy, though this is being addressed both by methods that add an empirical dispersion term and by the use of non-local density functionals. Difficult problems such as crystal structure prediction are already being tackled successfully in this way, though the computational cost is high.

An alternative is to use a classical potential but to deal with quantum effects by using Feynman path integral methods (Feynman and Hibbs 1965, Berendsen 2007). It can be shown that a thermal quantum particle is isomorphic to a ring of n fictitious classical particles ('beads') connected by harmonic springs—a *ring polymer* (Ceperley 1995, Chakravarty 2005). Each bead interacts with the rest of the system in the same way that the original particle would. The number of beads should be at least $\hbar\omega_{\max}/kT$, where $\omega_{\max}$ is the maximum frequency present in the problem. For H atoms, where quantum effects are most significant, $\omega_{\max}$ is of the order of $4000\,\mathrm{cm}^{-1}$, while at ambient temperature $kT \sim 200\,\mathrm{cm}^{-1}$, so n needs to be at least 20. In practice up to 40 beads may be required for a converged simulation, and more at lower temperatures. Since the simulation has to follow all the beads in the ring polymer, this implies an increase in computational time by a factor of the order of n. However, Markland and Manolopoulos (2008*a*,*b*) have shown that far fewer beads are needed for the more slowly varying parts of the potential—sometimes only one. Fanourgakis *et al.* (2009) showed that the same idea can be applied to polarizable potentials, and that the overall increase in computational cost over a conventional classical simulation is less than an order of magnitude.

13.4 Spectroscopic methods

The most important source of accurate data on intermolecular potentials is undoubtedly spectroscopy. Early progress in this area is illustrated by the Faraday discussion on the structure and dynamics of Van der Waals complexes (*Faraday* 1994), and by the review issues of *Chemical Reviews* on Van der Waals molecules (*Chemical Reviews* 1988, 1994, 2000), while more recent developments include chirped microwave pulse Fourier transform spectroscopy (Brown *et al.* 2008) and the use of state-to-state vibrational predissociation measurements with velocity map imaging to measure dissociation energies D_0 (Li *et al.* 2006), including an accurate value at last for the dissociation energy of the water dimer (Rocher-Casterline *et al.* 2011).

One long-standing technique is molecular beam microwave spectroscopy. The use of a molecular beam offers many advantages: the effects of collisions with other molecules are virtually eliminated, and the very low rotational–vibrational temperature (typically a few K) means that only a few rotational levels are occupied. This technique was pioneered by Klemperer and refined by Flygare, and has been used by them and many others to determine the microwave spectra of a wide variety of weakly bound molecular complexes. From these spectra the rotational constants can be obtained, and by using Stark spectroscopy it is possible to measure the magnitude of the components of the dipole moment of the complex along one or more of the inertial axes. A more recent development is the chirped microwave pulse Fourier

transform spectrometer (Brown *et al.* 2008), which uses a microwave pulse that varies linearly in frequency from 7 to 18 GHz over the pulse length of 1 μs. The wide frequency range and high resolution makes it possible to observe spectra in great detail very efficiently. If the molecules contain quadrupolar nuclei such as nitrogen or chlorine, there may be hyperfine splittings in the spectra that can be used to determine further features of the structure (Stephens *et al.* 2011).

The disadvantage of rotational microwave spectroscopy is that it yields averaged information for the vibrational ground state. The potential energy surface of a weakly bound complex is often very complex, with shallow minima separated by low barriers. There are numerous low-frequency vibrations, often anharmonic and large-amplitude, and the low barriers lead to tunnelling splittings. The structure that emerges from microwave spectroscopy is averaged over these large-amplitude vibrations, and so may give a quite misleading picture of the complex. In such cases, much more information can be obtained from far-infrared spectroscopy ('vibration–rotation–tunnelling' or FIR-VRT spectroscopy), where the energy levels depend on the details of the potential energy surface far from the minima. The development of tunable far-infrared lasers and sensitive detectors has made it possible to obtain detailed information on potential energy surfaces (Saykally and Blake 1993).

Molecular beam vibrational spectroscopy can be used to measure dissociation energies (D_0) of complexes. The method involves vibrational predissociation: that is, an internal vibrational mode of one of the molecules in the complex is excited (for example the donor HF stretch in HF dimer) and the vibrational energy becomes redistributed among the intermolecular modes, so that the complex dissociates. By observing the rotational states of the fragments and their kinetic energy, the dissociation energy is obtained as the difference between the vibrational excitation energy and the energy carried away by the fragments. The dissociation energy D_0 of HF dimer was found in this way to be $1065 \pm 5\,\mathrm{cm}^{-1}$ (Dayton *et al.* 1989). Complexes of polyatomic molecules are more difficult, as some of the initial vibrational energy can end up in lower-energy vibrational modes of the monomers, and the rotational spectrum may be more complicated, but Rocher-Casterline *et al.* (2011) were able to measure D_0 for a number of complexes, including water dimer, for which $D_0 = 1105 \pm 10\,\mathrm{cm}^{-1}$ ($13.2 \pm 0.12\,\mathrm{kJ\,mol}^{-1}$).

Systems that have been studied using spectroscopy include Ar···DCl, for which Hutson (1992) determined an accurate potential energy surface using microwave, FIR-VRT and mid-infrared data. This system has a global minimum about $170\,\mathrm{cm}^{-1}$ deep at the hydrogen-bonded geometry (Ar···HCl), and a secondary minimum about $145\,\mathrm{cm}^{-1}$ deep at the linear Ar···ClH configuration. Hutson's potential predicts the energy levels extremely accurately, though Elrod *et al.* (1993) found small inaccuracies in the description of the secondary minimum.

Other systems where detailed potential energy surfaces have been obtained from far infrared spectroscopy include Ar···H_2O (Cohen and Saykally 1993), Ar···H_3N (Schmuttenmaer *et al.* 1994), Ar···CO_2 (Hutson *et al.* 1996) and Ar···H_2 (Bissonnette *et al.* 1996). In these systems there is no first-order electrostatic interaction, and the binding is due to a balance between induction, dispersion and repulsion. As Saykally and Blake (1993) have pointed out, the anisotropy of the repulsion is particularly important in determining the structure. A combination of spectroscopic and other experimental data may be needed for a full characterization of the potential. For example, the work on Ar···H_2 cited above used virial coefficients and vibrational transition pressure-shifting coefficients as well as the spectroscopic data.

As with other methods, the experimental data are not usually enough to determine the potential energy surface directly. It is more usual to compare the data with calculated spectra using a potential energy surface, either empirical or *ab initio*, and to refine the potential until agreement is obtained.

Goldman *et al.* (2002, 2005) used FIR-VRT spectroscopy to refine the parameters in the ASP-W *ab initio* potential (§12.4.1). The calculation of the spectrum is much less straightforward than for ordinary semi-rigid molecules, where all the vibrational motion takes place in a small region around the equilibrium geometry. In water dimer there are eight equivalent minima: any of the four H nuclei may occupy the hydrogen bond, and for each of these the H nuclei in the acceptor may be exchanged. The barriers between the minima are low, so all are accessible, and the potential energy surface has a rather complicated structure (Wales 2003). The symmetry group for systems such as this comprises permutations of identical nuclei, possibly combined with the inversion of the whole system in the centre of mass, and the energy levels can be classified under this group. The line splittings in the spectrum give information about the barrier heights. Wormer and van der Avoird (2000) have given a detailed account of the methods used to calculate the spectrum from the potential energy surface, for this and other Van der Waals complexes. Other water clusters up to the hexamer have been studied in the same way (Saykally and Wales 2012). In the case of the hexamer, there are several possible structures, of which the lowest-energy ones, usually called the cage, prism and book isomers, are very close in energy according to theoretical calculations (p. 185). Pérez *et al.* (2012), using chirped microwave pulse Fourier transform spectrometry, were able to obtain the rotational spectra of cage, prism and book isomers of the water hexamer, which were all seen in the same molecular beam, together with the octamer and nanomer, and to identify the cage as the lowest in energy.

An interesting puzzle was presented by the ammonia dimer, studied by Nelson *et al.* (1985) using rotational spectroscopy. They interpreted their results in terms of a structure in which the NH_3 symmetry axes were nearly, but not quite, antiparallel, aligned at angles of 48.6° and 64.5° to the line joining centres of mass. This structure was quite different from the expected classical hydrogen-bonded structure, which was also predicted by *ab initio* calculation. It appeared to explain the observed dipole moment of the dimer, much smaller, at 0.75 D, than the value of 1.47 D for a single NH_3 molecule, but it did not explain why there was apparently a barrier preventing passage through the symmetrical structure (both molecules tilted at about 57°) to an equivalent geometry with the dipole in the opposite direction. Since only a small displacement separated the two equivalent geometries, a very low barrier would be expected. The *ab initio* calculations find a very small barrier between the classical structure where one NH_3 is the proton donor and the structure in which the other NH_3 takes that role.

The puzzle was only solved 10 years later (Van der Avoird *et al.* 1994). The key lay in the realization that the states could be classified in terms of approximate quantum numbers k_A and k_B for the rotation of the monomers about their respective symmetry axes. The monomer states can be labelled as *ortho* ($|k| = 0 \bmod 3$) and *para* ($|k| \neq 0 \bmod 3$). If both molecules are *ortho* or both *para*, the states are symmetric or antisymmetric between the two molecules, the dipole moment is zero, and no rotational spectrum is observed. If one is *ortho* and the other *para*, however, there is an asymmetry that leads to a small non-zero dipole moment. Using a model that took account of the full symmetry of the problem, Olthof *et al.* (1994) were able to account for the spectrum in detail. This example shows that a conflict between an *ab initio*

calculation of the potential energy surface and experiment does not necessarily mean that one or the other is wrong; it may mean that the calculation of the spectrum from the potential is inadequate.

It is also possible to use infrared spectroscopy at more conventional frequencies, by observing combination bands between the intermolecular and intramolecular vibrations, or by studying the changes in frequency and rotational structure of the intramolecular bands on complex formation. The early work involved conventional gas-phase absorption spectroscopy with very long path lengths (Watanabe and Welsh 1964, McKellar 1994), but most later work has used molecular beam spectroscopy. This method has been used to study the intermolecular vibrational modes in $(HF)_2$ and $(DF)_2$ (Nesbitt 1994) and in Ar_nHF (McIlroy *et al.* 1991, McIlroy and Nesbitt 1992), where in conjunction with far infrared vibration–rotation–tunnelling spectroscopy (Elrod *et al.* 1991, 1993) it provides accurate information about many-body terms in the potential (see Chapter 10).

13.4.1 Rotational Rydberg–Klein–Rees method

In a few favourable cases, the spectroscopic measurements can be used directly to determine the intermolecular potential. The method is a version of the RKR method for determining the potential function for a diatomic molecule. This is a semi-classical procedure that uses the Bohr quantization condition:

$$\frac{\sqrt{2\mu}}{\hbar}\int_{a_{vJ}}^{b_{vJ}}[E(v,J)-V(R;J)]^{1/2}\,\mathrm{d}R=\left(v+\tfrac{1}{2}\right)\pi, \tag{13.4.1}$$

where a_{vJ} and b_{vJ} are the classical turning points of the vibrational motion in the state with vibrational quantum number v and rotational quantum number J, and $V(R;J)$ is the effective vibrational potential in rotational state J:

$$V(R;J)=V(R)+\frac{J(J+1)}{2\mu R^2}. \tag{13.4.2}$$

The standard RKR treatment (Child 1991) leads to the formulae

$$b_{vJ}-a_{vJ}=\frac{2\hbar}{\sqrt{2\mu}}\int_{-1/2}^{v}\frac{dv'}{[E(v,J)-E(v',J)]^{1/2}},$$

$$\frac{1}{a_{vJ}}-\frac{1}{b_{vJ}}=\frac{2\sqrt{2\mu}}{\hbar}\int_{-1/2}^{v}\frac{B(v',J)dv'}{[E(v,J)-E(v',J)]^{1/2}},$$

where $B(v,J)$ is the generalized rotational constant:

$$B(v,J)=\frac{1}{2J+1}\left(\frac{\partial E}{\partial J}\right)_v.$$

This treatment normally relies on information about rotational levels of a series of vibrational states. Nesbitt *et al.* (1989) and Nesbitt and Child (1993) showed that a similar method can be used when the rotational levels are available only for a single vibrational state. It relies on centrifugal stretching data to supply the missing information, so it needs high-precision rotational energy levels. Furthermore it can be used not just for atom–atom potentials but for

complexes such as Ar···HF and N_2···HF, which are linear and relatively stiff; in this case the method provides a radial potential that is averaged over the angular motions. For most Van der Waals molecules, unfortunately, the angular motions are very floppy and strongly coupled to the radial motion, so an average radial potential is not very helpful in understanding the details of the potential energy surface.

13.4.2 Atom–diatom clusters

Usually, therefore, the determination of potential energy surfaces from spectroscopic data involves the calculation of energy levels from a postulated potential energy surface, which is then modified iteratively to bring the calculated levels into agreement with experiment (Le Roy and Van Kranendonk 1974). This is a difficult calculation, but where it can be carried out it gives high-quality information about the potential energy surface. In the most favourable cases, such as Ar···HCl, the potential surface obtained this way is believed to be very accurate (Hutson 1992).

Systems like this, comprising an atom and a diatomic molecule, are the simplest Van der Waals complexes where orientation-dependent potentials arise, but they will serve to illustrate the methods used and the approximations needed to determine the energy levels from the potential energy surface.

We follow the notation of Hutson (1990*b*), which should be consulted for further details. The position of the atom A relative to the centre of mass of the diatomic molecule B is described by the vector $\mathbf{R}$, or (R,β,α) in space-fixed polar coordinates. We can define a body-fixed axis system with its z axis in the direction of $\mathbf{R}$; the x and y axes of this system are arbitrary. The vector from one atom of the diatomic to the other is $\mathbf{r}$, or (r,θ,φ) in polar coordinates referred to the body-fixed frame. Consequently r is the bond-length, and θ is the angle between $\mathbf{r}$ and $\mathbf{R}$.

The Hamiltonian for the system is now

$$\begin{aligned}\mathcal{H} &= -\frac{\hbar^2}{2\mu}\nabla_R^2 + \mathcal{H}_B + V(\mathbf{R},\mathbf{r}) \\ &= -\frac{\hbar^2}{2\mu}R^{-1}\frac{\partial^2}{\partial R^2}R + \frac{\hbar^2\mathbf{l}^2}{2\mu R^2} + \mathcal{H}_B + V(R,r,\theta),\end{aligned} \tag{13.4.3}$$

where $\mathcal{H}_B$ is the Hamiltonian for the isolated diatom B, $\mu = M_A M_B/(M_A + M_B)$ is the reduced mass of the whole system, V is the intermolecular potential, and $\mathbf{l}$ is the angular momentum operator for the end-over-end rotation of the complex. The r-dependence of the potential can normally be ignored: it causes mixing between the diatom vibrational states, but not usually to a significant extent.

However, V depends on the orientation of the diatom relative to the intermolecular vector $\mathbf{R}$, and the rotation of the diatom is approximately quantized along $\mathbf{R}$. That is, the appropriate wavefunctions are the spherical harmonics $Y_{jK}(\theta,\varphi)$ with component K of angular momentum along the body-fixed z axis, though they are mixed by the intermolecular interaction. Rotation of the system as a whole, relative to the space-fixed frame, changes the angles α and β; the third Euler angle γ is the same as φ. Accordingly the appropriate basis functions to describe the rotational motion are

$$\Phi_{jK}^{JM}(\alpha,\beta,\theta,\varphi) = \left(\frac{2J+1}{4\pi}\right)^{1/2} D_{MK}^{J}(\alpha,\beta,0)^* Y_{jK}(\theta,\varphi). \tag{13.4.4}$$

Here D^J_{MK} is a Wigner function used as a rotational wavefunction (see Appendix B). The total angular momentum $\mathbf{J}$ is the vector sum of the angular momentum $\mathbf{j}$ of the diatom and the angular momentum $\mathbf{l}$ of the end-over-end rotation of the complex.

The wavefunction for the system is then written as

$$\psi^{JM}_n(\mathbf{R},\mathbf{r}) = \frac{1}{R}\sum_{jK}\Phi^{JM}_{jK}(\alpha,\beta,\theta,\varphi)\chi^n_{jKJ}(R),$$

where n is a label distinguishing different solutions with the same rotational quantum numbers. If we substitute this into the Schrödinger equation $\mathcal{H}\psi_n = E\psi_n$, multiply by $\Phi^{JM*}_{jK}(\alpha,\beta,\theta,\varphi)$ and integrate, we get

$$\left\{-\frac{\hbar^2}{2\mu}\frac{\mathrm{d}^2}{\mathrm{d}R^2} + (jKJ|V|jKJ) + \frac{\hbar^2}{2\mu R^2}(jKJ|(\mathbf{J}-\mathbf{j})^2|jKJ) + E^0_j - E\right\}\chi^n_{jKJ}(R)$$
$$= -{\sum_{j'}}'(jKJ|V|j'KJ)\chi^n_{j'KJ}(R) - \sum_{K'=K\pm1}\frac{\hbar^2}{2\mu R^2}(jKJ|(\mathbf{J}-\mathbf{j})^2|jK'J)\chi^n_{jK'J}(R). \quad (13.4.5)$$

Here $\mathbf{l}^2$ of eqn (13.4.3) has been replaced by $(\mathbf{J}-\mathbf{j})^2$, and the use of parentheses rather than angle brackets in the matrix elements denotes integration over the angular variables only. The prime on the summation over j' indicates that $j' = j$ is excluded. Eqn (13.4.5) is a set of coupled differential equations in R for the radial functions $\chi^n_{jKJ}(R)$; they are called the *close-coupling equations* or the *coupled-channel equations*. The matrix elements $(jKJ|(\mathbf{J}-\mathbf{j})^2|jK'J)$ that occur in them can be evaluated by standard techniques of angular momentum theory, not discussed here; they are

$$(jKJ\big|(\mathbf{J}-\mathbf{j})^2\big|jKJ) = J(J+1) + j(j+1) - 2K^2,$$
$$(jKJ\big|(\mathbf{J}-\mathbf{j})^2\big|j,K\pm1,J) = [J(J+1) - K(K\pm1)]^{1/2}[j(j+1) - K(K\pm1)]^{1/2}.$$

The matrix elements $(jKJ|V|j'KJ)$ are more troublesome in general, but for small molecules, the potential can be expanded in Legendre polynomials:

$$V(R,\theta) = \sum_\lambda V_\lambda(R)P_\lambda(\cos\theta), \quad (13.4.6)$$

and then the angular integration can again be carried out by standard techniques to give

$$(jKJ|V|j'K'J) = \sum_\lambda V_\lambda(R)g_\lambda(jj'K)\delta_{KK'}, \quad (13.4.7)$$

where

$$g_\lambda(jj'K) = (-)^K[(2j+1)(2j'+1)]\begin{pmatrix} j & \lambda & j' \\ 0 & 0 & 0\end{pmatrix}\begin{pmatrix} j & \lambda & j' \\ -K & 0 & K\end{pmatrix}.$$

Thus the matrix elements are independent of J and diagonal in K.

There are two interrelated aspects to the solution of eqn (13.4.5). One concerns the method to be used to find the radial functions $\chi^n_{jKJ}(R)$, and the other concerns the dimension of the problem. If the $\chi^n_{jKJ}(R)$ are included only up to some maximum value $j_{\max}$ of j, there are $2j+1$

values of K for each j, giving nearly $(2j_{\max} + 1)^2$ coupled equations in all. (Values of $j < K$ cannot occur, but K is usually small for the states of interest.) This truncation of the problem, with no other approximations made, is called the *close-coupling approximation*. It is usually impracticable to carry out the calculations without further approximations, because the time required is proportional to the cube of the number of coupled equations, i.e., to $(2j_{\max} + 1)^6$, and further approximations are then needed to reduce the dimension. The most important of these is the *helicity decoupling* approximation, in which the Coriolis terms coupling K with $K \pm 1$ on the right of eqn (13.4.5) are neglected. There is then only one value of K in the equations, so that the dimension is reduced substantially, from $(2j_{\max} + 1)^2$ to $j_{\max} + 1 - K$. This is a good approximation if the coupling term between K and K' is sufficiently small.

One way to solve the coupled equations of eqn (13.4.5) uses the formalism of scattering theory. For a given value of the energy, the differential equations are solved numerically, starting in the classically forbidden regions at large and small R and approaching the classically allowed region around the potential minimum. The large-R and small-R solutions have to match, and this is only possible for certain values of the energy, which are the eigenvalues of the problem. The strategy for finding the eigenvalues efficiently has been described by Johnson (1978) and Manolopoulos (1988), and a program is available for carrying out the whole calculation by this method (Hutson 1990*a*).

This is a laborious procedure, because of the need to iterate towards an acceptable value of the energy and because the numerical integration of the radial differential equations is itself a time-consuming process. An alternative is to assume that the radial and angular motions are approximately separable, so that a Born–Oppenheimer-like treatment can be used. The wavefunction is written in the form $\chi_{nJ}(R)\psi_J(\Omega; R)$; that is, the angular equations are solved at a particular value of R, ignoring the radial kinetic energy term in the Hamiltonian. This leads to a set of secular equations whose solutions are the rotational wavefunctions ψ_J and the rotational energies, as a function of R. The rotational energy serves as the potential energy for the radial motion, and (numerical) solution of the radial problem gives the radial wavefunction $\chi_{nJ}(R)$ and the total energy. This procedure is like the conventional Born–Oppenheimer separation of electronic and nuclear motion, but it does not depend, as that approximation does, on the very different timescales of the two kinds of motion. Rather it relies on the anisotropy of the interaction being only weakly dependent on R. The method was introduced by Holmgren *et al.* (1977) and called by them the Born–Oppenheimer angular–radial separation, or BOARS, method. Hutson and Howard (1980) showed that this adiabatic approximation leads to significant errors, but that they can be effectively corrected by perturbation theory, leading to a much more accurate procedure that they called the corrected Born–Oppenheimer (CBO) method.

An alternative procedure that does not require this approximation is to expand the radial wavefunction in terms of some basis set. The whole problem then reduces to the solution of a set of secular equations. This is feasible if the number of rotational states that have to be included is not too great, which in turn requires that the potential is not very anisotropic. The reason for this is that a term in P_λ in eqn (13.4.6) couples state j with states from $|j-\lambda|$ to $j+\lambda$, so if the expansion of the potential converges slowly it will be necessary to take a large value of $j_{\max}$ to describe its effects. This increases the dimension of the problem, as we have seen. Consequently the method has been used only for near-spherical molecules like H_2 (Bačić and Light 1989).

13.4.3 Larger systems

So far we have been considering the simplest case of a complex like Ar···HCl, formed from an atom and a diatomic molecule. Complexes comprising an atom and any linear molecule can be treated by similar methods, if the molecule can be treated as rigid, but as soon as we contemplate a complex of two diatomics, or of an atom and a non-linear molecule, the problem becomes very much less tractable. For an atom and a non-linear molecule we require two angular coordinates, for two linear molecules we need three. and for two non-linear molecules we need five. The number of angular functions needed for an adequate description increases by an order of magnitude for each new variable, and the computational effort is roughly proportional to the cube of the number of basis functions. Nevertheless the method has been used to obtain the vibration–rotation–tunnelling spectrum of water dimer, treating the molecules as rigid (Huang *et al.* 2008) (see p. 228).

If the internal vibrational motion of the molecules is to be taken into account, it is necessary to provide additional basis functions for the vibrational coordinates. The usual procedure is to use a direct product basis: a set of one-dimensional basis functions is used for each coordinate, and the overall basis function is a product comprising one function from each set. The number of such basis functions evidently becomes very large as the number of degrees of freedom increases. However, it is possible to reduce the size of the problem considerably by truncating the basis, discarding those product functions that are expected to make a negligible contribution to the wavefunction (Avila and Carrington 2011).

A further difficulty concerns the intermolecular potential. The single-site expansion of the potential converges more slowly for larger molecules, and eventually ceases to converge at all, as we have seen for the electrostatic interaction. It then becomes necessary to use multisite potentials of the type discussed in Chapter 7, and the calculation of the matrix elements becomes much more difficult. Some calculations have been carried out with such potentials; for example a site–site potential was used in calculations of the vibration–rotation–tunnelling spectrum of NH_3 dimer (Van Bladel *et al.* 1992, Olthof *et al.* 1994), but it was necessary to expand the potential in terms of single-site angular functions in order to calculate the matrix elements, truncating the expansion at quite low rank to keep the calculation tractable. As a result of the truncation the error in the expanded potential was about 8%.

13.4.4 Discrete variable representation

The discrete variable representation (DVR) method (Heather and Light 1982, Light and Carrington 2000, Császár *et al.* 2012) is one way to overcome the problem of matrix element evaluation. In simple terms, this describes the wavefunction by its value at each of a large array of points. The relationship to conventional expansion in terms of a set of basis functions is that if such a set of (orthonormal) functions is given, a DVR can be constructed using the gaussian quadrature points and weights derived from that set of basis functions, and the two procedures—DVR and basis function expansion—are then precisely equivalent. The advantage of the DVR over the conventional procedure is that the matrix elements of the intermolecular potential energy involve no integrations, but only the evaluation of the potential energy at the DVR points. It therefore becomes possible to handle potential energy functions of arbitrary complexity. Moreover the size of the problem can be reduced by deleting points in regions of high potential energy where the wavefunction is known to be negligible—a much simpler and safer procedure than dropping expansion functions from a conventional basis.

The difficulty with the DVR is that the gaussian quadrature points are only easily obtained for functions of one variable, and no generalization to systems of more than one dimension has yet been found. A system with many degrees of freedom is usually described in a direct-product fashion; that is, if we have a set of quadrature points $x_i,\ 1 \le i \le n_x$, in coordinate x, a set $y_j,\ 1 \le j \le n_y$, for coordinate y, and so on, the DVR points for the many-dimensional problem will be $(x_i, y_j, \ldots),\ 1 \le i \le n_x,\ 1 \le j \le n_y, \ldots$. Although points can be deleted from this set as already mentioned, the remaining points may not cover the space very efficiently. An example of this is the case of two linear molecules: their rotational wavefunctions can be described by products of spherical harmonics $Y_{l_1 m_1}(\theta_1, \varphi_1) Y_{l_2 m_2}(\theta_2, \varphi_2)$, and a DVR for this basis can be set up. However, it uses the four variables θ_1, φ_1, θ_2 and φ_2, and only three variables are of interest, the potential energy of the system being independent of $\varphi_1 + \varphi_2$. No three-dimensional DVR for this system has been found. See Althorpe and Clary (1995) or Light and Carrington (2000) for a fuller discussion.

Again, the inclusion of internal molecular vibrations complicates the calculation considerably. Leforestier *et al.* (2009) dealt with this problem by means of an adiabatic separation of intermolecular and intramolecular coordinates. At a given position in intermolecular coordinates, the vibrational problem for each molecule was solved in the field due to the other, using the DVR method. The sum of the energies of one vibrational level from each molecule was then treated as the value of the intermolecular potential for the vibration–rotation–tunnelling problem (in which the vibrations are now intermolecular).

Variants on the DVR include the collocation method, a less efficient but much simpler approach (Peet and Yang 1989, Cohen and Saykally 1990, Leforestier 1994). Here one expands the wavefunction in the usual way in terms of a set of basis functions:

$$\Psi = \sum c_j \varphi_j,$$

and then solves the eigenvalue equation

$$\mathbf{Hc} = E\mathbf{Rc},$$

where the elements of the matrices **H** and **R** are simply the functions $\mathcal{H}\varphi_j$ and φ_j evaluated at a point $\mathbf{r}_i$ in configuration space:

$$H_{ij} = (\mathcal{H}\varphi_j)|_{\mathbf{r}=\mathbf{r}_i}, \qquad R_{ij} = \varphi_j(\mathbf{r}_i).$$

If there are N basis functions it is necessary to choose N points in configuration space so that the matrices are square, but they are not symmetrical and the eigenvalues and eigenvectors may be complex. In practice the imaginary parts are small if the basis functions and sampling points are well chosen, and this provides a criterion for judging the quality of the calculation. Leforestier's method cited above involves using more points than functions; in this case there are more equations than unknowns and they are solved by a least-squares procedure. The increased number of points allows for higher accuracy but the computational effort remains modest.

13.4.5 Diffusion Monte Carlo

The quantum Monte Carlo method for solving the Schrödinger equation, also known as diffusion Monte Carlo (DMC), was first set out by Anderson (1975, 1976, 1980), though it had

been discussed much earlier. Later reviews were given by Suhm and Watts (1991) and Anderson (1995), who discuss the technical details involved in making the method work efficiently and accurately.

The time-dependent Schrödinger equation for the motion of the nuclei is, in atomic units,

$$\mathrm{i}\frac{\partial \Psi}{\partial t} = -\sum_k \nabla_k^2 \Psi + V\Psi, \tag{13.4.8}$$

where V is the potential energy. If we change variables, setting $\tau = \mathrm{i}t$, this takes the form of a diffusion equation:

$$\frac{\partial \Psi}{\partial \tau} = \sum_k \nabla_k^2 \Psi - V\Psi. \tag{13.4.9}$$

Any linear combination of the exact stationary-state wavefunctions is a solution of eqn (13.4.8):

$$\Psi = \sum_n \varphi_n \exp(-\mathrm{i}t(E_n - E_R)),$$

where E_R is an arbitrary reference energy, and when expressed in terms of the imaginary time variable τ this becomes a sum of decaying functions, provided that we choose E_R so that all the $E_n - E_R$ are positive:

$$\Psi(\mathbf{r}, \tau) = \sum_n \varphi_n \exp(-(E_n - E_R)\tau).$$

The ground-state term has the smallest E_n and so decays most slowly, so we can start from an arbitrary initial guess and follow the diffusion process until all the other terms have disappeared. Ideally we wish to choose the E_R equal to E_0, and then the ground state term will not decay at all, but initially we do not know E_0; the object of the calculation is usually to find it.

The procedure that is used to solve eqn (13.4.9) is a type of random walk; hence the term 'Monte Carlo'. An initial guess at the wavefunction is made by choosing a large set of points, sometimes called walkers, or psi-particles or 'psips', in configuration space; the local density of the points is proportional to the wavefunction. In the absence of the potential-energy term, the wavefunction evolves by diffusion: a delta function $\prod_k \delta(\mathbf{r}_k - \mathbf{r}_k(0))$ becomes, after (imaginary) time τ, a gaussian distribution:

$$U(\mathbf{r}, \tau) = \prod_k (4\pi D_k \tau)^{-3/2} \exp\left[-\frac{(\mathbf{r}_k - \mathbf{r}_k(0))^2}{4D_k\tau}\right], \tag{13.4.10}$$

where $D_k = 1/2m_k$ is an effective diffusion coefficient for nucleus k. This can be modelled by making each point follow a random walk: each point is displaced randomly in configuration space at each step of the process, with a probability distribution given by eqn (13.4.10). The influence of the potential energy is then taken into account for a point at $\mathbf{r}$ by either destroying or replicating it according to a random number whose probability density is proportional to $\exp[E_R - V(\mathbf{r})]$. That is, points in regions of high potential energy are likely to be destroyed and points in regions of low potential energy are likely to be replicated. The replicas then evolve independently of their parents.

One attraction of this method is that it provides the energy E_0 of the vibrational ground state, including anharmonicity effects, with no need to supply a basis set of vibrational functions. Since potential energy surfaces for weakly bound clusters are strongly anharmonic this is an important advantage. The other important feature is that no integrations are needed; all that is required is the value of the potential energy at randomly generated points in configuration space. Consequently the intermolecular potential can be as elaborate as necessary, and need not be constrained into mathematically convenient but physically unsound forms. For example, calculations have been carried out on the water dimer by Gregory and Clary (1994) using the potential of Millot and Stone (1992) (see §12.4.1), and the tunnelling splittings so obtained were in good agreement with more conventional calculations using the same potential (Althorpe and Clary 1994). More recently, Jaeger *et al.* (2006) have used the method to find binding energies of clusters of quadrupolar molecules, and Shank *et al.* (2009) used it to obtain the zero-point energy of the water dimer and hence a very accurate estimate of $D_0 = 1103\,\mathrm{cm}^{-1} = 13.2\,\mathrm{kJ\,mol}^{-1}$ for the dissociation energy.

Because the method is statistical there are errors, which decrease only slowly ($\propto N^{-1/2}$) as the number of steps N in the calculation is increased; but reliable estimates of the errors can be obtained, and there are methods of reducing the error by biasing the calculation using an approximate wavefunction obtained by some other method (Suhm and Watts 1991). It is also possible to reduce the error by eliminating the internal motions of the molecules from the calculation and using only the intermolecular coordinates; this is the rigid body diffusion Monte Carlo (RBDMC) method (Buch 1992).

The main limitation is the difficulty of handling excited states. The wavefunction is treated by the method as a probability density, represented by the density of walkers, which must be positive, so the method can only handle a region of the wavefunction which has the same sign everywhere—it cannot cross nodes. States whose symmetry is different from the ground state can be handled relatively easily by the fixed-node method: that is, by rejecting any random step that would cross a nodal surface. This ensures that the wavefunction goes to zero at the nodal surface. States with the same symmetry as the ground state or some other lower-energy state are much more difficult to handle, though methods have been suggested (Suhm and Watts 1991). The difficulty is that the positions of the nodes in the wavefunction are unknown unless they are determined by symmetry, and it is usually necessary to estimate them by carrying out an approximate calculation by some other method. This introduces an error whose magnitude is hard to estimate.

An important variant of the fixed-node method is the method of correlated sampling for calculating small energy differences such as tunnelling splittings (Wells 1985). When a system tunnels through a symmetrical barrier, as in the donor–acceptor inversion of HF dimer, there are two wavefunctions, one symmetric and one antisymmetric with respect to the barrier, but both very similar except for sign everywhere except in the barrier region. If both states are described using the same set of diffusing points, the statistical uncertainties are strongly correlated and the energy difference can be calculated much more accurately than the absolute energy. The method has been used to calculate tunnelling splittings in water dimer and trimer (Gregory and Clary 1995*a*). In the case of the trimer, the non-additive induction energy and the triple-dipole dispersion, both three-body terms, can be included (Gregory and Clary 1995*b*). The evaluation of the necessary matrix elements would be very difficult using a conventional basis-set expansion, even if the dimension of the problem were not prohibitive.

13.4.6 Feynman path-integral methods

Another method for obtaining spectroscopic information, in particular tunnelling splittings, from a potential energy surface is based on Feynman's path integral approach to quantum mechanics (see §13.3, p. 249). The particular variant of this idea that is used for calculating tunnelling splittings is the instanton approximation (Richardson and Althorpe 2009, 2011), which is based on a steepest-descent integral about the minimum-energy ring polymer. Its attraction as a method is that it is much simpler to implement and faster to carry out than the DVR or DMC methods, and it can handle the tunnelling through barriers between pairs of minima on an arbitrary potential energy surface without making any assumptions about the paths between the minima. It does make the approximation that the potential energy surface is harmonic in directions orthogonal to the tunnelling path. It has been applied to the calculation of tunnelling splittings in water dimer and trimer (Richardson *et al.* 2011) and on larger clusters up to the octamer (Richardson *et al.* 2012). The results are very good for D_2O dimer, but not quite as good for H_2O dimer and for the trimer, where the neglect of anharmonicity orthogonal to the path is more troublesome. Nevertheless the calculations on the trimer were able to explore all of the distinct tunnelling pathways between pairs of the 96 symmetry-equivalent minima on the potential energy surface due to Wang *et al.* (2009), currently the best available. The results showed that the tunnelling-splitting pattern is more complex than previously thought, and explained the appearance of so-called anomalous quartets in the experimental spectrum. Diffusion Monte Carlo, on the other hand, can only handle clusters up to pentamer and even for the trimer is limited to an incomplete treatment, while the DVR approach cannot be used even for the trimer.

13.5 Molecular beam scattering

In molecular-beam spectroscopy (§13.4), a single beam is used; if a mixed complex is to be studied, a mixture of gases is fed to the nozzle. An alternative way to study molecular interactions is to use two crossed beams, one for each component of the complex, and to study the scattering of the molecules following collisions at the crossing-point. The scattering is most conveniently studied mathematically in the centre-of-mass coordinate system, which moves relative to the laboratory frame, so a transformation between these coordinate systems is necessary; see, for example, Murrell and Bosanac (1989). In the centre-of-mass frame the position of one molecule relative to the other is described by a distance R and an angle ϑ (Fig. 13.2), and we can think of a particle of mass μ, the reduced mass of the system, being scattered from a fixed point at the origin. A classical scattering event begins with R large and $\vartheta = \pi$; as the molecules collide R reaches a minimum value R_c, and then the molecules separate again to large R along a path at $\vartheta = \theta$. The parameters describing the collision of two atoms are the kinetic energy E and the 'impact parameter' b which is the distance by which the centres of mass would miss each other if there were no interaction. The angular momentum of the system is related to E and b: its magnitude is $L = b\mu v = b\sqrt{2\mu E}$, where v is the initial relative velocity and μ the reduced mass. The collision angle θ is therefore a function of E and b. For a purely repulsive potential, $\theta = \pi$ when $b = 0$; that is, in a head-on collision the atoms rebound along their approach paths. As b increases, the scattering angle decreases from π, and is zero when b is so large that the atoms do not influence each other.

If the atom–atom potential has an attractive long-range part, as is usual, then it is possible for θ to become negative for some values of b; that is, the trajectory is pulled towards the

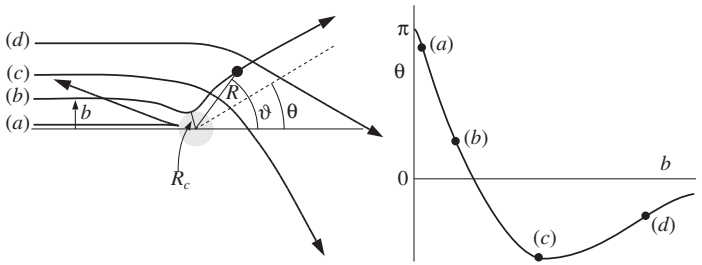

Fig. 13.2 (Left) Classical scattering trajectories for several values of the impact parameter b. (Right) Scattering angle as a function of impact parameter.

origin instead of being repelled from it. Since the limit for large b is still $\theta = 0$, the deflection angle reaches a minimum for some value of b and then increases again to zero. The scattering intensity near the minimum value of θ is high, because a range of values of b all contribute to the scattering near this angle; this effect is called a rainbow, because it is analogous to the refraction of sunlight in rain droplets that causes an optical rainbow. It occurs when the trajectory passes through the deepest part of the attractive well without experiencing the repulsive wall, and therefore the position of the rainbow gives information about the depth of the well (Mason 1957).

The observed scattering (still in the centre-of-mass coordinate system) is described by the *cross-section* σ. A particle will be scattered into a direction between θ and $\theta + \mathrm{d}\theta$ if its impact parameter falls in some range b to $b + \mathrm{d}b$. The area of a cross-section through the incoming beam corresponding to this range of b values is $2\pi b\,\mathrm{d}b$, so the flux of particles is $F.2\pi b\,\mathrm{d}b$, where F is the incident flux per unit area. The corresponding outgoing flux is spread over solid angle $2\pi \sin\theta\,\mathrm{d}\theta$, so the outgoing flux per unit solid angle for unit incident flux per unit area is

$$\sigma(\theta) = 2\pi b\,\mathrm{d}b/2\pi \sin\theta\,\mathrm{d}\theta = \left|\frac{b}{\sin\theta\,\mathrm{d}\theta/\mathrm{d}b}\right|; \tag{13.5.1}$$

the modulus sign appears because it is immaterial whether θ increases or decreases as b is increased. $\sigma(\theta)$ is called the *differential cross-section*.

In an observation we cannot distinguish between trajectories like (*b*) and (*d*) in Fig. 13.2, for which the scattering angles are θ_b and $\theta_d = -\theta_b$. Similarly, a scattering angle of θ is indistinguishable from $\theta + 2\pi$, where the trajectory orbits the origin. The experimental scattering angle Θ is obtained from the microscopic scattering angle θ by constructing $\Theta = |\theta - 2n\pi|$, choosing n so that the result is between 0 and π. The experimental differential cross-section is a sum over all the values of b that scatter into a given experimental angle Θ:

$$\sigma(\Theta) = \sum_i \left|\frac{b_i}{\sin\theta\,(\mathrm{d}\theta/\mathrm{d}b)_i}\right|. \tag{13.5.2}$$

The differential cross-section is a function of the collision energy E, so a further integration over the collision energy profile is needed to yield the observed property, though it is sometimes possible to carry out time-of-flight measurements to isolate the scattering at a particular collision energy. The integral of the differential scattering over all directions is the total scattering cross-section:

$$\sigma = 2\pi \int_0^{\pi} \sigma(\Theta) \sin\Theta \, \mathrm{d}\Theta.$$

The differential cross-section (13.5.2) is singular when either $\mathrm{d}\theta/\mathrm{d}b = 0$ or $\sin\theta = 0$. In practice, because of the variability of the collision energies, one just sees a maximum in the differential cross-section. When $\mathrm{d}\theta/\mathrm{d}b = 0$ this is called a rainbow, as already discussed; when $\sin\theta = 0$ it is known as a *glory*, again by analogy with the atmospheric phenomenon.

It will be apparent that the scattering data do not provide information directly about the intermolecular potential. Rather it is necessary, as for other experimental properties, to postulate some form of interatomic potential and to calculate the differential cross-section from it, modifying the potential until agreement with the observations is achieved. In a few cases the classical cross-section can be calculated analytically; alternatively it can be found by constructing a large number of collision trajectories by solving the classical equations of motion.

For atoms, the potential depends only on the centre-of-mass separation R, and atomic beam scattering provides useful information about it. For molecules, as usual, the problem is complicated by the presence of rotational and vibrational degrees of freedom, and trajectory calculations have to sample a range of initial conditions for these degrees of freedom as well as for the collision parameter and the energy.

A further complication is that classical mechanics is often inadequate; this is so especially for light atoms and molecules and for molecules with small moments of inertia. In such cases interference effects appear, for example between scattered waves at a particular Θ that arise from different values of b. The possibility of inelastic scattering also arises: the collision may transfer energy from the translational motion into rotational or vibrational degrees of freedom of the molecules. At very low collision energies, and with the molecules in their ground states, no such transfer is possible, because there is not enough energy to excite the molecules, but as the collision energy is increased, more and more excited states become accessible. Each possible internal state of the scattered molecules is called a *channel* in the language of scattering theory, and as the collision energy increases more channels open.

The quantum-mechanical solution of the scattering problem starts from the same point as the calculation of spectra, namely the coupled-channel equations—eqn (13.4.5) for the scattering of an atom from a diatomic. In the scattering problem, however, the collision energy E can take any positive value. The standard procedure is to integrate the equations outwards from small R, where the wavefunction is zero because of the large repulsion energy, to large R, where the wavefunctions become plane waves. The difficulty with this is the same as in the spectroscopic calculation: there are usually too many possible states or channels to consider. At long range only the open channels can contribute to the wavefunction, but at short range the closed channels may also contribute. It is always necessary to truncate the set of coupled-channel equations, but further approximations are usually needed. It is not necessary here to explore the details; they can be found, for instance, in the book by Murrell and Bosanac (1989). They also give an account of semi-classical methods in scattering theory, described in more detail by Child (1991); such methods can be used for simple atomic scattering problems but unfortunately they are not easily applied to systems with rotational and vibrational degrees of freedom.

An example of the use of molecular beam scattering to verify the accuracy of a calculated potential is the case of $H_2 \cdots D_2$ (Buck *et al.* 1983). Here an accurate *ab initio* potential was used in close-coupling calculations to obtain the differential cross-sections, not only for elastic

scattering, but also for inelastic scattering, in which one or both molecules were excited to a higher rotational state. These different types of scattering event can be distinguished by time-of-flight techniques: following inelastic scattering, where the molecules become excited, they have less translational energy and so travel more slowly and reach the detector later than elastically scattered molecules. In this case the agreement between experiment and theoretical calculation was complete, so the measurements validated the calculation but did not provide new information about the potential.

Usually it is not possible to calculate the potential so accurately. An example of the use of molecular beam scattering to study intermolecular potentials involving a polyatomic molecule is the study by Yang and Watts (1994) of the interactions between acetylene and Ar, H_2 and N_2. In the case of $Ar\cdots C_2H_2$, a potential determined by Thornley and Hutson (1992) was used to calculate the differential cross-section, and was found to give the rainbow peak in the wrong place, at about 9° in laboratory coordinates instead of 7° as observed. The rotational spectra from which the potential was derived depend mainly on the vibrationally averaged structure, and are not sensitive to the depth of the well, which, as we have seen, is the main factor determining the position of the rainbow angle. Yang and Watts were able to reproduce the differential cross-section using a different potential with several adjustable parameters, but this is not necessarily a better potential since it is fitted only to the scattering, and takes no account of the spectroscopic data. Clearly the most satisfactory procedure for determining intermolecular potentials is to use experimental data from as many sources as possible, so as to take advantage of the sensitivity of different measurements to different features of the potential.

The conclusion is that molecular beam scattering data can provide useful information about potentials, and in principle a given potential can be used to calculate scattering cross-sections for comparison with experimental data. For practical purposes, however, the potential often needs to be described by a single-site spherical-harmonic expansion, and this faces the same convergence limitations as in calculations of spectra. Consequently it is difficult to study molecules unless they are 'nearly spherical'—that is, unless any anisotropies are small and can be described by just a few terms of a spherical harmonic expansion.

13.6 Measurements on liquids and solids

Experiments on condensed phases can also provide information about intermolecular potentials, but they are complicated by the effects of the many-body terms. It has been usual to attempt to describe the properties of solids in terms of an effective pair potential that includes the many-body effects in some averaged fashion, but it is becoming increasingly common to include some many-body effects explicitly, especially induction.

13.6.1 Liquids

Liquid structure can be investigated by both X-ray and neutron scattering experiments. The experiments yield the structure factor $S(\mathbf{k})$, which is related to the intensity of the scattering at wave vector $\mathbf{k}$. (For particles of wavelength λ scattered through an angle α the wave vector is $(4\pi/\lambda)\sin\frac{1}{2}\alpha$.) The structure factor is the Fourier transform of the radial distribution function $g(r)$ (§13.3), which is the probability density for finding a second atom at distance r from a given first atom, and the Fourier transform can be inverted to derive the distribution function

from the structure factor. In the case of molecules, the scattering is a superposition of contributions from pairs of atoms, including scattering by pairs of atoms in the same molecule. In neutron scattering, the amplitude of the scattering is usually very different for different isotopes, so isotopic substitution can be used to separate the structure factors for different types of atom, and hence their radial distribution functions.

The radial distribution function and the structure factor involve an average over the ensemble, so as with many other properties it is not possible to derive much information about the potential directly from the measurement. The positions of the peaks in the radial distribution function correspond to favoured atom–atom distances, which gives a guide to the value of R_m and the coordination shell structure in the liquid, but generally it is necessary to postulate a potential and calculate the radial distribution function from it by computer simulation. Adopting this approach, Pusztai *et al.* (2008) found that of several water potentials investigated, the TIP4P-2005 potential was the most consistent with the neutron scattering data for liquid D_2O, and that none were seriously inconsistent.

13.6.2 Crystals

Crystal structures can be investigated by X-ray or neutron diffraction. Single crystals give very detailed diffraction patterns, and the procedures for determining the crystal structure from the diffraction pattern are well established. Where single crystals are not available, X-ray or neutron diffraction from a crystalline powder can be used, but the diffraction pattern is then an average over crystal orientations and is harder to interpret. X-rays are scattered by the electrons, so hydrogen atoms contribute weakly to the diffraction pattern and their positions are not determined reliably. Moreover the electron density around hydrogen is largely in the bond, so bond lengths to hydrogen appear systematically too short in X-ray structures. Neutrons, on the other hand, are scattered from the nuclei, so neutron diffraction gives more reliable atom positions and is preferred, especially for organic crystals, though larger samples are needed so powder diffraction usually has to be used.

The scattering angle 2θ and wavelength λ are related by Bragg's law:

$$\lambda = 2d_{hkl} \sin\theta, \tag{13.6.1}$$

where d_{hkl} is the spacing between crystal planes labelled by the crystallographic indices hkl. A spallation neutron source provides pulses of neutrons, each comprising a range of wavelengths. The wavelength is related to the neutron momentum $p = mv$ by $\lambda = h/p$, and the speed of the scattered neutrons can be measured by time of flight to one or more detectors at fixed scattering angles (Willis 1994).

Crystal structures can provide quite direct information about some aspects of the potential. The distance between neighbouring atoms in a simple solid such as that of an inert gas is close to the equilibrium separation R_m of the pair potential, though it is not quite the same because the attractions between more distant pairs of atoms tend to make the interatomic distance slightly shorter, while the repulsive effect of the triple-dipole dispersion tends to increase it. Similarly the lattice energy per atom is close to the value of $-\frac{1}{2}n\epsilon$ obtained by counting nearest-neighbour pair interactions only. (n is the number of nearest neighbours of each atom.) However, this too is modified by the same effects as the interatomic distance, and also by the zero-point energy associated with the lattice vibrations. For any given potential and crystal structure it is easy to calculate the optimum interatomic separation. The corresponding lattice

energy can also be calculated, though it is rather more difficult to determine accurately because of the need to estimate the zero-point energy. The lattice vibration frequencies can however be determined from the potential, and provide a further point of comparison with experiment, both through direct spectroscopic measurement and via measurements of the heat capacity. Spectroscopy normally yields only the $\mathbf{k} = 0$ vibration frequency, in which the molecules in different unit cells all move in phase.

The prediction of the crystal structures of small organic molecules has provided a powerful test of methods of calculating intermolecular interactions, and has important applications in the pharmaceutical industry. Such molecules often have more than one known crystal structure (polymorphs) and may have others not yet discovered (Bernstein 2011). Properties such as solubility, which affect drug dosage, can differ significantly between polymorphs. The lowest-energy polymorphs often differ in energy by a few $\mathrm{kJ\,mol^{-1}}$ or less, so a good global optimization procedure such as basin-hopping is needed as well as a high-quality potential energy function, and exploration of the crystal energy landscape, including not just the energy minima but the barriers between them, may be needed for a full understanding of the possible polymorphs (Wales 2011). In recent years it has become practicable to use density functional theory calculations with empirical dispersion (DFT-D) as a tool for crystal structure prediction (Kendrick *et al.* 2011), but it is expensive in computational resources, so analytical force fields are first derived from DFT-D calculations for the initial structure screening, and the selected structures are then refined with DFT-D. Analytical models of the intermolecular interactions are needed in any case, not only for finding crystal structures but for predicting morphology (crystal shape) and mechanical properties (Beyer *et al.* 2001).

The structures of molecular crystals are sensitive to details of the potential and are difficult to predict (Gavezzotti 2007, Oganov 2011), but techniques have advanced considerably since the classic book by Pertsin and Kitaigorodsky (1987). Price (2009) and Day (2011) give detailed accounts of the methods in current use. Point-charge models of the electrostatics are inadequate, so distributed multipoles are essential (Coombes *et al.* 1996, Day *et al.* 2005*b*). We have seen (p. 212) that the anisotropies of both repulsion and electrostatic terms were essential for a successful prediction of the crystal structure of molecular chlorine. The same principles apply to the chlorobenzenes, where a model using transferable electrostatic, dispersion and anisotropic repulsion terms accounted very successfully for 13 crystal structures of chlorobenzenes, including the three polymorphs of *p*-dichlorobenzene (Day and Price 2003) and a polymorph of 1,2,4,5-tetrachlorobenzene that was only characterized later (Barnett *et al.* 2006).

The use of anisotropic site–site models to describe the intermolecular potentials in crystals calls for the development of new techniques, as in other applications. The optimization of the structure requires the first and possibly the second derivatives of the potential, and these can be obtained as described in §12.6; further details of the application to crystal structure prediction are given by Willock *et al.* (1995), in work that led to the development of the DMACRYS program (Price *et al.* 2010). One feature that requires attention is that the interaction with other molecules involves a summation over all the unit cells of the lattice, out to infinity. For terms with R^{-n} distance dependence this summation is absolutely convergent only when $n > 3$. When $n \leq 3$, that is, for charge–charge, charge–dipole and dipole–dipole interactions, it is only conditionally convergent, and it is necessary to use the Ewald summation technique (Allen and Tildesley 1987). Its original application was to charge–charge interactions in ionic

crystals (Ewald 1921), but the extension to charge–dipole and dipole–dipole interactions has been described by Smith (1982*a*,*b*), and to higher multipoles, for technical reasons concerned with cutoff discontinuities, by Leslie (2008).

Ideally one wishes to compare the free energies of the various polymorphs, but this is not usually possible in practice, and it is more usual to compare static lattice energies, i.e., minima on the crystal potential energy surface. The zero-point vibrational energy and the vibrational contribution to the free energy may differ between polymorphs; the differences are small—of the order of 1 kJ mol^{-1}—but comparable with typical energy differences between polymorphs. They can be estimated using the harmonic approximation (Gavezzotti and Filippini 1995, van Eijck 2001). For flexible molecules the molecules may be forced by packing effects into structures very different from the gas-phase minimum-energy structure, so the deformation energy needs to be included (van Eijck *et al.* 2001). Furthermore the actual crystal structure that is observed may be influenced by kinetic effects, so the observed structure may not always be the thermodynamically most stable one. The crystallization environment too may affect the crystal structure; for example crystallization from a hydrogen-bonding solvent may lead to a different polymorph than from a non-polar solvent.

All of these issues make crystal structure prediction a difficult task, but one in which accurate intermolecular potential energy surfaces have an important part to play. There has been a series of blind tests in which research groups are challenged to predict the structures of a small number of molecular crystals—structures that have been determined but not revealed—and the reports on these blind tests (Lommerse *et al.* 2000, Motherwell *et al.* 2002, Day *et al.* 2005*a*, 2009, Bardwell *et al.* 2011) document the steady improvement in methods of crystal structure prediction based on accurate intermolecular potentials.

Appendix A
Cartesian Tensors

The essential feature of tensor algebra is that it expresses physical ideas in a form which is independent of coordinate system. It is then often unnecessary to specify a coordinate system at all, and when one is needed, it can be chosen to simplify the treatment of the problem. The description of a physical problem in terms of tensors has two further virtues:

- It is very compact, making the essential features of the mathematics more apparent;
- It is immediately obvious from the form of an expression whether it has the correct (e.g. scalar or vector) behaviour.

This is a condensed summary of the basic ideas. For a fuller account see, for example, Jeffreys (1931).

A.1 Basic definitions

A *scalar* is a quantity described by a single number, whose value is the same in all coordinate systems. Example: energy.

A *vector* is a quantity described by three numbers (labelled by a subscript taking values 1, 2 or 3 (or x, y, z)) whose values in one (primed) coordinate system are related to those in a rotated (unprimed) system by

$$v_{\alpha'} = \sum_{\alpha=1}^{3} a_{\alpha'\alpha} v_\alpha. \tag{A.1.1}$$

Examples are velocity; angular momentum; dipole moment. The quantities $a_{\alpha'\alpha}$ form an orthogonal matrix A describing the rotation. Consequently

$$\begin{aligned} &\sum_{\alpha=1}^{3} a_{\alpha'\alpha} a_{\beta'\alpha} = \delta_{\alpha'\beta'} \qquad (AA^T = I \text{ in matrix notation}), \\ &\sum_{\alpha'=1}^{3} a_{\alpha'\alpha} a_{\alpha'\beta} = \delta_{\alpha\beta} \qquad (A^T A = I). \end{aligned} \tag{A.1.2}$$

The coefficient $a_{\alpha'\alpha}$ is the cosine of the angle between the α' and α axes. In the equivalent matrix notation, T denotes the transpose.

It is customary to use the *repeated-suffix summation convention*, due originally to Einstein, according to which any subscript appearing twice in one term is automatically summed over. Thus (A.1.2) can be written

$$a_{\alpha'\alpha} a_{\beta'\alpha} = \delta_{\alpha'\beta'}, \tag{A.1.3a}$$

$$a_{\alpha'\alpha} a_{\alpha'\beta} = \delta_{\alpha\beta}. \tag{A.1.3b}$$

No subscript may occur more than twice in a term. Thus the expression $(\mathbf{r}\cdot\mathbf{s})^2$ may not be written as $r_\alpha s_\alpha r_\alpha s_\alpha$ (because of the possibility of ambiguity with $(\mathbf{r}\cdot\mathbf{r})(\mathbf{s}\cdot\mathbf{s})$) but must be written as, e.g., $r_\alpha s_\alpha r_\beta s_\beta$. α and β here are *dummy suffixes*; since they are summed over, the actual symbol used is irrelevant. α and β in (A.1.3b), on the other hand, are *free suffixes*; each such suffix must occur precisely once in each term of the equation, and the equation holds for each value (1, 2 or 3) that they can take.

A *tensor* of rank n is a quantity described by 3^n numbers (labelled by n subscripts each taking the value 1, 2 or 3). Tensors of rank 2 often describe the relationship between two vectors; e.g. the polarizability $\alpha_{\xi\eta}$ describes the dipole μ_ξ induced by an electric field F_η:

$$\mu_\xi = \alpha_{\xi\eta} F_\eta. \tag{A.1.4}$$

In order that such equations remain valid in any coordinate system, it is necessary that the values of tensor components in the primed coordinate system are related to those in the unprimed system by

$$T_{\alpha'\beta'\ldots\nu'} = a_{\alpha'\alpha} a_{\beta'\beta} \ldots a_{\nu'\nu} T_{\alpha\beta\ldots\nu}. \tag{A.1.5}$$

It follows from (A.1.2) that the converse relationship holds:

$$T_{\alpha\beta\ldots\nu} = a_{\alpha\alpha'} a_{\beta\beta'} \ldots a_{\nu\nu'} T_{\alpha'\beta'\ldots\nu'}. \tag{A.1.6}$$

[Proof: substitute (A.1.5) into the r.h.s. of (A.1.6) and use (A.1.2).] We see that scalars and vectors are tensors of rank 0 and 1 respectively. Note that the order of subscripts on $a_{\alpha\alpha'}$ is immaterial: $a_{\alpha\alpha'}$ is the same as $a_{\alpha'\alpha}$, being the direction cosine between the two axes concerned. Thus $a_{1'2} = a_{21'}$, but neither of course is the same as $a_{12'} = a_{2'1}$.

However, the order of the subscripts on the tensor itself is usually significant; that is, $T_{\alpha\beta\gamma\ldots\nu} \neq T_{\beta\alpha\gamma\ldots\nu}$ in general. If in a particular case $T_{\alpha\beta\gamma\ldots\nu} = T_{\beta\alpha\gamma\ldots\nu}$ for any choice of coordinate system, and for all values of the remaining suffixes $\gamma\ldots\nu$, then the tensor T is said to be *symmetric* with respect to the first two subscripts.

Addition and *subtraction* of tensors is straightforward: the quantity

$$W_{\alpha\beta\ldots\nu} = T_{\alpha\beta\ldots\nu} + U_{\alpha\beta\ldots\nu} \tag{A.1.7}$$

is a component of a tensor W which is the sum of the tensors T and U.

The *outer product* of two tensors is obtained by multiplying components without summing:

$$X_{\alpha\beta\ldots\lambda\mu\nu\pi\ldots\zeta} = T_{\alpha\beta\ldots\lambda\mu} U_{\nu\pi\ldots\zeta}, \tag{A.1.8}$$

and is readily shown to be a tensor (use (A.1.5)), with a rank which is the sum of the ranks of the factors.

Contraction involves setting two subscripts equal and performing the sum implied by the notation; e.g.

$$Y_{\gamma\delta\ldots\nu} = T_{\alpha\alpha\gamma\delta\ldots\nu} \equiv \sum_\alpha T_{\alpha\alpha\gamma\delta\ldots\nu}. \tag{A.1.9}$$

It is easy to show that if T is a tensor of rank n, then Y is a tensor of rank $n-2$. (Use (A.1.5) and (A.1.2).) Applying this procedure to an outer product, taking the contracted suffices one from each factor, yields an *inner product*, e.g.

$$Z_{\alpha\beta\ldots\lambda\pi\ldots\zeta} = X_{\alpha\beta\ldots\lambda\mu\mu\pi\ldots\zeta} = T_{\alpha\beta\ldots\lambda\mu}U_{\mu\pi\ldots\zeta}. \tag{A.1.10}$$

Clearly Z is a tensor: it is a contraction of X which is a tensor, as stated above. It is also true that if (A.1.10) holds in all coordinate systems, and Z and T are known to be tensors, then it follows that U is a tensor (*quotient rule*).

The simplest case of an inner product is the scalar product of two vectors: for example $s = u_\alpha v_\alpha = \mathbf{u}\cdot\mathbf{v}$. It is a quantity of rank 0, i.e., a scalar—it is independent of coordinate system. Another common case is the vector formed by taking the inner product of a second-rank tensor with a vector, as in (A.1.4) above.

A.1.1 Isotropic tensors

Normally the application of (A.1.5) yields a set of numbers, describing the tensor in the new axes, which are different from those describing it in the old axes—e.g. $T_{1'1'\ldots1'} \neq T_{11\ldots1}$. However, some tensors retain the same numerical values in all axis systems, and are called *isotropic*. Apart from scalar multiplicative factors (scalars being always isotropic by definition) the important isotropic tensors are the *Kronecker* tensor or Kronecker delta:

$$\delta_{\alpha\beta} = \begin{cases} 1 & \text{when } \alpha = \beta, \\ 0 & \text{otherwise,} \end{cases} \tag{A.1.11}$$

and the *Levi-Civita* tensor:

$$\epsilon_{\alpha\beta\gamma} = \begin{cases} 1 & \text{when } \alpha\beta\gamma \text{ is a cyclic permutation of 123,} \\ -1 & \text{when } \alpha\beta\gamma \text{ is a cyclic permutation of 321,} \\ 0 & \text{otherwise.} \end{cases} \tag{A.1.12}$$

There are no other isotropic tensors of rank less than 4; moreover all isotropic tensors of any rank can be expressed in terms of outer products of δ's and ϵ's.

Notice that $\delta_{\alpha\beta}$ behaves like a subscript substitution operator: in $\delta_{\alpha\beta}t_{\beta\gamma}$, for example, there is only one term in the implied sum over β that does not vanish, namely the one for which $\beta = \alpha$. Consequently $\delta_{\alpha\beta}t_{\beta\gamma} = t_{\alpha\gamma}$. Notice also that $\delta_{\alpha\alpha} = 3$.

An important use of the Levi-Civita tensor occurs in the *vector product* of two vectors; in tensor notation $\mathbf{v} = \mathbf{r}\wedge\mathbf{s}$ is $v_\alpha = \epsilon_{\alpha\beta\gamma}r_\beta s_\gamma$.

A.1.2 Polar and axial tensors

The transformation rule in (A.1.1) or (A.1.5) is appropriate only for proper rotations of the axes. For improper rotations, which involve a reflection and change the handedness of the coordinate system, two possibilities arise. Either the rule in (A.1.5) may apply as it stands, in which case we have a *polar* tensor, or there may be an additional change of sign for improper rotations, in which case we have an *axial* tensor. (A.1.5) may be written in a more general form to take account of these possibilities:

$$T_{\alpha'\beta'\ldots\nu'} = \det(a)^p a_{\alpha'\alpha}a_{\beta'\beta}\ldots a_{\nu'\nu}T_{\alpha\beta\ldots\nu}, \tag{A.1.13}$$

where $\det(a)$ is the determinant of the matrix whose elements are the direction cosines $a_{\alpha'\alpha}$, and p is 0 for a polar tensor and 1 for an axial one. Since $\det(a)$ is +1 for a proper rotation and

-1 for an improper one, this gives the extra change of sign for an axial tensor under improper rotation.

It follows that any product, outer or inner, of two polar tensors or two axial tensors is polar, while the product of a polar tensor with an axial tensor is axial. The fundamental axial tensor is the Levi-Civita tensor, which is axial by definition in order that $\epsilon_{123} = +1$ in left-handed coordinate systems as well as right-handed ones. Therefore the vector product of two polar tensors is axial. The prime example of this is angular momentum: $\mathbf{l} = \mathbf{r} \wedge \mathbf{p}$ is the vector product of the polar vectors $\mathbf{r}$ and $\mathbf{p}$ describing position and momentum, expressed in tensor notation as $l_\alpha = \epsilon_{\alpha\beta\gamma} r_\beta p_\gamma$.

Appendix B
Spherical Tensors

Here we summarize the basic concepts of the spherical-tensor formalism. This is not intended as an explanatory account, but merely as a summary of the principal formulae and definitions that we need. A fuller account may be found in one of the many textbooks on angular momentum theory, such as Brink and Satchler (1993) or Zare (1988).

B.1 Spherical harmonics

Recall that the spherical harmonics, usually denoted $Y_{lm}(\theta,\varphi)$, are the functions of θ and φ that satisfy the eigenvalue equations for the angular momentum operators:

$$\hat{\mathbf{L}}^2 Y_{lm} = \hbar^2 l(l+1) Y_{lm},$$
$$\hat{L}_z Y_{lm} = \hbar m Y_{lm}.$$

They are normalized so that $\int |Y_{lm}|^2 \, \sin\theta \, \mathrm{d}r \, \mathrm{d}\theta \, \mathrm{d}\varphi = 1$, and because they are eigenfunctions of the hermitian operators $\hat{\mathbf{L}}^2$ and $\hat{L}_z$, they are orthogonal:

$$\int Y^*_{lm} Y_{l'm'} \, \sin\theta \, \mathrm{d}r \, \mathrm{d}\theta \, \mathrm{d}\varphi = \delta_{ll'}\delta_{mm'}.$$

The angular momentum operator $\hat{\mathbf{L}} = \mathbf{r} \times \hat{\mathbf{p}}$ has components defined by

$$\begin{aligned}
\hat{L}_x &= y p_z - z p_y = -\mathrm{i}\hbar\Big(y\frac{\partial}{\partial z} - z\frac{\partial}{\partial y}\Big),\\
\hat{L}_y &= z p_x - x p_z = -\mathrm{i}\hbar\Big(z\frac{\partial}{\partial x} - x\frac{\partial}{\partial z}\Big),\\
\hat{L}_z &= x p_y - y p_x = -\mathrm{i}\hbar\Big(x\frac{\partial}{\partial y} - y\frac{\partial}{\partial x}\Big).
\end{aligned} \tag{B.1.1}$$

In spherical polar coordinates, $\hat{L}_z = -\mathrm{i}\hbar\partial/\partial\varphi$, while

$$\hat{\mathbf{L}}^2 = -\hbar^2\Big(\frac{1}{\sin\theta}\frac{\partial}{\partial\theta}\sin\theta\frac{\partial}{\partial\theta} + \frac{1}{\sin^2\theta}\frac{\partial^2}{\partial\varphi^2}\Big).$$

The operators $\hat{L}_\pm = \hat{L}_x \pm \hat{L}_y$ are important in the theory. The spherical harmonics satisfy

$$\hat{L}_\pm Y_{lm} = +\sqrt{l(l+1) - m(m\pm1)}\,\hbar Y_{l,m\pm1}, \tag{B.1.2}$$

so that $\hat{L}_+$ and $\hat{L}_-$ have the effect of shifting the eigenvalue m up or down by one unit. For this reason they are called shift or ladder operators.

It is more convenient for our purposes to use renormalized spherical harmonics, first defined by Racah, which differ from the Y_{lm} by a constant factor:

$$C_{lm}(\theta,\varphi) = \sqrt{\frac{4\pi}{2l+1}}Y_{lm}(\theta,\varphi).$$

These evidently satisfy the same eigenvalue equations, but their normalization is different: they satisfy $C_{l0}(0,0) = 1$. The use of these functions avoids the factors of $\sqrt{4\pi}$ that otherwise clutter up the equations. The explicit form of the spherical harmonics is derived in some elementary texts on quantum mechanics, and is

$$C_{lm}(\theta,\varphi) = \epsilon_m\left[\frac{(l-|m|)!}{(l+|m|)!}\right]^{1/2}P_l^m(\cos\theta)\mathrm{e}^{im\varphi}, \tag{B.1.3}$$

where $P_l^m(\cos\theta)$ is an associated Legendre function (Abramowitz and Stegun 1965, Zare 1988), and the phase factor ϵ_m, important for maintaining the phase relationships required by eqn (B.1.2), is $(-1)^m$ for $m > 0$ and 1 for $m \le 0$.

We can also define related functions called the regular and irregular spherical harmonics:

$$\begin{aligned} R_{lm}(\mathbf{r}) &= r^l C_{lm}(\theta,\varphi), \\ I_{lm}(\mathbf{r}) &= r^{-l-1}C_{lm}(\theta,\varphi), \end{aligned} \tag{B.1.4}$$

where r, θ and φ form the spherical polar representation of the vector argument $\mathbf{r}$. These functions satisfy Laplace's equation: $\nabla^2 R_{lm} = 0$ everywhere, while $\nabla^2 I_{lm} = 0$ except at the origin. This is easily demonstrated using the fact that

$$\nabla^2 = \frac{1}{r^2}\frac{\partial}{\partial r}r^2\frac{\partial}{\partial r} - \frac{\hat{\mathbf{L}}^2}{\hbar^2 r^2}.$$

The first few of the regular spherical harmonics are

$$\begin{aligned} R_{00}(\mathbf{r}) &= 1, \\ R_{10}(\mathbf{r}) &= z = r\cos\theta, \\ R_{11}(\mathbf{r}) &= -\sqrt{\tfrac{1}{2}}(x+iy) = -\sqrt{\tfrac{1}{2}}r\sin\theta\mathrm{e}^{\mathrm{i}\varphi}, \\ R_{1,-1}(\mathbf{r}) &= \sqrt{\tfrac{1}{2}}(x-iy) = \sqrt{\tfrac{1}{2}}r\sin\theta\mathrm{e}^{-\mathrm{i}\varphi}, \\ R_{20}(\mathbf{r}) &= \tfrac{1}{2}(3z^2-r^2) = \tfrac{1}{2}r^2(3\cos^2\theta - 1). \end{aligned}$$

Here x, y and z are the cartesian components of $\mathbf{r}$. As the functions with non-zero m are complex, it is helpful to define real functions R_{lmc} and R_{lms}, for $m > 0$, by

$$\left.\begin{aligned} R_{lmc} &= \sqrt{\tfrac{1}{2}}[(-1)^m R_{lm} + R_{l,-m}], \\ \mathrm{i}R_{lms} &= \sqrt{\tfrac{1}{2}}[(-1)^m R_{lm} - R_{l,-m}], \end{aligned}\right\} \quad m > 0. \tag{B.1.5}$$

This relationship between the real and complex components can be written in the form

$$R_{lm} = \sum_{\kappa} R_{l\kappa} X_{\kappa m}. \tag{B.1.6}$$

Here we use the Greek label κ generically for the real components; for a given value of l it takes the values 0, $1c$, $1s$, …, lc, ls. The transformation coefficients $X_{\kappa m}$ are zero except for $X_{00} = 1$ and

$$\left.\begin{aligned} X_{mc,m} &= (-1)^m \sqrt{\tfrac{1}{2}}, \quad & X_{mc,-m} &= \sqrt{\tfrac{1}{2}}, \\ X_{ms,m} &= (-1)^m \mathrm{i} \sqrt{\tfrac{1}{2}}, \quad & X_{ms,-m} &= -\mathrm{i} \sqrt{\tfrac{1}{2}}, \end{aligned}\right\} \quad m > 0. \tag{B.1.7}$$

The matrix X is unitary.

It is sometimes more convenient to express the relationship between real and complex components differently:

$$\begin{aligned} R_{lmc} &= b_m R_{lm} + b_{\overline{m}} R_{l\overline{m}}, \\ \mathrm{i} R_{lms} &= b_m R_{lm} - b_{\overline{m}} R_{l\overline{m}}, \end{aligned} \tag{B.1.8}$$

where

$$b_m = \begin{cases} (-1)^m \sqrt{\tfrac{1}{2}}, & m > 0, \\ \tfrac{1}{2}, & m = 0, \\ \sqrt{\tfrac{1}{2}}, & m < 0, \end{cases} \tag{B.1.9}$$

and $\overline{m} \equiv -m$. If this is done, there is no need to restrict m in eqn (B.1.8) to be positive, and the definitions ensure that $R_{l\overline{m}c} = R_{lmc}$ and $R_{l\overline{m}s} = -R_{lms}$. We also see that

$$R_{lm} = (R_{lmc} + \mathrm{i} R_{lms})/2b_m, \tag{B.1.10}$$

for all m, and that $R_{l0c} = R_{l0}$ and $R_{l0s} = 0$.

The labels c and s stand for 'cosine' and 'sine' respectively, since R_{lmc} and R_{lms} are proportional to $\cos m\varphi$ and $\sin m\varphi$ respectively. Some of these functions are tabulated in Table E.1. Real irregular spherical harmonics are defined similarly, and can be obtained from the corresponding regular harmonics by dividing by r^{2l+1}. We shall also use real forms C_{lmc} and C_{lms} of the ordinary spherical harmonics.*

B.2 Rotations of the coordinate system

The spherical harmonics Y_{lm} and C_{lm} and the regular and irregular solid harmonics R_{lm} and I_{lm} all depend on the angular coordinates in the same way. Accordingly they all transform under

*Some authors use a different notation, writing, for example, Z_{lm} for C_{lmc} and $Z_{l\overline{m}}$ for C_{lms}. This notation has several disadvantages: it requires a new letter, Z instead of C, so that the link with the complex form is less apparent; the form Z_{lm} is not obviously a real rather than complex component; and the regular and irregular harmonics either require two new, less mnemonic, letters than R and I, or must be expressed less compactly as $r^l Z_{lm}$ and $r^{-l-1} Z_{lm}$. The only compensating advantage, if indeed it is an advantage, is the loss of the c or s suffix.

rotations in the same way. A rotation is described by the Euler angles defined in Fig. 1.2, and the effect of such a rotation on a spherical harmonic is

$$R(\alpha,\beta,\gamma)Y_{lm} = \sum_{m'} Y_{lm'} D^l_{m'm}(\alpha,\beta,\gamma), \tag{B.2.1}$$

where the $D^l_{m'm}(\alpha,\beta,\gamma)$ are the *Wigner rotation matrices*. That is, the rotated function $R(\alpha,\beta,\gamma)Y_{lm}$ can be expressed as a linear combination of the original set of functions, with coefficients that are elements of the Wigner rotation matrix. Here we are using the active convention for rotations; that is, the l.h.s. of eqn (B.2.1) describes the function that we obtain by rotating the spherical harmonic Y_{lm} according to the Euler angles α, β and γ, while the r.h.s. is a linear combination of the original set of unrotated functions. The alternative passive convention involves rotating the axes rather than the functions; see Brink and Satchler or Zare. The Wigner rotation matrices are defined by eqn (B.2.1); since $D^l_{m'm}(\alpha,\beta,\gamma)$ is the coefficient of $Y_{lm'}$ in the rotated function $R(\alpha,\beta,\gamma)Y_{lm}$, we can use the orthogonality of the spherical harmonics to write

$$D^l_{m'm}(\alpha,\beta,\gamma) = \int Y^*_{lm'} R(\alpha,\beta,\gamma) Y_{lm} \sin\theta \,\mathrm{d}\theta \,\mathrm{d}\varphi.$$

Explicit tables of the Wigner rotation matrices are given in Brink and Satchler for $l \leq 2$.

B.3 Spherical tensors

A spherical tensor of rank l is now defined as any set of $2l + 1$ quantities, labelled by $m = l, l-1, \ldots, -l$ like the spherical harmonics, for which the same transformation law holds as for the spherical harmonics. That is, if

$$R(\alpha,\beta,\gamma)T_{lm} = \sum_{m'} T_{lm'} D^l_{m'm}(\alpha,\beta,\gamma),$$

where the $D^l_{m'm}$ are the Wigner rotation matrices as in eqn (B.2.1), then the set T_{lm} is a spherical tensor of rank l.

For our purposes, the main importance of this is that the multipole moments, when expressed in spherical-tensor form, do satisfy this requirement. However, any quantum-mechanical operator can be expressed in spherical-tensor form. For example, the spherical-tensor components of a vector operator with cartesian components v_x, v_y and v_z are

$$\begin{aligned} v_{11} &= -\sqrt{\tfrac{1}{2}}(v_x + \mathrm{i}v_y), \\ v_{10} &= v_z, \\ v_{1,-1} &= \sqrt{\tfrac{1}{2}}(v_x - \mathrm{i}v_y). \end{aligned} \tag{B.3.1}$$

Instead of regarding the $D^l_{mk}(\alpha,\beta,\gamma)$ as matrices, defined for particular values of α,β and γ, it is possible to regard them as functions of α,β and γ for particular values of l, m and k. In this context they are called Wigner functions. In fact it turns out that $[(2l+1)/8\pi^2]^{1/2} D^l_{mk}(\alpha,\beta,\gamma)^*$ is the normalized rotational wavefunction of a symmetric top whose orientation is described

by the Euler angles α, β and γ and which has angular momentum quantum number l, with component m in the global z direction and component k in the molecule-fixed z direction. From this it follows that the set of $D^l_{mk}(\alpha,\beta,\gamma)^*$, for any fixed k, is a spherical tensor of rank l.

B.4 Coupling of wavefunctions and spherical tensors

Given a set of eigenfunctions $\varphi_{l_1 m_1}$ with angular momentum eigenvalues l_1 and m_1, and another set $\psi_{l_2 m_2}$ with eigenvalues l_2 and m_2, it is possible to construct from the products $\varphi_{l_1 m_1}\psi_{l_2 m_2}$ a set of angular momentum functions Ψ_{LM} for each value of the eigenvalue L from $l_1 + l_2$ by integer steps down to $|l_1 - l_2|$ (the Clebsch–Gordan series). For example, from the 15 products $Y_{1m_1}Y_{2m_2}$ of the rank 1 and rank 2 spherical harmonics, such as arise in the wavefunction for an atom with one p electron and one d electron outside closed shells, we can construct functions with $L = 3$, 2 and 1. The formula for the new functions is

$$\Psi_{LM} = \sum_{m_1 m_2} \langle l_1 l_2 m_1 m_2 | LM \rangle \varphi_{l_1 m_1}\psi_{l_2 m_2},$$

where the coefficient $\langle l_1 l_2 m_1 m_2 | LM \rangle$ is called a *Wigner* or *Clebsch–Gordan* or *vector coupling* coefficient. It is zero unless $m = m_1 + m_2$ and L is one of the values $l_1 + l_2, l_1 + l_2 - 1, \ldots, |l_1 - l_2|$. The latter condition is called the triangle condition, and can be expressed symmetrically: $l_1 + l_2 + L$ must be an integer, and none of the three may exceed the sum of the other two. There is a formula for the Wigner coefficient (Brink and Satchler 1993, Zare 1988), but it is quite complicated and values are usually obtained from tables, for example in Varshalovich *et al.* (1988, pp. 271–278).

The same procedure can be applied when the factors in the products are not wavefunctions $\varphi_{l_1 m_1}$ and $\psi_{l_2 m_2}$ but spherical-tensor operators $R_{l_1 m_1}$ and $S_{l_2 m_2}$. In this case it often happens that $l_1 = l_2$ and we require $L = 0$. In this case the coupled function is a scalar: it is invariant under rotations. The Wigner coefficients take a particularly simple form in this case, and the coupled operator is

$$(R \times S)_{00} = \sum_m (2l+1)^{-1/2}(-1)^{l-m} R_{lm} S_{l,-m}. \tag{B.4.1}$$

The reason for the importance of this case is that the Hamiltonian for an isolated system is invariant under rotations, so these invariant combinations of operators are the only ones that can occur in such a Hamiltonian. It occurs so often, in fact, that it is usual to define the 'scalar product' of two sets of spherical-tensor operators as

$$R \cdot S = \sum_m (-1)^m R_{lm} S_{l,-m}, \tag{B.4.2}$$

i.e., with a different phase and normalization from eqn (B.4.1). In the particular case where R and S are vectors (rank 1), this expression yields, using (B.3.1),

$$R \cdot S = -R_{11}S_{1,-1} + R_{10}S_{10} - R_{1,-1}S_{11} = R_x S_x + R_y S_y + R_z S_z,$$

in agreement with the conventional cartesian definition. Indeed, this is the main reason for the use of the definition (B.4.2), the scalar product of two vectors being then the same whether the cartesian or the spherical tensor formulation is used.

Where we have a spherical-tensor 'scalar product' of the form $\sum_m (-1)^m A_{l,-m} B_{lm}$, it can always be replaced by a scalar product in terms of the real components. For any $m > 0$ we can use eqn (B.1.5) to show that

$$\begin{aligned} A_{lmc}B_{lmc} + A_{lms}B_{lms} &= \tfrac{1}{2}((-1)^m A_{lm} + A_{l,-m})((-1)^m B_{lm} + B_{l,-m}) \\ &\quad - \tfrac{1}{2}((-1)^m A_{lm} - A_{l,-m})((-1)^m B_{lm} - B_{l,-m}) \\ &= (-1)^m (A_{lm}B_{l,-m} + A_{l,-m}B_{lm}). \end{aligned}$$

When we sum over m from 1 to l and add the $m = 0$ term we get

$$\sum_m (-1)^m A_{l,-m} B_{lm} = \sum_\kappa A_{l\kappa} B_{l\kappa}. \tag{B.4.3}$$

B.4.1 Wigner $3j$ symbols

A similar situation sometimes arises when we have three sets of spherical tensor quantities, $R_{l_1 m_1}$, $S_{l_2 m_2}$ and $T_{l_3 m_3}$ and we wish to construct a scalar from them. In this case we can begin by constructing a rank l_3 tensor from R and S (this is possible only if l_1, l_2 and l_3 satisfy the triangle condition) and then form the scalar product of this with T:

$$\begin{aligned} (R \times S \times T)_{00} &= (2l_3 + 1)^{-1/2} \sum_{m_3} (-1)^{l_3 - m_3} \sum_{m_1 m_2} \langle l_1 l_2 m_1 m_2 | l_3 m_3 \rangle R_{l_1 m_1} S_{l_2 m_2} T_{l_3, -m_3} \\ &= (-1)^{l_1 - l_2 + l_3} \sum_{m_1 m_2 m_3} \begin{pmatrix} l_1 & l_2 & l_3 \\ m_1 & m_2 & m_3 \end{pmatrix} R_{l_1 m_1} S_{l_2 m_2} T_{l_3 m_3}, \end{aligned} \tag{B.4.4}$$

where the quantity in parentheses is a *Wigner 3j symbol*, defined by

$$\begin{pmatrix} l_1 & l_2 & l_3 \\ m_1 & m_2 & m_3 \end{pmatrix} = (2l_3 + 1)^{-1/2} (-1)^{l_1 - l_2 - m_3} \langle l_1 l_2 m_1 m_2 | l_3, -m_3 \rangle.$$

The phase factor here is chosen to make the $3j$ symbol as symmetric as possible: it is invariant under even permutations of its columns, while odd permutations multiply it by a factor $(-1)^{l_1 + l_2 + l_3}$.

One example is the S function introduced in §3.3. It takes the form

$$S^{k_1 k_2}_{l_1 l_2 j} = i^{l_1 - l_2 - j} \sum_{m_1 m_2 m} [D^{l_1}_{m_1 k_1}(\Omega_1)]^* [D^{l_2}_{m_2 k_2}(\Omega_2)]^* C_{jm}(\theta, \varphi) \begin{pmatrix} l_1 & l_2 & j \\ m_1 & m_2 & m \end{pmatrix}. \tag{B.4.5}$$

Here θ and φ are the polar angles describing the direction of the intermolecular vector $\mathbf{R}$. We see that apart from some additional numerical constants, this has the form of eqn (B.4.4), with j and m taking the place of l_3 and m_3. (Remember that $[D^{l_1}_{m_1 k_1}(\Omega_1)]^*$ is the m_1 component of a spherical tensor of rank l_1.)

When three or more sets of spherical tensor quantities are coupled together, there are usually several ways of doing it. The relationship between the different 'coupling schemes' is expressed by Wigner $6j$ and $9j$ symbols. For an explanation of these quantities, consult Brink and Satchler (1993) or Zare (1988).

Appendix C
Introduction to Perturbation Theory

C.1 Non-degenerate perturbation theory

We give here a summary of the principles of perturbation theory, for reference and to define the notation.

We are faced with a Hamiltonian $\mathcal{H}$ that is too complicated to handle directly. We suppose that it differs by a small 'perturbation' $\mathcal{H}'$ from a closely related unperturbed or 'zeroth-order' Hamiltonian $\mathcal{H}^0$ describing a problem that we can solve:

$$\mathcal{H} = \mathcal{H}^0 + \lambda\mathcal{H}'. \tag{C.1.1}$$

Here λ may be a physical quantity describing the strength of the perturbation, such as the magnitude of an electric or magnetic field, but often it is just a parameter that we can vary hypothetically from 0 for the unperturbed problem to 1 for the problem that we want to solve.

Suppose that the eigenfunctions of the unperturbed problem are $|n^0\rangle$, with eigenvalues W_n^0:

$$\mathcal{H}^0|n^0\rangle = W_n^0|n^0\rangle. \tag{C.1.2}$$

We want to find $|n\rangle$ and W_n satisfying $\mathcal{H}|n\rangle = W_n|n\rangle$. We assume at this stage that $|n\rangle$ is a non-degenerate state, well separated in energy from other states. Expand $|n\rangle$ and W_n as power series in λ:

$$|n\rangle = |n^0\rangle + \lambda|n'\rangle + \lambda^2|n''\rangle + \cdots, \tag{C.1.3}$$

$$W_n = W_n^0 + \lambda W_n' + \lambda^2 W_n'' + \cdots. \tag{C.1.4}$$

Without loss of generality, we can require that $|n^0\rangle$ is normalized and that all the corrections to the zeroth-order wavefunction are orthogonal to it:

$$\langle n^0|n'\rangle = \langle n^0|n''\rangle = \cdots = 0, \tag{C.1.5}$$

so that $\langle n|n^0\rangle = \langle n^0|n^0\rangle = 1$. This is *intermediate normalization*. Substitute the expressions (C.1.3) and (C.1.4) into $(\mathcal{H} - W_n)|n\rangle = 0$, and we get

$$((\mathcal{H}^0 - W_n^0) + \lambda(\mathcal{H}' - W_n') - \lambda^2 W_n'' + \cdots)(|n^0\rangle + \lambda|n'\rangle + \lambda^2|n''\rangle + \cdots) = 0. \tag{C.1.6}$$

For sufficiently small λ, we expect the power series to converge, and in that case we can equate coefficients of powers of λ:

$$(\mathcal{H}^0 - W_n^0)|n^0\rangle = 0, \tag{C.1.7}$$

$$(\mathcal{H}^0 - W_n^0)|n'\rangle + (\mathcal{H}' - W_n')|n^0\rangle = 0, \tag{C.1.8}$$

$$(\mathcal{H}^0 - W_n^0)|n''\rangle + (\mathcal{H}' - W_n')|n'\rangle - W_n''|n^0\rangle = 0, \tag{C.1.9}$$

$$(\mathcal{H}^0 - W_n^0)|n'''\rangle + (\mathcal{H}' - W_n')|n''\rangle - W_n''|n'\rangle - W_n'''|n^0\rangle = 0, \tag{C.1.10}$$

and so on. The first of these equations is the *zeroth-order* problem, an eigenvalue equation which we suppose solved. The rest are inhomogeneous differential equations. Multiply the first-order equation (C.1.8) by $\langle n^0|$ and integrate:

$$\langle n^0|\mathcal{H}^0 - W_n^0|n'\rangle + \langle n^0|\mathcal{H}' - W_n'|n^0\rangle = 0. \tag{C.1.11}$$

Because $\mathcal{H}^0 - W_n^0$ is hermitian, it follows that for any wavefunction ψ,

$$\langle n^0|\mathcal{H}^0 - W_n^0|\psi\rangle = \langle\psi|\mathcal{H}^0 - W_n^0|n^0\rangle^* = 0, \tag{C.1.12}$$

and since $|n^0\rangle$ is normalized we obtain

$$W_n' = \langle n^0|\mathcal{H}'|n^0\rangle. \tag{C.1.13}$$

Thus the *first-order energy* W_n' is the expectation value of the perturbation operator for the unperturbed wavefunction $|n^0\rangle$. Indeed the total energy to first order is

$$W_n^0 + \lambda W_n' = \langle n^0|\mathcal{H}^0 + \lambda\mathcal{H}'|n^0\rangle. \tag{C.1.14}$$

An alternative way to write this result is:

$$W_n = \langle n^0|\mathcal{H}|n^0\rangle + O(\lambda^2). \tag{C.1.15}$$

Thus the expectation value of the complete Hamiltonian over the unperturbed wavefunction gives the total energy correct to first order in λ.

Now multiply the second-order equation (C.1.9) by $\langle n^0|$, to give

$$\langle n^0|\mathcal{H}^0 - W^0|n''\rangle + \langle n^0|\mathcal{H}' - W_n'|n'\rangle - \langle n^0|W_n''|n^0\rangle = 0. \tag{C.1.16}$$

Once again, the first term is zero. Moreover W_n' disappears from the second term because of the orthogonality between the unperturbed wavefunction and the corrections, eqn (C.1.5), so (C.1.16) becomes

$$W_n'' = \langle n^0|\mathcal{H}'|n'\rangle, \tag{C.1.17}$$

and we have the *second-order energy*. To evaluate this, we need the first-order wavefunction $|n'\rangle$, and to obtain it, we have to solve the inhomogeneous differential equation (C.1.8).

C.1.1 Rayleigh–Schrödinger perturbation theory

The standard way to do this, used by Rayleigh for classical oscillators and adapted for quantum mechanics by Schrödinger, is to expand $|n'\rangle$ in terms of the unperturbed eigenfunctions:

$$|n'\rangle = \sum_k{}' c_k|k^0\rangle, \tag{C.1.18}$$

where the prime on the summation sign conventionally indicates that we are to omit the term with $k = n$. This is to ensure that $\langle n^0|n'\rangle = 0$, in accordance with (C.1.5). Substitute this expression into (C.1.8) and remember that $\mathcal{H}^0|k^0\rangle = W_k^0|k^0\rangle$:

$$\sum_k{}' c_k(W_k^0 - W_n^0)|k^0\rangle + (\mathcal{H}' - W_n')|n^0\rangle = 0. \tag{C.1.19}$$

Multiply by $\langle p^0|$, and remember that the eigenfunctions $|k^0\rangle$ of the unperturbed Hamiltonian are orthonormal. We obtain

$$c_p = -\frac{\langle p^0|\mathcal{H}'|n^0\rangle}{W_p^0 - W_n^0} = -\frac{H'_{pn}}{\Delta_{pn}}, \tag{C.1.20}$$

so that the first-order wavefunction is

$$\begin{aligned} |n'\rangle &= -{\sum_p}' |p^0\rangle \frac{\langle p^0|\mathcal{H}'|n^0\rangle}{W_p^0 - W_n^0} \\ &= -{\sum_p}' |p^0\rangle \frac{H'_{pn}}{\Delta_{pn}}. \end{aligned} \tag{C.1.21}$$

Here the second form introduces an abbreviated notation for the 'energy denominator' $\Delta_{pn} = W_p^0 - W_n^0$ and for the matrix element $H'_{pn} = \langle p^0|\mathcal{H}'|n^0\rangle$. We substitute this result into (C.1.17) to obtain the second-order energy:

$$\begin{aligned} W_n'' &= \langle n^0|\mathcal{H}'|n'\rangle = -{\sum_p}' \frac{\langle n^0|\mathcal{H}'|p^0\rangle\langle p^0|\mathcal{H}'|n^0\rangle}{W_p^0 - W_n^0} \\ &= -{\sum_p}' \frac{H'_{np}H'_{pn}}{\Delta_{pn}} \\ &= -{\sum_p}' \frac{|H'_{pn}|^2}{\Delta_{pn}}. \end{aligned} \tag{C.1.22}$$

Here we have a sum over the excited states of the system. It is important to realize that this extends over *all* excited states, including continuum states.

C.1.2 Unsöld's average-energy approximation

A crude but useful approximation to the second-order energy can be obtained by replacing all the energy denominators in the Rayleigh–Schrödinger expression (C.1.22) for the second-order energy by some 'average' value Δ:

$$\begin{aligned} W_n'' = -{\sum_p}' \frac{|H'_{pn}|^2}{\Delta_{pn}} &\approx -{\sum_p}' \frac{|H'_{pn}|^2}{\Delta} \\ &= -\frac{1}{\Delta}\Big(\sum_p H'_{np}H'_{pn} - H'_{nn}H'_{nn}\Big) \\ &= -\frac{1}{\Delta}\Big(\langle n^0|(\mathcal{H}')^2|n^0\rangle - \langle n^0|\mathcal{H}'|n^0\rangle^2\Big). \end{aligned} \tag{C.1.23}$$

If $|n\rangle$ is the ground state and Δ the first excitation energy, then $\Delta_{pn} \geq \Delta$ and the approximate expression must be larger in magnitude than the exact. Often Δ is taken to be the first ionization energy, but this does not give a lower bound to $|W_n''|$ because the sum over states includes an integral over the continuum states.

C.2 The resolvent

We study here a formal treatment of the perturbation problem which is sometimes useful. It is used in §6.3.1 in the development of iterative symmetry-forcing perturbation methods. First consider the operator $P_k \equiv |k^0\rangle\langle k^0|$, where $|k^0\rangle$ is one of the normalized eigenstates of $\mathcal{H}^0$. If we apply this to a wavefunction $\sum_j c_j|j^0\rangle$, we obtain $\sum_j c_j|k^0\rangle\langle k^0|j^0\rangle = \sum_j c_j|k^0\rangle\delta_{jk} = c_k|k^0\rangle$. That is, P_k projects from a general wavefunction the $|k^0\rangle$ component. It is a *projection operator*. All projection operators satisfy $P_k^2 = P_k$, easily verified in this case. We can also define a complementary projection operator $Q_k = 1 - P_k$, which removes the $|k^0\rangle$ component from any wavefunction, leaving the rest of the wavefunction unchanged. It is easy to verify that $Q_k^2 = Q_k$ also.

Now consider the operator

$$R_n = \frac{Q_n}{(W_n^0 - \mathcal{H}^0)}.$$

Operating on state $|n^0\rangle$ this gives zero, because $Q_n|n^0\rangle = 0$. (This can be made rigorous by replacing W_n^0 by z in the denominator, and taking the limit $z \to W_n^0$ after applying the operator (McWeeny 1989).) Otherwise it behaves like an inverse of the operator $W_n^0 - \mathcal{H}^0$. It is called the *reduced resolvent*.

Apply this operator to eqns (C.1.8–C.1.10). The result is

$$\begin{aligned}
|n'\rangle &= -R_n(\mathcal{H}' - W_n')|n^0\rangle \\
&= -R_n\mathcal{H}'|n^0\rangle, && \text{(C.2.1)}\\
|n''\rangle &= -R_n(\mathcal{H}' - W_n')|n'\rangle + R_nW_n''|n^0\rangle \\
&= -R_n(\mathcal{H}' - W_n')|n'\rangle, && \text{(C.2.2)}\\
|n'''\rangle &= -R_n(\mathcal{H}' - W_n')|n''\rangle + R_nW_n''|n'\rangle + R_nW_n'''|n^0\rangle \\
&= -R_n(\mathcal{H}' - W_n')|n''\rangle + R_nW_n''|n'\rangle, && \text{(C.2.3)}
\end{aligned}$$

and in general

$$|n^{(m)}\rangle = -R_n(\mathcal{H}' - W_n')|n^{(m-1)}\rangle + R_n\sum_{t=1}^{m-2} W_n^{(m-t)}|n^{(t)}\rangle. \qquad \text{(C.2.4)}$$

By expressing R_n in the form $R_n = \sum_k{}'|k^0\rangle(W_n^0 - W_k^0)^{-1}\langle k^0|$ (with the prime on the sum denoting as usual that the term $k = n$ is omitted from the sum) we can recover the formulae of Rayleigh–Schrödinger perturbation theory.

C.3 Degenerate perturbation theory

If the state $|n^0\rangle$ is degenerate (a set of components $|n\alpha^0\rangle$ all with energy W_n^0) then we cannot apply the Rayleigh–Schrödinger formulae (C.1.21) and (C.1.17) because some of the energy denominators vanish. Also, if we take a particular perturbed state and allow λ to tend to zero, there is no reason to expect that the resulting zeroth-order state $|nm^0\rangle$ will coincide with one of the $|n\alpha^0\rangle$. Rather we expect to get a linear combination of them:

$$|nm^0\rangle = \sum_\alpha c_{\alpha m}|n\alpha^0\rangle. \qquad \text{(C.3.1)}$$

The first-order perturbation equation (C.1.8) now becomes, for the perturbed state $|nm\rangle$,

$$(\mathcal{H}^0 - W_n^0)|nm'\rangle + (\mathcal{H}' - W'_{nm}) \sum_\alpha c_{\alpha m}|n\alpha^0\rangle = 0. \tag{C.3.2}$$

If we multiply by $\langle n\beta^0|$, the first term disappears as before, because $(\mathcal{H}^0 - W_n^0)|n\beta^0\rangle = 0$, and we get a set of secular equations:

$$\langle n\beta^0|\mathcal{H}' - W'_{nm}|n\alpha^0\rangle c_{\alpha m} = 0. \tag{C.3.3}$$

Consequently we need to solve these secular equations to find the first-order energies W'_{nm} and the corresponding eigenvectors $c_{\alpha m}$. Alternatively, since $(\mathcal{H}^0 - W_n^0)|n\alpha^0\rangle = 0$, we can replace (C.3.3) by

$$\langle n\beta^0|\mathcal{H}^0 + \lambda\mathcal{H}' - W_n^0 - \lambda W'_{nm}|n\alpha^0\rangle c_{\alpha m} = 0. \tag{C.3.4}$$

That is,

$$\sum_\alpha (H_{n\beta,n\alpha} - W\delta_{\beta\alpha})c_{\alpha m} = 0, \tag{C.3.5}$$

where $H_{n\beta,n\alpha}$ is the matrix element of the complete Hamiltonian and W is the energy correct to first order. Note that (C.3.5) is the result we would get from a variational treatment using the trial function (C.3.1), and that consequently the same result applies in the 'nearly degenerate' case, where the energy separations among a set of unperturbed states, although non-zero, are not large compared with the matrix elements of the perturbation. In such a case the formulae don't blow up, but the perturbation series fails to converge and the degenerate version must be used.

Now we can follow the Rayleigh–Schrödinger procedure to find the first-order wavefunction as before:

$$|nm'\rangle = -{\sum_{pq}}' \frac{\mathcal{H}'_{pq,nm}}{\Delta_{pn}}|pq^0\rangle, \tag{C.3.6}$$

where the sum is taken over the components $|pq^0\rangle$ of the other unperturbed states, and $\Delta_{pn} = W_p^0 - W_n^0$ as before. Similarly

$$W''_{nm} = -{\sum_{pq}}' \frac{|\mathcal{H}'_{pq,nm}|^2}{\Delta_{pn}}. \tag{C.3.7}$$

C.4 Time-dependent perturbation theory

Here we consider a Hamiltonian $\mathcal{H} = \mathcal{H}^0 + \mathcal{H}'$ consisting of a time-independent part $\mathcal{H}^0$ and a time-dependent perturbation $\mathcal{H}'$. The unperturbed states are stationary:

$$\Psi_n = \psi_n \exp(-\mathrm{i}W_n t/\hbar) = |n\rangle \exp(-\mathrm{i}\omega_n t), \tag{C.4.1}$$

where the $|n\rangle$ are the eigenstates of the unperturbed Hamiltonian: $\mathcal{H}^0|n\rangle = W_n|n\rangle$. The perturbed problem does not have stationary states; the solution Ψ must satisfy Schrödinger's time-dependent equation:

$$\mathcal{H}\Psi = \mathrm{i}\hbar\frac{\partial}{\partial t}\Psi. \tag{C.4.2}$$

To solve this, we use Dirac's method of *variation of constants*: let

$$\Psi = \sum_k a_k(t)\Psi_k(t) = \sum_k a_k(t)\psi_k \exp(-\mathrm{i}\omega_k t). \tag{C.4.3}$$

If the Hamiltonian were time-independent the a_k would be constant (and their values would be arbitrary). In the presence of the small time-dependent perturbation they evolve slowly with time. Substituting (C.4.3) into (C.4.2) gives

$$\mathcal{H}\sum_k a_k(t)\Psi_k(t) = \mathrm{i}\hbar\frac{\partial}{\partial t}\sum_k a_k(t)\Psi_k(t), \tag{C.4.4}$$

or

$$\sum_k [a_k W_k\Psi_k + a_k\mathcal{H}'(t)\Psi_k] = \sum_k [\mathrm{i}\hbar\frac{\partial a_k}{\partial t}\Psi_k + a_k W_k\Psi_k]. \tag{C.4.5}$$

Multiply by $\Psi_p^* = \langle p|\exp(+\mathrm{i}W_p t/\hbar)$ and integrate over variables other than time:

$$\sum_k a_k\langle p|\mathcal{H}'(t)|k\rangle \exp(\mathrm{i}\omega_{pk}t) = \mathrm{i}\hbar\frac{\partial a_p}{\partial t}, \tag{C.4.6}$$

where $\omega_{pk} = (W_p - W_k)/\hbar$. We can integrate this formally to obtain

$$a_p(t) - a_p(0) = -\frac{\mathrm{i}}{\hbar}\sum_k \int_0^t a_k(\tau)\langle p|\mathcal{H}'(\tau)|k\rangle \exp(\mathrm{i}\omega_{pk}\tau)\,\mathrm{d}\tau. \tag{C.4.7}$$

If $\mathcal{H}'$ takes the form $\mathcal{H}' = \hat{V}f(t)$, where $\hat{V}$ is an operator independent of time and $f(t)$ is a function only of the time, then

$$a_p(t) - a_p(0) = -\frac{\mathrm{i}}{\hbar}\sum_k V_{pk}\int_0^t a_k(\tau)f(\tau)\exp(\mathrm{i}\omega_{pk}\tau)\,\mathrm{d}\tau. \tag{C.4.8}$$

All of this is *exact*, but is rarely useful as it stands since the expression for $a_p(t)$ involves all the a_k (including a_p) at times from 0 to t. We must therefore approximate: we assume that $\hat{V}$ is sufficiently small that the a_k will not change much over the interval from 0 to t, so that we can put $a_k(\tau) = a_k(0)$ in (C.4.8), giving

$$a_p(t) - a_p(0) = -\frac{\mathrm{i}}{\hbar}\sum_k V_{pk}a_k(0)\int_0^t f(\tau)\exp(\mathrm{i}\omega_{pk}\tau)\,\mathrm{d}\tau. \tag{C.4.9}$$

If necessary we could substitute this result back into the r.h.s. of (C.4.8) to obtain a second-order formula, but in practice (C.4.9) is usually adequate.

For simplicity we now consider the case where the system is definitely in the stationary state n at time 0, so that $a_k(0) = \delta_{kn}$. Then $a_p(t)$ is the probability amplitude for a transition to state p having occurred by time t:

$$a_p(t) = -\frac{\mathrm{i}}{\hbar}V_{pn}\int_0^t f(\tau)\exp(\mathrm{i}\omega_{pn}\tau)\,\mathrm{d}\tau, \quad p \neq n. \tag{C.4.10}$$

The development of the theory from this point depends on the form of the function $f(t)$ that describes the time-dependence of the perturbation. See, for example, the discussion in §2.5 of the response of a molecule to an oscillating electric field.

Appendix D
Conversion Factors

The conversion factors in this appendix have been derived using the 2010 CODATA recommended values of the fundamental constants. The uncertainties in these values are generally a few parts in the last digit quoted.

D.1 Multipole moments

Dipole moment

The debye is defined as 10^{-18} esu (electrostatic units). The esu of length is the centimetre, while the esu of charge is numerically equal to $10/c$ C, but with c expressed in cm s^{-1} (Cohen *et al.* 2008*b*).

	10^{-30} C m	debye	a.u. (ea_0)	e Å
10^{-30} C m	1	0.299792458	0.11794743	0.062415093
1 debye	3.33564095	1	0.39343029	0.20819434
1 a.u. (ea_0)	8.4783533	2.5417464	1	0.529177211
1 e Å	16.021766	4.8032045	1.88972612	1

Quadrupole moment

The buckingham unit of quadrupole moment was introduced by Debye and named after A. D. Buckingham. It is the same as the debye ångström = 10^{-26} esu.

	10^{-40} C m^2	D Å	a.u. (ea_0^2)	e Å^2
10^{-40} C m^2	1	0.299792458	0.222888345	0.062415093
1 B = 1 D Å	3.33564095	1	0.743475491	0.208194342
1 a.u. (ea_0^2)	4.4865513	1.3450342	1	0.280028521
1 e Å^2	16.021766	4.8032045	3.57106483	1

Octopole moment

	10^{-50} C m^3	a.u. (ea_0^3)	e Å^3
10^{-50} C m^3	1	0.42119793	0.062415093
1 a.u. (ea_0^3)	2.3741807	1	0.14818471
1 e Å^3	16.021766	6.74833449	1

D.2 Polarizabilities

The dipole–dipole polarizability has dimensions of $[4\pi\epsilon_0] \times [\text{length}^3]$. In the electrostatic unit system, $4\pi\epsilon_0$ is dimensionless and is equal to 1, so that the polarizability has units of volume, typically Å^3. In atomic units, $4\pi\epsilon_0$ is numerically equal to 1, but it is not dimensionless; nevertheless, polarizabilities in atomic units are often wrongly quoted as being in units of a_0^3. When converting any of these to SI, it is necessary to insert the factor of $4\pi\epsilon_0$. The SI unit of permittivity, i.e., of $4\pi\epsilon_0$, is F m^{-1}, where $\text{F} = \text{C V}^{-1}$ is the farad, so the SI unit of polarizability is F m^2.

	$10^{-40}\,\text{F m}^2$	a.u. $(4\pi\epsilon_0 a_0^3)$	$\text{Å}^3 = 10^{-24}\,\text{cm}^3$
$10^{-40}\,\text{F m}^2$	1	6.0651006	0.89875518
1 a.u.	0.16487773	1	0.14818471
$1\,\text{Å}^3 = 10^{-24}\,\text{cm}^3$	1.11265006	6.7483335	1

In general, the SI unit of rank-l–rank-l' polarizability is $\text{F m}^{l+l'}$, and the atomic unit is $4\pi\epsilon_0 \times a_0^{l+l'+1}$. Conversion factors for these are easily derived from those for dipole–dipole polarizability by applying the appropriate power of $a_0 = 0.52917725 \times 10^{-10}\,\text{m}$. Thus for dipole–quadrupole polarizability:

$$1\,\text{a.u.} = 4\pi\epsilon_0 a_0^4 = 0.08725 \times 10^{-50}\,\text{F m}^3.$$

D.3 Dispersion coefficients

C_6 coefficients have the form [energy]×[length]^6, and various length and energy units have been used. Only the conversions between atomic units and SI are given here; E_h is the Hartree energy $e^2/4\pi\epsilon_0 a_0$:

$$E_\text{h} a_0^6 = 57.65261 \times 10^{-60}\,\text{kJ mol}^{-1}\,\text{m}^6 = 57.65261\,\text{kJ mol}^{-1}\,\text{Å}^6;$$

$$\text{kJ mol}^{-1}\,\text{Å}^6 = 0.0173453 E_\text{h} a_0^6.$$

Appendix E
Cartesian–Spherical Conversion Tables

Table E.1 Regular spherical harmonics and multipole moments.

$R_{00} = 1$	$Q_{00} = q$
$R_{10} = z$	$Q_{10} = \mu_z$
$R_{11c} = x$	$Q_{11c} = \mu_x$
$R_{11s} = y$	$Q_{11s} = \mu_y$
$R_{20} = \frac{1}{2}(3z^2 - r^2)$	$Q_{20} = \Theta_{zz}$
$R_{21c} = \sqrt{3}xz$	$Q_{21c} = \frac{2}{\sqrt{3}}\Theta_{xz}$
$R_{21s} = \sqrt{3}yz$	$Q_{21s} = \frac{2}{\sqrt{3}}\Theta_{yz}$
$R_{22c} = \frac{1}{2}\sqrt{3}(x^2 - y^2)$	$Q_{22c} = \frac{1}{\sqrt{3}}(\Theta_{xx} - \Theta_{yy})$
$R_{22s} = \sqrt{3}xy$	$Q_{22s} = \frac{2}{\sqrt{3}}\Theta_{xy}$
$R_{30} = \frac{1}{2}(5z^3 - 3zr^2)$	$Q_{30} = \Omega_{zzz}$
$R_{31c} = \frac{1}{4}\sqrt{6}x(5z^2 - r^2)$	$Q_{31c} = \sqrt{\frac{3}{2}}\Omega_{xzz}$
$R_{31s} = \frac{1}{4}\sqrt{6}y(5z^2 - r^2)$	$Q_{31s} = \sqrt{\frac{3}{2}}\Omega_{yzz}$
$R_{32c} = \frac{1}{2}\sqrt{15}z(x^2 - y^2)$	$Q_{32c} = \sqrt{\frac{3}{5}}(\Omega_{xxz} - \Omega_{yyz})$
$R_{32s} = \sqrt{15}xyz$	$Q_{32s} = 2\sqrt{\frac{3}{5}}\Omega_{xyz}$
$R_{33c} = \frac{1}{4}\sqrt{10}(x^3 - 3xy^2)$	$Q_{33c} = \sqrt{\frac{1}{10}}(\Omega_{xxx} - 3\Omega_{xyy})$
$R_{33s} = \frac{1}{4}\sqrt{10}(3x^2y - y^3)$	$Q_{33s} = \sqrt{\frac{1}{10}}(3\Omega_{xxy} - \Omega_{yyy})$

continued ...

Table E.1 continued

$R_{40} = \frac{1}{8}[8z^4 - 24(x^2+y^2)z^2 + 3(x^4+2x^2y^2+y^4)]$	$Q_{40} = \Phi_{zzzz}$
$R_{41c} = \frac{1}{4}\sqrt{10}[4xz^3 - 3xz(x^2+y^2)]$	$Q_{41c} = \sqrt{\frac{8}{5}}\Phi_{xzzz}$
$R_{41s} = \frac{1}{4}\sqrt{10}[4yz^3 - 3yz(x^2+y^2)]$	$Q_{41s} = \sqrt{\frac{8}{5}}\Phi_{yzzz}$
$R_{42c} = \frac{1}{4}\sqrt{5}(x^2-y^2)(6z^2-x^2-y^2)$	$Q_{42c} = 2\sqrt{\frac{1}{5}}(\Phi_{xxzz} - \Phi_{yyzz})$
$R_{42s} = \frac{1}{2}\sqrt{5}xy(6z^2-x^2-y^2)$	$Q_{42s} = 4\sqrt{\frac{1}{5}}\Phi_{xyzz}$
$R_{43c} = \frac{1}{4}\sqrt{70}z(x^3-3xy^2)$	$Q_{43c} = 2\sqrt{\frac{2}{35}}(\Phi_{xxxz} - 3\Phi_{xyyz})$
$R_{43s} = \frac{1}{4}\sqrt{70}z(3x^2y-y^3)$	$Q_{43s} = 2\sqrt{\frac{2}{35}}(3\Phi_{xxyz} - \Phi_{yyyz})$
$R_{44c} = \frac{1}{8}\sqrt{35}(x^4-6x^2y^2+y^4)$	$Q_{44c} = \sqrt{\frac{1}{35}}(\Phi_{xxxx} - 6\Phi_{xxyy} + \Phi_{yyyy})$
$R_{44s} = \frac{1}{2}\sqrt{35}xy(x^2-y^2)$	$Q_{44s} = 4\sqrt{\frac{1}{35}}(\Phi_{xxxy} - \Phi_{xyyy})$

Table E.2 Conversion from spherical multipole moments to cartesian.

$$\Theta_{xx} = -\tfrac{1}{2}Q_{20} + \tfrac{1}{2}\sqrt{3}Q_{22c}$$
$$\Theta_{yy} = -\tfrac{1}{2}Q_{20} - \tfrac{1}{2}\sqrt{3}Q_{22c}$$
$$\Theta_{zz} = Q_{20}$$
$$\Theta_{xy} = \tfrac{1}{2}\sqrt{3}Q_{22s}$$
$$\Theta_{xz} = \tfrac{1}{2}\sqrt{3}Q_{21c}$$
$$\Theta_{yz} = \tfrac{1}{2}\sqrt{3}Q_{21s}$$

$$\Omega_{xxx} = \sqrt{\tfrac{5}{8}}Q_{33c} - \sqrt{\tfrac{3}{8}}Q_{31c}$$
$$\Omega_{xxy} = \sqrt{\tfrac{5}{8}}Q_{33s} - \sqrt{\tfrac{1}{24}}Q_{31s}$$
$$\Omega_{xyy} = -\sqrt{\tfrac{5}{8}}Q_{33c} - \sqrt{\tfrac{1}{24}}Q_{31c}$$
$$\Omega_{yyy} = -\sqrt{\tfrac{5}{8}}Q_{33s} - \sqrt{\tfrac{3}{8}}Q_{31s}$$
$$\Omega_{xxz} = \sqrt{\tfrac{5}{12}}Q_{32c} - \tfrac{1}{2}Q_{30}$$
$$\Omega_{xyz} = \sqrt{\tfrac{5}{12}}Q_{32s}$$
$$\Omega_{yyz} = -\sqrt{\tfrac{5}{12}}Q_{32c} - \tfrac{1}{2}Q_{30}$$
$$\Omega_{xzz} = \sqrt{\tfrac{2}{3}}Q_{31c}$$
$$\Omega_{yzz} = \sqrt{\tfrac{2}{3}}Q_{31s}$$
$$\Omega_{zzz} = Q_{30}$$

$$\Phi_{xxxx} = \tfrac{3}{8}Q_{40} - \tfrac{1}{4}\sqrt{5}Q_{42c} + \tfrac{1}{8}\sqrt{35}Q_{44c}$$
$$\Phi_{xxxy} = \tfrac{1}{8}(-\sqrt{5}Q_{42s} + \sqrt{35}Q_{44s})$$
$$\Phi_{xxyy} = \tfrac{1}{8}Q_{40} - \tfrac{1}{8}\sqrt{35}Q_{44c}$$
$$\Phi_{xyyy} = -\tfrac{1}{8}(\sqrt{5}Q_{42s} + \sqrt{35}Q_{44s})$$
$$\Phi_{yyyy} = \tfrac{3}{8}Q_{40} + \tfrac{1}{4}\sqrt{5}Q_{42c} + \tfrac{1}{8}\sqrt{35}Q_{44c}$$
$$\Phi_{xxxz} = \tfrac{1}{16}(-3\sqrt{10}Q_{41c} + \sqrt{70}Q_{43c})$$
$$\Phi_{xxyz} = \tfrac{1}{16}(-\sqrt{10}Q_{41s} + \sqrt{70}Q_{43s})$$
$$\Phi_{xyyz} = -\tfrac{1}{16}(\sqrt{10}Q_{41c} + \sqrt{70}Q_{43c})$$
$$\Phi_{yyyz} = -\tfrac{1}{16}(3\sqrt{10}Q_{41s} + \sqrt{70}Q_{43s})$$
$$\Phi_{xxzz} = -\tfrac{1}{2}Q_{40} + \tfrac{1}{4}\sqrt{5}Q_{42c}$$
$$\Phi_{xyzz} = \tfrac{1}{4}\sqrt{5}Q_{42s}$$
$$\Phi_{yyzz} = -\tfrac{1}{2}Q_{40} - \tfrac{1}{4}\sqrt{5}Q_{42c}$$
$$\Phi_{xzzz} = \sqrt{\tfrac{5}{8}}Q_{41c}$$
$$\Phi_{yzzz} = \sqrt{\tfrac{5}{8}}Q_{41s}$$
$$\Phi_{zzzz} = Q_{40}$$

Table E.3 Origin-shift coefficients for multipole moments in real spherical-tensor form (eqn (2.7.8)).

$W_{tu}(\mathbf{x})$	u								
t	00	10	$11c$	$11s$	20	$21c$	$21s$	$22c$	$22s$
00	1								
10	R_{10}	1	0	0					
$11c$	R_{11c}	0	1	0					
$11s$	R_{11s}	0	0	1					
20	R_{20}	$2R_{10}$	$-R_{11c}$	$-R_{11s}$	1	0	0	0	0
$21c$	R_{21c}	$\sqrt{3}R_{11c}$	$\sqrt{3}R_{10}$	0	0	1	0	0	0
$21s$	R_{21s}	$\sqrt{3}R_{11s}$	0	$\sqrt{3}R_{10}$	0	0	1	0	0
$22c$	R_{22c}	0	$\sqrt{3}R_{11c}$	$-\sqrt{3}R_{11s}$	0	0	0	1	0
$22s$	R_{22s}	0	$\sqrt{3}R_{11s}$	$\sqrt{3}R_{11c}$	0	0	0	0	1
30	R_{30}	$3R_{20}$	$-\sqrt{3}R_{21c}$	$-\sqrt{3}R_{21s}$	$3R_{10}$	$-\sqrt{3}R_{11c}$	$-\sqrt{3}R_{11s}$	0	0
$31c$	R_{31c}	$\sqrt{8}R_{21c}$	$\sqrt{6}R_{20} - \sqrt{\frac{1}{2}}R_{22c}$	$-\sqrt{\frac{1}{2}}R_{22s}$	$\sqrt{6}R_{11c}$	$\sqrt{8}R_{10}$	0	$-\sqrt{\frac{1}{2}}R_{11c}$	$-\sqrt{\frac{1}{2}}R_{11s}$
$31s$	R_{31s}	$\sqrt{8}R_{21s}$	$-\sqrt{\frac{1}{2}}R_{22s}$	$\sqrt{6}R_{20} + \sqrt{\frac{1}{2}}R_{22c}$	$\sqrt{6}R_{11s}$	0	$\sqrt{8}R_{10}$	$\sqrt{\frac{1}{2}}R_{11s}$	$-\sqrt{\frac{1}{2}}R_{11c}$
$32c$	R_{32c}	$\sqrt{5}R_{22c}$	$\sqrt{5}R_{21c}$	$-\sqrt{5}R_{21s}$	0	$\sqrt{5}R_{11c}$	$-\sqrt{5}R_{11s}$	$\sqrt{5}R_{10}$	0
$32s$	R_{32s}	$\sqrt{5}R_{22s}$	$\sqrt{5}R_{21s}$	$\sqrt{5}R_{21c}$	0	$\sqrt{5}R_{11s}$	$\sqrt{5}R_{11c}$	0	$\sqrt{5}R_{10}$
$33c$	R_{33c}	0	$\sqrt{\frac{15}{2}}R_{22c}$	$-\sqrt{\frac{15}{2}}R_{22s}$	0	0	0	$\sqrt{\frac{15}{2}}R_{11c}$	$-\sqrt{\frac{15}{2}}R_{11s}$
$33s$	R_{33s}	0	$\sqrt{\frac{15}{2}}R_{22s}$	$\sqrt{\frac{15}{2}}R_{22c}$	0	0	0	$\sqrt{\frac{15}{2}}R_{11s}$	$\sqrt{\frac{15}{2}}R_{11c}$

Table E.4 Conversion from spherical dipole–quadrupole polarizabilities to cartesian.

$A_{\alpha,\beta\gamma}$	α		
$\beta\gamma$	x	y	z
xx	$-\frac{1}{2}\alpha_{11c,20} + \frac{1}{2}\sqrt{3}\alpha_{11c,22c}$	$-\frac{1}{2}\alpha_{11s,20} + \frac{1}{2}\sqrt{3}\alpha_{11s,22c}$	$-\frac{1}{2}\alpha_{10,20} + \frac{1}{2}\sqrt{3}\alpha_{10,22c}$
yy	$-\frac{1}{2}\alpha_{11c,20} - \frac{1}{2}\sqrt{3}\alpha_{11c,22c}$	$-\frac{1}{2}\alpha_{11s,20} - \frac{1}{2}\sqrt{3}\alpha_{11s,22c}$	$-\frac{1}{2}\alpha_{10,20} - \frac{1}{2}\sqrt{3}\alpha_{10,22c}$
zz	$\alpha_{11c,20}$	$\alpha_{11s,20}$	$\alpha_{10,20}$
xy	$\frac{1}{2}\sqrt{3}\alpha_{11c,22s}$	$\frac{1}{2}\sqrt{3}\alpha_{11s,22s}$	$\frac{1}{2}\sqrt{3}\alpha_{10,22s}$
xz	$\frac{1}{2}\sqrt{3}\alpha_{11c,21c}$	$\frac{1}{2}\sqrt{3}\alpha_{11s,21c}$	$\frac{1}{2}\sqrt{3}\alpha_{10,21c}$
yz	$\frac{1}{2}\sqrt{3}\alpha_{11c,21s}$	$\frac{1}{2}\sqrt{3}\alpha_{11s,21s}$	$\frac{1}{2}\sqrt{3}\alpha_{10,21s}$

Table E.5 Conversion from cartesian quadrupole–quadrupole polarizabilities to spherical.

$\alpha_{2\kappa,2\kappa'}$	κ'				
κ	0	$1c$	$1s$	$2c$	$2s$
0	$3C_{zz,zz}$	$2\sqrt{3}C_{zz,xz}$	$2\sqrt{3}C_{zz,yz}$	$\sqrt{3}(C_{zz,xx} - C_{zz,yy})$	$2\sqrt{3}C_{zz,xy}$
$1c$	$2\sqrt{3}C_{xz,zz}$	$4C_{xz,xz}$	$4C_{xz,yz}$	$2(C_{xz,xx} - C_{xz,yy})$	$4C_{xz,xy}$
$1s$	$2\sqrt{3}C_{yz,zz}$	$4C_{yz,xz}$	$4C_{yz,yz}$	$2(C_{yz,xx} - C_{yz,yy})$	$4C_{yz,xy}$
$2c$	$\sqrt{3}(C_{xx,zz} - C_{yy,zz})$	$2(C_{xx,xz} - C_{yy,xz})$	$2(C_{xx,yz} - C_{yy,yz})$	$(C_{xx,xx} - 2C_{xx,yy} + C_{yy,yy})$	$2(C_{xx,xy} - C_{yy,xy})$
$2s$	$2\sqrt{3}C_{xy,zz}$	$4C_{xy,xz}$	$4C_{xy,yz}$	$2(C_{xy,xx} - C_{xy,yy})$	$4C_{xy,xy}$

Table E.6 Conversion from spherical quadrupole–quadrupole polarizabilities to cartesian.

$$
\begin{aligned}
12C_{xx,xx} &= \alpha_{20,20} - 2\sqrt{3}\alpha_{20,22c} + 3\alpha_{22c,22c} \\
12C_{xx,xy} &= -\sqrt{3}\alpha_{20,22s} + 3\alpha_{22c,22s} \\
12C_{xx,xz} &= -\sqrt{3}\alpha_{20,21c} + 3\alpha_{22c,21c} \\
12C_{xx,yy} &= \alpha_{20,20} - 3\alpha_{22c,22c} \\
12C_{xx,yz} &= -\sqrt{3}\alpha_{20,21s} + 3\alpha_{22c,21s} \\
12C_{xx,zz} &= -2\alpha_{20,20} + 2\sqrt{3}\alpha_{22c,20} \\
12C_{xy,xy} &= 3\alpha_{22s,22s} \\
12C_{xy,xz} &= 3\alpha_{22s,21c} \\
12C_{xy,yy} &= -\sqrt{3}\alpha_{22s,20} - 3\alpha_{22s,22c} \\
12C_{xy,yz} &= 3\alpha_{22s,21s} \\
12C_{xy,zz} &= 2\sqrt{3}\alpha_{22s,20} \\
12C_{xz,xz} &= 3\alpha_{21c,21c} \\
12C_{xz,yy} &= -\sqrt{3}\alpha_{21c,20} - 3\alpha_{21c,22c} \\
12C_{xz,yz} &= 3\alpha_{21c,21s} \\
12C_{xz,zz} &= 2\sqrt{3}\alpha_{21c,20} \\
12C_{yy,yy} &= \alpha_{20,20} + 2\sqrt{3}\alpha_{20,22c} + 3\alpha_{22c,22c} \\
12C_{yy,yz} &= -\sqrt{3}\alpha_{20,21s} - 3\alpha_{22c,21s} \\
12C_{yy,zz} &= -2\alpha_{20,20} - 2\sqrt{3}\alpha_{22c,20} \\
12C_{yz,yz} &= 3\alpha_{21s,21s} \\
12C_{yz,zz} &= 2\sqrt{3}\alpha_{21s,20} \\
12C_{zz,zz} &= 4\alpha_{20,20}
\end{aligned}
$$

Appendix F
Interaction Functions

Here are listed the interaction functions T^{ab}_{tu} that arise in the spherical-tensor formulation of electrostatic interactions (see Chapter 3). The terms in R^{-n} up to $n = 5$ have been given previously by Stone (1991), but there were misprints in the formulae for $T_{21c,21c}$ and $T_{21s,21s}$: the coefficient +6 in the last term should have been −6 in each case. The formulae given here for these two functions and for $T_{21c,21s}$ are in a different and more symmetrical form given by Hättig and Heß (1994), but the two versions are equivalent. All the formulae for $n = 6$ were derived by Hättig and Heß.

The interaction function T^{ab}_{tu} for the electrostatic interaction between a multipole moment Q_t on site a and a moment Q_u on site b, both referred to local axes, is given in terms of the direction cosines r^a_α, r^b_β and $c_{\alpha\beta}$. If $\mathbf{e}^a_x$, $\mathbf{e}^a_y$ and $\mathbf{e}^a_z$ are the unit vectors defining the local axis system for site a, $\mathbf{e}^b_x$, $\mathbf{e}^b_y$ and $\mathbf{e}^b_z$ are the unit vectors for site b, and $\mathbf{e}_{ab}$ is a unit vector in the direction from a to b, then $r^a_\alpha = \mathbf{e}^a_\alpha \cdot \mathbf{e}_{ab}$, $r^b_\beta = \mathbf{e}^b_\beta \cdot \mathbf{e}_{ba} = -\mathbf{e}^b_\beta \cdot \mathbf{e}_{ab}$ (note the minus sign) and $c_{\alpha\beta} = \mathbf{e}^a_\alpha \cdot \mathbf{e}^b_\beta$. Thus r^a_α, $\alpha = x, y, z$, are the components of a unit vector in the direction from a to b, expressed in the local axis system of site a, and r^b_β, $\beta = x, y, z$, are the components of a unit vector in the direction from b to a, expressed in the local axis system of site b.

With this notation, it is possible to obtain $T^{ab}_{ut} = T^{ba}_{tu}$ from T^{ab}_{tu} merely by replacing a by b and vice versa, and exchanging the suffixes in every $c_{\alpha\beta}$.

The components of a dipole moment may be written as Q_{10}, Q_{11c} and Q_{11s} or as Q_{1z}, Q_{1x} and Q_{1y}. The latter notation is used here, with the usual cartesian-tensor convention of α to mean x, y or z.

Table F.1 Interaction functions $T^{ab}_{t\,u}$ for all terms in R^{-n} up to $n = 6$.

t	u	$4\pi\epsilon_0 T^{ab}_{tu}$
00	00	R^{-1}
1α	00	$R^{-2}.r^a_\alpha$
20	00	$R^{-3}.\frac{1}{2}(3{r^a_z}^2 - 1)$
$21c$	00	$R^{-3}.\sqrt{3}r^a_x r^a_z$
$21s$	00	$R^{-3}.\sqrt{3}r^a_y r^a_z$
$22c$	00	$R^{-3}.\frac{1}{2}\sqrt{3}({r^a_x}^2 - {r^a_y}^2)$
$22s$	00	$R^{-3}.\sqrt{3}r^a_x r^a_y$
1α	1β	$R^{-3}.(3r^a_\alpha r^b_\beta + c_{\alpha\beta})$
30	00	$R^{-4}.\frac{1}{2}(5{r^a_z}^3 - 3r^a_z)$
$31c$	00	$R^{-4}.\frac{1}{4}\sqrt{6}r^a_x(5{r^a_z}^2 - 1)$
$31s$	00	$R^{-4}.\frac{1}{4}\sqrt{6}r^a_y(5{r^a_z}^2 - 1)$
$32c$	00	$R^{-4}.\frac{1}{2}\sqrt{15}r^a_z({r^a_x}^2 - {r^a_y}^2)$
$32s$	00	$R^{-4}.\sqrt{15}r^a_x r^a_y r^a_z$
$33c$	00	$R^{-4}.\frac{1}{4}\sqrt{10}r^a_x({r^a_x}^2 - 3{r^a_y}^2)$
$33s$	00	$R^{-4}.\frac{1}{4}\sqrt{10}r^a_y(3{r^a_x}^2 - {r^a_y}^2)$
20	1β	$R^{-4}.\frac{1}{2}(15{r^a_z}^2 r^b_\beta + 6r^a_z c_{z\beta} - 3r^b_\beta)$
$21c$	1β	$R^{-4}.\sqrt{3}(r^a_x c_{z\beta} + c_{x\beta}r^a_z + 5r^a_x r^a_z r^b_\beta)$
$21s$	1β	$R^{-4}.\sqrt{3}(r^a_y c_{z\beta} + c_{y\beta}r^a_z + 5r^a_y r^a_z r^b_\beta)$
$22c$	1β	$R^{-4}.\frac{1}{2}\sqrt{3}(5({r^a_x}^2 - {r^a_y}^2)r^b_\beta + 2r^a_x c_{x\beta} - 2r^a_y c_{y\beta})$
$22s$	1β	$R^{-4}.\sqrt{3}(5r^a_x r^a_y r^b_\beta + r^a_x c_{y\beta} + r^a_y c_{x\beta})$
40	00	$R^{-5}.\frac{1}{8}(35{r^a_z}^4 - 30{r^a_z}^2 + 3)$
$41c$	00	$R^{-5}.\frac{1}{4}\sqrt{10}(7r^a_x {r^a_z}^3 - 3r^a_x r^a_z)$
$41s$	00	$R^{-5}.\frac{1}{4}\sqrt{10}(7r^a_y {r^a_z}^3 - 3r^a_y r^a_z)$
$42c$	00	$R^{-5}.\frac{1}{4}\sqrt{5}(7{r^a_z}^2 - 1)({r^a_x}^2 - {r^a_y}^2)$

continued ...

Table F.1 continued

t	u	$4\pi\epsilon_0 T^{ab}_{tu}$
$42s$	00	$R^{-5}.\frac{1}{2}\sqrt{5}(7r_z^{a\,2}-1)r_x^a r_y^a$
$43c$	00	$R^{-5}.\frac{1}{4}\sqrt{70}r_x^a r_z^a(r_x^{a\,2}-3r_y^{a\,2})$
$43s$	00	$R^{-5}.\frac{1}{4}\sqrt{70}r_y^a r_z^a(3r_x^{a\,2}-r_y^{a\,2})$
$44c$	00	$R^{-5}.\frac{1}{8}\sqrt{35}(r_x^{a\,4}-6r_x^{a\,2}r_y^{a\,2}+r_y^{a\,4})$
$44s$	00	$R^{-5}.\frac{1}{2}\sqrt{35}r_x^a r_y^a(r_x^{a\,2}-r_y^{a\,2})$
30	1β	$R^{-5}.\frac{1}{2}(35r_z^{a\,3}r_\beta^b+15r_z^{a\,2}c_{z\beta}-15r_z^a r_\beta^b-3c_{z\beta})$
$31c$	1β	$R^{-5}.\frac{1}{4}\sqrt{6}(35r_x^a r_z^{a\,2}r_\beta^b+5r_z^{a\,2}c_{x\beta}+10r_x^a r_z^a c_{z\beta}-5r_x^a r_\beta^b-c_{x\beta})$
$31s$	1β	$R^{-5}.\frac{1}{4}\sqrt{6}(35r_y^a r_z^{a\,2}r_\beta^b+5r_z^{a\,2}c_{y\beta}+10r_y^a r_z^a c_{z\beta}-5r_y^a r_\beta^b-c_{y\beta})$
$32c$	1β	$R^{-5}.\frac{1}{2}\sqrt{15}((r_x^{a\,2}-r_y^{a\,2})(7r_z^a r_\beta^b+c_{z\beta})+2r_z^a(r_x^a c_{x\beta}-r_y^a c_{y\beta}))$
$32s$	1β	$R^{-5}.\sqrt{15}(r_x^a r_y^a(7r_z^a r_\beta^b+c_{z\beta})+r_z^a(r_x^a c_{y\beta}+r_y^a c_{x\beta}))$
$33c$	1β	$R^{-5}.\frac{1}{4}\sqrt{10}(7r_x^{a\,3}r_\beta^b+3(r_x^{a\,2}-r_y^{a\,2})c_{x\beta}-21r_x^a r_y^{a\,2}r_\beta^b-6r_x^a r_y^a c_{y\beta})$
$33s$	1β	$R^{-5}.\frac{1}{4}\sqrt{10}(-7r_y^{a\,3}r_\beta^b+3(r_x^{a\,2}-r_y^{a\,2})c_{y\beta}+21r_x^{a\,2}r_y^a r_\beta^b+6r_x^a r_y^a c_{x\beta})$
20	20	$R^{-5}.\frac{3}{4}(35r_z^{a\,2}r_z^{b\,2}-5r_z^{a\,2}-5r_z^{b\,2}+20r_z^a r_z^b c_{zz}+2c_{zz}^2+1)$
20	$21c$	$R^{-5}.\frac{1}{2}\sqrt{3}(35r_z^{a\,2}r_x^b r_z^b-5r_x^b r_z^b+10r_z^a r_x^b c_{zz}+10r_z^a r_z^b c_{zx}+2c_{zx}c_{zz})$
20	$21s$	$R^{-5}.\frac{1}{2}\sqrt{3}(35r_z^{a\,2}r_y^b r_z^b-5r_y^b r_z^b+10r_z^a r_y^b c_{zz}+10r_z^a r_z^b c_{zy}+2c_{zy}c_{zz})$
20	$22c$	$R^{-5}.\frac{1}{4}\sqrt{3}(35r_z^{a\,2}r_x^{b\,2}-35r_z^{a\,2}r_y^{b\,2}-5r_x^{b\,2}+5r_y^{b\,2}+20r_z^a r_x^b c_{zx}-20r_z^a r_y^b c_{zy}+2c_{zx}^2-2c_{zy}^2)$
20	$22s$	$R^{-5}.\frac{1}{2}\sqrt{3}(35r_z^{a\,2}r_x^b r_y^b-5r_x^b r_y^b+10r_z^a r_x^b c_{zy}+10r_z^a r_y^b c_{zx}+2c_{zx}c_{zy})$
$21c$	$21c$	$R^{-5}.(35r_x^a r_z^a r_x^b r_z^b+5r_x^a r_x^b c_{zz}+5r_x^a r_z^b c_{zx}+5r_z^a r_x^b c_{xz}+5r_z^a r_z^b c_{xx}+c_{xx}c_{zz}+c_{xz}c_{zx})$
$21c$	$21s$	$R^{-5}.(35r_x^a r_z^a r_y^b r_z^b+5r_x^a r_y^b c_{zz}+5r_x^a r_z^b c_{zy}+5r_z^a r_y^b c_{xz}+5r_z^a r_z^b c_{xy}+c_{xy}c_{zz}+c_{xz}c_{zy})$
$21c$	$22c$	$R^{-5}.\frac{1}{2}(35r_x^a r_z^a r_x^{b\,2}-35r_x^a r_z^a r_y^{b\,2}+10r_x^a r_x^b c_{zx}-10r_x^a r_y^b c_{zy}+10r_z^a r_x^b c_{xx}-10r_z^a r_y^b c_{xy}+2c_{xx}c_{zx}-2c_{xy}c_{zy})$
$21c$	$22s$	$R^{-5}.(35r_x^a r_z^a r_x^b r_y^b+5r_x^a r_x^b c_{zy}+5r_x^a r_y^b c_{zx}+5r_z^a r_x^b c_{xy}+5r_z^a r_y^b c_{xx}+c_{xx}c_{zy}+c_{xy}c_{zx})$
$21s$	$21s$	$R^{-5}.(35r_y^a r_z^a r_y^b r_z^b+5r_y^a r_y^b c_{zz}+5r_y^a r_z^b c_{zy}+5r_z^a r_y^b c_{yz}+5r_z^a r_z^b c_{yy}+c_{yy}c_{zz}+c_{yz}c_{zy})$
$21s$	$22c$	$R^{-5}.\frac{1}{2}(35r_y^a r_z^a r_x^{b\,2}-35r_y^a r_z^a r_y^{b\,2}+10r_y^a r_x^b c_{zx}-10r_y^a r_y^b c_{zy}+10r_z^a r_x^b c_{yx}-10r_z^a r_y^b c_{yy}+2c_{yx}c_{zx}-2c_{yy}c_{zy})$
$21s$	$22s$	$R^{-5}.(35r_y^a r_z^a r_x^b r_y^b+5r_y^a r_x^b c_{zy}+5r_y^a r_y^b c_{zx}+5r_z^a r_x^b c_{yy}+5r_z^a r_y^b c_{yx}+c_{yx}c_{zy}+c_{yy}c_{zx})$

continued ...

Table F.1 continued

t	u	$4\pi\epsilon_0 T^{ab}_{tu}$
$22c$	$22c$	$R^{-5}.\frac{1}{4}(35r_x^{a2}r_x^{b2} - 35r_x^{a2}r_y^{b2} - 35r_y^{a2}r_x^{b2} + 35r_y^{a2}r_y^{b2} + 20r_x^a r_x^b c_{xx} - 20r_x^a r_y^b c_{xy} - 20r_y^a r_x^b c_{yx} + 20r_y^a r_y^b c_{yy} + 2c_{xx}^2 - 2c_{xy}^2 - 2c_{yx}^2 + 2c_{yy}^2)$
$22c$	$22s$	$R^{-5}.\frac{1}{2}(35r_x^{a2}r_x^b r_y^b - 35r_y^{a2}r_x^b r_y^b + 10r_x^a r_x^b c_{xy} + 10r_x^a r_y^b c_{xx} - 10r_y^a r_x^b c_{yy} - 10r_y^a r_y^b c_{yx} + 2c_{xx}c_{xy} - 2c_{yx}c_{yy})$
$22s$	$22s$	$R^{-5}.(35r_x^a r_y^a r_x^b r_y^b + 5r_x^a r_x^b c_{yy} + 5r_x^a r_y^b c_{yx} + 5r_y^a r_x^b c_{xy} + 5r_y^a r_y^b c_{xx} + c_{xx}c_{yy} + c_{xy}c_{yx})$
50	00	$R^{-6}.\frac{1}{8}(63r_z^{a5} - 70r_z^{a3} + 15r_z^a)$
$51c$	00	$R^{-6}.\frac{1}{8}\sqrt{15}(21r_x^a r_z^{a4} - 14r_x^a r_z^{a2} + r_x^a)$
$51s$	00	$R^{-6}.\frac{1}{8}\sqrt{15}(21r_y^a r_z^{a4} - 14r_y^a r_z^{a2} + r_y^a)$
$52c$	00	$R^{-6}.\frac{1}{4}\sqrt{105}(3r_x^{a2}r_z^{a3} - 3r_y^{a2}r_z^{a3} - r_x^{a2}r_z^a + r_y^{a2}r_z^a)$
$52s$	00	$R^{-6}.\frac{1}{2}\sqrt{105}(3r_x^a r_y^a r_z^{a3} - r_x^a r_y^a r_z^a)$
$53c$	00	$R^{-6}.\frac{1}{16}\sqrt{70}(9r_x^{a3}r_z^{a2} - 27r_x^a r_y^{a2}r_z^{a2} - r_x^{a3} + 3r_x^a r_y^{a2})$
$53s$	00	$R^{-6}.\frac{1}{16}\sqrt{70}(27r_x^{a2}r_y^a r_z^{a2} - 9r_y^{a3}r_z^{a2} - 3r_x^{a2}r_y^a + r_y^{a3})$
$54c$	00	$R^{-6}.\frac{3}{8}\sqrt{35}(r_x^{a4}r_z^a - 6r_x^{a2}r_y^{a2}r_z^a + r_y^{a4}r_z^a)$
$54s$	00	$R^{-6}.\frac{3}{2}\sqrt{35}(r_x^{a3}r_y^a r_z^a - r_x^a r_y^{a3}r_z^a)$
$55c$	00	$R^{-6}.\frac{3}{16}\sqrt{14}(r_x^{a5} - 10r_x^{a3}r_y^{a2} + 5r_x^a r_y^{a4})$
$55s$	00	$R^{-6}.\frac{3}{16}\sqrt{14}(5r_x^{a4}r_y^a - 10r_x^{a2}r_y^{a3} + r_y^{a5})$
40	1β	$R^{-6}.\frac{5}{8}(63r_z^{a4}r_\beta^b - 42r_z^{a2}r_\beta^b + 28r_z^{a3}c_{z\beta} + 3r_\beta^b - 12r_z^a c_{z\beta})$
$41c$	1β	$R^{-6}.\frac{1}{4}\sqrt{10}(63r_x^a r_z^{a3}r_\beta^b - 21r_x^a r_z^a r_\beta^b + 21r_x^a r_z^{a2}c_{z\beta} + 7r_z^{a3}c_{x\beta} - 3r_x^a c_{z\beta} - 3r_z^a c_{x\beta})$
$41s$	1β	$R^{-6}.\frac{1}{4}\sqrt{10}(63r_y^a r_z^{a3}r_\beta^b - 21r_y^a r_z^a r_\beta^b + 21r_y^a r_z^{a2}c_{z\beta} + 7r_z^{a3}c_{y\beta} - 3r_y^a c_{z\beta} - 3r_z^a c_{y\beta})$
$42c$	1β	$R^{-6}.\frac{1}{4}\sqrt{5}(63r_x^{a2}r_z^{a2}r_\beta^b - 63r_y^{a2}r_z^{a2}r_\beta^b - 7r_x^{a2}r_\beta^b + 7r_y^{a2}r_\beta^b + 14r_x^{a2}r_z^a c_{z\beta} + 14r_x^a r_z^{a2}c_{x\beta} - 14r_y^{a2}r_z^a c_{z\beta} - 14r_y^a r_z^{a2}c_{y\beta} - 2r_x^a c_{x\beta} + 2r_y^a c_{y\beta})$
$42s$	1β	$R^{-6}.\frac{1}{2}\sqrt{5}(63r_x^a r_y^a r_z^{a2}r_\beta^b - 7r_x^a r_y^a r_\beta^b + 14r_x^a r_y^a r_z^a c_{z\beta} + 7r_x^a r_z^{a2}c_{y\beta} + 7r_y^a r_z^{a2}c_{x\beta} - r_x^a c_{y\beta} - r_y^a c_{x\beta})$
$43c$	1β	$R^{-6}.\frac{1}{4}\sqrt{70}(9r_x^{a3}r_z^a r_\beta^b - 27r_x^a r_y^{a2}r_z^a r_\beta^b + r_x^{a3}c_{z\beta} + 3r_x^{a2}r_z^a c_{x\beta} - 3r_x^a r_y^{a2}c_{z\beta} - 6r_x^a r_y^a r_z^a c_{y\beta} - 3r_y^{a2}r_z^a c_{x\beta})$
$43s$	1β	$R^{-6}.\frac{1}{4}\sqrt{70}(27r_x^{a2}r_y^a r_z^a r_\beta^b - 9r_y^{a3}r_z^a r_\beta^b + 3r_x^{a2}r_y^a c_{z\beta} + 3r_x^{a2}r_z^a c_{y\beta} + 6r_x^a r_y^a r_z^a c_{x\beta} - r_y^{a3}c_{z\beta} - 3r_y^{a2}r_z^a c_{y\beta})$

continued ...

Table F.1 continued

t	u	$4\pi\epsilon_0 T^{ab}_{tu}$
$44c$	1β	$R^{-6}.\frac{1}{8}\sqrt{35}(9r_x^{a\,4}r_\beta^b - 54r_x^{a\,2}r_y^{a\,2}r_\beta^b + 9r_y^{a\,4}r_\beta^b + 4r_x^{a\,3}c_{x\beta} - 12r_x^{a\,2}r_y^a c_{y\beta} - 12r_x^a r_y^{a\,2}c_{x\beta} + 4r_y^{a\,3}c_{y\beta})$
$44s$	1β	$R^{-6}.\frac{1}{2}\sqrt{35}(9r_x^{a\,3}r_y^a r_\beta^b - 9r_x^a r_y^{a\,3}r_\beta^b + r_x^{a\,3}c_{y\beta} + 3r_x^{a\,2}r_y^a c_{x\beta} - 3r_x^a r_y^{a\,2}c_{y\beta} - r_y^{a\,3}c_{x\beta})$
30	20	$R^{-6}.\frac{5}{4}(63r_z^{a\,3}r_z^{b\,2} - 7r_z^{a\,3} - 21r_z^a r_z^{b\,2} + 42r_z^{a\,2}r_z^b c_{zz} + 3r_z^a - 6r_z^b c_{zz} + 6r_z^a c_{zz}^2)$
30	$21c$	$R^{-6}.\frac{5}{2}\sqrt{3}(21r_z^{a\,3}r_x^b r_z^b - 7r_z^a r_x^b r_z^b + 7r_z^{a\,2}r_x^b c_{zz} + 7r_z^{a\,2}r_z^b c_{zx} - r_x^b c_{zz} - r_z^b c_{zx} + 2r_z^a c_{zx}c_{zz})$
30	$21s$	$R^{-6}.\frac{5}{2}\sqrt{3}(21r_z^{a\,3}r_y^b r_z^b - 7r_z^a r_y^b r_z^b + 7r_z^{a\,2}r_y^b c_{zz} + 7r_z^{a\,2}r_z^b c_{zy} - r_y^b c_{zz} - r_z^b c_{zy} + 2r_z^a c_{zy}c_{zz})$
30	$22c$	$R^{-6}.\frac{5}{4}\sqrt{3}(21r_z^{a\,3}r_x^{b\,2} - 21r_z^{a\,3}r_y^{b\,2} - 7r_z^a r_x^{b\,2} + 7r_z^a r_y^{b\,2} + 14r_z^{a\,2}r_x^b c_{zx} - 14r_z^{a\,2}r_y^b c_{zy} - 2r_x^b c_{zx} + 2r_y^b c_{zy} + 2r_z^a c_{zx}^2 - 2r_z^a c_{zy}^2)$
30	$22s$	$R^{-6}.\frac{5}{2}\sqrt{3}(21r_z^{a\,3}r_x^b r_y^b - 7r_z^a r_x^b r_y^b + 7r_z^{a\,2}r_x^b c_{zy} + 7r_z^{a\,2}r_y^b c_{zx} - r_x^b c_{zy} - r_y^b c_{zx} + 2r_z^a c_{zx}c_{zy})$
$31c$	20	$R^{-6}.\frac{5}{8}\sqrt{6}(63r_x^a r_z^{a\,2}r_z^{b\,2} - 7r_x^a r_x^{a\,2} - 7r_x^a r_z^{b\,2} + 28r_x^a r_z^a r_z^b c_{zz} + 14r_z^{a\,2}r_z^b c_{xz} + r_x^a - 2r_z^b c_{xz} + 2r_x^a c_{zz}^2 + 4r_z^a c_{xz}c_{zz})$
$31c$	$21c$	$R^{-6}.\frac{5}{4}\sqrt{2}(63r_x^a r_z^{a\,2}r_x^b r_z^b - 7r_x^a r_x^b r_z^b + 14r_x^a r_z^a r_x^b c_{zz} + 14r_x^a r_z^a r_z^b c_{zx} + 7r_z^{a\,2}r_x^b c_{xz} + 7r_z^{a\,2}r_z^b c_{xx} - r_x^b c_{xz} - r_z^b c_{xx} + 2r_x^a c_{zx}c_{zz} + 2r_z^a c_{xx}c_{zz} + 2r_z^a c_{xz}c_{zx})$
$31c$	$21s$	$R^{-6}.\frac{5}{4}\sqrt{2}(63r_x^a r_z^{a\,2}r_y^b r_z^b - 7r_x^a r_y^b r_z^b + 14r_x^a r_z^a r_y^b c_{zz} + 14r_x^a r_z^a r_z^b c_{zy} + 7r_z^{a\,2}r_y^b c_{xz} + 7r_z^{a\,2}r_z^b c_{xy} - r_y^b c_{xz} - r_z^b c_{xy} + 2r_x^a c_{zy}c_{zz} + 2r_z^a c_{xy}c_{zz} + 2r_z^a c_{xz}c_{zy})$
$31c$	$22c$	$R^{-6}.\frac{5}{8}\sqrt{2}(63r_x^a r_z^{a\,2}r_x^{b\,2} - 63r_x^a r_z^{a\,2}r_y^{b\,2} - 7r_x^a r_x^{b\,2} + 7r_x^a r_y^{b\,2} + 28r_x^a r_z^a r_x^b c_{zx} - 28r_x^a r_z^a r_y^b c_{zy} + 14r_z^{a\,2}r_x^b c_{xx} - 14r_z^{a\,2}r_y^b c_{xy} - 2r_x^b c_{xx} + 2r_y^b c_{xy} + 2r_x^a c_{zx}^2 - 2r_x^a c_{zy}^2 + 4r_z^a c_{xx}c_{zx} - 4r_z^a c_{xy}c_{zy})$
$31c$	$22s$	$R^{-6}.\frac{5}{4}\sqrt{2}(63r_x^a r_z^{a\,2}r_x^b r_y^b - 7r_x^a r_x^b r_y^b + 14r_x^a r_z^a r_x^b c_{zy} + 14r_x^a r_z^a r_y^b c_{zx} + 7r_z^{a\,2}r_x^b c_{xy} + 7r_z^{a\,2}r_y^b c_{xx} - r_x^b c_{xy} - r_y^b c_{xx} + 2r_x^a c_{zx}c_{zy} + 2r_z^a c_{xx}c_{zy} + 2r_z^a c_{xy}c_{zx})$
$31s$	20	$R^{-6}.\frac{5}{8}\sqrt{6}(63r_y^a r_z^{a\,2}r_z^{b\,2} - 7r_y^a r_z^{a\,2} - 7r_y^a r_z^{b\,2} + 28r_y^a r_z^a r_z^b c_{zz} + 14r_z^{a\,2}r_z^b c_{yz} + r_y^a - 2r_z^b c_{yz} + 2r_y^a c_{zz}^2 + 4r_z^a c_{yz}c_{zz})$
$31s$	$21c$	$R^{-6}.\frac{5}{4}\sqrt{2}(63r_y^a r_z^{a\,2}r_x^b r_z^b - 7r_y^a r_x^b r_z^b + 14r_y^a r_z^a r_x^b c_{zz} + 14r_y^a r_z^a r_z^b c_{zx} + 7r_z^{a\,2}r_x^b c_{yz} + 7r_z^{a\,2}r_z^b c_{yx} - r_x^b c_{yz} - r_z^b c_{yx} + 2r_y^a c_{zx}c_{zz} + 2r_z^a c_{yx}c_{zz} + 2r_z^a c_{yz}c_{zx})$
$31s$	$21s$	$R^{-6}.\frac{5}{4}\sqrt{2}(63r_y^a r_z^{a\,2}r_y^b r_z^b - 7r_y^a r_y^b r_z^b + 14r_y^a r_z^a r_y^b c_{zz} + 14r_y^a r_z^a r_z^b c_{zy} + 7r_z^{a\,2}r_y^b c_{yz} + 7r_z^{a\,2}r_z^b c_{yy} - r_y^b c_{yz} - r_z^b c_{yy} + 2r_y^a c_{zy}c_{zz} + 2r_z^a c_{yy}c_{zz} + 2r_z^a c_{yz}c_{zy})$
$31s$	$22c$	$R^{-6}.\frac{5}{8}\sqrt{2}(63r_y^a r_z^{a\,2}r_x^{b\,2} - 63r_y^a r_z^{a\,2}r_y^{b\,2} - 7r_y^a r_x^{b\,2} + 7r_y^a r_y^{b\,2} + 28r_y^a r_z^a r_x^b c_{zx} - 28r_y^a r_z^a r_y^b c_{zy} + 14r_z^{a\,2}r_x^b c_{yx} - 14r_z^{a\,2}r_y^b c_{yy} - 2r_x^b c_{yx} + 2r_y^b c_{yy} + 2r_y^a c_{zx}^2 - 2r_y^a c_{zy}^2 + 4r_z^a c_{yx}c_{zx} - 4r_z^a c_{yy}c_{zy})$

continued ...

Table F.1 continued

t	u	$4\pi\epsilon_0 T^{ab}_{tu}$
$31s$	$22s$	$R^{-6}.\frac{5}{4}\sqrt{2}(63r_y^a r_z^{a2} r_x^b r_y^b - 7r_y^a r_x^b r_y^b + 14r_y^a r_z^a r_x^b c_{zy} + 14r_y^a r_z^a r_y^b c_{zx} + 7r_z^{a2} r_x^b c_{yy} + 7r_z^{a2} r_y^b c_{yx} - r_x^b c_{yy} - r_y^b c_{yx} + 2r_y^a c_{zx} c_{zy} + 2r_z^a c_{yx} c_{zy} + 2r_z^a c_{yy} c_{zx})$
$32c$	20	$R^{-6}.\frac{1}{4}\sqrt{15}(63r_x^{a2} r_z^a r_z^{b2} - 63r_y^{a2} r_z^a r_z^{b2} - 7r_x^{a2} r_z^a + 7r_y^{a2} r_z^a + 14r_x^{a2} r_z^b c_{zz} + 28r_x^a r_z^a r_z^b c_{xz} - 14r_y^{a2} r_z^b c_{zz} - 28r_y^a r_z^a r_z^b c_{yz} + 4r_x^a c_{xz} c_{zz} - 4r_y^a c_{yz} c_{zz} + 2r_z^a c_{xz}^2 - 2r_z^a c_{yz}^2)$
$32c$	$21c$	$R^{-6}.\frac{1}{2}\sqrt{5}(63r_x^{a2} r_z^a r_x^b r_z^b - 63r_y^{a2} r_z^a r_x^b r_z^b + 7r_x^{a2} r_x^b c_{zz} + 7r_x^{a2} r_z^b c_{zx} + 14r_x^a r_z^a r_x^b c_{xz} + 14r_x^a r_z^a r_z^b c_{xx} - 7r_y^{a2} r_x^b c_{zz} - 7r_y^{a2} r_z^b c_{zx} - 14r_y^a r_z^a r_x^b c_{yz} - 14r_y^a r_z^a r_z^b c_{yx} + 2r_x^a c_{xx} c_{zz} + 2r_x^a c_{xz} c_{zx} - 2r_y^a c_{yx} c_{zz} - 2r_y^a c_{yz} c_{zx} + 2r_z^a c_{xx} c_{xz} - 2r_z^a c_{yx} c_{yz})$
$32c$	$21s$	$R^{-6}.\frac{1}{2}\sqrt{5}(63r_x^{a2} r_z^a r_y^b r_z^b - 63r_y^{a2} r_z^a r_y^b r_z^b + 7r_x^{a2} r_y^b c_{zz} + 7r_x^{a2} r_z^b c_{zy} + 14r_x^a r_z^a r_y^b c_{xz} + 14r_x^a r_z^a r_z^b c_{xy} - 7r_y^{a2} r_y^b c_{zz} - 7r_y^{a2} r_z^b c_{zy} - 14r_y^a r_z^a r_y^b c_{yz} - 14r_y^a r_z^a r_z^b c_{yy} + 2r_x^a c_{xy} c_{zz} + 2r_x^a c_{xz} c_{zy} - 2r_y^a c_{yy} c_{zz} - 2r_y^a c_{yz} c_{zy} + 2r_z^a c_{xy} c_{xz} - 2r_z^a c_{yy} c_{yz})$
$32c$	$22c$	$R^{-6}.\frac{1}{4}\sqrt{5}(63r_x^{a2} r_z^a r_x^{b2} - 63r_x^{a2} r_z^a r_y^{b2} - 63r_y^{a2} r_z^a r_x^{b2} + 63r_y^{a2} r_z^a r_y^{b2} + 14r_x^{a2} r_x^b c_{zx} - 14r_x^{a2} r_y^b c_{zy} + 28r_x^a r_z^a r_x^b c_{xx} - 28r_x^a r_z^a r_y^b c_{xy} - 14r_y^{a2} r_x^b c_{zx} + 14r_y^{a2} r_y^b c_{zy} - 28r_y^a r_z^a r_x^b c_{yx} + 28r_y^a r_z^a r_y^b c_{yy} + 4r_x^a c_{xx} c_{zx} - 4r_x^a c_{xy} c_{zy} - 4r_y^a c_{yx} c_{zx} + 4r_y^a c_{yy} c_{zy} + 2r_z^a c_{xx}^2 - 2r_z^a c_{xy}^2 - 2r_z^a c_{yx}^2 + 2r_z^a c_{yy}^2)$
$32c$	$22s$	$R^{-6}.\frac{1}{2}\sqrt{5}(63r_x^{a2} r_z^a r_x^b r_y^b - 63r_y^{a2} r_z^a r_x^b r_y^b + 7r_x^{a2} r_x^b c_{zy} + 7r_x^{a2} r_y^b c_{zx} + 14r_x^a r_z^a r_x^b c_{xy} + 14r_x^a r_z^a r_y^b c_{xx} - 7r_y^{a2} r_x^b c_{zy} - 7r_y^{a2} r_y^b c_{zx} - 14r_y^a r_z^a r_x^b c_{yy} - 14r_y^a r_z^a r_y^b c_{yx} + 2r_x^a c_{xx} c_{zy} + 2r_x^a c_{xy} c_{zx} - 2r_y^a c_{yx} c_{zy} - 2r_y^a c_{yy} c_{zx} + 2r_z^a c_{xx} c_{xy} - 2r_z^a c_{yx} c_{yy})$
$32s$	20	$R^{-6}.\frac{1}{2}\sqrt{15}(63r_x^a r_y^a r_z^a r_z^{b2} - 7r_x^a r_y^a r_z^a + 14r_x^a r_y^a r_z^b c_{zz} + 14r_x^a r_z^a r_z^b c_{yz} + 14r_y^a r_z^a r_z^b c_{xz} + 2r_x^a c_{yz} c_{zz} + 2r_y^a c_{xz} c_{zz} + 2r_z^a c_{xz} c_{yz})$
$32s$	$21c$	$R^{-6}.\sqrt{5}(63r_x^a r_y^a r_z^a r_x^b r_z^b + 7r_x^a r_y^a r_x^b c_{zz} + 7r_x^a r_y^a r_z^b c_{zx} + 7r_x^a r_z^a r_x^b c_{yz} + 7r_x^a r_z^a r_z^b c_{yx} + 7r_y^a r_z^a r_x^b c_{xz} + 7r_y^a r_z^a r_z^b c_{xx} + r_x^a c_{yx} c_{zz} + r_x^a c_{yz} c_{zx} + r_y^a c_{xx} c_{zz} + r_y^a c_{xz} c_{zx} + r_z^a c_{xx} c_{yz} + r_z^a c_{xz} c_{yx})$
$32s$	$21s$	$R^{-6}.\sqrt{5}(63r_x^a r_y^a r_z^a r_y^b r_z^b + 7r_x^a r_y^a r_y^b c_{zz} + 7r_x^a r_y^a r_z^b c_{zy} + 7r_x^a r_z^a r_y^b c_{yz} + 7r_x^a r_z^a r_z^b c_{yy} + 7r_y^a r_z^a r_y^b c_{xz} + 7r_y^a r_z^a r_z^b c_{xy} + r_x^a c_{yy} c_{zz} + r_x^a c_{yz} c_{zy} + r_y^a c_{xy} c_{zz} + r_y^a c_{xz} c_{zy} + r_z^a c_{xy} c_{yz} + r_z^a c_{xz} c_{yy})$
$32s$	$22c$	$R^{-6}.\frac{1}{2}\sqrt{5}(63r_x^a r_y^a r_z^a r_x^{b2} - 63r_x^a r_y^a r_z^a r_y^{b2} + 14r_x^a r_y^a r_x^b c_{zx} - 14r_x^a r_y^a r_y^b c_{zy} + 14r_x^a r_z^a r_x^b c_{yx} - 14r_x^a r_z^a r_y^b c_{yy} + 14r_y^a r_z^a r_x^b c_{xx} - 14r_y^a r_z^a r_y^b c_{xy} + 2r_x^a c_{yx} c_{zx} - 2r_x^a c_{yy} c_{zy} + 2r_y^a c_{xx} c_{zx} - 2r_y^a c_{xy} c_{zy} + 2r_z^a c_{xx} c_{yx} - 2r_z^a c_{xy} c_{yy})$
$32s$	$22s$	$R^{-6}.\sqrt{5}(63r_x^a r_y^a r_z^a r_x^b r_y^b + 7r_x^a r_y^a r_x^b c_{zz} + 7r_x^a r_y^a r_z^b c_{zx} + 7r_x^a r_z^a r_x^b c_{yy} + 7r_x^a r_z^a r_y^b c_{yx} + 7r_y^a r_z^a r_x^b c_{xy} + 7r_y^a r_z^a r_z^b c_{xx} + r_x^a c_{yx} c_{zz} + r_x^a c_{yy} c_{zx} + r_y^a c_{xx} c_{zz} + r_y^a c_{xy} c_{zx} + r_z^a c_{xx} c_{yy} + r_z^a c_{xy} c_{yx})$

continued ...

Table F.1 continued

t	u	$4\pi\epsilon_0 T^{ab}_{tu}$
$33c$	20	$R^{-6}.\frac{1}{8}\sqrt{10}(63r_x^{a\,3}r_z^{b\,2} - 189r_x^a r_y^{a\,2}r_z^{b\,2} - 7r_x^{a\,3} + 21r_x^a r_y^{a\,2} + 42r_x^{a\,2}r_z^b c_{xz} - 84r_x^a r_y^a r_z^b c_{yz} - 42r_y^{a\,2}r_z^b c_{xz} + 6r_x^a c_{xz}^2 - 6r_x^a c_{yz}^2 - 12r_y^a c_{xz}c_{yz})$
$33c$	$21c$	$R^{-6}.\frac{1}{4}\sqrt{30}(21r_x^{a\,3}r_x^b r_z^b - 63r_x^a r_y^{a\,2}r_x^b r_z^b + 7r_x^{a\,2}r_x^b c_{xz} + 7r_x^{a\,2}r_z^b c_{xx} - 14r_x^a r_y^a r_x^b c_{yz} - 14r_x^a r_y^a r_z^b c_{yx} - 7r_y^{a\,2}r_x^b c_{xz} - 7r_y^{a\,2}r_z^b c_{xx} + 2r_x^a c_{xx}c_{xz} - 2r_x^a c_{yx}c_{yz} - 2r_y^a c_{xx}c_{yz} - 2r_y^a c_{xz}c_{yx})$
$33c$	$21s$	$R^{-6}.\frac{1}{4}\sqrt{30}(21r_x^{a\,3}r_y^b r_z^b - 63r_x^a r_y^{a\,2}r_y^b r_z^b + 7r_x^{a\,2}r_y^b c_{xz} + 7r_x^{a\,2}r_z^b c_{xy} - 14r_x^a r_y^a r_y^b c_{yz} - 14r_x^a r_y^a r_z^b c_{yy} - 7r_y^{a\,2}r_y^b c_{xz} - 7r_y^{a\,2}r_z^b c_{xy} + 2r_x^a c_{xy}c_{xz} - 2r_x^a c_{yy}c_{yz} - 2r_y^a c_{xy}c_{yz} - 2r_y^a c_{xz}c_{yy})$
$33c$	$22c$	$R^{-6}.\frac{1}{8}\sqrt{30}(21r_x^{a\,3}r_x^{b\,2} - 21r_x^{a\,3}r_y^{b\,2} - 63r_x^a r_y^{a\,2}r_x^{b\,2} + 63r_x^a r_y^{a\,2}r_y^{b\,2} + 14r_x^{a\,2}r_x^b c_{xx} - 14r_x^{a\,2}r_y^b c_{xy} - 28r_x^a r_y^a r_x^b c_{yx} + 28r_x^a r_y^a r_y^b c_{yy} - 14r_y^{a\,2}r_x^b c_{xx} + 14r_y^{a\,2}r_y^b c_{xy} + 2r_x^a c_{xx}^2 - 2r_x^a c_{xy}^2 - 2r_x^a c_{yx}^2 + 2r_x^a c_{yy}^2 - 4r_y^a c_{xx}c_{yx} + 4r_y^a c_{xy}c_{yy})$
$33c$	$22s$	$R^{-6}.\frac{1}{4}\sqrt{30}(21r_x^{a\,3}r_x^b r_y^b - 63r_x^a r_y^{a\,2}r_x^b r_y^b + 7r_x^{a\,2}r_x^b c_{xy} + 7r_x^{a\,2}r_y^b c_{xx} - 14r_x^a r_y^a r_x^b c_{yy} - 14r_x^a r_y^a r_y^b c_{yx} - 7r_y^{a\,2}r_x^b c_{xy} - 7r_y^{a\,2}r_y^b c_{xx} + 2r_x^a c_{xx}c_{xy} - 2r_x^a c_{yx}c_{yy} - 2r_y^a c_{xx}c_{yy} - 2r_y^a c_{xy}c_{yx})$
$33s$	20	$R^{-6}.\frac{1}{8}\sqrt{10}(189r_x^{a\,2}r_y^a r_z^{b\,2} - 63r_y^{a\,3}r_z^{b\,2} - 21r_x^{a\,2}r_y^a + 7r_y^{a\,3} + 42r_x^{a\,2}r_z^b c_{yz} + 84r_x^a r_y^a r_z^b c_{xz} - 42r_y^{a\,2}r_z^b c_{yz} + 12r_x^a c_{xz}c_{yz} + 6r_y^a c_{xz}^2 - 6r_y^a c_{yz}^2)$
$33s$	$21c$	$R^{-6}.\frac{1}{4}\sqrt{30}(63r_x^{a\,2}r_y^a r_x^b r_z^b - 21r_y^{a\,3}r_x^b r_z^b + 7r_x^{a\,2}r_x^b c_{yz} + 7r_x^{a\,2}r_z^b c_{yx} + 14r_x^a r_y^a r_x^b c_{xz} + 14r_x^a r_y^a r_z^b c_{xx} - 7r_y^{a\,2}r_x^b c_{yz} - 7r_y^{a\,2}r_z^b c_{yx} + 2r_x^a c_{xx}c_{yz} + 2r_x^a c_{xz}c_{yx} + 2r_y^a c_{xx}c_{xz} - 2r_y^a c_{yx}c_{yz})$
$33s$	$21s$	$R^{-6}.\frac{1}{4}\sqrt{30}(63r_x^{a\,2}r_y^a r_y^b r_z^b - 21r_y^{a\,3}r_y^b r_z^b + 7r_x^{a\,2}r_y^b c_{yz} + 7r_x^{a\,2}r_z^b c_{yy} + 14r_x^a r_y^a r_y^b c_{xz} + 14r_x^a r_y^a r_z^b c_{xy} - 7r_y^{a\,2}r_y^b c_{yz} - 7r_y^{a\,2}r_z^b c_{yy} + 2r_x^a c_{xy}c_{yz} + 2r_x^a c_{xz}c_{yy} + 2r_y^a c_{xy}c_{xz} - 2r_y^a c_{yy}c_{yz})$
$33s$	$22c$	$R^{-6}.\frac{1}{8}\sqrt{30}(63r_x^{a\,2}r_y^a r_x^{b\,2} - 63r_x^{a\,2}r_y^a r_y^{b\,2} - 21r_y^{a\,3}r_x^{b\,2} + 21r_y^{a\,3}r_y^{b\,2} + 14r_x^{a\,2}r_x^b c_{yx} - 14r_x^{a\,2}r_y^b c_{yy} + 28r_x^a r_y^a r_x^b c_{xx} - 28r_x^a r_y^a r_y^b c_{xy} - 14r_y^{a\,2}r_x^b c_{yx} + 14r_y^{a\,2}r_y^b c_{yy} + 4r_x^a c_{xx}c_{yx} - 4r_x^a c_{xy}c_{yy} + 2r_y^a c_{xx}^2 - 2r_y^a c_{xy}^2 - 2r_y^a c_{yx}^2 + 2r_y^a c_{yy}^2)$
$33s$	$22s$	$R^{-6}.\frac{1}{4}\sqrt{30}(63r_x^{a\,2}r_y^a r_x^b r_y^b - 21r_y^{a\,3}r_x^b r_y^b + 7r_x^{a\,2}r_x^b c_{yy} + 7r_x^{a\,2}r_y^b c_{yx} + 14r_x^a r_y^a r_x^b c_{xy} + 14r_x^a r_y^a r_y^b c_{xx} - 7r_y^{a\,2}r_x^b c_{yy} - 7r_y^{a\,2}r_y^b c_{yx} + 2r_x^a c_{xx}c_{yy} + 2r_x^a c_{xy}c_{yx} + 2r_y^a c_{xx}c_{xy} - 2r_y^a c_{yx}c_{yy})$

References

Abramowitz, M. and Stegun, I. A. (1965) *Handbook of Mathematical Functions*, Dover, New York. 144, 272

Acevedo, O. and Jorgensen, W. L. (2009) 'Advances in quantum and molecular mechanical (QM/MM) simulations for organic and enzymatic reactions,' *Acc. Chem. Res.* **43**, 142–151. 220

Adamo, C. and Barone, V. (1999) 'Toward reliable density functional methods without adjustable parameters: The PBE0 model,' *J. Chem. Phys.* **110**, 6158–6170. 79

Adams, W. H. (1990) 'Perturbation theory of intermolecular interactions—what is the problem, are there solutions?' *International Journal of Quantum Chemistry* **S24**, 531–547. 106

Adams, W. H. (1994) 'The polarization approximation and the Amos–Musher intermolecular perturbation theories compared to infinite order at finite separation,' *Chem. Phys. Lett.* **229**, 472–480. 113

Adams, W. H. (2002*a*) 'True or false? Order is not uniquely defined in symmetry adapted perturbation theory,' *J. Mol. Struct. (TheoChem)* **591**, 59–65. 104

Adams, W. H. (2002*b*) 'Two new symmetry-adapted perturbation theories for the calculation of intermolecular interaction energies,' *Theor. Chem. Acc.* **108**, 225–231. 114, 115, 117

Addicoat, M. A. and Collins, M. A. (2009) 'Accurate treatment of non-bonded interactions within systematic molecular fragmentation,' *J. Chem. Phys.* **131**, 104103. 219, 220

Ahlrichs, R. (1976) 'Convergence properties of the intermolecular force series ($1/r$ expansion),' *Theor. Chim. Acta* **41**, 7–15. 63, 148

Ahlrichs, R., Furche, F., Hättig, C., Klopper, W., Sierka, M. and Weigend, F. (2011) *Turbomole 6.3.1*, Karlsruhe, http://www.turbomole-gmbh.com/. 91

Ahlrichs, R., Penco, R. and Scoles, G. (1977) 'Intermolecular forces in simple systems,' *Chem. Phys.* **19**, 119–130. 205

Alemán, C., Orozco, M. and Luque, F. J. (1994) 'Multicentric charges for the accurate representation of electrostatic interactions in force-field calculations for small molecules,' *Chem. Phys.* **189**, 573–584. 139

Allen, M. J. and Tozer, D. J. (2000) 'Kohn–Sham calculations using hybrid exchange–correlation functionals with asymptotically corrected potentials,' *J. Chem. Phys.* **113**, 5185–5192. 79

Allen, M. J. and Tozer, D. J. (2002) 'Helium dimer dispersion forces and correlation potentials in density functional theory,' *J. Chem. Phys.* **117**, 11113–11120. 93

Allen, M. P. and Tildesley, D. J. (1987) *Computer Simulation of Liquids*, Clarendon Press, Oxford. 247, 248, 265

Allinger, N. L. (1976) 'Calculation of molecular structure and energy by force-field methods,' *Adv. Phys. Org. Chem.* **13**, 1–82. 221

Allinger, N. L. (1977) 'Conformational analysis. 130. MM2. A hydrocarbon force field utilizing V_1 and V_2 torsional terms,' *J. Amer. Chem. Soc.* **99**, 8127–8134. 221

Allinger, N. L., Yuh, Y. H. and Lii, J.-H. (1989) 'Molecular mechanics. The MM3 force field for hydrocarbons. I.' *J. Amer. Chem. Soc.* **111**, 8551–8566. 221

Althorpe, S. C. and Clary, D. C. (1994) 'Calculation of the intermolecular bound states for water dimer,' *J. Chem. Phys.* **101**, 3603–3609. 259

Althorpe, S. C. and Clary, D. C. (1995) 'A new method for calculating the rovibrational states of polyatomics with application to water dimer,' *J. Chem. Phys.* **102**, 4390–4399. 257

Altman, R. S., Marshall, M. D. and Klemperer, W. (1982) *Disc. Faraday Soc.* **73**, 116. 169

Altman, R. S., Marshall, M. D. and Klemperer, W. (1983*a*) 'Electric dipole moment and quadrupole hyperfine structure of OC – HCl and OC – DCl.' *J. Chem. Phys.* **79**, 52–56. 169

Altman, R. S., Marshall, M. D. and Klemperer, W. (1983*b*) 'Microwave spectrum and molecular structure of N_2 – HCl,' *J. Chem. Phys.* **79**, 57–64. 169

Altmann, S. L. (1986) *Rotations, Quaternions and Double Groups*, Oxford University Press, New York. 234

Amos, A. T. (1970) 'The derivation of symmetry-adapted perturbation theories,' *Chem. Phys. Lett.* **5**, 587–590. 111

Amos, A. T. and Crispin, R. J. (1976*a*) 'Calculations of intermolecular interaction energies,' *Theoretical Chemistry: Advances and Perspectives* **2**, 1–66, Note that eqn (A2) is incorrect. 122

Amos, A. T. and Crispin, R. J. (1976*b*) 'Intermolecular forces between large molecules,' *Molec. Phys.* **31**, 159–176. 124

Amos, R. D. (1985) 'Multipole moments of N_2 and F_2 using SCF and Møller–Plesset calculation,' *Chem. Phys. Lett.* **113**, 19–22. 124

Anderson, J. B. (1975) 'A random-walk simulation of the Schrödinger equation: H_3^+,' *J. Chem. Phys.* **63**, 1499–1503. 257

Anderson, J. B. (1976) 'Quantum chemistry by random walk,' *J. Chem. Phys.* **65**, 4121. 257

Anderson, J. B. (1980) 'Quantum chemistry by random walk: higher accuracy,' *J. Chem. Phys.* **73**, 3897–3899. 257

Anderson, J. B. (1995) 'Fixed-node quantum Monte Carlo,' *Int. Rev. Phys. Chem.* **14**, 85–112. 258

Ángyán, J. G. (2007) 'On the exchange-hole model of London dispersion forces,' *J. Chem. Phys.* **127**, 024108. 95

Ángyán, J. G., Jansen, G., Loos, M., Hättig, C. and Heß, B. A. (1994) 'Distributed polarizabilities using the topological theory of atoms in molecules,' *Chem. Phys. Lett.* **219**, 267–273. 170

Applequist, J. (1983) 'Cartesian polytensors,' *J. Math. Phys.* **24**, 736–741. 163

Applequist, J. (1985) 'A multipole interaction theory of electric polarization of atomic and molecular assemblies.' *J. Chem. Phys.* **83**, 809–826. 163

Applequist, J., Carl, J. R. and Fung, K.-K. (1972) 'An atom dipole interaction model for molecular polarizability. Application to polyatomic molecules and determination of atom polarizabilities,' *J. Amer. Chem. Soc.* **94**, 2952–2960. 161, 163

Arfken, G. (1970) *Mathematical Methods for Physicists*, Academic Press, New York, London. 47

Arnautova, Y. A., Jagielska, A. and Scheraga, H. A. (2006) 'A new force field (ECEPP-05) for peptides, proteins, and organic molecules,' *J. Phys. Chem. B* **110**, 5025–5044. 221

Arunan, E., Desiraju, G. R., Klein, R. A., Sadlej, J., Scheiner, S., Alkorta, I., Clary, D. C., Crabtree, R. H., Dannenberg, J. J., Hobza, P., Kjaergaard, H. G., Legon, A. C., Mennucci, B. and Nesbitt, D. J. (2011) 'Defining the hydrogen bond,' *Pure Appl. Chem.* **83**, 1619–1636. 153

Avila, G. and Carrington, T., Jr (2011) 'Using nonproduct quadrature grids to solve the vibrational Schrödinger equation in 12D,' *J. Chem. Phys.* **134**, 054126. 256

Axilrod, P. M. and Teller, E. (1943) 'Interaction of the Van der Waals type between three atoms,' *J. Chem. Phys.* **11**, 299–300. 188

Aziz, R. A. (1984) in *Inert Gases, Potentials, Dynamics, and Energy Transfer in Doped Crystals*, ed. M. L. Klein, chap. 2, Springer, Berlin. 207

Bačić, Z. and Light, J. C. (1989) 'Theoretical methods for rovibrational spectra of floppy molecules,' *Ann. Rev. Phys. Chem.* **40**, 469–498. 255

Bader, R. F. W. (1990) *Atoms in Molecules*, Clarendon Press, Oxford. 129, 170, 241

Bak, K. L., Halkier, A., Jørgensen, P., Olsen, J., Helgaker, T. and Klopper, W. (2001) 'Chemical accuracy from 'Coulomb hole' extrapolated molecular quantum-mechanical calculations,' *J. Mol. Struct.* **567**, 375–384. 81

Bardwell, D. A., Adjiman, C. S., Arnautova, Y. A., Bartashevich, E., Boerrigter, S. X. M., Braun, D. E., Cruz-Cabeza, A. J., Day, G. M., Valle, R. G. D., Desiraju, G. R., van Eijck, B. P., Facelli, J. C., Ferraro, M. B., Grillo, D., Habgood, M., Hofmann, D. W. M., Hofmann, F., Jose, K. V. J., Karamertzanis, P. G., Kazantsev, A. V., Kendrick, J., Kuleshova, L. N., Leusen, F. J. J., Maleev, A. V., Misquitta, A. J., Mohamed, S., Needs, R. J., Neumann, M. A., Nikylov, D., Orendt, A. M., Pal, R., Pantelides, C. C., Pickard, C. J., Price, L. S., Price, S. L., Scheraga, H. A., van de Streek, J., Thakur, T. S., Tiwari, S., Venuti, E. and Zhitkov, I. K. (2011) 'Towards crystal structure prediction of complex organic compounds – a report on the fifth blind test,' *Acta Cryst. B* **67**, 535–551. 266

Barker, J. A. (1953) 'Statistical mechanics of interacting dipoles,' *Proc. Roy. Soc. A* **219**, 367–372. 176, 179

Barker, J. A. (1986) 'Many-body interactions in rare gases,' *Molec. Phys.* **57**, 755–760. 190

Barker, J. A., Fisher, R. A. and Watts, R. O. (1971) 'Liquid argon: Monte Carlo and molecular dynamics calculations,' *Molec. Phys.* **21**, 657–673. 204

Barnes, P., Finney, J. L., Nicholas, J. D. and Quinn, J. E. (1979) 'Cooperative effects in simulated water,' *Nature* **282**, 459–464. 227

Barnett, S. A., Broder, C. K., Shankland, K., David, W. I. F., Ibberson, R. M. and Tocher, D. A. (2006) 'Single-crystal X-ray and neutron powder diffraction investigation of the phase transition in tetrachlorobenzene,' *Acta Cryst. B* **62**, 287–295. 265

Bartlett, R. J. (2010) 'The coupled-cluster revolution,' *Molec. Phys.* **108**, 2905–2920. 77

Bartolomei, M., Hernández, M. I., Campos-Martínez, J., Carmona-Novillo, E. and Hernández-Lamoneda, R. (2008) 'The intermolecular potentials of the $O_2 \cdots O_2$ dimer: a detailed *ab initio* study of the energy splittings for the three lowest multiplet states,' *Phys. Chem. Chem. Phys* **10**, 7374–5380. 200

Basilevsky, M. V. and Berenfeld, M. M. (1972*a*) 'Intermolecular interactions in the region of small overlap,' *Int. J. Quantum Chem.* **6**, 23–45. 107

Basilevsky, M. V. and Berenfeld, M. M. (1972*b*) 'SCF perturbation theory and intermolecular interactions,' *Int. J. Quantum Chem.* **6**, 555–574. 107

Battaglia, M. R., Buckingham, A. D., Neumark, D., Pierens, R. K. and Williams, J. H. (1981) 'The quadrupole moments of carbon dioxide and carbon disulphide,' *Molec. Phys.* **43**, 1015–1020. 16

Becke, A. D. (1988) 'A multicenter numerical integration scheme for polyatomic molecules,' *J. Chem. Phys.* **88**, 2547–2553. 81, 128

Becke, A. D. (1993*a*) 'A new mixing of Hartree–Fock and local density-functional theories,' *J. Chem. Phys.* **98**, 1372–1377. 79

Becke, A. D. (1993*b*) 'Density-functional thermochemistry. III. The role of exact exchange,' *J. Chem. Phys.* **98**, 5648–5652. 79

Becke, A. D. and Johnson, E. R. (2005) 'Exchange-hole dipole moment and the dispersion interaction,' *J. Chem. Phys.* **122**, 154104. 94

Becke, A. D. and Johnson, E. R. (2006) 'Exchange-hole dipole moment and the dispersion interaction: High-order dispersion coefficients,' *J. Chem. Phys.* **124**, 014104. 94

Becke, A. D. and Johnson, E. R. (2007) 'Exchange-hole dipole moment and the dispersion interaction revisited,' *J. Chem. Phys.* **127**, 154108. 94

Bell, R. J. (1970) 'Multipolar expansion for the non-additive third-order interaction energy of three atoms,' *J. Phys. B* **3**, 751–62. 189

Ben-Naim, A. (1980) *Hydrophobic Interactions*, Plenum Press, New York. 192

Berendsen, H. J. C. (2007) *Simulating the Physical World*, Cambridge University Press, Cambridge. 249

Berendsen, H. J. C., Postma, J. P. M., van Gunsteren, W. F. and Hermans, J. (1981) 'Interaction models for water in relation to protein hydration,' in *Intermolecular Forces*, ed. B. Pullman, 331–342, D. Reidel, Dordrecht, Holland. 226

Bernal, J. D. and Fowler, R. H. (1933) 'A theory of water and ionic solutions,' *J. Chem. Phys.* **1**, 515–548. 225

Berne, B. J. and Pechukas, P. (1972) 'Gaussian model potentials for molecular interactions,' *J. Chem. Phys.* **56**, 4213–4216. 209

Bernstein, J. (2011) 'Polymorphism – a perspective,' *Cryst. Growth Des.* **11**, 627–631. 265

Berweger, C. D., van Gunsteren, W. F. and Müller-Plathe, F. (1995) 'Force field parametrisation by weak coupling: re-engineering SPC water,' *Chem. Phys. Lett.* **232**, 429–436. 226

Best, R. B., Buchete, N.-V. and Hummer, G. (2008) 'Are current molecular dynamics force fields too helical?' *Biophys. J.* **95**, L07–L09. 223

Best, R. B. and Hummer, G. (2009) 'Optimized molecular dynamics force fields applied to the helix–coil transition of polypeptides,' *J. Phys. Chem. B* **113**, 9004–9015. 223

Beyer, T., Day, G. M. and Price, S. L. (2001) 'The prediction, morphology, and mechanical properties of the polymorphs of paracetamol,' *J. Amer. Chem. Soc.* **123**, 5086–5094. 265

Bickelhaupt, F. M. and Baerends, E. J. (2000) 'Kohn–Sham density functional theory: predicting and understanding chemistry,' *Rev. Comput. Chem.* **15**, 1–86. 98

Birge, R. R. (1980) 'Calculation of molecular polarizabilities using an anisotropic atom point dipole interaction model which includes the effect of electron repulsion,' *J. Chem. Phys.* **72**, 5312–5319. 161

Birnbaum, G. and Cohen, E. R. (1975) 'Far infrared collision-induced absorption in gaseous methane. II. Determination of the octopole and hexadecapole moments,' *J. Chem. Phys.* **62**, 3807–3812. 242

Bissonnette, C., Chuaqui, C. E., Crowell, K. G., Roy, R. J. L., Wheatley, R. J. and Meath, W. J. (1996) 'A reliable new potential energy surface for $H_2\cdots Ar$,' *J. Chem. Phys.* **105**, 2639–2653. 250

Bogaard, M. P., Buckingham, A. D., Pierens, R. K. and White, A. H. (1978) 'Rayleigh scattering depolarization ratio and molecular polarizability anisotropy for gases,' *J. Chem. Soc. Faraday Trans. I* **74**, 3008–3015. 169

Böhm, H.-J. and Ahlrichs, R. (1982) 'A study of short-range repulsions,' *J. Chem. Phys.* **77**, 2028–2034. 214, 215

Bondi, A. (1964) 'Van der Waals volumes and radii,' *J. Phys. Chem.* **68**, 441–451. 154, 202

Bone, R. G. A. and Handy, N. C. (1990) '*Ab initio* studies of internal rotation barriers and vibrational frequencies of $(C_2H_2)_2$, $(CO_2)_2$ and $C_2H_2\cdots CO_2$,' *Theor. Chim. Acta* **78**, 133–163. 53, 54

Bone, R. G. A., Rowlands, T. W., Handy, N. C. and Stone, A. J. (1991) 'Transition states from molecular symmetry groups: analysis of non-rigid acetylene trimer,' *Molec. Phys.* **72**, 33–73. 7, 53

Born, M. and Mayer, J. E. (1932) 'Zur Gittertheorie der Ionenkristalle,' *Z. Phys.* **75**, 1–18. 204

Böttcher, C. J. F., van Belle, O. C., Bordewijk, P. and Rip, A. (1972) *Theory of Electric Polarization*, Elsevier. 176

Boys, S. F. (1950) 'Electronic wave functions. I. A general method of calculation for the stationary states of any molecular system,' *Proc. Roy. Soc. A* **200**, 542–554. 125

Boys, S. F. (1960) 'Construction of some molecular orbitals to be approximately invariant for changes from one molecule to another,' *Rev. Mod. Phys.* **32**, 296–299. 174

Boys, S. F. and Bernardi, F. (1970) 'The calculation of small molecular interactions by the difference of separate total energies. Some procedures with reduced errors,' *Molec. Phys.* **19**, 553–566. 89, 151

Boys, S. F. and Shavitt, I. (1959) 'Report WIS–AF–13,' Tech. rep., University of Wisconsin, Madison, WI, USA. 82

Braun, D. E., Karamertzanis, P. G. and Price, S. L. (2011) 'Which, if any, hydrates will crystallise? Predicting hydrate formation of two dihydroxybenzoic acids,' *Chem. Comm.* **47**, 5443–5445. 225

Breneman, C. M. and Wiberg, K. B. (1990) 'Determining atom-centered monopoles from molecular electrostatic potentials – the need for high sampling density in formamide conformational analysis,' *J. Comput. Chem.* **11**, 361–373. 138

Bridge, N. J. and Buckingham, A. D. (1966) 'The polarization of laser light scattered by gases,' *Proc. Roy. Soc. A* **295**, 334–349. 166

Brink, D. M. and Satchler, G. R. (1993) *Angular Momentum*, Clarendon Press, Oxford, 3rd edn. 22, 40, 271, 274, 275, 276

Brooks, B. R., Bruccoleri, R. E., Olafson, B. D., States, D. J., Swaminathan, S. and Karplus, M. (1983) 'CHARMM: A program for macromolecular energy, minimization and dynamics calculations,' *J. Comput. Chem.* **4**, 187–217. 221

Brooks, F. C. (1952) 'Convergence of intermolecular force series,' *Phys. Rev.* **86**, 92–97. 63, 148

Brown, G. G., Dian, B. C., Douglass, K. O., Geyer, S. M., Shipman, S. T. and Pate, B. H. (2008) 'A broadband Fourier transform microwave spectrometer based on chirped pulse excitation,' *Rev. Sci. Instr.* **79**, 053103. 249, 250

Buch, V. (1992) 'Treatment of rigid bodies by diffusion Monte Carlo: application to the para–$H_2 \cdots H_2O$ and ortho–$H_2 \cdots H_2O$ clusters,' *J. Chem. Phys.* **97**, 726–729. 259

Buck, U., Huisken, F., Kohlhase, A., Otten, D. and Schaefer, J. (1983) 'State resolved rotational excitations in $D_2 \cdots H_2$ collisions,' *J. Chem. Phys.* **78**, 4439–4450. 262

Buckingham, A. D. (1960) 'Solvent effects in vibrational spectroscopy,' *Trans. Faraday Soc.* **56**, 753–760. 157

Buckingham, A. D. (1967) 'Permanent and induced molecular moments and long-range intermolecular forces,' *Adv. Chem. Phys.* **12**, 107–143. 39, 46, 57, 66, 241

Buckingham, A. D. (1978) 'Basic theory of intermolecular forces: applications to small molecules,' in *Intermolecular Interactions from Diatomics to Biopolymers*, ed. B. Pullman, 1–67, Wiley, Chichester. 33

Buckingham, A. D., del Bene, J. E. and McDowell, S. A. C. (2008) 'The hydrogen bond,' *Chem. Phys. Lett.* . 153

Buckingham, A. D. and Disch, R. L. (1963) 'The quadrupole moment of carbon dioxide,' *Proc. Roy. Soc. A* **273**, 275–289. 23, 242

Buckingham, A. D., Disch, R. L. and Dunmur, D. A. (1968) 'The quadrupole moments of some simple molecules,' *J. Amer. Chem. Soc.* **90**, 3104–3107. 132

Buckingham, A. D. and Fowler, P. W. (1983) 'Do electrostatic interactions predict structures of Van der Waals molecules?' *J. Chem. Phys.* **79**, 6426–6428. 154, 203

Buckingham, A. D. and Fowler, P. W. (1985) 'A model for the geometries of Van der Waals complexes,' *Canad. J. Chem.* **63**, 2018–2025. 154, 203

Buckingham, A. D., Fowler, P. W. and Stone, A. J. (1986) 'Electrostatic predictions of shapes and properties of Van der Waals molecules,' *Internat. Rev. Phys. Chem.* **5**, 107–114. 170

Buckingham, A. D., Graham, C. and Williams, J. H. (1983) 'Electric field-gradient-induced birefringence in N_2, C_2H_6, C_3H_6, Cl_2, N_2O and CH_3F,' *Molec. Phys.* **49**, 703–710. 23, 124

Buckingham, A. D. and Longuet-Higgins, H. C. (1968) 'The quadrupole moments of polar molecules,' *Molec. Phys.* **14**, 63–72. 42

Buckingham, R. A. and Corner, J. (1947) 'Tables of second virial and low-pressure Joule–Thompson coefficients for intermolecular potentials with exponential repulsion,' *Proc. Roy. Soc. A* **189**, 118–129. 204

Bukowski, R., Szalewicz, K., Groenenboom, G. C. and van der Avoird, A. (2008*a*) 'Polarizable interaction potential for water from coupled cluster calculations. I. Analysis of dimer potential energy surface,' *J. Chem. Phys.* **128**, 094313. 228

Bukowski, R., Szalewicz, K., Groenenboom, G. C. and van der Avoird, A. (2008*b*) 'Polarizable interaction potential for water from coupled cluster calculations. II. Applications to dimer spectra, virial coefficients, and simulations of liquid water,' *J. Chem. Phys.* **128**, 094314. 228

Bultinck, P., Alsenoy, C. V., Ayers, P. W. and Carbó-Dorca, R. (2007) 'Critical analysis and extension of the Hirshfeld atoms in molecules,' *J. Chem. Phys.* **126**, 144111. 129

Bundgen, P., Thakkar, A. J., Kumar, A. and Meath, W. J. (1997) 'Reliable anisotropic dipole properties and dispersion energy coefficients for NO, evaluated using constrained dipole oscillator strength techniques,' *Molec. Phys.* **90**, 721–728. 244

Burnham, C. J. and Xantheas, S. S. (2002*a*) 'Development of transferable interaction models for water. I. Prominent features of the water dimer potential energy surface,' *J. Chem. Phys.* **116**, 1479–1492. 227, 229

Burnham, C. J. and Xantheas, S. S. (2002*b*) 'Development of transferable interaction models for water. III. Reparametrization of an all-atom polarizable rigid model (TTM2–R) from first principles,' *J. Chem. Phys.* **116**, 1500–1510. 227

Burnham, C. J. and Xantheas, S. S. (2002*c*) 'Development of transferable interaction models for water. IV. A flexible, all-atom polarizable potential (TTM2–F) based on geometry dependent charges derived from an *ab initio* monomer dipole moment surface,' *J. Chem. Phys.* **116**, 5115–5124. 227

Caldwell, J. W. and Kollman, P. A. (1995) 'Structure and properties of neat liquids using nonadditive molecular dynamics: Water, methanol, and N-methylacetamide,' *J. Phys. Chem.* **99**, 6208–6219. 227

Cammi, R., Bonaccorsi, R. and Tomasi, J. (1985) 'Counterpoise corrections to the interaction energy components in bimolecular complexes,' *Theor. Chim. Acta* **68**, 271–283. 98

Car, R. and Parrinello, M. (1985) 'Unified approach for molecular dynamics and density functional theory,' *Phys. Rev. Lett.* **55**, 2471–2474. 248

Case, D. A., Cheatham, T. E., III, Darden, T. A., Gohlke, H., Luo, R., Merz, K. M., Jr., Onufriev, A., Simmerling, C., Wang, B. and Woods, R. (2005) 'The Amber biomolecular simulation programs,' *J. Comput. Chem.* **26**, 1668–1688. 221

Casida, M. E. (1995) 'Time-dependent density-functional response theory for molecules,' in *Recent Advances in Density-Functional Theory*, ed. D. P. Chong, World Scientific. 85

Casida, M. E. and Salahub, D. R. (2000) 'Asymptotic correction approach to improving approximate exchange–correlation potentials: Time-dependent density-functional theory calculations of molecular excitation spectra,' *J. Chem. Phys.* **113**, 8918–8935. 79

Casimir, H. B. G. and Polder, D. (1948) 'The influence of retardation on the London–Van der Waals forces,' *Phys. Rev.* **73**, 360–372. 65, 67

Celebi, N., Ángyán, J. G., Dehez, F., Millot, C. and Chipot, C. (2000) 'Distributed polarizabilities derived from induction energies: a finite perturbation approach,' *J. Chem. Phys.* **112**, 2709–2717. 172

Cencek, W., Szalewicz, K., Leforestier, C., van Harrevelt, R. and van der Avoird, A. (2008) 'An accurate analytic representation of the water pair potential,' *Phys. Chem. Chem. Phys* **10**, 4716–4731. 228

Ceperley, D. M. (1995) 'Path integrals in the theory of condensed helium,' *Rev. Mod. Phys.* **67**, 279–355. 249

Cerjan, C. J. and Miller, W. H. (1981) 'On finding transition states,' *J. Chem. Phys.* **75**, 2800–2806. 229, 236

Chai, J.-D. and Head-Gordon, M. (2008) 'Long-range corrected hybrid density functionals with damped atom–atom dispersion corrections,' *Phys. Chem. Chem. Phys* **10**, 6615–6620. 94

Chakrabarti, D. and Wales, D. J. (2009) 'Simulations of rigid bodies in an angle-axis framework,' *Phys. Chem. Chem. Phys* **11**, 1970–1976. 234

Chakravarty, C. (2005) 'Hybrid Monte Carlo implementation of the Fourier path integral algorithm,' *J. Chem. Phys.* **123**, 024104. 249

Chałasiński, G., Rak, J., Szczęśniak, M. M. and Cybulski, S. M. (1997) 'Origins and modeling of many-body exchange effects in Van der Waals clusters,' *J. Chem. Phys.* **106**, 3301–3310. 190

Chałasiński, G. and Szczęśniak, M. M. (2000) 'State of the art and challenges of the *ab initio* theory of intermolecular interactions,' *Chem. Rev.* **100**, 4227–4252. 191, 240

Champagne, B., Perpète, E. A., van Gisbergen, S. J. A., Baerends, E. J., Snijders, J. G., Soubra-Ghaoui, C., Robins, K. A. and Kirtman, B. (1998) 'Assessment of conventional density functional schemes for computing the polarizabilities and hyperpolarizabilities of conjugated oligomers: An *ab initio* investigation of polyacetylene chains,' *J. Chem. Phys.* **109**, 10489–10498. 68

Chandler, D. (2005) 'Interfaces and the driving force of hydrophobic assembly,' *Nature* **437**, 640–647. 192

Cheatham, T. E., III and Young, M. A. (2000) 'Molecular dynamics simulation of nucleic acids: Successes, limitations, and promise,' *Biopolymers* **56**, 232–256, AMBER; nucleic acids. 221

Chemical Reviews (1988) 'Van der Waals molecules,' *Chem. Rev.* **88**, 815–988. 249

Chemical Reviews (1994) 'Van der Waals molecules II,' *Chem. Rev.* **94**, 1721–2160. 249

Chemical Reviews (2000) 'Van der Waals molecules III,' *Chem. Rev.* **100**, 3861–4264. 249

Child, M. S. (1991) *Semiclassical Mechanics with Molecular Applications*, Clarendon Press, Oxford. 252, 262

Chipot, C., Ángyán, J. G., Maigret, A. and Scheraga, H. A. (1994) 'Modelling amino-acid side-chains. 3. Influence of intramolecular and intermolecular environment on point charges,' *J. Phys. Chem.* **98**, 1518. 139

Christiansen, O., Olsen, J., Jorgensen, P., Koch, H. and Malmqvist, P. A. (1996) 'On the inherent divergence in the Møller–Plesset series: the neon atom – a test case,' *Chem. Phys. Letters* **261**, 369–378. 77

Cioslowski, J. (1989*a*) 'General and unique partitioning of molecular electronic properties into atomic contributions,' *Phys. Rev. Lett.* **62**, 1469–1471. 137

Cioslowski, J. (1989*b*) 'A new population analysis based on atomic polar tensors,' *J. Amer. Chem. Soc.* **111**, 8333–8336. 137

Cisneros, G. A., Elking, D. M., Piquemal, J.-P. and Darden, T. A. (2007) 'Numerical fitting of molecular properties to Hermite gaussians,' *J. Phys. Chem. A* **111**, 12049–12056. 145

Čižek, J. and Paldus, J. (1980) 'The coupled-cluster approach,' *Physica Scripta* **21**, 251. 77

Claverie, P. (1971) 'Theory of intermolecular forces. I. On the inadequacy of the usual Rayleigh–Schrödinger perturbation method for the treatment of intermolecular forces,' *Int. J. Quantum Chem.* **5**, 273–296. 104, 106

Claverie, P. (1978) 'Elaboration of approximate formulas for the interactions between large molecules: applications in organic chemistry,' in *Intermolecular Interactions: from Diatomics to Biopolymers*, ed. B. Pullman, 69–305, Wiley. 106

Cochran, W. (1959) 'Theory of the lattice vibrations of germanium,' *Proc. Roy. Soc. A* **253**, 260–276. 208

Cohen, A. J., Mori-Sánchez, P. and Yang, W. (2008*a*) 'Insights into current limitations of density functional theory,' *Science* **321**, 792–794. 95

Cohen, E. R., Cvitaš, T., Frey, J. G., Holmström, B., Kuchitsu, K., Marquardt, R., Mills, I. M., Pavese, F., Quack, M., Stohner, J., Strauss, H. L., Takami, M. and Thor, A. J., eds. (2008*b*) *Quantities, Units and Symbols in Physical Chemistry*, IUPAC and RSC Publishing, Cambridge, 3rd edn. 283

Cohen, R. C. and Saykally, R. J. (1990) 'Extending the collocation method to multidimensional molecular dynamics: direct determination of the intermolecular potential of Ar – H_2O from tunable far infrared laser spectroscopy,' *J. Phys. Chem.* **94**, 7991–8000. 257

Cohen, R. C. and Saykally, R. J. (1993) 'Determination of an improved global potential energy surface for Ar – H_2O from vibration–rotation–tunnelling spectroscopy,' *J. Chem. Phys.* **98**, 6007–6030. 250

Colwell, S. M., Handy, N. C. and Lee, A. M. (1996) 'Determination of frequency-dependent polarizabilities using current density-functional theory,' *J. Chem. Phys.* **53**, 1316–1322. 85

Colwell, S. M., Murray, C. W., Handy, N. C. and Amos, R. D. (1993) 'The determination of hyperpolarisabilities using density functional theory,' *Chem. Phys. Lett.* **210**, 261–268. 85

Coombes, D. S., Price, S. L., Willock, D. J. and Leslie, M. (1996) 'Role of electrostatic interactions in determining the crystal structures of polar organic molecules. a distributed multipole study,' *J. Phys. Chem.* **100**, 7352–7360. 265

Cooper, A. R. and Hutson, J. M. (1993) 'Non-additive intermolecular forces from the spectroscopy of Van der Waals trimers: calculations on $Ar_2\cdots HCl$,' *J. Chem. Phys.* **98**, 5337–5351. 191

Cooper, D. L. and Stutchbury, N. C. J. (1985) 'Distributed multipole analysis from charge partitioning by zero-flux surfaces: the structure of HF complexes,' *Chem. Phys. Lett.* **120**, 167–172. 129

Corner, J. (1948) 'The second virial coefficient of a gas of non-spherical molecules,' *Proc. Roy. Soc. A* **192**, 275–292. 209

Cox, S. R. and Williams, D. E. (1981) 'Representation of the molecular electrostatic potential by a net atomic charge model,' *J. Comput. Chem.* **2**, 304–323. 138

Cozzi, F., Cinquini, M., Annunziata, R. and Siegel, J. S. (1993) 'Dominance of polar/π over charge transfer effects: stacked phenyl interactions,' *J. Amer. Chem. Soc.* **115**, 5330–5331. 151

Craig, D. P. and Thirumachandran, T. (1984) *Molecular Quantum Electrodynamics*, Academic Press. 65

Craig, S. L. and Stone, A. J. (1994) 'Stereoselectivity and regioselectivity in Diels–Alder reactions studied by intermolecular perturbation theory,' *J. Chem. Soc. Faraday Trans.* **90**, 1663–1668. 153

Császár, A. G., Fábri, C., Szidarovszky, T., Mátyus, E., Furtenbacher, T. and Czakó, G. (2012) 'The fourth age of quantum chemistry: molecules in motion,' *Phys. Chem. Chem. Phys* **14**, 1085–1106. 256

Cwiok, T., Jeziorski, B., Kołos, W., Moszynski, R., Rychlewski, J. and Szalewicz, K. (1992) 'Convergence properties and large-order behavior of the polarization expansion for the interaction energy of hydrogen atoms,' *Chem. Phys. Lett.* **195**, 67–76. 105, 113

Cybulski, S. M., Bledson, T. M. and Toczyłowski, R. R. (2002) 'Comment on "hydrogen bonding and stacking interactions of nucleic acid base pairs: A density-functional-theory treatment" [*J. Chem. Phys.* **114**, 5149 (2001),' *J. Chem. Phys.* **116**, 11039–11040. 94

Cybulski, S. M. and Scheiner, S. (1990) 'Comparison of Morokuma and perturbation-theory approaches to decomposition of interaction energy: $NH_4^+\cdots NH_3$,' *Chem. Phys. Lett.* **166**, 57–64. 97

Cybulski, S. M. and Seversen, C. E. (2003) 'An interaction energy decomposition approach for the supermolecule density functional theory calculations,' *J. Chem. Phys.* **119**, 12704–12707. 92, 93, 99

Cybulski, S. M. and Seversen, C. E. (2005) 'Critical examination of the supermolecule density functional theory calculations of intermolecular interactions,' *J. Chem. Phys.* **122**, 014117. 93

Dalgarno, A. (1967) 'New methods for calculating long-range intermolecular forces,' *Adv. Chem. Phys.* **12**, 143–166. 244

Dalgarno, A. and Lynn, N. (1957*a*) 'An exact calculation of second order long range forces,' *Proc. Phys. Soc. (London)* **A70**, 223–225. 63, 148

Dalgarno, A. and Lynn, N. (1957*b*) 'Properties of the helium atom,' *Proc. Phys. Soc. (London)* **A70**, 802–808. 244

Darden, T. A., Perera, L., Li, L. and Pedersen, L. G. (1999) 'New tricks for modelers from the crystallography toolkit: the particle mesh Ewald algorithm and its use in nucleic acid simulations,' *Structure* **7**, R55–R60. 222

Davidson, E. R. and Chakravorty, S. J. (1994) 'A possible definition of basis set superposition error,' *Chem. Phys. Lett.* **217**, 48–54. 88

Davydov, A. S. (1962) *Theory of Molecular Excitons*, McGraw-Hill, New York, translated by M. Kasha and M. Oppenheimer, Jr. from the Russian edition of 1951. 196

Day, G. M. (2011) 'Current approaches to predicting molecular organic crystal structures,' *Cryst. Rev.* **17**, 3–52. 265

Day, G. M., Cooper, T. G., Cruz-Cabeza, A. J., Hejczyk, K. E., Ammon, H. L., Boerrigter, S. X. M., Tan, J. S., Della Valle, R. G., Venuti, E., Jose, K. V. J., Gadre, S. R., Desiraju, G. R., Thakur, T. S., van Eijck, B. P., Facelli, J. C., Bazterra, V. E., Ferraro, M. B., Hofmann, D. W. M., Neumann, M. A., Leusen, F. J. J., Kendrick, J., Price, S. L., Misquitta, A. J., Karamertzanis, P. G., Welch, G. W. A., Scheraga, H. A., Arnautova, Y. A., Schmidt, M. U., van de Streek, J., Wolf, A. K. and Schweizer, B. (2009) 'Significant progress in predicting the crystal structures of small organic molecules — a report on the fourth blind test,' *Acta Cryst. B* **65**, 107–125. 266

Day, G. M., Motherwell, W. D. S., Ammon, H. L., Boerrigter, S. X. M., Valle, R. G. D., Venuti, E., Dzyabchenko, A., Dunitz, J. D., Schweizer, B., van Eijck, B. P., Erk, P., Facelli, J. C., Bazterra, V. E., Ferraro, M. B., Hofmann, D. W. M., Leusen, F. J. J., Liang, C., Pantelides, C. C., Karamertzanis, P. G., Price, S. L., Lewis, T. C., Nowell, H., Torrisi, A., Scheraga, H. A., Arnautova, Y. A., Schmidt, M. U. and Verwer, P. (2005*a*) 'A third blind test of crystal structure prediction,' *Acta Cryst. B* **61**, 511–527. 266

Day, G. M., Motherwell, W. D. S. and Jones, W. (2005*b*) 'Beyond the isotropic atom model in crystal structure prediction of rigid molecules: atomic multipoles versus point charges,' *Cryst. Growth Des.* **5**, 1023–1033. 265

Day, G. M. and Price, S. L. (2003) 'A nonempirical anisotropic atom–atom model potential for chlorobenzene crystals,' *J. Amer. Chem. Soc.* **125**, 16434–16443. 213, 265

Dayton, D. C., Jucks, K. W. and Miller, R. E. (1989) 'Photofragment angular distributions for HF dimer: scalar J-J correlations in state-to-state photodissociation,' *J. Chem. Phys.* **90**, 2631–2638. 6, 250

del Bene, J. E., Person, W. B. and Szczepaniak, K. (1995) 'Properties of hydrogen-bonded complexes obtained from the B3LYP functional with 6–31G(d,p) and 6–31+G(d,p) basis sets,' *J. Phys. Chem.* **99**, 10705–10707. 92

Dewar, M. J. S. and Thompson, C. C. (1966) 'π–molecular complexes. III. A critique of charge transfer, and stability constants for some TCNE–hydrocarbon complexes,' *Tetrahedron* **22 (S7)**, 97–114. 150

Dewar, M. J. S., Zoebisch, E. G., Healy, E. F. and Stewart, J. J. P. (1985) 'AM1: a new general-purpose quantum mechanical molecular model,' *J. Amer. Chem. Soc.* **107**, 3902–3909. 95

Dham, A. K., Allnatt, A. R., Meath, W. J. and Aziz, R. A. (1989) 'The Kr–Kr potential energy curve and related physical properties: the XC and HFD-B potential models,' *Molec. Phys.* **67**, 1291–1307. 207, 208

Dick, B. G. and Overhauser, A. W. (1958) 'Theory of the dielectric constants of alkali halide crystals,' *Phys. Rev.* **112**, 90–103. 208

Dinur, U. and Hagler, A. T. (1989) 'Determination of atomic point charges and point dipoles from the Cartesian derivatives of the molecular dipole moment and second moments, and from energy second derivatives of planar dimers. I. Theory,' *J. Chem. Phys.* **91**, 2949–2958. 137

Dixit, S., Crain, J., Poon, W. C. K., Finney, J. L. and Soper, A. K. (2002) 'Molecular segregation observed in a concentrated alcohol–water solution,' *Nature* **416**, 829–832. 192

Dobson, J. F. (2007) 'Unusual features of the dispersion force in layered and striated nanostructures,' *Surface Sci.* **601**, 5667–5672. 180

Doran, M. B. and Zucker, I. J. (1971) 'Higher-order multipole three-body Van der Waals interactions and stability of rare gas solids,' *J. Phys. C* **4**, 307–312. 189

Douketis, C., Scoles, G., Marchetti, S., Zen, M. and Thakkar, A. J. (1982) 'Intermolecular forces *via* hybrid Hartree–Fock-SCF plus damped dispersion (HFD) energy calculations: an improved spherical model,' *J. Chem. Phys.* **76**, 3057–3063. 205, 207

Du, Q., Freysz, E. and Shen, Y. R. (1994) 'Surface vibrational spectroscopic studies of hydrogen bonding and hydrophobicity,' *Science* **264**, 826–828. 193

Dulmage, W. J. and Lipscomb, W. N. (1951) 'The crystal structures of hydrogen cyanide, HCN,' *Acta. Cryst.* **4**, 330–334. 52

Dunlap, B. I. (2000) 'Robust and variational fitting,' *Phys. Chem. Chem. Phys* **2**, 2113–2116. 82

Dunlap, B. I., Connolly, J. W. D. and Sabin, J. R. (1979) 'On first-row diatomic molecules and local density models,' *J. Chem. Phys.* **71**, 4993–4999. 82

Dyke, T. R., Howard, B. J. and Klemperer, W. (1972) 'Radiofrequency and microwave spectrum of HF dimer,' *J. Chem. Phys.* **56**, 2442–2454. 55

Eberly, J. H. (1989) 'Quantum optics at very high laser intensities,' *Adv. Chem. Phys.* **73**, 801–822. 30

Eggenberger, R., Gerber, S., Huber, H. and Searles, D. (1991) 'Basis set superposition errors in intermolecular structures and force constants,' *Chem. Phys. Lett.* **183**, 223–226. 91

Eisenschitz, L. and London, F. (1930) 'Über das Verhältnis der van der Waalsschen Kräfte zu den homöopolaren Bindungskräften,' *Z. Phys.* **60**, 491–527. 110

Elking, D. M., Cisneros, G. A., Piquemal, J.-P., Darden, T. A. and Pedersen, L. G. (2010) 'Gaussian multipole model (GMM),' *J. Chem. Theory Comput.* **6**, 190–202. 145

Elliott, J. P. and Dawber, P. G. (1979) *Symmetry in Physics*, MacMillan, London. 34

Elrod, M. J. and Saykally, R. J. (1994) 'Many-body effects in intermolecular forces,' *Chem. Rev.* **94**, 1975–1997. 187

Elrod, M. J., Steyert, D. W. and Saykally, R. J. (1991) 'Tunable far-infrared laser spectroscopy of a ternary Van der Waals cluster Ar_2HCl: a sensitive probe of three-body forces,' *J. Chem. Phys.* **94**, 58–66. 252

Elrod, M. J., Host, B. C., Steyert, D. W. and Saykally, R. J. (1993) 'Far-infrared vibration-rotation-tunnelling spectroscopy of ArDCl. A critical test of the H6(4,3,0) potential surface,' *Molec. Phys.* **79**, 245–251. 250

Elrod, M. J., Loeser, J. G. and Saykally, R. J. (1993) 'An investigation of three-body effects in intermolecular forces. III. Far infrared laser vibration–rotation–tunnelling spectra of the lowest internal rotor state of Ar_2HCl,' *J. Chem. Phys.* **98**, 5352–5361. 252

Epstein, S. T. and Johnson, R. E. (1968) 'The application of perturbation theories for exchange forces to a simple model,' *Chem. Phys. Lett.* **1**, 602–604. 111

Ernesti, A. and Hutson, J. M. (1994) 'Non-additive intermolecular forces from the spectroscopy of Van der Waals trimers: the effect of monomer vibrational excitation in $Ar_2\cdots HF$ and $Ar_2\cdots HCl$,' *J. Chem. Soc. Faraday Disc.* **97**, 119–129. 191

Etters, R. D. and Danilowicz, R. (1979) 'Three-body interactions in small rare-gas clusters,' *J. Chem. Phys.* **71**, 4767–4768. 189

Ewald, P. (1921) *Ann. Phys. (Leipzig)* **64**, 253–287. 266

Ewing, J. J., Tigelaar, H. L. and Flygare, W. H. (1972) 'Molecular Zeeman effect, magnetic properties and electric quadrupole moments in ClF, BrF, ClCN, BrCN and ICN,' *J. Chem. Phys.* 1957–1966. 241

Fanourgakis, G. S., Markland, T. E. and Manolopoulos, D. E. (2009) 'A fast path integral method for polarizable force fields,' *J. Chem. Phys.* **131**, 094102. 249

Faraday (2010) 'Multiscale modelling of soft matter,' *Faraday Disc.* **144**. 229

Faraday (1994) 'Structure and dynamics of Van der Waals complexes,' *Faraday Disc.* **97**, 1–461. 249

Feller, D. (1992) 'Application of systematic sequences of wavefunctions to the water dimer,' *J. Chem. Phys.* **96**, 6104–6114. 82

Ferenczy, G. G. (1991) 'Charges derived from distributed multipole series,' *J. Comp. Chem.* **12**, 913–917. 131

Ferenczy, G. G., Winn, P. J. and Reynolds, C. A. (1997) 'Toward improved force fields. 2. Effective distributed multipoles,' *J. Phys. Chem. A* **101**, 5446–5455. 131

Feynman, R. P. (1939) 'Forces in molecules,' *Phys. Rev.* **56**, 340. 83

Feynman, R. P. and Hibbs, A. R. (1965) *Quantum Mechanics and Path Integrals*, McGraw-Hill, New York. 249

Figari, G. and Magnasco, V. (1985) 'On the evaluation of the cofactors occurring in the matrix elements between multiply-excited determinantal wavefunctions of non-orthogonal orbitals,' *Molec. Phys.* **55**, 319–330. 109

Filippini, G. and Gavezzotti, A. (1993) 'Empirical intermolecular potentials for organic crystals: the '6-exp' approximation revisited,' *Acta Cryst.* **B49**, 868–880. 212

Finney, J. L. (2001) 'The water molecule and its interactions: the interaction between theory, modelling, and experiment,' *J. Mol. Liq.* **90**, 303–312. 225

Fischer, F. R., Wood, P. A., Allen, F. H. and Diederich, F. (2008) 'Orthogonal dipolar interactions between amide carbonyl groups,' *Proc. Nat. Acad. Sci. (US)* **105**, 17290–17294. 117

Fleming, I. (1976) *Frontier Orbitals and Organic Chemical Reactions*, Wiley, London, New York. 153

Fleming, I. (2009) *Molecular Orbitals and Organic Chemical Reactions*, Wiley, Chichester. 153

Forster, T. and Kasper, K. (1955) 'Ein Konzentrationsumschlag der Fluoreszenz des Pyrens,' *Z. Elektrochem.* **59**, 976–980. 197

Fowler, P. W. and Madden, P. A. (1984) 'In-crystal polarizabilities of alkali and halide ions,' *Phys. Rev. B* **29**, 1035–1042. 185, 186

Fowler, P. W. and Madden, P. A. (1985) 'In-crystal polarizability of O^{2-},' *J. Phys. Chem.* **89**, 2581–2585. 185

Fowler, P. W. and Stone, A. J. (1987) 'Induced dipole moments of Van der Waals complexes,' *J. Phys. Chem.* **91**, 509–511. 170, 241

Francl, M. M., Carey, C., Chirlian, L. E. and Gange, D. M. (1996) 'Charges fit to electrostatic potentials. II. Can atomic charges be unambiguously fit to electrostatic potentials?' *J. Comput. Chem.* **17**, 367–383. 139

Francl, M. M., Pietro, W. J., Hehre, W. J., Binkley, J. S., Gordon, M. S., DeFrees, D. J. and Pople, J. A. (1982) 'SCF MO methods. 23. A polarization-type basis set for second-row elements,' *J. Chem. Phys.* **77**, 3654–3665. 80

Frank, H. S. and Evans, M. W. (1945) 'Free volume and entropy in condensed systems. III. Entropy in binary liquid mixtures; partial molal entropy in dilute solutions; structure and thermodynamics in aqueous electrolytes,' *J. Chem. Phys.* **13**, 507–532. 193

Fraser, G. T., Suenram, R. D., Lovas, F. J., Pine, A. S., Hougen, J. T., Lafferty, W. J. and Muenter, J. S. (1988) 'Infrared and microwave investigations of interconversion tunnelling in the acetylene dimer,' *J. Chem. Phys.* **89**, 6028–6045. 53

Freitag, M. A., Gordon, M. S., Jensen, J. H. and Stevens, W. J. (2000) 'Evaluation of charge penetration between distributed multipole expansions,' *J. Chem. Phys.* **112**, 7300–7306. 145

Frey, R. F. and Davidson, E. R. (1989) 'Energy partitioning of the self-consistent-field interaction energy of ScCO,' *J. Chem. Phys.* **90**, 5555–5562. 97

Freyriafava, C., Dovesi, F., Saunders, V. R., Leslie, M. and Roetti, C. (1993) 'Ca and Be substitution in bulk MgO: *ab initio* Hartree–Fock and ionic model supercell calculations,' *J. Phys. Condensed Matter* **5**, 4793–4804. 209

Frisch, H. L. and Helfand, E. (1960) 'Conditions imposed by gross properties on the intermolecular potential,' *J. Chem. Phys.* **32**, 269–270. 245

Frisch, M. J., del Bene, J. E., Binkley, J. S. and Schaefer, H. F., III (1986) 'Extensive theoretical studies of the hydrogen-bonded complexes $(H_2O)_2$, $(H_2O)_2H^+$, $(HF)_2$, F_2H^- and $(NH_3)_2$,' *J. Chem. Phys.* **84**, 2279–2289. 90

Frisch, M. J., Trucks, G. W., Schlegel, H. B., Scuseria, G. E., Robb, M. A., Cheeseman, J. R., Montgomery, J. A., Jr., Vreven, T., Kudin, K. N., Burant, J. C., Millam, J. M., Iyengar, S. S., Tomasi, J., Barone, V., Mennucci, B., Cossi, M., Scalmani, G., Rega, N., Petersson, G. A., Nakatsuji, H., Hada, M., Ehara, M., Toyota, K., Fukuda, R.,

Hasegawa, J., Ishida, M., Nakajima, T., Honda, Y., Kitao, O., Nakai, H., Klene, M., Li, X., Knox, J. E., Hratchian, H. P., Cross, J. B., Bakken, V., Adamo, C., Jaramillo, J., Gomperts, R., Stratmann, R. E., Yazyev, O., Austin, A. J., Cammi, R., Pomelli, C., Ochterski, J. W., Ayala, P. Y., Morokuma, K., Voth, G. A., Salvador, P., Dannenberg, J. J., Zakrzewski, V. G., Dapprich, S., Daniels, A. D., Strain, M. C., Farkas, O., Malick, D. K., Rabuck, A. D., Raghavachari, K., Foresman, J. B., Ortiz, J. V., Cui, Q., Baboul, A. G., Clifford, S., Cioslowski, J., Stefanov, B. B., Liu, G., Liashenko, A., Piskorz, P., Komaromi, I., Martin, R. L., Fox, D. J., Keith, T., Al-Laham, M. A., Peng, C. Y., Nanayakkara, A., Challacombe, M., Gill, P. M. W., Johnson, B. G., Chen, W., Wong, M. W., Gonzalez, C. and Pople, J. A. (2004) 'Gaussian 03,' Gaussian, Inc., Wallingford, CT. 81

Fukui, K. and Fujimoto, H. (1968) 'An MO-theoretical interpretation of the nature of chemical reaction. I. Partitioning analysis of the interaction energy,' *Bull. Chem. Soc. Japan* **41**, 1989–1997. 153

Garmer, D. R. and Stevens, W. J. (1989) 'Transferability of molecular distributed polarizabilities from a simple localized orbital based method,' *J. Phys. Chem.* **93**, 8263–8270. 174

Garrido, N. M., Jorge, M., Queimada, A. J., Gomes, J. R. B., Economou, I. G. and Macedo, E. A. (2011) 'Predicting hydration Gibbs energies of alkyl-aromatics using molecular simulation,' *Phys. Chem. Chem. Phys* **13**, 17384–17394. 223

Gavezzotti, A. (2007) *Molecular Aggregation*, Oxford University Press. 265

Gavezzotti, A. and Filippini, G. (1994) 'Geometry of the intermolecular X–H···Y (X, Y = N, O) hydrogen bond and the calibration of empirical hydrogen-bond potentials,' *J. Phys. Chem.* **98**, 4831–4837. 212

Gavezzotti, A. and Filippini, G. (1995) 'Polymorphic forms of organic crystals at room conditions: thermodynamic and structural implications,' *J. Amer. Chem. Soc.* **117**, 12299–12305. 266

Gerratt, J. and Mills, I. M. (1968) 'Force constants and dipole moment derivatives of molecules from perturbed Hartree–Fock calculations,' *J. Chem. Phys.* **49**, 1719–1729. 85, 170

Ghanty, T. K., Staroverov, V. N., Koren, P. R. and Davidson, E. R. (2000) 'Is the hydrogen bond in water dimer and ice covalent?' *J. Amer. Chem. Soc.* **122**, 1210–1214. 151, 156

Goldman, N., Fellers, R. S., Brown, M. G., Braly, L. B., Keoshian, C. J., Leforestier, C. and Saykally, R. J. (2002) 'Spectroscopic determination of the water dimer intermolecular potential-energy surface,' *J. Chem. Phys.* **116**, 10148–10163. 228, 251

Goldman, N., Leforestier, C. and Saykally, R. J. (2005) 'A 'first principles' potential energy surface for liquid water from VRT spectroscopy of water clusters,' *Phil. Trans. Roy. Soc. A* **363**, 493–508. 228, 251

Goldman, N. and Saykally, R. J. (2004) 'Elucidating the role of many-body forces in liquid water. I. Simulations of water clusters on the VRT–(ASP-W) potential surfaces,' *J. Chem. Phys.* **120**, 4777–4789. 189

Gordon, M. S., Fedorov, D. G., Pruitt, S. R. and Slipchenko, L. V. (2012) 'Fragmentation methods: a route to accurate calculations on large systems,' *Chem. Rev.* **112**, 632–672. 219

Gouyet, J. F. (1973) 'Use of biorthogonal orbitals in calculation by perturbation of intermolecular interactions,' *J. Chem. Phys.* **59**, 4637–4641. 108

Gray, C. G. and Gubbins, K. E. (1984) *Theory of Molecular Fluids*, vol. 1: Fundamentals, Oxford University Press, Oxford. 14, 17, 19, 27, 28, 72, 240, 243

Gray, C. G., Gubbins, K. E. and Joslin, C. G. (2011) *Theory of Molecular Fluids*, vol. 2: Applications, Oxford University Press, Oxford. 240

Gray, N. A. B. and Stone, A. J. (1970) 'Justifiability of the ZDO approximation in terms of a power series expansion,' *Theor. Chim. Acta* **18**, 389–390. 107

Gregory, J. K. and Clary, D. C. (1994) 'A comparison of conventional and rigid body diffusion Monte Carlo techniques. Application to water dimer.' *Chem. Phys. Lett.* **228**, 547–554. 259

Gregory, J. K. and Clary, D. C. (1995*a*) 'Calculations of the tunnelling splittings in water dimer and trimer using diffusion Monte Carlo,' *J. Chem. Phys.* **102**, 7817–7829. 259

Gregory, J. K. and Clary, D. C. (1995*b*) 'Three-body effects on molecular properties in the water trimer,' *J. Chem. Phys.* **103**, 8924–8930. 259

Gresh, N. (1995) 'Energetics of Zn^{2+} binding to a series of biologically relevant ligands: a molecular mechanics investigation grounded on *ab initio* self-consistent field supermolecular computations,' *J. Comput. Chem.* **16**, 856–882. 219

Gresh, N., Claverie, P. and Pullman, A. (1984) 'Theoretical studies of molecular conformation – derivation of an additive procedure for the computation of intramolecular interaction energies – comparison with *ab initio* SCF computations,' *Theor. Chim. Acta* **66**, 1–20. 219

Griffiths, G. I. G., Misquitta, A. J., Needs, R. J., Pickard, C. J. and Fortes, A. D. (2012) 'Theoretical study of ammonia monohydrate at pressures up to 12 GPa,' *J. Chem. Phys.* submitted. 95

Grimme, S. (2011) 'Density functional theory with London dispersion corrections,' *WIREs Comp. Molec. Sci.* **1**, 211–228. 94

Grimme, S., Antony, J., Ehrlich, S. and Krieg, H. (2010) 'A consistent and accurate *ab initio* parametrization of density functional dispersion correction (DFT-D) for the 94 elements H–Pu,' *J. Chem. Phys.* **132**, 154104. 94

Gritsenko, O. V. and Baerends, E. J. (2004) 'Asymptotic correction of the exchange–correlation kernel of time-dependent density functional theory for long-range charge-transfer excitations,' *J. Chem. Phys.* **121**, 655–660. 79

Guerra, C. F., Handgraaf, J.-W., Baerends, E. J. and Bickelhaupt, F. M. (2004) 'Voronoi deformation density (VDD) charges: Assessment of the Mulliken, Bader, Hirshfeld, Weinhold, and VDD methods for charge analysis,' *J. Comput. Chem.* **25**, 189–210. 129

Guillot, B. (2002) 'A reappraisal of what we have learnt during three decades of computer simulations on water,' *J. Mol. Liq.* **101**, 219–260. 225

Gunning, M. J. and Raab, R. E. (1997) 'Physical implications of the use of primitive and traceless electric quadrupole moments,' *Molec. Phys.* **91**, 589–595. 42

Gussoni, M., Castiglioni, C. and Zerbi, G. (1986) 'Molecular point charges as derived from infrared intensities and from *ab initio* calculations,' *Theochem (J. Mol. Struct.)* **31**, 203–212. 136

Gutowski, M. and Piela, L. (1988) 'Interpretation of the Hartree–Fock interaction energy between closed-shell systems,' *Molec. Phys.* **64**, 337–355. 97, 98

Gutowski, M., Van Duijneveldt, F. B., Chałasiński, G. and Piela, L. (1987) 'Proper correction for the basis set superposition error in SCF calculations of intermolecular interactions,' *Molec. Phys.* **61**, 233–247. 89

Gutowski, M., van Duijneveldt-van de Rijdt, J. G. C. M., van Lenthe, J. H. and van Duijneveldt, F. B. (1993) 'Accuracy of the Boys and Bernardi function counterpoise method,' *J. Chem. Phys.* **98**, 4728–4737. 90

Halkier, A., Klopper, W., Helgaker, T. and Jørgensen, P. (1999) 'Basis-set convergence of the molecular electric dipole moment,' *J. Chem. Phys.* **111**, 4424–4430. 14

Hamermesh, M. (1989) *Group Theory and Its Application to Physical Problems*, Dover, New York. 34

Handy, N. C. and Schaefer, H. F., III (1984) 'On the evaluation of analytic energy derivatives for correlated wavefunctions,' *J. Chem. Phys.* **81**, 5031–5033. 85

Hariharan, P. C. and Pople, J. A. (1973) 'Self-consistent-field molecular orbital methods. XII. Further extension of Gaussian-type basis sets for use in molecular-orbital studies of organic molecules,' *Theor. Chim. Acta* **28**, 213–222. 80

Harvey, A. H. and Lemmon, E. W. (2004) 'Correlation for the second virial coefficient of water,' *J. Phys. Chem. Ref. Data* **33**, 369–376. 246

Hättig, C. (1996) 'Recurrence relations for the direct calculation of spherical multipole interaction tensors and Coulomb-type interaction energies,' *Chem. Phys. Lett.* **260**, 341–351. 51, 231

Hättig, C. (1997) 'On the calculation of derivatives for Coulomb-type interaction energies and general anisotropic pair potentials,' *Chem. Phys. Lett.* **268**, 521–530. 52

Hättig, C. and Heß, B. A. (1994) 'Calculation of orientation dependent double-tensor moments for Coulomb-type molecular interactions,' *Molec. Phys.* **81**, 813–824. 50, 230, 291

Haverkort, J. E. M., Baas, F. and Beenakker, J. J. M. (1983) 'Measurements of depolarization ratios of linear chain molecules: a test of the principle of additivity of bond polarizabilities,' *Chem. Phys.* **79**, 105–109. 159

Hayes, I. C. and Stone, A. J. (1984*a*) 'An intermolecular perturbation theory for the region of moderate overlap,' *Molec. Phys.* **53**, 83–105. 107, 109, 117, 146

Hayes, I. C. and Stone, A. J. (1984*b*) 'Matrix elements between determinantal wavefunctions of non-orthogonal orbitals,' *Molec. Phys.* **53**, 69–82. 109

Heather, R. W. and Light, J. C. (1982) 'Discrete variable theory of triatomic photodissociation,' *J. Chem. Phys.* **79**, 147–159. 256

Hehre, W. J., Ditchfield, R. and Pople, J. A. (1971) 'Self-consistent-field molecular-orbital methods. XII. Further extensions of Gaussian-type basis sets for use in molecular orbital studies of organic molecules,' *J. Chem. Phys.* **56**, 2257–2261. 80

Helgaker, T., Jørgensen, P. and Olsen, J. (2000) *Molecular Electronic-Structure Theory*, Wiley, Chichester. 74, 75, 76

Helgaker, T., Klopper, W., Koch, H. and Noga, J. (1997) 'Basis-set convergence of correlated calculations on water,' *J. Chem. Phys.* **106**, 9639–9646. 77

Hellmann, H. (1937) *Einführung in die Quantenchemie*, Deuticke, Leipzig. 83

Hepburn, J., Scoles, G. and Penco, R. (1975) 'A simple but reliable method for prediction of intermolecular potentials,' *Chem. Phys. Lett.* **36**, 451–456. 93, 205

Hermans, J., Berendsen, H. J. C., van Gunsteren, W. F. and Postma, J. P. M. (1984) 'A consistent empirical potential for water–protein interactions,' *Biopolymers* **23**, 1513–1518. 221

Hesselmann, A. (2009) 'Derivation of the dispersion energy as an explicit density- and exchange-hole functional,' *J. Chem. Phys.* **130**, 084104. 95

Hesselmann, A. and Jansen, G. (2002*a*) 'First-order intermolecular interaction energies from Kohn–Sham orbitals,' *Chem. Phys. Lett.* **357**, 464–470. 79, 117, 119

Hesselmann, A. and Jansen, G. (2002*b*) 'Intermolecular induction and exchange-induction energies from coupled-perturbed Kohn–Sham density functional theory,' *Chem. Phys. Lett.* **362**, 319–325. 119

Hesselmann, A. and Jansen, G. (2003) 'Intermolecular dispersion energies from time-dependent density functional theory,' *Chem. Phys. Lett.* **367**, 778–784. 119

Hills, R. D., Jr, Lu, L. and Voth, G. A. (2010) 'Multiscale coarse-graining of the protein energy landscape,' *PLoS Comput. Biol.* **6**, e1000827. 229

Hinde, R. J. (2008) 'Three-body interactions in solid parahydrogen,' *Chem. Phys. Lett.* **460**, 141–145. 190

Hirschfelder, J. O. (1967) 'Perturbation theory for exchange forces,' *Chem. Phys. Lett.* **1**, 325–329, 363–368. 59, 111

Hirschfelder, J. O., Curtiss, C. F. and Bird, R. B. (1954) *Molecular Theory of Liquids and Gases*, Wiley, New York and London. 46, 247

Hirschfelder, J. O. and Silbey, R. (1966) 'New type of molecular perturbation treatment,' *J. Chem. Phys.* **45**, 2188–2192. 111

Hirshfeld, F. L. (1977) 'Bonded-atom fragments for describing molecular charge densities,' *Theor. Chim. Acta* **44**, 129–138. 128

Hodges, M. P., Stone, A. J. and Xantheas, S. S. (1997) 'The contribution of many-body terms to the energy for small water clusters — a comparison of *ab initio* and accurate model potentials,' *J. Phys. Chem. A* **101**, 9163–9168. 183

Hohenberg, P. and Kohn, W. (1964) 'Inhomogeneous electron gas,' *Phys. Rev.* **136**, B864–B871. 78

Holmgren, S. L., Waldman, M. and Klemperer, W. (1977) 'Internal dynamics of Van der Waals complexes. I. Born–Oppenheimer separation of radial and angular motion,' *J. Chem. Phys.* **67**, 4414–4422. 255

Huang, D. M. and Chandler, D. (2002) 'The hydrophobic effect and the influence of solute–solvent attractions,' *J. Phys. Chem. B* **106**, 2047–2053. 193

Huang, X., Braams, B. J. and Bowman, J. M. (2005) '*Ab initio* potential energy and dipole moment surfaces for $(H_5O_2)^+$,' *J. Chem. Phys.* **122**, 044308. 228

Huang, X., Braams, B. J. and Bowman, J. M. (2006) '*Ab initio* potential energy and dipole moment surfaces for $(H_2O)_2$,' *J. Phys. Chem. A* **110**, 445–451. 96, 228

Huang, X., Braams, B. J., Bowman, J. M., Kelly, R. E. A., Tennyson, J., Groenenboom, G. C. and van der Avoird, A. (2008) 'New *ab initio* potential energy surface and the vibration-rotation-tunneling levels of $(H_2O)_2$ and $(D_2O)_2$,' *J. Chem. Phys.* **128**, 034312. 96, 228, 256

Huang, Z. S. and Miller, R. E. (1989) 'The structure of CO_2–HCCH from near infrared spectroscopy,' *Chem. Phys.* **132**, 185–196. 54

Hujo, W. and Grimme, S. (2011) 'Performance of the Van der Waals density functional VV10 and (hybrid) GGA variants for thermochemistry and noncovalent interactions,' *J. Chem. Theory Comput.* **7**, 3866–3871. 93

Hunter, C. A. (1993) 'Sequence-dependent DNA structure: the role of base stacking interactions,' *J. Molec. Biol.* **230**, 1025–1054. 140

Hunter, C. A. (1994) 'The role of aromatic interactions in molecular recognition,' *Chem. Soc. Rev.* **23**, 101–109. 140, 198

Hunter, C. A. and Sanders, J. K. M. (1990) 'The nature of $\pi - \pi$ interactions,' *J. Amer. Chem. Soc.* **112**, 5525–5534. 140

Hunter, C. A., Sanders, J. K. M. and Stone, A. J. (1989) 'Exciton coupling in porphyrin dimers,' *Chem. Phys.* **133**, 395–404. 199

Hunter, C. A., Singh, J. and Thornton, J. M. (1991) '$\pi - \pi$ interactions: the geometry and energetics of phenylalanine–phenylalanine interactions in proteins,' *J. Molec. Biol.* **218**, 837–846. 140

Huot, J. and Bose, T. K. (1991) 'Determination of the quadrupole moment of nitrogen from the dielectric second virial coefficient,' *J. Chem. Phys.* **94**, 3849–3854. 124

Hutson, J. M. (1989*a*) 'The intermolecular potential of Ne–HCl: determination from high-resolution spectroscopy,' *J. Chem. Phys.* **91**, 4448–4454. 210

Hutson, J. M. (1989*b*) 'Anisotropic intermolecular forces. III. Rare gas–hydrogen bromide systems,' *J. Chem. Phys.* **91**, 4455–4461. 210

Hutson, J. M. (1990*a*) 'BOUND,' A computer program distributed by EPSRC Collaborative Computational Project No. 6 on Heavy Particle Dynamics. 255

Hutson, J. M. (1990*b*) 'Dynamics of Van der Waals complexes: beyond atom-diatom systems,' in *Dynamics of Polyatomic Van der Waals Complexes*, eds. N. Halberstadt and K. C. Janda, 67–79, NATO ASI, Plenum. 253

Hutson, J. M. (1992) 'Vibrational dependence of the anisotropic intermolecular potential of Ar–HCl,' *J. Phys. Chem.* **96**, 4237–4247. 250, 253

Hutson, J. M., Ernesti, A., Law, M. M., Roche, C. F. and Wheatley, R. J. (1996) 'The intermolecular potential energy surface for $CO_2\cdots$Ar: fitting to high-resolution spectroscopy of Van der Waals complexes and second virial coefficients,' *J. Chem. Phys.* **105**, 9130–9140. 250

Hutson, J. M. and Howard, B. J. (1980) 'Spectroscopic properties and potential surfaces for atom–diatom Van der Waals molecules,' *Molec. Phys.* **41**, 1123–1141. 255

Hylleraas, E. A. (1929) 'New calculation of the energy of helium in the ground-state, and the deepest terms of ortho-helium,' *Zeit. Phys.* **54**, 347–366. 77

Isaacs, E. D., Shukla, A., Platzman, P. M., Hamann, D. R., Barbiellini, B. and Tulk, C. A. (1999) 'Covalency of the hydrogen bond in ice: a direct X-ray measurement,' *Phys. Rev. Lett.* **82**, 600–603. 150, 156

Israelachvili, J. N. (1992) *Intermolecular and Surface Forces*, Academic Press, London, 2nd edn. 65

Jaeger, H. M., Swenson, D. W. H. and Dykstra, C. E. (2006) 'Remarkable features in the interactions of quadrupolar molecules,' *J. Phys. Chem. A* **110**, 6399–6407. 259

Jalink, H., Parker, D. H. and Stolte, S. (1987) 'Experimental verification of the sign of the electric dipole moment of N_2O.' *J. Mol. Spectr.* **121**, 236–237. 170, 241

Janda, K. C., Klemperer, W. and Novick, S. E. (1976) 'Measurement of the sign of the dipole moment of ClF,' *J. Chem. Phys.* **64**, 2698–2699. 241

Jankowski, P. (2004) 'Approximate generation of full-dimensional *ab initio* Van der Waals surfaces for high-resolution spectroscopy,' *J. Chem. Phys.* **121**, 1655–1662. 224

Jansen, L. (1957) 'Interactions between permanent multipole moments,' *Physica* **23**, 599–604. 46

Jansen, L. (1958) 'Tensor formalism for Coulomb interaction and asymptotic properties of multipole expansions,' *Phys. Rev.* **110**, 661–669. 46

Jarque, C. and Buckingham, A. D. (1989) 'Ion–ion interaction in a polarizable lattice,' *Chem. Phys. Lett.* **164**, 485–490. 191

Jarque, C. and Buckingham, A. D. (1992) 'Ion–ion interaction in a polarizable medium,' in *Molecular Liquids: New Perspectives in Physics and Chemistry*, ed. J. J. C. Teixeira-Dias, 253–265, Kluwer, Dordrecht. 191

Jeffreys, H. (1931) *Cartesian Tensors*, Cambridge University Press. 267

Jensen, F. (1999) *Introduction to Computational Chemistry*, Wiley, Chichester. 74, 76, 78, 83, 85

Jensen, F. (2001) 'Polarization consistent basis sets: Principles,' *J. Chem. Phys.* **115**, 9113–9125. 81

Jensen, F. (2002*a*) 'Polarization consistent basis sets. II. Estimating the Kohn–Sham basis set limit,' *J. Chem. Phys.* **116**, 7372–7379. 81

Jensen, F. (2002*b*) 'Polarization consistent basis sets. III. The importance of diffuse functions,' *J. Chem. Phys.* **117**, 9234–9240. 81

Jensen, F. (2003) 'Polarization consistent basis sets. IV. The basis set convergence of equilibrium geometries, harmonic vibrational frequencies, and intensities,' *J. Chem. Phys.* **118**, 2459–2463. 81

Jensen, F. (2007) 'Polarization consistent basis sets. 4: the elements He, Li, Be, B, Ne, Na, Mg, Al, and Ar,' *J. Phys. Chem. A* . 81

Jensen, J. H. and Gordon, M. S. (1996) 'An approximate formula for the intermolecular Pauli repulsion between closed shell molecules,' *Molec. Phys.* **89**, 1313–1325. 219

Jeziorska, M., Jeziorski, B. and Čižek, J. (1987) 'Direct calculation of the Hartree–Fock interaction energy via exchange perturbation expansion—the He···He interaction,' *Int. J. Quantum Chem.* **32**, 149–164. 116

Jeziorski, B. and Kołos, W. (1977) 'On symmetry forcing in the perturbation theory of weak intermolecular interactions,' *Int. J. Quantum Chem.* **12, Suppl. 1**, 91–117. 111, 112, 113

Jeziorski, B., Moszynski, R., Ratkiewicz, A., Rybak, S., Szalewicz, K. and Williams, H. L. (1993) 'SAPT: a program for many-body symmetry-adapted perturbation theory calculations of intermolecular interaction energies,' in *Methods and Techniques in Computational Chemistry: METECC94*, ed. E. Clementi, vol. B, 79, STEF, Cagliari. 117, 119

Jeziorski, B., Moszynski, R. and Szalewicz, K. (1994) 'Perturbation theory approach to intermolecular potential energy surfaces of Van der Waals complexes,' *Chem. Rev.* **94**, 1887–1930. 117

Jeziorski, B., Szalewicz, K. and Chałasinski, G. (1978) 'Symmetry forcing and convergence properties of perturbation expansions for molecular interaction energies,' *Int. J. Quantum Chem.* **14**, 271–287. 111, 113

Jhanwar, B. L. and Meath, W. J. (1982) 'Dipole oscillator strength distributions, sums and dispersion energy coefficients for CO and CO_2,' *Chem. Phys.* **67**, 185–199. 244

Jhanwar, B. L., Meath, W. J. and MacDonald, J. C. F. (1981) 'Dipole oscillator strength distributions and sums for C_2H_6, C_3H_8, *n*-C_4H_{10}, *n*-C_5H_{12}, *n*-C_6H_{14}, *n*-C_7H_{16}, and *n*-C_8H_{18},' *Canad. J. Phys.* **59**, 185–197. 159

Johnson, B. R. (1978) 'The renormalized Numerov method applied to calculations of bound states of the coupled-channel Schrödinger equation,' *J. Chem. Phys.* **69**, 4678–4688. 255

Johnson, R. E. and Epstein, S. T. (1968) 'Connection between several perturbation theories of intermolecular forces,' *Chem. Phys. Lett.* **1**, 599–601. 111

Jordan, M. J. T., Thompson, K. C. and Collins, M. A. (1995) 'Convergence of molecular potential energy surfaces by interpolation: Application to the OH + H_2 → H_2O + H reaction,' *J. Chem. Phys.* **102**, 5647–5657. 96

Jorgensen, W. L., Chandrasekhar, J., Madura, J. D., Impey, R. W. and Klein, M. L. (1983) 'Comparison of simple model potentials for simulating liquid water,' *J. Chem. Phys.* **79**, 926–935. 226

Jorgensen, W. L. and Tirado-Rives, J. (1988) 'The OPLS potential function for proteins. Energy minimization for crystals of cyclic peptides and crambin,' *J. Amer. Chem. Soc.* **110**, 1657–1666. 221

Joslin, C. G., Gray, C. G. and Singh, S. (1985) 'Far infrared absorption in gaseous CH_4 and CF_4. A theoretical study.' *Molec. Phys.* **54**, 1469–1489. 242

Joubert, L. and Popelier, P. L. A. (2002) 'Improved convergence of the 'atoms in molecules' multipole expansion of the electrostatic interaction,' *Molec. Phys.* **100**, 3357–3365. 130

Jurečka, P., Černý, J., Hobza, P. and Salahub, D. R. (2007) 'Density functional theory augmented with an empirical dispersion term. Interaction energies and geometries of 80 noncovalent complexes compared with *ab initio* quantum mechanics calculations,' *J. Comput. Chem.* **28**, 555–569. 94

Jurečka, P., Šponer, J., Černý, J. and Hobza, P. (2006) 'Benchmark database of accurate (MP2 and CCSD(T) complete basis set limit) interaction energies of small model complexes, DNA base pairs, and amino acid pairs,' *Phys. Chem. Chem. Phys* **8**, 1985–1993. 94

Kaczmarek, A., Sadlej, A. J. and Leszczynski, J. (2004) 'Monomer basis-set truncation effects in calculations of interaction energies: A model study,' *J. Chem. Phys.* **120**, 7837–7848. 89

Kaczmarek, A., Sadlej, A. J. and Leszczynski, J. (2006) 'First-order interaction energies and basis set truncation effects,' *Molec. Phys.* **104**, 395–407. 89

Kato, T. (1957) 'On the eigenfunctions of many-particle systems in quantum mechanics,' *Commun. pure appl. math.* **10**, 151–177. 77

Kazantsev, A. V., Karamertzanis, P. G., Adjiman, C. S. and Pantelides, C. C. (2011*a*) 'Efficient handling of molecular flexibility in lattice energy minimization of organic crystals,' *J. Chem. Theory Comput.* **7**, 1998–2016. 225

Kazantsev, A. V., Karamertzanis, P. G., Adjiman, C. S., Pantelides, C. C., Price, S. L., Galek, P. T. A., Day, G. M. and Cruz-Cabeza, A. J. (2011*b*) 'Successful prediction of a model pharmaceutical in the fifth blind test of crystal structure prediction,' *Int. J. Pharm.* **418**, 168–178. 225

Keller, J. B. and Zumino, B. (1959) 'Determination of intermolecular potentials from thermodynamic data and the law of corresponding states,' *J. Chem. Phys.* **30**, 1351–1353. 245

Kendrick, J., Leusen, F. J. J., Neumann, M. A. and van de Streek, J. (2011) 'Progress in crystal structure prediction,' *Chem. Eur. J* **17**, 10735–10743. 265

Khaliullin, R. Z., Cobar, E. A., Lochan, R. C., Bell, A. T. and Head-Gordon, M. (2007) 'Unravelling the origin of intermolecular interactions using absolutely localized molecular orbitals,' *J. Phys. Chem.* **111**, 8753–8765. 99, 152

Kihara, T. (1978) *Intermolecular Forces*, Wiley. 209

Kim, H.-Y., Sofod, J. O., Velegol, D., Cole, M. W. and Lucas, A. A. (2006) 'Van der Waals forces between nanoclusters: importance of many-body effects,' *J. Chem. Phys.* **124**, 074504. 190

Kim, Y. S., Kim, S. K. and Lee, W. D. (1981) 'Dependence of the closed-shell repulsive interaction on the overlap of the electron densities,' *Chem. Phys. Lett.* **80**, 574–575. 216

King, B. F. and Weinhold, F. (1995) 'Structure and spectroscopy of $(HCN)_n$ clusters: cooperative and electronic delocalization effects in C–H···N hydrogen bonding,' *J. Chem. Phys.* **103**, 333–347. 108

Kita, S., Noda, K. and Inouye, H. (1976) 'Repulsion potentials for Cl^-–R and Br^-–R (R = He, Ne and Ar) derived from beam experiments,' *J. Chem. Phys.* **64**, 3446–3449. 216

Kitaura, K., Ikeo, E., Asada, T., Nakano, T. and Uebayasi, M. (1999) 'Fragment molecular orbital method: an approximate computational method for large molecules,' *Chem. Phys. Lett.* **313**, 701–708. 219

Kitaura, K. and Morokuma, K. (1976) 'A new energy decomposition scheme for molecular interactions within the Hartree–Fock approximation,' *Int. J. Quantum Chem.* **10**, 325–340. 97

Kittel, C. (1987) *Quantum theory of solids*, Wiley, New York & Chichester. 196

Klopman, G. (1968) 'Chemical reactivity and the concept of charge- and frontier-controlled reactions,' *J. Amer. Chem. Soc.* **90**, 223–234. 153

Klopman, G. and Hudson, R. F. (1967) 'Polyelectronic perturbation theory of chemical reactivity,' *Theor. Chim. Acta* **8**, 165 174. 153

Klopper, W. and Lüthi, H. P. (1999) 'The MP2 limit correction applied to coupled cluster calculations of the electronic dissociation energies of the hydrogen fluoride and water dimers,' *Molec. Phys.* **96**, 559–570. 83

Klopper, W., Manby, F. R., Ten-no, S. and Valeev, E. F. (2006) 'R12 methods in explicitly correlated molecular electronic structure theory,' *Int. Rev. Phys. Chem.* **25**, 427. 77

Klopper, W., van Duijneveldt-van de Rijdt, J. G. C. M. and van Duijneveldt, F. B. (2000) 'Computational determination of equilibrium geometry and dissociation energy of the water dimer,' *Phys. Chem. Chem. Phys* **2**, 2227–2234. 91, 229

Knizia, G., Adler, T. B. and Werner, H.-J. (2009) 'Simplified CCSD(T)-F12 methods: Theory and benchmarks,' *J. Chem. Phys.* **130**, 054104. 77

Knowles, P. J. and Meath, W. J. (1986*a*) 'Non-expanded dispersion and induction energies, and damping functions, for molecular interactions, with application to HF···He,' *Molec. Phys.* **59**, 965–984. 149, 207

Knowles, P. J. and Meath, W. J. (1986*b*) 'Non-expanded dispersion energies and damping functions for Ar_2 and Li_2,' *Chem. Phys. Lett.* **124**, 164–171. 149, 207

Knowles, P. J. and Meath, W. J. (1987) 'A separable method for the calculation of dispersion and induction energy damping functions with applications to the dimers arising from He, Ne and HF,' *Molec. Phys.* **60**, 1143–1158. 149, 207

Koch, U., Popelier, P. L. A. and Stone, A. J. (1995) 'Conformational dependence of atomic multipole moments,' *Chem. Phys. Lett.* **238**, 253–260. 224

Koch, W. and Holthausen, M. C. (2000) *A Chemist's Guide to Density Functional Theory*, Wiley-VCH Verlag GmbH, Weinheim. 78

Kochanski, E. and Gouyet, J. F. (1975*a*) '*Ab initio* calculation of the first order term of the intermolecular energy near the Van der Waals minimum,' *Theor. Chim. Acta* **39**, 329–337. 108

Kochanski, E. and Gouyet, J. F. (1975*b*) '*Ab initio* studies of the intermolecular interactions between two hydrogen molecules near the Van der Waals minimum from a perturbation procedure using biorthogonal orbitals,' *Molec. Phys.* **29**, 693–701. 108

Kohn, W. and Sham, L. J. (1965) 'Self-consistent equations including exchange and correlation effects,' *Phys. Rev.* **140**, A1133–A1138. 78

Koide, A., Meath, W. J. and Allnatt, A. R. (1981) 'Second-order charge overlap effects and damping functions for isotropic atomic and molecular interactions,' *Chem. Phys.* **58**, 105–119. 206, 207

Kołos, W. and Wolniewicz, L. (1974) 'Variational calculations of the long-range interaction between two ground state hydrogen atoms,' *Chem. Phys. Lett.* **24**, 457–460. 205

Korona, T., Hesselmann, A. and Dodziuk, H. (2009) 'Symmetry-adapted perturbation theory applied to endohedral fullerene complexes: A stability study of $H_2@C_{60}$ and $2H_2@C_{60}$,' *J. Chem. Theory Comput.* **5**, 1585–1596. 121

Korona, T., Williams, H. L., Bukowski, R., Jeziorski, B. and Szalewicz, K. (1997) 'Helium dimer potential from symmetry-adapted perturbation theory calculations using large gaussian geminal and orbital basis sets,' *J. Chem. Phys.* **106**, 5109–5122. 110

Kreek, H. and Meath, W. J. (1969) 'Charge-overlap effects. Dispersion and induction forces,' *J. Chem. Phys.* **50**, 2289–2302. 148, 205

Kuharsky, R. A. and Rossky, P. J. (1985) 'A quantum mechanical study of structure in liquid H_2O and D_2O,' *J. Chem. Phys.* **82**, 5164–5177. 229

Kumar, A. and Meath, W. J. (1984) 'Pseudo-spectral dipole oscillator-strength distributions for SO_2, CS_2 and OCS and values of some related dipole–dipole and triple-dipole dispersion energy constants,' *Chem. Phys.* **91**, 411–418. 188

Kumar, A. and Meath, W. J. (1985) 'Pseudo-spectral dipole oscillator strengths and dipole–dipole and triple-dipole dispersion energy coefficients for HF, HCl, HBr, He, Ne, Ar, Kr and Xe,' *Molec. Phys.* **54**, 823–833. 188

Kumar, A. and Meath, W. J. (1992) 'Dipole oscillator strength properties and dispersion energies for acetylene and benzene,' *Molec. Phys.* **75**, 311–324. 244

Kumar, A. and Meath, W. J. (1994) 'Reliable isotropic and anisotropic dipole properties, and dipolar dispersion energy coefficients, for CO evaluated using constrained dipole oscillator strength techniques,' *Chem. Phys.* **189**, 467–477. 244

Kumar, A., Meath, W. J., Bundgen, P. and Thakkar, A. J. (1996) 'Reliable anisotropic dipole properties, and dispersion energy coefficients, for O_2 evaluated using constrained dipole oscillator strength techniques,' *J. Chem. Phys.* **105**, 4927–4937. 244

Kumar, A. and Thakkar, A. J. (2010) 'Dipole oscillator strength distributions with improved high-energy behavior: Dipole sum rules and dispersion coefficients for Ne, Ar, Kr, and Xe revisited,' *Canad. J. Chem.* **132**, 074301. 243, 244

Kutzelnigg, W. (1980) 'The 'primitive' wavefunction in the theory of intermolecular interactions,' *J. Chem. Phys.* **73**, 343–359. 113

Kutzelnigg, W. (1985) 'r_{12}-dependent terms in the wave function as closed sums of partial wave amplitudes for large L,' *Theor. Chim. Acta* **68**, 445. 77

Kutzelnigg, W. (1992) 'Does the polarization approximation converge for large r to a primitive or a symmetry-adapted function?' *Chem. Phys. Lett.* **195**, 77–84. 105

Kvasnicka, V., Laurinc, H. and Hubac, I. (1974) 'Many-body perturbation theory of intermolecular interactions,' *Phys. Rev. A* **10**, 2016–2026. 107

Lange, O. L. D. and Raab, R. E. (2006) 'On the theory of the Buckingham effect,' *Molec. Phys.* **104**, 607–611. 42

Langreth, D. C., Lundqvist, B. I., Chakarova-Kack, S. D., Cooper, V. R., Dion, M., Hyldgaard, P., Kelkkanen, A., Kleis, J., Kong, L., Li, S., Moses, P. G., Murray, E., Puzder, A., Rydberg, H., Schroder, E. and Thonhauser, T. (2009) 'A density functional for sparse matter,' *J. Phys. Condens. Matter* **21**, 084203. 93

Le, H.-A. and Bettens, R. P. A. (2011) 'Distributed multipoles and energies of flexible molecules,' *J. Chem. Theory Comput.* **7**, 921–930. 224

Le Fèvre, R. J. W. (1965) 'Molecular polarizability and refractivity,' *Adv. Phys. Org. Chem.* **3**, 1–90. 160

Le Roy, R. J. and Van Kranendonk, J. (1974) 'Anisotropic intermolecular potentials from an analysis of spectra of H_2– and D_2–inert-gas complexes,' *J. Chem. Phys.* **61**, 4750–4769. 253

Le Sueur, C. R. and Stone, A. J. (1993) 'Practical schemes for distributed polarizabilities,' *Molec. Phys.* **78**, 1267–1291. 170

Le Sueur, C. R. and Stone, A. J. (1994) 'Localization methods for distributed polarizabilities,' *Molec. Phys.* **83**, 293–308. 173

Le Sueur, C. R., Stone, A. J. and Fowler, P. W. (1991) 'Induced dipole moments in acetylene complexes,' *J. Phys. Chem.* **95**, 3519–3522. 170

Leavitt, R. P. (1980) 'An irreducible tensor method of deriving the long-range anisotropic interactions between molecules of arbitrary symmetry,' *J. Chem. Phys.* **72**, 3472–3482. 46

Leforestier, C. (1994) 'Grid method for the Wigner functions. Application to the Van der Waals system Ar–H_2O,' *J. Chem. Phys.* **101**, 7357–7363. 257

Leforestier, C., van Harrevelt, R. and van der Avoird, A. (2009) 'Vibration–rotation–tunneling levels of the water dimer from an *ab initio* potential surface with flexible monomers,' *J. Phys. Chem. A* . 228, 257

Legon, A. C. (2010) 'The halogen bond: an interim perspective,' *Phys. Chem. Chem. Phys* **12**, 7736–7747. 157

Legon, A. C. and Millen, D. J. (1982) 'Determination of properties of hydrogen-bonded dimers by rotational spectroscopy and a classification of dimer geometries,' *Faraday Disc. Chem. Soc.* **73**, 71–87, 127, 128. 153

Legon, A. C., Millen, D. J. and Mjöberg, P. J. (1977) 'The hydrogen cyanide dimer: Identification and structure from microwave spectroscopy,' *Chem. Phys. Lett.* **47**, 589–591. 52

Leighton, P., Cowan, J. A., Abraham, R. J. and Sanders, J. K. M. (1988) 'Geometry of porphyrin–porphyrin interactions,' *J. Org. Chem.* **53**, 733–740. 198

Leslie, M. (1983) 'A symmetry-adapted method for the determination of the lattice energy and properties of ionic crystals,' *Solid State Ionics* **8**, 243–246. 209

Leslie, M. (2008) 'DL_MULTI—a molecular dynamics program to use distributed multipole electrostatic models to simulate the dynamics of organic crystals,' *Molec. Phys.* **106**, 1567–1578. 51, 230, 266

Li, G., Parr, J., Fedorov, I. and Reisler, H. (2006) 'Imaging study of vibrational predissociation of the HCl–acetylene dimer: pair-correlated distributions,' *Phys. Chem. Chem. Phys* **8**, 2915–2924. 249

Light, J. C. and Carrington, T., Jr (2000) 'Discrete-variable representations and their utilization,' *Advances in Chem. Phys.* **114**, 263–310. 256, 257

Lighthill, M. J. (1958) *Fourier Analysis and Generalized Functions*, Cambridge University Press, Cambridge. 20

Lii, J.-H. and Allinger, N. L. (1991) 'The MM3 force field for amides, polypeptides and proteins,' *J. Comput. Chem.* **12**, 186–199. 221

Lillestolen, T. C. and Wheatley, R. (2008) 'Redefining the atom: atomic charge densities produced by an iterative stockholder approach,' *Chem. Comm.* **2008**, 5909–5911. 129

Lillestolen, T. C. and Wheatley, R. (2009) 'Atomic charge densities generated using an iterative stockholder approach,' *J. Chem. Phys.* **131**, 144101. 129

Lillestolen, T. C. and Wheatley, R. J. (2007) 'First-principles calculation of local atomic polarizabilities,' *J. Phys. Chem. A* **111**, 11141–11146. 174

Linder, B. (1962) 'Generalized form for dispersion interaction,' *J. Chem. Phys.* **37**, 963–966. 67

Lindorff-Larsen, K., Maragakis, P., Piana, S., Eastwood, M. P., Dror, R. O. and Shaw, D. E. (2012) 'Systematic validation of protein force fields against experimental data,' *PLoS ONE* **7**, e32131. 223

Lommerse, J. P. M., Motherwell, W. D. S., Ammon, H. L., Dunitz, J. D., Gavezzotti, A., Hofmann, D. W. M., Leusen, F. J. J., Mooij, W. T. M., Price, S. L., Schweizer, B., Schmidt, M. U., van Eijck, B. P., Verwer, P. and Williams, D. E. (2000) 'A test of crystal structure prediction of small organic molecules,' *Acta Cryst. B* **56**, 697–714. 266

London, F. (1930*a*) 'Über einige Eigenschaften und Anwendungen der Molekularkräfte,' *Z. Physik. Chem. B* **11**, 222–251. 64, 65

London, F. (1930*b*) 'Zur Theorie und Systematik der Molekularkräfte,' *Z. Phys.* **63**, 245–279. 57

London, F. (1937) 'The general theory of molecular forces,' *Trans. Faraday Soc.* **33**, 8–26. 57, 64

Longuet-Higgins, H. C. (1956) 'The electronic states of composite systems,' *Proc. Roy. Soc. A* **235**, 537–543. 57, 58

Longuet-Higgins, H. C. (1965) 'Intermolecular forces,' *Disc. Faraday Soc.* **40**, 7–18. 27

Loudon, R. (1973) *The Quantum Theory of Light*, Clarendon Press, Oxford. 33

Löwdin, P.-O. (1950) 'On the non-orthogonality problem connected with the use of atomic wavefunctions in the theory of molecules and crystals,' *J. Chem. Phys.* **18**, 365–375. 107

Lu, L. and Voth, G. A. (2011) 'The multiscale coarse-graining method. VII. Free energy decomposition of coarse-grained effective potentials,' *J. Chem. Phys.* **134**, 224107. 229

Magnasco, V. and Figari, G. (1986) 'Epstein–Nesbet calculation of interatomic interactions in the Van der Waals region,' *Molec. Phys.* **59**, 689–705. 109

Mahoney, M. W. and Jorgensen, W. L. (2000) 'A five-site model for liquid water and the reproduction of the density anomaly by rigid, nonpolarizable potential functions,' *J. Chem. Phys.* **112**, 8910–8922. 226

Maitland, G. C., Rigby, M., Smith, E. B. and Wakeham, W. A. (1981) *Intermolecular Forces: their origin and determination*, Clarendon Press, Oxford. 203, 204, 246, 247

Manolopoulos, D. E. (1988) 'Close coupled equations,' Ph.D. thesis, Cambridge University. 255

Mantina, M., Chamberlin, A. C., Valero, R., Cramer, C. J. and Truhlar, D. G. (2009) 'Consistent Van der Waals radii for the whole main group,' *J. Phys. Chem. A* **113**, 5806–5812. 202

Margenau, H. (1939) 'Van der Waals forces,' *Rev. Mod. Phys.* **11**, 1–35. 57

Margoliash, D. J., Proctor, T. R., Zeiss, G. D. and Meath, W. J. (1978) 'Triple-dipole energies for H, He, Li, N, O. H_2, N_2, O_2, NO, N_2O, H_2O, NH_3 and CH_4 evaluated using pseudo-spectral dipole oscillator strength distributions.' *Molec. Phys.* **35**, 747–757. 189

Markland, T. E. and Manolopoulos, D. E. (2008*a*) 'An efficient ring polymer contraction scheme for imaginary time path integral simulations,' *J. Chem. Phys.* **129**, 024105. 249

Markland, T. E. and Manolopoulos, D. E. (2008*b*) 'A refined ring polymer contraction scheme for systems with electrostatic interactions,' *Chem. Phys. Lett.* **464**, 256–261. 249

Maroulis, G. (2003) 'Accurate electric multipole moment, static polarizability and hyperpolarizability derivatives for N_2,' *J. Chem. Phys.* **118**, 2673–2687. 124

Marx, D. and Hutter, J. (2009) *Ab initio molecular dynamics: basic theory and advanced methods*, Cambridge University Press. 249

Mas, E. M., Bukowski, R., Szalewicz, K., Groenenboom, G. C., Groenenboom, G. C., Wormer, P. E. S. and van der Avoird, A. (2000) 'Water pair potential of near spectroscopic accuracy. I. Vibration–rotation–tunneling levels of the water dimer,' *J. Chem. Phys.* **113**, 6687–6701. 228

Mason, E. A. (1957) 'Scattering of low-velocity molecular beams in gases,' *J. Chem. Phys.* **26**, 667–677. 261

Matsuoka, O., Clementi, E. and Yoshimine, M. (1976) 'Configuration interaction study of the water dimer potential surface,' *J. Chem. Phys.* **64**, 1351–1367. 226

Mavroyannis, C. and Stephen, M. J. (1962) 'Dispersion forces,' *Molec. Phys.* **5**, 629–638. 67, 68

Mayer, I. and Surjan, P. R. (1993) 'Handling overlap as a perturbation,' *Croatica Chem. Acta* **66**, 161–165. 107

McClellan, A. L. (1963) *Tables of Experimental Dipole Moments*, vol. 1, Freeman. 14, 240

McClellan, A. L. (1974) *Tables of Experimental Dipole Moments*, vol. 2, Rahara Enterprises, El Cerrito. 14, 240

McClellan, A. L. (1989) *Tables of Experimental Dipole Moments*, vol. 3, Rahara Enterprises, El Cerrito. 14, 240

McDowell, S. A. C., Le Sueur, C. R., Buckingham, A. D. and Stone, A. J. (1992) 'Using monomer properties to obtain integrated intensities for vibrational transitions of Van der Waals complexes,' *Molec. Phys.* **77**, 823–835. 157

McGurk, J., Norris, C. L., Tigelaar, H. L. and Flygare, W. H. (1973) 'Molecular magnetic properties of FCl,' *J. Chem. Phys.* **58**, 3118–3120. 241

McIlroy, A., Lascola, R., Lovejoy, C. M. and Nesbitt, D. J. (1991) 'Structural dependence of HF vibrational red shifts in Ar_nHF, n = 1–4, via high-resolution slit jet infrared spectroscopy,' *J. Phys. Chem.* **95**, 2636–2644. 252

McIlroy, A. and Nesbitt, D. J. (1992) 'Intermolecular motion in Ar_nHF micromatrices,' *J. Chem. Phys.* **97**, 6044–6056. 252

McKellar, A. R. W. (1994) 'Long-path equilibrium IR spectra of weakly bound complexes at low temperatures,' *Faraday Disc.* **97**, 69–80. 252

McLachlan, A. D. (1963) 'Retarded dispersion forces between molecules,' *Proc. Roy. Soc. A* **271**, 387–401. 67

McQuarrie, D. A. (1976) *Statistical Mechanics*, Harper & Row, New York. 245, 247

McWeeny, R. (1984) 'Weak interactions between molecules,' *Croatica Chem. Acta* **57**, 865–878. 180

McWeeny, R. (1989) *Methods of Molecular Quantum Mechanics*, Academic Press, London, 2nd edn. 280

Meath, W. J. and Aziz, R. A. (1984) 'On the importance and problems in the construction of many-body potentials.' *Molec. Phys.* **52**, 225–243. 190

Meath, W. J. and Koulis, M. (1991) 'On the construction and use of reliable two-body and many-body interatomic and intermolecular potentials,' *Theochem. (J. Mol. Struct.)* **72**, 1–37. 93, 190, 207

Meath, W. J. and Kumar, A. (1990) 'Reliable isotropic and anisotropic dipole dispersion energies, evaluated using constrained dipole oscillator strength techniques, with application to interactions involving H_2, N_2, and the rare gases,' *Int. J. Quantum Chem.* **38, issue S24**, 501–520. 244

Meath, W. J., Margoliash, D. J., Jhanwar, B. L., Koide, A. and Zeiss, G. D. (1981) 'Accurate molecular properties, their additivity, and their use in constructing intermolecular potentials,' in *Intermolecular forces*, ed. B. Pullman, 101–115, Reidel, Dordrecht. 243

Meerts, W. L., de Leeuw, F. H. and Dymanus, A. (1977) 'Electric and magnetic properties of carbon monoxide by molecular-beam electric-resonance spectroscopy,' *Chem. Phys.* **22**, 319–324. 133

Miller, K. J. (1990) 'Additivity methods in molecular polarizability,' *J. Amer. Chem. Soc.* **112**, 8533–8542. 160

Millot, C., Soetens, J.-C., Martins Costa, M. T. C., Hodges, M. P. and Stone, A. J. (1998) 'Revised anisotropic site potentials for the water dimer, and calculated properties,' *J. Phys. Chem. A* **102**, 754–770. 183, 228

Millot, C. and Stone, A. J. (1992) 'Towards an accurate intermolecular potential for water,' *Molec. Phys.* **77**, 439–462. 156, 213, 227, 259

Milonni, P. W. and Eberly, J. H. (1988) *Lasers*, Wiley, New York. 197

Mirsky, K. (1978) 'The determination of the intermolecular interaction energy by empirical methods,' in *Computing in Crystallography*, eds. R. Schenk, R. Olthof-Hazenkamp, H. van Koningsveld and G. C. Bassi, 169–182, Delft University Press. 211

Misquitta, A. J., Jeziorski, B. and Szalewicz, K. (2003) 'Dispersion energy from density-functional theory description of monomers,' *Phys. Rev. Lett.* **91**, 33201. 117, 119

Misquitta, A. J., Jeziorski, B. and Szalewicz, K. (2005*a*) 'Dispersion energy from density-functional theory description of monomers,' *Phys. Rev. Lett.* **91**, 033201. 86

Misquitta, A. J., Podeszwa, R., Jeziorski, B. and Szalewicz, K. (2005*b*) 'Intermolecular potentials based on symmetry-adapted perturbation theory with dispersion energies from time-dependent density-functional calculations,' *J. Chem. Phys.* **123**, 214103. 86

Misquitta, A. J., Spencer, J., Stone, A. J. and Alavi, A. (2010) 'Dispersion interactions between semiconducting wires,' *Phys. Rev. B* **82**, 075312. 181

Misquitta, A. J. and Stone, A. J. (2008) 'Accurate induction energies for small organic molecules: 1. Theory,' *J. Chem. Theory Comput.* **4**, 7–18. 116, 175, 180

Misquitta, A. J. and Stone, A. J. (2012) '*Ab initio* atom–atom potentials using CamCASP: pyridine,' in preparation. See also www-stone.ch.cam.ac.uk/programs/camcasp.html. 175, 217, 219

Misquitta, A. J., Stone, A. J. and Price, S. L. (2008*a*) 'Accurate induction energies for small organic molecules. 2. Development and testing of distributed polarizability models against sapt(dft) energies,' *J. Chem. Theory Comput.* **4**, 19–32. 175, 176

Misquitta, A. J. and Szalewicz, K. (2002) 'Intermolecular forces from asymptotically corrected density functional description of monomers,' *Chem. Phys. Lett.* **357**, 301–306. 119, 120

Misquitta, A. J. and Szalewicz, K. (2005) 'Symmetry-adapted perturbation-theory calculations of intermolecular forces employing density-functional description of monomers,' *J. Chem. Phys.* **122**, 214109. 119

Misquitta, A. J., Welch, G. W. A., Stone, A. J. and Price, S. L. (2008*b*) 'A first principles prediction of the crystal structure of $C_6Br_2ClFH_2$,' *Chem. Phys. Lett.* **456**, 105–109. 219

Momany, F. A. (1978) 'Determination of partial atomic charge from *ab initio* molecular electrostatic potentials. Application to formamide, methanol and formic acid,' *J. Phys. Chem.* **82**, 592. 138

Morgan, J. D., III and Simon, B. (1980) 'Behaviour of molecular potential energy curves for large molecular separation,' *Int. J. Quantum Chem.* **17**, 1143–1166. 106

Morokuma, K. (1971) 'Molecular orbital studies of hydrogen bonds. III. C=O···H–O hydrogen bond in $H_2CO{\cdots}H_2O$ and $H_2CO{\cdots}2H_2O$,' *J. Chem. Phys.* **55**, 1236–1244. 97

Morokuma, K. and Kitaura, K. (1981) 'Energy decomposition analysis of molecular interactions,' in *Chemical Applications of Atomic and Molecular Eletrostatic Potentials*, eds. P. Politzer and D. G. Truhlar, 215–242, Plenum Press, New York. 97

Moszynski, R., Heijmen, T. G. A. and Jeziorski, B. (1996) 'Symmetry-adapted perturbation theory for the calculation of Hartree–Fock interaction energies,' *Molecular Phys.* **88**, 741–758. 116

Moszynski, R., Wormer, P. E. S., Heijmen, T. G. A. and van der Avoird, A. (1998) 'Symmetry-adapted perturbation theory of non-additive three-body interactions in Van der Waals molecules. II. Application to the $Ar_2{\cdots}HF$ interaction,' *J. Chem. Phys.* **108**, 579–589. 121

Moszynski, R., Wormer, P. E. S., Jeziorski, B. and van der Avoird, A. (1995*a*) 'Symmetry-adapted perturbation theory of non-additive three-body interactions in Van der Waals molecules. I. General theory,' *J. Chem. Phys.* **103**, 8058–8074. 121

Moszynski, R., Wormer, P. E. S. and Van der Avoird, A. (1995*b*) '*Ab initio* potential-energy surface and near infrared spectrum of the He–C_2H_2 complex,' *J. Chem. Phys.* **102**, 8385–8397. 119

Motherwell, W. D. S., Ammon, H. L., Dunitz, J. D., Dzyabchenko, A., Erk, P., Gavezzotti, A., Hofmann, D. W. M., Leusen, F. J. J., Lommerse, J. P. M., Mooij, W. T. M., Price, S. L., Scheraga, H. A., Schweizer, B., Schmidt, M. U., van Eijck, B. P., Verwer, P. and Williams, D. E. (2002) 'Crystal structure prediction of small organic molecules: a second blind test,' *Acta Cryst. B* **58**, 647–661. 266

Muenter, J. S. (1989) 'Radio-frequency and microwave spectroscopy of the HCCH–CO_2 and DCCD–CO_2 Van der Waals complexes,' *J. Chem. Phys.* **90**, 4048–4053. 54

Mulliken, R. S. (1952) 'Molecular compounds and their spectra,' *J. Amer. Chem. Soc.* **74**, 811–824. 150

Munro, L. J. and Wales, D. J. (1999) 'Defect migration in crystalline silicon,' *Phys. Rev. B* **59**, 3969–3980. 229

Murray, C. W., Handy, N. C. and Laming, G. J. (1993) 'Quadrature schemes for integrals of density functional theory,' *Molec. Phys.* **78**, 997–1014. 81, 128

Murrell, J. N. and Bosanac, S. D. (1989) *Introduction to the Theory of Atomic and Molecular Collisions*, Wiley. 260, 262

Murrell, J. N. and Laidler, K. J. (1968) 'Symmetries of activated complexes,' *Trans. Faraday Soc.* **64**, 371–377. 7

Murrell, J. N. and Shaw, G. (1967) 'Intermolecular forces in the region of small orbital overlap,' *J. Chem. Phys.* **46**, 1768–1772. 111

Murthy, C. S., O'Shea, S. F. and McDonald, I. R. (1983) 'Electrostatic interactions in molecular crystals: lattice dynamics of solid nitrogen and carbon dioxide,' *Molec. Phys.* **50**, 531–541. 138

Musher, I. J. and Amos, A. T. (1967) 'Theory of weak atomic and molecular interactions,' *Phys. Rev.* **164**, 31–43. 111

Muto, Y. (1943) *Proc. Phys.-Math. Soc. Japan* **17**, 629–631. 188

Neiss, C. and Hättig, C. (2007) 'Frequency-dependent nonlinear optical properties with explicitly correlated coupled-cluster response theory using the CCSD(R12) model,' *J. Chem. Phys.* **126**, 154101. 77

Nelson, D. D., Fraser, G. T. and Klemperer, W. (1985) 'Ammonia dimer – a surprising structure,' *J. Chem. Phys.* **83**, 6201–6208. 251

Némethy, G., Pottle, M. S. and Scheraga, H. A. (1983) 'Energy parameters in polypeptides. 9. Updating of geometrical parameters, nonbonded interactions and hydrogen-bond interactions for the naturally occurring amino acids,' *J. Phys. Chem.* **87**, 1883–1887. 221

Nesbitt, D. J. (1994) 'Probing potential energy surfaces *via* high-resolution IR laser spectroscopy,' *Faraday Discuss. Chem. Soc.* **97**, 1–18. 252

Nesbitt, D. J. and Child, M. S. (1993) 'Rotational RKR inversion of intermolecular stretching potentials: extension to linear hydrogen-bonded complexes,' *J. Chem. Phys.* **98**, 478–486. 252

Nesbitt, D. J., Child, M. S. and Clary, D. C. (1989) 'Rydberg–Klein–Rees inversion of high-resolution Van der Waals infrared spectra: an intermolecular potential energy surface for Ar···HF (v = 1),' *J. Chem. Phys.* **90**, 4855–4864. 252

Neumann, M. A. and Perrin, M.-A. (2005) 'Energy ranking of molecular crystals using density functional theory calculations and an empirical Van der Waals correction,' *J. Phys. Chem. B* **109**, 3181–3183. 94

Nevins, N., Chen, K. and Allinger, N. L. (1996) 'Molecular mechanics (MM4) calculations on alkenes,' *J. Comput. Chem.* **17**, 669–694. 221

Ng, K.-C., Meath, W. J. and Allnatt, A. R. (1979) 'A reliable semi-empirical approach for evaluating the isotropic intermolecular forces between closed-shell systems,' *Molec. Phys.* **37**, 237–253. 207

Novick, S. E., Janda, K. C. and Klemperer, W. (1976) 'HF–ClF: structure and bonding,' *J. Chem. Phys.* **65**, 5115–5121. 155

Novoa, J. J., Planas, M. and Whangbo, M.-H. (1994) 'A numerical evaluation of the counterpoise method on hydrogen bond complexes using near complete basis sets,' *Chem. Phys. Lett.* **225**, 240–246. 90

Nyburg, S. C. and Faerman, C. H. (1985) 'A revision of Van der Waals radii for molecular crystals: N, O, F, S, Cl, Se, Br and I bonded to carbon,' *Acta Cryst. B: Struct. Sci.* **B41**, 274–279. 212

Oganov, A. R., ed. (2011) *Modern Methods of Crystal Structure Prediction*, Wiley-VCH, Weinheim. 265, 322

Ogilvie, J. F. (1988) 'The electric dipole moment function of HF,' *J. Phys. B* **21**, 1663–1671. 134

Ohashi, N. and Pine, A. S. (1984) 'High resolution spectrum of the HCl dimer,' *J. Chem. Phys.* **81**, 73–84. 55

Ohshima, Y., Masumoto, Y., Takami, M. and Kuchitsu, K. (1988) 'The structure and tunneling motion of acetylene dimer studied by free-jet infrared absorption spectroscopy in the 14 μm region,' *Chem. Phys. Lett.* **147**, 1–6. 53

Olsen, J., Christiansen, O., Koch, H. and Jorgensen, P. (1996) 'Surprising cases of divergent behavior in Møller–Plesset perturbation-theory,' *J. Chem. Phys.* **105**, 5082–5090. 77

Olthof, E. H. T., van der Avoird, A. and Wormer, P. E. S. (1994) 'Structure, internal mobility, and spectrum of the ammonia dimer: calculation of the vibration–rotation–tunneling states,' *J. Chem. Phys.* **101**, 8430–8442. 251, 256

Onuchic, J. N., Luthey-Schulten, Z. and Wolynes, P. G. (1997) 'Theory of protein folding: the energy landscape perspective,' *Ann. Rev. Phys. Chem.* **48**, 545–600. 7

Pack, R. T. (1978) 'Anisotropic potentials and the damping of rainbow and diffraction oscillations in differential cross-sections,' *Chem. Phys. Lett.* **55**, 197–201. 210

Pack, R. T., Piper, E., Pfeffer, G. A. and Toennies, J. P. (1984) 'Multiproperty empirical anisotropic intermolecular potentials. II. He···SF_6 and Ne···SF_6,' *J. Chem. Phys.* **80**, 4940–4950. 210

Pack, R. T., Valentini, J. J. and Cross, J. D. (1982) 'Multiproperty empirical anisotropic intermolecular potentials. I. Ar···SF_6 and Kr···SF_6,' *J. Chem. Phys.* **77**, 5486–5499. 210

Patel, A. J., Varilly, P., Jamadagni, S. N., Acharya, H., Garde, S. and Chandler, D. (2011) 'Extended surfaces modulate hydrophobic interactions of neighboring solutes,' *Proc. Nat. Acad. Sci. (US)* **108**, 17678–17683. 193

Patkowski, K., Jeziorski, B. and Szalewicz, K. (2001*a*) 'Symmetry-adapted perturbation theory with regularized Coulomb potential,' *J. Mol. Struct. (TheoChem)* **547**, 293–307. 114, 115

Patkowski, K., Jeziorski, B. and Szalewicz, K. (2004) 'Unified treatment of chemical and Van der Waals forces via symmetry-adapted perturbation expansion,' *J. Chem. Phys.* **120**, 6849–6862. 114

Patkowski, K., Korona, T. and Jeziorski, B. (2001*b*) 'Convergence behavior of the symmetry-adapted perturbation theory for states submerged in Pauli forbidden continuum,' *J. Chem. Phys.* **115**, 1137–1152. 113

Patkowski, K., Murdachaew, G., Fou, C.-M. and Szalewicz, K. (2005) 'Accurate *ab initio* potential for argon dimer including the highly repulsive region,' *Molec. Phys.* **103**, 2031–2045. 77

Pauling, L. (1928) 'The shared-electron chemical bond,' *Proc. Nat. Acad. Sci.* **14**, 359–362. 153

Pauling, L. (1960) *The Nature of the Chemical Bond*, Cornell University Press, 3rd edn. 154, 202

PCCP (2009) 'Coarse-grained modeling of soft condensed matter,' *Phys. Chem. Chem. Phys* **11**, 1855–2125, (special issue). 229

Peet, A. C. and Yang, W. (1989) 'An adapted form of the collocation method for calculating energy levels of rotating atom–diatom complexes,' *J. Chem. Phys.* **91**, 6598–6603. 257

Perdew, J. P., Burke, K. and Ernzerhof, M. (1996) 'Generalized gradient approximation made simple,' *Phys. Rev. Lett.* **77**, 3865–3868, also see erratum, *Phys. Rev. Lett.* **78**, 1396 (1996). 79

Perdew, J. P., Parr, R. G., Levy, M. and Balduz, J. L., Jr. (1982) 'Density-functional theory for fractional particle number: derivative discontinuities of the energy,' *Phys. Rev. Lett.* **49**, 1691–1694. 79

Pérez, C., Muckle, M. T., Zaleski, D. P., Seifert, N. A., Temelso, B., Shields, G. C., Kisiel, Z. and Pate, B. H. (2012) 'Structures of cage, prism, and book isomers of water hexamer from broadband rotational spectroscopy,' *Science* **336**, 897–901. 251

Pérez-Jordá, J. M. and Becke, A. D. (1995) 'A density-functional study of Van der Waals forces: rare gas diatomics,' *Chem. Phys. Lett.* **233**, 134–137. 92

Pertsin, A. J. and Kitaigorodsky, A. I. (1987) *The atom–atom potential method: applications to organic molecular solids*, vol. 43 of *Springer series in chemical physics*, Springer-Verlag, Berlin, New York. 265

Petersilka, M., Gossmann, U. J. and Gross, E. K. U. (1996) 'Excitation energies from time-dependent density-functional theory,' *Phys. Rev. Lett.* **76**, 1212–1215. 85

Peterson, K. A. and Dunning, T. H. (1995) 'Benchmark calculations with correlated molecular wave functions. VII. Binding energy and structure of the HF dimer,' *J. Chem. Phys.* **102**, 2032–2041. 6

Piana, S., Lindorff-Larsen, K. and Shaw, D. E. (2011) 'How robust are protein folding simulations with respect to force field parameterization?' *Biophys. J.* **100**, L47–L49. 223

Pimentel, G. C. and McClellan, A. L. (1960) *The Hydrogen Bond*, W. H. Freeman, San Francisco. 153

Piquemal, J.-P., Chevreau, H. and Gresh, N. (2007) 'Toward a separate reproduction of the contributions to the Hartree–Fock and DFT intermolecular interaction energies by polarizable molecular mechanics with the SIBFA potential,' *J. Chem. Theory Comput.* **3**, 824–837. 219

Piquemal, J.-P., Cisneros, G. A., Reinhardt, P., Gresh, N. and Darden, T. A. (2006) 'Towards a force field based on density fitting,' *J. Chem. Phys.* **124**, 104101. 145

Piquemal, J.-P., Gresh, N. and Giessner-Prettre, C. (2003) 'Improved formulas for the calculation of the electrostatic contribution to the intermolecular interaction energy from multipolar expansion of the electronic distribution,' *J. Phys. Chem.* **107**, 10353–10359. 145

Pitzer, K. S. (1959) 'Inter- and intramolecular forces and molecular polarizabilities,' *Adv. Chem. Phys.* **2**, 59–83. 68

Podeszwa, R. and Szalewicz, K. (2007) 'Three-body symmetry-adapted perturbation theory based on Kohn–Sham description of the monomers,' *J. Chem. Phys.* **126**, 194101. 121, 189

Poll, J. D. and Hunt, J. L. (1981) 'Analysis of the far infrared spectrum of gaseous N_2,' *Canad. J. Phys.* **59**, 1448–1458. 124

Ponder, J. W. (2009) 'TINKER – software tools for molecular design,' Tech. rep., http://dasher.wustl.edu/tinker/. 223, 230

Ponder, J. W. and Case, D. A. (2003) 'Force fields for protein simulations,' in *Protein Simulations*, vol. 66 of *Advances in Protein Chemistry*, 27. 221, 223

Ponder, J. W., Wu, C., Ren, P., Pande, V. S., Chodera, J. D., Schnieders, M. J., Haque, I., Mobley, D. L., Lambrecht, D. S., DiStasio, R. A., Jr., Head-Gordon, M., Clark, G. N. I., Johnson, M. E. and Head-Gordon, T. (2010) 'Current status of the AMOEBA polarizable force field,' *J. Phys. Chem. B* **114**, 2549–2564. 223

Popelier, P. L. A. (2000) *Atoms in Molecules: an Introduction*, Prentice-Hall, Harlow, UK. 129

Popelier, P. L. A. and Stone, A. J. (1994) 'Formulae for the first and second derivatives of anisotropic potentials with respect to geometrical parameters,' *Molec. Phys.* **82**, 411–425, Erratum, Molec. Phys. (1995) **84**, 811. 235

Pople, J. A., Schneider, W. G. and Bernstein, H. J. (1959) *High-Resolution Nuclear Magnetic Resonance*, McGraw-Hill, New York. 157

Price, S. L. (2009) 'Computational prediction of organic crystal structures and polymorphism,' *Int. Rev. Phys. Chem.* **27**, 541–568. 265

Price, S. L., Leslie, M., Welch, G. W. A., Habgood, M., Price, L. S., Karamertzanis, P. G. and Day, G. M. (2010) 'Modelling organic crystal structures using distributed multipole and polarizability-based model intermolecular potentials,' *Phys. Chem. Chem. Phys* **12**, 8478–8490. 265

Price, S. L. and Stone, A. J. (1980) 'Evaluation of anisotropic model intermolecular pair potentials using an *ab initio* SCF-CI surface,' *Molec. Phys.* **40**, 805–822. 212

Price, S. L. and Stone, A. J. (1982) 'The anisotropy of the $Cl_2 \cdots Cl_2$ pair potential as shown by the crystal structure—evidence for intermolecular bonding or lone-pair effects?' *Molec. Phys.* **47**, 1457–1470. 212, 213

Price, S. L. and Stone, A. J. (1983) 'A distributed multipole analysis of the charge densities of the azabenzene molecules,' *Chem. Phys. Lett.* **98**, 419–423. 134

Price, S. L. and Stone, A. J. (1984) 'A six-site intermolecular potential scheme for the azabenzene molecules, derived by crystal structure analysis,' *Molec. Phys.* **51**, 569–583. 134

Price, S. L. and Stone, A. J. (1987) 'The electrostatic interactions in Van der Waals complexes involving aromatic molecules,' *J. Chem. Phys.* **86**, 2859–2868. 154

Price, S. L., Stone, A. J. and Alderton, M. (1984) 'Explicit formulae for the electrostatic energy, forces and torques between a pair of molecules of arbitrary symmetry,' *Molec. Phys.* **52**, 987–1001. 50

Prichard, J. S., Nandi, R. N., Muenter, J. S. and Howard, B. J. (1988) 'Vibration–rotation spectrum of the carbon-dioxide acetylene Van der Waals complex in the 3μ region,' *J. Chem. Phys.* **89**, 1245–1250. 54

Pu, M., Garrahan, J. P. and Hirst, J. D. (2011) 'Comparison of implicit solvent models and force fields in molecular dynamics simulations of the PB1 domain,' *Chem. Phys. Lett.* **515**, 283–289. 223

Pusztai, L., Pizio, O. and Sokolowski, S. (2008) 'Comparison of interaction potentials of liquid water with respect to their consistency with neutron diffraction data of pure heavy water,' *J. Chem. Phys.* **129**, 184103. 264

Rauk, A., Allen, L. C. and Clementi, E. (1970) 'Electronic structure and inversion barrier of ammonia,' *J. Chem. Phys.* **52**, 4133–4144. 88

Reed, A. E., Curtiss, L. A. and Weinhold, F. (1988) 'Intermolecular interactions from a natural bond orbital, donor–acceptor viewpoint,' *Chem. Rev.* **88**, 899–926. 108, 156

Reed, A. E., Weinhold, F., Curtiss, L. A. and Pochatko, D. J. (1986) 'Natural bond orbital analysis of molecular interactions: theoretical studies of binary complexes of HF, H_2O, NH_3, N_2, O_2, F_2, CO and CO_2 with HF, H_2O and NH_3,' *J. Chem. Phys.* **84**, 5687–5705. 107, 108

Reimers, J. R., Watts, R. O. and Klein, M. L. (1982) 'Intermolecular potential functions and the properties of water,' *Chem. Phys.* **64**, 95–114. 226, 227

Rein, R. (1973) 'Physical properties and interactions of polyatomic molecules: with applications to molecular recognition in biology,' *Adv. Quantum Chem.* **7**, 335–396. 124

Ren, P. and Ponder, J. W. (2002) 'Consistent treatment of inter- and intramolecular polarization in molecular mechanics calculations,' *J. Comput. Chem.* **23**, 1497–1506. 223

Ren, P. and Ponder, J. W. (2003) 'Polarizable atomic multipole water model for molecular mechanics simulation,' *J. Phys. Chem. B* **107**, 5933–5947. 51, 223

Reynolds, C. A., Essex, J. W. and Richards, W. G. (1992*a*) 'Atomic charges for variable molecular-conformations,' *J. Amer. Chem. Soc.* **114**, 9075–9079. 224

Reynolds, C. A., Essex, J. W. and Richards, W. G. (1992*b*) 'Errors in free energy perturbation calculations due to neglecting the conformational variation of atomic charges,' *Chem. Phys. Letters* **199**, 257–260. 224

Rezus, Y. L. and Bakker, H. J. (2007) 'Observation of immobilized water molecules around hydrophobic groups,' *Phys. Rev. Lett.* **99**, 148301. 193

Richardson, J. O. and Althorpe, S. C. (2009) 'Ring-polymer molecular dynamics rate-theory in the deep-tunneling regime: connection with semiclassical instanton theory,' *J. Chem. Phys.* **131**, 214106 . 260

Richardson, J. O. and Althorpe, S. C. (2011) 'Ring-polymer instanton method for calculating tunneling splittings,' *J. Chem. Phys.* **134**, 054109. 260

Richardson, J. O., Althorpe, S. C. and Wales, D. J. (2011) 'Instanton calculations of tunneling splittings for water dimer and trimer,' *J. Chem. Phys.* **135**, 124109. 260

Richardson, J. O., Althorpe, S. C. and Wales, D. J. (2012) in preparation. 260

Rijks, W. and Wormer, P. E. S. (1989) 'Correlated Van der Waals coefficients. II. Dimers consisting of CO, HF, H_2O and NH_3,' *J. Chem. Phys.* **90**, 6507–6519, Note Erratum below, correcting many of the tabulated values. 68, 227

Rijks, W. and Wormer, P. E. S. (1990) 'Erratum: Correlated Van der Waals coefficients. II. Dimers consisting of CO, HF, H_2O and NH_3,' *J. Chem. Phys.* **92**, 5754. 228

Rob, F., Podeszwa, R. and Szalewicz, K. (2007) 'Electrostatic interaction energies with overlap effects from a localized approach,' *Chem. Phys. Lett.* **445**, 315–320. 145

Rocher-Casterline, B. E., Ch'ng, L. C., Mollner, A. K. and Reisler, H. (2011) 'Determination of the bond dissociation energy (D_0) of the water dimer, $(H_2O)_2$, by velocity map imaging,' *J. Chem. Phys.* **134**, 211101. 228, 249, 250

Rodger, P. M., Stone, A. J. and Tildesley, D. J. (1987) 'Atomic anisotropy and the structure of liquid chlorine,' *J. Chem. Soc. Faraday Trans. II* **83**, 1689–1702. 248

Rodger, P. M., Stone, A. J. and Tildesley, D. J. (1988*a*) 'The intermolecular potential of chlorine—a three-phase study,' *Molec. Phys.* **63**, 173–188. 212, 213

Rodger, P. M., Stone, A. J. and Tildesley, D. J. (1988*b*) 'Intermolecular interactions in halogens: bromine and iodine,' *Chem. Phys. Lett.* **145**, 365–370. 212, 213

Roterman, I. K., Gibson, K. D. and Scheraga, H. A. (1989*a*) 'A comparison of the CHARMm, AMBER and ECEPP potentials for peptides. 1. Conformational predictions for the tandemly repeated peptide $(Asn–Ala–Asn–Pro)_9$,' *J. Biomol. Struct. Dyn.* **7**, 391–419. 138, 223

Roterman, I. K., Lambert, M. H., Gibson, K. D. and Scheraga, H. A. (1989*b*) 'A comparison of the CHARMm, AMBER and ECEPP potentials for peptides. 2. Phi-psi maps for normal-acetyl alanine N′-methyl amide—comparisons, contrasts and simple experimental tests,' *J. Biomol. Struct. Dyn.* **7**, 421–453. 138, 223

Rowlinson, J. S. (1949) 'The second virial coefficient of polar gases,' *Trans. Faraday Soc.* **45**, 974. 225

Rowlinson, J. S. (1951) 'The lattice energy of ice and the second virial coefficient of water vapour,' *Trans. Faraday Soc.* **47**, 120. 226

Rybak, S., Jeziorski, B. and Szalewicz, K. (1991) 'Many-body symmetry-adapted perturbation theory of intermolecular interactions—H_2O and HF dimers,' *J. Chem. Phys.* **95**, 6576–6601. 113

Sadlej, A. J. (1988) 'Medium-size polarized basis sets for high-level correlated calculations of molecular electric properties,' *Coll. Czech Chem. Commun.* **53**, 1995–2016. 87

Sadlej, A. J. (1991) 'Medium-sized polarized basis sets for high-level correlated calculations of molecular electric properties. II. Second-row atoms Si–Cl,' *Theor. Chim. Acta* **79**, 123–140. 87

Salem, L. (1968) 'Intermolecular orbital theory of the interaction between conjugated systems. I. General theory,' *J. Amer. Chem. Soc.* **90**, 543–552. 153

Sandorfy, C. (1976) *Anharmonicity and Hydrogen Bonding*, North-Holland, Amsterdam, 613–654. 157

Saykally, R. J. and Blake, G. A. (1993) 'Molecular interactions and hydrogen-bond tunneling dynamics—some new perspectives,' *Science* **259**, 1570–1575. 250

Saykally, R. J. and Wales, D. J. (2012) 'Pinning down the water hexamer,' *Science* **336**, 814–815. 251

Schäffer, R. and Jansen, G. (2012) 'Intermolecular exchange-induction energies without overlap expansion,' *Theor. Chim. Acta* submitted. 110

Schmuttenmaer, C. A., Cohen, R. C. and Saykally, R. J. (1994) 'Spectroscopic determination of the intermolecular potential energy surface for Ar···NH_3,' *J. Chem. Phys.* **101**, 146–173. 250

Schnieders, M. J., Fenn, T. D., Pande, V. S. and Brunger, A. T. (2009) 'Polarizable atomic multipole X-ray refinement: application to peptide crystals,' *Acta Cryst D* **65**, 952–965. 241

Schwenke, D. W. and Truhlar, D. G. (1985) 'Systematic study of basis set superposition errors in the calculated interaction energy of two HF molecules,' *J. Chem. Phys.* **82**, 2418–2426. 90

Shank, A., Wang, Y., Kaledin, A., Braams, B. J. and Bowman, J. M. (2009) 'Accurate *ab initio* and "hybrid" potential energy surfaces, intramolecular vibrational energies, and classical IR spectrum of the water dimer,' *J. Chem. Phys.* **130**, 144314. 228, 259

Shaw, D. E. *et al.* (2008) 'Anton, a special-purpose machine for molecular dynamics simulation,' *Comm. ACM* **51**, 91–97. 248

Sherrill, C. D., Sumpter, B. G., Sinnokrot, M. O., Marshall, M. S., Hohenstein, E. G., Walker, R. C. and Gould, I. R. (2009) 'Assessment of standard force field models against high-quality *ab initio* potential curves for prototypes of π–π, CH–π, and SH–π interactions,' *J. Comput. Chem.* **30**, 2187–2193. 223

Sholl, D. and Steckel, J. A. (2009) *Density Functional Theory: A Practical Introduction*, Wiley, New Jersey. 78

Sikora, P. T. (1970) 'Combining rules for spherically symmetrical intermolecular potentials,' *J. Phys. B* **3**, 1475–1482. 215

Silberstein, L. (1917) 'Molecular refractivity and atomic interaction,' *Phil. Mag.* **33**, 92–128. 61, 161

Simon, S., Duran, M. and Dannenberg, J. J. (1996) 'How does basis set superposition error change the potential surfaces for hydrogen-bonded dimers?' *J. Chem. Phys.* **105**, 11024. 91

Singh, U. C. and Kollman, P. A. (1984) 'An approach to computing electrostatic charges for molecules,' *J. Comput. Chem.* **5**, 129–145. 138

Sippl, M., Némethy, G. and Scheraga, H. A. (1984) 'Intermolecular potentials from crystal data. 6. Determination of empirical potentials for OH···O=C hydrogen bond from packing considerations,' *J. Phys. Chem.* **88**, 6231–6233. 221

Slater, J. C. (1951) 'A simplification of the Hartree–Fock method,' *Phys. Rev.* **81**, 385–390. 94

Slater, J. C. and Kirkwood, J. G. (1931) 'The Van der Waals forces in gases,' *Phys. Rev.* **37**, 682–697. 68

Slipchenko, L. V. and Gordon, M. S. (2006) 'Electrostatic energy in the effective fragment potential method: Theory and application to benzene dimer,' *J. Comput. Chem.* **28**, 276–291. 145

Smith, W. (1982*a*) 'Point multipoles in the Ewald summation,' *CCP5 Quarterly* **4**, 13–25. 266

Smith, W. (1982*b*) 'The program MDMULP,' Tech. rep., Daresbury Laboratory. 266

Smith, W., Leslie, M. and Forester, T. R. (2003) 'The DL–POLY–2 user manual,' Tech. rep., CCLRC, Daresbury Laboratory, Warrington WA4 4AD, UK. 51

Söderhjelm, P., Kongsted, J. and Ryde, U. (2011) 'Conformational dependence of isotropic polarizabilities,' *J. Chem. Theory Comput.* **7**, 1404–1414. 224

Söderhjelm, P. and Ryde, U. (2009) 'How accurate can a force field become? A polarizable multipole model combined with fragment-wise quantum-mechanical calculations,' *J. Phys. Chem. A* **113**, 617–627. 223

Sokalski, W. A., Hariharan, P. C. and Kaufman, J. J. (1983*a*) 'A self-consistent field interaction energy decomposition study of twelve hydrogen-bonded dimers,' *J. Phys. Chem.* **87**, 2803–2810. 98

Sokalski, W. A. and Poirier, R. A. (1983) 'Cumulative atomic multipole representation of the molecular charge distribution and its basis set dependence,' *Chem. Phys. Lett.* **98**, 86–92. 124, 126

Sokalski, W. A., Roszak, S., Hariharan, P. C. and Kaufman, J. J. (1983*b*) 'Improved SCF interaction energy decomposition scheme corrected for basis set superposition effect,' *Int. J. Quantum Chem.* **23**, 847–854. 98

Sokalski, W. A. and Sawaryn, A. (1992) 'Cumulative multicenter multipole moment databases and their applications,' *J. Mol. Struct.* **256**, 91–112. 139

Solheim, H., Ruud, K. and Åstrand, P.-O. (2004) 'Atomic dipole moments calculated using analytical molecular second-moment gradients,' *J. Chem. Phys.* **120**, 10368–10378. 137

Spackman, M. A. (1992) 'Molecular electric moments from X-ray diffraction data,' *Chemical Reviews* **92**, 1769–1797. 136, 241

Spackman, M. A. (2006) 'The use of the promolecular charge density to approximate the penetration contribution to intermolecular electrostatic energies,' *Chem. Phys. Lett.* **418**, 158–162. 145

Spackman, M. A. and Jayatilaka, D. (2009) 'Hirshfeld surface analysis,' *CrystEngComm* **11**, 19–32. 241

Spackman, M. A., Munshi, P. and Dittrich, B. (2007) 'Dipole moment enhancement in molecular crystals from X-ray diffraction data,' *ChemPhysChem* **8**, 2051–2063. 241

Sprik, M. (1991) 'Hydrogen bonding and the static dielectric constant in liquid water,' *J. Chem. Phys.* **95**, 6762–6769. 227

Sprik, M. and Klein, M. L. (1988) 'A polarizable model for water using distributed charge sites,' *J. Chem. Phys.* **89**, 7556–7560. 209, 227

Steinmann, C., Fedorov, D. G. and Jensen, J. H. (2010) 'Effective fragment molecular orbital method: A merger of the effective fragment potential and fragment molecular orbital methods,' *J. Phys. Chem. A* **114**, 8705–8712. 219

Stephens, P. J., Devlin, J. F., Chabalowski, C. F. and Frisch, M. J. (1994) '*Ab Initio* calculation of vibrational absorption and circular dichroism spectra using density functional force fields,' *J. Phys. Chem.* **98**, 11623–11627. 79

Stephens, S. L., Walker, N. R. and Legon, A. C. (2011) 'Internal rotation and halogen bonds in $CF_3I\cdots NH_3$ and $CF_3I\cdots N(CH_3)_3$ probed by broadband rotational spectroscopy,' *Phys. Chem. Chem. Phys* **13**, 20736–20744. 250

Stevens, R. M., Pitzer, R. and Lipscomb, W. N. (1963) 'Perturbed Hartree–Fock calculations. I. Magnetic susceptibility and shielding in the HF molecule,' *J. Chem. Phys.* **38**, 550–560. 85, 170

Stewart, J. J. P. (1989) 'Optimization of parameters for semi-empirical methods. I. Method. II. Applications,' *J. Comput. Chem.* 209–264. 95

Stillinger, F. H. and Rahman, A. (1974) 'Improved simulation of liquid water by molecular dynamics,' *J. Chem. Phys.* **60**, 1545. 226

Stogryn, D. E. (1971) 'Higher order interaction energies for systems of asymmetric molecules,' *Molec. Phys.* **22**, 81–103. 189

Stone, A. J. (1978*a*) 'The description of bimolecular potentials, forces and torques: the S and V function expansions,' *Molec. Phys.* **36**, 241–256. 70

Stone, A. J. (1978*b*) 'Theories of organic reactions,' *Chem. Soc. Spec. Periodical Rep. Theor. Chem.* **3**, 39–69. 153

Stone, A. J. (1979) 'Intermolecular forces,' in *The Molecular Physics of Liquid Crystals*, eds. G. R. Luckhurst and G. W. Gray, 31–50, Academic Press. 212

Stone, A. J. (1981) 'Distributed multipole analysis; or how to describe a molecular charge distribution,' *Chem. Phys. Lett.* **83**, 233–239. 124

Stone, A. J. (1985) 'Distributed polarizabilities,' *Molec. Phys.* **56**, 1065–1082. 27, 166

Stone, A. J. (1991) 'Classical electrostatics in molecular interactions,' in *Theoretical Models of Chemical Bonding, vol. 4*, ed. Z. B. Maksić, 103–131, Springer-Verlag. 50, 291

Stone, A. J. (1993) 'Computation of charge-transfer energies by perturbation theory,' *Chem. Phys. Lett.* **211**, 101–109. 151, 152, 153, 156

Stone, A. J. (2005) 'Distributed multipole analysis: Stability for large basis sets,' *J. Chem. Theory Comput.* **1**, 1128–1132. 127, 219

Stone, A. J. (2011) 'Electrostatic damping functions and the penetration energy,' *J. Phys. Chem. A* **115**, 7017–7027. 144

Stone, A. J. and Alderton, M. (1985) 'Distributed multipole analysis—methods and applications,' *Molec. Phys.* **56**, 1047–1064. 123, 124, 127, 129

Stone, A. J. and Erskine, R. W. (1980) 'Intermolecular self-consistent-field perturbation theory for organic reactions. I. Theory and implementation; nucleophilic attack on carbonyl compounds,' *J. Amer. Chem. Soc.* **102**, 7185–7192. 107

Stone, A. J., Hättig, C., Jansen, G. and Ángyán, J. G. (1996) 'Transferability of topologically partitioned polarizabilities: the case of *n*-alkanes,' *Molec. Phys.* **89**, 595–605. 173

Stone, A. J. and Misquitta, A. J. (2009) 'Charge transfer in symmetry-adapted perturbation theory,' *Chem. Phys. Lett.* **473**, 201–205. 151, 152

Stone, A. J. and Tong, C.-S. (1989) 'Local and non-local dispersion models,' *Chem. Phys.* **137**, 121–135. 179, 180

Stone, A. J. and Tong, C.-S. (1994) 'Anisotropy of atom–atom repulsions,' *J. Comput. Chem.* **15**, 1377–1392. 215, 216

Stone, A. J. and Tough, R. J. A. (1984) 'Spherical tensor theory of long-range intermolecular forces,' *Chem. Phys. Lett.* **110**, 123–129. 72

Storer, J. W., Giesen, D. J., Cramer, C. J. and Truhlar, D. G. (1995) 'Class IV charge models: a new semiempirical approach in quantum chemistry,' *J. Comp.-Aided Molec. Design* **9**, 87–110. 136

Stouch, T. R. (2012) 'The errors of our ways: taking account of error in computer-aided drug design to build confidence intervals for our next 25 years,' *J. Comput. Aided Mol. Des.* **26**, 125–134. 223

Strodel, B. and Wales, D. J. (2008) 'Implicit solvent models and the energy landscape for aggregation of the amyloidogenic KFFE peptide,' *Phys. Chem. Chem. Phys* **4**, 657–672. 225

Strømsheim, M. D., Kumar, N., Coriani, S., Sagvolden, E., Teale, A. M. and Helgaker, T. (2011) 'Dispersion interactions in density-functional theory: An adiabatic-connection analysis,' *J. Chem. Phys.* **135**, 194109. 93

Suhm, M. A. and Watts, R. O. (1991) 'Quantum Monte-Carlo studies of vibrational states in molecules and clusters,' *Phys. Reports* **204**, 293–329. 258, 259

Surjan, P. R. and Mayer, I. (1991) 'Intermolecular interactions: biorthogonal perturbation theory revisited,' *Theochem* **72**, 47–58. 108

Surjan, P. R., Mayer, I. and Lukovits, I. (1985) 'Second-quantization-based perturbation theory for intermolecular interactions without basis set superposition error,' *Chem. Phys. Lett.* **119**, 538–542. 108

Surjan, P. R. and Poirier, R. A. (1986) 'Intermolecular interactions using small basis sets: perturbation theory calculations avoiding basis set superposition error,' *Chem. Phys. Lett.* **128**, 358–362. 108

Svensson, M., Humbel, S., Froese, R. D. J., Matsubara, T., Sieber, S. and Morokuma, K. (1996) 'ONIOM: A multilayered integrated MO + MM method for geometry optimizations and single point energy predictions. a test for Diels–Alder reactions and $Pt(P(t\text{-}Bu)_3)_2+H_2$ oxidative addition,' *J. Phys. Chem.* **100**, 19357–19363. 220

Szabo, A. and Ostlund, N. S. (1989) *Modern Quantum Chemistry*, McGraw-Hill. 74

Szalewicz, K. (2012) 'Symmetry-adapted perturbation theory of intermolecular forces,' *WIREs Comp. Molec. Sci.* **2**, 254–272. 117

Szalewicz, K., Cole, S. J., Kołos, W. and Bartlett, R. J. (1988) 'A theoretical study of the water dimer interaction,' *J. Chem. Phys.* **89**, 3662–3673. 90, 91

Szalewicz, K., Leforestier, C. and van der Avoird, A. (2009) 'Towards the complete understanding of water by a first-principles computational approach,' *Chem. Phys. Lett.* **482**, 1–14. 227

Szalewicz, K., Patkowski, K. and Jeziorski, B. (2005) 'Intermolecular interactions via perturbation theory: from diatoms to biomolecules,' in *Intermolecular Forces and Clusters II*, ed. D. J. Wales, vol. 116 of *Structure and Bonding*, 43–117. 106

Tang, K. T. (1969) 'Dynamic polarizabilities and Van der Waals coefficients,' *Phys. Rev.* **177**, 108–114. 68, 188

Tang, K. T. and Toennies, J. P. (1978) 'A simple model of the Van der Waals potential at intermediate distances. II. Anisotropic potential of $He\cdots H_2$ and $Ne\cdots H_2$,' *J. Chem. Phys.* **68**, 5501–5517. 73

Tang, K. T. and Toennies, J. P. (1984) 'An improved simple model for the Van der Waals potential based on universal damping functions for the dispersion coefficients,' *J. Chem. Phys.* **80**, 3726–3741. 206

Tekin, A. and Jansen, G. (2007) 'How accurate is density functional theory combined with symmetry-adapted perturbation theory approach for ch–π and π–πp interactions? a comparison to supermolecular calculations for the acetylene–benzene dimer,' *Phys. Chem. Chem. Phys* **9**, 1680–1687. 121

Temelso, B., Archer, K. A. and Shields, G. C. (2011) 'Benchmark structures and binding energies of small water clusters with anharmonicity corrections,' *J. Phys. Chem. A* **115**, 12034–12046. 185

Thakkar, A. J. (1988) 'Higher dispersion coefficients: accurate values for the hydrogen atom and simple estimates for other systems,' *J. Chem. Phys.* **89**, 2092–2098. 73

Thakkar, A. J., Hettema, H. and Wormer, P. E. S. (1992) '*Ab initio* dispersion coefficients for interactions involving rare-gas atoms,' *J. Chem. Phys.* **97**, 3252–3264. 68

Thole, B. T. (1981) 'Molecular polarizabilities calculated with a modified dipole interaction,' *Chem. Phys.* **59**, 341–350. 164

Thomas, G. F. and Meath, W. J. (1977) 'Dipole spectrum, sums and properties of ground-state methane and their relation to the molar refractivity and dispersion energy constant,' *Molec. Phys.* **34**, 113–125. 159

Thompson, K. C., Jordan, M. J. T. and Collins, M. A. (1998) 'Polyatomic molecular potential energy surfaces by interpolation in local internal coordinates,' *J. Chem. Phys.* **108**, 8302–8315. 96, 224

Thornley, A. E. and Hutson, J. M. (1992) 'The intermolecular potential of Ar–acetylene. Information from infrared and microwave spectroscopy,' *Chem. Phys. Lett.* **198**, 1–8. 263

Tinkham, M. (1964) *Group Theory and Quantum Mechanics*, McGraw-Hill, New York. 34

Tkatchenko, A., DiStasio, R. A., Jr., Head-Gordon, M. and Scheffler, M. (2009) 'Dispersion-corrected Møller–Plesset second-order perturbation theory,' *J. Chem. Phys.* **131**, 094106. 93

Tough, R. J. A. and Stone, A. J. (1977) 'Properties of the regular and irregular solid harmonics,' *J. Phys. A* **10**, 1261–1269. 19, 45

Townes, C. H., Dousmanis, G. C., White, R. L. and Schwarz, R. F. (1955) 'Connections between molecular structure and certain magnetic effects in molecules,' *Disc. Faraday Soc.* **19**, 56–64. 15, 241

Tozer, D. J. and Handy, N. C. (1998*a*) 'The development of new exchange-correlation functionals,' *J. Chem. Phys.* **108**, 2545–2555. 79

Tozer, D. J. and Handy, N. C. (1998*b*) 'Improving virtual Kohn–Sham orbitals and eigenvalues: Application to excitation energies and static polarizabilities,' *J. Chem. Phys.* **109**, 10180–10189. 79

Tsuzuki, S. and Lüthi, H. P. (2001) 'Interaction energies of Van der Waals and hydrogen bonded systems calculated using density functional theory: assessing the PW91 model,' *J. Chem. Phys.* **114**, 3949–3957. 92

Unsöld, A. (1927) 'Quantentheorie des Wasserstoffmolekülions und der Born–Landéschen Abstossunskräfte,' *Z. Physik.* **43**, 563–574. 65

Valiev, M., Bylaska, E. J., Govind, N., Kowalski, K., Straatsma, T. P., van Dam, H. J. J., Wang, D., Nieplocha, J., Apra, E., Windus, T. L. and de Jong, W. A. (2010) 'NWChem: a comprehensive and scalable open-source solution for large scale molecular simulations,' *Comp. Phys. Comm.* **181**, 14771489. 91

Van Bladel, J. W. I., Van der Avoird, A., Wormer, P. E. S. and Saykally, R. J. (1992) 'Computational exploration of the six-dimensional vibration–rotation–tunnelling dynamics of $(NH_3)_2$,' *J. Chem. Phys.* **97**, 4750–4763. 256

Van Caillie, C. and Amos, R. D. (1998) 'Static and dynamic polarisabilities, Cauchy coefficients and their anisotropies: a comparison of standard methods,' *Chem. Phys. Lett.* **291**, 71–77. 68

Van Caillie, C. and Amos, R. D. (2000) 'Static and dynamic polarisabilities, Cauchy coefficients and their anisotropies: an evaluation of DFT functionals,' *Chem. Phys. Lett.* **328**, 446–452. 68

Van de Streek, J., Neumann, M. A. and Perrin, M.-A. (2010) 'Energy ranking of molecular crystals using density functional theory calculations and an empirical Van der Waals correction,' *CrystEngComm* **12**, 3827–3833. 94

Van der Avoird, A. (1967*a*) 'Intermolecular interactions by perturbation theory including exchange effects,' *Chem. Phys. Lett.* **1**, 24–27. 110

Van der Avoird, A. (1967*b*) 'Note on a perturbation theory for intermolecular interactions in the wave operator formalism,' *Chem. Phys. Lett.* **1**, 411–412. 110

Van der Avoird, A. (1967*c*) 'A perturbation theory for intermolecular interactions in the wave-operator formalism,' *J. Chem. Phys.* **47**, 3649–3653. 110

Van der Avoird, A., Olthof, E. H. T. and Wormer, P. E. S. (1994) 'Is the $NH_3 \cdots NH_3$ riddle solved?' *Faraday Discussions* **97**, 43–55. 251

van Duijneveldt, F. B., van Duijneveldt-van de Rijdt, J. G. C. M. and van Lenthe, J. H. (1994) 'State of the art in counterpoise theory,' *Chem. Rev.* **94**, 1873–1885. 89, 90

van Eijck, B. P. (2001) '*Ab initio* crystal structure predictions for flexible hydrogen-bonded molecules. Part III. Effect of lattice vibrations,' *J. Comput. Chem.* **22**, 816–826. 266

van Eijck, B. P., Mooij, W. T. M. and Kroon, J. (2001) '*Ab initio* crystal structure predictions for flexible hydrogen-bonded molecules. Part II. Accurate energy minimization,' *J. Comput. Chem.* **22**, 805–815. 266

van Gisbergen, S. J. A., Schipper, P. R. T., Gritsenko, O. V., Baerends, E. J., Snijders, J. G., Champagne, B. and Kirtman, B. (1999) 'Electric field dependence of the exchange–correlation potential in molecular chains,' *Phys. Rev. Lett.* **83**, 694–697. 68

van Hemert, M. C., Wormer, P. E. S. and van der Avoird, A. (1983) '*Ab initio* calculation of the Heisenberg exchange interaction between O_2 molecules,' *Phys. Rev. Lett.* **51**, 1167–1170. 200

VandeVondele, J., Krack, M., Mohamed, F., Parrinello, M., Chassaing, T. and Hutter, J. (2005) 'Quickstep: Fast and accurate density functional calculations using a mixed Gaussian and plane waves approach,' *Comp. Phys. Comm.* **167**, 103–128. 82

Varshalovich, D. A., Moskalev, A. N. and Khersonskii, V. K. (1988) *Quantum Theory of Angular Momentum*, World Scientific, Singapore. 275

Vigné-Maeder, F. and Claverie, P. (1988) 'The exact multicentre multipolar part of a molecular charge distribution and its simplified representations,' *J. Chem. Phys.* **88**, 4934–4948. 123, 124

Voisin, C. and Cartier, A. (1993) 'Determination of distributed polarizabilities to be used for peptide modelling,' *Theochem (J. Mol. Struct.)* **105**, 35–45. 165

Volkov, A., King, H. F. and Coppens, P. (2006) 'Dependence of the intermolecular electrostatic interaction energy on the level of theory and the basis set,' *J. Chem. Theory Comput.* **2**, 81–89. 145

Volkov, A., Koritsanszky, T. and Coppens, P. (2004) 'Combination of the exact potential and multipole methods (EP/MM) for evaluation of intermolecular electrostatic interaction energies with pseudoatom representation of molecular electron densities,' *Chem. Phys. Lett.* **391**, 170–175. 145

Vydrov, O. A. and Van Voorhis, T. (2010*a*) 'Dispersion interactions from a local polarizability model,' *Phys. Rev. A* **81**, 062708. 93

Vydrov, O. A. and Van Voorhis, T. (2010*b*) 'Nonlocal Van der Waals density functional: the simpler the better,' *J. Chem. Phys.* **133**, 244103. 93

Waldman, M. and Hagler, A. T. (1993) 'New combining rules for rare gas Van der Waals parameters,' *J. Comput. Chem.* **14**, 1077–1084. 203

Wales, D. J. (1991) 'Theoretical study of some small Van der Waals complexes containing inert gas atoms,' *Molec. Phys.* **74**, 1–25. 229, 236

Wales, D. J. (2003) *Energy Landscapes*, Cambridge University Press, Cambridge. 251

Wales, D. J. (2004) *Energy Landscapes: Applications to Clusters, Biomolecules and Glasses*, Cambridge University Press, Cambridge, England. 7

Wales, D. J. (2011) 'Energy landscapes and structure prediction using basin-hopping,' in (Oganov 2011), 29–54. 265

Wang, J., Cieplak, P., Li, J., Hou, T., Luo, R. and Duan, Y. (2011) 'Development of polarizable models for molecular mechanical calculations. I. Parameterization of atomic polarizability,' *J. Phys. Chem. B* **115**, 3091–3099. 165

Wang, J., Wolf, R. M., Caldwell, J. W., Kollman, P. A. and Case, D. A. (2004) 'Development and testing of a general Amber force field,' *J. Comput. Chem.* **25**, 1157–1174. 221

Wang, Y., Shepler, B. C., Braams, B. J. and Bowman, J. M. (2009) 'Full-dimensional, *ab initio* potential energy and dipole moment surfaces for water,' *J. Chem. Phys.* **131**, 054511. 228, 260

Warshel, A. and Parson, W. W. (1987) 'Spectroscopic properties of photosynthetic reaction centres,' *J. Amer. Chem. Soc.* **109**, 6143–6163. 198

Watanabe, A. and Welsh, H. L. (1964) 'Direct spectroscopic evidence of bound states of $(H_2)_2$ complexes at low temperature,' *Phys. Rev. Lett.* **13**, 810–812. 252

Watson, M. A., Sałek, P., Macak, P. and Helgaker, T. (2004) 'Linear-scaling formation of the Kohn–Sham Hamiltonian: application to the calculation of excitation energies and polarizabilities of large molecular systems,' *J. Chem. Phys.* **121**, 2915–2931. 80

Weiner, S. J., Kollman, P. A., Case, D. A., Singh, U. C., Ghio, C., Alagona, G., Profeta, S. and Weiner, P. (1984) 'A new force field for molecular mechanical simulation of nucleic acids and proteins,' *J. Amer. Chem. Soc.* **106**, 765–784. 221

Weiner, S. J., Kollman, P. A., Nguyen, D. T. and Case, D. A. (1986) 'An all atom force field for simulations of proteins and nucleic acids,' *J. Comput. Chem.* **7**, 230–252. 221

Welch, G. W. A., Karamertzanis, P. G., Misquitta, A. J., Stone, A. J. and Price, S. L. (2008) 'Is the induction energy important for modelling organic crystals?' *J. Chem. Theory Comput.* **4**, 522–532. 218

Wells, A. F. (1975) *Structural Inorganic Chemistry*, Clarendon Press, Oxford, 4th edn. 185, 186

Wells, B. H. (1985) 'The differential Green's function Monte Carlo method. The dipole moment of LiH,' *Chem. Phys. Lett.* **115**, 89–94. 259

Wells, B. H. and Wilson, S. (1986) 'Van der Waals interaction potentials: many-body effects in rare gas mixtures,' *Molec. Phys.* **57**, 421–426. 190

Wells, B. H. and Wilson, S. (1989*a*) 'Van der Waals interaction potentials. Many-body effects in Ne_4,' *Molec. Phys.* **66**, 457–464. 190

Wells, B. H. and Wilson, S. (1989*b*) 'Van der Waals potentials: convergence of the many-body expansion,' *Molec. Phys.* **65**, 1363–1376. 190

Werner, H.-J. and Meyer, W. (1976) 'PNO–CI and PNO–CEPA studies of electron correlation effects. V. Static dipole polarizabilities of small molecules,' *Molec. Phys.* **31**, 855–872. 86

Wheatley, R. J. (1993*a*) 'Gaussian multipole functions for describing molecular charge distributions,' *Molec. Phys.* **79**, 597–610. 142

Wheatley, R. J. (1993*b*) 'A new distributed multipole procedure for linear molecules,' *Chem. Phys. Lett.* **208**, 159–166. 128

Wheatley, R. J. and Lillestolen, T. C. (2007) 'Calculating intermolecular potentials with SIMPER: the water–nitrogen and water–oxygen interactions, dispersion energy coefficients, and preliminary results for larger molecules,' *Int. Rev. Phys. Chem.* **26**, 449–485. 219

Wheatley, R. J. and Lillestolen, T. C. (2009) 'Calculating intermolecular potentials with SIMPER: the water–nitrogen and water–oxygen interactions, dispersion energy coefficients, and preliminary results for larger molecules,' *Int. Rev. Phys. Chem.* **26**, 449–485. 246

Wheatley, R. J. and Meath, W. J. (1993*a*) 'Dispersion energy damping functions, and their relative scale with interatomic separation, for (H, He, Li)–(H, He, Li) interactions,' *Molec. Phys.* **80**, 25–54. 207

Wheatley, R. J. and Meath, W. J. (1993*b*) 'On the relationship between first-order exchange and Coulomb interaction energies for closed shell atoms and molecules,' *Molec. Phys.* **79**, 253–275. 214

Wheatley, R. J. and Price, S. L. (1990*a*) 'An overlap model for estimating the anisotropy of repulsion,' *Molec. Phys.* **69**, 507–533. 216, 217

Wheatley, R. J. and Price, S. L. (1990*b*) 'A systematic intermolecular potential method applied to chlorine,' *Molec. Phys.* **71**, 1381–1404. 213

Wheatley, R. J., Tulegenov, A. S. and Bichoutskaia, E. (2004) 'Intermolecular potentials from supermolecule and monomer calculations,' *Int. Rev. Phys. Chem.* **23**, 151–185. 219

White, C. A., Johnson, B. G., Gill, P. M. and Head-Gordon, M. (1994) 'The continuous fast multipole method,' *Chem. Phys. Lett.* **230**, 8–16. 80

Wiberg, K. B. and Rablen, P. R. (1993) 'Comparison of atomic charges derived by different procedures,' *J. Comput. Chem.* **14**, 1504–1518. 139

Wilkinson, J. H. (1965) *The Algebraic Eigenvalue Problem*, Clarendon Press, Oxford. 107

Williams, D. E. (1965) 'Repulsion center of a bonded hydrogen atom,' *J. Chem. Phys.* **43**, 4424–4426. 210

Williams, D. E. (1967) 'Non-bonded potential parameters derived from crystalline hydrocarbons,' *J. Chem. Phys.* **47**, 4680–4684. 211

Williams, D. E. (1993) 'Net atomic charge and multipole models for the *ab initio* molecular electrostatic potential,' *Rev. Comput. Chem.* **2**, 219–271. 54, 139

Williams, D. E. (1999) 'Improved intermolecular force field for crystalline hydrocarbons containing four- or three-coordinated carbon,' *J. Mol. Struct.* **485-486**, 321–347. 211

Williams, D. E. (2001) 'Improved intermolecular force field for molecules containing H, C, N, and O atoms, with applications to nucleoside and peptide crystals,' *J. Comput. Chem.* **22**, 1154–1166. 211

Williams, G. J. (2004) 'Molecular distributed polarizabilities,' Ph.D. thesis, University of Cambridge. 70, 180

Williams, G. J. and Stone, A. J. (2003) 'Distributed dispersion: a new approach,' *J. Chem. Phys.* **119**, 4620–4628. 172

Williams, G. J. and Stone, A. J. (2004) 'Transferable polarizabilities for the alkanes,' *Molec. Phys.* **102**, 985–991. 173

Williams, H. L. and Chabalowski, C. F. (2001) 'Using Kohn–Sham orbitals in symmetry-adapted perturbation theory to investigate intermolecular interactions,' *J. Phys. Chem. A* **105**, 646–659. 119

Williams, H. L., Szalewicz, K., Jeziorski, B., Moszynski, R. and Rybak, S. (1993) 'Symmetry-adapted perturbation theory calculation of the Ar$\cdots$$H_2$ intermolecular potential energy surface,' *J. Chem. Phys.* **98**, 1279–1292. 113, 119

Willis, B. T. M. (1994) 'Crystallography with a pulsed neutron source,' *Zeit. Krist.* **209**, 385–389. 264

Willock, D. J., Leslie, M., Price, S. L. and Catlow, C. R. A. (1993) 'The need for realistic electrostatic models to predict the crystal structures of NLO molecules,' *Mol. Cryst. Liq. Cryst.* **234**, 499–506. 230

Willock, D. J., Price, S. L., Leslie, M. and Catlow, C. R. A. (1995) 'The relaxation of molecular crystal structures using a distributed multipole electrostatic model.' *J. Comput. Chem.* **16**, 628–647. 230, 265

Wilson, E. B., Jr (1968) 'Some remarks on quantum chemistry,' in *Structural Chemistry and Molecular Biology*, eds. A. Rich and N. Davidson, 753–760, W. H. Freeman, San Francisco. 78

Wilson, E. B., Jr, Decius, J. C. and Cross, P. C. (1955) *Molecular Vibrations*, McGraw-Hill, New York. 8

Wilson, M. and Madden, P. A. (1994) 'Anion polarization and the stability of layered structures in MX_2 systems,' *J. Phys. Condensed Matter* **6**, 159–170. 185, 187, 209

Woodward, R. B. and Hoffmann, R. (1970) *The Conservation of Orbital Symmetry*, Verlag Chemie, Weinheim. 153

Wormer, P. E. S. and Hettema, H. (1992) 'Many-body perturbation theory of frequency-dependent polarizabilities and Van der Waals coefficients: application to $H_2O\cdots H_2O$ and Ar$\cdots NH_3$,' *J. Chem. Phys.* **97**, 5592–5606. 68

Wormer, P. E. S., Kłos, J. A., Groenenboom, G. C. and van der Avoird, A. (2005) '*Ab initio* computed diabatic potential energy surfaces of OH$\cdots$HCl,' *J. Chem. Phys.* **122**, 244325. 200

Wormer, P. E. S. and van der Avoird, A. (1984) 'Heisenberg exchange and electrostatic interactions between O_2 molecules: an *ab initio* study,' *J. Chem. Phys.* **81**, 1929–1939. 200

Wormer, P. E. S. and van der Avoird, A. (2000) 'Intermolecular potentials, internal motions, and spectra of Van der Waals and hydrogen-bonded complexes,' *Chem. Rev.* **100**, 4109–4143. 251

Xantheas, S. S. (1995) '*Ab initio* studies of cyclic water clusters $(H_2O)_n$, n = 1–6. III. Comparison of density functional with MP2 results,' *J. Chem. Phys.* **102**, 4505–4517. 92

Yang, J. and Hättig, C. (2009) 'Highly accurate CCSD(R12) and CCSD(F12) optical response properties using standard triple-ζ basis sets,' *J. Chem. Phys.* **131**, 074102. 77

Yang, J. and Hättig, C. (2010) 'Recent advances in explicitly correlated coupled-cluster response theory for excited states and optical properties,' *Zeit. Phys. Chem.* **224**, 383–395. 77

Yang, M. B. and Watts, R. O. (1994) 'The anisotropic potential energy surfaces of H_2, N_2, and Ar with C_2H_2 from total differential scattering experiments,' *J. Chem. Phys.* **100**, 3582–3593. 263

Yashonath, S., Price, S. L. and McDonald, I. R. (1988) 'A six-site anisotropic atom–atom potential model for the condensed phases of benzene,' *Molec. Phys.* **64**, 361–376. 134

Zare, R. N. (1988) *Angular Momentum*, Wiley Interscience. 9, 22, 47, 271, 272, 274, 275, 276

Zuchowski, P. S., Podeszwa, R., Moszynski, R., Jeziorski, B. and Szalewicz, K. (2008) 'Symmetry-adapted perturbation theory utilizing density functional description of monomers for high-spin open-shell complexes,' *JCP* **129**, 084101. 200

Author Index

Page numbers listed here may refer to pages where the author is included under '*et al.*' in one or more citations.

Abraham R. J. 198
Abramowitz M. 144, 272
Acevedo O. 220
Acharya H. 193
Adamo C. 79
Adams W. H. 104, 106, 113, 114, 115, 117
Addicoat M. A. 219, 220
Adjiman C. S. 225, 266
Adler T. B. 77
Ahlrichs R. 63, 91, 148, 205, 214, 215
Alagona G. 221
Alavi A. 181
Alderton M. 50, 123, 124, 127, 129
Alemán C. 139
Allen F. H. 117
Allen L. C. 88
Allen M. J. 79, 93
Allen M. P. 247, 248, 265
Allinger N. L. 221
Allnatt A. R. 206, 207, 208
Alsenoy C. V. 129
Althorpe S. C. 257, 259, 260
Altman R. S. 169
Altmann S. L. 234
Ammon H. L. 266
Amos A. T. 111, 122, 124
Amos R. D. 68, 85, 124
Anderson J. B. 257, 258
Ángyán J. G. 95, 139, 170, 172, 173
Annunziata R. 151
Antony J. 94
Applequist J. 161, 163
Apra E. 91
Archer K. A. 185
Arfken G. 47
Arnautova Y. A. 221, 266
Arunan E. 153
Asada T. 219
Åstrand P.-O. 137
Avila G. 256
Axilrod P. M. 188
Ayers P. W. 129
Aziz R. A. 190, 207, 208

Baas F. 159
Bačić Z. 255
Bader R. F. W. 129, 170, 241
Baerends E. J. 68, 79, 98, 129
Bak K. L. 81
Bakker H. J. 193
Balduz J. L., Jr. 79
Barbiellini B. 150, 156
Bardwell D. A. 266
Barker J. A. 176, 179, 190, 204
Barnes P. 227
Barnett S. A. 265
Barone V. 79
Bartlett R. J. 77, 90, 91
Bartolomei M. 200
Basilevsky M. V. 107
Battaglia M. R. 16
Becke A. D. 79, 81, 92, 94, 128
Beenakker J. J. M. 159
Bell A. T. 99, 152
Bell R. J. 189
Ben-Naim A. 192
Berendsen H. J. C. 221, 226, 249
Berenfeld M. M. 107
Bernal J. D. 225
Bernardi F. 89, 151
Berne B. J. 209
Bernstein H. J. 157
Bernstein J. 265
Berweger C. D. 226
Best R. B. 223
Bettens R. P. A. 224
Beyer T. 265
Bichoutskaia E. 219
Bickelhaupt F. M. 98, 129
Binkley J. S. 80, 90
Bird R. B. 46, 247
Birge R. R. 161
Birnbaum G. 242
Bissonnette C. 250
Blake G. A. 250
Bledson T. M. 94
Bogaard M. P. 169
Böhm H.-J. 214, 215
Bonaccorsi R. 98
Bondi A. 154, 202
Bone R. G. A. 7, 53, 54

Bordewijk P. 176
Born M. 204
Bosanac S. D. 260, 262
Bose T. K. 124
Böttcher C. J. F. 176
Bowman J. M. 96, 228, 256, 259, 260
Boys S. F. 82, 89, 125, 151, 174
Braams B. J. 96, 228, 256, 259, 260
Braly L. B. 228, 251
Braun D. E. 225
Breneman C. M. 138
Bridge N. J. 166
Brink D. M. 22, 40, 271, 274, 275, 276
Broder C. K. 265
Brooks B. R. 221
Brooks F. C. 63, 148
Brown G. G. 249, 250
Brown M. G. 228, 251
Bruccoleri R. E. 221
Brunger A. T. 241
Buch V. 259
Buchete N.-V. 223
Buck U. 262
Buckingham A. D. 16, 23, 33, 39, 42, 46, 57, 66, 124, 132, 153, 154, 157, 166, 169, 170, 191, 203, 241, 242
Buckingham R. A. 204
Bukowski R. 110, 228
Bultinck P. 129
Bundgen P. 244
Burke K. 79
Burnham C. J. 227, 229
Bylaska E. J. 91

Caldwell J. W. 221, 227
Cammi R. 98
Campos-Martínez J. 200
Car R. 248
Carbó-Dorca R. 129
Carey C. 139
Carl J. R. 161, 163
Carmona-Novillo E. 200
Carrington T., Jr 256, 257

Cartier A. 165
Case D. A. 221, 223
Casida M. E. 79, 85
Casimir H. B. G. 65, 67
Castiglioni C. 136
Catlow C. R. A. 230, 265
Celebi N. 172
Cencek W. 228
Ceperley D. M. 249
Cerjan C. J. 229, 236
Černý J. 94
Ch'ng L. C. 228, 249, 250
Chabalowski C. F. 79, 119
Chai J.-D. 94
Chakarova-Kack S. D. 93
Chakrabarti D. 234
Chakravarty C. 249
Chakravorty S. J. 88
Chałasinski G. 89, 111, 113, 190, 191, 240
Chamberlin A. C. 202
Champagne B. 68
Chandler D. 192, 193
Chandrasekhar J. 226
Chassaing T. 82
Cheatham T. E., III 221
Chen K. 221
Chevreau H. 219
Child M. S. 252, 262
Chipot C. 139, 172
Chirlian L. E. 139
Chodera J. D. 223
Christiansen O. 77
Chuaqui C. E. 250
Cieplak P. 165
Cinquini M. 151
Cioslowski J. 137
Cisneros G. A. 145
Čižek J. 77, 116
Clark G. N. I. 223
Clary D. C. 252, 257, 259
Claverie P. 104, 106, 123, 124, 219
Clementi E. 88, 226
Cobar E. A. 99, 152
Cochran W. 208
Cohen A. J. 95
Cohen E. R. 242, 283
Cohen R. C. 250, 257
Cole M. W. 190
Cole S. J. 90, 91
Collins M. A. 96, 219, 220, 224
Colwell S. M. 85
Connolly J. W. D. 82
Coombes D. S. 265
Cooper A. R. 191
Cooper D. L. 129
Cooper T. G. 266
Cooper V. R. 93
Coppens P. 145
Coriani S. 93
Corner J. 204, 209
Cowan J. A. 198
Cox S. R. 138
Cozzi F. 151
Craig D. P. 65
Craig S. L. 153
Crain J. 192
Cramer C. J. 136, 202
Crispin R. J. 122, 124
Cross J. D. 210
Cross P. C. 8
Crowell K. G. 250
Cruz-Cabeza A. J. 225, 266
Császár A. G. 256
Curtiss C. F. 46, 247
Curtiss L. A. 107, 108, 156
Cvitaš T. 283
Cwiok T. 105, 113
Cybulski S. M. 92, 93, 94, 97, 99, 190
Czakó G. 256

Dalgarno A. 63, 148, 244
Danilowicz R. 189
Dannenberg J. J. 91
Darden T. A. 145, 221, 222
David W. I. F. 265
Davidson E. R. 88, 97, 151, 156
Davydov A. S. 196
Dawber P. G. 34
Day G. M. 213, 225, 265, 266
Dayton D. C. 6, 250
de Jong W. A. 91
de Leeuw F. H. 133
Decius J. C. 8
DeFrees D. J. 80
Dehez F. 172
del Bene J. E. 90, 92, 153
Devlin J. F. 79
Dewar M. J. S. 95, 150
Dham A. K. 207, 208
Dian B. C. 249, 250
Dick B. G. 208
Diederich F. 117
Dinur U. 137
Dion M. 93
Disch R. L. 23, 132, 242
DiStasio R. A., Jr. 93, 223
Ditchfield R. 80
Dittrich B. 241
Dixit S. 192
Dobson J. F. 180
Dodziuk H. 121
Doran M. B. 189
Douglass K. O. 249, 250
Douketis C. 205, 207
Dousmanis G. C. 15, 241
Dovesi F. 209
Dror R. O. 223
Du Q. 193
Duan Y. 165
Dulmage W. J. 52
Dunitz J. D. 266
Dunlap B. I. 82
Dunmur D. A. 132
Dunning T. H. 6
Duran M. 91
Dyke T. R. 55
Dykstra C. E. 259
Dymanus A. 133

Eastwood M. P. 223
Eberly J. H. 30, 197
Economou I. G. 223
Eggenberger R. 91
Ehrlich S. 94
Eisenschitz L. 110
Elking D. M. 145
Elliott J. P. 34
Elrod M. J. 187, 250, 252
Epstein S. T. 111
Ernesti A. 191, 250
Ernzerhof M. 79
Erskine R. W. 107
Essex J. W. 224
Etters R. D. 189
Evans M. W. 193
Ewald P. 266
Ewing J. J. 241

Fábri C. 256
Faerman C. H. 212
Fanourgakis G. S. 249
Fedorov D. G. 219
Fedorov I. 249
Feller D. 82
Fellers R. S. 228, 251
Fenn T. D. 241
Ferenczy G. G. 131
Feynman R. P. 83, 249, 260
Figari G. 109
Filippini G. 212, 266
Finney J. L. 192, 225, 227
Fischer F. R. 117
Fisher R. A. 204
Fleming I. 153
Flygare W. H. 241
Forester T. R. 51
Forster T. 197
Fortes A. D. 95
Fou C.-M. 77
Fowler P. W. 154, 170, 185, 186, 203, 241
Fowler R. H. 225
Francl M. M. 80, 139
Frank H. S. 193
Fraser G. T. 53, 251
Freitag M. A. 145
Frey J. G. 283

Frey R. F. 97
Freyriafava C. 209
Freysz E. 193
Frisch H. L. 245
Frisch M. J. 79, 90
Froese R. D. J. 220
Fujimoto H. 153
Fukui K. 153
Fung K.-K. 161, 163
Furche F. 91
Furtenbacher T. 256

Galek P. T. A. 225
Gange D. M. 139
Garde S. 193
Garmer D. R. 174
Garrahan J. P. 223
Garrido N. M. 223
Gavezzotti A. 212, 265, 266
Gerber S. 91
Gerratt J. 85, 170
Geyer S. M. 249, 250
Ghanty T. K. 151, 156
Ghio C. 221
Gibson K. D. 138, 223
Giesen D. J. 136
Giessner-Prettre C. 145
Gill P. M. 80
Gohlke H. 221
Goldman N. 189, 228, 251
Gomes J. R. B. 223
Gordon M. S. 80, 145, 219
Gossmann U. J. 85
Gould I. R. 223
Gouyet J. F. 108
Govind N. 91
Graham C. 23, 124
Gray C. G. 14, 17, 19, 27, 28, 72, 240, 242, 243
Gray N. A. B. 107
Gregory J. K. 259
Gresh N. 145, 219
Griffiths G. I. G. 95
Grimme S. 93, 94
Gritsenko O. V. 68, 79
Groenenboom G. C. 96, 200, 228, 256
Gross E. K. U. 85
Gubbins K. E. 14, 17, 19, 27, 28, 72, 240, 243
Guerra C. F. 129
Guillot B. 225
Gunning M. J. 42
Gussoni M. 136
Gutowski M. 89, 90, 97, 98

Habgood M. 265
Hagler A. T. 137, 203
Halkier A. 14, 81
Hamann D. R. 150, 156
Hamermesh M. 34
Handgraaf J.-W. 129
Handy N. C. 7, 53, 54, 79, 81, 85, 128
Haque I. 223
Hariharan P. C. 80, 98
Harvey A. H. 246
Hättig C. 50, 51, 52, 77, 91, 170, 173, 230, 231, 291
Haverkort J. E. M. 159
Hayes I. C. 107, 109, 117, 146
Head-Gordon M. 80, 93, 94, 99, 152, 223
Head-Gordon T. 223
Healy E. F. 95
Heather R. W. 256
Hehre W. J. 80
Heijmen T. G. A. 116, 121
Helfand E. 245
Helgaker T. 14, 74, 75, 76, 77, 80, 81, 93
Hellmann H. 83
Hepburn J. 93, 205
Hermans J. 221, 226
Hernández M. I. 200
Hernández-Lamoneda R. 200
Heß B. A. 50, 170, 230, 291
Hesselmann A. 79, 95, 117, 119, 121
Hettema H. 68
Hibbs A. R. 249
Hills R. D., Jr 229
Hinde R. J. 190
Hirschfelder J. O. 46, 59, 111, 247
Hirshfeld F. L. 128
Hirst J. D. 223
Hobza P. 94
Hodges M. P. 183, 228
Hoffmann R. 153
Hohenberg P. 78
Hohenstein E. G. 223
Holmgren S. L. 255
Holmström B. 283
Holthausen M. C. 78
Host B. C. 250
Hou T. 165
Hougen J. T. 53
Howard B. J. 54, 55, 255
Huang D. M. 193
Huang X. 96, 228, 256
Huang Z. S. 54
Hubac I. 107
Huber H. 91
Hudson R. F. 153
Huisken F. 262
Hujo W. 93
Humbel S. 220
Hummer G. 223
Hunt J. L. 124
Hunter C. A. 140, 198, 199
Huot J. 124
Hutson J. M. 191, 210, 250, 253, 255, 263
Hutter J. 82, 249
Hyldgaard P. 93
Hylleraas E. A. 77

Ibberson R. M. 265
Ikeo E. 219
Impey R. W. 226
Inouye H. 216
Isaacs E. D. 150, 156
Israelachvili J. N. 65

Jaeger H. M. 259
Jagielska A. 221
Jalink H. 170, 241
Jamadagni S. N. 193
Janda K. C. 155, 241
Jankowski P. 224
Jansen G. 79, 110, 117, 119, 121, 170, 173
Jansen L. 46
Jarque C. 191
Jayatilaka D. 241
Jeffreys H. 267
Jensen F. 74, 76, 78, 81, 83, 85
Jensen J. H. 145, 219
Jeziorska M. 116
Jeziorski B. 86, 105, 106, 110, 111, 112, 113, 114, 115, 116, 117, 119, 121, 200
Jhanwar B. L. 159, 243, 244
Johnson B. G. 80
Johnson B. R. 255
Johnson E. R. 94
Johnson M. E. 223
Johnson R. E. 111
Jones W. 265
Jordan M. J. T. 96, 224
Jorge M. 223
Jorgensen P. 77
Jorgensen W. L. 220, 221, 226
Joslin C. G. 240, 242
Joubert L. 130
Jucks K. W. 6, 250
Jurečka P. 94
Jørgensen P. 14, 74, 75, 76, 81

Kaczmarek A. 89
Kaledin A. 228, 259
Karamertzanis P. G. 218, 225, 265
Karplus M. 221
Kasper K. 197
Kato T. 77
Kaufman J. J. 98
Kazantsev A. V. 225
Kelkkanen A. 93
Keller J. B. 245
Kelly R. E. A. 96, 228, 256

Kendrick J. 265
Keoshian C. J. 228, 251
Khaliullin R. Z. 99, 152
Khersonskii V. K. 275
Kihara T. 209
Kim H.-Y. 190
Kim S. K. 216
Kim Y. S. 216
King B. F. 108
King H. F. 145
Kirkwood J. G. 68
Kirtman B. 68
Kisiel Z. 251
Kita S. 216
Kitaigorodsky A. I. 265
Kitaura K. 97, 219
Kittel C. 196
Klein M. L. 209, 226, 227
Kleis J. 93
Klemperer W. 55, 155, 169, 241, 251, 255
Klopman G. 153
Klopper W. 14, 77, 81, 83, 91, 229
Kłos J. A. 200
Knizia G. 77
Knowles P. J. 149, 207
Koch H. 77
Koch U. 224
Koch W. 78
Kochanski E. 108
Kohlhase A. 262
Kohn W. 78
Koide A. 206, 207, 243
Kollman P. A. 138, 221, 227
Kołos W. 90, 91, 105, 111, 112, 113, 205
Kong L. 93
Kongsted J. 224
Koren P. R. 151, 156
Koritsanszky T. 145
Korona T. 110, 113, 121
Koulis M. 93, 190, 207
Kowalski K. 91
Krack M. 82
Kreek H. 148, 205
Krieg H. 94
Kroon J. 266
Kuchitsu K. 53, 283
Kuharsky R. A. 229
Kumar A. 188, 243, 244
Kumar N. 93
Kutzelnigg W. 77, 105, 113
Kvasnicka V. 107

Lafferty W. J. 53
Laidler K. J. 7
Lambert M. H. 138, 223
Lambrecht D. S. 223
Laming G. J. 81, 128
Lange O. L. D. 42
Langreth D. C. 93
Lascola R. 252
Laurinc H. 107
Law M. M. 250
Le Fèvre R. J. W. 160
Le H.-A. 224
Le Roy R. J. 253
Le Sueur C. R. 157, 170, 173
Leavitt R. P. 46
Lee A. M. 85
Lee W. D. 216
Leforestier C. 227, 228, 251, 257
Legon A. C. 52, 153, 157, 250
Leighton P. 198
Lemmon E. W. 246
Leslie M. 51, 209, 230, 265, 266
Leszczynski J. 89
Leusen F. J. J. 265
Levy M. 79
Li G. 249
Li J. 165
Li L. 222
Li S. 93
Light J. C. 255, 256, 257
Lighthill M. J. 20
Lii J.-H. 221
Lillestolen T. C. 129, 174, 219, 246
Linder B. 67
Lindorff-Larsen K. 223
Lipscomb W. N. 52, 85, 170
Lochan R. C. 99, 152
Loeser J. G. 252
Lommerse J. P. M. 266
London F. 57, 64, 65, 110
Longuet-Higgins H. C. 27, 42, 57, 58
Loos M. 170
Loudon R. 33
Lovas F. J. 53
Lovejoy C. M. 252
Löwdin P.-O. 107
Lu L. 229
Lucas A. A. 190
Lukovits I. 108
Lundqvist B. I. 93
Luo R. 165, 221
Luque F. J. 139
Luthey-Schulten Z. 7
Lüthi H. P. 83, 92
Lynn N. 63, 148, 244

Macak P. 80
MacDonald J. C. F. 159
Macedo E. A. 223
Madden P. A. 185, 186, 187, 209
Madura J. D. 226
Magnasco V. 109
Mahoney M. W. 226
Maigret A. 139
Maitland G. C. 203, 204, 246, 247
Malmqvist P. A. 77
Manby F. R. 77
Manolopoulos D. E. 249, 255
Mantina M. 202
Maragakis P. 223
Marchetti S. 205, 207
Margenau H. 57
Margoliash D. J. 189, 243
Markland T. E. 249
Maroulis G. 124
Marquardt R. 283
Marshall M. D. 169
Marshall M. S. 223
Martins Costa M. T. C. 183, 228
Marx D. 249
Mas E. M. 228
Mason E. A. 261
Masumoto Y. 53
Matsubara T. 220
Matsuoka O. 226
Mátyus E. 256
Mavroyannis C. 67, 68
Mayer I. 107, 108
Mayer J. E. 204
McClellan A. L. 14, 153, 240
McDonald I. R. 134, 138
McDowell S. A. C. 153, 157
McGurk J. 241
McIlroy A. 252
McKellar A. R. W. 252
McLachlan A. D. 67
McQuarrie D. A. 245, 247
McWeeny R. 180, 280
Meath W. J. 93, 148, 149, 159, 188, 189, 190, 205, 206, 207, 208, 214, 243, 244, 250
Meerts W. L. 133
Merz K. M., Jr. 221
Meyer W. 86
Millen D. J. 52, 153
Miller K. J. 160
Miller R. E. 6, 54, 250
Miller W. H. 229, 236
Millot C. 156, 172, 183, 213, 227, 228, 259
Mills I. M. 85, 170, 283
Milonni P. W. 197
Mirsky K. 211
Misquitta A. J. 86, 95, 116, 117, 119, 120, 151, 152, 175, 176, 180, 181, 217, 218, 219
Mjöberg P. J. 52
Mobley D. L. 223
Mohamed F. 82
Mollner A. K. 228, 249, 250
Momany F. A. 138
Mooij W. T. M. 266

Morgan J. D., III 106
Mori-Sánchez P. 95
Morokuma K. 97, 220
Moses P. G. 93
Moskalev A. N. 275
Moszynski R. 105, 113, 116, 117, 119, 121, 200
Motherwell W. D. S. 265, 266
Muckle M. T. 251
Muenter J. S. 53, 54
Müller-Plathe F. 226
Mulliken R. S. 150
Munro L. J. 229
Munshi P. 241
Murdachaew G. 77
Murray C. W. 81, 85, 128
Murray E. 93
Murrell J. N. 7, 111, 260, 262
Murthy C. S. 138
Musher I. J. 111
Muto Y. 188

Nakano T. 219
Nandi R. N. 54
Needs R. J. 95
Neiss C. 77
Nelson D. D. 251
Némethy G. 221
Nesbitt D. J. 252
Neumann M. A. 94, 265
Neumark D. 16
Nevins N. 221
Ng K.-C. 207
Nguyen D. T. 221
Nicholas J. D. 227
Nieplocha J. 91
Noda K. 216
Noga J. 77
Norris C. L. 241
Novick S. E. 155, 241
Novoa J. J. 90
Nyburg S. C. 212

O'Shea S. F. 138
Oganov A. R. 265, 322
Ogilvie J. F. 134
Ohashi N. 55
Ohshima Y. 53
Olafson B. D. 221
Olsen J. 74, 75, 76, 77, 81
Olthof E. H. T. 251, 256
Onuchic J. N. 7
Onufriev A. 221
Orozco M. 139
Ostlund N. S. 74
Otten D. 262
Overhauser A. W. 208

Pack R. T. 210
Paldus J. 77
Pande V. S. 223, 241
Pantelides C. C. 225
Parker D. H. 170, 241
Parr J. 249
Parr R. G. 79
Parrinello M. 82, 248
Parson W. W. 198
Pate B. H. 249, 250, 251
Patel A. J. 193
Patkowski K. 77, 106, 113, 114, 115
Pauling L. 153, 154, 202
Pavese F. 283
Pechukas P. 209
Pedersen L. G. 145, 222
Peet A. C. 257
Penco R. 93, 205
Perdew J. P. 79
Perera L. 222
Pérez C. 251
Pérez-Jordá J. M. 92
Perpète E. A. 68
Perrin M.-A. 94
Person W. B. 92
Pertsin A. J. 265
Petersilka M. 85
Peterson K. A. 6
Pfeffer G. A. 210
Piana S. 223
Pickard C. J. 95
Piela L. 89, 97, 98
Pierens R. K. 16, 169
Pietro W. J. 80
Pimentel G. C. 153
Pine A. S. 53, 55
Piper E. 210
Piquemal J.-P. 145, 219
Pitzer K. S. 68
Pitzer R. 85, 170
Pizio O. 264
Planas M. 90
Platzman P. M. 150, 156
Pochatko D. J. 107, 108
Podeszwa R. 86, 121, 145, 189, 200
Poirier R. A. 108, 124, 126
Polder D. 65, 67
Poll J. D. 124
Ponder J. W. 51, 221, 223, 230
Poon W. C. K. 192
Popelier P. L. A. 129, 130, 224, 235
Pople J. A. 80, 157
Postma J. P. M. 221, 226
Pottle M. S. 221
Price L. S. 265
Price S. L. 50, 134, 154, 175, 176, 212, 213, 216, 217, 218, 219, 225, 230, 265
Prichard J. S. 54
Proctor T. R. 189
Profeta S. 221
Pruitt S. R. 219
Pu M. 223
Pullman A. 219
Pusztai L. 264
Puzder A. 93

Quack M. 283
Queimada A. J. 223
Quinn J. E. 227

Raab R. E. 42
Rablen P. R. 139
Rahman A. 226
Rak J. 190
Ratkiewicz A. 117, 119
Rauk A. 88
Reed A. E. 107, 108, 156
Reimers J. R. 226, 227
Rein R. 124
Reinhardt P. 145
Reisler H. 228, 249, 250
Ren P. 51, 223
Reynolds C. A. 131, 224
Rezus Y. L. 193
Richards W. G. 224
Richardson J. O. 260
Rigby M. 203, 204, 246, 247
Rijks W. 68, 227, 228
Rip A. 176
Rob F. 145
Robins K. A. 68
Roche C. F. 250
Rocher-Casterline B. E. 228, 249, 250
Rodger P. M. 212, 213, 248
Roetti C. 209
Rossky P. J. 229
Roszak S. 98
Roterman I. K. 138, 223
Rowlands T. W. 7, 53
Rowlinson J. S. 225, 226
Roy R. J. L. 250
Ruud K. 137
Rybak S. 113, 117, 119
Rychlewski J. 105, 113
Rydberg H. 93
Ryde U. 223, 224

Sabin J. R. 82
Sadlej A. J. 87, 89
Sagvolden E. 93
Salahub D. R. 79, 94
Sałek P. 80
Salem L. 153
Sanders J. K. M. 140, 198, 199
Sandorfy C. 157
Satchler G. R. 22, 40, 271, 274, 275, 276

Saunders V. R. 209
Sawaryn A. 139
Saykally R. J. 187, 189, 228, 250, 251, 252, 256, 257
Schaefer H. F., III 85, 90
Schaefer J. 262
Schäffer R. 110
Scheffler M. 93
Scheiner S. 97
Scheraga H. A. 138, 139, 221, 223
Schipper P. R. T. 68
Schmuttenmaer C. A. 250
Schneider W. G. 157
Schnieders M. J. 223, 241
Schroder E. 93
Schwarz R. F. 15, 241
Schwenke D. W. 90
Scoles G. 93, 205, 207
Searles D. 91
Seifert N. A. 251
Seversen C. E. 92, 93, 99
Sham L. J. 78
Shank A. 228, 259
Shankland K. 265
Shavitt I. 82
Shaw D. E. 223, 248
Shaw G. 111
Shen Y. R. 193
Shepler B. C. 228, 260
Sherrill C. D. 223
Shields G. C. 185, 251
Shipman S. T. 249, 250
Sholl D. 78
Shukla A. 150, 156
Sieber S. 220
Siegel J. S. 151
Sierka M. 91
Sikora P. T. 215
Silberstein L. 61, 161
Silbey R. 111
Simmerling C. 221
Simon B. 106
Simon S. 91
Singh J. 140
Singh S. 242
Singh U. C. 138, 221
Sinnokrot M. O. 223
Sippl M. 221
Slater J. C. 68, 94
Slipchenko L. V. 145, 219
Smith E. B. 203, 204, 246, 247
Smith W. 51, 266
Snijders J. G. 68
Söderhjelm P. 223, 224
Soetens J.-C. 183, 228
Sofod J. O. 190
Sokalski W. A. 98, 124, 126, 139
Sokolowski S. 264
Solheim H. 137
Soper A. K. 192
Soubra-Ghaoui C. 68
Spackman M. A. 136, 145, 241
Spencer J. 181
Šponer J. 94
Sprik M. 209, 227
Staroverov V. N. 151, 156
States D. J. 221
Steckel J. A. 78
Stegun I. A. 144, 272
Steinmann C. 219
Stephen M. J. 67, 68
Stephens P. J. 79
Stephens S. L. 250
Stevens R. M. 85, 170
Stevens W. J. 145, 174
Stewart J. J. P. 95
Steyert D. W. 250, 252
Stillinger F. H. 226
Stogryn D. E. 189
Stohner J. 283
Stolte S. 170, 241
Stone A. J. 7, 19, 27, 45, 50, 53, 70, 72, 107, 109, 116, 117, 123, 124, 127, 129, 134, 144, 146, 151, 152, 153, 154, 156, 157, 166, 170, 172, 173, 175, 176, 179, 180, 181, 183, 199, 212, 213, 215, 216, 217, 218, 219, 224, 227, 228, 235, 241, 248, 259, 291
Storer J. W. 136
Stouch T. R. 223
Straatsma T. P. 91
Strauss H. L. 283
Strodel B. 225
Strømsheim M. D. 93
Stutchbury N. C. J. 129
Suenram R. D. 53
Suhm M. A. 258, 259
Sumpter B. G. 223
Surjan P. R. 107, 108
Svensson M. 220
Swaminathan S. 221
Swenson D. W. H. 259
Szabo A. 74
Szalewicz K. 77, 86, 90, 91, 105, 106, 110, 111, 113, 114, 115, 117, 119, 120, 121, 145, 189, 200, 227, 228
Szczepaniak K. 92
Szczęśniak M. M. 190, 191, 240
Szidarovszky T. 256

Takami M. 53, 283
Tang K. T. 68, 73, 188, 206
Teale A. M. 93
Tekin A. 121
Teller E. 188
Temelso B. 185, 251
Ten-no S. 77
Tennyson J. 96, 228, 256
Thakkar A. J. 68, 73, 205, 207, 243, 244
Thirumachandran T. 65
Thole B. T. 164
Thomas G. F. 159
Thompson C. C. 150
Thompson K. C. 96, 224
Thonhauser T. 93
Thor A. J. 283
Thornley A. E. 263
Thornton J. M. 140
Tigelaar H. L. 241
Tildesley D. J. 212, 213, 247, 248, 265
Tinkham M. 34
Tirado-Rives J. 221
Tkatchenko A. 93
Tocher D. A. 265
Toczyłowski R. R. 94
Toennies J. P. 73, 206, 210
Tomasi J. 98
Tong C.-S. 179, 180, 215, 216
Tough R. J. A. 19, 45, 72
Townes C. H. 15, 241
Tozer D. J. 79, 93
Trouton, F. T. 2
Truhlar D. G. 90, 136, 202
Tsuzuki S. 92
Tulegenov A. S. 219
Tulk C. A. 150, 156

Uebayasi M. 219
Unsöld A. 65

Valeev E. F. 77
Valentini J. J. 210
Valero R. 202
Valiev M. 91
van Belle O. C. 176
Van Bladel J. W. I. 256
Van Caillie C. 68
van Dam H. J. J. 91
Van de Streek J. 94, 265
Van der Avoird A. 96, 110, 119, 121, 200, 227, 228, 251, 256, 257
Van der Waals, J. D. 2
van Duijneveldt F. B. 89, 90, 91, 229
van Duijneveldt-van de Rijdt J. G. C. M. 89, 90, 91, 229
van Eijck B. P. 266
van Gisbergen S. J. A. 68
van Gunsteren W. F. 221, 226
van Harrevelt R. 228, 257
van Hemert M. C. 200
Van Kranendonk J. 253
van Lenthe J. H. 89, 90

Van Voorhis T. 93
VandeVondele J. 82
Varilly P. 193
Varshalovich D. A. 275
Velegol D. 190
Vigné-Maeder F. 123, 124
Voisin C. 165
Volkov A. 145
Voth G. A. 229
Vydrov O. A. 93

Wakeham W. A. 203, 204, 246, 247
Waldman M. 203, 255
Wales D. J. 7, 225, 229, 234, 236, 251, 260, 265
Walker N. R. 250
Walker R. C. 223
Wang B. 221
Wang D. 91
Wang J. 165, 221
Wang Y. 228, 259, 260
Warshel A. 198
Watanabe A. 252
Watson M. A. 80
Watts R. O. 204, 226, 227, 258, 259, 263
Weigend F. 91
Weiner P. 221
Weiner S. J. 221
Weinhold F. 107, 108, 156
Welch G. W. A. 218, 219, 265
Wells A. F. 185, 186
Wells B. H. 190, 259
Welsh H. L. 252
Werner H.-J. 77, 86
Whangbo M.-H. 90
Wheatley R. 129
Wheatley R. J. 128, 142, 174, 207, 213, 214, 216, 217, 219, 246, 250
White A. H. 169
White C. A. 80
White R. L. 15, 241
Wiberg K. B. 138, 139
Wilkinson J. H. 107
Williams D. E. 54, 138, 139, 210, 211
Williams G. J. 70, 172, 173, 180
Williams H. L. 110, 113, 117, 119
Williams J. H. 16, 23, 124
Willis B. T. M. 264
Willock D. J. 230, 265
Wilson E. B., Jr 8, 78
Wilson M. 185, 187, 209
Wilson S. 190
Windus T. L. 91
Winn P. J. 131
Wolf R. M. 221
Wolniewicz L. 205
Wolynes P. G. 7
Wood P. A. 117
Woods R. 221
Woodward R. B. 153
Wormer P. E. S. 68, 119, 121, 200, 227, 228, 251, 256
Wu C. 223

Xantheas S. S. 92, 183, 227, 229

Yang J. 77
Yang M. B. 263
Yang W. 95, 257
Yashonath S. 134
Yoshimine M. 226
Young M. A. 221
Yuh Y. H. 221

Zaleski D. P. 251
Zare R. N. 9, 22, 47, 271, 272, 274, 275, 276
Zeiss G. D. 189, 243
Zen M. 205, 207
Zerbi G. 136
Zoebisch E. G. 95
Zuchowski P. S. 200
Zucker I. J. 189
Zumino B. 245

Index

Page numbers in italic followed by *n*, *f* or *t* refer to footnotes, figures and tables respectively.

3 *j* symbols, 276

ab initio methods, 74–99
  for molecular properties, 83–87
acetylene, 16, *215f, 216f*
  complexes
    with CO_2, 54
    with He, 119
  dimer, 53, *54f*
  trimer, 53
additivity and non-additivity, 3
AIM, *see* atoms in molecules
alkaline earth halides, 185
allocation algorithms
  for distributed multipoles, 126–130
    Bader, 129
    Hirshfeld, 128
    hybrid, 127
    Mulliken, 126
    nearest-site, 127
    stockholder, 128
    Voronoi polyhedra, 129
    Wheatley, 128
  for distributed polarizabilities, 170
AM1, 95
AMBER force field, 220
ammonia dimer spectrum, 251
angular momentum operators, 271
angular–radial separation, 255
anisotropic site potential, 227
anisotropy, 8
  in electrostatic interactions, 139
  of dispersion coefficients, 244
  of polarizabilities, 27, 160, 165
  of repulsion, 212, 216, *216f*, 250
  of three-body interactions, 189
anthracene
  crystal structure, 53
antisymmetrization
  consequences for perturbation theory, 103–106
Anton computer, 248
Applequist model, 161–166
  damped, 164
  for CO, 165
  higher ranks, 163
  singularities, 163
APT, *see* atomic polar tensor method
Ar, 263
  potential, 204
Ar···H_2, 119
Ar···HCl, 253
ASP model for water, 227
asymptotic correction
  in density functional theory, 79
atom shapes, *215f, 216f*
atom–atom models, 210–218
  isotropic models inadequate, 212
  of dispersion, 217
  parameters for, 211
  see also site–site models
atom–diatom spectra
  intermolecular potential from, 253
atomic polar tensor method, 136–137
atomic polarizabilities, 159, 242, *243t*
atomic unit, 283
  of dipole moment, 14
  of octopole moment, 18
  of polarizability, 27
  of quadrupole moment, 16
atoms in molecules, 129, 241
average-energy approximation, 279
  for the dispersion energy, 65
axes, *see* coordinate systems
axial tensors, 269
Axilrod–Teller–Muto, *see* triple-dipole dispersion
azabenzenes
  distributed multipoles, 134

bacteriochlorophyll, 197, *198f*
Bader partitioning, 129, 241
balanced basis sets, 82
Barker–Fisher–Watts potential for argon, 204
basis set superposition error, 88–91, 121
  and charge transfer, 151
  and geometry optimization, 90, *90f*
  counterpoise correction, 89
  in energy decomposition analysis, 98
basis sets, 79–83
  auxiliary, 81
  balance, 82
  correlation consistent, 81
  extrapolation, 81
  for properties, 86
  for SAPT and SAPT-DFT, 121
  plane-wave, 82
  polarization-consistent, 81

benzene
  complex with hexafluorobenzene, 54
  crystal structure, 53
Berthelot combining rule, 203
binding energies, *3t*
biorthogonal functions, 108
Bloch functions, 196
BOARS, *see* angular–radial separation
bond polarizabilities, 159
Born–Mayer potential, 204, 212
Born–Oppenheimer, 74
boundary conditions
  periodic, 247
Boyle temperature, 245
BSSE, *see* basis set superposition error
Buckingham unit of quadrupole moment, 283
Buckingham–Corner potential, 204
Buckingham–Fowler model, 154–155

C_2H_2, *see* acetylene
C_6 coefficient, *see* dispersion coefficient
$C_6F_6\cdots C_6H_6$, 54
C_6H_6, 16
  distributed multipoles, 134
$C_6H_6\cdots C_6F_6$, 123
C_9 coefficient, *see* triple-dipole dispersion
CamCASP, 219
CAMM, *see* cumulative atomic multipole moments
Car–Parrinello molecular dynamics, 248
carbon monoxide, 14
cartesian tensors, 267–270
  contraction, 268
  definition, 268
  isotropic, 269
  Kronecker tensor, 269
  Levi-Civita tensor, 269
  outer product, 268
  polar and axial, 269
  quotient rule, 269
CASSCF, 76
CBO, *see* angular–radial separation
CCSD, *see* coupled-cluster
$CdCl_2$
  crystal structure, *186f*
centre of charge, 39
CH_4, 17, *18f*
change of origin, *see also* origin dependence
  origin-shift coefficients, *288t*
channel, 262
charge
  centre of, 39
charge density operator, 20
charge density susceptibility, 27–29
  frequency-dependent, 34, 85, 189
  imaginary frequency, 34
    in the dispersion energy, 69
charge penetration, 141–145
charge transfer, 5, 150–153
  and basis set superposition error, 151
  and frontier-orbital theory, 153
  postulated in alkaline earth halides, 185
charge-transfer complexes, 150
charge-transfer energy, 150
  in the water dimer, *156f*
charge-transfer spectra, 150
charge-flow polarizabilities, 160, 167
CHARMM force field, 221
CHELPG, 138
chlorophyll, 197
CISD, *see* configuration interaction
CKS, *see* coupled perturbation theory
Cl_2, *215f*, 248, 265
Clebsch–Gordan coefficient, 275
ClF···HF, 154, *155f*
close-coupling approximation, 255
close-coupling equations, 254
CO, 14
  Applequist polarizabilities, 165
  distributed multipoles, 132
  distributed polarizabilities, 168
CO_2, 16
  complex with acetylene, 54
coarse-graining, 229
collision-induced absorption, 242
combining rules, 202, 221
  energy-dependent hard-core model, 215
  for Lennard-Jones potential, 203
  for site–site repulsion, 214
    limitations of, 216
  for W99 force field, 211
  Lorentz–Berthelot, 203
Compton scattering
  and charge transfer, 150
configuration interaction, 75
  CISD, 76, 87
  size consistency, 91
convergence
  of the multipole expansion, 122, *122f*
    of the induction energy, 62, 148
conversion tables
  between spherical and cartesian, 285–286
  between units, 283
cooperative effects, *see* non-additivity
coordinate systems, 8–11
  atom and linear molecule, *10f*
  global and local, 8, 48
  molecule-fixed and space-fixed, 8
  two linear molecules, *11f*
  two non-linear molecules, *11f*
Coriolis, 255
Corner potential, 209
correlated sampling, 259
correlation, *see* electron correlation
correlation corrections
  to exchange–repulsion, 119
correlation energy, 92
coupled perturbation theory, 85
coupled-channel equations, 254, 262
coupled-cluster, 77
coupling of spherical tensors, 275–276

CPMD, *see* Car–Parrinello molecular dynamics
cross-section, 261
  differential, 261
crystal structures
  prediction, 265
crystals, *see also* molecular crystals
  alkaline earth halides, 185
cumulative atomic multipole moments, 139

D_e and D_0, 6, 228, 250, 259
damping, 5
  of induction and dispersion, 148
damping functions
  ab initio calculations, 149
  for Ar···Ar, *149f*
  for the electrostatic interaction, 144
  Hartree–Fock–dispersion, 205
  Koide–Meath–Allnatt, 205
  Tang–Toennies, 206, *206f*
  Thole, 164
debye unit of dipole moment, 14, 283
deformation energy, 4
delta function, 20
δ^{HF} correction, 116
density functional theory
  and dispersion energy, 92
  asymptotic correction, 79
  B3LYP, 79
  DFT-D method, 93, 265
  exact exchange, 95
  for interaction energies, 92–95
  general principles, 78–79
  hybrid functionals, 79
  in symmetry-adapted perturbation theories, 115
  Kohn–Sham method, 78
  limitations, 92
  non-local functionals, 93
  PBE0, 79
density overlap model, 216
density susceptibility, *see* charge density susceptibility
density-fitting, 81
  for distributed polarizabilities, 171
  for the FDDS, 86
depletion force, 193
DFT, *see* density functional theory
DFT-SAPT, *see* SAPT-DFT
dielectric constant
  in molecular mechanics, 222
differential cross-section, 261
diffusion coefficients, 246
diffusion Monte Carlo, 257–259
  excited states, 259
  rigid body, 259
dipole moment, 13
  from Mulliken charges, 138
  measurement, 240
  sign
    Debye convention, *15n*
  units, 14, 283
  see also multipole moments
dipole moments
  induced, in molecular complexes, 169
  table of values, *14t*
dipole oscillator strength distributions, 188, 243
  sum rules, 243
dipole–dipole interactions, 46, 51, 52
  favourable and unfavourable, *52f*
dipole–quadrupole interactions, 47, 55
  favourable and unfavourable, *55f*
Dirac delta function, 20
discrete variable representation, 256
dispersion coefficient, 66
  combining rules, 68, 72
  measurement, 244
  numerical values, 72, *73t*
  recursion formula, 73
  sign convention, *66n*
  Slater–Kirkwood formula, 68
  units, 284
dispersion energy, 4, 59, 64–73
  atom–atom models, 217
  correlation effects, 148
  damping, *see* damping functions
  derivatives, 236
  distributed, 179
    localized, 180
  Drude model, 64
  higher-rank terms, 70
  London formula, 65
  many-body terms, 187–190
  McLachlan formula, 67
  models for atoms, 205–207
  non-expanded, 69
  orientation dependence, 69
  penetration effects, 148
  retardation effect, 65
  Slater–Kirkwood formula
    Tang's version, 68
  spherical-tensor form, 69
  triple-dipole, *see* triple-dipole dispersion
  Unsöld approximation, 65
distributed dispersion, 179
  localized, 180
distributed multipole analysis, 124–134
distributed multipole expansions, 123–157
  empirical, 123
distributed multipoles
  and electron correlation, 132
  and porphin dimer, 198
  CO, 132
  HF, 133
  hybrid allocation algorithm, 127
  N_2, 131
  sensitivity to basis set, 127
  simplified, 130
    formamide, *130f*
  symmetry, 135
distributed polarizabilities, 166–176, 209
  and induction energy, 176–179

Applequist model, *see* Applequist model
computation, 170–176
density-fitting, 171
for CO, 168
from polarization responses, 172
localized, 173, 180
relationship to molecular polarizabilities, 168
theory, 166
distributed transition moments, 197–199
divergence spheres, 122
for regions, 126
DMA, *see* distributed multipole analysis
DMC, *see* diffusion Monte Carlo
DNA, 140
DOSD, *see* dipole oscillator strength distribution
dummy suffixes, 268
DVR, *see* discrete variable representation
DZP, *see* basis sets

ϵ, *see* well depth
ECEPP force field, 221
Eckart conditions, 8
effective fragment potential, 219
EFMO, *see* fragment molecular orbital
EFP, *see* effective fragment potential
eigenvector-following
for structure optimization, 229
Einstein summation convention, 17, 267
EL–HAV perturbation theory, 111
electric field
magnitudes, 30
of a molecule, 43, 45
electric field gradient, 23
of a molecule, 45
electron correlation, 75–77
explicit, 77
r12 methods, 77
size consistency, 91–92
and CISD, 91
electrostatic energy, 4, 45–56, 141–145
derivatives, 230
electrostatic interaction
in a polar solvent, *192f*
in a polarizable solvent, *191f*
electrostatic potential
charges fitted to, 138
of a molecule, 43–44
electrostatic units, 283
energy decomposition analysis, 96–99
basis set superposition error, 98
energy derivatives, 51, 229–239
asymmetry of second derivatives, 236
basic first derivative formulae, *235t*
basic second derivative formulae, *237t*
induction, 238
repulsion and dispersion, 236
energy landscape, 6–7
entropy, 191, 192
esu, 283
ethyne, *see* acetylene
Euler angles, *8f*
and quaternions, 9
definition, 8
Ewald summation, 265
exchange
neglect at long range, 57
exchange hole, 94
exchange perturbation theories, 106
exchange–dispersion, 148
exchange–induction, 148
exchange–repulsion energy, 5, 146–147
and spin, 103
and the charge density, 102
correlation effects, 119
distance dependence, *147f*
in H_2, 100–102
see also repulsion energy
exchange-coulomb model, 201, 207, 214
excimer lasers, 197
excimers, 197
potential curves, *198f*
excited states
interactions involving, 194–199
exciton splitting, 197
excitons, 196–197
exp-6 potential, 204
parameters for, *211t*
experimental measurement
of dispersion coefficients, 244
of multipole moments, 240–242
of polarizabilities, 242–244

far-infrared spectroscopy, 250
FDDS, *see* charge density susceptibility
Fermi hole, 94
FIR-VRT spectroscopy, 250
fixed-node method, 259
FMO, *see* fragment molecular orbital
force fields, 220–223
polarizable, 223
W99, 211, *211t*
forces, calculation of, 229
fragment molecular orbital, 219
free energy, 191
frontier orbitals, 153

GAPT, *see* atomic polar tensor method
gaussian basis functions, 80
gaussian multipoles, 142–145
non-multipolar components, 143
gaussian overlap model, 209
geometric-mean combining rule, 203
geometries, choice of, 95
global coordinate system, 8
global minimum, 6
GROMOS force field, 221

H_2O, *see* water
halogen bond, 157
hard-sphere model, 202

Hartree–Fock limit, 115
Hartree–Fock–dispersion model, 93, 201, 205, 207, 226
HCN, 52
helicity decoupling, 255
Hellmann–Feynman theorem, 83, 103
Hessian
  electric and magnetic, 85
  of the potential energy surface, 7
    calculation, 229
Hessian index, 7
hexadecapole moment, *see* multipole moments
hexafluorobenzene
  complex with benzene, 54
HF, 16
  dimer, 55, 153
    structure, *55f*
    zero-point energy, 6
  distributed multipoles, 133
HF···ClF, 154, *155f*
HFD, *see* Hartree–Fock–dispersion model
Hirshfeld partitioning, 128, 241
HOMO, *see* frontier orbitals
HS perturbation theory, 111
hydrogen bond, 153–157
  Buckingham–Fowler model, 154–155
  charge transfer, 156
  electrostatic picture, 153
  in molecular mechanics, 222
  in the water dimer, *155f*
  Legon–Millen rule, 153
  non-additive effects, 157
hydrophobic effect, 192–193
hyperpolarizability, 30

ice
  Compton scattering, 150
  triple-dipole dispersion, 189
impact parameter, 260
incomplete gamma function, 164, 206
induction energy, 4, 59–64
  and distributed polarizabilities, 176–179
  and non-uniform fields, 160
  and the charge density susceptibility, 63
  classical model, 116
  correlation effects, 148
  δ^{HF} correction, 116
  derivatives, 238
  in alkaline earth halides, 185–187
  in symmetry-adapted perturbation theory, 116
  in water clusters, *183f, 184f*
  multipole expansion, 60
    asymptotic convergence, 62, 148
  non-additivity, 61, 182–187
    example, *61f*
  penetration effects, 148
  schematic representation, *179f*
  the ZI method, 117
inelastic scattering, 243, 247, 262, 263
instanton method, 260
intensities
  and resonance interactions, 195
interaction functions, 46–47, 50, *291–297t*
interaction tensors
  cartesian, 44
  spherical, 50
interference effects
  in molecular beam scattering, 262
intermediate normalization, 277
intermolecular forces
  classification, 4, *5t*
  long-range and short-range, 4
intermolecular potentials
  from spectroscopy, 249–260
internal coordinates, 11, 219
isotropic tensors, 269
iterative symmetry-forcing procedures, 111–115
  regularized, 114–115

Kohn–Sham method, 78
Koopmans' theorem, 79
Kronecker delta, 17, 269

lattice vibrations, 264
Legon–Millen rule, 153
Lennard-Jones potential, 203
Levi-Civita tensor, 269
linear response, 30
local coordinate system, 8
local minima, 6
localized polarizabilities, 180
long-range approximation, 58
long-range forces, 4
long-range perturbation theory, 57–73
Lorentz combining rule, 203
LUMO, *see* frontier orbitals

magnetic effects, 4
many-body effects, 182–193
  in Ar_2HCl, 190
  in water clusters, *183f, 184f*
  solvent effects, 191
many-body perturbation theory, 76
many-body terms, 3
  in the dispersion energy, 187–190
  in the repulsion energy, 190
  in the SAPT method, 121
Mayer function, 245, *245f*
MBPT, 76
McLachlan identity, 67
measurement
  of dispersion coefficients, 244
  of multipole moments, 240–242
  of polarizabilities, 242–244
Metropolis sampling, 248
$MgCl_2$, 185, *185f*
  crystal structure, *186f*
microwave spectroscopy, 249, 251
minima
  and the Hessian, 7

local and global, 6
symmetry-related, 6, 7
MM4 force field, 221
models
atom–atom, *see* atom–atom models
coarse-grained, 229
Corner potential, 209
density overlap, 216
DFT-D, 93, 265
exchange-coulomb, 201, 207, 214
for dispersion, 205–207
for repulsion, 207–208
for small molecules, 209–218
gaussian overlap model, 209
hard-sphere, 202
Hartree–Fock–dispersion, 93, 201, 205, 207, 226
repulsive potentials, 214–217
site–site, *see* site–site models
test particle model, 214
molecular beams
scattering, 260
spectroscopy, 249, 251
molecular crystals
polymorphs, 265
resonance interactions, 196–197
structure prediction, 265
structures, 264–266
molecular dynamics, 247
molecular mechanics, 220–223
molecular properties, 13–42
ab initio calculation, 83–87
finite field method, 84
measurement, 240–244
molecule–molecule potentials, 209–210
Møller–Plesset, 76
monopole moment, *see* charge
Monte Carlo, 247, 257
Morokuma analysis, *see* energy decomposition analysis
MP2, *see* Møller–Plesset
MRCI, 76
MS–MA perturbation theory, 111
Mulfit program, 131, 139
Mulliken allocation algorithm, 126
Mulliken population analysis
for point charge models, 138
multipole expansion
cartesian form, 43–47
convergence, 122, *122f*
molecular, 123
of the electrostatic interaction, 45
single-site, 123
spherical tensor form, 47–52
multipole interactions
dipole–dipole, 46, 51, 52
dipole–quadrupole, 47, 55
quadrupole–quadrupole, 47, 51–54
T functions, 50, *291–297t*
multipole moments, 13–22
cartesian formulation, 13–19
chiral molecules, 36
conformational dependence, 224
conversion between spherical and cartesian, *285t, 286t*
general definition, 18
in an electric field, 21
local and global axes, 48
measurement, 240–242
number of components, 18
origin dependence, 39
spherical-tensor formulation, 19
symmetry, 34–37
tracelessness, 21
see also dipole moment, quadrupole moment, etc.; distributed multipoles
MX_2 structures, 185–187

N_2, *215f*
distributed multipoles, 124, 131
point charge models, 137
naphthalene
crystal structure, 53
nearest-site allocation algorithm, 127
neutron diffraction, 264
neutron scattering, 263
NH_3
dimer, 256
inversion, 6, 88
non-additivity
in hydrogen bonding, 157
of the induction energy, 61, 182–187
example, *61f*
see also many-body effects

O_2 dimer, 199
octopole moment, 17, *18f*
spelling, *15n*
units, 283
see also multipole moments
ONIOM, 220
open-shell systems, 199
OPLS force field, 221
origin dependence, 39–42
of multipoles, 39
of polarizabilities, 41
of the quadrupole moment, 40, 42
oscillator strength, *see* dipole oscillator strength distributions

π–π interactions, 140
pairwise additivity and non-additivity, 3, 182–193
path integral methods, 249, 260
penetration effects, 5
electrostatic, 141–145
in induction and dispersion, 148
periodic boundary conditions, 247
permittivity
units, 284
perturbation theory
coupled Hartree–Fock, 85

coupled Kohn–Sham, 85
degenerate, 280–281
failure of the long-range theory, 100
long-range, 57–73
non-degenerate, 277–280
first-order, 278
second-order, 278
Rayleigh–Schrödinger, 278, 281
short-range, 100–121
symmetric, *see* symmetric perturbation theories
Rayleigh–Schrödinger, 113
symmetry-adapted, *see* symmetry-adapted perturbation theories
time-dependent, 31–34, 281–282
PES, *see* potential energy surfaces
phenylalanine, 140
PM3, 95
point charge models, 136–140
cumulative atomic multipole moments, 139
for π systems, 140
Mulliken population analysis, 138
potential-fitted charges, 138
polar tensors, 269
polarizabilities, 24–34, 242–244
additivity, 159
anisotropy, 27
Applequist model, 161–166
damped, 164
for CO, 165
higher ranks, 163
singularities, 163
atom and bond, 159
atomic, 242
cartesian form, 24
charge-flow, 160, 167
conformational dependence, 224
conversion between spherical and cartesian, 25, *286t*, *289t, 290t*
distributed, 166–176, 209
localized, 173
frequency-dependent, 31–34
imaginary frequency, 33–34, 67, 70, 85, 243
inversion symmetry, 38
local, 173
local molecular orbital, 174
magnitude, 27
measurement, 242–244
models for atoms and ions, 208–209
origin dependence, 41
response to non-uniform fields, 160
shell model, 208
spherical tensor form, 25
static and optical-frequency, *243t*
symmetry, 37–39
table of values, *28t*
units, 284
vibrational, 242
polarizable continuum model, 220
polarization approximation, 58
polarization catastrophe, 62
polarization functions, 81
porphin, 197, *198f*
position vectors
definition, *43f*
potential energy surfaces, 6–7, 74, 240
ab initio, 95–96
for water, 225–229
from experiment, 250–253
potential models, *see* models
potential of mean force, 191
potential-fitted charges, 138
promolecule, 128
pseudopotentials, 82
psips, 258

QM/MM, 220
quadrupole moment, 15–17
examples, *15f*
measurement, 241
origin dependence, 40, 42
spelling, *15n*
table of values, *17t*
units, 283
see also multipole moments
quadrupole–quadrupole interactions, 47, 51–54
and crystal structures, 53
favourable and unfavourable, *53f*
quantum Monte Carlo, 257–259
quaternions, 9
and Euler angles, 9

Racah spherical harmonics, 272
radial distribution function, 248, 263
radius ratio, 185
rainbow
in molecular beam scattering, 261
random walk, 258
Rayleigh–Schrödinger perturbation theory, 278, 281
symmetrized, 113
region, 123
regular spherical harmonics, 19, *285t*
regularized Coulomb functions, 115
regularized symmetry-forcing procedures, 114–115
relativistic effects ignored, 74
relay matrix, 161
repeated-suffix summation convention, 17, 267
repulsion energy
derivatives, 236
many-body terms, 190
models for atoms, 207–208
see also exchange–repulsion energy
resolvent, 280
resonance energy, 4
resonance interactions, 194–199
energy levels and allowed transitions, *195f*
in molecular crystals, 196–197
retardation, effect on dispersion energy, 65
rigid body diffusion Monte Carlo, 259
ring polymer, 249, 260
RKR, *see* Rydberg–Klein–Rees

R_m, 1
rotation matrices, Wigner, 274
rotations
  angle–axis, 9
  Euler angles, 8
  quaternions, 9
rotations of the coordinate system, 273
Rydberg–Klein–Rees method, 252

σ, 1
S functions
  definition, 49
  for real components, 50
  in repulsion models, 217
saddle points, 6
  and the Hessian, 7
SAPT, *see also* symmetry-adapted perturbation theories
  for water dimer, 228
  implementation, 117
  many-body corrections, 121
  summary of terms, *118t*
SAPT(DFT), *see* SAPT-DFT
SAPT-DFT, 119
  summary of terms, *120t*
scalar product
  of spherical tensors, 275
scattering
  classical trajectories, *261f*
  inelastic, 243, 247, 262, 263
  neutron and X-ray, 263
  of molecular beams, 260–263
SCF, *see* self-consistent field
second moment, 21
second virial coefficient, *see* virial coefficient
self-consistent field, 75
semi-classical methods, 262
semi-empirical methods, 95
short-range effects, 141–158
short-range forces, 4
short-range perturbation theory, 100–121
  and antisymmetrization, 103
  at second order, 147–153
  correlation corrections, 118
  exchange–repulsion, 146–147
SIBFA, 145, 219
simulation methods, 247–249
  Car–Parrinello, 248
  molecular dynamics, 247
  Monte Carlo, 247
single-exchange approximation, 109
site, 123
site–site models, 210–218
  combining rules for, 214
  shape and hardness, 212
  test particle, *215t*
  test particle model, 214
  see also atom–atom models
size consistency, 91–92
  and CISD, 91
Slater–Kirkwood formula, 68
  Tang's version, 68
Slater-type orbitals, 80
solvent effects, 191
Soret band, 199
special pair, 197
spectroscopy
  and intermolecular potentials, 249–260
spherical harmonic addition theorem, 47
spherical harmonics, 271–273
  Racah normalization, 272
  real form, 272
  regular and irregular, 272
  transformation under rotations, 273
spherical tensors, 274–276
  coupling, 275–276
  scalar product, 275
SRS perturbation theory, 113
Stark effect, 240
stationary points, 7
stockholder partitioning, 128
structure factor, 263
structure optimization, 229
sum rules, 243
  Thomas–Reiche–Kuhn, 243
summation convention, 267
supermolecule method, 74, 87–92
susceptibility
  charge density, *see* charge density susceptibility
symmetric perturbation theories, 106–110
  biorthogonal functions, 108
  expansion in exchange, 109
  expansion in overlap, 106
  non-orthogonal perturbation theory, 108
  orthogonalization, 107
symmetrized Rayleigh–Schrödinger perturbation theory, 113
symmetry
  of distributed multipoles, 135
  of multipole moments, 34–37
  of polarizabilities, 37–39
symmetry-adapted perturbation theories, 106, 110–117
  and density functional theory, 115
  and electron correlation, 115
  EL–HAV, 110
  induction, 116
  iterative symmetry-forcing procedures, 111–115

$T_{\alpha\beta\ldots\nu}$, 44
T functions, 50, *291–297t*
Tang–Toennies damping functions, 206
TDDFT, *see* coupled perturbation theory
tensors
  cartesian, *see* cartesian tensors
  interaction, 44
  spherical, *see* spherical tensors
test particle model, 214, *215f*, *215t*
tetrahedral molecules
  non-zero multipole moments, 35

thermal conductivity, 246
Thole damping, 164
Thomas–Reiche–Kuhn sum rule, 243
three-body terms, *see* many-body terms
time correlation functions, 248
time-dependent perturbation theory, 281–282
  for polarizabilities, 31–34
time-of-flight
  in molecular beam scattering, 263
torques, calculation of, 229
transition dipoles
  in resonance interactions, 195–196
transition moments
  distributed monopole model, 197–199
transition states, 6
transport coefficients, 246–247
  from time correlation functions, 248
triple-dipole dispersion, 188
  coefficient, 188
    combining rule, 188
  geometrical factor, 188
  in solid argon, 188
Trouton's rule, 2
tunnelling, 6
tunnelling splittings, 259
two-wire cell, *23f*, 241
TZ2P, *see* basis sets

units
  conversion between, 283–284
  of dipole moment, 14
  of octopole moment, 18
  of polarizability, 27
  of quadrupole moment, 16
Unsöld approximation, 279
  for the dispersion energy, 65

Van der Waals, 2
variation principle, 87
  and energy differences, 88
vector coupling coefficient, 275
versions
  of a structure, 7
vibration–rotation–tunnelling spectroscopy, 250
vibrational polarizabilities, 242, *243t*
vibrations, 11
virial coefficient
  pressure, 245–246
viscosity, 246
Voronoi polyhedra, 129
VRT, *see* vibration–rotation–tunnelling spectroscopy

water
  dimer, 259
    charge transfer energy, *156f*
    dissociation energy, 229, 259
    energy terms, 155
    potential models, 227–229
    spectrum, 251
  dimer and trimer
    tunnelling splittings, 260
  hexamer
    structures, *184f*
    triple-dipole dispersion, 189
  interaction sites, *225f*
  potentials, 225–229
  quadrupole moment, 16
  Sprik–Klein potential, 209
  tetramer
    many-body corrections, *184f*
  trimer, 259
    many-body corrections, *183f*
  trimer and tetramer
    many-body corrections, 183
  triple-dipole dispersion, 189
well depth, 1, 2, *3t*
Wheatley allocation algorithm, 128
Wigner 3*j* symbols, 276
Wigner coefficient, 275
Wigner functions, 274
Wigner rotation matrices, 274
Woodward–Hoffmann rules, 153

X-ray diffraction, 264
  multipole moments from, 136, 241
X-ray scattering, 263
  inelastic, 150
XC, *see* exchange-Coulomb
xenon excimer laser, 197
Xe···Xe, *198f*

zero-point energy, 6, 229